THE DEVELOPMENT OF A NOVEL *IN VITRO* MODEL SUITABLE FOR THE PREDICTION OF BIOAVAILABILITY

by

LANCE R. SHAW

A thesis submitted for the degree
of Doctor of Philosophy
at
ASTON UNIVERSITY

February 2001

Aston University

THE DEVELOPMENT OF A NOVEL *IN VITRO* MODEL SUITABLE FOR THE PREDICTION OF BIOAVAILABILITY

By
LANCE RAYMOND SHAW

Submitted for the degree of Doctor of Philosophy, 2001

SUMMARY

In vitro studies of drug absorption processes are undertaken to assess drug candidate or formulation suitability, mechanism investigation, and ultimately for the development of predictive models. This study included each of these approaches, with the aim of developing novel *in vitro* methods for inclusion in a drug absorption model. Two model analgesic drugs, ibuprofen and paracetamol, were selected. The study focused on three main areas, the interaction of the model drugs with co-administered antacids, the elucidation of the mechanisms responsible for the increased absorption rate observed in a novel paracetamol formulation and the development of novel ibuprofen tablet formulations containing alkalising excipients as dissolution promoters.

Several novel dissolution methods were developed. A method to study the interaction of drug/excipient mixtures in the powder form was successfully used to select suitable dissolution enhancing excipients. A method to study intrinsic dissolution rate using paddle apparatus was developed and used to study dissolution mechanisms. Methods to simulate stomach and intestine environments in terms of media composition and volume and drug/antacid doses were developed. Antacid addition greatly increased the dissolution of ibuprofen in the stomach model.

Novel methods to measure drug permeability through rat stomach and intestine were developed, using sac methodology. The methods allowed direct comparison of the apparent permeability values obtained. Tissue stability, reproducibility and integrity was observed, with selectivity between paracellular and transcellular markers and hydrophilic and lipophilic compounds within an homologous series of beta-blockers.

The diffusion of the model drugs through native pig gastric mucus was characterised. For both drugs the barrier was found to be significantly more than an unstirred water layer. For paracetamol, the addition of each antacid did not significantly affect either the lag-time or diffusion rate. For ibuprofen, the addition of aluminium hydroxide eliminated the diffusion of the drug. The addition of the other antacids reduced the long lag-time observed and modified the diffusion rate. Also, the effect of changing pH (2-8) was studied. A correlation existed between increasing pH, reduced lag-time and increased diffusion rate. The lag time/diffusion rate changes correlated with a drug/mucus hydrophobic interaction that was eliminated with increasing pH.

In vitro model and literature data were combined to produce a computer simulation which modelled oral absorption. The model output was compared to *in vivo* pharmacokinetic data . A statistically significant correlation for predicted and observed t_{max} was observed with R^2=0.9139 and P<0.0001.

The role of sodium bicarbonate, the primary excipient in the novel paracetamol formulation was investigated. Dissolution rate was the only absorption parameter found to be modified (increased) in its presence.

Novel ibuprofen tablet formulations were produced containing tri-sodium phosphate and/or sodium carbonate as dissolution promoting excipients. The tablets generally met pharmacopoeia specifications and were stable after extended storage. Computer modelling predicted increased absorption rate compared to a commercial product.

KEYWORDS: ibuprofen, paracetamol, antacids, absorption, IVIVC, dissolution

Acknowledgements

I would like to express sincere gratitude to Dr. Barbara Conway for her supervision, guidance, support, interest and freedom in the development of this project. I am also grateful to Professor Bill Irwin for his interest and advice. I would like to thank Dr. Tim Grattan for his interest and support and Smithkline Beecham and the Engineering and Physical Sciences Research Council for financial support.

I would also like to thank Dr. John Slack for use of the stability chambers located at OSI pharmaceuticals and Mr. Ian Williams for use of the atomic absorption spectrophotometer located at Upjohn Ltd. I would also like to thank Dr. Karen Lewis for use of the tabletting equipment located at Smithkline Beecham (Harlow) and her assistance during tablet manufacture. Finally, I would also like to thank the staff of Rowley's abattoir for the supply of animal tissues.

Contents

Figure **Page**

Report summary 2
Acknowledgements 3
Contents 4
List of figures 13
List of tables 29
Abbreviations 32

CHAPTER 1 INTRODUCTION

1.1 Oral drug delivery route 34
1.1.1 Anatomy and Physiology of the Stomach 34
1.1.1.1 Anatomy of the stomach 34
1.1.1.2 Stomach histology 36
1.1.1.3 Stomach physiology 36
1.1.1.3.1 Gastric secretions 36
1.1.1.3.2 Cephalic motility phase 37
1.1.1.3.3 Gastric motility phase 38
1.1.1.3.4 Intestinal motility phase 40
1.1.1.3.5 Interdigestive migrating motility complex 41
1.1.2 Gastric emptying 41
1.1.2.1 Gastric emptying of digestible solids and liquids 41
1.1.2.2 Gastric emptying of liquid dosage forms in the fasted state 43
1.1.2.3 Gastric emptying of solid dosage forms in the fasted state 43
1.1.2.4 Gastric emptying of solid dosage forms during the fed state 44
1.1.3 Anatomy and physiology of the small intestine 44
1.1.3.1 Anatomy of the small intestine 45
1.1.3.2 Small intestine histology 45
1.1.3.3 Small intestine physiology 46
1.1.3.3.1 Small intestine secretions 46
1.1.3.3.2 Digestion in the small intestine 47
1.1.3.3.3 Absorption from the small intestine 47

1.1.4 Physicochemical properties of drugs and their application to dissolution and absorption in the GI tract 49
1.1.4.1 Solubility/pH relationships for weak acids and bases..... 49
1.1.4.2 Partition coefficient..... 51
1.2 Bioequivalence and bioavailability 52
1.3 *In vitro in vivo* correlations..... 54
1.3.1 Biopharmaceutics classification system..... 54
1.3.1.1 Class I - high solubility/high permeability drugs..... 55
1.3.1.2 Class II - low solubility/high permeability drugs..... 55
1.3.1.3 Class III - high solubility/low permeability drugs..... 55
1.3.1.4 Class IV - low solubility/low permeability drugs..... 56
1.3.2 Development of IVIVC on a product-by-product basis..... 57
1.3.3 Development of IVIVC using official apparatus..... 58
1.3.4 Dissolution apparatus developments..... 59
1.3.5 Experimental design and optimisation techniques..... 61
1.4 Profiles of selected drug models..... 61
1.4.1 Paracetamol 61
1.4.2 Ibuprofen 68
1.4.3 Selection of antacids..... 72
1.5 Project objectives 72
1.5.1 Development of *in vitro* model to predict drug bioavailability. Validation of model by *in vitro* characterisation of the effect of antacids on the bioavailability of analgesic drugs, during co-administration, and correlation with literature data..... 73
1.5.2 The characterisation of sodium bicarbonate as an absorption enhancing excipient in paracetamol and ibuprofen solid dosage formulations. 76
1.5.3 The development of novel analgesic tablet formulations utilising alkalising excipients. Prediction of bioavailability using novel *in vitro* model. 76

CHAPTER 2 GENERAL METHODS

2.1 Paracetamol assay by HPLC 77

2.1.1 Experimental 77
2.1.1.1 Materials 77
2.1.1.2 Equipment 77
2.1.1.3 Method/chromatographic conditions 78
2.1.2 Example data 78
2.2 Ibuprofen assay by HPLC 80
2.2.1 Experimental 80
2.2.1.1 Materials 80
2.2.1.2 Equipment 81
2.2.1.3 Method/chromatographic conditions 81
2.2.2 Example data 81
2.3 Ibuprofen Impurities by HPLC 83
2.3.1 Experimental 83
2.3.1.1 Materials 83
2.3.1.2 Equipment 83
2.3.1.3 Method/chromatographic conditions 83
2.4 Miscellaneous HPLC Methods 84
2.4.1 Experimental 84
2.4.1.1 Materials 84
2.4.1.2 Equipment 84
2.4.1.3 Method/chromatographic conditions 84
2.5 pH measurements 84
2.6 Kinematic viscosity determination 85
2.7 Scintillation Counting 85

CHAPTER 3 PHYSICOCHEMICAL ANALYSES

3.1 Introduction 86
3.2 Solubility/pH profile of model drugs 86
3.2.1 Experimental 86
3.2.1.1 Materials 86
3.2.1.2 Equipment 86
3.2.1.3 Method 87
3.2.2 Results and discussion 87

3.3 Solubility of antacids in selected buffers 90
3.3.1 Experimental 90
3.3.1.1 Materials 90
3.3.1.2 Equipment 90
3.3.1.3 Method 90
3.3.2 Results and discussion 91
3.4 Dissolved drug adsorption onto antacids 92
3.4.1 Experimental 92
3.4.1.1 Materials 92
3.4.1.2 Equipment 92
3.4.1.3 Method 92
3.4.2 Results and discussion 93
3.5 Solubility of model drugs in excipient-containing solutions 93
3.5.1 Experimental 93
3.5.1.1 Materials 93
3.5.1.2 Equipment 94
3.5.1.3 Method 94
3.5.2 Results and discussion 94

4 DISSOLUTION STUDIES

4.1 Introduction 98
4.2 Theoretical Considerations 99
4.3 Factors affecting the dissolution rate of a drug 101
4.3.1 Dissolution volume 101
4.3.2 Intrinsic dissolution rate constant 101
4.3.3 Surface area of the drug 101
4.3.4 Saturated solubility 102
4.4 Dissolution method development 103
4.4.1 Controlled powder dissolution method 103
4.4.2 Drug/antacid interaction 105
4.4.3 Determination of IDR utilising USP paddle apparatus 105
4.4.4 Commercial tablet dissolution method 108
4.5 Methods for calculation of the dissolution rate of drugs 108

4.5.1 Physical methods 108
4.5.2 Mathematical models 109
4.6 Controlled powder dissolution study 111
4.6.1 Introduction 111
4.6.2 Selection of excipients 111
4.6.3 Experimental 114
4.6.3.1 Materials 114
4.6.3.2 Equipment 114
4.6.3.3 Method 114
4.6.4 Results and discussion 115
4.7 Drug/antacid interaction dissolution study 147
4.7.1 Introduction 147
4.7.2 Experimental 147
4.7.2.1 Materials 147
4.7.2.2 Equipment 148
4.7.2.3 Method 148
4.7.3 Results and discussion 149
4.8 The role of sodium bicarbonate on the dissolution of model drugs from solid dosage formulations 162
4.8.1 Introduction 162
4.8.2 Validation of IDR dissolution method and elucidation of the mechanism controlling the dissolution of model drugs 163
4.8.2.1 Experimental 163
4.8.2.1.1 Materials 163
4.8.2.1.2 Equipment 163
4.8.2.1.3 Method 163
4.8.2.2 Results and discussion 164
4.8.3 Sensitivity of IDR method to pH modification 168
4.8.3.1 Experimental 168
4.8.3.1.1 Materials 168
4.8.3.1.2 Equipment 168
4.8.3.1.3 Method 168
4.8.3.2 Results and discussion 169

4.8.4 Effect of dissolved excipients on the IDR of paracetamol 171
4.8.4.1 Experimental 171
4.8.4.1.1 Materials 171
4.8.4.1.2 Equipment 172
4.8.4.1.3 Method 172
4.8.4.2 Results and discussion 172
4.8.5 Comparison of a novel paracetamol formulation, containing sodium bicarbonate *versus* commercially available paracetamol tablet formulations 175
4.8.5.1 Experimental 175
4.8.5.1.1 Materials 175
4.8.5.1.2 Equipment 176
4.8.5.1.3 Method 176
4.8.5.2 Results and discussion 177
4.8.6 The role of sodium bicarbonate on the dissolution of model drugs from solid dosage forms 181
4.8.7 Summary 190

CHAPTER 5 DRUG DIFFUSION THROUGH MUCUS

5.1 Introduction 194
5.2 Theoretical considerations 196
5.3 Selection of mucus model and diffusion method 201
5.4 Validation of native pig gastric mucus 203
5.4.1 Preparation of mucus 204
5.4.2 Mucus inter-batch variation and stability 204
5.4.2.1 Experimental 204
5.4.2.1.1 Materials 204
5.4.2.1.2 Equipment 204
5.4.2.1.3 Method 206
5.4.2.2 Results and discussion 207
5.5 Drug diffusion through mucus layer 209
5.5.1 Experimental 210
5.5.1.1 Materials 210

5.5.1.2 Equipment 210
5.5.1.3 Method 210
5.5.2 Results and discussion 212
5.5.2.1 Mucus retardation of diffusion rate of model drugs 212
5.5.2.2 The effect of dissolved excipients/antacids on the diffusion rate of model drugs, and the role of pH 214
5.6 Summary 231

CHAPTER 6 DRUG PERMEABILITY THROUGH THE STOMACH AND SMALL INTESTINE

6.1 Introduction 233
6.2 Theoretical considerations 234
6.3 Development of *in vitro* stomach and intestine models 237
6.4 Validation of stomach and intestine models 242
6.4.1 Tight junction integrity 242
6.4.1.1 Experimental 242
6.4.1.1.1 Materials 242
6.4.1.1.2 Equipment 242
6.4.1.1.3 Method 243
6.4.1.2 Results and Discussion 244
6.4.2 Method reproducibility and tissue stability 247
6.4.2.1 Experimental 247
6.4.2.1.1 Materials 247
6.4.2.1.2 Equipment 248
6.4.2.1.3 Method 248
6.4.2.2 Results and discussion 249
6.4.3 Membrane barrier drug permeability selectivity 253
6.4.3.1 Experimental 253
6.4.3.1.1 Materials 253
6.4.3.1.2 Equipment 254
6.4.3.1.3 Method 254
6.4.3.2 Results and discussion 255
6.5 The effect of dissolved excipients/antacids on model drugs' permeability 266

6.5.1 Introduction 266
6.5.2 Experimental 266
6.5.2.1 Materials 266
6.5.2.2 Equipment 266
6.5.2.3 Method 266
6.5.3 Results and discussion 267
6.6 Summary 284

CHAPTER 7 TABLET FORMULATION DEVELOPMENT

7.1 Introduction 286
7.2 Granule formulation development 287
7.2.1 Paracetamol granule development 287
7.2.1.1 Experimental 287
7.2.1.1.1 Materials 287
7.2.1.1.2 Equipment 287
7.2.1.1.3 Method 288
7.2.1.2 Results and Discussion 288
7.2.2 Ibuprofen granule development 294
7.2.2.1 Experimental 294
7.2.2.1.1 Materials 294
7.2.2.1.2 Equipment 294
7.2.2.1.3 Method 294
7.2.2.2 Results and Discussion 294
7.3 Novel ibuprofen tablet formulation development program 298
7.3.1 Experimental 298
7.3.1.1 Materials 298
7.3.1.2 Equipment 299
7.3.1.3 Method 299
7.3.2 Results and discussion 300
7.4 Novel ibuprofen tablet formulation stability program 309
7.4.1 Experimental 309
7.4.1.1 Materials 309
7.4.1.2 Equipment 309

7.4.1.3 Method 310
7.4.2 Results and discussion 310
7.5 Summary 323

CHAPTER 8 DEVELOPMENT OF DRUG ABSORPTION MODEL

8.1 Introduction 326
8.2 Experimental 328
8.2.1 Equipment 328
8.2.2 Method 328
8.3 Results and Discussion 333
8.4 Summary 356

CHAPTER 9 GENERAL SUMMARY

9.1 IVIVC development 359
9.2 Mechanism elucidation of Zapp tablets rapid absorption 362
9.3 Tablet formulation development 363
9.4 Future work 365

References 366
Appendices
Appendix 1 - Composition of buffers 383
Appendix 2 - Radio-labelled materials manufacture and certificates of analysis ... 384

LIST OF FIGURES

Figure		Page
1.1	A schematic illustrating the peristaltic contractions that act to mix and propel stomach contents	39
1.2	A schematic of the gastric and duodenal BER electrical activity	40
1.3	An example of the gastric emptying patterns of co-administered solid and liquid tracers	42
1.4	The structural formula of paracetamol	62
1.5	The structural formula of ibuprofen	68
1.6	Schematic of the developed *in vitro* model	75
2.1	HPLC chromatogram of paracetamol peak with caffeine internal standard obtained using assay method	79
2.2	HPLC chromatogram demonstrating the resolution of paracetamol from its impurity 4-aminophenol	79
2.3	Typical calibration plot for paracetamol assay method	80
2.4	HPLC chromatogram of ibuprofen peak with fenoprofen internal standard obtained using assay method	82
2.5	Typical calibration plot for ibuprofen assay method	82
3.1	Solubility/pH data for paracetamol	89
3.2	Solubility/pH data for ibuprofen	89
3.3	Saturated solubility of paracetamol in 0.05M HCl containing dissolved excipients	96
3.4	Saturated solubility of ibuprofen in USP buffer pH6.8 containing dissolved excipients	97
4.1	Diagram of pellet holders as used in novel IDR method	107
4.2	Dissolution data (F_1 fit-factors) illustrating the effects of excipients/antacids on the dissolution rate of powders with paracetamol used as the model drug	120
4.3	Dissolution profiles of ground Zapp *versus* pure paracetamol using controlled powder dissolution method	121
4.4	Dissolution profiles of sodium bicarbonate/paracetamol mix *versus* pure paracetamol using controlled powder dissolution method	122

4.5	Dissolution profiles of sodium bicarbonate (33%)/paracetamol mix *versus* pure paracetamol using controlled powder dissolution method	122
4.6	Dissolution profiles of sodium bicarbonate (66%)/paracetamol mix *versus* pure paracetamol using controlled powder dissolution method	122
4.7	Dissolution profiles of sodium bicarbonate/paracetamol mix *versus* pure paracetamol using controlled powder dissolution method with water as the dissolution medium	123
4.8	Dissolution profiles of citric acid/paracetamol mix *versus* pure paracetamol using controlled powder dissolution method	123
4.9	Dissolution profiles of lactose/paracetamol mix *versus* pure paracetamol using controlled powder dissolution method	123
4.10	Dissolution profiles of tartaric acid/paracetamol mix *versus* pure paracetamol using controlled powder dissolution method	124
4.11	Dissolution profiles of sodium chloride/paracetamol mix *versus* pure paracetamol using controlled powder dissolution method	124
4.12	Dissolution profiles of di-calcium phosphate/paracetamol mix *versus* pure paracetamol using controlled powder dissolution method	124
4.13	Dissolution profiles of magnesium hydroxide/paracetamol mix *versus* pure paracetamol using controlled powder dissolution method	125
4.14	Dissolution profiles of starch/paracetamol mix *versus* pure paracetamol using controlled powder dissolution method	125
4.15	Dissolution profiles of microcrystalline cellulose/paracetamol mix *versus* pure paracetamol using controlled powder dissolution method	125
4.16	Dissolution profiles of calcium carbonate/paracetamol mix *versus* pure paracetamol using controlled powder dissolution method	126

4.17	Dissolution profiles of aluminium hydroxide/paracetamol mix *versus* pure paracetamol using controlled powder dissolution method	126
4.18	Dissolution profiles of magnesium oxide/paracetamol mix *versus* pure paracetamol using controlled powder dissolution method	126
4.19	Dissolution profiles of L-arginine/paracetamol mix *versus* pure paracetamol using controlled powder dissolution method	127
4.20	Dissolution profiles of glycine/paracetamol mix *versus* pure paracetamol using controlled powder dissolution method	127
4.21	Dissolution profiles of L-lysine/paracetamol mix *versus* pure paracetamol using controlled powder dissolution method	127
4.22	Dissolution profiles of tri-sodium phosphate/paracetamol mix *versus* pure paracetamol using controlled powder dissolution method	128
4.23	Dissolution profiles of sodium carbonate/paracetamol mix *versus* pure paracetamol using controlled powder dissolution method	128
4.24	Dissolution profiles of potassium bicarbonate/paracetamol mix *versus* pure paracetamol using controlled powder dissolution method	128
4.25	Dissolution profiles of ground Tylenol® *versus* pure paracetamol using controlled powder dissolution method	129
4.26	Dissolution profiles of potassium bicarbonate/paracetamol mix *versus* pure paracetamol using controlled powder dissolution method with water as the dissolution medium	129
4.27	Linear section of the dissolution profile of aluminium hydroxide/paracetamol mix generated using controlled powder dissolution method	132
4.28	Linear section of the dissolution profile of pure paracetamol generated using controlled powder dissolution method	132
4.29	Linear section of the dissolution profile of aluminium hydroxide/paracetamol mix generated using controlled powder	132

	dissolution method	
4.30	Dissolution data (F_1 fit-factors) illustrating the effects of excipients/antacids on the dissolution rate of powders with ibuprofen used as the model drug	136
4.31	Dissolution profiles of aluminium hydroxide/ibuprofen mix *versus* pure ibuprofen using controlled powder dissolution method	137
4.32	Dissolution profiles of sodium bicarbonate/ibuprofen mix *versus* pure ibuprofen using controlled powder dissolution method	138
4.33	Dissolution profiles of sodium chloride/ibuprofen mix *versus* pure ibuprofen using controlled powder dissolution method	138
4.34	Dissolution profiles of magnesium hydroxide/ibuprofen mix *versus* pure ibuprofen using controlled powder dissolution method	138
4.35	Dissolution profiles of calcium carbonate/ibuprofen mix *versus* pure ibuprofen using controlled powder dissolution method	139
4.36	Dissolution profiles of lactose/ibuprofen mix *versus* pure ibuprofen using controlled powder dissolution method	139
4.37	Dissolution profiles of starch/ibuprofen mix *versus* pure ibuprofen using controlled powder dissolution method	139
4.38	Dissolution profiles of di-calcium phosphate/ibuprofen mix *versus* pure ibuprofen using controlled powder dissolution method	140
4.39	Dissolution profiles of microcrystalline cellulose/ibuprofen mix *versus* pure ibuprofen using controlled powder dissolution method	140
4.40	Dissolution profiles of potassium bicarbonate/ibuprofen mix *versus* pure ibuprofen using controlled powder dissolution method	140
4.41	Dissolution profiles of citric acid/ibuprofen mix *versus* pure ibuprofen using controlled powder dissolution method	141

4.42	Dissolution profiles of tartaric acid/ibuprofen mix *versus* pure ibuprofen using controlled powder dissolution method	141
4.43	Dissolution profiles of sodium bicarbonate (33%)/ibuprofen mix *versus* pure ibuprofen using controlled powder dissolution method	141
4.44	Dissolution profiles of sodium bicarbonate (66%)/ibuprofen mix *versus* pure ibuprofen using controlled powder dissolution method	142
4.45	Dissolution profiles of L-arginine/ibuprofen mix *versus* pure ibuprofen using controlled powder dissolution method	142
4.46	Dissolution profiles of L-lysine/ibuprofen mix *versus* pure ibuprofen using controlled powder dissolution method	142
4.47	Dissolution profiles of glycine/ibuprofen mix *versus* pure ibuprofen using controlled powder dissolution method	143
4.48	Dissolution profiles of tri-basic sodium phosphate/ibuprofen mix *versus* pure ibuprofen using controlled powder dissolution method	143
4.49	Dissolution profiles of sodium carbonate/ibuprofen mix *versus* pure ibuprofen using controlled powder dissolution method	143
4.50	Dissolution profiles of ground Hedex® *versus* pure ibuprofen using controlled powder dissolution method	144
4.51	Dissolution profiles of magnesium oxide/ibuprofen mix *versus* pure ibuprofen using controlled powder dissolution method	144
4.52	Linear section of the dissolution profile of aluminium 0hydroxide/ibuprofen mix generated using controlled powder dissolution method	146
4.53	Linear section of the dissolution profile of pure ibuprofen generated using controlled powder dissolution method	146
4.54	Linear section of the dissolution profile of lactose/ibuprofen mix generated using controlled powder dissolution method	146

4.55	Effect of co-administered magnesium oxide on the dissolution of paracetamol tablets in simulated stomach method	152
4.56	Effect of co-administered sodium bicarbonate on the dissolution of paracetamol tablets in simulated stomach method	152
4.57	Effect of co-administered calcium carbonate on the dissolution of paracetamol tablets in simulated stomach method	153
4.58	Effect of co-administered aluminium hydroxide on the dissolution of paracetamol tablets in simulated stomach method	153
4.59	Effect of co-administered magnesium hydroxide on the of dissolution paracetamol tablets in simulated intestine method	154
4.60	Effect of co-administered magnesium oxide on the dissolution of paracetamol tablets in simulated intestine method	154
4.61	Effect of co-administered sodium bicarbonate on the dissolution of paracetamol tablets in simulated intestine method	155
4.62	Effect of co-administered calcium carbonate on the dissolution of paracetamol tablets in simulated intestine method	155
4.63	Effect of co-administered aluminium hydroxide on the dissolution of paracetamol tablets in simulated intestine method	156
4.64	Effect of co-administered magnesium hydroxide on the of dissolution paracetamol tablets in simulated intestine method	156
4.65	Effect of co-administered aluminium hydroxide on the dissolution of ibuprofen tablets in simulated stomach method	157
4.66	Effect of co-administered magnesium hydroxide on the of dissolution ibuprofen tablets in simulated stomach method	157
4.67	Effect of co-administered magnesium oxide on the dissolution of ibuprofen tablets in simulated stomach method	158
4.68	Effect of co-administered calcium carbonate on the dissolution of ibuprofen tablets in simulated stomach method	158
4.69	Effect of co-administered sodium bicarbonate on the dissolution of ibuprofen tablets in simulated stomach method	159
4.70	Effect of co-administered sodium bicarbonate on the dissolution of ibuprofen tablets in simulated intestine method	159

4.71	Effect of co-administered calcium carbonate on the dissolution of ibuprofen tablets in simulated intestine method	160
4.72	Effect of co-administered magnesium oxide on the dissolution of ibuprofen tablets in simulated intestine method	160
4.73	Effect of co-administered magnesium hydroxide on the dissolution of ibuprofen tablets in simulated intestine method	161
4.74	Effect of co-administered aluminium hydroxide on the dissolution of ibuprofen tablets in simulated intestine method	161
4.75	IDR dissolution profiles of paracetamol illustrating the effect of changing the stirrer rate	164
4.76	IDR dissolution profiles of ibuprofen illustrating the effect of changing the stirrer rate	165
4.77	Illustration of the linear relationship between IDR of paracetamol and the hydrodynamic conditions	167
4.78	Illustration of the linear relationship between IDR of ibuprofen and the hydrodynamic conditions	167
4.79	The effect of pH on the IDR of paracetamol	170
4.80	IDR of paracetamol in 0.05M HCl containing various excipients	174
4.81	IDR of ibuprofen in 0.05M HCl containing various excipients	174
4.82	Dissolution data (F_1 fit-factors) illustrating the variation between the dissolution characteristics of commercially formulated paracetamol 500mg tablets	178
4.83	Dissolution profiles of selected paracetamol 500mg tablets	179
4.84	Dissolution profiles of Panadol® 500mg tablets under different stirrer conditions	179
4.85	Dissolution profiles of Zapp 500mg tablets under different stirrer conditions	180
4.86	Comparison of Zapp and Panadol® tablets dissolution using simulated stomach model	180
4.87	Calculated values of k_2 constant for the dissolution of paracetamol in excipient-containing medium	185
4.88	Histogram of calculated values of k_2 constant for the dissolution of paracetamol in excipient-containing medium	186

4.89	Schematic of aspects of the dissolution process detailing the effect of dissolved sodium bicarbonate on ibuprofen dissolution	188
4.90	Calculated values of k_2 constant for the dissolution of ibuprofen in excipient-containing medium	189
4.91	Histogram of calculated values of k_2 constant for the dissolution of ibuprofen in excipient-containing medium	190
5.1	Schematic representation of a typical diffusion profile through a membrane	197
5.2	Diagram of a side-on three-compartment diffusion cell	205
5.3	Diagram of central compartment of side-on three-compartment diffusion cell	206
5.4	Calculated flux values for the diffusion of paracetamol through three batches of mucus	208
5.5	Calculated flux values for the diffusion of paracetamol through one batch of mucus over 4 days	209
5.6	The diffusion of paracetamol through a single membrane filter, an unstirred aqueous layer and a mucus layer	213
5.7	The diffusion of ibuprofen through a single membrane filter, an unstirred aqueous layer and a mucus layer	214
5.8	Effect of dissolved antacid/excipient on the lag times for paracetamol diffusion	216
5.9	Effect of dissolved antacid/excipient on the diffusion rate for paracetamol diffusion	216
5.10	Effect of saturated aluminium hydroxide solution on the diffusion of paracetamol	217
5.11	Effect of saturated calcium carbonate solution on the diffusion of paracetamol	217
5.12	Effect of saturated magnesium hydroxide solution on the diffusion of paracetamol	218
5.13	Effect of saturated magnesium oxide solution on the diffusion of paracetamol	218
5.14	Effect of 15mmol/200ml sodium bicarbonate on the diffusion of paracetamol	218

5.15	Effect of dissolved antacids/excipients on the lag-time for ibuprofen diffusion	220
5.16	Effect of dissolved antacids/excipients on the diffusion rate for ibuprofen diffusion	221
5.17	Effect of 15mmol/200ml sodium bicarbonate on the diffusion of ibuprofen	221
5.18	Effect of saturated magnesium hydroxide solution on the diffusion of ibuprofen	222
5.19	Effect of saturated magnesium oxide solution on the diffusion of ibuprofen	222
5.20	Effect of saturated aluminium hydroxide solution on the diffusion of ibuprofen	222
5.21	Effect of saturated calcium carbonate solution on the diffusion of paracetamol	223
5.22	Effect of pH on the lag time for ibuprofen diffusion	224
5.23	Effect of pH on the diffusion rate of ibuprofen diffusion	225
5.24	Effect of pH on the diffusion profile of ibuprofen	225
5.25	Percent ionised with changing pH for ibuprofen paracetamol and mucus	227
6.1	Schematic representation of paracellular and diffusive components of passive drug absorption across the gastrointestinal mucosa	237
6.2	Permeability of mannitol through stomach in presence and absence of calcium ions	246
6.3	Permeability of mannitol through intestine in presence and absence of calcium ions	246
6.4	Stomach permeability frequency distribution of mannitol controls measured throughout the experimental series	252
6.5	Intestine permeability frequency distribution of mannitol controls measured throughout the experimental series	253
6.6	Permeability of various drugs through the stomach model	256
6.7	Permeability of various drugs through the intestine model	257

6.8	Effect of molecular weight on the efficiency of drug transport by the paracellular route, expressed as the sieving coefficient	259
6.9	Relationship between % absorbed in humans and the apparent permeability in the stomach model	261
6.10	Relationship between % absorbed in humans and the apparent permeability in the intestine model	261
6.11	Relationship between logD, determined in a water:propylene glycol dipelargonate system and $\log k_A$. Data is for a compound set with a wide range of structural diversity. Absorption determined *in-situ* in rat ileum	263
6.12	Correlation between oral absorption in man and the permeability co-efficients in vascularly perfused whole rat small intestine	263
6.13	Transport profiles of drugs through the stomach model	264
6.14	Transport profiles of drugs through the stomach model	264
6.15	Transport profiles of drugs through the intestine model	265
6.16	Transport profiles of drugs through the intestine model	265
6.17	Effect of antacid/excipient on the relative permeability of paracetamol compared to mannitol through intestine	271
6.18	Effect of antacid/excipient on the relative permeability of ibuprofen compared to mannitol through intestine	272
6.19	Effect of antacid/excipient on the relative permeability of paracetamol compared to mannitol through stomach	273
6.20	Effect of antacid/excipient on the relative permeability of ibuprofen compared to mannitol through stomach	274
6.21	Transport profiles of mannitol and paracetamol through the stomach, with donor solution containing buffer only (control)	275
6.22	Transport profiles of mannitol and paracetamol through the stomach, with donor solution containing sodium bicarbonate	275
6.23	Transport of mannitol and paracetamol through the stomach, with donor solution saturated with calcium carbonate	276
6.24	Transport profiles of mannitol and paracetamol through the stomach, with donor solution saturated with aluminium hydroxide	276

6.25	Transport profiles of mannitol and paracetamol through the stomach, with donor solution saturated with magnesium hydroxide	276
6.26	Transport profiles of mannitol and paracetamol through the stomach, with donor solution saturated with magnesium oxide	277
6.27	Transport profiles of mannitol and ibuprofen through the stomach, with donor solution containing buffer only (control)	277
6.28	Transport profiles of mannitol and ibuprofen through the stomach, with donor solution containing sodium bicarbonate	277
6.29	Transport of mannitol and ibuprofen through the stomach, with donor solution saturated with calcium carbonate	278
6.30	Transport of mannitol and ibuprofen through the stomach, with donor solution saturated with aluminium hydroxide	278
6.31	Transport of mannitol and ibuprofen through the stomach, with donor solution saturated with magnesium hydroxide	278
6.32	Transport of mannitol and ibuprofen through the stomach, with donor solution saturated with magnesium oxide	279
6.33	Transport of mannitol and ibuprofen through the stomach, with donor solution containing Formulation 5 ibuprofen tablet	279
6.34	Transport of mannitol and paracetamol through the intestine, with donor solution containing buffer only (control)	279
6.35	Transport of mannitol and paracetamol through the intestine, with donor solution containing sodium bicarbonate	280
6.36	Transport of mannitol and paracetamol through the intestine, with donor solution saturated with calcium carbonate	280
6.37	Transport of mannitol and paracetamol through the intestine, with donor solution saturated with aluminium hydroxide	280
6.38	Transport of mannitol and paracetamol through the intestine, with donor solution saturated with magnesium hydroxide	281
6.39	Transport of mannitol and paracetamol through the intestine, with donor solution saturated with magnesium oxide	281
6.40	Transport of mannitol and ibuprofen through the intestine, with donor solution containing buffer only (control)	281

6.41	Transport of mannitol and ibuprofen through the intestine, with donor solution containing sodium bicarbonate	282
6.42	Transport of mannitol and ibuprofen through the intestine, with donor solution saturated with calcium carbonate	282
6.43	Transport of mannitol and ibuprofen through the intestine, with donor solution saturated with aluminium hydroxide	282
6.44	Transport of mannitol and ibuprofen through the intestine, with donor solution saturated with magnesium hydroxide	283
6.45	Transport of mannitol and ibuprofen through the intestine, with donor solution saturated with magnesium oxide	283
6.46	Transport of mannitol and ibuprofen through the intestine, with donor solution containing Formulation 5 ibuprofen tablet	283
7.1	Relationship between the granule dissolution rate expressed as F_1 *versus* the excipient composition, for ibuprofen granule development study	292
7.2	Example of a response line when two factors, crushing strength and composition, are investigated	295
7.3	Dissolution profiles of ibuprofen granules with varying dissolution promoting excipients compositions	296
7.4	Dissolution of two commercial and one experimental (Formulation5) ibuprofen tablet formulations in simulated intestine fluid (USP buffer 6.8)	306
7.5	Dissolution of two commercial ibuprofen tablet formulations in simulated stomach fluid (0.05M HCl).	306
7.6	Dissolution of formulation 1 and two commercial ibuprofen tablet formulations in simulated stomach fluid (0.05M HCl)	307
7.7	Dissolution of formulation 2 and two commercial ibuprofen tablet formulations in simulated stomach fluid (0.05M HCl)	307
7.8	Dissolution of formulation 3 and two commercial ibuprofen tablet formulations in simulated stomach fluid (0.05M HCl)	308
7.9	Dissolution of formulation 4 and two commercial ibuprofen tablet formulations in simulated stomach fluid (0.05M HCl)	308

7.10	Dissolution of Formulation 5 and two commercial ibuprofen tablet formulations in simulated stomach fluid (0.05M HCl)	309
7.11	Effect of long term storage at 25°C/60%RH on the assay of each ibuprofen formulation	317
7.12	Effect of long term storage at 40°C/75%RH on the assay of each ibuprofen formulation	317
7.13	Effect of long term storage at 25°C/60%RH on the dissolution of each ibuprofen formulation	318
7.14	Effect of long term storage at 40°C/75%RH on the dissolution of each ibuprofen formulation	318
7.15	Effect of long term storage at 25°C/60%RH on dissolution solution pH for each ibuprofen formulation	319
7.16	Effect of long term storage at 40°C/75%RH on dissolution pH for each ibuprofen formulation	319
7.17	Effect of long term storage at 25°C/60%RH on the ATW of each ibuprofen formulation	320
7.18	Effect of long term storage at 40°C/75%RH on the ATW of each ibuprofen formulation	320
7.19	Effect of long term storage at 25°C/60%RH on the measured LOD for each ibuprofen formulation	321
7.20	Effect of long term storage at 40°C/75%RH on the measured LOD for each ibuprofen formulation	321
7.21	Effect of long term storage at 25°C/60%RH on the crushing strength for each ibuprofen formulation	322
7.22	Effect of long term storage at 40°C/75%RH on the crushing strength for each ibuprofen formulation	322
8.1	Developed model to simulate the drug absorption process for drugs administered *via* the oral route	330
8.2	Predicted drug plasma concentration/time profile for paracetamol control simulated PK study	339
8.3	Predicted parameter values during paracetamol control simulated PK study	339

8.4	Predicted %dissolved/%absorbed relationship during paracetamol control simulated PK study	339
8.5	Predicted drug plasma concentration/time profile for paracetamol/ magnesium oxide simulated PK study	340
8.6	Predicted parameter values during paracetamol/magnesium oxide simulated PK study	340
8.7	Predicted %dissolved/%absorbed relationship during paracetamol/ magnesium oxide simulated PK study	340
8.8	Predicted drug plasma concentration/time profile for paracetamol/ magnesium hydroxide simulated PK study	341
8.9	Predicted parameter values during paracetamol/magnesium hydroxide simulated PK study	341
8.10	Predicted %dissolved/%absorbed relationship during paracetamol/ magnesium hydroxide simulated PK study	341
8.11	Predicted drug plasma concentration/time profile for paracetamol/ aluminium hydroxide simulated PK study	342
8.12	Predicted parameter values during paracetamol/aluminium hydroxide simulated PK study	342
8.13	Predicted %dissolved/%absorbed relationship during paracetamol/ aluminium hydroxide simulated PK study	342
8.14	Predicted drug plasma concentration/time profile for paracetamol/ calcium carbonate simulated PK study	343
8.15	Predicted parameter values during paracetamol/calcium carbonate simulated PK study	343
8.16	Predicted %dissolved/%absorbed relationship during paracetamol/ calcium carbonate simulated PK study	343
8.17	Predicted drug plasma concentration/time profile for paracetamol/ sodium bicarbonate simulated PK study	344
8.18	Predicted parameter values during paracetamol/sodium bicarbonate simulated PK study	344
8.19	Predicted %dissolved/%absorbed relationship during paracetamol/ sodium bicarbonate simulated PK study	344

8.20	Predicted drug plasma concentration/time profile for paracetamol Zapp simulated PK study	345
8.21	Predicted parameter values during paracetamol Zapp simulated PK study	345
8.22	Predicted %dissolved/%absorbed relationship during paracetamol Zapp simulated PK study	345
8.23	Predicted drug plasma concentration/time profile for ibuprofen control simulated PK study	346
8.24	Predicted parameter values during ibuprofen control simulated PK study	346
8.25	Predicted %dissolved/%absorbed relationship during ibuprofen control simulated PK study	346
8.26	Predicted drug plasma concentration/time profile for ibuprofen/ magnesium oxide simulated PK study	347
8.27	Predicted parameter values during ibuprofen /magnesium oxide simulated PK study	347
8.28	Predicted %dissolved/%absorbed relationship during ibuprofen/ magnesium oxide simulated PK study	347
8.29	Predicted drug plasma concentration/time profile for ibuprofen/ magnesium hydroxide simulated PK study	348
8.30	Predicted parameter values during ibuprofen/magnesium hydroxide simulated PK study	348
8.31	Predicted %dissolved/%absorbed relationship during ibuprofen/ magnesium hydroxide simulated PK study	348
8.32	Predicted drug plasma concentration/time profile for ibuprofen/ aluminium hydroxide simulated PK study	349
8.33	Predicted parameter values during ibuprofen/aluminium hydroxide simulated PK study	349
8.34	Predicted %dissolved/%absorbed relationship during ibuprofen/ aluminium hydroxide simulated PK study	349
8.35	Predicted drug plasma concentration/time profile for ibuprofen/ calcium carbonate simulated PK study	350

8.36	Predicted parameter values during ibuprofen/calcium carbonate simulated PK study	350
8.37	Predicted %dissolved/%absorbed relationship during ibuprofen/ calcium carbonate simulated PK study	350
8.38	Predicted drug plasma concentration/time profile for ibuprofen/ sodium bicarbonate simulated PK study	351
8.39	Predicted parameter values during ibuprofen/sodium bicarbonate simulated PK study	351
8.40	Predicted %dissolved/%absorbed relationship during ibuprofen/ sodium bicarbonate simulated PK study	351
8.41	Predicted drug plasma concentration/time profile for ibuprofen formulation 5 simulated PK study	352
8.42	Predicted parameter values during ibuprofen formulation 5 simulated PK study	352
8.43	Predicted %dissolved/%absorbed relationship during ibuprofen formulation 5 simulated PK study	352
8.44	Predicted effects of changing dissolution and gastric emptying rates on the T_{max} of paracetamol, with gastric emptying lag time set at 16 minutes	355
8.45	Predicted effects of changing dissolution and gastric emptying rates on the T_{max} of paracetamol, with gastric emptying lag time set at 8 minutes	355
8.46	Correlation between predicted T_{max} values, obtained form the model, and values referenced from *in vivo* studies	356

LIST OF TABLES

Table		Page
1.1	Pharmacokinetics of paracetamol	67
1.2	Pharmacokinetics of ibuprofen	71
3.1	Solubility/pH relationship for ibuprofen and paracetamol	88
3.2	Solubility of antacids in simulated gastric (0.05MHCl) and simulated intestinal buffer (USP buffer pH6.8)	91
3.3	The adsorption of model drugs (dissolved) onto solid antacids	93
3.4	The solubility of model drugs in excipient-containing buffer solutions	95
4.1	Details of excipient group properties used for powder dissolution study	113
4.2	F_1 fit-factors for paracetamol:excipient mixtures compared to pure paracetamol	116
4.3	Categorisation of excipient with respect to its effect on the dissolution rate of paracetamol	117
4.4	Illustration of the effect of alkalising excipients on the dissolution of paracetamol from powder mixes	118
4.5	Calculated dissolution rates of paracetamol powder mixes	131
4.6	F_1 fit factors for ibuprofen:excipient mixtures compared to pure ibuprofen	133
4.7	Categorisation of excipient with respect to its effect on the dissolution rate of ibuprofen	134
4.8	Calculated dissolution rates of ibuprofen powder mixes	145
4.9	F_1 fit-factors comparing dissolution profiles of model drugs in antacid containing simulated gastric and intestinal environments	151
4.10	Paracetamol IDR with changing hydrodynamic conditions	166
4.11	Ibuprofen IDR with changing hydrodynamic conditions	166
4.12	The effect of increasing pH on the IDR of paracetamol	170
4.13	The effect of dissolved excipients on the IDR of model drugs	173
4.14	Contribution of the measured factors to the dissolution of paracetamol from pellets using IDR paddle method	183

4.15	Contribution of the measured factors to the dissolution of ibuprofen from pellets using IDR paddle method	186
5.1	The effects of dissolved antacid/excipient additives on the diffusion of paracetamol through mucus	215
5.2	The effects of dissolved antacid/excipient additives on the diffusion of ibuprofen through mucus	220
5.3	The effects of pH on the diffusion of ibuprofen through mucus	224
5.4	Calculated values of species ionised at experimental pH, for mucus and paracetamol	228
5.5	Calculated values of species ionised at experimental pH, for mucus and ibuprofen	230
6.1	Effect of calcium-free-buffer on the transport of mannitol through rat stomach and intestine tissue	245
6.2	Summary of the calculated apparent permeability of mannitol control during the study of the effects of antacids/excipients on the permeability of model drugs through rat Gi tissue samples	250
6.3	Selected drugs' apparent permeability values through rat stomach and intestine tissues	255
6.4	The effects of added antacids/excipients on the apparent permeability of ibuprofen/mannitol through rat intestine	269
6.5	The effects of added antacids/excipients on the apparent permeability of paracetamol/mannitol through rat intestine	269
6.6	The effects of added antacids/excipients on the apparent permeability of ibuprofen/mannitol through rat stomach	270
6.7	The effects of added antacids/excipients on the apparent permeability of paracetamol/mannitol through rat stomach	270
7.1	Factor (excipient) combinations for paracetamol granules development study	290
7.2	Physical characterisation of paracetamol granule formulations	293
7.3	Factor (excipient) combinations for ibuprofen granules development study	296
7.4	Physical characterisation of ibuprofen granule formulations	298

7.5	Physical and chemical characterisation of ibuprofen tablet formulations	305
7.6	Summary of the effect of long term storage on the physical and chemical characteristics of ibuprofen formulation 1	314
7.7	Summary of the effect of long term storage on the physical and chemical characteristics of ibuprofen formulation 2	314
7.8	Summary of the effect of long term storage on the physical and chemical characteristics of ibuprofen formulation 3	315
7.9	Summary of the effect of long term storage on the physical and chemical characteristics of ibuprofen formulation 4	315
7.10	Summary of the effect of long term storage on the physical and chemical characteristics of ibuprofen formulation 5	316
8.1	Summary of developed *in vivo-in vitro* model's functionality	331
8.2	Summary of rate constants used in modelling study	332
8.3	Summary of t_{max} data generated from drug absorption model	338

ABBREVIATIONS

AAS	Atomic Absorption Spectroscopy
ATW	Average tablet weight
BCS	Biopharmaceutics Classification System
BER	Basic electrical rhythm
Bq	Bequerel
BP	British Pharmacopoeia
CCK	Cholecystokin
Ci	Curie
CI	Confidence interval
cm	Centimetre
Conc^{n}	Concentration
C of A	Certificate of Analysis
DDRG	Drug Delivery Research Group
Diss^{n}	Dissolution
DPM	Disintegrations *per* minute
EGTA	Ethylene glycol-bis(β-aminoethylether)-N,N,N',N'-tetra acetic acid
FDA	Federal Drug Administration
G	Giga
GI	Gastrointestinal
GIP	Gastric inhibitory peptide
GE	Gastric emptying
GLP	Good Laboratory Practice
h or hr	Hour
HCl	Hydrochloric acid
HEPES	N-2-hydroxyethylpiperazine-N'-2-ethane sulphonic acid
IDR	Intrinsic dissolution rate
IMMC	Interdigestive migrating motility complex
IR	Immediate release
IVIVC	*In vitro-In vivo* Correlation
kcal	Kilocalories
kg	Kilograms

LOD	Loss on drying
M	Molar
MBS	Modified buffer solution
mg	Milligrammes
min	Minutes
ml	Millilitres
mM	Millmolar
mmol	Millimoles
NSAID	Non-steroidal anti-inflammatory drug
PGM	Pig gastric mucus
PK	Pharmacokinetics
R	Correlation coefficient
RH	Relative humidity
RPM	Revolutions *per* minute
RSD	Relative standard deviation
s	Seconds
SB	Smithkline Beecham Pharmaceuticals
SD	Standard Deviation
SEM	Standard error of the mean
SUPAC	Scale-up post-approval change
USP	United States Pharmacopoeia
UV	Ultraviolet
µg	Micrograms
µl	Microlitres
°C	Degrees Celsius
%	Percentage
"at least"	For experiments this implies 5-6 replicates for dissolution studies and 3-5 replicates for all other studies

CHAPTER 1
INTRODUCTION

1.1 Oral drug delivery route

The oral drug delivery route is the most frequently used route of administration. Oral dosage forms are usually intended for systemic effects resulting from drug absorption through the various mucosa of the GI tract. Factors affecting the absorption of drugs by this route include the physicochemical properties of the drug and formulations, the changing chemical environment, nature and degree of barrier and drug permeability through the GI mucosa. Any study related to this route of administration requires a review of these factors.

1.1.1 Anatomy and physiology of the human stomach

The stomach is a 'j' shaped enlargement of the GI tract, located directly inferior to the diaphragm in the epigastric, umbilical and left hypochondriac regions of the abdomen. The stomach connects the oesophagus to the duodenum, the first part of the small intestine. One of the primary functions of the stomach is to act as a mixing and holding area for recently ingested food. As appropriate, the stomach forces small quantities of partially digested material into the first portion of the small intestine, the duodenum. The stomach begins the digestion of proteins, continues the digestion of triglycerides and converts the ingested material into a mass of liquid called chyme, and absorbs some substances.

1.1.1.1 Anatomy of the stomach

The stomach can vary its size to accommodate a volume of between approximately 0.5 and 5.0 litres (Sanford 1982). The stomach consists of four main regions: the cardia, fundus, body and pylorus. The rounded portion at the top of the structure, at the opening, is the cardia. The rounded portion above and to the left of the cardia is the fundus. Inferior to the fundus is located the large central portion of the stomach, which is termed the body. The lower region of the stomach which connects to the duodenum is the pylorus. The pylorus can be further subdivided into the pyloric

antrum, which connects to the body of the stomach and the pyloric canal, which connects to the duodenum. Between the pyloric canal and the duodenum is the pyloric sphincter - a valve for regulating flow from the stomach. The concave medial border of the stomach is known as the lesser curvature and the convex lateral border is the greater curvature. When the stomach is empty, the mucosae lie in large folds, called rugae, which are visible to the naked eye (Tortora 1996).

For discussions relating to motility, the stomach is divided into two regions: the orad area, consisting of the fundus, cardia and upper portion of the body, and the caudad area consisting of the distal body and pylorus. The gastric aspect of the emptying process is the result of contraction of smooth muscle cells arranged in three layers: an outer longitudinal layer, a middle circular layer and an inner oblique layer. The longitudinal layer is absent on the anterior and posterior surfaces of the stomach. The circular layer is the most prominent and is present in all areas of the stomach except the paraoesophagal region. The oblique layer is the least complete, being formed from two bands of muscle lying on the anterior and posterior surfaces of the stomach. These two bands meet at the mouth of the pyloric sphincter and fan out to fuse with the circular muscle layer in the caudad. Both the circular and the longitudinal muscle layers increase in thickness towards the duodenum (Johnson 1991).

The stomach is innervated with both intrinsic and extrinsic nerves. The intrinsic nerves lie within a large number of networks or plexuses. The most prominent of these is the myenteric plexus that lies in a three dimensional matrix between the longitudinal and circular muscle layers and throughout the circular muscle layer. Extrinsically the stomach is innervated by branches of the vagus nerves and by fibres originating in the coeliac plexus of the sympathetic nervous system. The bundle of circular muscle located at the gastroduodenal junction is separated from the duodenum *via* a connective tissue septum. However, some longitudinal muscle fibres connect the pyloric antrum to muscle cells within the duodenum. The pylorus is richly innervated with both extrinsic and intrinsic nerves, particularly the thickened circular muscle layer. The proximal duodenum is similar to the rest of the intestine except that again it is richly innervated with intrinsic nerves (Tortora 1996).

1.1.1.2 Stomach histology

The stomach wall is composed of four basic layers, as in the rest of the GI tract, but with some modifications. The surface layer of the mucosa consists of a layer of columnar epithelial cells called mucus surface cells. Epithelial cells also extend down to form narrow channels called gastric pits. Within these gastric pits are columns of secretory cells called gastric glands. These glands consist of three types of exocrine gland cells namely mucus neck cells, chief cells and parietal cells, whose secretions are deployed into the stomach lumen. In addition the gastric glands include one of the hormone producing enteroendocrine cell types, known as G cells, these cells being especially prolific in the pyloric antrum. The submucosa of the stomach consists of areolar connective tissue, which connects the mucosa to the muscularis (Tortora 1996).

1.1.1.3 Stomach physiology

1.1.1.3.1 Gastric secretions

Four constituents of the gastric juice have physiological functions, intrinsic factor, hydrogen ions, pepsin and mucus. Intrinsic factor is produced by parietal cells and is required for the absorption of vitamin B_{12}. The hydrochloric acid is required for the conversion of pepsinogen into pepsin and it acts to kill microbes and denature proteins, it is also secreted by parietal cells (Johnson *et al.* 1991). The acid can traverse the mucus layer, from the gastric gland to the lumen, by diffusing through the mucus at pHs above 4, forming viscous fingering patterns as it moves. At a pH of 2, the acid is unable to diffuse back towards the mucosa due to the high viscosity of the gastric mucus (Bhaskar *et al.* 1992). The unstimulated human stomach secretes acid at a rate equal to 10 to 15 % of that present during maximal stimulation. The empty stomach contains a relatively small volume of gastric juice usually at a pH of less than 2. Mucus is secreted by gastric neck and surface cells. It covers the whole of the stomach wall and acts as a protective barrier for the underlying mucosa against the acidic conditions in the lumen. The mucus mode of action is as a high viscosity, mechanical barrier and through the mucus-bicarbonate barrier whereby bicarbonate ions secreted by the gastric epithelium, form a pH gradient from pH 1-2 at the lumen to pH 6-7 at the cell surface (Bhaskar *et al.* 1992; Desai and Vadgamma, 1992; Rees

1987; and Williams and Turnberg, 1981). Pepsin, converted from pepsinogen at pH below 5, is produced by the chief cells and is utilised to break down certain bonds in proteins.

Both neural and hormonal mechanisms control the secretion of gastric juice and contraction of smooth muscle in the stomach wall. During digestion, events occur in three overlapping phases; the cephalic, gastric and intestinal phases. During the cephalic phase parasympathetic impulses from nuclei in the medulla oblongata are transmitted *via* the vagus nerves. These impulses promote peristalsis in the stomach and smooth muscle and stimulate gastric glands to secrete pepsinogen, hydrochloric acid and mucus into stomach chyme and gastrin into the blood. Then, during the intestinal phase, neural and hormonal reflexes initiated in the small intestine exert an inhibitory effect on secretory activity and motility of the stomach (Tortora 1996). A second digestive pattern occurs during the fasting state known as the interdigestive migrating motility complex (IMMC).The stomach generates these 'housekeeping' mechanical waves which act to clear the stomach of indigestible solids (Moore 1989).

1.1.1.3.2 Cephalic motility phase

Chemoreceptors and mechanoreceptors located in the tongue and the buccal and nasal cavities are stimulated by tasting, smelling, chewing and swallowing food. The cerebal cortex and feeding centre in the hypothalamus send impulses to and from the brain. The efferent nerve impulses are relayed through the vagal nucleus and vagal efferent fibres to the stomach. Parasympathetic fibres innervate parietal cells, chief cells and mucous cells and increase secretions from all the gastric glands. They also innervate smooth muscle of the stomach and stimulate gastric motility. The cephalic phase has been studied by a procedure known as sham-feeding. A dog is prepared with oesophageal and gastric fistulas. When the oesophageal fistula is open, swallowed food does not enter the stomach. Gastric secretion can be collected from the gastric fistula and its volume and acid content measured. From these studies it has been deduced that the cephalic phase accounts for approximately 30% of the stimulation (Tortora 1996 and Johnson 1991).

1.1.1.3.3 Gastric motility phase

When swallowed food first enters the stomach and mixes with the small volume of gastric juice present, buffers, primarily in the form of proteins contained in the food, neutralise the acid. The volume of the food also acts to distend the stomach wall. The rise in pH is monitored by chemoreceptors which send nerve impulses to the submucosal plexus where they activate parasympathetic fibres which stimulate gastrin release which in turn stimulates the release of hydrochloric acid and pepsinogen. According to Johnson (1991) the increase in pH of the contents of the gastric juice does not, in itself, cause a stimulus for release of gastrin but acts to allow other stimuli to be effective, thus it is proposed that the distension of the stomach and bathing the mucosa with certain chemicals, primarily amino acids and peptides, are the effective stimuli of the gastric phase. Tortora (1996) does not make this distinction and reports the change in pH to be the controlling mechanism, although of course this is affected by the buffering action of proteins etc. This system acts as a negative control loop to regulate the release of gastric juices.

The stretch receptors, activated by the intake of food, regulate and increase the waves of peristalsis that act to mix the food with the gastric juice by promoting the release of gastrin. The orad region of the stomach exhibits little contractile activity during the digestive state. Food in this region tends to remain in relatively undisturbed layers for an hour or more after eating. The predominant motor activity in this region is concerned with the accommodation of the ingested material (Johnson 1991). The caudad region exhibits marked activity during the gastric phase. After eating contractions of varying amplitudes occur almost continuously. Contractions normally begin in the mid-stomach and move toward the gastroduodenal junction. During the first hour of digestion these waves are shallow over both the body and pylorus antrum regions. Subsequently, as they approach the junction they increase in both force and velocity. Thus, the primary contractile event in the stomach is a peristaltic contraction. Between contractions, pressure in the caudad region is near intraabdominal levels. When contractions begin they can be observed as rhythmic increases and decreases in pressure. In humans the duration of these contractions ranges between 12 and 20 seconds and the maximum frequency is 3 to 5 contractions *per* minute as illustrated in figure 1.1.

Figure 1.1
Intraluminal pressures recorded from five areas of the stomach. A sensor in the orad region records little phasic activity. Sensors in the caudad region detect peristaltic contractions, as they begin in the middle stomach and progress towards the gastroduodenal junction. It is noted that the contractions increase in force and velocity as they near the junction.

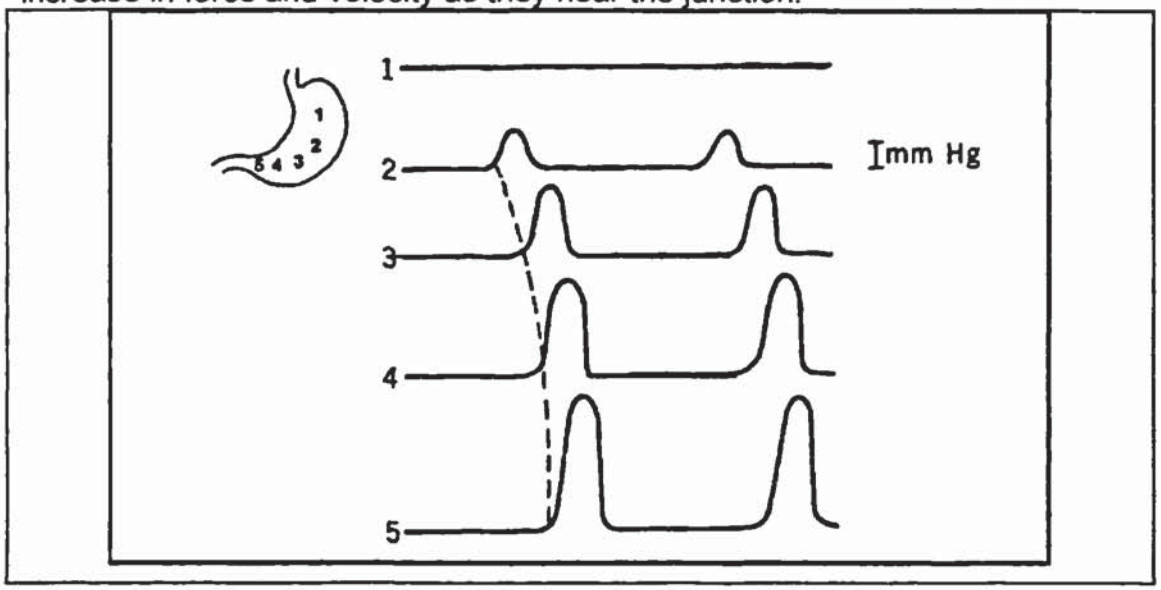

Reproduced from Johnson (1991)

Contractions of the caudad region of the stomach serve to both mix and propel gastric contents. The gastric contents are pushed ahead of the contraction, starting from the middle stomach, towards the gastroduodenal junction. The pressure in the pyloric antrum increases as the viscous gastric contents are pushed into it by the peristaltic wave, resulting in the evacuation of some of the gastric contents into the duodenum, beyond the pyloric sphincter. However, the increase in the peristaltic wave velocity is such that it overtakes the gastric contents and therefore occlusion of the gastric contents by the wave does not occur. In fact most of the contents are repulsed back to the main body of the stomach. This process has been termed 'retropulsion' and it causes thorough mixing of the gastric contents and mechanically reduces the size of solid particles. Thus the peristaltic contractions of the caudad stomach both mix and empty gastric contents (Sanford 1982 and Johnson 1991).
The frequency of peristaltic contractions depends on an electrical event originating in the cells of the longitudinal muscle layer. The event, a rhythmical depolarisation and repolarisation of the resting membrane potential, does not occur simultaneously over

the caudad stomach, its tract is from a point on the greater curvature towards the lesser curvature and the pyloric region. It is commonly referred to as either the basic electrical rhythm (BER), slow wave or pacesetter potential. The BER is always measurable whether peristalsis is occurring or not. The relationship between the BER and peristalsis can be characterised as follows; the action potentials of peristalsis can be correlated with the maximum depolarisation of the BER, *i.e.* when the smooth muscle is at its most excitable. Thus the BER sets the frequency of peristalsis. This is fairly constant although it can be increased by gastrin. The force of contraction is regulated by hormonal and neural mechanisms, gastrin, motilin and vagal activity all being excitatory and secretin being inhibitory. Also the lag time between BER waves decreases as the gastroduodenal junction is approached, leading to the increase in velocity. Figure 1.2 illustrates these relationships. It is noted that figures 1.1 and 1.2 demonstrate the same characteristics (Johnson 1991 and Sanford 1982).

Figure 1.2
The recordings of gastric and duodenal BER electrical activity from electrodes placed at equal intervals on the surface of the stomach of a dog. It can be observed that the electrical frequency remains unchanged but the amplitude increases in the pyloric antrum. The velocity of the BER potential is indicated by the slope of the line connecting the cycles.

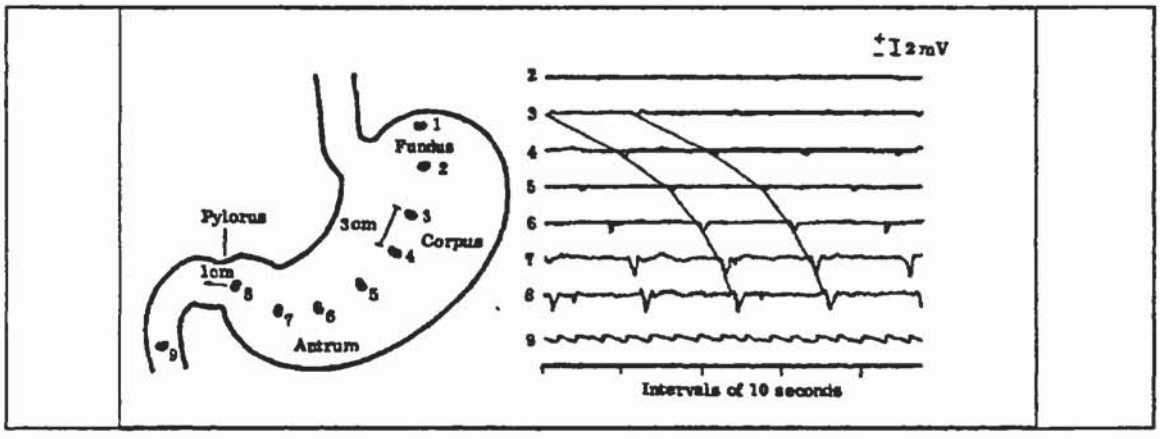

Reproduced from Kelly *et al.* (1969).

1.1.1.3.4 Intestinal motility phase

The intestinal phase is due to activation of receptors in the small intestine. Whereas reflexes initiated during the cephalic and gastric phases stimulate stomach secretory activity and motility, those occurring during the intestinal phase have inhibitory effects

which decrease the exit of chyme from the stomach and prevent overloading the duodenum with more chyme than can be processed. In addition, responses occurring during the intestinal phase promote the continued digestion of foods that have reached the small intestine. When chyme containing fatty acids and glucose leaves the stomach and enters the small intestine, it triggers enteroendocrine in the mucosa to release three hormones into the blood - gastric inhibitory peptide (GIP), secretin and cholecystokinin (CCK). With respect to the stomach, GIP inhibits gastric secretions and motility, secretin mainly decreases gastric secretions and CCK mainly inhibits stomach emptying. The presence of food in the small intestine also inhibits gastric secretion and motility through a neural reflex called the enterogastric reflex (Tortora 1996).

1.1.1.3.5 Interdigestive migrating motility complex

The IMMC dominates in the fasted state. The primary function of this pattern is to periodically clear the residual content of the upper GI tract. Each cycle lasts between 90-120 minutes and consists of four phases. The duration of each phase is controlled by the hormone motilin. Phase I consists of a relatively limited number of weak intensity contractions and corresponds to 40-50% of the cycle time. Phase II is characterised by amplitude increase such that discharge of gastric contents commences. Phase III covers the period of maximum amplitude and frequency of contractions - three to four contractions *per* minute. Discharge of cellular debris, mucus and particles greater than 1.0mm in diameter, which are unable to pass through the pylorus by normal peristaltic action is completed during this phase. Phase IV is a transitional phase corresponding to a decrease in amplitude and frequency of contractions. The IMMC is interrupted by the administration of food. (Maceras *et al.* 1995 and Moore 1989).

1.1.2 Gastric emptying

1.1.2.1 Gastric emptying of digestible solids and liquids

The introduction of radionuclide-based methods has greatly enhanced the understanding of the emptying of ordinary meals and has been utilised for the measurement of drug transit throughout the gastrointestinal tract. It has been

demonstrated by Moore *et al.* (1983) that liquids empty more quickly than solids, and that the solid emptying pattern is linear. Initially, the liquid emptying is more rapid, it then becomes more linear and in parallel with solid phase emptying. It was suggested that this was due to thorough mixing of the two phases and to simultaneous emptying. It was considered that this effect would be more pronounced with longer gastric residence times of larger meals. These findings are illustrated in figure 1.3.

Figure 1.3
The percentage retention of liquid and solid tracers in 10 healthy young (mean=31) males. Subjects were fed 900g, 633-kcal meals. Each datapoint represents a mean of the normalised counts ± SEM.

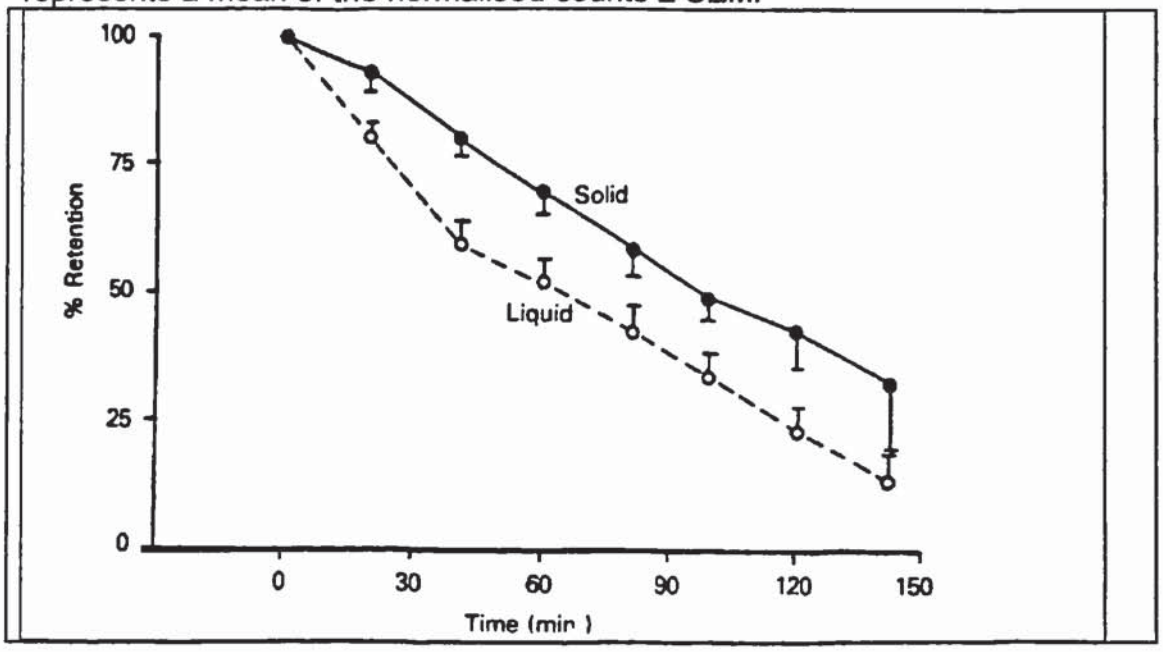

Reproduced from Moore *et al.* (1983)

Studies by Moore *et al.* (1981) and Hunt (1975) have shown that the calorific content of a meal is proportional to the emptying rate and that the size of the meal does not affect the rate of emptying, over the tested range. It has also been demonstrated that the ingestion of 600ml of test solutions containing increasing concentrations of glucose led to a delay in the gastric emptying rate, at concentrations of 40g/litre or higher (Vist and Maughan 1994).

1.1.2.2 Gastric emptying of liquid dosage forms in the fasted state

Liquids less than 50ml in volume are emptied by the IMMC, mainly during phase III of the cycle. As the volume increases the emptying becomes less dependent on the IMMC. At volumes of 200ml or larger, first-order kinetics apply and the rate is controlled by negative feedback mechanisms from the small intestine. The first of these is controlled by the pH and the other by the osmolality of the gastric chyme that reaches the small intestine. Generally, the lower the pH and the further from iso-osmotic is the liquid, the slower the emptying rate (Macheras *et al.* 1995). Sodium chloride solution (200mosmol/kg) is considered the most rapidly emptied solution, in terms of osmolarity, by Sanford (1982). The half-life of 400ml saline solution has been measured as typically between 5-10 minutes by Macheras *et al.* (1995) and the mean gastric emptying time of 300ml of water measured as 24.9±4.7 minutes by Dorlars *et al.* (1994).

1.1.2.3 Gastric emptying of solid dosage forms in the fasted state

The mechanism of emptying of solid dosage forms from the stomach is dependent on the volume of water taken concurrently to the administration. For volumes of less than 50ml the dosage form is emptied by the IMMC cycle, substantially during phase III. When the dosage form is administered with volumes of more than 50ml, gastric emptying depends on the physical characteristics of the solids. For immediate release formulations drug particles or granules may disperse over the intragastric area. Different fates may await the particles, depending on the particle size. For particles less than 0.5mm it is possible that they may become trapped in the mucus layer, with subsequent emptying occurring only during phase III of the IMMC. For particles generally between 2-6mm, emptying again occurs only during phase III of the IMMC. Particles less than or equal to 1mm in size and about 1g/ml density empty first with the water according to the pattern detailed in section 1.1.2.2. Other particles are emptied with a dependency on the phase of the IMMC. A significant consequence of the non-uniform pattern of gastric emptying of solids is the observation of two peaks in plots of drug concentration in serum as a function of time, in the absorptive phase (Macheras *et al.* 1995; Moore 1989; Johnson 1991). For example, Mummanenni *et al.* (1995) studied the role of antacids on the appearance of double peaks in plasma-time

profiles for cimetidine, concluding that the gastric pH did affect their presence such that for pH's less than 3, 80% of the profiles exhibited double peaks whereas a pH of 5 or above eliminated the double peak. Double peaks were also present 2-2.5hrs post-dosing, in 7 of the 11 profiles, in subjects receiving a dispersible formulation of diclofenac in a study carried out by Macia *et al.* (1995).

1.1.2.4 Gastric emptying of solid dosage forms during the fed state

Gastric emptying of oral drugs is delayed when the drugs are administered with meals and is controlled by the intragastric hydrodynamics. Variables affecting the emptying rate are the size and density of the solids, as well as the viscosity and emptying rate of the liquid fraction of the gastric contents. Generally particles of less than 1mm empty with the liquid fraction of the meal. Particles of a larger size show a lag time prior to onset of emptying. If the diameter is 2-5mm and density about 1g/ml the particles enter the duodenum with rate inversely proportional to their size according to a pattern similar to that followed by the liquid fraction of a meal. The density of the dosage form, if significantly different from the liquid food, can delay gastric emptying. If the size is greater than 5mm the particles remain in the stomach until the digestive motility pattern is replaced with the IMMC fasting pattern and phase III contractions occur (Macheras *et al.* 1995).

1.1.3 Anatomy and physiology of the small intestine

The primary site of digestion and absorption in the body is the small intestine. The structure is specially adapted for this purpose, the outstanding feature of the small intestine being its very large surface area, due to its length, which is further increased by circular folds, villi and microvilli. The small intestine begins at the pyloric sphincter of the stomach, coils through the central and inferior part of the abdominal cavity, and eventually opens into the large intestine. The main functions of the small intestine are the mechanical and chemical digestion of food, followed by the absorption of nutrients, with approximately 90% of all nutrients being absorbed, the remaining 10% being absorbed in the stomach and large intestine (Tortora 1996).

1.1.3.1 Anatomy of the small intestine

The small intestine averages approximately 2.5cm in diameter and is 3m long in a living person and about 6.5m long in a cadaver, due to loss of smooth muscle tone after death. The small intestine is divided into three segments. The duodenum is the shortest segment. It starts at the pyloric sphincter of the stomach and extends about 25 cm until it merges with the jejunum. Duodenum means "12"; the structure is 12 fingers' breadth in length. The jejunum is about 1m long and extends to the ileum. The final portion of the small intestine, the ileum is about 2m long and joins the large intestine at the ileocecal sphincter (valve). Projections called circular folds, or *plicae eirculares* are permanent ridges in the mucosa, about 10mm high. Some extend all the way around the circumference of the intestine, and others extend only part of the way around. The circular folds begin near the proximal portion of the duodenum and end at about the midportion of the ileum. They enhance absorption by increasing surface area and causing the chyme to spiral, rather than to move in a straight line, as it passes through the small intestine (Tortora 1996).

1.1.3.2 Small intestine histology

The wall of the small intestine is composed of the same four coats that make up most of the GI tract. However, special features of both the mucosa and submucosa facilitate processes of digestion and absorption. The mucosa forms a series of fingerlike villi. These projections are 0.5-1mm long and give the intestinal mucosa a velvety appearance. The large number of villi (20-40 *per* mm^2) vastly increases the surface area of the epithelium available for absorption and digestion. The epithelium of the mucosa consists of simple columnar epithelium that contains absorptive cells, goblet cells, enteroendocrine cells, and Paneth cells. The apical membrane of the absorptive cells features microvilli. Each microvillus is a 1μm long cylindrical, membrane-covered projection that contains a bundle of 20-30 actin filaments. In a photomicrograph taken through a light microscope, the microvilli are too small to be seen individually. They form a fuzzy line, called the brush border, at the apical surface of the absorptive cells, next to the lumen of the small intestine. Larger amounts of digested nutrients can diffuse into the absorptive cells of the intestinal wall because the miicrovilli greatly increase the surface area of the plasma membrane. There are

an estimated 200 million microvilli *per* square millimeter of small intestine. The brush border also contains several digestive enzymes. The mucosa contains many cavities lined with glandular epithelium. Cells lining the cavities form the intestinal glands (crypts of Lieberkuhn) and secrete intestinal juice. Paneth cells are found in the deepest parts of the intestinal glands. They secrete lysozyme, a bactericidal enzyme, and are also capable of phagocytosis. They may have a role in regulating the microbial population in the intestines. Enteroendocrine cells, also in the deepest part of the intestinal glands, secrete three hormones: secretin (S cells), cholecystokinin (CCK cells), and gastric inhibitory peptide (K cells). The submucosa of the duodenum contains duodenal (Brunner's) glands. They secrete an alkaline mucus that helps neutralise gastric acid in the chyme. Many of the epithelial cells in the mucosa are goblet cells, which secrete additional mucus. The lamina propria of the small intestine has an abundance of mucosa-associated lymphoid tissue (MALT). Solitary lymphatic nodules are most numerous in the distal part of the ileum. Groups of lymphatic nodules, referred to as aggregated lymphatic follicles (Peyer's patches), are numerous in the ileum. The muscularis mucosae consists of smooth muscle. The muscularis of the small intestine consists of two layers of smooth muscle. The outer, thinner layer contains longitudinally arranged fibres. The inner, thicker layer contains circularly arranged fibres. Except for a major portion of the duodenum, the serosa (or *visceral peritoneum*) completely surrounds the small intestine (Tortora 1996 and Johnson 1991).

1.1.3.3 Small intestine physiology

1.1.3.3.1 Small intestine secretions

Intestinal juice is a clear liquid yellow fluid with a slightly alkaline pH(7.6), which is secreted at a rate of 1-2 litres *per* day and contains water and mucus. Together, pancreatic and intestinal juices provide a vehicle for the absorption of substances from chyme as they come into contact with the microvilli. Among the brush-border enzymes are four carbohydrate-digesting enzymes, three protein-digesting enzymes and two types of nucleotide-digesting enzymes. Cells that slough off from the lumen release enzymes that digest nutrients in the chyme (Tortora 1996).

1.1.3.3.2 Digestion in the small intestine

Digestion is the mechanical and chemical breakdown of food. Mechanical digestion can be divided into divided into two types: segmentation and peristalsis. Segmentation is the major movement of the small intestine. It is strictly a localised contraction in areas containing food. Its action is to mix chyme with the digestive juices and bring the particles of food into contact with the mucosa for absorption. Segmentation starts with the contractions of circular muscle fibres in a portion of the small intestine, an action that constricts the intestine into segments. Following this muscle fibres that encircle the middle of each segment also contract, dividing each segment again. Finally, the fibres that contracted first relax, and each small segment unites with an adjoining small segment so that large segments are formed. This sequence of events is repeated 12-16 times a minute, sloshing the chyme back and forth. An analogy for this movement would be to alternately squeeze opposite ends of a tube of toothpaste. Peristalsis propels the chyme onward through the intestinal tract. Peristaltic contractions in the small intestine are normally very weak compared with those in the oesophagus or stomach, and chyme remains in the small intestine for 3-5 hours. Peristalsis, like segmentation, is controlled by the autonomic nervous system. Chemical digestion begins in the mouth, salivary amylase converts starch to maltose, maltotriose, and dextrins. In the stomach, pepsin converts proteins to peptides and lingual and gastric lipases convert some triglycerides into fatty acids and monoglycerides. Thus chyme entering the small intestine contains partially digested carbohydrates, proteins, and lipids. The completion of the digestion of carbohydrates, proteins, and lipids is a collective effort of pancreatic juice, bile, and intestinal juice in the small intestine (Tortora 1996 and Johnson 1991).

1.1.3.3.3 Small intestinal absorption

Essentially, all carbohydrates are absorbed as monosaccharides. They pass through the apical surface by an active transport mechanism. Most proteins are absorbed as amino acids by active processes that occur mainly in the duodenum and jejenum. Dietary lipids are absorbed by passive diffusion. Triglycerides having been emulsified and digested are broken down into monoglycerides and fatty acids. Short-chain fatty acids having fewer than 10-12 carbon atoms pass into the epithelial cells by passive diffusion. Longer chained fatty acids and monoglycerides reach the bloodstream by a

different route and require bile for adequate absorption. Bile forms micelles which have a non-polar core and can 'dissolve' monoglycerides and long chain fatty acids. The micelles act to transport these agents to the apical surface of the epithelial cells, where diffusion of the fatty acids and monoglycerides across into the cells occurs, leaving the bile behind in chyme. Water absorption occurs by osmosis in the GI tract with approximately 9 litres entering the small intestine, with approximately 2 litres being ingested and 7 litres being secreted further up the GI tract. About 8 litres are reabsorbed through the small intestine (Tortora 1996 and Johnson 1991).

1.1.4 Physicochemical properties of drugs and their application to dissolution and absorption in the gastrointestinal tract

1.1.4.1 Solubility/pH relationships for weak acids and bases

Many drugs are weak acids or weak bases and when dissolved in solutions they exist in equilibrium between their undissociated molecules and their ions. In solution, a weakly acidic drug *HA* may be simply represented by :

$$HA \leftrightharpoons H^+ + A^-$$

Similarly, the protonation of a weakly basic drug *B* may be represented by:

$$B + H^+ \rightleftharpoons BH^+$$

The ionisation constant, also commonly referred to as the dissociation constant, K_a, of a weak acid may be described by applying the Law of Mass Action to the first equation above to yield:

$$K_a = \frac{[H^+][A^-]}{[HA]}$$

equation 1.1

Taking logarithms of both sides gives:

$$\log K_a = \log [H^+] + \log [A^-] - \log [HA]$$

The signs in this equation can be reversed to give

$$-\log K_a = -\log [H^+] - \log [A^-] + \log [HA]$$

The symbol pK_a is used to represent the negative logarithm of the acid dissociation constant K_a in the same way that the negative logarithm of the hydrogen ion concentration is represented by the symbol pH thus:

$$pK_a = pH + log\ [HA] - log\ [A^-]$$

or

$$pK_a = pH + \log\frac{[HA]}{[A^-]}$$

Thus a general equation that is applicable to any acidic drug with one ionisable group may be written, where C_u and C_i represent the concentrations of the unionised and ionised species, respectively. This equation is known as the Henderson-Hasselbalch equation thus:

$$pK_a = pH + \log\frac{C_u}{C_i}$$

It is noted that when the solution pH equals the pK_a the ratio of unionised and ionised species is unity. It can be shown by a similar derivation that for weak bases:

$$pK_a = pH + \log\frac{C_i}{C_u}$$

The solubility of the ionised and unionised forms of drug are different as the undissociated form of the drug does not interact with the water molecules to the same extent as the ionised form. With the total solubility of the drug S and the solubility of the unionised form S_o it can be stated that:

$$S = S_o + (concentration\ of\ ionised\ species)$$

Rearranging equation 1.1 and substituting S_o for $[HA]$ and $S\text{-}S_o$ for $[A]$ it can be deduced that

$$\frac{K_a}{[H_3O^+]} = \left\{\frac{S - S_o}{S_o}\right\}$$

taking logarithms

$$pH - pKa = \log\left\{\frac{S - S_o}{S_o}\right\}$$

equation 1.2

It can be shown by a similar derivation that for weak bases

$$pH - pK_a = \log\left\{\frac{S_o}{S - S_o}\right\}$$

It can be observed from these equations that the solubility of a weak acid will increase exponentially with increasing pH above the pK_a value. For bases, the solubility will increase exponentially with decreasing pH below the pK_a value. As the solubility of a drug affects its dissolution rate, it is apparent that manipulation of solution pH across the pK_a of a weakly acidic or basic drug will dramatically alter the rate of dissolution (Aulton 1988; Florence and Attwood 1988).

1.1.4.2 Partition coefficient

The membranes of the gastrointestinal tract act as lipophillic barriers to the absorption of drugs. Non-active absorption occurs by a process of partitioning into the membrane and diffusion across the barrier. Mucosal membranes are more permeable to unionised drug compared to the ionised form due to highly charged nature of the cell membrane which may act to repel or bind ionised species. The degree of partitioning is also governed by the relative solubilities of the drug in aqueous and lipophillic environments. A standardised coefficient has been adopted which measures the

relative solubilities of a drug in octanol:water and is described as the partition coefficient thus:

$$P = \frac{C_o}{C_w}$$

where C_o and C_w are the solubilities in the octanol and water phases respectively. The coefficient is usually described in its logarithmic form (log P).

The combination of the Henderson-Hasselbalch equations with the partition coefficient form the basis of the widely accepted pH-partition theory, used as a simplified model for drug absorption.

1.2 Bioequivalence and Bioavailability

For immediate release dosage forms regulatory bodies, including the United States Federal Drug Administration (FDA), require that new formulations of an existing product are required to be demonstrated to be bioequivalent to the currently marketed (reference) product. Common to all agencies is the requirement for an *in vivo* bioequivalence study. Generally, the criteria include an open-label crossover study, conducted using healthy male volunteers, with a random treatment sequence and allowance of a washout period (at least 10 half-lives of the active drug). Dosing to steady state may be required for drugs that exhibit non-linear absorption or disposition characteristics. In some instances, subject to regulatory approval, the use of animals in bioequivalence studies is required, when the drug is unsuitable for administration to healthy volunteers. However, regardless of the individual criteria used the bioequivalence study is the definitive measure of whether the new formulation (test) is therapeutically equivalent and can be directly substituted for the reference product (Williams 1991).

Blood or urine samples taken throughout the bioequivalence study are analysed to yield concentration-time curves. From these data, pharmacokinetic parameters are derived to generate information regarding the rate and extent of absorption. Various methods are employed to compare drug absorption between the reference and test

products, *i.e.* compartmental, graphical and observational methods. For compartmental methods, it is assumed that absorption occurs by a specific rate process, *e.g.* zero or first order. Graphical methods, *e.g.* the Wagner-Nelson method, compare the percentage drug absorbed *versus* time for the reference and test products. Neither of these methods can assess the extent of absorption and both require data to be generated, from I.V. dosing, to derive the elimination rate constant(s). Observational methods assess the rate of absorption directly from a comparison of drug, or metabolite, concentration *vs.* time after administration (Williams 1991). At present, the method most commonly utilised is the observational method, *i.e.* direct determination of the peak concentration (C_{max}) and its time of occurrence (t_{max}). The extent of drug absorption is measured by area under the plasma concentration-time curve (AUC) with extrapolation to a time (t) or infinity (Williams 1991). The determination of bioavailability (F) requires the bioequivalence study to include an intravenous dose. This is not usually performed and only the relative bioavailability is usually determined. Together C_{max}, t_{max} and AUC provide an almost complete description of the drug concentration-time profile and they are used substantially for bioequivalence and bioavailability studies (Welling 1986).

Historically, the FDA requirements for the statistical determination of bioequivalence was by use of the so called "75/75-125" rule. According to this rule the relative AUC and C_{max} for the test product, *i.e.* the test/reference ratio must be within 0.75-1.25 for 75% of the subjects. The rule was an attempt to consider the individual variability in the rate and extent of absorption. In the 1980s the *power approach* (Schuirmann 1987) was applied to AUC and C_{max} parameters. The power approach consisted of two statistical tests: an F test with the null hypothesis of no difference between the two formulations and the evaluation of the power of the test to detect a 20% mean difference in treatments. In addition, the plasma concentration-time profiles had to be 'reasonably superimposible'. Statistically, these criteria have been demonstrated to have poor performance. The use of these methods was discontinued by the FDA Division of Bioequivalence in 1986. The currently used rule is termed the *two one-sided tests procedure*. By custom and regulatory precedent, mean treatment difference of 20% or less are generally considered to be of no clinical significance. The current statistical test's null hypothesis is that the difference between the test and

reference means is not more than 20%. By this procedure, if the test and reference product are not bioequivalent (difference >20%) there is a 5% chance of concluding that they are bioequivalent (Dighe and Adams 1991).

1.3 *In vivo/In vitro* Correlations

The development of *in vivo/in vitro* correlations (IVIVCs) is an area within biopharmaceutics receiving considerable interest and effort by industrial, regulatory and academic sectors. The reasons for this include the reduction of development costs, avoiding excessive use of human volunteers in bioavailability and bioequivalence studies and the speeding up of submission dates, leading to the earlier availability of products. Work has focused on two key areas: 1) the development of a general set of guidelines linking drug dissolution, absorption and bioavailability and 2) development of IVIVCs on a product-by-product basis utilising existing technology and through the development of specific apparatus suitable for the drug under investigation.

1.3.1 Biopharmaceutics Classification System

Although correlations between *in vitro* dissolution and *in vivo* bioavailability for oral products have been produced general methods for predicting oral drug absorption have been limited. The reasons for this lie within the complex nature of the processes occurring during drug dissolution and absorption within the GI tract and the complex pharmacokinetics of drugs making it difficult to obtain accurate absorption estimates from systemic availability. Any model would require consideration of the variation within the GI tract, *e.g.* fasted/fed state, cyclical fasted state motility, gastric emptying and intestinal transit, variable lumen contents including pH, enzymes, surfactants and dietary lipids, drug absorption mechanism, permeability and variation in drug physicochemical properties during GI transit (Amidon *et al.* 1995).

Fundamental parameters controlling the rate and extent of absorption are the drug dissolution and GI permeability. Sinko *et al.* (1991) have demonstrated a good correlation between extent of absorption and intestinal membrane permeability in an animal model, that is mechanism of absorption independent.

In addition, drug dissolution and absorption models have been developed for water insoluble drugs. Utilising these models Amidon *et al.* (1995) determined that the key parameters controlling drug absorption are three dimensionless numbers; an absorption number - An, a dissolution number - Dn and a dose number Do; representing the fundamental processes of membrane permeation, drug dissolution and dose, respectively. Briefly, these parameters can be defined as the ratio of absorption time to residence time in the intestine, a function of the particle size and solubility and the number of doses of drug that can be dissolved in the stomach contents (specified as 250ml), respectively (Swarbrick 1997). Amidon *et al.* (1995) have developed these concepts and formalised them into a system based on high/low solubility-permeability expectations. With this system drugs can be categorised and predictions relating to the likelihood of IVIVCs established. This system has been codified by the FDA (USA 1997). Four categories are listed below, along with a summary of the IVIVCs expectation:

1.3.1.1 Class I - high solubility/high permeability

An IVIVC is expected if the dissolution rate is slower than gastric emptying rate, otherwise a limited or no correlation is expected. A product having a dissolution rate of at least 85% within 15 minutes using 0.1M HCl under mild dissolution conditions, is considered to behave as a solution with no bioavailability issues. If the dissolution rate is slower than gastric emptying, a dissolution profile with multiple timepoints in multiple media is recommended.

1.3.1.2 Class II - low solubility/high permeability

IVIVC expected if *in vitro* dissolution rate is similar to *in vivo* dissolution rate. Dissolution profiles in multiple media are recommended for drug products in this category.

1.3.1.3 Class III - high solubility/low permeability

Absorption (permeability) is rate-determining and therefore limited or no IVIVC with dissolution rate is expected.

1.3.1.4 Class IV - low solubility/low permeability

Drugs in this category would be expected to present significant problems for delivery by the oral route. A limited or no IVIVC would be expected.

Note

A drug is considered highly soluble when the dose divided by the solubility does not exceed 250ml. High-permeability drugs are generally those where the extent of absorption is greater than 90% in the absence of documented instability in the GI tract (FDA 1997).

For immediate release (IR) products the generation of a IVIVC has two major benefits from a regulatory perspective. Firstly, the dissolution test used within the quality control environment is considered to be of more value if an IVIVC has been demonstrated previously. If this is the case the *in vitro* test can serve as a tool to distinguish between acceptable and unacceptable products, *i.e.* those demonstrated to be bioequivalent or non-bioequivalent. Generally, to achieve the IVIVC correlation three batches that show differences in the *in vivo* and *in vitro* characteristics are required and the *in vitro* conditions are modified, if required, to correspond with the *in vivo* data. Very often, the dissolution test is found to be more sensitive and discriminating than the *in vivo* test. This is considered extremely useful as it can be used to indicate changes in the product before the *in vivo* performance is affected (FDA 1997).

Secondly, SUPAC-IR guidance (FDA 1997) uses *in vitro* dissolution testing as the basis for justifying 'sameness' between the reference (pre-change) and test (post-change) product whose components or composition, site of manufacture, changes in scale, or manufacturing process and/or equipment is altered. Depending on the magnitude of change, the level of dissolution profile comparisons (single point, multiple points in one medium, or multiple points in several medium) required are selected to demonstrate sameness. Furthermore, under some circumstances, if an IVIVC has been demonstrated in the past, it can be used as a surrogate for *in vivo* bioequivalence studies (Swarbrick 1997). Additionally, where a IR product is available

in multiple strengths, comparative dissolution tests can be used to waive bioequivalence requirements for lower strengths of a dosage form if the drug has linear kinetics and the *in vitro* dissolution test is 'adequate', implying an IVIVC has been demonstrated (FDA 1995). To measure the product 'sameness' model-dependent or model-independent approaches are used and these will be discussed in chapter 4.

For modified-release products, *i.e.* delayed or extended, as for IR products, it is essential that there is a relationship between the *in vitro* dissolution profile and the bioavailability of a drug product to validate the dissolution test as a useful quality control tool. For the purposes of comparison, a system has been developed in which the relationship between the dissolution profile and in vivo profile is compared mathematically. The highest level of correlation, Level-A, is described as being when the two curves produced are super-imposable, either directly or through the appropriate use of time corrections or other mathematical functions. If this correlation is achieved then changes to manufacturing date, process and equipment, raw material supplier and minor formulation changes may be undertaken without recourse to additional bioavailability/bioequivalence studies (Skelly *et al.* 1990). Level-B correlations are defined as being the comparison of the mean *in vitro* dissolution time of the product to either the mean *in vivo* residence time or the mean *in vivo* dissolution time derived by using principles of statistical moment analysis. Level-C correlations are defined as the mean *in vitro* dissolution time of the product compared to one mean pharmacokinetic parameter, (noting that this does not reflect the complete dissolution profile or the plasma level profile which is important for controlled release products). As both Level-B and Level-C correlations are not point-to-point correlations, they cannot be used to justify changes allowed under Level-A. However they are justified insofar as they allow a framework for development groups working in this field (Swarbrick 1997).

1.3.2 Development of IVIVC on a product-by-product basis

There have been numerous attempts to produce an IVIVC for individual products. A general review by Welling (1991) concluded that of the drugs reviewed, covering seven therapeutic areas, the only correlation found to be of value in a clinical

environment was reported for digoxin products. However, he conceded that several of the studies showed moderate or rank order correlations, although they were based on limited formulations. Work conducted in this area concentrates on three areas; 1) utilisation of official dissolution apparatus, 2) the development of new apparatus, and 3) the use of experimental design and optimisation techniques.

1.3.3 IVIVC development using official apparatus

The USP has four official apparatus approved for dissolution testing: apparatus type I -rotating baskets, apparatus type II-rotating paddles, apparatus III-reciprocating cylinder and apparatus IV-flow-through cell system. The first two methods are simple, robust, standardised, used world-wide and flexible enough to allow dissolution testing for a variety of drugs. For this reason they are recommended unless proven to be unsatisfactory. As with all guidelines issued by regulatory authorities, the use of alternative or modified technologies is not discouraged, as long as the scientific rationale can be justified, ensuring scientific innovation is not stifled (FDA 1997).

To ensure maximum discriminating power, mild agitation conditions should be selected for dissolution studies. Dash *et al.* (1988) established that, for two bioequivalent Ibuprofen tablets, substituting paddle apparatus set at 50rpm for the test procedure described in the USP monograph, *i.e.* baskets at 150rpm, highlighted differences in the formulation not seen when tested to the standard. It was concluded that as the products were bioequivalent the discriminating test was not satisfactory. Currently, the conclusion is drawn that the discriminating method can be considered superior.

Work undertaken by Sotiropoulus *et al.* (1981) where the bioavailability of four different paracetamol products (three tablets and one solution) was compared to the dissolution rates using the paddle apparatus, set at 85rpm, and using 0.1N HCl as the dissolution medium, led to the conclusion that the rate and amount of paracetamol excreted may be related to the dissolution rate. Analysis of the data showed that one of the three brands tested dissolved significantly more slowly than the other two brands ($t_{50\%}$ of 50±0.00min *vs.* 1±1.73 & 1±2.70 min) and also produced the lowest observed excretion rate. The two remaining brands were indistinguishable from each other *in vitro.* This is considered a rank-order correlation, where elucidation is aided by apparent significant differences in one product from the other two.

In a study comparing naproxen tablets and caplets, Charles and Mogg (1994) compared the *in vitro* dissolution of the formulations utilising the paddle apparatus, at 50rpm, and pH 7.4 buffer, with a bioavailability study conducted on sixteen volunteers. The general conclusion was that despite a three-fold increase in dissolution rate between the caplet and the tablet the products could be considered bioequivalent from the pharmacokinetic data. It is noted from the data that C_{max} was 4% higher and t_{max} 20% lower for the caplet formulation although these differences were not significant at 90% CI. However, it can be concluded that a rank-order correlation was again in evidence.

To contrast with the above examples, Mattok *et al.* (1971) conducted an extensive study of eight different lots of paracetamol tablets where no type of correlation could be determined. Using rotating basket apparatus, set at 100rpm and using 0.1M HCl as the dissolution medium it was found that two batches, which were several years old, had significantly different $t_{50\%}$ dissolution times to the other batches ($\approx$ 20min vs. <5min) but when compared against the 'physiological availabilites', determined from blood levels and total urinary excretion, no correlation could be derived. In fact, the two batches demonstrating the longest dissolution times exhibited some of the highest 'physiological availabilities'.

1.3.4 Dissolution apparatus developments

The development of new dissolution apparatus is a wide and constantly growing area. Due to the enormous diversity of formulation types, differences in drug characteristics, limitations to the current official methods and the complex environment within the GI tract, specific systems have been developed to enable these various issues to be overcome. Examples of dissolution systems and their significance are discussed in this section.

The USP rotating paddle method is not considered particularly suitable for some dosage forms, including capsules, beads and pelletised formulations because of their tendency to float on the dissolution medium. To overcome this problem, the USP (1995) states 'a small loose piece of non-reactive material such as wire or glass helix

may be attached to dosage units that would otherwise float'. Baichwal *et al.* (1985) have found that this method could restrict the opening of capsules and was found to be cumbersome, non-reproducible and cause difficulties in placement of the dosage form. In addition, different types of dosage forms cannot be evaluated under identical experimental conditions. To overcome these issues Baichwal *et al.* (1985) developed a stationary basket-rotating paddle apparatus. After extensive comparison with the two official apparatus it was concluded that the system was superior for the following reasons: tablets and capsules could be evaluated under identical experimental conditions, sufficient agitation intensity was accomplished ensuring homogeneity throughout the dissolution fluid (even at a low stirrer speed of 50rpm), and as the agitation intensity did not significantly vary throughout the whole vessel, particles or granules expelled from the vessel during dissolution were not subjected to different agitation intensities.

The introduction of several oral mucosal drug delivery systems, including those of Bottenberg *et al.* (1992) and Bouckaert and Remon (1993), where the method of studying release of the drug from bioadhesive polymeric matrices was largely based on official dissolution tests, led to the development of a dissolution apparatus suitable for these dosage forms, by Mumtaz and Ch'ng (1995). Their aim was to develop a system which would give a more realistic assessment of the release of drug from a bioadhesive buccal tablet. Briefly, the apparatus consisted of a fresh chicken pouch being fastened to a glass slide followed by the binding of the buccal tablet to the tissue sample. This was placed within a cell which had previously been attached to the outer assembly at an angle of 40°. Water, preheated to 37°C, from a USP dissolution apparatus was circulated over the cell at a rate of 4ml min^{-1}. At regular time intervals samples were removed and analysed by U.V. absorption after which they were replaced into the dissolution medium reservoir. The apparatus was used to test the effect of varying concentrations of poly(acrylic acid-2,5-dimethyl-1,5-hexadiene) (PADH) and hydroxypropyl-methylcellulose (HPMC) in triamcinolone acetonide bioadhesive buccal tablets. Increasing concentrations of PADH are known to cause tablets to disintegrate more rapidly whereas increasing concentrations of HPMC are known to provide more prolonged release of the drug. The conclusion

drawn was that the results produced by the apparatus concurred with predicted patterns.

1.3.5 Experimental design and optimisation techniques

An alternative approach to obtaining an IVIVC for a specific product involves the use of experimental design where *in vitro* factors are varied systematically with the aim of studying the relationship between a dissolution response factor, *e.g.* t_{50}% and an *in vivo* variable such as the absorption rate constant. From the *in vitro* data various methods may be applied to determine the *in vitro* conditions that exhibit the highest level of correlation with the *in vivo* data. An example of this method involved the study of two ibuprofen capsule formulations *in vivo* in beagle dogs and *in vitro* using a standard paddle apparatus. The work carried out by Ishii *et al.* (1996) involved varying the pH of the dissolution medium and paddle speed of rotation in a two-factor experimental design, involving 12 experiments. A correlation between the *in vitro* and *in vivo* first-order rate constants (k_d) predicted that an IVIVC would be obtained using experimental conditions of pH 4.5 and a paddle speed of 56 rpm. Dissolution testing of both formulations at the predicted optimised experimental conditions was found in practice to be in good agreement with the *in vivo* data, hence an IVIVC was achieved.

1.4 Profiles of selected model drugs

1.4.1 Paracetamol

Paracetamol, which is also known as acetaminophen in North America and in several other countries, is a white, odourless crystalline powder with a melting point of 169-171°C and a molecular weight of 151.2. The partition coefficient in octanol and pH 7.2 buffer is 6.24. The empirical formula is $C_8H_9NO_2$ and the structural formula is illustrated in figure 1.4. It is soluble 1 in 70 of water, 1 in 7 to 1 in 10 of ethanol and 1 in 13 of acetone; it is very slightly soluble in chloroform and practically insoluble in ether. Paracetamol is a weak organic acid with a pK_a value 9-10.2 as summarised by Florey (1974).There are official standards for the identification, purity and stability of paracetamol in many Pharmacopoeias, including those of Britain, Europe and the United States of America. Paracetamol has analgesic and antipyretic actions and is available in a large number of official and proprietary products alone and in

combination with other analgesics and drugs such as caffeine, antihistamines and sympathomimetics. It is taken orally as tablets, capsules, effervescent solutions, suspensions and elixirs and rectally in suppository form (Prescott 1996; Martindale 1982; British National Formulary 1995).

Figure 1.4
The structural formula of paracetamol

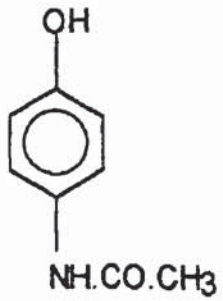

Paracetamol is absorbed from the GI tract by passive, non-ionic diffusion (Bagnall *et al.* 1979) and the rate of transfer depends, therefore, on factors such as the concentration gradient between the gastrointestinal lumen and the circulation, aqueous and lipid solubility and mucosal blood flow, permeability and surface area. The rate also depends on formulation factors because paracetamol must dissolve in gastrointestinal fluids before it can be absorbed. As paracetamol is a weak acid with a pK_a value 9-10.2 (Florey 1974) and as it is therefore largely unionised over the physiological range of pH, the rate of mucosal transfer would be independent of pH. Its water and lipid solubilities are such that rapid and complete absorption would be anticipated, and this has been confirmed in many studies. In studies in which paracetamol was given to rats with a non-absorbable marker, the most efficient site of absorption was found to be the mid-small intestine (Weikel and Lish 1959). Also, in rats, Bagnall *et al.* (1979) showed that paracetamol was absorbed by passive transport over a wide range of concentrations and pH, according to first-order kinetics. Absorption was greatest from the small intestine where 70% of the dose was absorbed in 30 minutes compared with 29% from the colon and 22% from the stomach over the same period of time. The small intestinal absorption of paracetamol was studied in four healthy volunteers using a segmental steady-state perfusion technique with a triple lumen tube. Absorption was similar from proximal and distal

sites, and the rate was directly related to the amount infused *per* unit time and the transmucosal water flux (Gramatte and Richter 1993).

The faster uptake of paracetamol from the small intestine than from the stomach can be attributed to the greater surface area and hence absorptive capacity at the former site. An important consequence of this is that unless the rate of absorption of paracetamol is very slow, it would be determined by the rate at which the drug was transferred from the stomach to the site of rapid absorption in the upper small intestine. Absorption also involves the process of dissolution from a solid dosage form and either of these two steps may be rate-limiting. Measures of absorption obtained by conventional pharmacokinetic analysis, such as mean absorption times and rate constants, therefore are usually hybrid terms that include dissolution, gastric emptying and uptake from the small intestine.

Heading *et al.* (1973) found that rapid gastric emptying in 14 convalescent patients was associated with the early appearance of high peak plasma paracetamol concentrations whereas peak concentrations were low and appeared late when gastric emptying was slow. This relationship between gastric emptying and paracetamol absorption has been confirmed in many subsequent studies. Paracetamol was absorbed very rapidly when it was given under conditions where gastric emptying was rapid such as in the fasting state with a large volume of fluid or an effervescent solution. In such circumstances there was little or no lag time and peak plasma concentrations occurred within 15 minutes of ingestion (Prescott 1980; Dougall *et al.* 1983; Borin and Ayres 1989) with absorption half times as short as 6-8 min (Divoll *et al.* 1982; Ameer *et al.* 1983). Gastric emptying in a group of hospital patients was delayed by intravenous injection of propantheline, and there was a corresponding marked slowing of the absorption of paracetamol. Conversely, its absorption was accelerated by intravenous metoclopramide, a drug which stimulates gastric emptying (Nimmo *et al.* 1973).

The close relationship between gastric emptying and paracetamol absorption was strengthened further when it was shown that narcotic analgesics strongly inhibited gastric emptying and grossly impaired the absorption of paracetamol given at the same time, summarised by Prescott (1996). Individual variation in the times of peak concentrations following administration of a standard formulation was attributed to individual variation in the rate of gastric emptying (Letley *et al.* 1980). Further

confirmatory studies included the reversal by naloxone of the inhibition of gastric emptying and paracetamol absorption induced by pentazocine (Nimmo *et al.* 1979), the slowing of gastric emptying and paracetamol absorption by guar gum and pectin gel fibre (Holt *et al.* 1979), the inhibition of gastric emptying and paracetamol absorption by levodopa in young and elderly subjects (Robertson *et al.* 1990 and 1992), and the delaying effects of intravenous atropine on gastric emptying and paracetamol absorption, also in young and fit elderly volunteers (Rashid and Bateman, 1990).

In the above studies, the paracetamol was taken as tablets or in solution, but a good correlation was also demonstrated between gastric emptying and the absorption of paracetamol taken with food (Koizumi *et al.* 1988a). A significant relationship was also found between the absorption of paracetamol taken in liquid and solid form with different liquid diets and gastric emptying as assessed by changes in blood glucose and gallbladder emptying (Walter-Sack *et al.* 1989). Other investigators have confirmed a significant correlation between the emptying of radionuclide-labelled test meals from the stomach and the plasma and saliva concentrations of simultaneously administered paracetamol (Harasawa *et al.* 1982; Maddern *et al.* 1985; Koizumi *et al.* 1988b). In contrast to the weight of evidence, Petring *et al.* (1986 and 1990) were unable to demonstrate a significant correlation between gastric emptying of semi-solid oatmeal in healthy volunteers of both sexes and any measure of the absorption of paracetamol incorporated into the meal.

There is conflicting evidence as to whether paracetamol absorption is dose-dependent, Rawlins *et al.* (1977) found that a 2g dose was absorbed more slowly than a 1 or 0.5g dose. Liedtke *et al.* (1979) also reported similar results, in which a 1g dose appeared to be more slowly absorbed than a 0.5g dose. A reason for this could be paracetamol-induced inhibition of gastric emptying proposed by Weikel and Lish (1959). However, other studies do not confirm these findings. Seideman *et al.* (1980) gave 0.5 and 1g tablet doses and Borin and Ayres (1989) administered oral doses of 0.325, 0.5, 1.0, 1.5 and 2.0g to 15 subjects. Neither found any significant effect of dose on absorption. A further study by Clements *et al.* (1984) who gave doses from 5-20mg kg^{-1}, orally in solution over 2 hours also found no differences. In practice, the rate of paracetamol absorption is subject to many variables and a range of values will be obtained depending on the circumstances. For example, in a survey of 43 fasting

convalescent hospital patients, there was an 80-fold range in plasma paracetamol concentrations one hour after administration of three 500 mg tablets (Prescott 1974).

In a study, conducted on healthy volunteers, in which paracetamol was taken orally in solution under different conditions with simultaneous isotopic measurement of gastric emptying, the absorption curves and emptying patterns indicated negligible absorption from the stomach. A pharmacokinetic model was proposed in which the conventional single compartment used to represent the gastrointestinal tract was replaced by two compartments, one representing the stomach and the other the small intestine from which the drug was absorbed rapidly. With this model there was good agreement between experimental and observed values, and the mean first-order rate constant for direct transfer of paracetamol from the intestinal lumen to the systemic circulation was equivalent to an absorption half-time of 6.8±0.9 min. As expected, this was shorter than the corresponding half time of gastric emptying (Clements *et al.* 1978).

In man, paracetamol had a mean distribution volume of 0.9 litre kg^{-1}, averaged by Prescott (1996) from an extensive literature review. The concentrations of paracetamol in different organs two hours after administration of 2.7g of phenacetin (a prodrug) to a dog showed a relatively even distribution with tissue:plasma concentration ratios close to unity. Concentrations were lowest in fat and cerebrospinal fluid and highest in liver and kidney. In another study in dogs, the findings were generally similar with a mean tissue water to plasma water concentration ratio of about 1:1 (Prescott 1996).

Although paracetamol is rapidly absorbed from the gastrointestinal tract, it is incompletely available to the systemic system after oral administration, a variable proportion being lost through first-pass metabolism. The proportion of the dose reaching the systemic circulation appears to be dose-dependent, decreasing from 90% with 1 to 3g to 68% after 0.5g (Forrest 1982). From a quantitative perspective, the major routes for the metabolism of paracetamol are through conversion to the O-glucuronide conjugate and the sulphate conjugate. Lesser metabolic pathways include conversion to the cysteine and mercapturic acid conjuates. In man, paracetamol is converted extensively to O-glucuronide and this product is the major urinary metabolite of the drug (Prescott 1996). Glucuronide conjugation is catalysed by a family of glucuronyltransferases and uridine 5'-diphosphoglucuronic acid (UDP-

GA) is an essential substrate. Miller and Fisher (1974), Clements *et al.* (1984) and Thomas *et al.* (1988) showed that the glucuronide conjugation of paracetamol occurred primarily in the liver, but the fraction of dose recovered in the urine was largely independent of the route of administration. Prescott (1996) summarised from others that some glucuronide conjugation of paracetamol occurred in the gastrointestinal tract, the kidney, the spleen and lung.

Sulphate conjugation is a major parallel route of non-toxic elimination of paracetamol in many species and there is usually a reciprocal relationship with the extent of glucuronide conjugation. Aryl sulphotransferases are ubiquitous cytosolic enzymes and although the sulphate conjugation occurs primarily in the liver, small amounts may be formed in other tissues as noted for glucuronidation. For example Ramakrishna *et al.* (1989) demonstrated the sulphate conjugation of paracetamol in human colonic mucosa. The mechanism of the hepatotoxicity of paracetamol is by its conversion to a reactive intermediate metabolite by NADPH-dependent microsomal cytochrome P450 mixed function oxidase. The toxic metabolite of paracetamol is widely accepted to be N-acetyl-p-benzo-quinoneimine, but its precise mode of formation and mechanism of toxicity are uncertain, (Prescott 1996). Paracetamol is extensively metabolised within the liver with only 2 to 5% of a therapeutic dose being excreted unchanged in the urine. In young healthy subjects, approximately 85 to 95% of a therapeutic dose is excreted in the urine within 24 hours with about 4, 55, 30, 4 and 4% appearing as unchanged paracetamol and its glucuronide, sulphate, cysteine and mercapturic acid conjugates, respectively (Forrest *et al.* 1982).

The pharmacokinetics of paracetamol commercial products in humans, obtained by analysis of plasma samples is detailed in Table 1.1.

Table 1.1
The pharmacokinetics of paracetamol using commercial product formulations (except solutions) and analysis of plasma samples.
Blanks indicate data were not collected by the authors.

Reference	Dose (mg)	Cmax ($\mu g\ ml^{-1}$)	t_{max} (hr)	$t_{1/2}$ (hr)	k_{el} (hr^{-1})	Fraction available	$AUC_{0\text{-}infinity}$ ($\mu g.hr\ ml^{-1}$)
Iqbal *et al.* (1995)	500	3.75	0.75	1.89	0.42		11.59
Muller *et al.* (1995)	1000	10.1	0.83	1.66			18.45
Ameer *et al.* (1983)	IV650			2.63			39.37
Ameer *et al.* (1983)	650	11.99	0.76	2.55		0.79	
Ameer *et al.* (1983)	650	8.56	1.06	2.62			26.82
Ameer *et al.* (1983)	650	8.89	0.78	2.43			27.37
Ameer *et al.* (1982)	650	10.1	0.9			0.814	
Rawlins *et al.* (1977)	650	6.7	1.7			0.769	
Rawlins *et al.* (1977)	500			2.79		0.63	15.6
Rawlins *et al.* (1977)	1000			2.68		0.89	44
Rawlins *et al.* (1977)	2000			2.31		0.87	87.6
Rawlins *et al.* (1977)	IV1000						50.5
Fritz *et al.* (1984)	1300			2.7	0.26	0.886	
Sack-Walter *et al.* (1989)	500	8.8	0.58	2.95			
Sack-Walter *et al.* (1989)	500	9.1	0.42	2.85			
Hong *et al.* (1994)	1000	9.79	1.48	2.51			40.6
Blume *et al.* (1995)	500	7.16	0.6	2.00			
Petring (1986)	20mg/kg	12.6	1.0				
Gugler and Allgayer (1990)	1000	20.4	1.82				63.07
Albin *et al.* (1985)	500	6.01	0.85	2.35			18.8

1.4.2 Ibuprofen

Ibuprofen is a chiral nonsteroidal anti-inflammatory drug (NSAID) of the 2-arylpropionic acid (2-APA) class. It is a white, or almost white, powder or crystals, melting point of 75-77.5°C, with a characteristic odour and a slight taste and a molecular weight of 206.3. Ibuprofen is a weak organic acid with a measured partition coefficient of between 52.0-20.8 over the pH range 1.2-7.0 (Ghosh *et al.* 1998) and a pK_a of between 4.4-5.3 (Moffat 1986; Lund 1994). The empirical formula is $C_{13}H_{18}O_2$ and the structural formula is illustrated in figure 1.5. It is practically insoluble in water, soluble 1 in 1.5 of alcohol, 1 in 1 of chloroform, 1 in 2 ether and 1 in 1.5 acetone; it is soluble in alkaline hydroxide and bicarbonate solutions. There are official standards for the identification, purity and stability of ibuprofen in many Pharmacopoeias, including those of Britain, Europe and the United States of America. Ibuprofen has analgesic, anti-inflammatory and antipyretic actions and is available in a large number of official and proprietary products. It is taken orally as tablets, syrups and capsules, and applied topically as a gel (Martindale 1982; British National Formulary 1995).

Figure 1.5
The structural formula of Ibuprofen

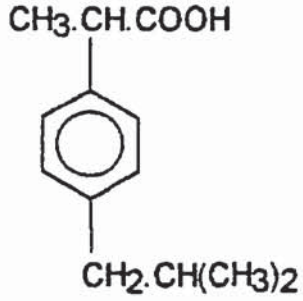

The solubility of ibuprofen varies significantly over physiological pH and therefore this is an important factor in drug absorption. In the stomach, ibuprofen is sparingly soluble and therefore the absorption profile will be affected by gastric emptying as demonstrated in a four-way crossover study, comparing ibuprofen 800mg tablets dissolved in water, with orange juice, diluted cherry syrup and Coca-Cola® solutions.

Insignificant pharmacokinetic differences were observed for the orange juice solution, though a delay in t_{max} was observed for the dilute cherry syrup solution. A reduced t_{max}, C_{max} and AUC were noted with a Coca-Cola® solution. High sugar loads, causing a delay in gastric emptying, were postulated to contribute in the delay in ibuprofen absorption (Small *et al.* 1988). It has been suggested that the rate of oral absorption may influence the pharmacokinetics of ibuprofen enantiomers. R(-)-ibuprofen undergoes an unidirectional metabolic inversion to the S(+)-ibuprofen. It is also thought that the inversion process is influenced by the rate of ibuprofen absorption and if the inversion takes place presystemically within the GI tract, the longer ibuprofen resides within this inversion site the more inversion will occur. Two studies summarised by Davies (1998) indicate a correlation between the S:R ratio and the residence time, measured by t_{max} correlation and comparison of tablets with ibuprofen solutions.

In man, ibuprofen has a distribution volume of between 0.1 to 0.2 l kg^{-1} which approximates to plasma volume. Ibuprofen is extensively bound (>98%) to whole human plasma with binding being stereoselective and a greater fraction of S-(+)-ibuprofen unbound. The synovial membrane is the proposed primary site of action for NSAIDs in patients with rheumatoid arthritis. In patients with rheumatoid and osteo-arthritis, ibuprofen had a longer t_{max} , a lower C_{max} and a higher elimination half-life in synovial fluid than plasma (Davies 1998). In one study ibuprofen concentrations were measured after administration of a single dose and at steady state in 8 patients with rheumatoid arthritis. Seven hours after a steady-state dose, the mean synovial fluid:plasma concentration ratios were constant with the concentration in the synovial fluid greater than plasma, on average. Also, protein binding was greater in plasma than in synovial fluid because of lower albumin and total protein concentrations in synovial fluid (Abernathy and Greenblatt 1985).

Ibuprofen undergoes extensive enantiomeric inversion in humans with between 53-65% reported in studies where each enantiomer was given individually and the amount calculated from the relative AUC. Two other methods (the stable isotope method and the stereochemical composition of urinary metabolites method) gave values of 56 and 60%, respectively, as summarised by Davies (1998).

Ibuprofen is extensively metabolised *via* formation of the two major metabolites, 2-hydroxy-ibuprofen and carboxy-ibuprofen and to a much less extent to 1-hydroxy-

ibuprofen and 3-hydroxy-ibuprofen. The metabolic pathway proceeds these compounds forming glucuronic acid conjugates. Ibuprofen is also metabolised to yield acyl glucuronides. The major metabolites have no significant pharmacological activity (Davies 1998).

Ibuprofen is rapidly excreted in both urine and faeces with between 70 to 90% of the administered dose excreted in urine after a 24 hour period. In one study, using 15 healthy volunteers approximately 12% of the dose was recovered as conjugated ibuprofen, ≈11% as the hydroxy metabolite, ≈15% as the conjugated hydroxy metabolite, ≈30% as the carboxy metabolite, and ≈12% as the conjugated carboxy metabolite. In 12 healthy volunteers 10 to15% was eliminated as ibuprofen, 25 to 30% as hydroxy ibuprofen, 30 to 40% as carboxy ibuprofen (free and conjugated). In 8 healthy volunteers ≈11% of the dose was excreted as ibuprofen, 20% as hydroxy ibuprofen and 43% as carboxy ibuprofen (Davies 1998).

The pharmacokinetics of ibuprofen commercial products in humans, obtained by analysis of plasma samples is detailed in Table 1.2.

Table 1.2
The pharmacokinetics of ibuprofen using commercial product formulations (except solutions) and analysis of plasma samples. Blanks indicate data were not collected by the authors.

Reference	Dose (mg)	C_{max} ($\mu g\ ml^{-1}$)	t_{max} (hr)	$t_{1/2abs}$ (hr)	$t_{1/2el}$ (hr)	k_{el} (hr^{-1})	$AUC_{0\text{-}infinity}$ ($\mu g.hr\ ml^{-1}$)	$AUC_{0\text{-}t}$ ($\mu g.hr\ ml^{-1}$)
El-Sayed *et al.* (1995)	600	54.9	2.08		2.79	0.248	234.7	221.2
El-Sayed *et al.* (1995)	600	53.7	1.92		2.69	0.258	222.5	209.9
Dash *et al.* (1988)	400	43.3	1.3				130	
Dash *et al.* (1988)	400	41	1.4				128	
SB (1998a)	400	32.4	1					
SB (1998a)	400	29.6	1.55					
Geisslinger *et al.* (1989)	600	50.8	0.89				205.5	
Stead *et al.* (1983)	200	27	1.38	2.31		0.35	76	
Stead *et al.* (1983)	300	20.1	1.7	0.99		0.33	93.6	
Stead *et al.* (1983)	400	25.6	2.48	0.86		0.33	113.6	
Stead *et al.* (1983)	200	19	1.95	1.76		0.32	63	
Stead *et al.* (1983)	400	36.4	2.07	1.45		0.32	128.8	
Lenhard *et al.*(1990)	600	40.32	1.5		1.4			
Lenhard *et al.*(1990)	600	52.03	1		1.8			
Saano *et al.* (1992)	200	17.8	2.04	1.04	1.42		81.1	
Saano *et al.* (1992)	200	24.6	1.36	0.6	1.29		81.3	
Saano *et al.* (1992)	200	17.3	1.46	1.19	1.46		84.3	
Walter *et al.* (1995)	800	45.2	2.6					
Kleinblesem *et al.* (1995)	400	36.7	1.1		1.8			
Jamali *et al.* (1988)	600	28.75	1.44		2.66			90.54
Jamali *et al.* (1988)	600	27.52	2.75		2.71			97.98
Jamali *et al.* (1988)	600	22.12	1.42		2.22			73.8
Jamali *et al.* (1988)	600	22.02	2.83		2.23			75.8
Jamali *et al.* (1988)	600	30.04	1.44		2.63			106.87
Jamali *et al.* (1988)	600	27.45	1.44		2.69			74.21
Jamali *et al.* (1988)	600	31.5	2.75		2.58			121.72
Jamali *et al.* (1988)	600	23.54	2.75		2.84			73.87
Jamali *et al.* (1988)	600	23.9	1.42		2.42			90.77
Jamali *et al.* (1988)	500	20.34	1.42		2.02			56.86
Jamali *et al.* (1988)	600	26.71	2.83		2.21			100.18
Jamali *et al.* (1988)	600	17.32	2.83		2.24			51.51
Albert and Gernaat (1984)	400	27.9	1.9		2.2		103	

1.43 Selection of antacids

Primarily, the interaction of antacids with the model drugs was chosen for study in order to validate the *in vitro* model developed for the purpose of generating IVIVCs. For this reason, antacids were selected for which pharmacokinetic data was available from studies where the effects of co-administration or use as a major excipient had been investigated. It was also considered valuable to characterise the antacid/drug interactions in their own right and for this reason several antacids, based on commercial availability, were selected. Selected antacids were used as non-formulated materials, supplied in powder form and used 'as is', allowing characterisation of the active material and excluding interferences due to formulation factors or excipients. On this basis the following were selected for investigation:

- calcium carbonate [$CaCO_3$]
- aluminium hydroxide [$Al(OH)_3$]
- magnesium hydroxide [$Mg(OH)_2$]
- magnesium oxide [MgO]
- sodium bicarbonate [$NaHCO_3$]

1.5 Project aims and objectives

The main aim of this project was to study and develop IVIVCs, based on physical and mathematical models. The industrial aspect and CASE award involved the *in vitro* study of a novel paracetamol formulation, Zapp, containing sodium bicarbonate as the main excipient, which had been found in pharmacokinetic studies to be absorbed far more quickly than conventional tablets and soluble formulations. With an understanding of the main physiological barriers to drug absorption, utilising available techniques and with a knowledge of current opinion, an objective was to utilise *in vitro* techniques to develop an overall model which could correlate with *in vivo* data. The generation of pharmacokinetic data was not within the scope of the project and it was therefore necessary to utilise data from literature, industrial sources and a parallel project running at Strathclyde University. For this reason the study focused on the effects of a group of antacids on the absorption of analgesic drugs during co-administration, an area which is well studied *in vivo*. This selection included sodium bicarbonate and therefore allowed concomitant study of the role of sodium bicarbonate in drug absorption. A second model drug, ibuprofen, was selected for

study, chosen on the basis that its physicochemical properties contrast with paracetamol, it is more readily ionisable over the physiological pH range and it is also a widely used and studied drug. Generally, as the antacids under study are alkalising agents and the drugs under investigation are weak acids, a third aim was to develop a tablet formulation screening program which focused on using pH modifying excipients as drug absorption enhancers for the model drugs. The objective here was to process successful candidates through the developed *in vitro* model to generate simulated pharmacokinetic data and predict *in vivo* bioavailability.

1.5.1 Development of *in vitro* model to predict drug bioavailability. Validation of model by *in vitro* characterisation of the effect of antacids on the bioavailability of analgesic drugs, during co-administration, and correlation with literature pharmacokinetic data.

Commonly used *in vitro* techniques for studying the absorption of drugs include: dissolution testing which determines a formulation's disintegration and dissolution, intubation, radiotelemetry, hydrogen-breath technique and gamma scintigraphy to study gastrointestinal transit, and diffusion cells, everted sac technique, cell culture techniques and Ussing chambers to study drug uptake/absorption. The development of IVIVCs for formulated products is largely based on dissolution testing, particularly for formulation changes to existing marketed drugs. This focus has been encouraged by regulatory bodies, especially the FDA, and the lead followed by industrial and academic workers. However, this approach has drawbacks in that many drugs, depending on their physicochemical properties, do not undergo dissolution rate-limiting absorption. When attempting to develop a model for the prediction of bioavailability, industry workers may be limited to currently approved and validated techniques which are robust and well established. However, in an academic environment, other techniques, mentioned above, could be included within the model to correlate more closely with the *in vivo* system. Utilising available techniques and with regard to resource limitations, the aim was to develop an *in vitro* absorption model, which could demonstrate IVIVCs and would therefore be useful as a predictive tool. Clearly, the development of an IVIVC requires data from both the *in vitro* model and the *in vivo* environment. The characterisation of antacid/analgesic co-administration using the model was chosen for the following reasons: sodium bicarbonate is frequently used as an antacid and is the proposed absorption enhancer

in the Zapp formulation and the drugs under study are widely used analgesics and substantial pharmacokinetic data for antacid/analgesic co-administration/co-formulation is available from literature to allow generation of an IVIVC.

Specifically:

- numerous pharmacokinetic and clinical trials have been conducted and are reported for commercial formulations of both drugs.
- Albin *et al.* (1985) studied the effects of aluminium hydroxide/magnesium hydroxide containing antacids on the absorption of paracetamol. Their results demonstrated delayed time to peak plasma concentration, and therefore reduced absorption rate, but were considered bioequivalent although a basis for this in fact was not discussed.
- pharmacokinetic data supplied by SB (1998b) demonstrated different absorption rates for paracetamol formulations containing sodium bicarbonate and calcium carbonate, the former being more quickly absorbed and the second being more slowly absorbed compared to the commercial formulation, demonstrated by differences in C_{max} and t_{max}.
- Neuvonen and Kivisto (1994) found that the co-administration of magnesium hydroxide with ibuprofen increased the drug absorption rate. The $AUC_{0\text{-}1hr}$ increased by 65% and the C_{max} increased by 31% although t_{max} was not significantly different.
- Hannula *et al.* (1990) studied the absorption of ibuprofen from capsules containing either aluminium hydroxide, calcium carbonate or sodium bicarbonate as the primary excipient. Their results demonstrated significant differences in absorption rate with formulations containing calcium carbonate or sodium bicarbonate being rapidly absorbed and the aluminium hydroxide containing formulation being very poorly absorbed. A dissolution study was also conducted which produced a rank correlation with the pharmacokinetic data.

The aims within this section can be summarised as the development of, and use of, currently available methods simulating the *in vivo* conditions for the characterisation of formulation, dissolution and drug transport through mucus and cell barriers, coupled with a literature review of gastric emptying parameters using paracetamol and ibuprofen as the model drugs and a group of antacids as potential absorption modifiers. Further to this an aim was that the model developed could be compared

with pharmacokinetic data available from the literature in an attempt to generate an IVIVC and so validate the model for further use as a predicative tool. The components of the model and strategy is illustrated in figure 1.6.

Figure 1.6
Illustrating schematically the developed *in vitro* model

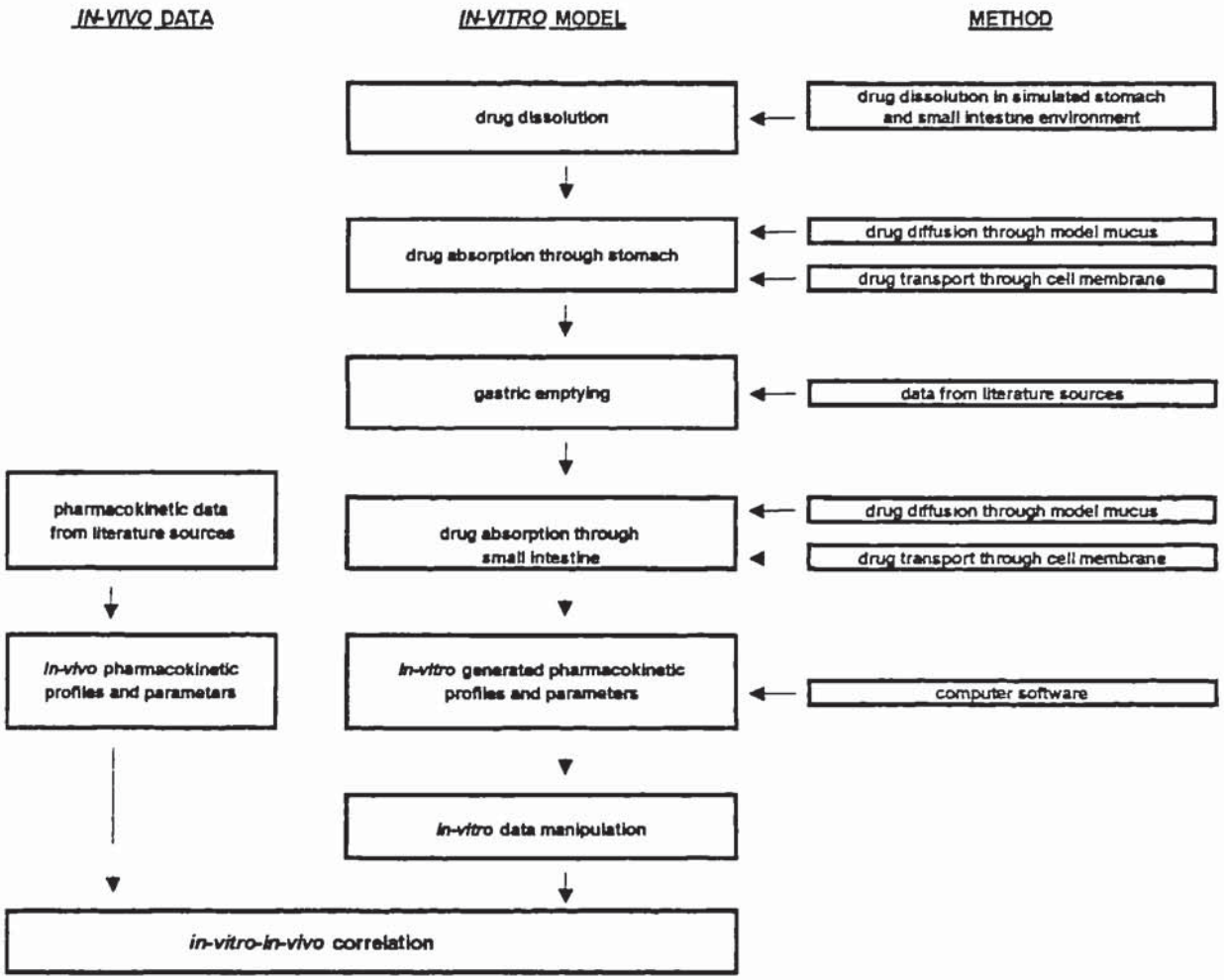

1.5.2 The characterisation of sodium bicarbonate as an absorption-enhancing excipient in paracetamol and ibuprofen solid dosage formulations

Clinically, a key requirement for analgesic products is that the product is fast acting to give rapid pain relief . Recent developments include the launch of ibuprofen lysinate tablets (Nurofen Advance®) which are clinically proven to be faster acting than conventional paracetamol commercial products (Mehlisch *et al.* 1995). SB have undertaken a development program to produce a fast-acting paracetamol formulation which yielded the Zapp formulation. Extensive *in vivo* assessment of Zapp tablets (Grattan *et al.* 2000) has demonstrated a significant increase in absorption rate (t_{max} 17.5 minutes) compared to standard products (t_{max} 35 minutes), in fact, the absorption rate was faster than that of the soluble form of the drug. Also, Ojantakanen *et al.* (1990) produced ibuprofen capsules containing sodium bicarbonate which demonstrated a faster t_{max} of 0.39hrs than ibuprofen solutions t_{max} 0.53hrs (Gillespie *et al.* 1982) and 0.71hrs (Lockwood *et al.* 1983). A solution containing dissolved drug would generally be expected to have the highest absorption rate and therefore the role of sodium bicarbonate in the absorption process of the model drugs is of great interest. On this basis, an aim was established to characterise fully the role sodium bicarbonate plays in the absorption process using methods developed as part of the IVIVC and others designed specifically for this purpose.

1.5.3 The development of novel analgesic tablet formulations utilising alkalising excipients. Prediction of bioavailability using novel *in vitro* model.

The previous studies' aims were to develop models and characterise effects based on and using alkalising agents and weakly acidic drugs. It was considered that an opportunity existed to utilise the knowledge gained and model developed to initiate a product development program for the model drugs based on alkalising excipients. The aim was to select potential absorption enhancers, develop methods to screen these from initial powder studies, through granulation and then tablet formulation studies. The final objective was to process successful candidates from the screening process through the *in vitro* model, with the aim of predicting *in vivo* parameters and estimating the potential improvement over currently available products.

CHAPTER 2
GENERAL METHODS

2.1 Paracetamol assay by HPLC

A number of methods are available for the determination of paracetamol by HPLC. If available, a pharmacopoeia method is usually a good starting point as the methods are generally robust having been widely used and refined. The USP has several paracetamol methods including the HPLC analysis of paracetamol and caffeine in this combined tablet monograph. This method was used as the starting point with caffeine selected as the internal standard and the solvent mixture selected for sample and reference standard preparation. The chromatographic conditions used were based on the method by Krieger (1987). The method was optimised to be stability indicating, *i.e.* separation of paracetamol's primary impurity, 4-aminophenol, from active and internal standard peaks and checked for possible interferences from the buffers and excipients used throughout this work.

2.1.1 Experimental

2.1.1.1 Materials

Paracetamol was supplied by SB (Weybridge, UK). Purity was assigned as 100.0% as the same batch of drug was used for sample and standard preparations throughout. Caffeine, methanol, 4-aminophenol and acetic acid were supplied by Aldrich (Poole, UK). All materials were of pharmaceutical, analytical or HPLC grade as appropriate. Double-distilled water was generated in-house using a Fison's Fi-Streem still.

2.1.1.2 Equipment

The HPLC system comprised a WISP 712 autoinjector, a Waters 484 ultraviolet variable wavelength detector and a Waters 600E system controller. Chromatograms were collected and integrated on a Waters chromatography 815 workstation.

2.1.1.3 Methods/chromatographic conditions

Working standards were prepared by serial dilution of a stock standard to produce standards within the range 0.005-0.2mg ml^{-1}, the exact concentration range dependent on the experiment. For all experiments preparation was designed to produce working solutions with concentrations in this range. The concentrations of internal standard (caffeine) in the working solutions for standards and samples was calculated to be approximately in the middle of the paracetamol range, to produce a peak of similar size to the active. All working solutions were diluted with solvent mixture (95:5 methanol:acetic acid). Samples and standards were injected once and calculations performed by the workstation by comparison of the samples response factor with the equation derived from the linear regression analysis of the standards.

The chromatographic conditions were:

injection volume	:	20µl
mobile phase	:	methanol:0.75% acetic acid (1:3)
wavelength	:	280nm
aufs	:	1.28abs
flow rate	:	1.0ml min^{-1}
runtime	:	15 minutes
column	:	techsphere ODS-2 5µm 150mm x 4.6mm ID (or equivalent)
sparge	:	helium 15ml min^{-1}

2.12 Example data

Typical chromatographic parameters were derived by application of the methods detailed in the USP (1995). Example parameter values, chromatograms and a calibration graph follow:

theoretical plates (i.std)	:	2400
theoretical plates (active)	:	2300
resolution factor (active/i.std)	:	6.1
resolution factor (impurity/active)	:	1.57
tail factor (active)	:	1.75
tail factor (i.std)	:	1.57
retention time (paracetamol)	:	≈4 min
retention time (internal standard)	:	≈9 min

Figure 2.1
Typical HPLC chromatogram of the paracetamol peak with the caffeine internal standard peak

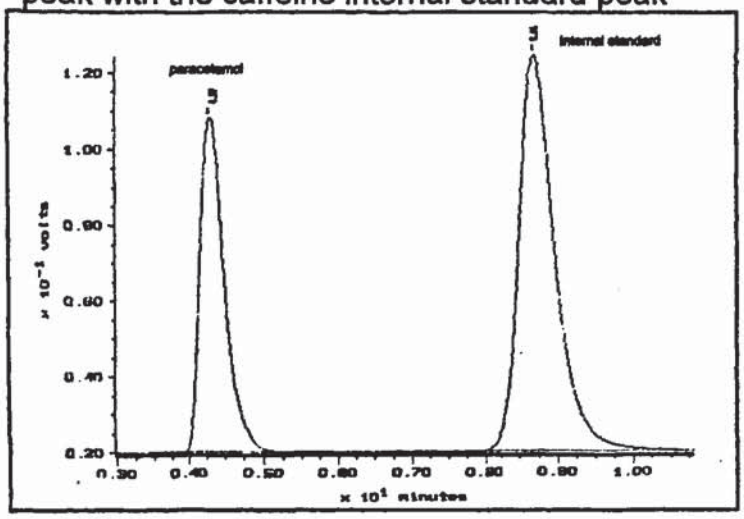

Figure 2.2
HPLC chromatogram demonstrating the resolution of paracetamol from its impurity 4-aminophenol.

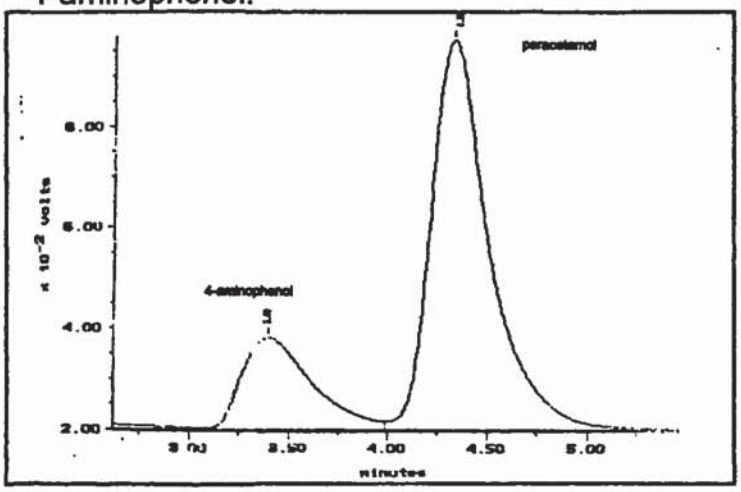

Figure 2.3
Typical calibration graph for paracetamol assay by HPLC. R^2=0.9999 and Y=0.6847X-0003. Note concentration scale corrected for dilution in this experiment.

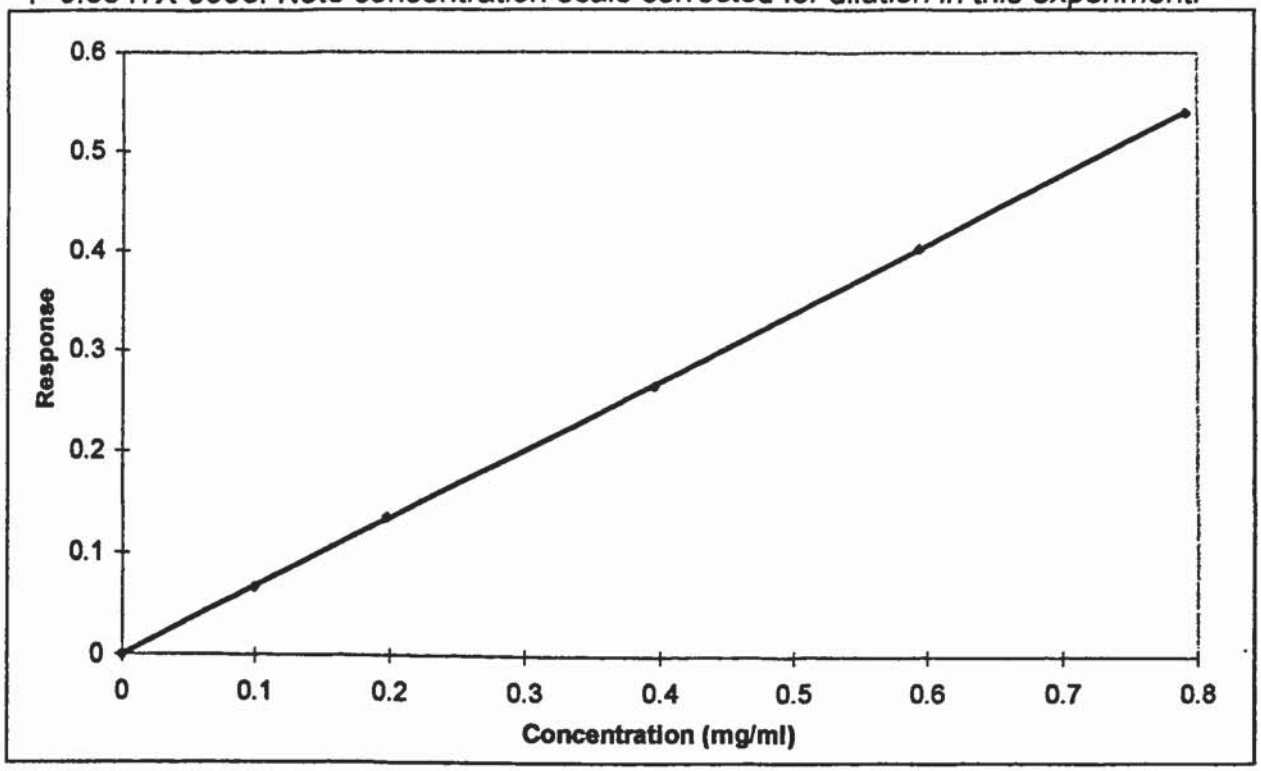

2.2 Ibuprofen assay by HPLC

A reversed phase HPLC method for ibuprofen assay has previously been developed within DDRG by Noble (1998). This method was selected for use in this study.

2.2.1 Experimental

2.2.1.1 Materials

Ibuprofen was supplied by SB (Weybridge, UK). Purity was assigned as 100.0% as the same batch of drug was used for sample and standard preparations throughout. Fenoprofen, acetonitrile and ortho-phosphoric acid were supplied from Aldrich (Poole,UK). All materials were of pharmaceutical, analytical or HPLC grade as appropriate. Double-distilled water was generated in-house using a Fison's Fi-Streem still.

2.2.1.2 Equipment

The HPLC equipment used was as detailed in section 2.1.1.2.

2.2.1.3 Method/chromatographic conditions

Working standards were prepared by serial dilution of a stock standard to produce standards within the range 0.001-0.1 mg ml^{-1}, the exact concentration range dependent on the experiment. For all experiments preparation was designed to produce working solutions with concentrations in this range. The concentrations of internal standard (fenoprofen) in the working solutions for standards and samples was calculated to be approximately in the middle of the ibuprofen range, to give a peak area similar in size to the active. All working solutions were diluted with solvent mixture (50:50 acetonitrile:water). Samples and standards were injected once and calculations performed by the workstation by comparison of the samples response factor with the equation derived from the linear regression analysis of the standards.

The chromatographic conditions were:

injection volume	:	100µl
mobile phase	:	acetonitrile:water:ortho-phosphoric acid (500:500:10)
wavelength	:	225nm
aufs	:	0.1abs
flow rate	:	1.0ml min^{-1}
runtime	:	7 minutes
column	:	Techsphere ODS-2 5µm 150mm x 4.6mm ID (or equivalent)
sparge	:	helium 15ml min^{-1}

2.22 Example data

Typical chromatographic parameters were derived by application of the methods detailed in the USP (1995). Example parameter values, chromatogram and calibration graph follow:

theoretical plates (i.std)	:	5400
theoretical plates (active)	:	5500
resolution factor (active/i.std)	:	4.8
tail factor (active)	:	1.03
tail factor (i.std)	:	1.15
retention time (ibuprofen	:	≈4 min
retention time (internal standard)	:	≈6 min

Figure 2.4
Typical HPLC chromatogram of the ibuprofen peak with the fenoprofen internal standard peak

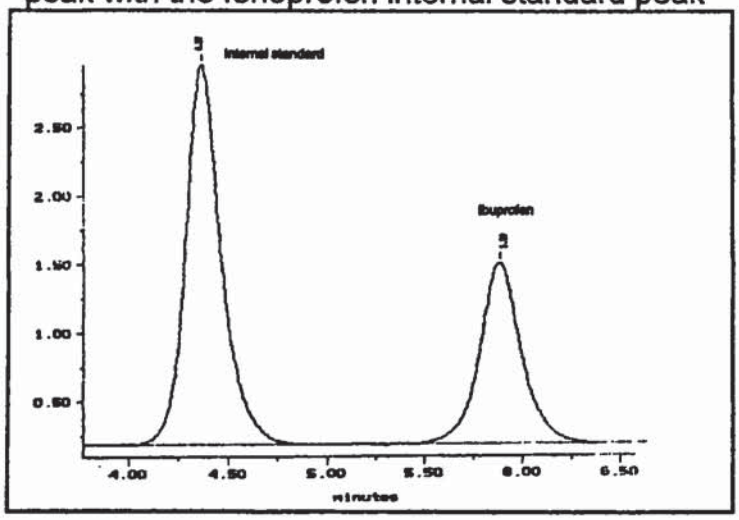

Figure 2.5
Typical calibration graph for ibuprofen assay by HPLC. R^2=0.9995, Y=121.1X-0.0331.

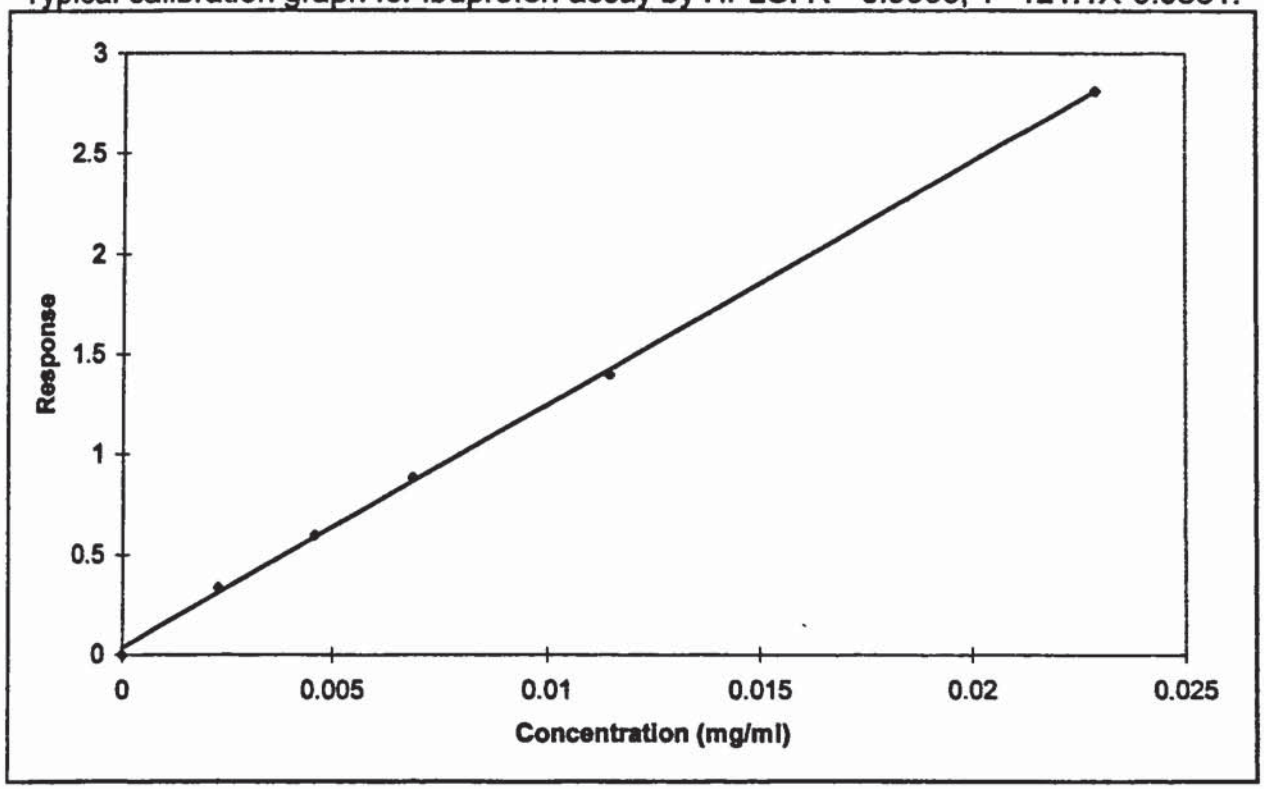

2.3 Ibuprofen Impurities by HPLC

2.3.1 Experimental

2.3.1.1 Materials

Ibuprofen was supplied by SB (Weybridge, UK). Acetonitrile and ortho-phosphoric acid were supplied by Aldrich (Poole,UK). All materials were of pharmaceutical, analytical or HPLC grade as appropriate. Double-distilled water was generated in-house using a Fison's Fi-Streem still.

2.3.1.2 Equipment

The HPLC equipment used was as detailed in section 2.1.1.2.

2.3.1.3 Method/chromatographic conditions

Tablet samples were ground and a sample containing approximately 0.1g of ibuprofen was dissolved in 20ml of acetonitrile. The samples were filtered through a 0.45μm HPLC filter (Gelman acrodisc® LC13PVDF) before use. The chromatographic conditions were:

injection volume	:	10μl
mobile phase	:	acetonitrile:water:ortho-phosphoric acid (340:660:0.5)
wavelength	:	214nm
aufs	:	0.02abs
flow rate	:	2.0ml min^{-1}
runtime	:	7 minutes
column	:	Techsphere ODS-2 5μm 150mm x 4.6mm ID (or equivalent)
sparge	:	helium 15ml min^{-1}

The area of any impurity peaks detected, excluding artefacts present in an injection of the solvent mixture (acetonitrile), were calculated as a percentage of the area due to the ibuprofen peak. No impurity peaks were observed, in all cases. The method sensitivity was investigated using a suitable dilution of one of the sample working solutions. It was found that peaks equivalent to 0.07% of the main peak could be easily detected. The methodology was supplied by SB (Product report PR/92/0018).

2.4 Miscellaneous HPLC Methods

2.4.1 Experimental

2.4.1.1 Materials

Propranolol, nadolol, cimetidine, ketoprofen, sodium lauryl sulphate, phosphoric acid, methanol, acetonitrile, procainamide HCl and sodium chloride were supplied by Aldrich (Poole,UK). All materials were of pharmaceutical, analytical or HPLC grade as appropriate. Double-distilled water was generated in-house using a Fison's Fi-Streem still.

2.4.1.2 Equipment

The HPLC equipment used was as detailed in section 2.1.1.2.

2.4.1.3 Methods

Samples obtained during permeability studies undertaken in chapter 7 for cimetidine, nadolol, and propranolol were analysed according to standard pharmacopoeia methods (USP 1995). Samples obtained for the study into ketoprofen permeability were analysed according to the method of Wong *et al.* (1992). Working standards were prepared by a serial dilution of a stock standard to produce standards covering the range of concentrations exhibited by the samples. Samples and standards were injected once and calculations performed by the workstation by comparison of the samples response factor with the equation derived from the linear regression analysis of the standards.

2.5 pH measurements

pH measurements were determined with Fisher Brand Hydros 400 pH meter (2 decimal places) connected to a Gallenkamp combination electrode. The instrument was calibrated before use with standard pH buffer solutions (Fisher, Loughborough, U.K), *i.e.* pH 7 and either pH 4 or 10 depending on the region of interest.

2.6 Kinematic viscosity

Kinematic viscosity was performed using a U-tube viscometer in accordance with the method detailed in the USP (1995). Measurements were conducted in triplicate at 37°C unless otherwise stated. U-tubes were calibrated in-house using double-distilled water at 20°C. Viscosities were calculated using the following equation:

$$\nu = \frac{kt}{\rho}$$

equation 2.1

where ν is the kinematic viscosity ($mm^2\ s^{-1}$), k is the calibration constant, t is the measured time and ρ is the measured density of the solution under test.

2.7 Scintillation Counter

A Packard liquid scintillation analyser 1900TR was used for measuring concentrations of the radio-labelled drugs in diffusion studies. Aliquots of the standard, the working solution added the donor cells, and samples were mixed thoroughly with 10mls of Optiphase 'Hi-safe' 3 scintillation fluid. DPMs were measured with the counter delay time set to at least 3 minutes.

CHAPTER 3
PHYSICOCHEMICAL STUDIES

3.1 Introduction

To fully characterise the absorption process it is essential to understand the physicochemical properties of the materials under investigation. The aim of this section was to measure key properties for the model drugs and antacids. The solubility/pH relationship has been discussed in section 1.1.4.1 and elucidation was important for initial selection of excipients as potential dissolution enhancers, for an understanding in the drug dissolution process, including the effect of dissolved excipients and also to characterise and potentially understand the mechanisms of action for the various effects caused by antacid co-administration. The results from this section were utilised in subsequent experimental and model development studies.

3.2 Solubility/pH profile of model drugs

3.2.1 Experimental

3.2.1.1 Materials

Paracetamol and ibuprofen were obtained from SB Pharmaceuticals (Weybridge, UK). Hydrochloric acid, sodium hydroxide, potassium chloride, boric acid, di-sodium phosphate, citric acid and mono-basic potassium phosphate were purchased from Aldrich (Poole, UK). All materials were of pharmaceutical or analytical grade as appropriate. Double-distilled water was generated in-house using a Fison's Fi-Streem still.

3.2.1.2 Equipment

A Techne SB-16 water bath/shaker was used for sample preparation. HPLC equipment was as detailed in section 2.1.1.2.

3.2.1.3 Method

The saturated solubilities of paracetamol and ibuprofen at 37°C, over the pH ranges of 1-11 and 1-7 respectively, were determined. The compositions of the buffers used are detailed in Appendix 1. Approximately 1g of drug was added to 30ml of buffer, each experiment being performed in triplicate. The suspensions were well shaken manually, and then placed in the water bath at 37°C, agitator setting 1 (70 cycles *per* minute), for 4 days. Each day, the vials were checked for the presence of solid, if necessary more drug was added. On the fifth day, and after a minimum of 96 hrs, sampling was undertaken. For paracetamol, 1.0 ml was withdrawn, visually ensuring no solid was collected (supernatant was clear), using a micropipette. Four 1.0ml aliquots of warm (40-50°C) water were used to wash-out the pipette tip. The aliquot and washings were combined in a single vial and 10.0ml of solvent mixture (95:5/methanol:acetic acid) added to give a total volume of 15.0ml. A 5.0 ml aliquot was taken and 2.0ml of the internal standard added. The samples were analysed by HPLC as detailed in section 2.1. For ibuprofen, 10ml was withdrawn and filtered through a 0.45μm cellulose filter into a pre-warmed beaker, the first 5ml being discarded. An aliquot of between 0.1-1.0ml was sampled to a volumetric flask (10.0-50.0ml) and four aliquots of warm (40-50°C) water used to wash-out the pipette tip. An internal standard quantity between 0.2-1.0ml was added, before dilution to volume. The aliquots and final volumes used were calculated from predicted solubility to ensure the HPLC data generated was within the calibrated region. Dilutions were repeated if necessary to ensure compliance. The pH values used were obtained by measuring the pH of the drug saturated buffer solutions, post sampling. The samples were analysed by HPLC as detailed in section 2.2.

3.2.2 Results and discussion

The solubility of paracetamol and ibuprofen were determined over the pH ranges of 1-11 and 1-7 respectively as summarised in table 3.1 and illustrated in figures 3.1 and 3.2. For paracetamol, literature values, summarised by Florey (1974), have been reported as 19 & 20 mg ml^{-1} in distilled water and 23.8 mg ml^{-1} in buffer pH 6.0, all at 37°C. The results here demonstrate that over the pH range 1-8, which is the range found *In vivo* in the GI tract, the solubility of paracetamol will not be affected by the systemic pH. The mean over the pH range 1.2-8.0 was calculated as 20.3±0.8 mg

ml^{-1}. As the pK_a was approached, variously reported as between 9.0-9.5 and also 10.15, as summarised by Florey (1974), a rapid increase in solubility was detected as predicted, as the solubility of a weak acid is affected by the pH of solution according to equation 1.2. For ibuprofen, solubility over the pH range 1-4 was determined as 0.058±0.004 mg ml^{-1} (henceforth referred to as ≈0.05 mg ml^{-1}), *i.e.* sparingly soluble in the stomach. A rapid and continual increase in solubility was recorded as the pK_a, summarised from others as 4.4 and 5.2 by Moffat (1986) and 5.3 by Lund (1994), was approached and thereafter. Herzfeldt and Kummel (1983) reported an average solubility of 0.02 mg ml^{-1} over the pH range 1-4 with the profile changing as recorded in this study, in terms of effect of pH but not in terms of magnitude. They conducted the experiment at room temperature with only a 48 hour dissolution time, possibly explaining the lower absolute solubility values obtained.

Table 3.1
Summarising the solubility/pH relationship for ibuprofen and paracetamol in buffer solutions. Results are the mean of 3 replicates±SD. *Used as x-axis in graph

Ibuprofen Buffer pH measured* /nominal	Ibuprofen solubility (mg ml^{-1}) ±SD	Paracetamol Buffer pH measured* /nominal	Paracetamol solubility (mg ml^{-1}) ±SD
1.51/1.2	0.058±0.001	1.46/1.2	21.0±0.3
1.83/2.0	0.053±0.004	1.92/2.0	20.9±0.5
2.82/3.0	0.062±0.017	2.93/3.0	20.5±0.3
3.85/4.0	0.058±0.007	4.00/4.0	19.5±0.1
4.77/5.0	0.166±0.027	5.06/5.0	18.7±0.2
5.45/6.0	0.713±0.018	6.09/6	20.4±0.1
5.55/8.0	0.938±0.008	7.14/7.0	20.9±0.8
6.16/9.0	4.20±0.23	7.93/8.0	22.4±0.2
6.28/7.0	3.89±0.46	9.32/9.0	24.8±0.3
6.52/9.7	10.3±1.59	9.82/13.0	40.8±0.3
7.02/11.0	27.5±3.3	10.80/13.5	120.5±7.8

Figure 3.1
Illustrating the solubility/pH relationship for paracetamol. Results are the mean of 3 replicates±SD

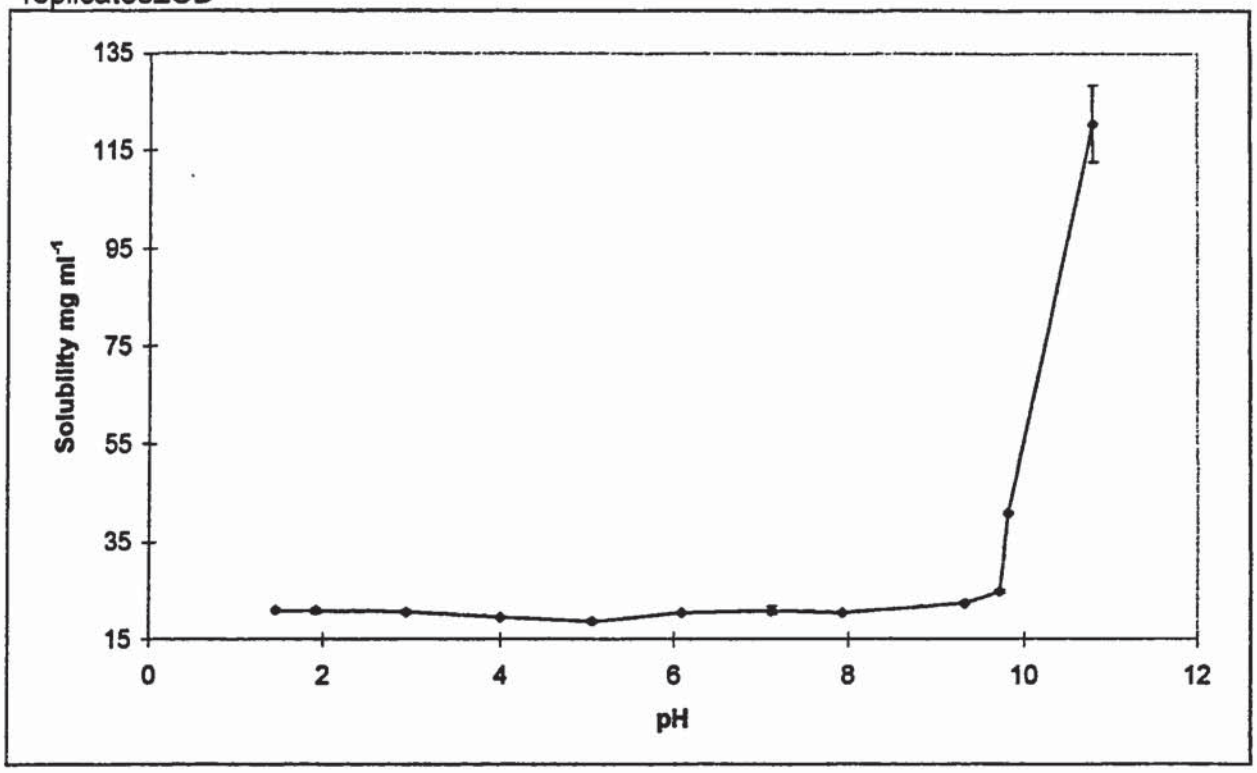

Figure 3.2
Illustrating the solubility/pH relationship for ibuprofen. Results are the mean of 3 replicates±SD

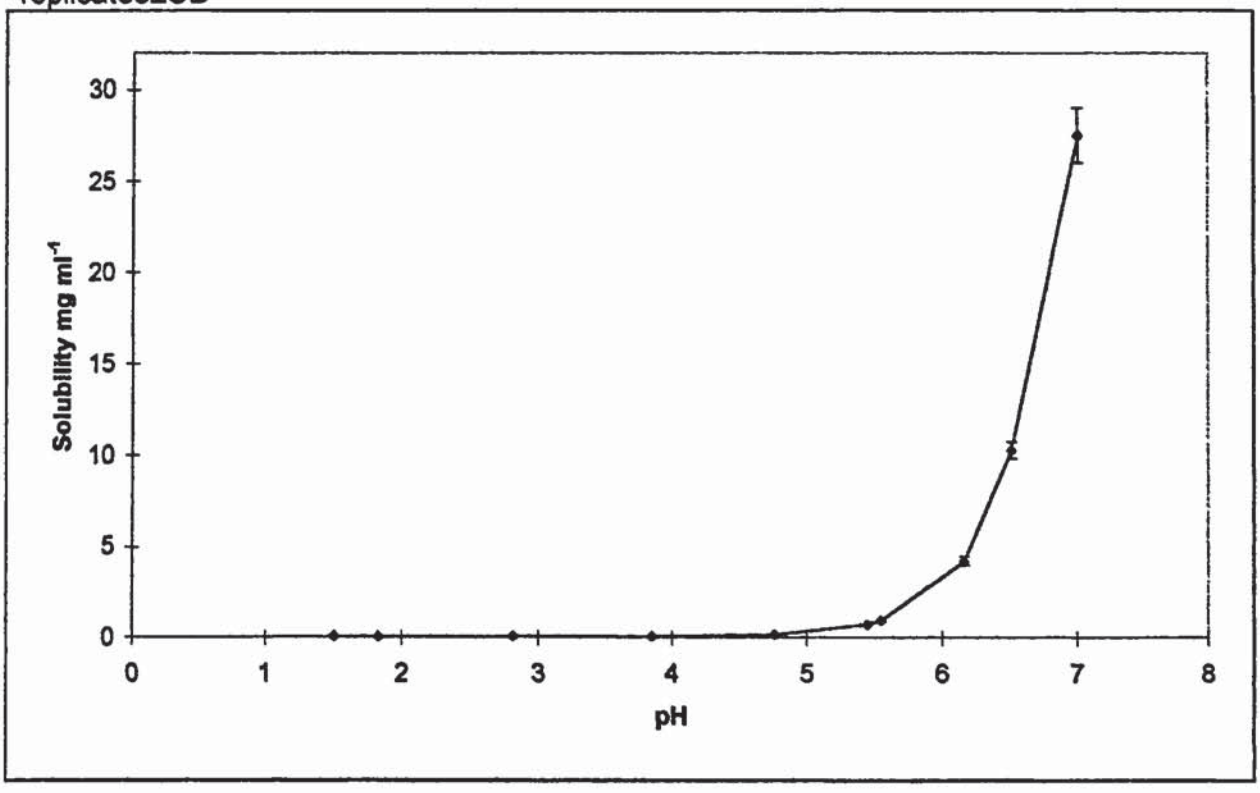

3.3 Solubility of antacids in selected buffers

3.3.1 Experimental

3.3.1.1 Materials

Hydrochloric acid, mono-basic potassium phosphate, sodium hydroxide, aluminium hydroxide, calcium carbonate, magnesium oxide and magnesium hydroxide were obtained from Aldrich (Poole,UK). Lanthanum oxide and 1000ppm reference standards (Magnesium and Calcium) were obtained from Fisher Scientific (Loughborough, UK). All materials were analytical or spectrosol grade as appropriate. Double-distilled water was generated in-house using a Fison's Fi-Streem still.

3.3.1.2 Equipment

A Techne SB-16 water bath/shaker was used for sample preparation. A Perkin-Elmer 2380 Atomic Absorption spectrophotometer, located at the Pharmacia and Upjohn Crawley facility, was used for AAS analysis.

3.3.1.3 Method

The four 'insoluble' antacids, calcium carbonate, aluminium hydroxide, magnesium oxide and magnesium hydroxide were selected for solubility studies. The antacids' solubility's were determined by AAS, except aluminium hydroxide which was determined gravimetrically. For the antacids, excluding aluminium hydroxide, excess antacid was added to 0.05M HCl or USP Buffer pH 6.8. The suspensions were shaken manually, and then placed in the water bath at 37°C, agitator setting 1 (70 cycles *per* minute), for 4 days. On the fifth day, and after a minimum of 96 hrs, sampling was undertaken. 10ml samples were withdrawn and filtered through a 0.45μm HPLC filter (Gelman acrodisc® LC13PVDF), discarding the first 5ml, into a pre-warmed beaker. 1.0ml aliquots were diluted to 100ml 0.5% w/v Lanthanum solution (5.87g lanthanum oxide, the ionisation suppressant, plus 25ml HCl *q.s.* final volume 1000ml). Further serial dilutions were undertaken as required until the working concentration of the cation under investigation was within the linear working range for the experimental conditions. The AAS conditions were:

- calcium analysis - wavelength 422.7nm, slit 0.7nm (air acetylene, oxidising lean blue flame) and 5 standards from 1-5ppm
- magnesium analysis- wavelength 285.2nm, slit 0.7nm (air acetylene, oxidising lean blue flame) and 5 standards from 0.1-0.5rpm

Results were calculated by comparison with a linear equation derived from the 6-point calibration data, followed by conversion from measured cation to parent compound. Aluminium hydroxide solubility was determined gravimetrically using the same solution preparation procedure, followed by filtration through acid washed No.4 crucible filters. This technique was limited in that it does not account for salt formation, *e.g.* possible conversion of aluminium hydroxide to aluminium chloride.

3.3.2 Results and discussion

The solutions were selected to simulate the gastric and intestinal environments *in vivo* (Dressman *et al.* 1998). The solubility results are detailed in table 3.2. They illustrate clearly that the antacids are all soluble in simulated gastric fluid and also that at the therapeutic doses standardised at 1g (British National Formulary 1995) the antacids are likely to be present in both dissolved and solid form. In simulated intestinal fluid the solubility is much lower and in the case of calcium carbonate considered as being at trace level. The results demonstrated greatly reduced antacid solubility as solvent pH is increased.

Table 3.2
The solubility of antacids in simulated gastric (0.05M HCl) and simulated intestinal fluid (USP buffer pH6.8). Results are mean of 3 replicates±SD

Antacid	Solubility in simulated stomach fluid (mg $200ml^{-1}$)	Solubility in simulated intestinal fluid (mg $200ml^{-1}$)
Magnesium oxide	190.1±4.5	12.0±0.1
Magnesium hydroxide	336.5±9.6	1.0±0.1
Aluminium hydroxide	400.0±5.2	11.4±10.9
Calcium Carbonate	660.0±25	<0.05

3.4 Dissolved drug adsorption onto antacids

3.4.1 Experimental

3.4.1.1 Materials

Paracetamol and ibuprofen were obtained from SB Pharmaceuticals (Weybridge, UK). Hydrochloric acid, sodium hydroxide, mono-basic potassium phosphate, aluminium hydroxide, calcium carbonate, magnesium oxide and magnesium hydroxide were purchased from Aldrich (Poole, UK). All materials were of pharmaceutical or analytical grade as appropriate. Double-distilled water was generated in-house using a Fison's Fi-Streem still.

3.4.1.2 Equipment

A Midde Laboratory Engineering Ltd water bath/shaker was used for sample preparation. HPLC equipment was as detailed in section 2.1.1.3.

3.4.1.3 Method

Drug/antacid concentrations were set to model *in vivo* concentrations. The experiment involved measuring the adsorption of dissolved drug onto the antacid under test from the following solutions; 5mg ml^{-1} paracetamol in 0.05M HCl, 5mg ml^{-1} paracetamol in USP buffer pH6.8 and 2mg ml^{-1} ibuprofen in USP buffer pH6.8. 250mg±5mg of each antacid was added to 50.0ml of the drug containing solution, followed by shaking overnight at 37°C and 60rpm. 10ml aliquots were filtered through a 0.45μm HPLC filter (Gelman acrodisc® LC13PVDF), discarding the first 5ml to waste. A 1.0ml aliquot was pipetted and diluted to 20.0ml including the addition of 1.0 ml of internal standard for paracetamol, for ibuprofen the 1.0ml aliquot was diluted to 10.0ml including the addition of 2.0ml of internal standard. Paracetamol and ibuprofen samples were analysed by HPLC according to the methods detailed in sections 2.1 and 2.2 respectively. The amounts of drug absorbed were calculated by difference from the measured drug concentration compared to the original drug concentration. The data were converted to give the % drug remaining in solution.

3.42 Results and Discussion

Firstly, the work did not include the analysis of ibuprofen adsorption in the stomach environment because of the very low (≈0.05 mg ml^{-1}) solubility of ibuprofen under these conditions, *i.e.* ibuprofen dissolution and hence absorption is minimal at this pH and any adsorption effect would be negligible. The results indicate that adsorption of dissolved drug by the antacids under test is not a major mechanism for altering the absorption of the model drugs. It is noted that, for paracetamol with all antacids, adsorption increases from the simulated stomach to the simulated intestinal environment, one reason for this could be decreased antacid solubility and hence increased surface area available for adsorption. The results are listed in table 3.3.

Table 3.3
The adsorption of dissolved drug onto solid antacid measured as the % remaining of drug in solution at nominal maximum concentration *In vivo*. Results are the mean of 3 replicates±SD.

Drug/ environment	Ibuprofen/ intestine	Paracetamol/ stomach	Paracetamol/ intestine
magnesium hydroxide	99.8±0.3	99.5±0.9	98.8±0.2
magnesium oxide	102±1.5	96.7±0.30	96.8±0.1
calcium carbonate	101.6±2.0	100.7±0.7	98.9±0.7
aluminium hydroxide	100.2±.0.2	100.2±0.4	99.1±0.1

3.5 Solubility of model drugs in excipient containing solutions

3.5.1 Experimental

3.5.1.1 Materials

Paracetamol, ibuprofen and sodium bicarbonate (extra fine grade) were obtained from SB Pharmaceuticals (Weybridge, UK). Hydrochloric acid, sodium hydroxide, mono-basic potassium phosphate, lactose, potassium bicarbonate, sodium chloride and tartaric acid were purchased from Aldrich (Poole, UK). All materials were of pharmaceutical or analytical grade as appropriate. Double-distilled water was generated in-house using a Fison's Fi-Streem still.

3.5.1.2 Equipment

A Techne SB-16 water bath/shaker was used for sample preparation. HPLC equipment was as detailed in section 2.1.1.2.

3.5.1.3 Method

The samples were prepared as detailed in 3.2.1.3 except the solutions used were 0.05M HCl for paracetamol and USP buffer pH6.8 for ibuprofen with the following additives:

lactose	- 15 and 75mmol *per* 200ml
sodium chloride	- 15, 75 and 150mmol *per* 200ml
tartaric acid	- 15, 75 and 150mmol *per* 200ml*
sodium bicarbonate	- 15,75, and 150mmol *per* 200ml
potassium bicarbonate	- 15,75, and 150mmol *per* 200ml

*Excipient not used in ibuprofen investigation due to analytical limitations relating to the very low intrinsic solubility of this drug.

The excipient-containing solutions were used 'as is', *i.e.* without readjustment of pH to the nominal value after addition of drug. Paracetamol and ibuprofen samples were analysed by HPLC according to the methods detailed in sections 2.1 and 2.2, respectively.

3.5.2 Results and discussion

The range chosen for excipient concentration was 15 to 150mmol of excipient *per* 200ml, selected on the basis that the sodium bicarbonate quantity in the Zapp formulation is set at approximately 15mmol (when diluted in gastric contents) and under dissolution conditions, the micro-environment around the tablet could have a higher concentration due to localised effects, hence the increase of one order of magnitude. The buffer solutions were chosen to simulate the primary dissolution site for each drug, *i.e.* simulated stomach fluid for paracetamol and simulated intestinal fluid for ibuprofen.

For paracetamol, the results demonstrate that potassium bicarbonate, sodium bicarbonate, and sodium chloride reduce the solubility of paracetamol, proportionally with increasing concentration for the latter two; lactose does not affect the solubility

and tartaric acid increases the solubility with increasing concentration. These results clearly indicate that sodium bicarbonate, in solution does not increase the solubility of paracetamol through the mechanisms of pH modification or the indifferent ion effect - through modification of the activity coefficient (James 1995). In fact, the effect is inhibitory, by a mechanism not yet defined. The results are illustrated in figure 3.3. For ibuprofen, both sodium bicarbonate and potassium bicarbonate enormously increase the solubility of the drug. The measured pH increased from pH≈6.8 to 7.3 as the concentration of these excipients was increased. With reference to figure 3.2 it is noted that this change in pH can be attributed as the cause of the dramatic increase and the dominant factor. Lactose does not effect the solubility of ibuprofen and sodium chloride decreases it proportionally with increasing concentration. The results are illustrated in figure 3.4. The results for both drugs are summarised in table 3.4.

Table 3.4
The solubility of model drugs in excipient containing buffer solutions. For paracetamol the buffer was 0.05M HCl and for ibuprofen USP buffer pH6.8 was used. Results are the mean of at least three replicates±SD. The final solution pH is also recorded.

Excipient concentration mmol/200ml	Paracetamol saturated solubility (mg ml^{-1})	Ibuprofen saturated solubility (mg ml^{-1})
lactose - 15	19.2±1.4 (pH=1.5)	3.11±0.0 (pH=6.3)
lactose - 75	19.2±0.3 (pH=1.5)	2.90±0.15 (pH=6.3)
sodium bicarbonate - 15	18.5±0.2 (pH=6.8)	11.3±0.01 (pH=6.9)
sodium bicarbonate - 75	16.5±0.2 (pH=7.8)	49.9±3.0 (pH=7.1)
sodium bicarbonate -150	14.1±0.3 (pH=8.1)	108.8±11.4 (pH=7.1)
potassium bicarbonate - 15	20.5±0.8 (pH=6.8)	9.75±1.50 (pH=6.9)
potassium bicarbonate - 75	20.3±0.3 (pH=7.8)	59.5±2.8 (pH=7.3)
potassium bicarbonate - 150	16.2±0.6 (pH=8.2)	205.6±9.4 (pH=7.3)
tartaric acid - 15	19.4±0.8 (pH=1.6)	*
tartaric acid - 75	19.8±0.8 (pH=1.5)	*
tartaric acid - 150	22.0±0.7 (pH=1.4)	*
sodium chloride - 15	18.7±0.4 (pH=1.5)	3.08±0.21 (pH=6.1)
sodium chloride - 75	16.5±0.1 (pH=1.4)	2.35±0.27 (pH=6.1)
sodium chloride - 150	14.2±0.3 (pH=1.2)	1.77±0.25 (pH=6.0)

* analysis not performed

Figure 3.3
Illustrating saturated solubility of paracetamol in 0.05M HCl containing dissolved excipients. Results are the mean of 3 replicates (±SD selected to aid visual clarity).

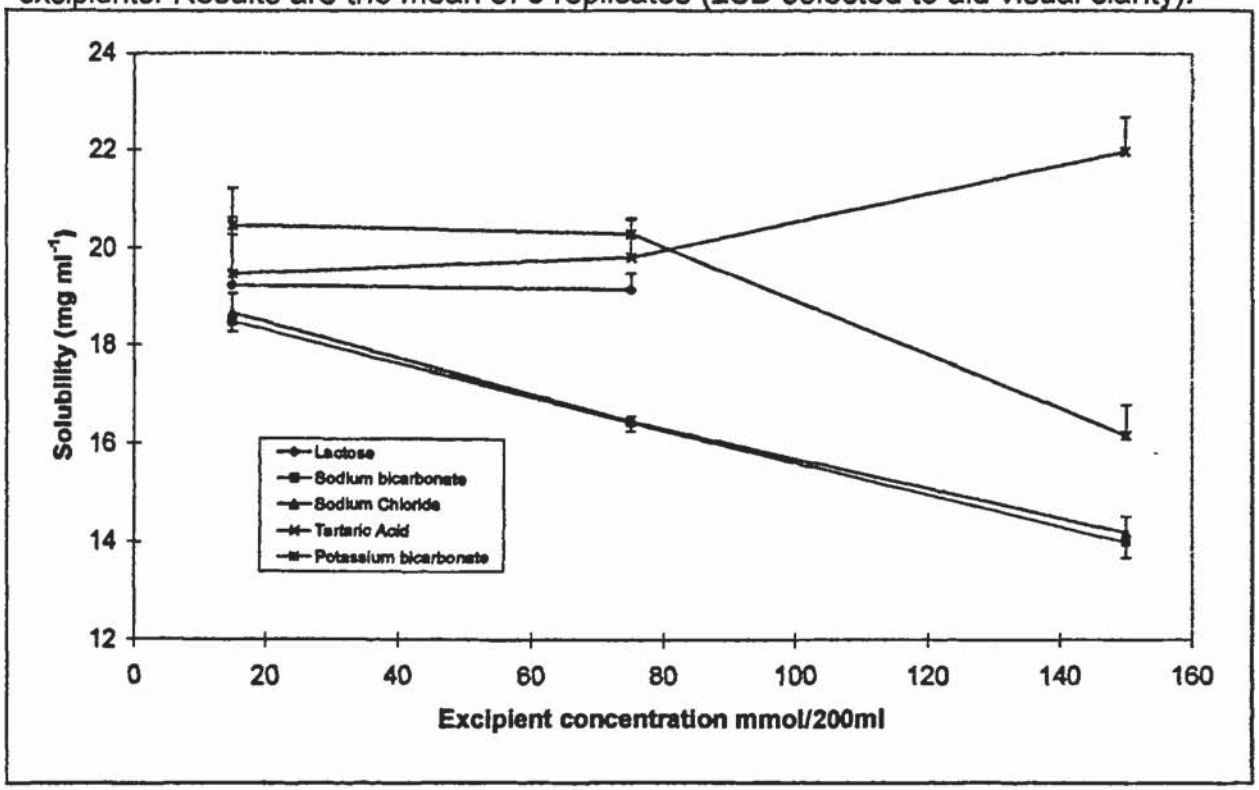

Figure 3.4
Illustrating saturated solubility of ibuprofen in USP buffer pH6.8 containing dissolved excipients. Results are the mean of 3 replicates (±SD selected to aid visual clarity).

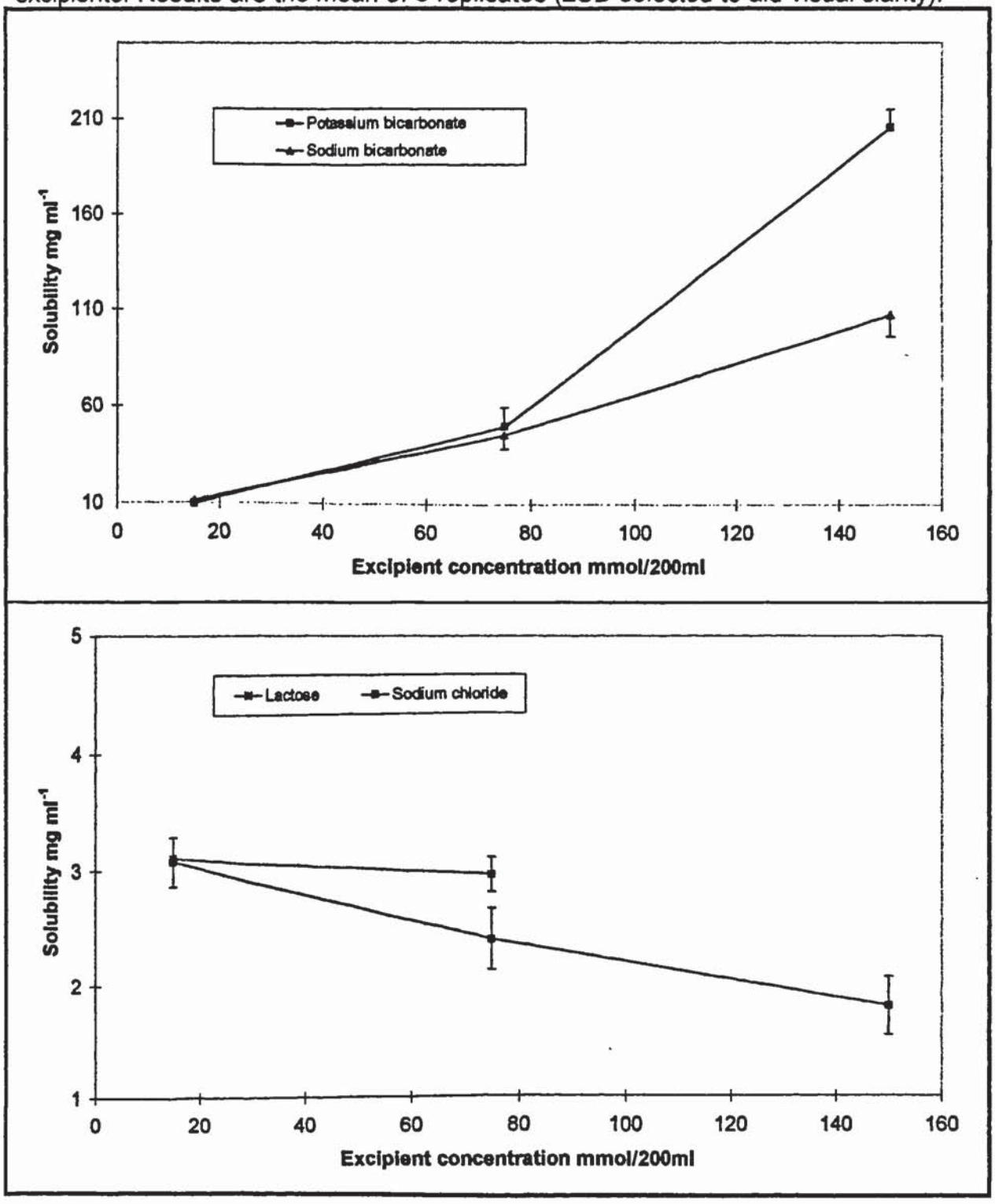

CHAPTER 4
DISSOLUTION STUDIES

4.1 Introduction

Considering the model drugs, for ibuprofen formulations, being BCS class II (Amidon *et al.* 1995), it is highly likely that the dissolution of the drug will be the rate-limiting step for drug absorption. For paracetamol formulations, BCS class I (Amidon *et al.* 1995), it is commonly assumed that the rate-limiting step is gastric emptying (Heading *et al.* 1973). However, there are examples where paracetamol dissolution has been found to correlate with bioavailability parameters, *e.g.*, Retaco *et al.* (1996); Sotiropoulus *et al.* (1981), although these examples generally have products with a wide variation in dissolution profile as well as relatively slow dissolution rates. These suggest that, generally for paracetamol, the rate-limiting step is in fine balance with the dissolution rate-becoming limiting for poorly dissolving formulations or conversely when large increases occur in the absorption rate, which may be applicable with the Zapp formulation. It is, therefore, likely that the dissolution process would be a very significant factor for both drugs during this investigation.

Also, the stated aims of the project are inter-related, particularly in terms of drug dissolution. Specifically, to meet these aims, the following investigations were undertaken:

- the variation between commercial products due to formula and formulation were investigated
- the role of sodium bicarbonate, the primary excipient in the Zapp formulation was characterised, by use of novel dissolution methods and physicochemical studies
- the effects of antacids on the dissolution processes of the model drugs was investigated, for inclusion in the overall IVIVC model.
- in combination with the characterisation study, excipients were selected for initial drug:excipient powder mixture dissolution study, to allow selection of suitable candidates for progression through the tablet formulation process, *i.e.* preparation of granules and formulated products.

Generally accepted theoretical models for the dissolution process (Macheras *et al.*, 1995) were used as basis for experimental design. On this basis four new methodologies were developed to study dissolution as detailed below:

- method to characterise drug IDR
- method to study the effect of excipients in close proximity to the drug during controlled powder dissolution
- method to study drug/antacid interactions
- method to discriminate between commercial tablet formulations

These methods were utilised to meet the aims outlined above.

4.2 Theoretical Considerations

The three basic models used to describe the dissolution process, *i.e.* the Noyes-Whitney, diffusion layer and interfacial barrier models are described by the following equation:

$$\frac{dm}{dt} = kA(C_s - C) \qquad \text{equation 4.1}$$

where m is the mass of solute passed into solution at time t, (therefore dm/dt represents the dissolution rate), A is the surface area of the undissolved solid in contact with the solvent, C_s is the saturated concentration of the solute at the experimental temperature, C is the solute concentration at time t and k is the generalised first-order rate constant (IDR rate constant). For the Noyes-Whitney and interfacial barrier models k is a generalised constant. However, for the diffusion layer model, constant k can be described as follows:

$$k = \frac{D}{h} \qquad \text{equation 4.2}$$

where D is the diffusion coefficient of the solute in the dissolution medium and h is the thickness of the boundary layer. The boundary layer is affected by the hydrodynamic conditions, *i.e.* degree of agitation - speed of stirring or shaking; size, shape and position of stirrer; volume of dissolution fluid; size and shape of container; and viscosity of dissolution medium. For the interfacial barrier model, where the process is

not diffusion rate limited, the hydrodynamic conditions do not contribute to the dissolution rate (Aulton,1988; Macheras *et al.*, 1995).

The diffusion coefficient can be described by the equation:

$$D = \frac{RT}{6Nr\pi\eta} \qquad \text{equation 4. 3}$$

where R is the universal gas constant, T is the absolute temperature, N is Avogadro's constant, η is the kinematic viscosity and r is the radius of the molecule in solution.

Reviewing equations 4.1 and 4.2, it is evident that the change in concentration of the dissolved drug is proportional to the IDR constant, the surface area and the concentration difference (C_s-C). Consequently any change to one or more of these variables or parameters will affect the rate of dissolution.

For these studies the theoretical diffusion layer and interfacial barrier models were applied. Experiments were designed to measure all factors within the model or, in some instances, some factors were reduced to constants by experimental design, to allow a specific assessment of individual, or a combination of, parameters.

4.3 Factors Affecting the Dissolution Rate

4.3.1 Dissolution Volume

Selection of the dissolution volume depends on the purpose of the experiment. Generally, if the experiment has been designed to model physiological conditions, the volume selected will compare to the physiological volume. If the purpose of the study is to evaluate defined factors it is usually desirable to conduct the dissolution study under 'sink' conditions (where the maximum value of C is at least 10 times smaller than C_S). This reduces the variable (C_S-C), in equation 4.1, to the constant C_S which simplifies the treatment of dissolution results (Macheras *et al.*, 1995).

4.3.2 Intrinsic Dissolution Rate (IDR) Constant

For the diffusion-layer model, the diffusion coefficient, the size of the diffusing molecules and the length of the boundary layer are included within the intrinsic term. The IDR constant is also inversely proportional to the viscosity of the liquid medium (Aulton, 1988). For the interfacial barrier model the IDR constant is a generalised rate constant.

4.3.3 Surface Area of the Drug

Depending on the purpose of the study, the surface area exposed to the dissolution medium may or may not be controlled. For example, in tablet dissolution studies all factors are of interest, including changes to surface area, for instance caused by disintegration. Conversely, if only the role of drug solubility is of interest the experimental design would aim to keep the surface area constant, simplifying evaluation of the data by removal of the area term from equation 4.1. The latter method would also be employed to evaluate changes in apparent surface area caused by, for example, the hydration capacity of tablet disintegrants, leading to aqueous penetration, and the swelling capacity leading to bursting of the formulation or a decrease in apparent area through the use of non-porous insoluble excipients.

4.3.4 Saturated Solubility

In the micro-environment surrounding the dissolving drug particle the pH and composition of the dissolution medium may be significantly different from the bulk solution. For weak acids, including ibuprofen and paracetamol, the pH of the dissolving medium may affect the saturated solubility and can be defined as

$$S = S_o + \frac{S_o K_a}{[H_3O^+]} \qquad \text{equation 4.4}$$

where S is the solubility at the experimental pH and S_o is the intrinsic solubility (Florence and Attwood 1988). Further to this, if the weak acid has a low pK_a, *e.g.,* ibuprofen, dissolution of the drug at the surface buffers the boundary layer to a value near the drugs own pK_a , significantly limiting the dissolution rate. This is one reason why many drugs are formulated as salts. Although salts do not provide higher solubility at a given pH, because of the buffering capacity of the ionised form of the drug in the salt, the pH of solution will be affected *e.g.*, it is higher in the case of a sodium salt of a weak acid. Although under *in vivo* conditions the amount of administered drug is likely to be insufficient to regulate the pH of the GI contents, the micro-environment of the solid particles will have a higher pH leading to an increased dissolution rate. If the total solubility in the micro-environment exceeds the solubility in the bulk solution, precipitation of fine particles of drug may occur. These fine particles of non-ionised acid have an increased rate of redissolution in terms of increased particle surface area (Macheras *et al.*, 1995). If the surrounding dissolution medium includes dissolved antacid/excipients, they may alter the pH of the micro-environment or bulk solution, form salts with the drug, change the nature of solvent leading to a change in solubility, through the 'common ion' or 'indifferent ion' phenomena (James, 1986) or cause macro changes to the nature of the solvent.

4.4 Dissolution method development

With reference to section 1.3.3, the approach adopted to develop dissolution methods, and potentially IVIVCs, was based on the official USP paddle and basket apparatus. When using these systems, the FDA (CDER 1997) recommend the use of the rotating paddle apparatus with a stirrer speed of 50rpm, which is considered to be capable of a high degree of discrimination (Dash *et al.*, 1988). Dressman *et al.*, (1998) recommend that simulated gastric fluid should contain between 0.01-0.05M HCl and the FDA recommend the use of USP pH1.2 buffer. 0.05M HCl (pH 1.3) was selected as the simulated gastric fluid. Intestinal fluid has a considerably higher pH than gastric fluid and has a significant buffering action due to bicarbonate ions. Therefore, USP buffer pH 6.8 as recommended by the FDA was selected as the simulated intestinal fluid. The use of these simulated media and the dissolution apparatus, where possible, allows correlation of data across the different methodologies, in this study.

4.4.1 Controlled powder dissolution method

As detailed in section 4.3, two factors by which an antacid/excipient may affect the dissolution rate are through modification of the microenvironment around a drug particle and through changes in the apparent surface area of the drug. Currently, two approaches are used to characterise these processes. The first is an extension of the rotating basket - IDR method, but involves the co-compression of the drug with the excipient of interest. While this method simulates the tablet formulation more closely than the proposed method, it is believed that there are also several disadvantages. It has been demonstrated for well mixed naproxen/phenytoin co-compressates that a simple linear relationship between dissolution rate and surface area is not valid, contradicting the stagnant-layer model predictions (Neervannan *et al.*1994a). Also, it has been shown that the particle size of an excipient will affect the dissolution rate of the drug and as this may be attributed to different mechanisms. These mechanisms include percolation theory, where pores of sufficient size and number are able to form networks which allow the solvent to penetrate and increase the contact area and where increase in excipient particle size produces more pores similar in dimensions or larger than the boundary layer whereby the diffusion layer curves into the pores

effectively increasing surface area. Also, the larger the excipient particle size the less uniform the mix, leaving areas of the disc unexposed to the effect of the excipient (Healy and Corrigan 1996). These phenomena are unlikely to be predictable. Finally, during the pellet-forming process the energy input may affect the morphology of both the drug and excipient. Whilst these properties are clearly of interest, without full characterisation of the processes involved, it would be difficult to attribute any changes in dissolution rate of drug to any specific property of the excipient under investigation.

The second approach can be demonstrated in the method developed by Hendriksen (1990), adapted from other workers, where the weighed samples were rapidly tipped from a glass vial onto the surface of the stirred dissolution medium. Disadvantages of this method include possible variation in addition technique, separation of the drug from the excipient and variable distribution of the material throughout the flask.

Considering the above points, neither of these approaches was deemed adequate. An alternative approach was attempted which used capsules filled with the powder mixes of interest and used the USP paddle apparatus at 50rpm. Unfortunately, dissolution profile variation between capsules was found to large and this approach was abandoned. A novel method based on the USP basket apparatus was developed. This involved sealing the lower part of the baskets, prepared by 'dipping' each basket into molten paraffin wax. Samples of the powder mix could then be located within the basket, and the weight selected to ensure the powder level was below the sealant line. The dissolution-medium pH was selected to simulate the stomach for paracetamol and the small intestine for ibuprofen, the primary dissolution sites for these drugs (ibuprofen being virtually insoluble in a strongly acidic environment). The dissolution volume was selected to ensure dissolution occurred under sink conditions for the drugs at the given pH. The basket rotational speed was then optimised such that minimal dispersal of powder occurred whilst retaining good mixing conditions, *i.e.* 100rpm This method ensured intimate contact between the mixture components and provided a similar surface area of powder exposed to the dissolution fluid throughout the experiment. As noted previously in the work by Dash *et al.* (1988), the USP basket method is not as discriminating as the USP paddle method. However, trials demonstrated the method to have sufficient sensitivity. The

method was thus suitable for evaluating compounds as potential dissolution rate modifiers and also as one tool in the evaluation of the role of antacids in the dissolution of the model drugs.

4.4.2 Drug antacid/interactions

To quantify the effect of the antacids on the dissolution of the model drugs it was decided to utilise dissolution systems based more closely on the *in vivo* environment. USP rotating paddle apparatus was selected with a stirrer speed of 50 rpm. Simulated gastric fluid or simulated intestinal fluid was used to model dissolution in the stomach or small intestine, as appropriate. The quantity of drug *versus* dissolution volume was selected to correspond to *in vivo* conditions as was the quantity of the antacid.

4.4.3 Determination of IDR utilising USP paddle apparatus

As stated previously, for research and preformulation activities it may be desirable to control the surface area of a dissolving drug. If this is controlled and sink conditions prevail the dissolution rate will be constant leading to a linear dissolution profile (% dissolved *vs.* time). Under these conditions it can be shown that

$$IDR = kCs \qquad \text{equation 4.5}$$

where the units of *IDR* are (mg cm^{-2} min^{-1}) and *k* is the IDR constant and *Cs* is the saturated solubility (Aulton 1988).

A commonly used method for the determination of the IDR is known as the rotating disc method. This method involves the fixing of a highly compacted drug disc to the underside of the basket holder using molten hard wax paraffin and also sealing of the edges. The hydrodynamic conditions of this system have been characterised by Levich and summarised by Macheras *et al.* (1995), allowing the determination of the diffusion coefficient (*D*). If a series of experiments are conducted over a range of hydrodynamic conditions, using this methodology, and changes in rotating basket speed *versus* the IDR are plotted against the square root of angular velocity, the diffusion constant (*D*) can be derived from the slope. A linear relationship also indicates that the mechanism of dissolution fits the diffusion layer model. Non-linearity

of this relationship is indicative of a interfacial boundary mechanism (Supabphol and Stewart 1996).

However, there are disadvantages to this system; the method of fixing the pellet to the base of the holder and the sealing of the exposed edges have been found to be difficult, in terms of the dexterity required, and could be liable to inter-operator variation. Also as stated previously, where possible, there is a preference for the USP paddle apparatus to be utilised.

Considering the above points, it was decided to investigate the suitability of a IDR system based on the paddle apparatus. For the system to be considered suitable, the IDR would have to be demonstrated to be linear, for the pure drug, over a working range, demonstrating that the stirring conditions were not producing turbulent flow. Levich plots (IDR *vs.* hydrodynamic conditions) could then be constructed to determine which mechanism suitably described the dissolution process, for the pure drug. This method could then be used to investigate the role of dissolved excipients on modification of the IDR through changes to the drug solubility or diffusion coefficient, through modification of its intrinsic terms, *i.e.* viscosity or radius of the molecule in solution (equation 4.3). Although not utilised in this series of experiments the system could, theoretically, also highlight changes in dissolution mechanism, when pure drug was co-compressed with excipients (Supabphol and Stewart 1996). Pellet holders were required to ensure the pellet surface area remained constant and the position of the pellet was similar to that of a tablet under experimental conditions.

Pellets for IDR methods should be produced to ensure zero porosity, high compaction and be sufficiently strong to withstand handling (Aulton 1988). Trial pellets of pure paracetamol were compressed using a 13mm punch and die set using conditions from Mahmud and Li Wan Po (1991), *i.e.* 10 minutes at 7000kg under vacuum. The pellets were found to fracture easily and therefore conditions were varied from 6000-8000kg and from 5-10 minutes to determine the optimum conditions.

Pellet preparation conditions for paracetamol were standardised at:

7000kg
6 minutes dwell time
300mg ± 3mg
24hr minimum elastic recovery period before use

For ibuprofen strong and hard pellets were obtained easily and it was found that acceptable pellets could be obtained in the range 1-10 minutes at 7000kg. Pellet preparation conditions were standardised for ibuprofen at:

7000kg
3 minutes dwell time
300mg ± 3mg
24hr minimum elastic recovery period before use

The pellets were fixed, using molten paraffin, into pellet holders. Paraffin was also used to seal the edges around the circumference of the pellet. The pellet holders are shown diagrammatically in figure 4.1.

Figure 4.1 Diagram of Poly tetra-fluoroethylene (PTFE) pellet holders

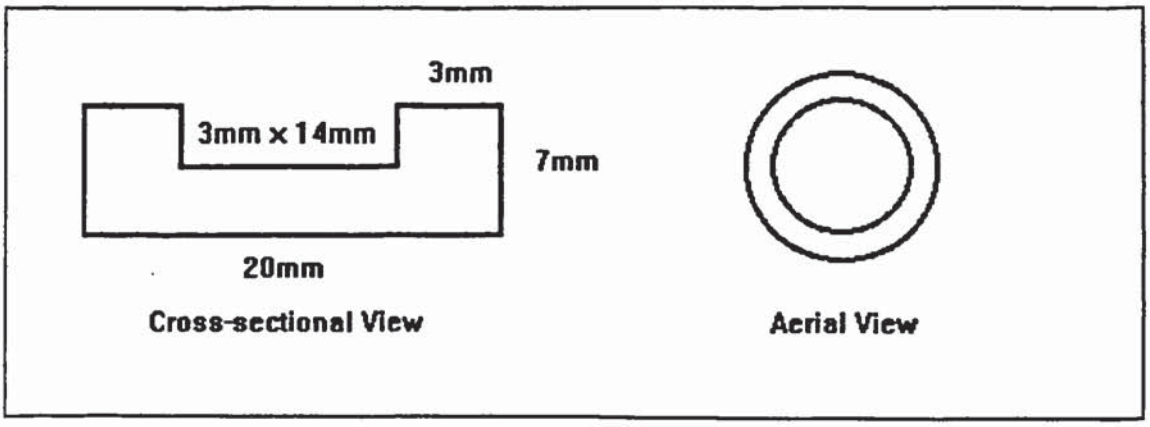

4.4.4 Commercial tablet dissolution method

Of the two model drugs, only a paracetamol formulation containing a specific pH-modifying agent has been commercially developed (Zapp). Therefore at present, it was decided to only investigate the differences in various paracetamol tablet formulations.

For paracetamol, the USP monograph for dissolution requires the use of the USP paddle apparatus with a stirrer speed of 50rpm and medium of USP buffer 5.8. The limits are set at 80% minimum dissolved at a 30 minute timepoint. This method was selected for the analysis of commercial products with one modification, the dissolution medium was changed to simulated stomach medium, *i.e.* 0.05M HCl.

4.5 Method for the calculation of the dissolution of drugs

Dissolution profiles are generally non-linear and this is usually due to a changing surface area or a decrease in C_s-C in non-sink conditions as the dissolution proceeds. Dissolution following such a process is difficult to analyse and various methods of both a physical and mathematical nature are employed to aid analysis.

4.5.1 Physical methods

Dissolution methods such as the standard rotating disc apparatus and the method developed and described in section 4.4.3 are designed to control the surface area of the drug to an effectively constant value. Experiments carried out using this technique generate linear dissolution profiles as long as sink conditions are maintained. Conventional powder dissolution studies are an extreme example of the changes in the surface area throughout the experiment, leading in some case to severe curvature in the dissolution profile. In an attempt to overcome this, the method described in section 4.4.1 was designed to limit the changes in surface area as the powders dissolved.

4.5.2 Mathematical models

Methods for the mathematical calculation of dissolution parameters fall into two categories, model dependent and model-independent approaches.

Model-dependent approaches for the dissolution of drug require a knowledge of several characteristics of the formulation, and may require some assumptions.

Commonly used treatments include:

- the Hixson-Crowell treatment, used for dissolution from hard gelatin capsules and suspensions, which linearises the data, but has been criticised for the assumption that the diffusion layer does not vary with particle size, when in fact it does (Macheras *et al.* 1995).
- the Weibull distribution function, a general function that can be applied to all common types of dissolution curves including those with a substantial lag time, which is capable of determining the curve type (exponential, sigmoidal or with a slope initially steeper than exponential) and can also define the time scale, which can be converted into a more useful dissolution time parameter. It requires minimal assumptions (Macheras *et al.* 1995).
- the statistical moment theory which can be applied to practically any type of dissolution data and makes very little assumptions (Macheras *et al.* 1995).

Two model-independent approaches have recently been introduced by Moore and Flanner (1996) and both have been approved by the FDA as acceptable mathematical tools for comparison of reference and post-change products (FDA(CDER)1997). The difference factor (F_1) calculates the percent difference between the two curves at each time point and is a measurement of the relative difference between the two curves:

$$F_1 = \left\{ \frac{\sum_{t=1}^{n} |R_t - T_t|}{\sum_{t=1}^{n} R_t} \right\} * 100\% \qquad \text{equation 4.6}$$

where R_t is the percentage drug dissolved for the reference product, at time t, T_t is the percentage drug dissolved for the test product, at time t, and n is the number of

where R_t is the percentage drug dissolved for the reference product, at time t, T_t is the percentage drug dissolved for the test product, at time t, and n is the number of timepoints. The similarity factor (F_2) is a logarithmic reciprocal square root transformation of the sum of the squared error and is a measurement of the similarity in the percent dissolution between the two curves:

$$F_2 = 50 * \log\left\{\left[1+(\frac{1}{n})\sum_{t=1}^{n}(R_t - T_t)^2\right]^{-0.5} * 100\right\} \quad \text{equation 4.7}$$

Although the similarity factor (F_2) is more sensitive to minor changes, as the relationship between F_2 *versus* the difference in the test and reference dissolution curves can be described by an exponential curve, the difference factor (F_1) will be used throughout this study, where the dissolution profile has not been linearised by the physical method. It was selected because it allows rapid assessment of differences in dissolution profiles by nature of its linear form and simple application. Also, although other approaches such as the statistical moment model may be more appropriate for IVIVC analysis, the development of correlations throughout this study will utilise the acquired dissolution profiles in their 'native' form, therefore not requiring mathematical transformation. Equation 4.6 measures differences between the two dissolution profiles under test without regard to sign. This is because the equation is utilised to measure any difference between the formulations under test as it was developed as a tool for use in product development/bioequivalence studies. The present study's aims require the measurement of differences in terms of magnitude but also in terms of inhibition or promotion of dissolution. Equation 4.6 was therefore modified as shown in equation 4.8. Thus, the sign of F_1 indicated either dissolution promotion (+) or dissolution inhibition (-), with the magnitude indicating the difference from the reference. This modification was used throughout for dissolution profile comparisons. Unless otherwise stated all points in the dissolution profiles are included in the calculation upto 1 measurement after 85% of both products had dissolved.

$$F_1 = -\left\{\frac{\sum_{t=1}^{n} R_t - T_t}{\sum_{t=1}^{n} R_t}\right\} * 100\% \quad \text{equation 4.8}$$

4.6 Controlled powder dissolution study

4.6.1 Introduction

As discussed in section 1.5.3, a primary project aim was to facilitate development of novel analgesic formulations based on pH-modifying excipients. Reviewing figures 3.1 and 3.2, it can be seen that increases in pH to >9 for paracetamol and >5 for ibuprofen may increase the dissolution rate by modification of the saturated solubility C_s. The three mechanisms of action for this are: (i) buffering or increasing the pH of the bulk solution; (ii) buffering or increasing the pH of the micro-environment and (iii) formation of salts of the drug either in the solid or liquid phase. The first aim was to assess excipients as part of a preformulation screening process. The suitability of the method to control the surface area of the drug sufficiently to produce linearisation of the dissolution profile was also assessed. The study was also designed to investigate the effects of drug/antacid interactions on the dissolution rate of the drug in an environment where interactions relating to the excipients found in the tablet formulations could be excluded from study, *i.e.* powder mixes containing drug and antacid only. Also, as part of the characterisation of sodium bicarbonate the role of changing excipient/drug ratios for sodium bicarbonate was determined. Lastly, a preliminary investigation into the role of any acid/base interaction between the paracetamol and basic excipient was undertaken to assess whether the pro-dissolution effervescence of the HCl/bicarbonate reaction was sustained by interaction of the bicarbonate with the weakly acid drug paracetamol in the absence of acidic medium. This was achieved by conducting the experiment with water as the dissolution medium. This experiment was not required for ibuprofen as the dissolution medium used for this drug was effectively neutral (USP buffer pH6.8).

4.6.2 Selection of excipients

pH-modifying excipients deemed as likely candidates for dissolution modification were selected on the basis of physicochemical properties. A range of supplementary excipients was also chosen from commonly used tabletting excipients. The antacids under investigation were also included and, finally, ground samples of one commercial formulation for each drug model were included as pseudo-controls. The

- changes to the intrinsic rate constant, through modification of solution pH or localised temperature changes
- changes to the saturated solubility, by adjustment of solution pH, or solvent properties
- changes to the apparent surface area through for example, physical shielding by 'caking' of the mixes or 'wetting' through hydration of tablet disintegrants.

The excipients chosen are detailed in table 4.1 and the reasons for their inclusion are also summarised:

Table 4.1

Details of excipient group used for powder dissolution study

Excipient	Reason for Inclusion/ Properties
lactose	Soluble (1 in 4.3) in water. Commonly used pH neutral tablet diluent.
sodium bicarbonate	Soluble (1 in 11) in water. Alkaline (0.1M pH 8.3). Used in effervescent formulations for production of carbon dioxide.
citric acid	Soluble (1 in 3.5) in water. Acidic (5%w/w pH 2.1-2.6). Used in effervescent formulations for production of carbon dioxide
sodium chloride	Soluble (1 in 2.8) in water. Neutral (saturated solution pH 6.7). Used as a diluent.
microcrystalline cellulose	Insoluble. Neutral (saturated solution pH 6.0). Insoluble Used as tablet disintegrant and diluent.
starch	Insoluble. Used as a tablet disintegrant
tartaric acid	Soluble (1 in 0.75) in water. Acidic (1.5%w/v pH2.2). Used as an acidulant.
calcium carbonate	Practically insoluble in water, soluble with effervescence in dilute mineral acids. Alkaline (saturated solution pH 8.9) Material used as diluent.
magnesium hydroxide	Practically insoluble in water, readily soluble in dilute acids. Alkaline (saturated solution pH 9.9). Commonly used as an antacid.
aluminium hydroxide	Practically insoluble in water, readily soluble in dilute acids. Alkaline (pH 7.2). Commonly used as an antacid.
magnesium oxide	Practically insoluble in water, readily soluble in dilute acids. Alkaline (saturated solution pH =10.3). Commonly used as an antacid.
L-arginine	Freely soluble in water. Alkaline (saturated solution pH=10.9). Used to prepare salts of drugs.
glycine	Freely soluble in water. Acidic (saturated solubility pH=6.3). Used to prepare salts of drugs.
L-lysine	Freely soluble in water. Alkaline (saturated solution pH=9.8). Used to prepare salts of drugs.
tri-basic sodium phosphate	Freely soluble in water. Strongly alkaline (pH≈11-12). Used therapeutically as an electrolyte.
sodium carbonate	Dissolves in water with evolution of heat. Alkaline (pH=11.6). Decomposed by acids with effervescence.
Potassium bicarbonate	Soluble (1 in 2.8) in water. Alkaline (0.1M pH=8.2) Decomposed by acids with effervescence.
di-calcium phosphate	Insoluble in water. Used extensively as a diluent.

Data sourced from Handbook of Pharmaceutical Excipients (1994), Martindale (1982) and Merck Index (1996). Saturated solution pHs performed in laboratory.

4.6.3 Experimental

4.6.3.1 Materials

Paracetamol, ibuprofen, starch, lactose (Pharmatose DCL 11), sodium bicarbonate (extra fine grade), microcrystalline cellulose (PH), Hedex® tablets (ibuprofen) B/N 1PH782 and Tylenol® caplets (paracetamol) B/N BBA151 were obtained from SB Pharmaceuticals (Weybridge, UK). Calcium carbonate, citric acid, sodium chloride, magnesium hydroxide, calcium hydrogen phosphate, hydrochloric acid, potassium chloride, methanol, acetic acid, L-arginine, glycine, L-lysine, tri-basic sodium phosphate, magnesium hydroxide, sodium carbonate, potassium bicarbonate, aluminium hydroxide, sodium hydroxide, mono-basic potassium phosphate and paraffin wax were purchased from Aldrich (Poole, UK). All materials were of pharmaceutical, analytical grade, AVS or HPLC grade as appropriate. Double-distilled water was generated in-house using a Fison's Fi-Streem still.

4.6.3.2 Equipment

The dissolution system consisted of a Caleva Model 7ST dissolution bath, equipped with 1 litre round-bottomed flasks and equipped with baskets conforming to Apparatus I-USP regulations (USP). Sampling was performed on a continuous loop basis, using a Watson-Marlow 5025 peristaltic pump set with a flow rate of 5ml min^{-1}. Analysis was performed automatically at desired time intervals using a LKB Biochrom Ultrospec II multi-cell UV/VIS spectrometer Quartz cells with 10mm pathlength. Data was collected by a computer using Tablet Dissolution Software V1.12 supplied by LKB Biochrom. Data printouts (absorbances) were collected.

4.6.3.3 Method

Initially, standard baskets as described in the USP were dipped in molten paraffin wax sealing the base and extending 10mm up the sides of the basket. These adapted baskets were used throughout the experimental series. Pure paracetamol, ibuprofen, the physical mixtures (50:50) and prepared by stirring with a spatula, or the ground tablets (prepared using a pestle and mortar with removal of the coating where possible), were weighed into the basket. The weights added were appropriate to give 300mg±3mg of paracetamol or ibuprofen. The baskets were gently tapped until the

powder was below the upper limit of the paraffin wax coated mesh. Dissolution medium (900ml *per* flask), 0.05M HCl for paracetamol and USP buffer pH6.8 for ibuprofen experiments, was prepared and thoroughly degassed. Dissolution fluid temperature was controlled at 37±0.5°C. After equilibration of dissolution medium, temperature and sampling flow-through system, each sampling station was background zeroed. The baskets were lowered slowly into the dissolution bath, and after a brief holding period (seconds), to allow entrapped air to exit from the powder, the rotational speed of the baskets was set to 100rpm. The data collection system was initiated, collecting absorbances at the appropriate wavelength, *i.e.* 237nm for ibuprofen and 295nm for paracetamol. For paracetamol, the experiment was conducted over 90 minutes, sampling at least every six minutes. F_1 values were calculated using data obtained at the 12 minute intervals from 6-84 minutes or until 1 interval after a minimum of 85% of the test mix had dissolved and 5 data pairs had been collected. For ibuprofen the experiment was conducted over 240 minutes, sampling at least every 12 minutes, F_1 values were calculated using data at the 12 minute intervals from 12-240 minutes or until 1 interval after a minimum of 85% of the test mix had dissolved and 5 data pairs had been collected.

4.6.4 Results and discussion

When comparing F_1 factors, a difference of >15 from the reference is usually considered to show non-equivalence (FDA (CDRA) 1997). This rule and visual analysis of diffusion profiles, including error bars ±SD, was utilised to judge whether the differences were significant. All F_1 values were calculated using the pure drug samples as the reference and averaging the data from all the replicates. Firstly, considering the results for paracetamol, the F_1 values obtained show a large spectrum of effects across the excipient set as detailed in table 4.2 and illustrated in figure 4.2

Table 4.2
F_1 Fit factors for paracetamol:excipient mixtures compared to pure paracetamol as reference. Sign indicates dissolution promoter (+) or inhibitor (-).

Reference number	Excipient	F_1 Factor
1	microcrystalline cellulose	-72.9
2	calcium carbonate	-62.7
3	starch	-52.1
4	magnesium hydroxide	-47.8
5	sodium carbonate	-40.7
6	magnesium oxide	-39.2
7	aluminium hydroxide	-37.0
8	di-calcium phosphate	-36.2
9	sodium chloride	-20.0
10	Tylenol®	-12.7
11	tartaric acid	-8.7
12	lactose	-6.8
13	citric acid	-4.1
14	pure paracetamol	0.0
15	glycine	16.7
16	sodium bicarbonate (water)	22.5
17	L-lysine	26.8
18	L-arginine	28.1
19	tri-basic sodium phosphate	39.5
20	sodium bicarbonate (66%)	172.6
21	sodium bicarbonate (33%)	186.9
22	potassium bicarbonate (water)	201.4
23	sodium bicarbonate pH 1.2	210.2
24	potassium bicarbonate pH 1.2	210.7
25	Zapp (100%)	215.3

The results indicate that the excipients fall into three broad categories as detailed in table 4.3.

Table 4.3

Categorisation of excipient with respect to its effect on the dissolution rate of paracetamol.

Significant inhibitory effect on dissolution rate	**Marginal effect on dissolution rate**	**Significant positive effect on dissolution rate**
microcrystalline cellulose	sodium chloride	sodium bicarbonate (all experiments)
calcium carbonate	tartaric acid	potassium bicarbonate (all experiments)
starch	lactose	L-lysine
magnesium hydroxide	Tylenol® tablets	L-arginine
sodium carbonate	citric acid	tri-basic sodium phosphate
aluminium hydroxide	glycine	Zapp prototype (100%)
magnesium hydroxide	-	-
di-calcium phosphate	-	-

Firstly, as the result for the Tylenol® tablets (10) is very similar to the pure paracetamol reference (14), the effect of each excipient *versus* the pure paracetamol indicates closely the likely performance against a standard formulated product. For compounds showing significant negative effects on the dissolution rate, including four of the antacids under study (2,4,6,7), it is proposed that this is likely to be related to the fact that these compounds are generally insoluble, *e.g.*, starch and microcrystalline cellulose (3 and 1), or soluble but with a slow dissolution rate, *e.g.*, magnesium oxide and hydroxide, aluminium hydroxide and calcium carbonate, which are all completely soluble under these conditions (see section 3.3), but where residue was observed in each basket on completion of the experiment. In fact, the calcium carbonate mix appeared completely impervious to water penetration, a surprising observation in view of the fact that calcium carbonate has a solubility of 264±10mg/200ml 0.05M HCl (see Section 3.3); all the other mixes in this group were observed to have become at least partially 'wetted-out'. The insolubility/slow dissolution rate and variable 'wetting' characteristics may contribute to an effect of

shielding the drug from the dissolution medium and thus reducing the effective surface area.

The experimental design meant that starch and microcrystalline cellulose did not act as disintegrants. However, the degree of inhibition was surprising as the both these materials have positive hydration as well as swelling capacity characteristics (Aulton, 1988). An unexpected member of this group was sodium carbonate (5), being soluble with effervescence in dilute acids and producing a solution with a pH significantly higher than the pK_a of paracetamol (pH=11.6, pK_a =9.5), it is generally considered as having potential as a dissolution promoter. The apparent inhibition by sodium carbonate cannot be readily explained but it is noted that it has a common anion with calcium carbonate, which also inhibited dissolution to an unexpected extent.

For compounds having a marginal effect on dissolution, it is noted that all are water-soluble, neutral or acidic. The closeness of the data does not allow for assessment of the role of excipient solubility but it is noted that all of these excipients are inhibitory, the likely mechanism being a reduction of the surface area of the drug in contact with the dissolution medium, due to the diluting effect of the excipient.

For the excipients having a positive effect on the dissolution of paracetamol, there are two sub-groups as illustrated in figure 4.2. The first sub-group consists mainly of non-effervescing, alkalising soluble excipients. An apparent trend between the alkalinity of an excipient and the dissolution rate is observed. This is in line with expectations as the drug solubility in the diffusion layer increases with increasing pH. Notably, both glycine and sodium bicarbonate (dissolution fluid water) exert a positive effect although they are not sufficiently alkaline to modify the solubility of paracetamol. These data are summarised in table 4.4.

Table 4.4
Illustrating the effect of alkalising soluble excipients on the dissolution of paracetamol from powder mixes

Excipient	pH (see table 4.1)	Difference factor F_1
glycine	5.9	16.7
sodium bicarbonate (water)	8.2	22.5
L-lysine	9.8	26.8
L-arginine	10.9	28.1
tri-sodium phosphate	11.5	39.5

The second sub-group consists of alkalising soluble excipients that effervesce in the dissolution medium used, namely sodium *bicarbonate and potassium bicarbonate in* 0.05M HCl. In acidic media, sodium bicarbonate and potassium bicarbonate react to form water and carbon dioxide. This gas generation is the basis of many effervescent formulations (Ansel *et al.* 1995). This has the effect of causing large changes in agitational force and increasing the surface area of the drug. They are likely to be the causes of the very significant differences in dissolution profile, *i.e.* difference factors F_1>200%, for both excipients. The design of the powder dissolution experiments meant that the gas generated was quickly released from the formulation. Visual inspection throughout the controlled basket dissolution indicated that undissolved powder was not removed from the bulk, therefore minimising the contribution of dispersal away from the baskets as the promoting factor. The Zapp prototype was found to be the fastest dissolving of all mixes tested with difference factor F_1=215.3, although not significantly different from the two bicarbonate 50:50 mixes.

The excipients found to have significant dissolution enhancing properties will be considered for inclusion in planned product formulation development work.

Figure 4.2
Illustrating the effects of excipients/antacids on the dissolution rate of powder mixtures *versus* pure paracetamol, by comparison of F_1 difference factors calculated using equation 4.8 from the mean dissolution profiles of at least five replicates.

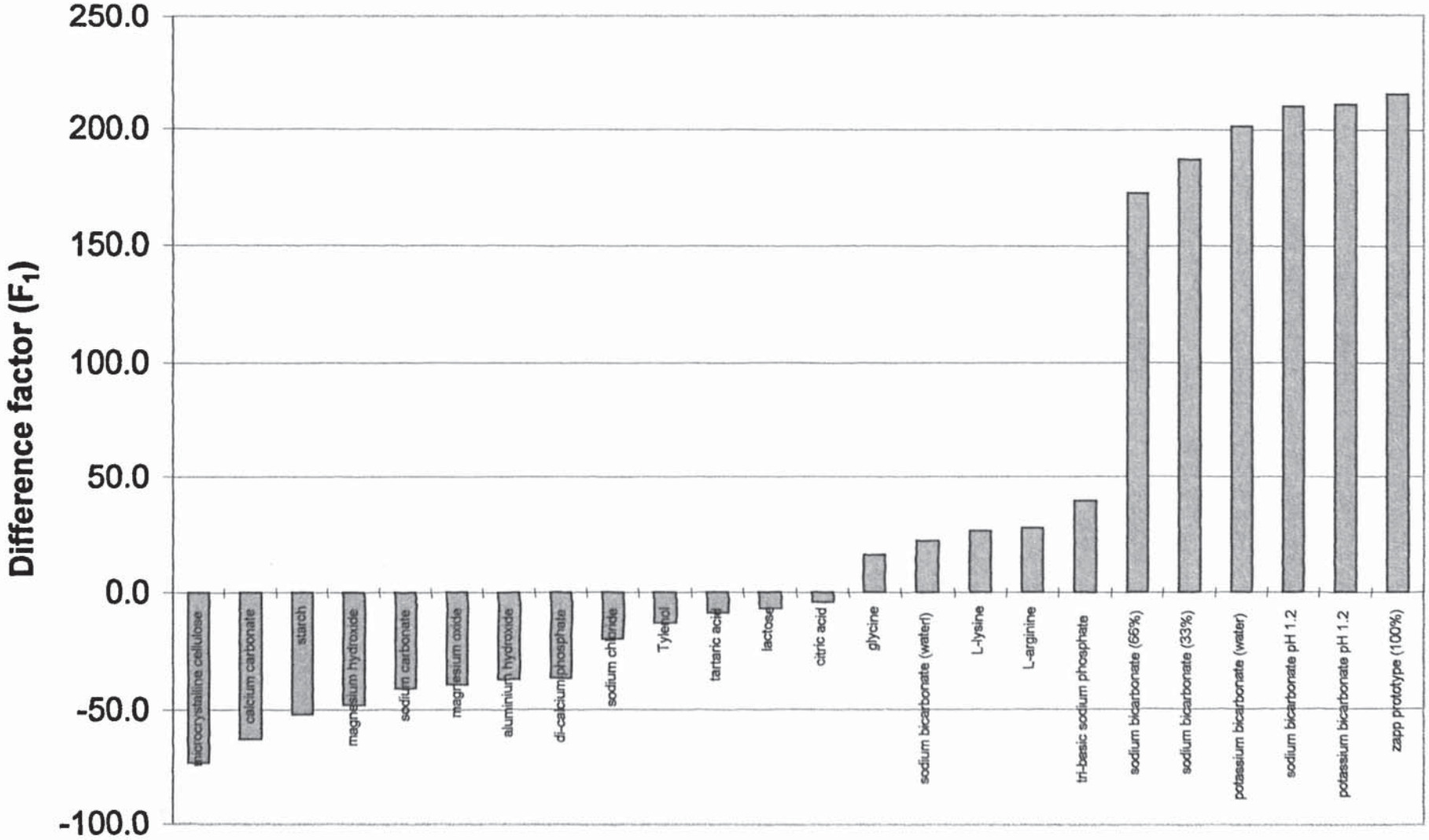

Interestingly, the paracetamol/potassium bicarbonate mix experiment conducted in water also demonstrated a difference factor of F_1>200. Visually, significantly more dispersal (loss of undissolved material from the baskets) was observed in this experiment, partly invalidating the results. However, it is possible that potassium bicarbonate, being a stronger base than sodium bicarbonate, due to the increasing ease of ionisation of the outer electron down group I of the periodic table (Wood and Holiday 1967), may to some extent undergo an acid/base reaction with paracetamol causing the generation of carbon dioxide. If this is the case, the suitability of potassium bicarbonate as an excipient for use with paracetamol would have to be assessed with regard to formulation stability.

The initial study into the role of excipient:drug ratio variation suggests the method can discriminate in this respect and also that it is a significant factor in the dissolution rate of paracetamol:sodium bicarbonate mixes thus:

- 66% sodium bicarbonate mix - F_1=172.6
- 33% sodium bicarbonate mix - F_1=186.9
- 50% sodium bicarbonate mix - F_1=210.2

Figures 4.3-4.26 illustrate the controlled powder mixes dissolution profiles compared to the pure paracetamol sample. Data points are the mean of at least five replicates with SD as appropriate for clarity.

Figure 4.3
Illustrating Zapp (100%) dissolution profile compared to pure paracetamol

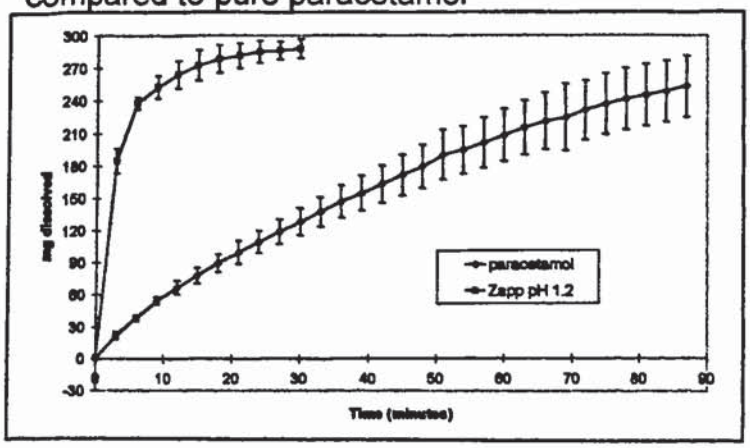

Figure 4.4
Illustrating sodium bicarbonate mix dissolution profile compared to pure paracetamol

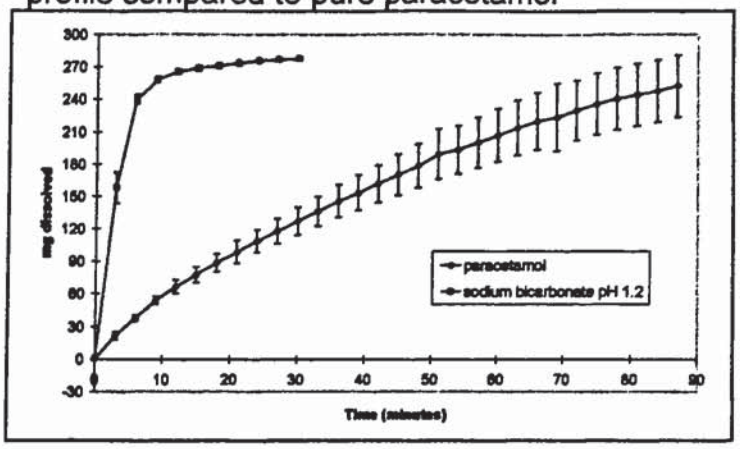

Figure 4.5
Illustrating sodium bicarbonate 33% mix dissolution profile compared to pure paracetamol

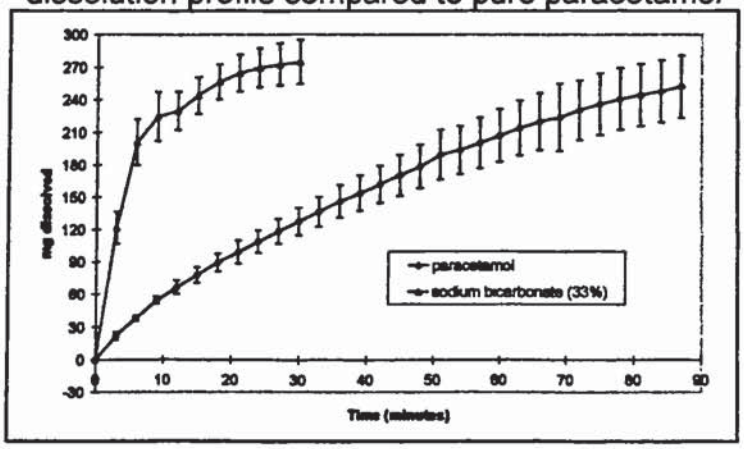

Figure 4.6
Illustrating sodium bicarbonate 66% mix dissolution profile compared to pure paracetamol

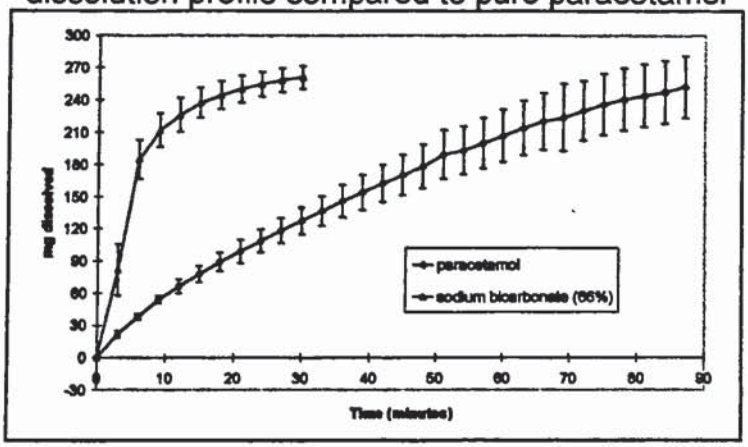

Figure 4.7
Illustrating sodium bicarbonate (water) mix dissolution profile compared to pure paracetamol

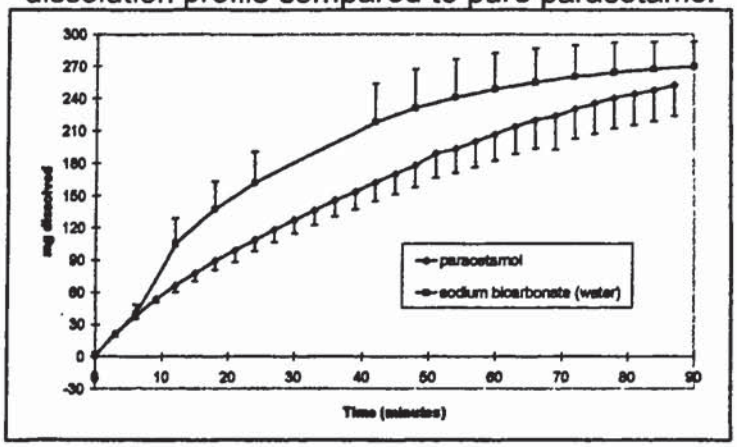

Figure 4.8
Illustrating citric acid mix dissolution profile compared to pure paracetamol

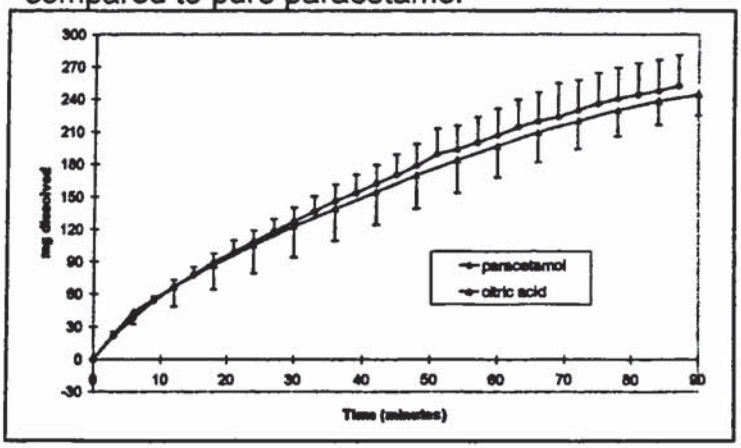

Figure 4.9
Illustrating lactose mix dissolution profile compared to pure paracetamol

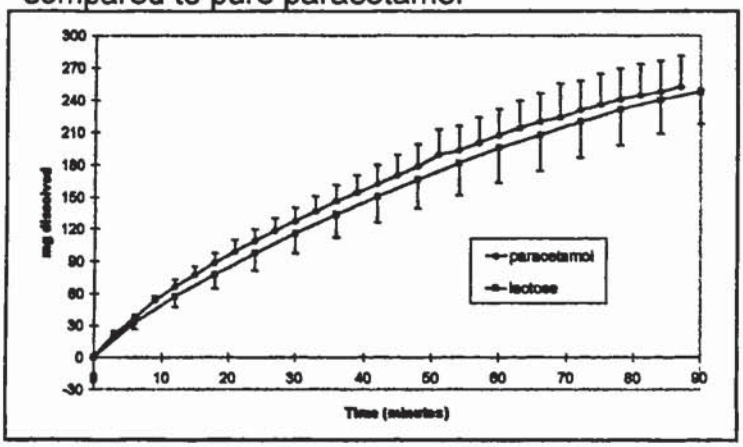

Figure 4.10
Illustrating tartaric acid mix dissolution profile compared to pure paracetamol

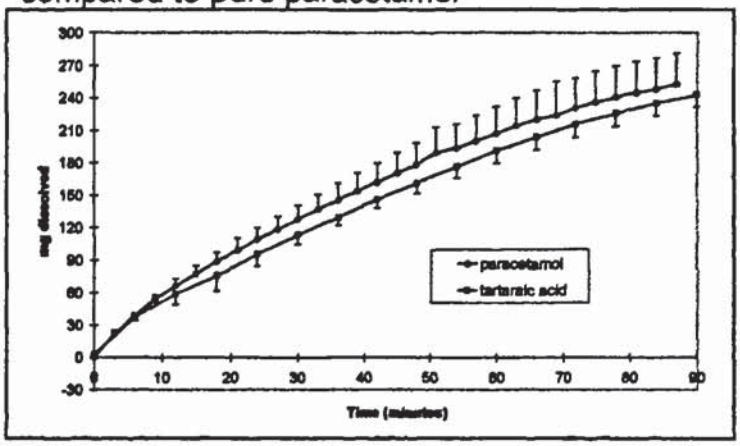

Figure 4.11
Illustrating sodium chloride mix dissolution profile compared to pure paracetamol

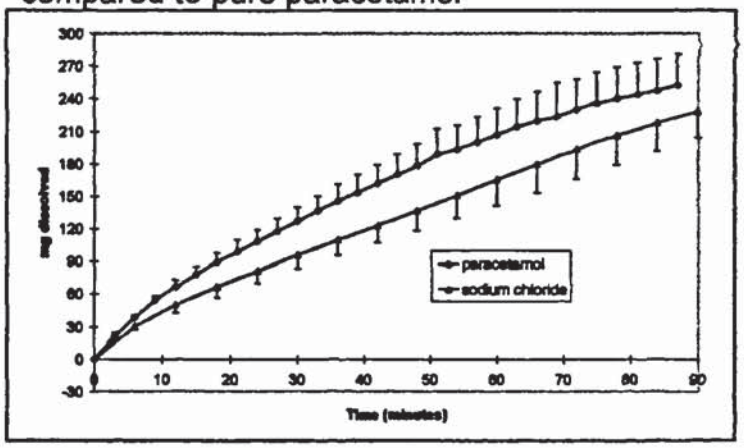

Figure 4.12
Illustrating di-calcium phosphate mix dissolution profile compared to pure paracetamol

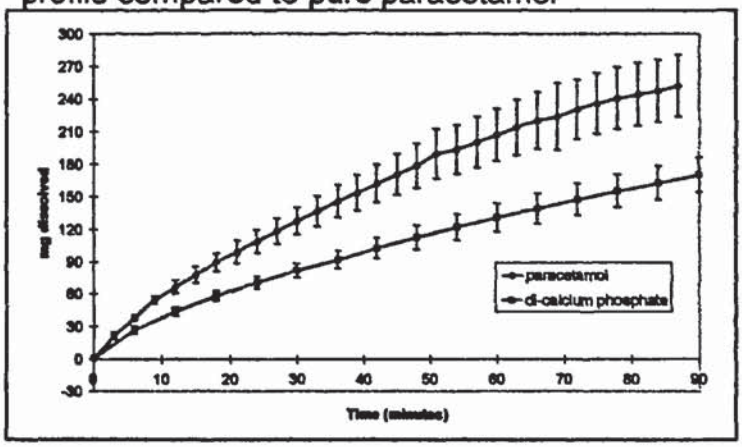

Figure 4.13
Illustrating magnesium hydroxide mix dissolution profile compared to pure paracetamol

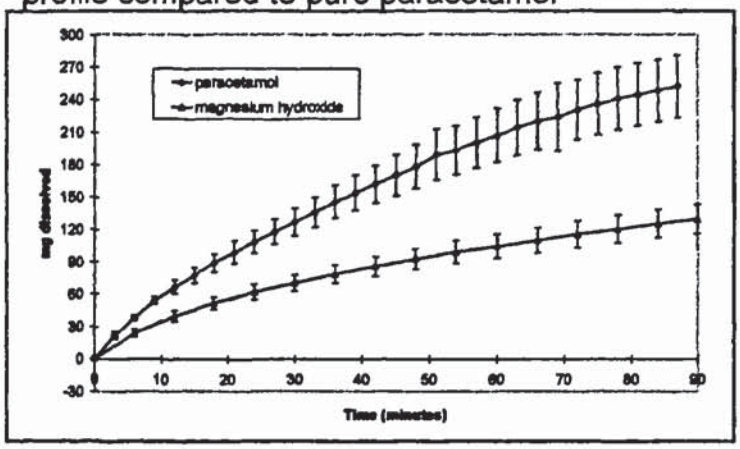

Figure 4.14
Illustrating starch mix dissolution profile compared to pure paracetamol

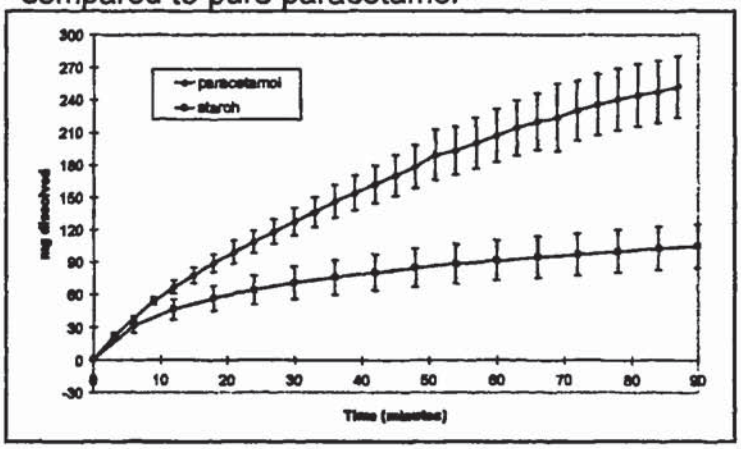

Figure 4.15
Illustrating microcrystalline cellulose mix dissolution profile compared to pure paracetamol

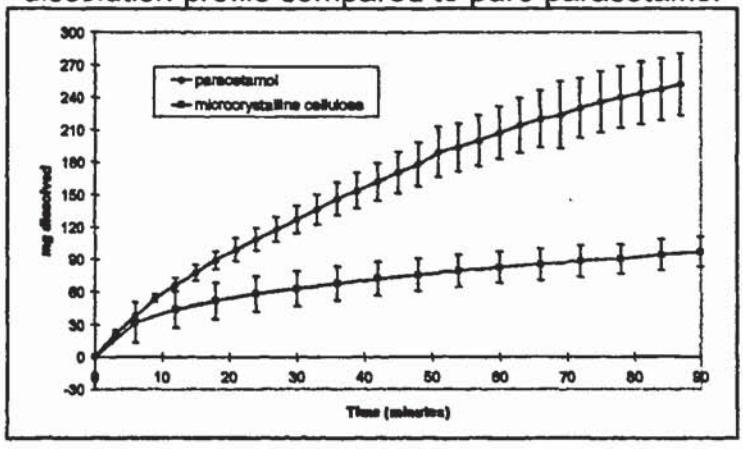

Figure 4.16
Illustrating calcium carbonate mix dissolution profile compared to pure paracetamol

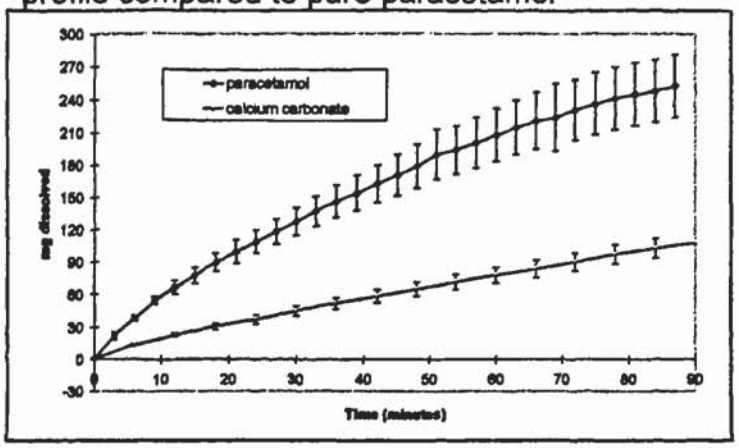

Figure 4.17
Illustrating aluminium hydroxide mix dissolution profile compared to pure paracetamol

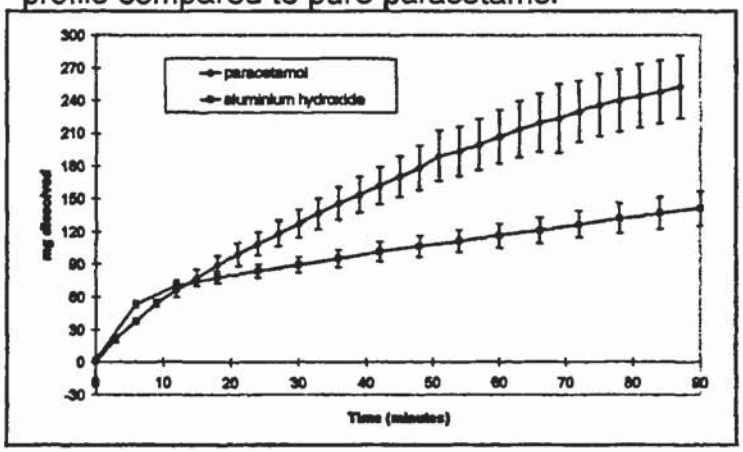

Figure 4.18
Illustrating magnesium oxide mix dissolution profile compared to pure paracetamol

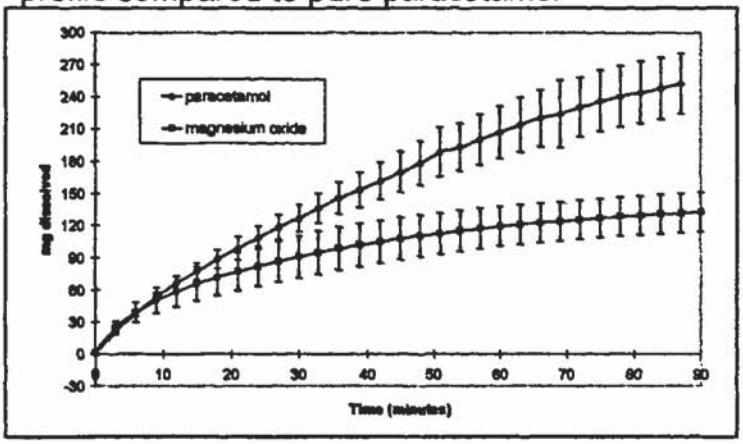

Figure 4.19
Illustrating L-arginine mix dissolution profile compared to pure paracetamol

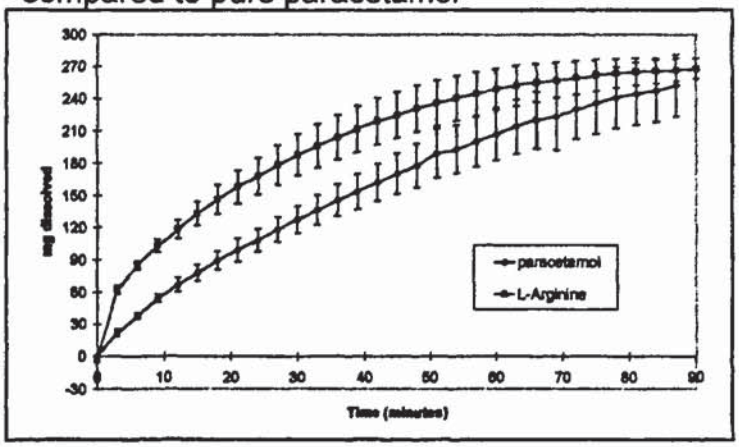

Figure 4.20
Illustrating glycine dissolution mix profile compared to pure paracetamol

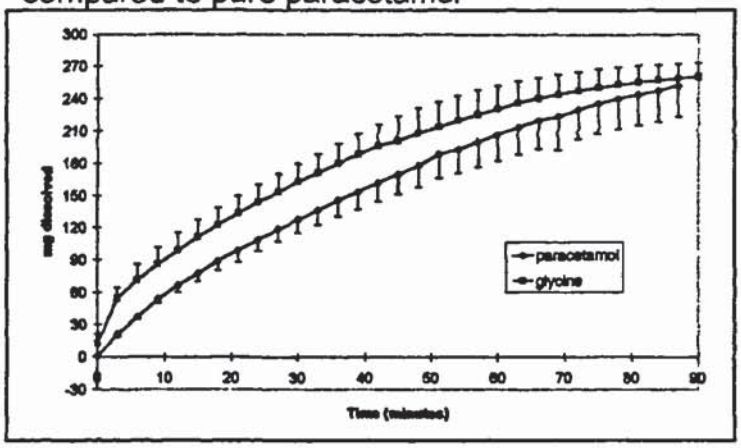

Figure 4.21
Illustrating L-lysine dissolution mix profile compared to pure paracetamol

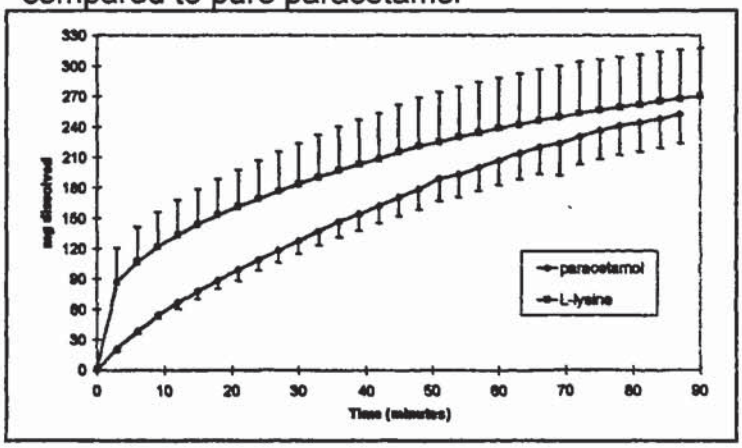

Figure 4.22
Illustrating tri-sodium phosphate mix dissolution profile compared to pure paracetamol

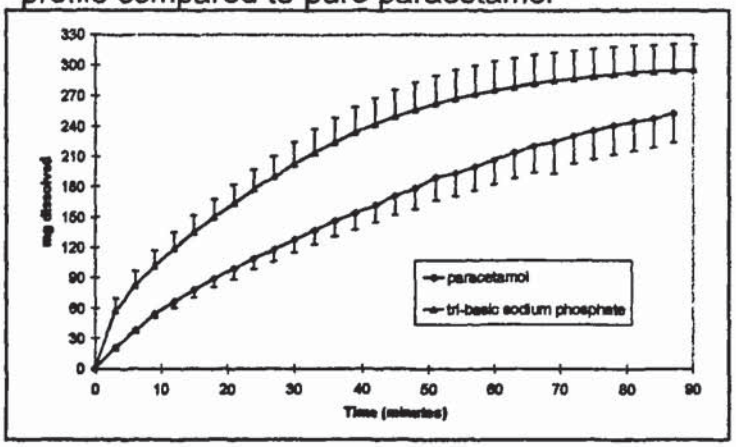

Figure 4.23
Illustrating sodium carbonate mix dissolution profile compared to pure paracetamol

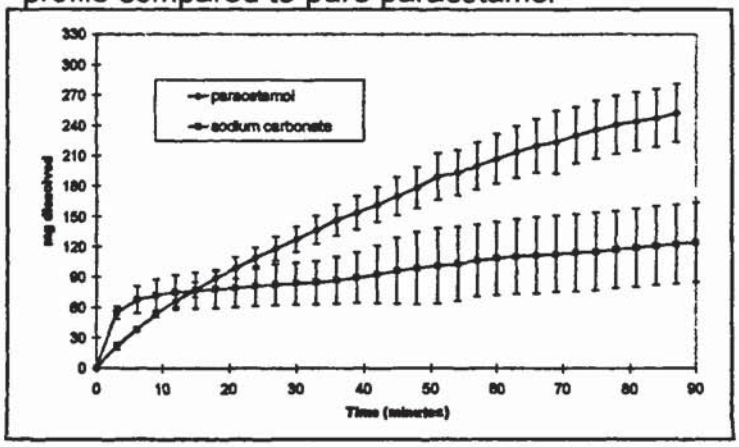

Figure 4.24
Illustrating potassium bicarbonate mix dissolution profile compared to pure paracetamol

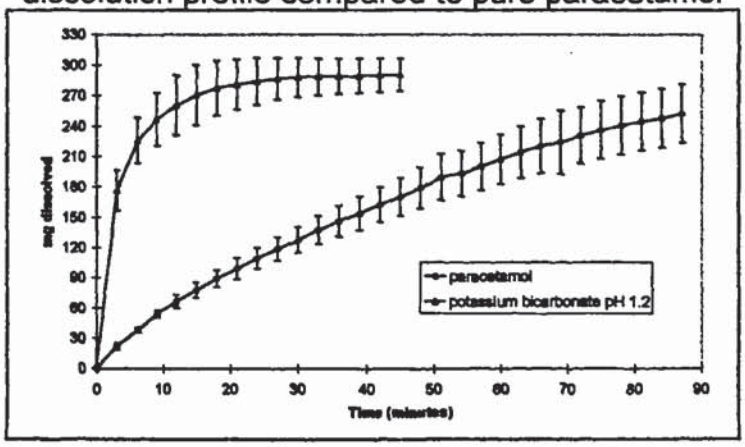

Figure 4.25
Illustrating ground Tylenol® dissolution profile compared to pure paracetamol

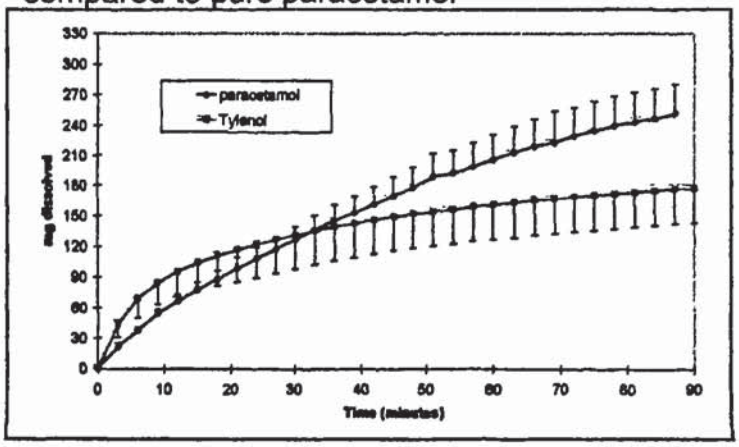

Figure 4.26
Illustrating potassium bicarbonate (water) mix dissolution profile compared to pure paracetamol

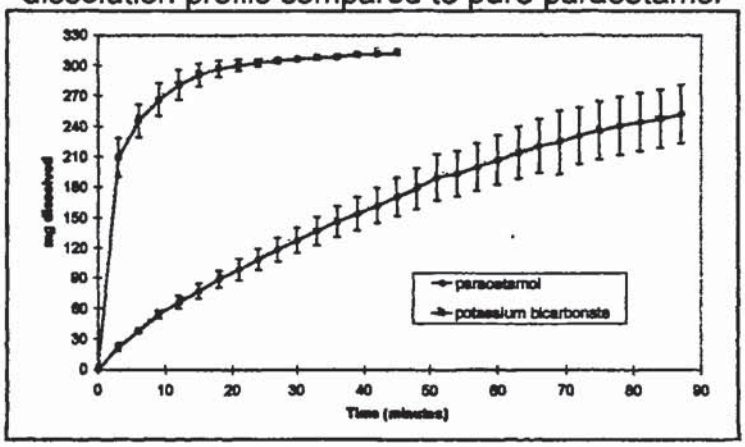

Generally, for the dissolution profiles generated by this method, three distinct phases are observed from the charts. The first phase corresponds to a 'dispersal' phase where some of the powdered material is lost from the basket during the initiation of the experiment, through for example the release of entrapped air bubbles. This leads to an increase in the initial rate. The second, most important phase, is the 'linear' phase which corresponds to a steady dissolution from the controlled surface of the powder mix. The third phase is apparent for the experiments where the dissolution rate is high and is due to a decreasing quantity of drug available to dissolve. This results in a decrease in the dissolution rate gradient. The F_1 fit-factor compared the complete profiles of powder mix *versus* the pure paracetamol sample. Further analysis of the dissolution profiles was conducted using the linear region of each graph. Firstly, visual analysis was performed to select the appropriate area, followed

by least-squares linear regression analysis of the selected region. Correlation coefficients (R^2) and dissolution-rate values were calculated for each profile. The calculated values are tabulated in table 4.5 and selected examples graphically illustrated in figures 4.27-4.29. It can be noted from the tabulated data that, in all cases where there are sufficient datapoints, R^2 >0.98 which demonstrates a very high level of linearity, as also shown in the graphical examples. The rank order of the dissolution rates generally corresponds to that found by the difference factor method, with the insoluble/slowly soluble compounds demonstrating the slowest rates followed by the neutral soluble compounds, then the alkalising soluble agents and finally the two bicarbonates. The Spearman rank correlation method (Miller and Miller 1993) was applied to the data and a correlation between the mathematical methods was found using a significance level of P=0.05 (ρ=0.930). This similarity indicates the usefulness of the dissolution method as both a qualitative and quantitative tool for the assessment of excipients for paracetamol formulations.

Table 4.5
Dissolution rate and correlation coefficient R^2 of paracetamol powder mixes, calculated from the linear section of the dissolution profile, generated using the controlled powder dissolution method. For comparison the fit-factors (F_1) are included

Excipient	Dissolution rate (mg min^{-1})	Fit-factor (F_1)	Correlation coefficient R^2
microcrystalline cellulose	0.439	-72.9	0.9899
starch	0.577	-52.1	0.9840
sodium carbonate	0.694	-40.7	0.9894
magnesium oxide	0.709	-39.2	0.9655
aluminium hydroxide	0.901	-37.0	0.9976
magnesium hydroxide	0.962	-47.8	0.9945
calcium carbonate	1.12	-62.7	0.9975
di-calcium phosphate	1.69	-36.2	0.9891
sodium chloride	2.37	-20.0	0.9983
L-lysine	2.39	26.8	0.9917
lactose	2.47	-6.8	0.9933
paracetamol	2.55	0	0.9923
citric acid	2.73	-4.1	0.9925
tartaric acid	2.76	-8.7	0.9964
glycine	3.04	16.7	0.9903
L-arginine	3.32	28.1	0.9864
tri-sodium phosphate	4.67	39.5	0.9914
potassium bicarbonate	37.5	210.7	0.9050*
sodium bicarbonate	40.1	210.2	0.9682*

*Due to high dissolution rate only 3 data-points were within the linear section.

Figure 4.27
Illustrating the linear section of the aluminium hydroxide mix dissolution profile. Results are mean of 5 replicates ±SD. R^2=0.9976

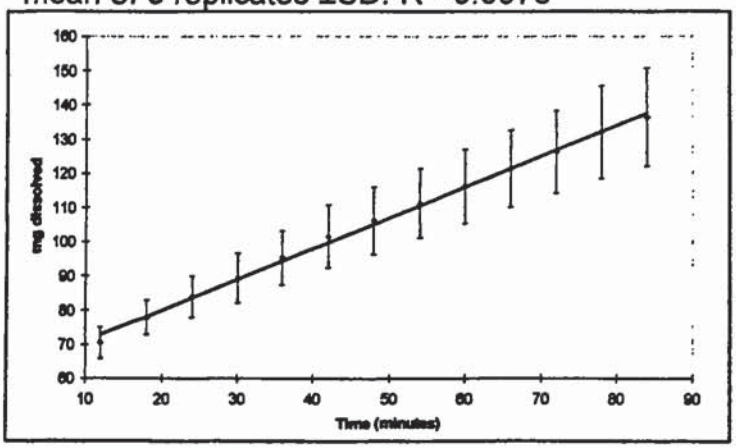

Figure 4.28
Illustrating the linear section of pure paracetamol dissolution profile. Results are mean of 5 replicates ±SD. R^2=0.9923

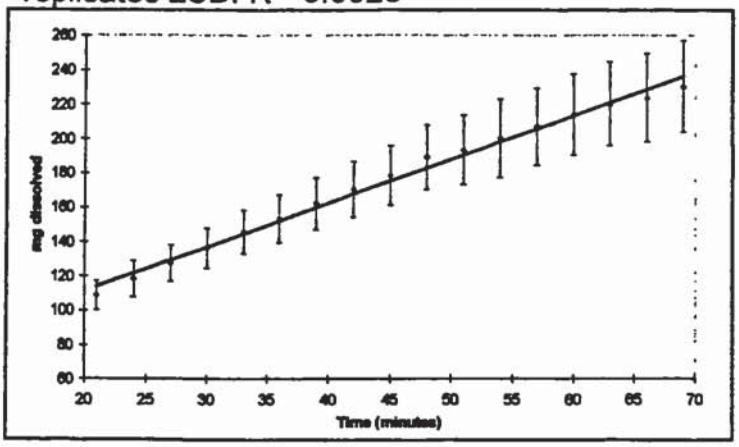

Figure 4.29
Illustrating the linear section of tri-sodium phosphate mix dissolution profile. Results are mean of 5 replicates ±SD. R^2=0.9914

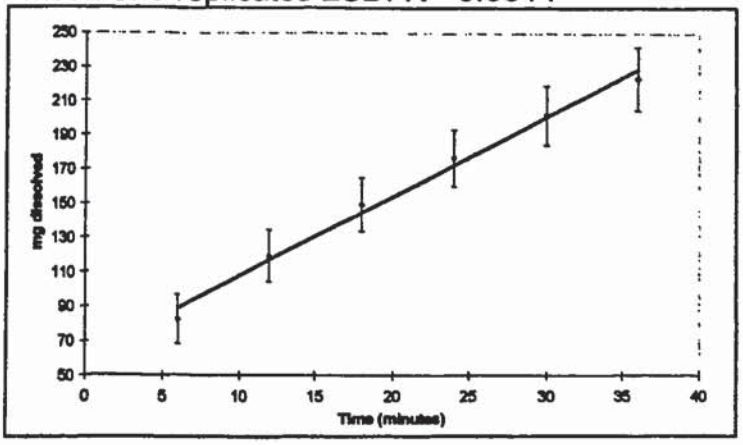

For ibuprofen, the calculated F_1 values obtained show a large spectrum of effects across the excipient set as detailed in table 4.6 and illustrated in figure 4.30.

Table 4.6
F_1 Fit factors for excipient powder mixtures compared to pure ibuprofen as reference

Reference number	Excipient	F_1 Factor
1	aluminium hydroxide	-91.0
2	tartaric acid	-70.7
3	citric acid	-61.8
4	calcium carbonate	-54.1
5	starch	-48.2
6	di-calcium phosphate	-47.2
7	magnesium hydroxide	-39.8
8	magnesium oxide	-23.8
9	pure ibuprofen	0.0
10	sodium chloride	19.0
11	microcrystalline cellulose	25.7
12	glycine	61.9
13	lactose	72.3
14	Hedex®	82.0
15	tri-basic sodium phosphate	328.5
16	sodium bicarbonate (33%)	331.6
17	potassium bicarbonate	347.4
18	L-arginine	350.2
19	sodium carbonate	373.9
20	sodium bicarbonate	389.2
21	sodium bicarbonate (66%)	398.7
22	L-lysine	401.2

The results indicate that the excipients fall into three broad categories as detailed in table 4.7.

Table 4.7
Categorisation of excipient with respect to its effect on the dissolution of ibuprofen.

Significant inhibitory effect on dissolution rate	**Positive effect on dissolution rate**	**Major positive effect on dissolution rate**
aluminium hydroxide	sodium chloride	tri-basic sodium phosphate
tartaric acid	microcrystalline cellulose	sodium bicarbonate (all experiments)
citric acid	glycine	potassium bicarbonate
calcium carbonate	lactose	L-arginine
starch	Hedex® tablets	sodium carbonate
di-calcium phosphate	-	L-lysine
magnesium hydroxide	-	-
magnesium oxide	-	-

Firstly, the formulated product, Hedex® tablets (14), showed superior dissolution characteristics to the unformulated pure powder ibuprofen (9). Its rank within the excipient group will therefore be used as an indicator as to whether each excipient may be suitable for further investigation as a dissolution promoter for formulated products. As for paracetamol, the group of antacids/excipients found to significantly inhibit dissolution included four of the antacids under study (1,4,7 and 8) and di-calcium phosphate (6). Of particular note was the presence of 'solid cakes' in the baskets on completion of the experiment for the magnesium oxide and hydroxide:ibuprofen mixes, the calcium carbonate:ibuprofen mix and particularly the aluminium hydroxide:ibuprofen mix, which was the found to be the most inhibitory of the compounds under test, and which was also observed to be completely dry and impervious to water on completion.

Their mode of action is likely to be as for paracetamol, *i.e.* reduction of apparent surface area by physical shielding and restriction of 'wetting' of drug. This group also contained both citric and tartaric acid. It is postulated that these may retard the dissolution of ibuprofen by limiting the buffering capacity of the dissolution medium,

i.e. act by maintaining the acidification of the boundary layer around each particle, in conjunction with the dissolving ibuprofen, hence reducing the concentration gradient C_s-C.

The remaining excipients/antacids were all found to be dissolution promoters when compared to the pure ibuprofen. The first sub-group (10-14), having a positive effect, were fairly diverse in nature, one common property being their neutrality. Secondly, of this group the formulated product (ground Hedex® tablets (14)) had the highest F_1 value, highlighting the limitations of all of the compounds in this group as potential dissolution promoters.

The second sub-group(15-22) were found to have a major promotive effect on the dissolution of ibuprofen. This group consists of the alkalising soluble compounds and also the two bicarbonates whose mode of action is likely to include modification of the dissolution hydrodynamics through effervescence (possibly reacting with the weakly acidic drug). Clearly, all of these compounds are likely to act by substantially increasing the solubility of ibuprofen by modification of the pH in both the bulk and diffusion layers as illustrated by the solubility/pH profile of ibuprofen in figure 3.2. The very rapid dissolution of all of the powder mixes within this group makes it impossible to verify the trends relating to pH. However, it is postulated that as ibuprofen is quite acidic and will be dissolution self-retarding (Macheras *et al.* 1995), the ability of each excipient to modify not only the bulk solution and therefore determine the overall solubility (which would be of critical importance in the *in vivo* stomach environment) but to buffer the diffusion layer to a high pH would contribute to the overall diffusion-enhancing ability of the excipient. This hypothesis is explored further in section 4.84. All of the excipients in the second sub-group are good candidates for use as dissolution promoters and will be considered for inclusion in the planned product formulation development work.

Figure 4.30
Illustrating the effects of excipients/antacids on the dissolution rate of powder mixtures *versus* pure ibuprofen, by comparison of F_1 difference factors calculated using equation 4.8 from the mean dissolution profiles of at least five replicates.

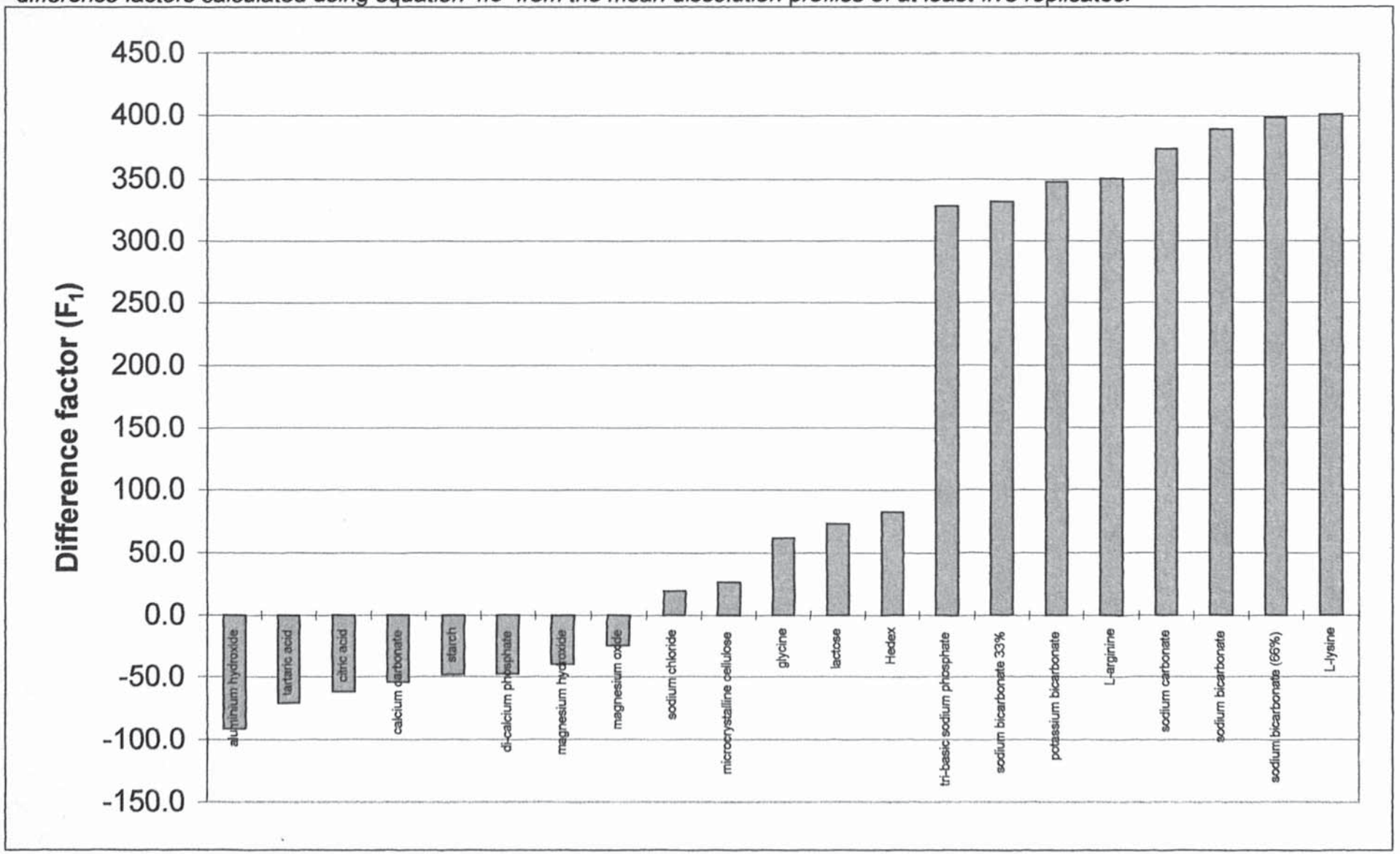

The initial study into the role of excipient:drug ratio variation suggests the method can discriminate in this respect and also that it is a significant factor in the dissolution rate of ibuprofen:sodium bicarbonate mixes thus:

- 33% sodium bicarbonate mix - F_1=331.6
- 66% sodium bicarbonate mix - F_1=398.7
- 50% sodium bicarbonate mix - F_1=389.2

As this method can discriminate between dissolution performance for both ibuprofen and paracetamol, with regard to drug:excipient ratio it may be suitable as a method for use during product formulation development studies.

Figures 4.31-4.51 illustrate the controlled powder mixes dissolution profiles compared to the pure ibuprofen. Data points are the mean of at least five replicates with SD as appropriate for clarity.

Figure 4.31
Illustrating aluminium hydroxide mix dissolution profile compared to pure ibuprofen

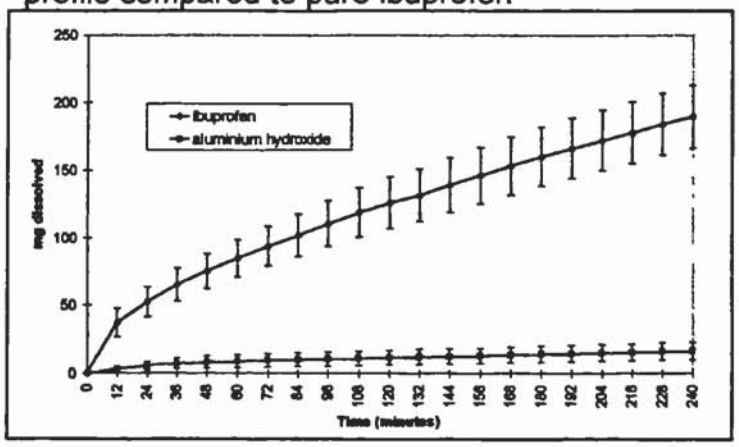

Figure 4.32
Illustrating sodium bicarbonate mix dissolution profile compared to pure ibuprofen

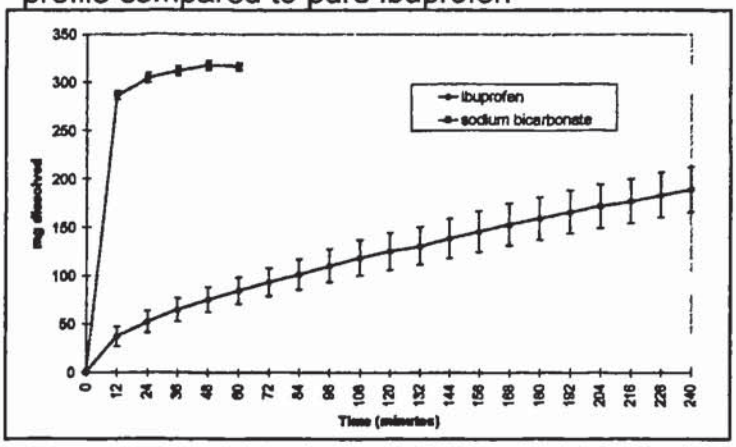

Figure 4.33
Illustrating sodium chloride mix dissolution profile compared to pure ibuprofen

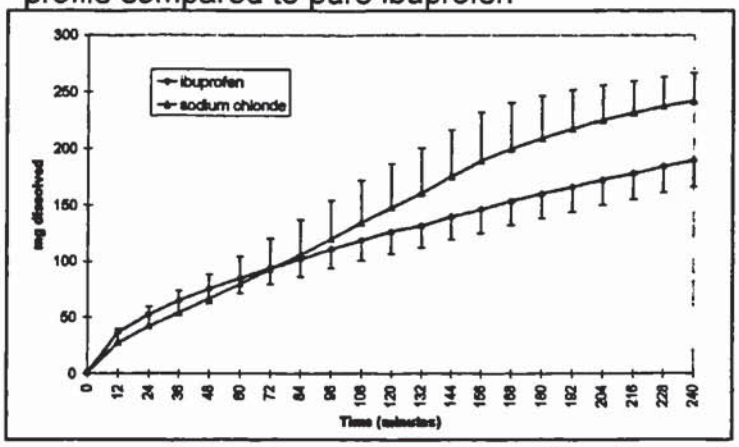

Figure 4.34
Illustrating magnesium hydroxide mix dissolution profile compared to pure ibuprofen

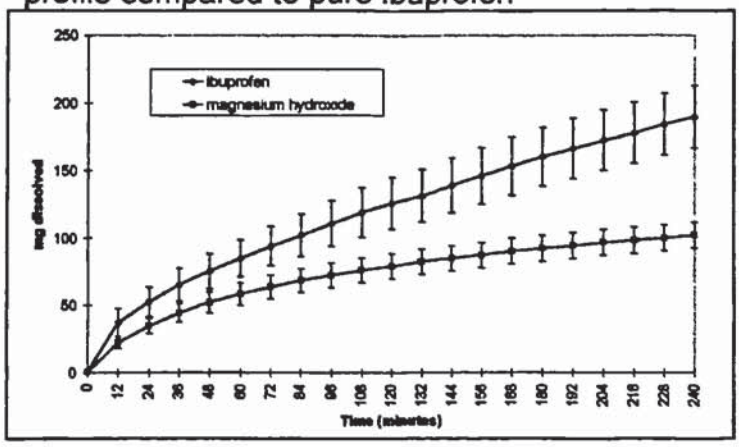

Figure 4.35
Illustrating calcium carbonate mix dissolution profile compared to pure ibuprofen

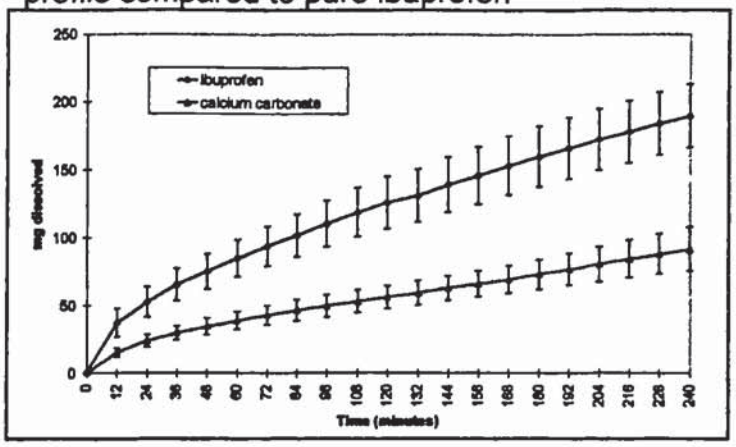

Figure 4.36
Illustrating lactose mix dissolution profile compared to pure ibuprofen

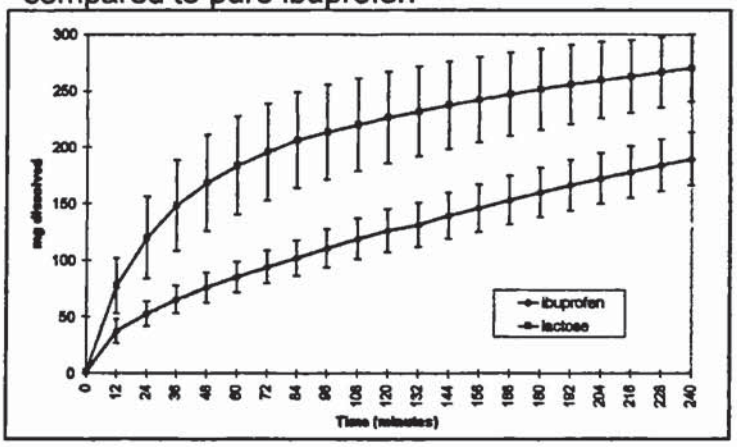

Figure 4.37
Illustrating starch mix dissolution profile compared to pure ibuprofen

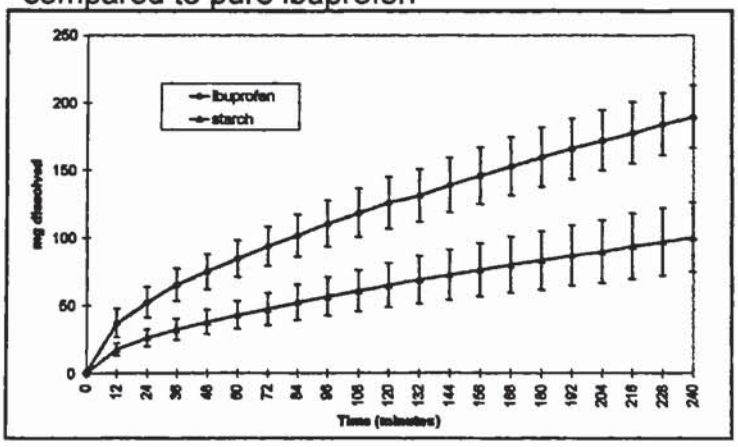

Figure 4.38
Illustrating di-calcium phosphate mix dissolution profile compared to pure ibuprofen

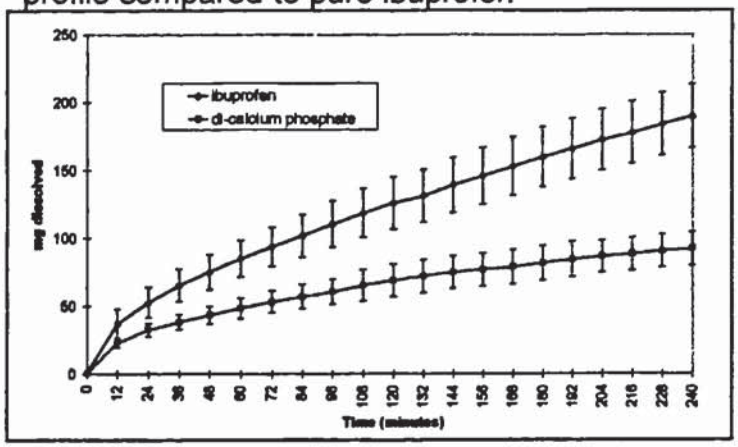

Figure 4.39
Illustrating microcrystalline cellulose mix dissolution profile compared to pure ibuprofen

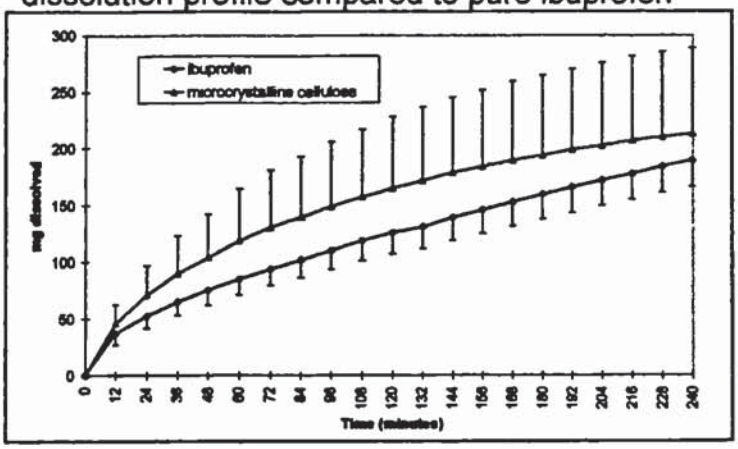

Figure 4.40
Illustrating potassium bicarbonate mix dissolution profile compared to pure ibuprofen

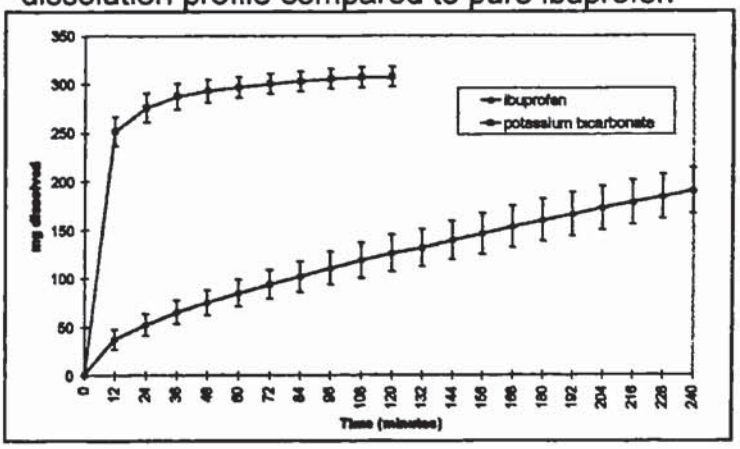

Figure 4.41
Illustrating citric acid mix dissolution profile compared to pure ibuprofen

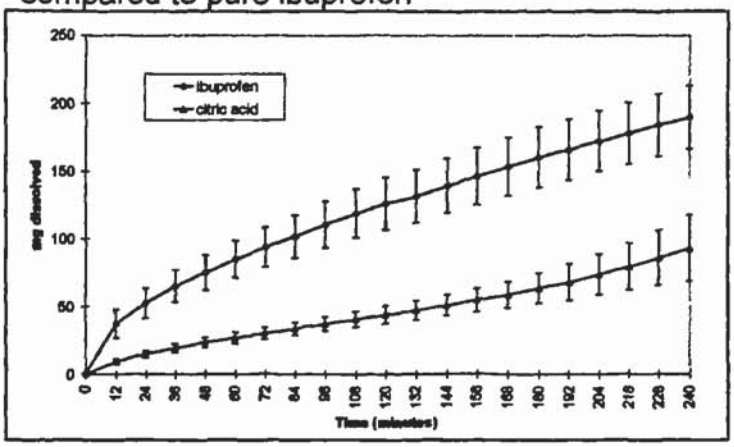

Figure 4.42
Illustrating tartaric acid mix dissolution profile compared to pure ibuprofen

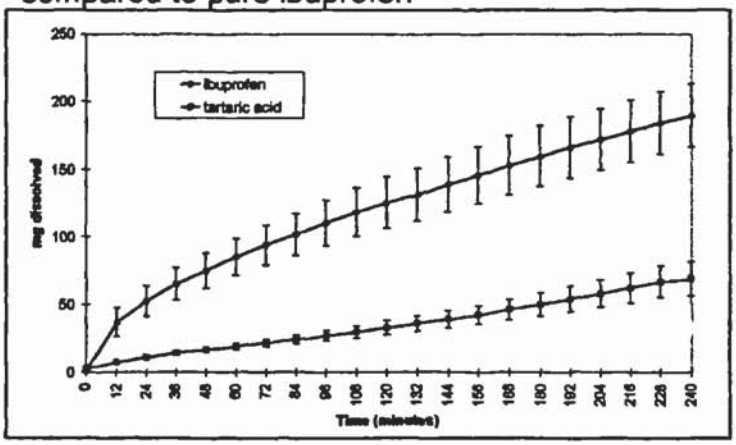

Figure 4.43
Illustrating sodium bicarbonate 33% mix dissolution profile compared to pure ibuprofen

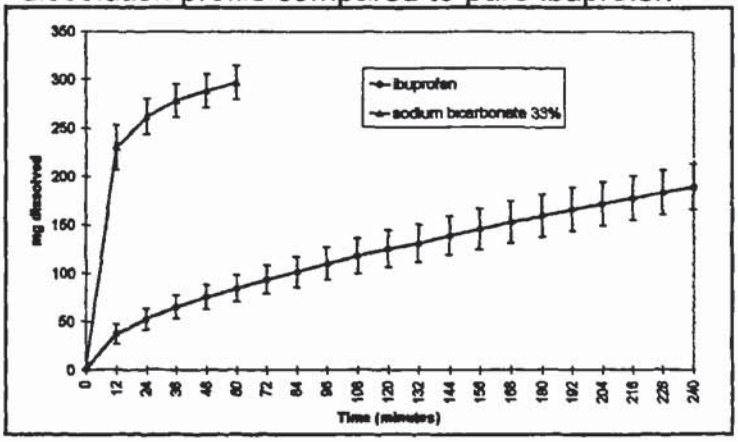

Figure 4.44
Illustrating sodium bicarbonate 66% mix dissolution profile compared to pure ibuprofen

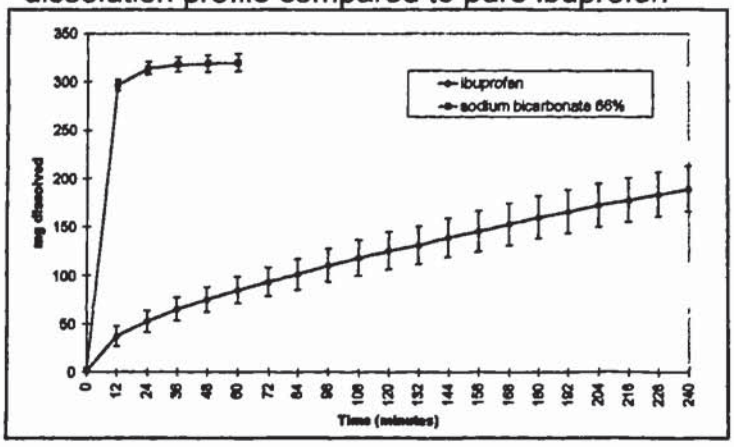

Figure 4.45
Illustrating L-arginine mix dissolution profile compared to pure ibuprofen

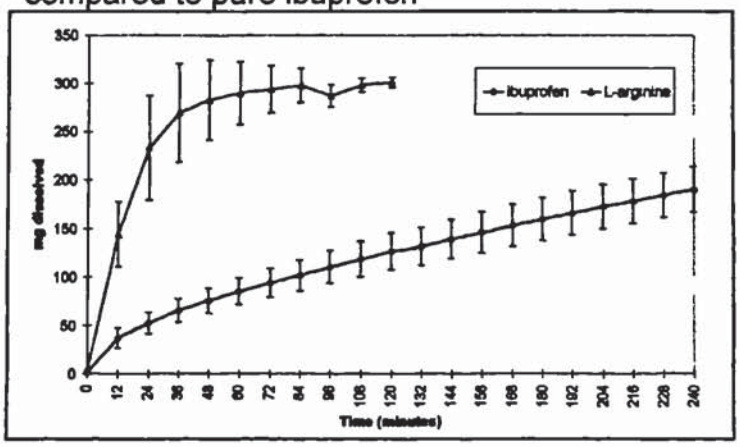

Figure 4.46
Illustrating L-lysine mix dissolution profile compared to pure ibuprofen

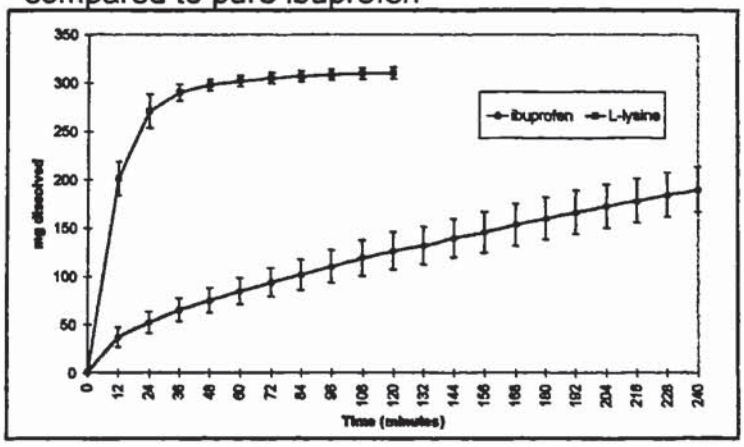

Figure 4.47
Illustrating glycine mix dissolution profile compared to pure ibuprofen

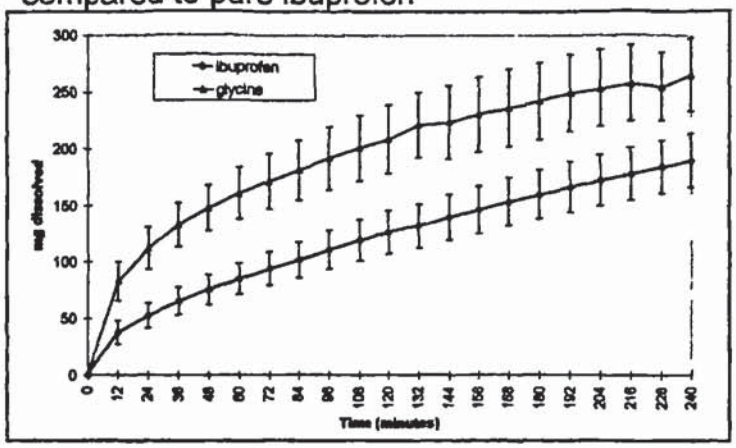

Figure 4.48
Illustrating tri-basic sodium phosphate mix dissolution profile compared to pure ibuprofen

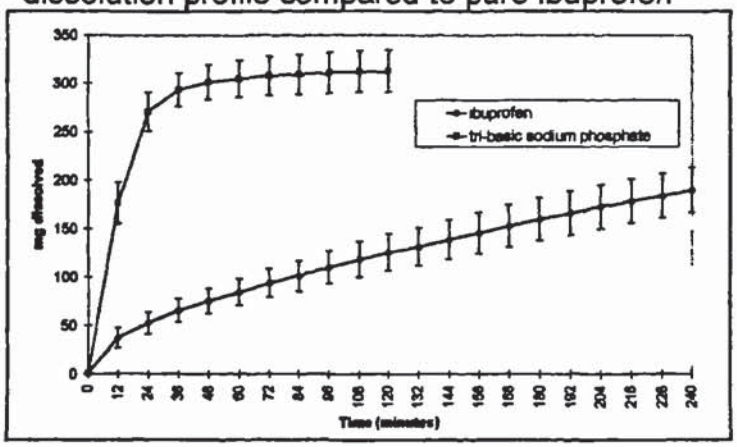

Figure 4.49
Illustrating sodium carbonate mix dissolution profile compared to pure ibuprofen

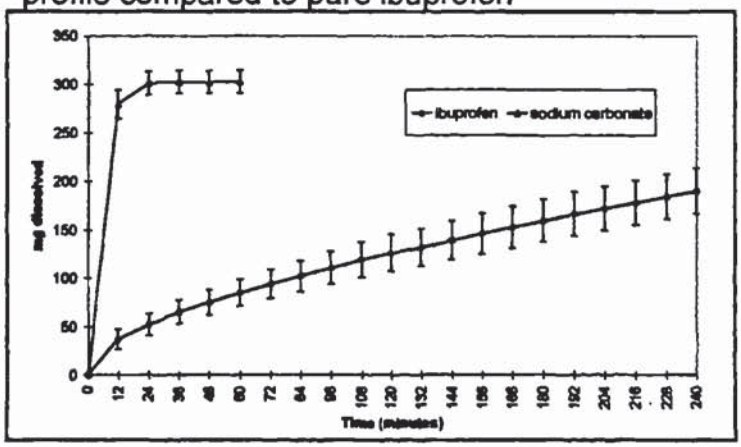

Figure 4.50
Illustrating ground Hedex® mix dissolution profile compared to pure ibuprofen

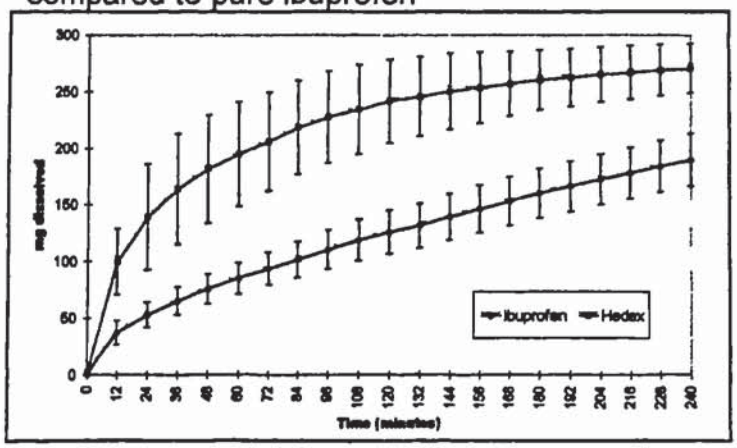

Figure 4.51
Illustrating magnesium oxide mix dissolution profile compared to pure ibuprofen

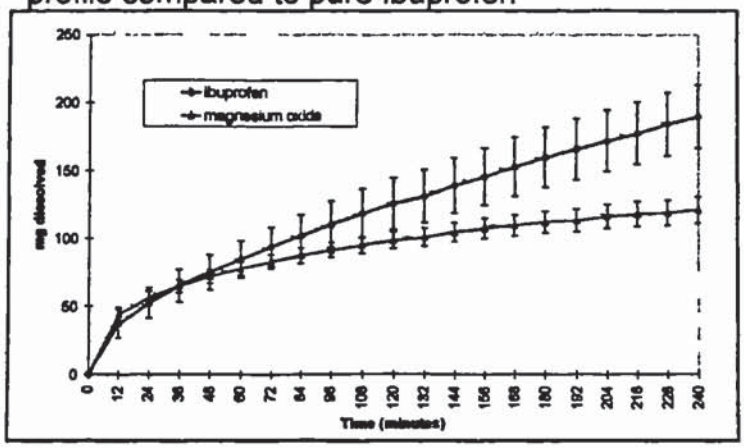

The criteria used for the analysis of the paracetamol powder mixes to obtain the linear portion of the dissolution profile were applied to the ibuprofen results. Correlation coefficients (R^2) and dissolution-rate values were calculated for each profile and are listed in table 4.8. Selected examples are graphically illustrated in figures 4.52-4.54.

Firstly, it is noted that for several of the fast-dissolving mixes the sampling rate was insufficient to collect enough datapoints to review the linearity of the dissolution profile. From the results in which enough datapoints were collected it is noted that in all cases R^2 >0.96 which demonstrates a very high level of linearity, as is also illustrated in the graphical examples. The rank order of dissolution rates generally corresponds to that found by the difference factor method, with the insoluble/slowly soluble and acidic compounds demonstrating the slowest rates followed by the neutral compounds, then the alkalising soluble agents and the two bicarbonates. The

Spearman rank correlation method (Miller and Miller 1993) was applied to the data, a correlation between the mathematical methods was found using a significance level of P=0.05 (ρ=0.851). This similarity indicates the usefulness of the dissolution method as both a qualitative and quantitative tool for the assessment of excipients for ibuprofen.

Table 4.8
Dissolution rate and correlation coefficient R^2 of ibuprofen powder mixes, calculated from the linear section of the dissolution profile, generated using the controlled powder dissolution method.

Excipient	Dissolution rate (mg min^{-1})	Fit-factor (F_1)	Correlation coefficient R^2
aluminium hydroxide	0.0432	-91.0	0.9989
magnesium hydroxide	0.233	-39.8	0.9735
magnesium oxide	0.235	-23.8	0.9719
di-calcium phosphate	0.257	-47.2	0.9736
tartaric acid	0.268	-70.7	0.9927
calcium carbonate	0.294	-54.1	0.9988
starch	0.333	-48.2	0.9932
citric acid	0.340	-61.8	0.9889
lactose	0.452	72.3	0.9702
microcrystalline cellulose	0.510	25.7	0.9683
ibuprofen	0.602	0.0	0.9940
glycine	0.623	61.9	0.9616
sodium chloride	1.06	19.0	0.9966
L-arginine	9.57	350.2	0.9834*
L-lysine	11.3	401.2	0.9272*
tri-sodium phosphate	11.3	328.5	0.9692*
potassium bicarbonate	11.5	347.4	0.8158*
sodium carbonate	12.5	373.9	0.8034*
sodium bicarbonate	12.7	389.2	0.7920*

* Due to high dissolution rate only 3 data-points were within the linear section.

Figure 4.52
Illustrating the linear section of the aluminium hydroxide mix dissolution profile. Results are mean of 5 replicates ±SD. R^2=0.9989

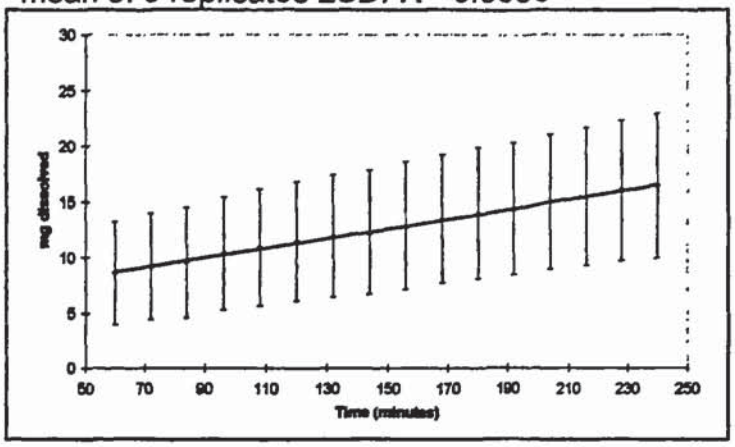

Figure 4.53
Illustrating the linear section of pure ibuprofen dissolution profile. Results are mean of 6 replicates ±SD. R^2=0.9940

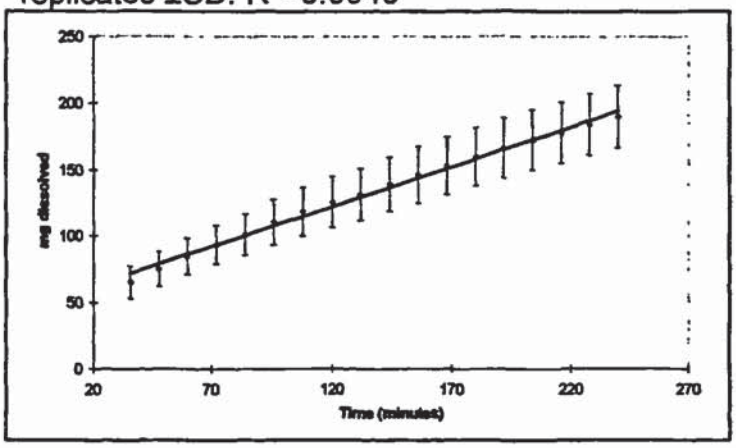

Figure 4.54
Illustrating the linear section of lactose mix dissolution profile. Results are mean of 6 replicates ±SD. R^2=0.9702

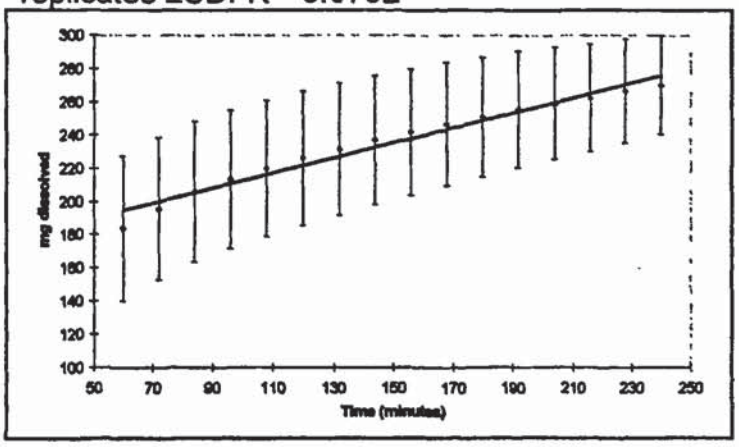

4.7 Drug/antacid interaction dissolution study

4.71 Introduction

The model used to describe the absorption process of a drug (developed in section 1.51) considers the dissolution of drug, firstly within the stomach environment, and then in some instances continued dissolution within the small intestine. The relative amount of dissolution in each environment is governed by several factors including the gastric emptying rate and solubility of the drug in each environment. The aim of this study was to determine specifically the effect of each antacid on the dissolution rate of the model drugs in both simulated gastric and intestinal environments, using a dissolution method based on the USP paddle apparatus, but with drug, antacid and dissolution volume set to represent *in vivo* concentrations during co-administration. Specifically, the dissolution volume was set at 400ml, twice the nominal volume in the fasted stomach (200ml derived from fasted stomach volume of 20-30ml (Dressman *et al.* 1998) with addition of 100-300ml of water taken with dose) and the lowest multiple of the stomach volume that could be used satisfactorily with this apparatus and therefore the antacid and tablets quantities used were adjusted to be twice the therapeutic dose. The IMMC has a duration of 90-120 minutes and therefore the maximum residence time in the stomach of 120 minutes was set as the experimental duration.

4.7.2 Experimental

4.7.2.1 Materials

Paracetamol, ibuprofen, sodium bicarbonate (extra fine grade), Hedex® tablets (ibuprofen 200mg) B/N 1PH782 were obtained from SB Pharmaceuticals (Weybridge). Panadol® tablets (paracetamol 500mg) B/N 1RB933 were obtained from a retail outlet. Calcium carbonate, magnesium hydroxide, hydrochloric acid, magnesium hydroxide, aluminium hydroxide, sodium hydroxide and mono-basic potassium phosphate were purchased from Aldrich (Poole,UK). All materials were of pharmaceutical or analytical grade as appropriate. Double-distilled water was generated in-house using a Fison's Fi-Streem still. Internal standards for HPLC analysis were prepared as detailed in sections 2.1 or 2.2 as appropriate.

4.7.2.2 Equipment

The dissolution system consisted of a Caleva Model 7ST dissolution bath, equipped with 1 litre round-bottomed flasks and with paddles conforming to Apparatus II- USP regulations (USP 1995). The HPLC system used for analysis of the samples was as described in section 2.1.1.2.

4.7.2.3 Method

Simulated gastric or intestinal fluid (0.05M HCl or pH6.8 USP buffer) dissolution medium, 400ml *per* flask, was prepared and thoroughly degassed using helium sparging. The temperature was controlled at 37±0.5°C. After equilibration of dissolution medium temperature the paddles were lowered slowly into the dissolution bath and then set to rotate at 50rpm. 2.0g of the antacid under investigation was added to each vessel followed by mixing for 10 minutes at 150rpm. The paddle speed was reset to 50rpm, the system hydrodynamics allowed to return to equilibrium (5 *minute hold time), followed by addition* of either four 500mg paracetamol tablets or four 200mg ibuprofen tablets as appropriate. 2.0ml samples were withdrawn using a syringe at the following timepoints, 5, 10, 15, 20, 30, 45, 60, 90 and 120 minutes, to be replaced by 2.0ml of fresh dissolution fluid. The samples were immediately filtered through a 0.45µm HPLC filter (Gelman acrodisc® LC13PVDF), the first 1ml being discarded and the remainder collected. 0.1ml aliquots were sampled and added to 2.0ml of the appropriate internal standard, both measured using micropipettes. For paracetamol tablets the samples were assayed by the HPLC method detailed in section 2.1 and for ibuprofen tablets the samples were assayed by the HPLC method detailed in section 2.2. The sampling procedure caused a dilution in the bulk dissolution samples. It was therefore necessary to adjust each successive sample concentration for the dilution caused by all the previous samples.

This was performed, using an Excel spreadsheet, by applying the following correction factor:

$$C_t = C_m + V_s * \frac{\sum_{t=1}^{t=n-1} C_m}{V_r} \qquad \text{equation 4.9}$$

where C_t is the true concentration of the drug at timepoint t, which would be found without dilution, C_{mt} is the current measured concentration of drug, V_s is the volume of sample removed for analysis, V_r is the volume of experimental solution, and $\sum C_m$ is the summed total of the previous measured concentrations (t=1 to n-1).

4.7.3 Results and discussion

The dissolution profiles for both drugs, in the two simulated environments containing antacid were compared against the control (drug without antacid) and the F_1 values calculated. These are summarised in table 4.9. The dissolution profiles are illustrated in figures 4.55-4.74.

For ibuprofen tablets dissolving in the simulated stomach (figures 4.65-4.69), it is noted from figure 4.65 that the dissolution profile reached a plateau after 20 minutes with only ≈1.3% of the active dissolved. This very low level of dissolution is in line with expectations, based on the determined saturated solubility of ibuprofen of 0.06mg ml^{-1} at the experimental pH, the maximum theoretical amount dissolved would be ≈ 2.5%. This can also be applied to the experiment simulating the co-administration of aluminium hydroxide. The shape of the dissolution curve is interesting, an initial increase followed by a decrease, and a large difference factor is obtained. However, these differences are inconsequential as the dissolution of drug is still negligible, compared with the available dose.

For all the other antacids, a profound increase in dissolution rate is observed. Significantly, the lowest of these is seen with calcium carbonate. This may be explained by the fact that the experimental pH on completion of the study was 5.6. At this pH, it is estimated from the pH/solubility profile of ibuprofen in section 3.2 that the solubility of ibuprofen would be ≈1.2mg ml^{-1}. Theoretically, the maximum solubility would be ≈60% of the available drug (*cf.* 67% experimentally measured after 120 minutes), therefore the dissolution is limited by the saturated solubility obtained under these conditions. For all the other antacids, the measured pH was sufficiently high for complete solubilisation of the drug.

As ibuprofen absorption is dissolution rate-limiting, all of the antacids, except aluminium hydroxide, are likely to significantly alter the absorption profile of ibuprofen *in vivo*. The magnitude of this effect will be investigated in the IVIVC development study.

For ibuprofen tablets dissolving in the intestinal environment, analysis of the dissolution profiles (figures 4.70-4.74) and the F_1 values indicates that all co-administered antacids, except aluminium hydroxide, act as dissolution promoters, the trend agreeing with solution pH values. The promoting effect is far smaller than that seen in the previous stomach simulation. Interestingly, it was observed that the ibuprofen dissolution profile reached a plateau of ≈70-80% (fig 4.74) when aluminium hydroxide was co-administered. This could not be explained in terms of saturated solubility or in terms of adsorption of dissolved drug onto the antacid as this phenomenon has been discounted by the work undertaken in section 3.4.

For paracetamol tablets dissolving in the stomach environment (figures 4.55-4.59), it is noted that a slight, but not significant, improvement in dissolution rate is recorded for co-administered magnesium hydroxide, calcium carbonate, sodium bicarbonate or aluminium hydroxide. The results for co-administered magnesium oxide show a steady rate of drug dissolution until a plateau of between 60-70% is reached as illustrated in figure 4.55. This may be partly explained by adsorption of dissolved drug onto the antacid as magnesium oxide was found to have the largest adsorptive capacity of the antacids under test (section 3.4.) The phenomenon is unlikely to be the sole factor responsible though as only ≈3% of drug was adsorbed, although it is recognised that a direct comparison cannot be made as the experimental protocols employed were different.

For paracetamol tablets dissolving in the intestinal environment (figures 4.60-4.64), it is noted that the co-administration of magnesium oxide or aluminium hydroxide produced paracetamol dissolution profiles which plateaued at between 75-85% as illustrated in figures 4.60 and 4.63. Sodium bicarbonate, calcium carbonate and magnesium hydroxide were found to have a negligible effect on the dissolution rate of paracetamol.

Iwuagwu and Aloko (1992) have also studied the effect of co-administered antacids on paracetamol tablet dissolution *in vitro.* Their work showed a large reduction in the total drug dissolved in 120 minutes for both aluminium hydroxide and magnesium oxide, being ≈30% and ≈20% of available dose respectively. Their protocol was similar in that they used Panadol® tablets and unformulated powdered antacids, however they used water as a dissolution fluid. There are several disadvantages to using water as the dissolution medium, the solubility of antacids varies significantly with pH, as investigated in section 3.3, therefore the quantities of dissolved and undissolved antacid are dependent on the medium used. Also, the pH-modifying effect of each antacid may be modified *In vivo* by the buffering actions of the GI fluids especially intestinal fluid which has a buffering capacity due to the presence of bicarbonate (Macheras *et. al.* 1995), and the pH and surface tension of water may vary with the source and during the dissolution itself, due to the influence of active and excipients. The FDA cite the last two reasons as a basis for discouraging the use of water as a dissolution medium (FDA(CDER) 1997). On this basis the results obtained in this study supersede those obtained by Iwuagwu and Aloko (1992).

Table 4.9
Summary of F_1 values comparing dissolution profiles of model drugs in antacid-containing simulated gastric and intestinal environments, with controls, where antacid addition was omitted. Table also includes pH values of dissolution medium, measured on completion of experiment.

Drug Simulated environment	**Ibuprofen Stomach**		**Ibuprofen Intestine**		**Paracetamol Stomach**		**Paracetamol Intestine**	
Antacid	F_1	pH	F_1	pH	F_1	pH	F_1	pH
sodium bicarbonate	6554	7.6	24.1	7.0	4.3	6.2	-11.1	7.3
calcium carbonate	3746	5.6	12.7	6.6	4.9	6.1	-2.5	7.0
magnesium oxide	6232	9.5	16.4	11.5	-32.9	9.4	-17.6	10.3
magnesium hydroxide	6140	8.9	25.9	6.7	11.6	9.0	5.7	8.4
aluminium hydroxide	78.5	3.4	-5.0	6.7	10.5	3.4	-18.7	7.0

Figure 4.55
Illustrating the effect of co-administered magnesium oxide on the dissolution of paracetamol tablets in simulated stomach fluid (0.05M HCl). Results are the mean of three replicates±SD

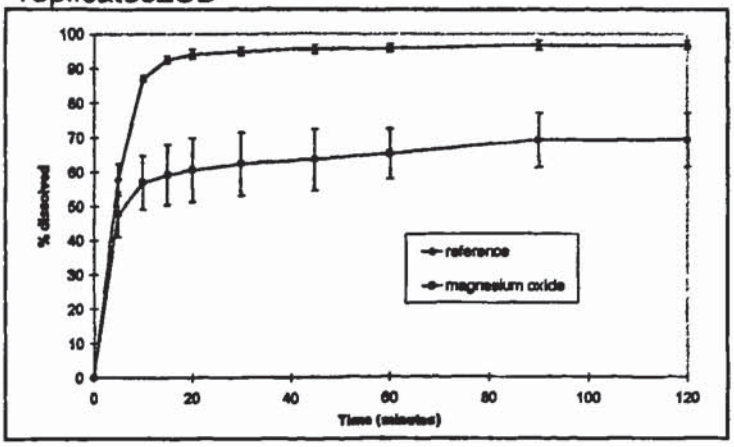

Figure 4.56
Illustrating the effect of co-administered sodium bicarbonate on the dissolution of paracetamol tablets in simulated stomach fluid (0.05M HCl). Results are the mean of three replicates±SD

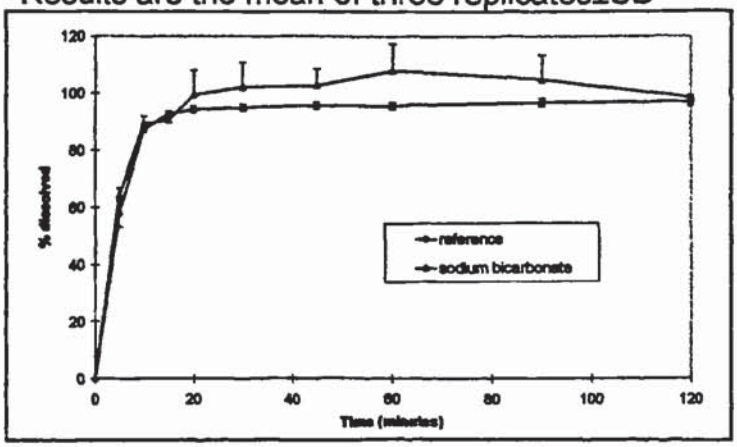

Figure 4.57
Illustrating the effect of co-administered calcium carbonate on the dissolution of paracetamol tablets in simulated stomach fluid (0.05M HCl). Results are the mean of three replicates±SD

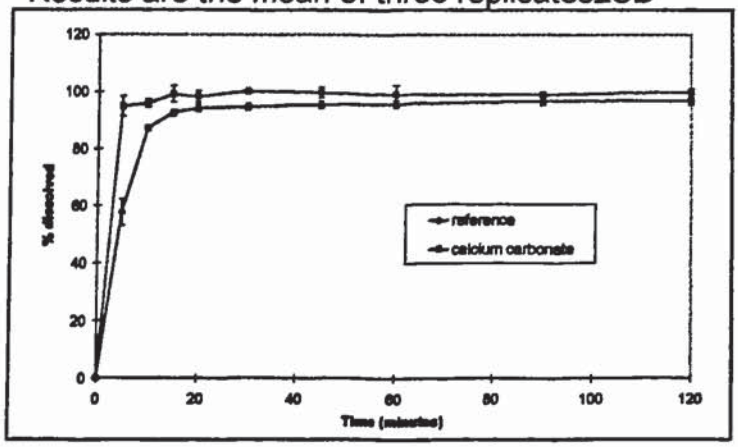

Figure 4.58
Illustrating the effect of co-administered aluminium hydroxide on the dissolution of paracetamol tablets in simulated stomach fluid (0.05M HCl). Results are the mean of three replicates±SD

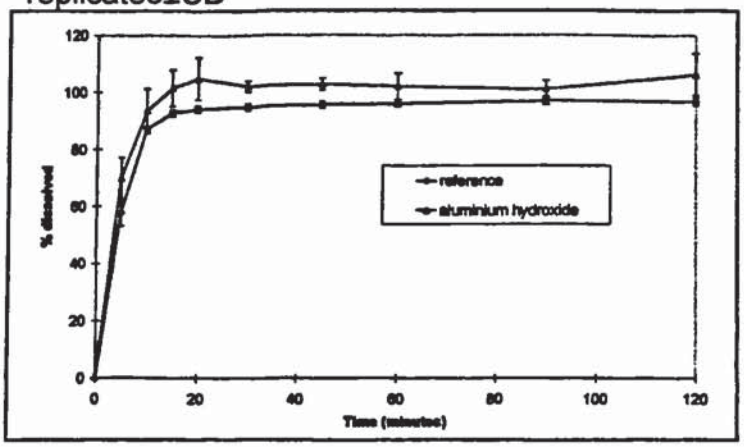

Figure 4.59
Illustrating the effect of co-administered magnesium hydroxide on the dissolution of paracetamol tablets in simulated stomach fluid (0.05M HCl). Results are the mean of three replicates±SD

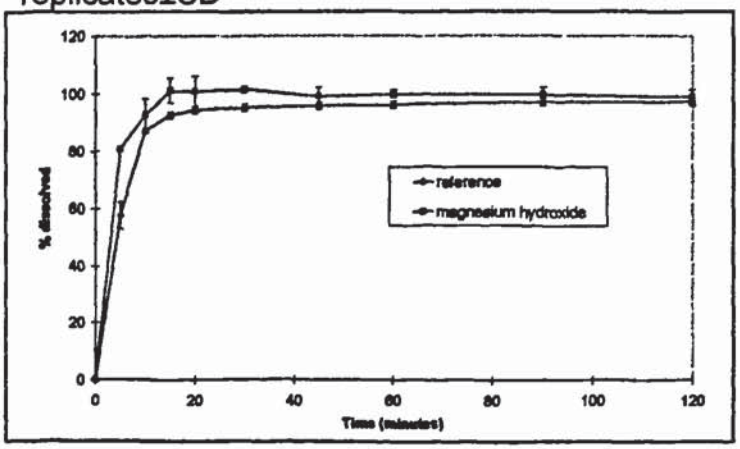

Figure 4.60
Illustrating the effect of co-administered magnesium oxide on the dissolution of paracetamol tablets in simulated intestinal fluid (USP buffer pH6.8). Results are the mean of three replicates±SD

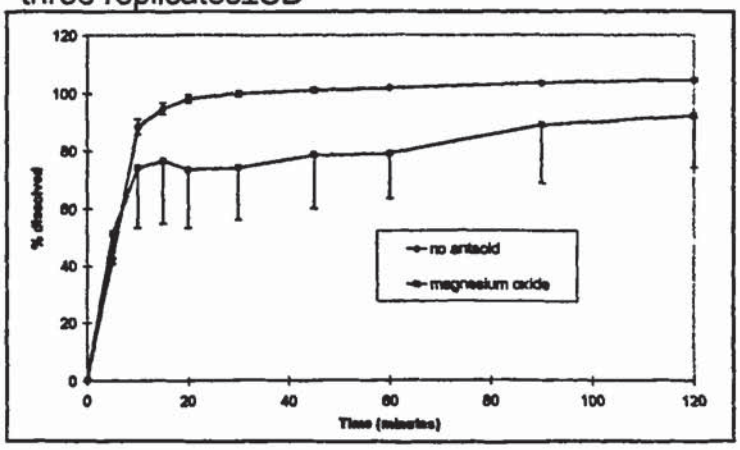

Figure 4.61
Illustrating the effect of co-administered sodium bicarbonate on the dissolution of paracetamol tablets in simulated intestinal fluid (USP buffer pH6.8). Results are the mean of three replicates±SD

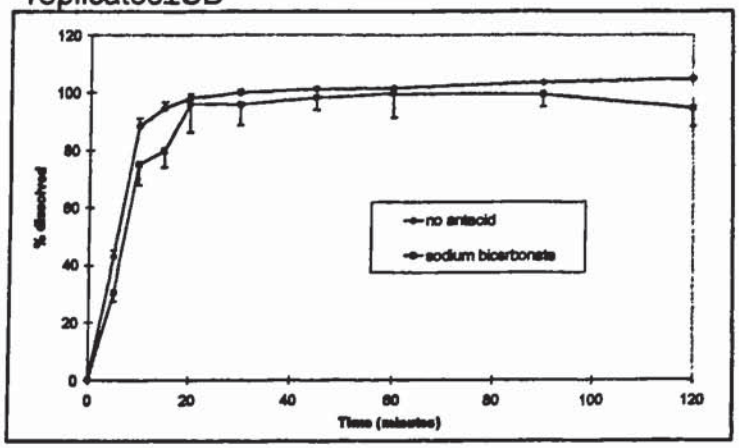

Figure 4.62
Illustrating the effect of co-administered calcium carbonate on the dissolution of paracetamol tablets in simulated intestinal fluid (USP buffer pH6.8). Results are the mean of three replicates±SD

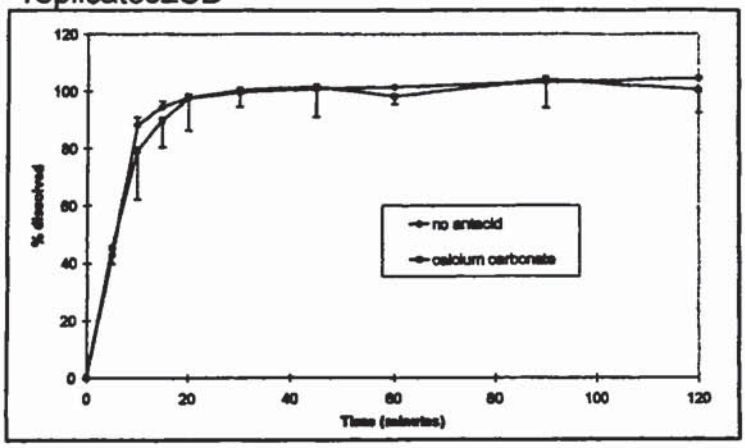

Figure 4.63
Illustrating the effect of co-administered aluminium hydroxide on the dissolution of paracetamol tablets in simulated intestinal fluid (USP buffer pH6.8). Results are the mean of three replicates±SD

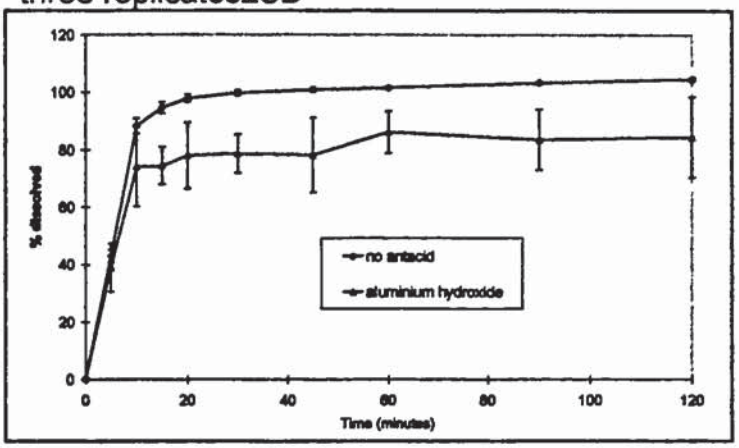

Figure 4.64
Illustrating the effect of co-administered magnesium hydroxide on the dissolution of paracetamol tablets in simulated intestinal fluid (USP buffer pH6.8). Results are the mean of three replicates±SD

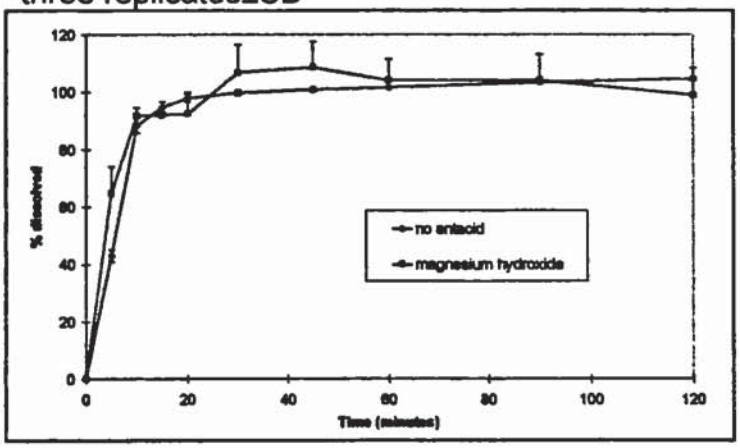

Figure 4.65
Illustrating the effect of co-administered aluminium hydroxide on the dissolution of ibuprofen tablets in simulated intestinal fluid (0.05M HCl). Results are the mean of three replicates±SD

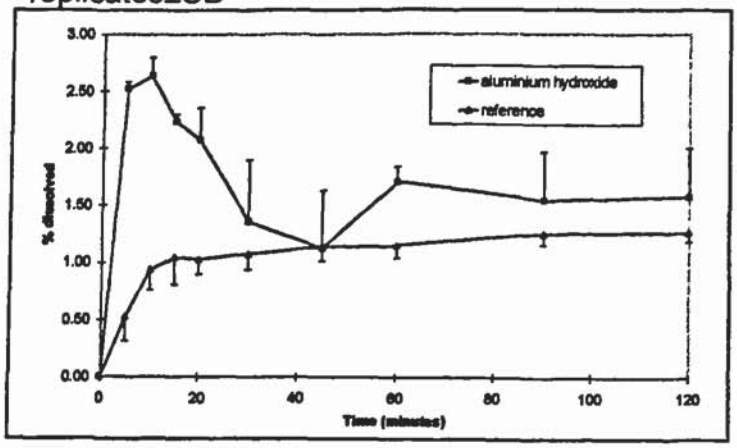

Figure 4.66
Illustrating the effect of co-administered magnesium hydroxide on the dissolution of ibuprofen tablets in simulated stomach fluid (0.05M HCl). Results are the mean of three replicates±SD

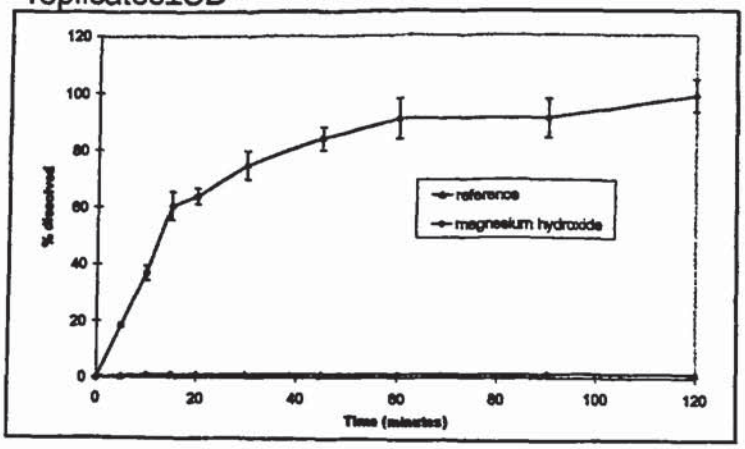

Figure 4.67
Illustrating the effect of co-administered magnesium oxide on the dissolution of ibuprofen tablets in simulated stomach fluid (0.05M HCl). Results are the mean of three replicates±SD

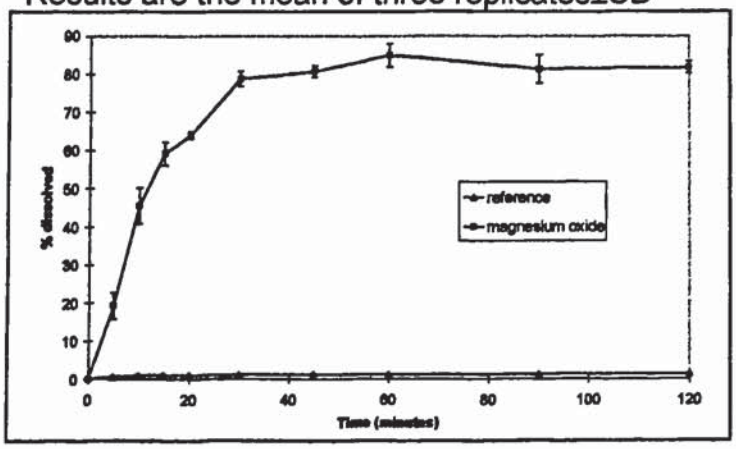

Figure 4.68
Illustrating the effect of co-administered calcium carbonate on the dissolution of ibuprofen tablets in simulated stomach fluid (0.05M HCl). Results are the mean of three replicates±SD

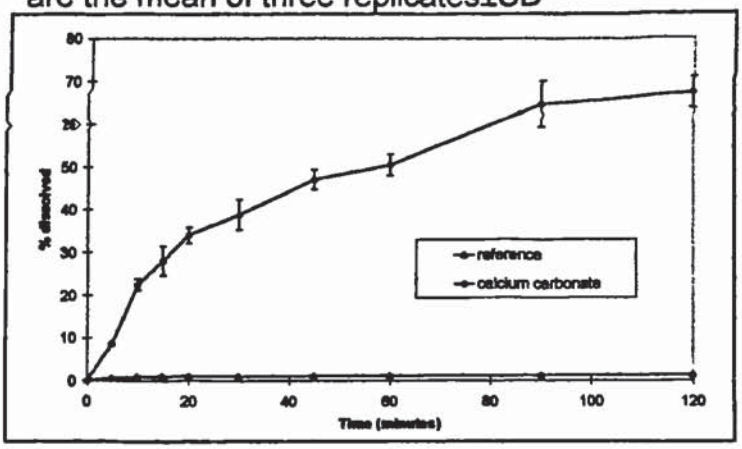

Figure 4.69
Illustrating the effect of co-administered sodium bicarbonate on the dissolution of ibuprofen tablets in simulated stomach fluid (0.05M HCl). Results are the mean of three replicates±SD

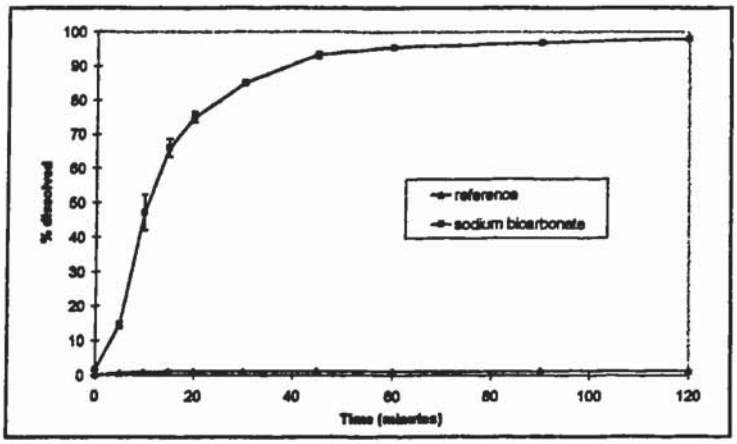

Figure 4.70
Illustrating the effect of co-administered sodium bicarbonate on the dissolution of ibuprofen tablets in simulated intestinal fluid (USP buffer pH6.8). Results are the mean of three replicates±SD

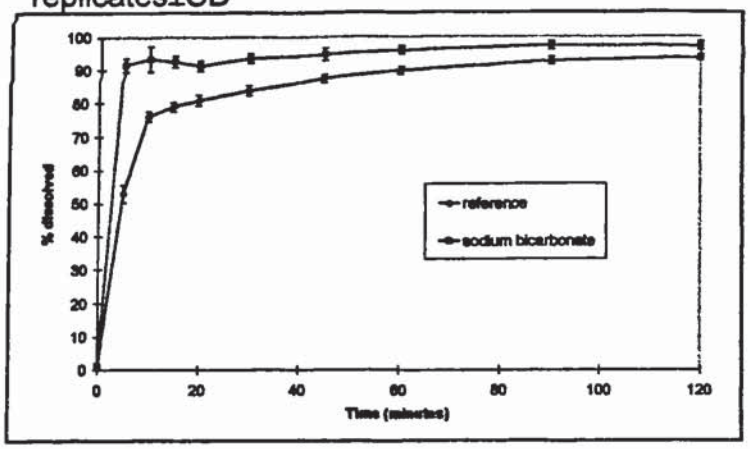

Figure 4.71
Illustrating the effect of co-administered calcium carbonate on the dissolution of ibuprofen tablets in simulated intestinal fluid (USP buffer pH6.8). Results are the mean of three replicates±SD

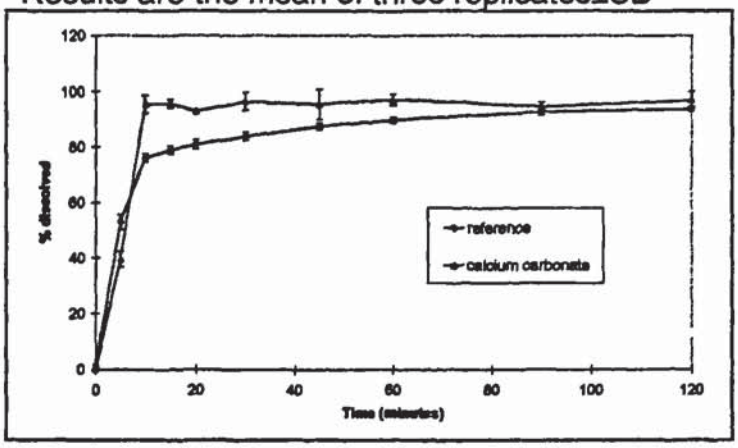

Figure 4.72
Illustrating the effect of co-administered magnesium oxide on the dissolution of ibuprofen tablets in simulated intestinal fluid (USP buffer pH6.8). Results are the mean of three replicates±SD

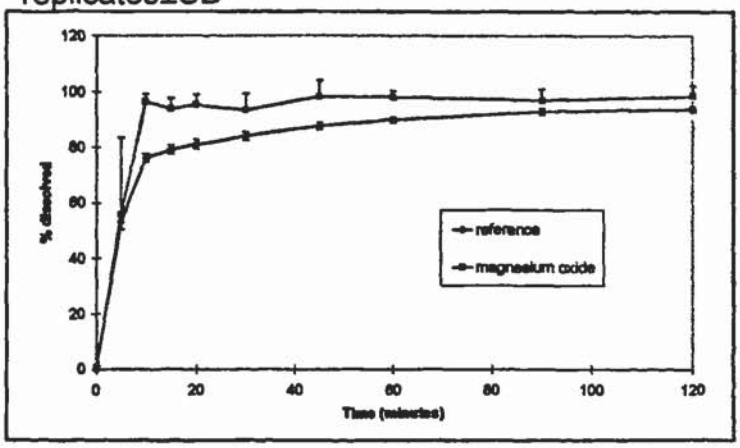

Figure 4.73
Illustrating the effect of co-administered magnesium hydroxide on the dissolution of ibuprofen tablets in simulated intestinal fluid (USP buffer pH6.8). Results are the mean of three replicates±SD

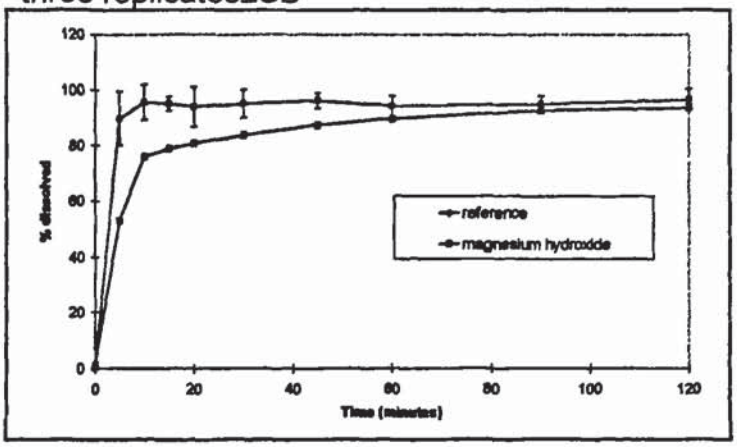

Figure 4.74
Illustrating the effect of co-administered aluminium hydroxide on the dissolution of ibuprofen tablets in simulated intestinal fluid (USP buffer pH6.8). Results are the mean of three replicates±SD

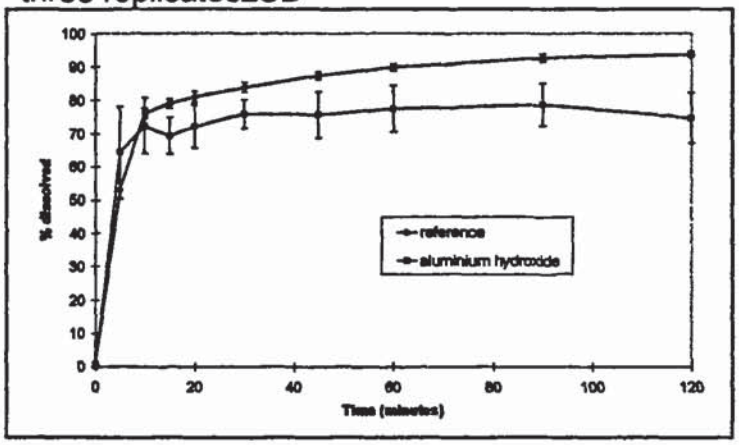

4.8 The role of sodium bicarbonate on the dissolution of model drugs from solid dosage forms

4.8.1 Introduction

It has been demonstrated in section 4.6 that the primary excipient in the Zapp formulation, sodium bicarbonate, promotes dissolution significantly through the generation of carbon dioxide gas on contact with acidic media. For ibuprofen, a combination of effervescence and alkalisation of the medium is the likely mechanism for promotion of dissolution. If the model drugs dissolve according to the diffusion-layer theory, the increase in dissolution rate due to effervescence can be explained in terms of a modification of the hydrodynamics and hence a change in the boundary layer (see equation 4.2). If the drugs dissolve according the interfacial boundary method, another explanation would have to be postulated. It was also observed in section 4.6 that sodium bicarbonate appeared to promote dissolution of paracetamol through a mechanism other than effervescence (dissolution of paracetamol in water experiment). The aims of this section were to validate the new IDR method, elucidate the mechanism controlling the dissolution process of the model drugs and then determine to what extent the other factors having importance in the dissolution process, were modified by the presence of sodium bicarbonate. In particular, the use of the IDR method, limiting the surface area meant that only changes to the saturated solubility C_s or IDR constant k would be investigated as they were not controlled by the method. Other excipients were chosen and also characterised for comparative purposes. The data from the saturated solubility studies (see section 3.2), viscosity studies and observations from the controlled powder dissolution study were combined with the results generated by the IDR study to characterise the mechanisms by which sodium bicarbonate promotes the dissolution process of the model drugs.

4.8.2 Validation of IDR method and elucidation of the mechanism controlling the dissolution of model drugs.

4.8.2.1 Experimental

4.8.2.1.1 Materials

Paracetamol, ibuprofen and sodium bicarbonate (extra fine grade) were obtained from SB Pharmaceuticals (Weybridge, UK). Hydrochloric acid, sodium hydroxide and mono-basic potassium phosphate were purchased from Aldrich (Poole, UK). All materials were of pharmaceutical or analytical grade as appropriate. Double-distilled water was generated in-house using a Fison's Fi-Streem still.

4.8.2.1.2 Equipment

The dissolution system consisted of a Caleva Model 7ST dissolution bath, equipped with 1 litre round-bottomed flasks and paddles conforming to Apparatus II - USP regulations (USP 1995). Sampling was performed on a continuous loop basis, using a Watson Marlow 5025 peristaltic pump set with a flow rate of 5ml min^{-1}. Analysis was performed automatically at desired time intervals using a LKB Biochrom Ultrospec II multi-cell UV/VIS spectrometer and Quartz cells with 10mm pathlength. Data was collected by a computer using Tablet Dissolution Software V1.12 supplied by LKB Biochrom. Data printouts (absorbances) were collected.

4.8.2.1.3 Method

Pellets were prepared and the methodology used as detailed in 4.43. Replicate IDR assays were performed at paddle speeds of 10, 30, 40, 50, 60 and 70rpm using 0.05M HCl and USP buffer pH6.8, controlled at 37±0.5°C, as the dissolution medium for paracetamol and ibuprofen respectively. For paracetamol, data was collected at 5 minute intervals for 90 minutes and absorbances were obtained at 295nm. For ibuprofen, data was collected at 6-minute intervals for 120 minutes and absorbances were obtained at 233nm. For both drugs the mass of drug dissolved (mg) *versus* dissolution time was calculated by comparison with a linear or polynomial equation derived from the 6-point calibration data. Standards were matrix-matched for pH.

4.8.2.2 Results and Discussion

The main requirement for a dissolution method designed to determine IDRs is that a significant part of the dissolution profile is linear, indicating that a fixed surface area of drug is exposed to the dissolution medium and the stirring conditions are not causing turbulent flow. Figures 4.75 and 4.76 illustrate typical dissolution profiles at 10, 30, 50 and 70rpm paddle speeds for the model drugs. On the basis of these data, all experiments conducted using this technique were carried out using a stirrer speed of 50rpm, using the data collected from timepoints 10-85 minutes for paracetamol and 18-120 minutes for ibuprofen.

Figure 4.75
IDR dissolution profiles of paracetamol illustrating the effect of changing stirrer speed. Results are the mean of at least five replicates.

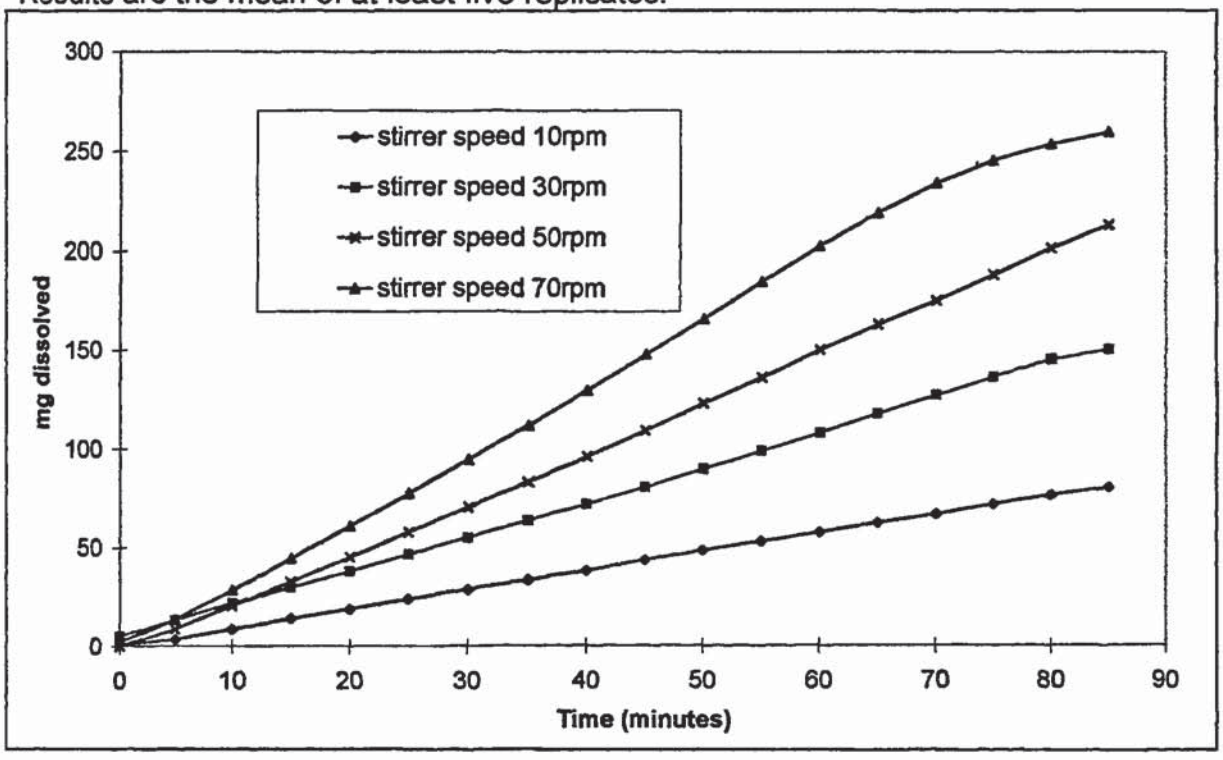

Figure 4.76
IDR dissolution profiles of ibuprofen illustrating the effect of changing stirrer speed. Results are the mean of at least five replicates.

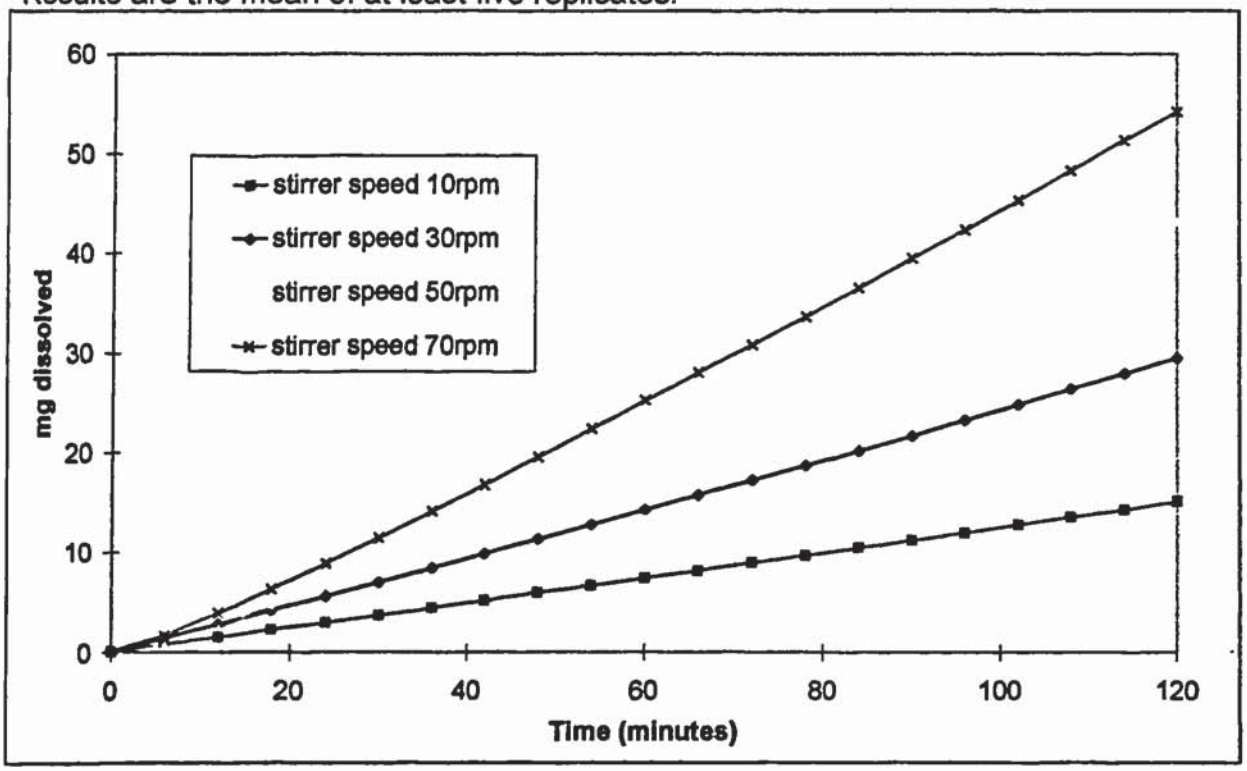

A change in hydrodynamic conditions, with any resultant change in the IDR, will allow elucidation of the dissolution mechanism. This technique is applied to the rotating basket apparatus, in the form of Levich plots as discussed in section 4.43. This technique is frequently used to determine whether the dissolution mechanism is diffusion/convection controlled, more closely follows the interfacial boundary model, or is described by a combination model (Supabphol and Stewart 1996). An empirical equation is frequently used to relate the IDR constant *k* to the stirring rate *N*, (Macheras *et al.* 1995):

$$k = a(N)^b \qquad \text{equation 4.10}$$

where *a* and *b* are constants. The values of b depend on the model considered. For the interfacial barrier model, where dissolution is not diffusion rate limited, *b*=0 and therefore *k* (the dissolution rate constant) is not dependent on the stirring conditions.

For the diffusion layer model b=1 and k is proportional to the stirring rate. If the value of b lies between zero and unity a combination model is usually considered.

The IDR (mg min^{-1} cm^{-2}) of both drugs at each paddle speed was calculated by dividing the gradient obtained from each linear profile by the surface area (1.327cm^2) of the exposed drug. The data are summarised in tables 4.10 and 4.11 and illustrated in figures 4.77 and 4.78. The calculated correlation coefficients demonstrate excellent linearity for the IDR over the whole speed range of the paddles. Also, the constructed Levich plots, IDR *versus* hydrodynamics expressed as paddle speed, show a very strong linear relationship, *i.e.* for paracetamol R^2=0.9887 and ibuprofen R^2=0.9734. From this it can be concluded that for both drugs the rate constant k is proportional to the stirrer speed, therefore b=1 and the dissolution process for both drugs can be described by the diffusion layer model.

Table 4.10
Summary of paracetamol IDR with changing hydrodynamic conditions. Assessment of linearity of IDR by use of correlation coefficient R^2.

Paddle Stirrer Speed (rpm)	IDR (mg min^{-1} cm^{-2}) ±SD	Correlation Coefficient R^2
10	0.730±0.07	0.9999
30	1.28±0.01	0.9996
40	1.76±0.01	0.9994
50	1.94±0.20	0.9997
60	2.18±0.20	0.9984
70	2.62±0.26	0.9991

Table 4.11
Summary of ibuprofen IDR with changing hydrodynamic conditions. Assessment of linearity of IDR by use of correlation coefficient R^2..

Paddle Stirrer Speed (rpm)	IDR (mg min^{-1} cm^{-2}) ±SD	Correlation Coefficient R^2
10	0.0952±0.0051	0.9997
30	0.1872±0.0079	0.9996
40	0.2189±0.0108	0.9981
50	0.2844±0.0176	0.9998
60	0.2817±0.0198	0.9997
70	0.3537±0.0180	0.9994

Figure 4.77
Illustrating the linear relationship between the IDR of paracetamol and the hydrodynamic conditions (paddle speed). Results are the mean of at least 5 replicates ±SD. Y=0.0308X+0.4146.

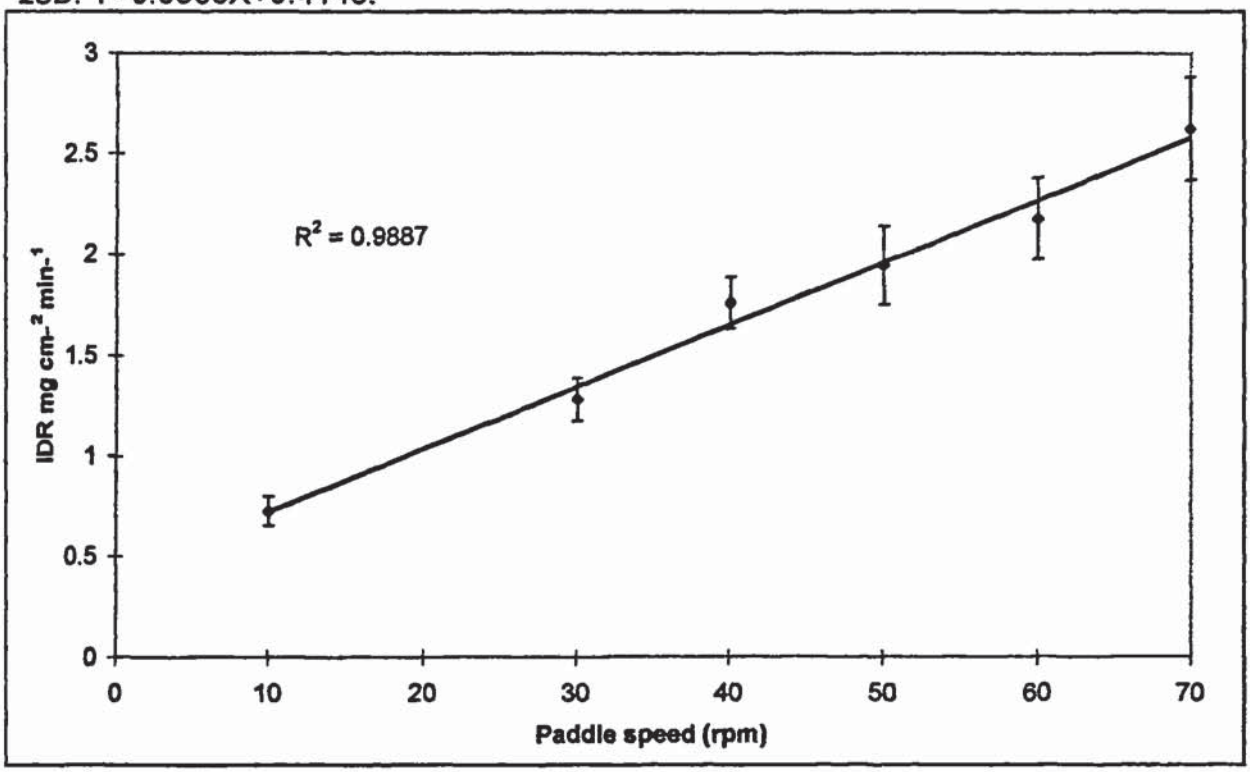

Figure 4.78
Illustrating the linear relationship between the IDR of ibuprofen and the hydrodynamic conditions (paddle speed). Results are the mean of at least 5 replicates±SD. Y=0.0041X+0.0581

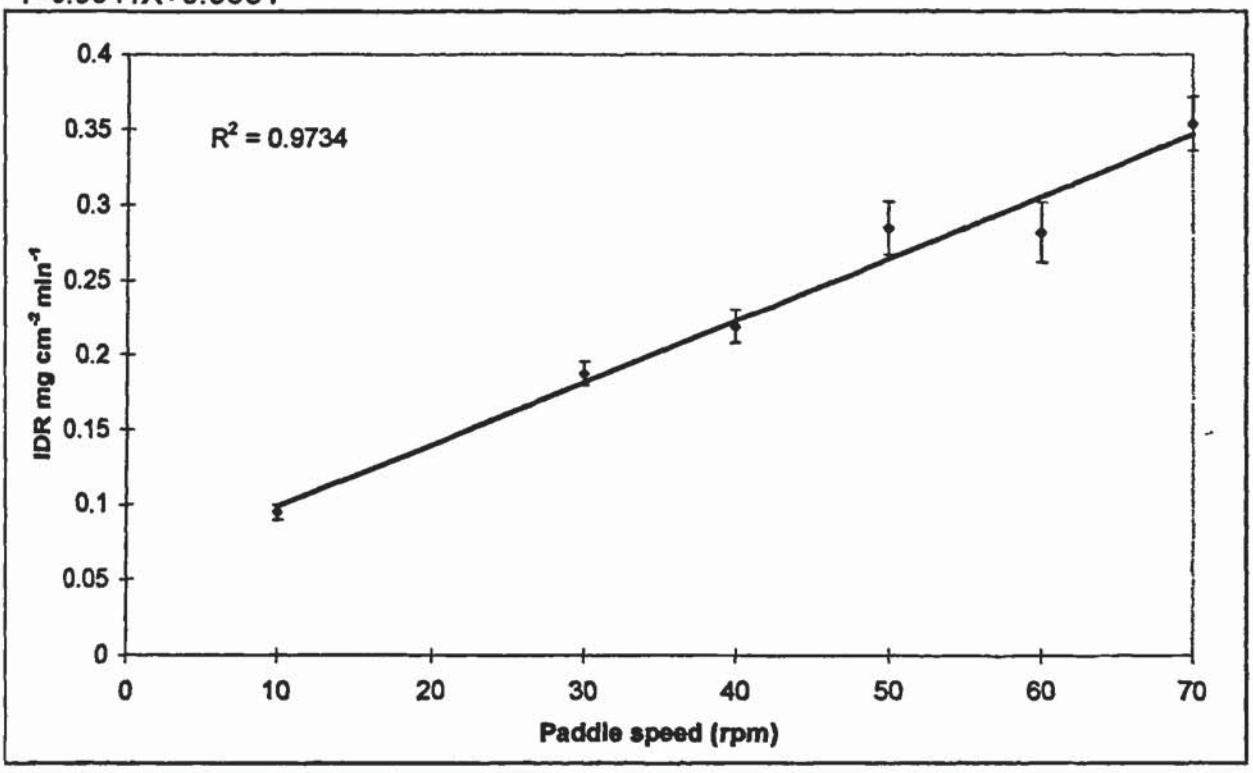

4.8.3 Sensitivity of IDR method to pH modification

As sodium bicarbonate, or any other pH-modifying excipient, may affect the dissolution rate of the model drugs by increasing the pH to values above the pK_a, thereby increasing the saturated solubility, it was necessary to ensure that the new IDR paddle method was sensitive enough to highlight these changes before proceeding to investigate sodium bicarbonate and the comparative excipients. This was achieved by measuring the IDR of paracetamol at various pHs using a range of buffers.

4.8.3.1 Experimental

4.8.3.1.1 Materials

Paracetamol was obtained from SB Pharmaceuticals (Weybridge). Hydrochloric acid, sodium hydroxide, potassium chloride, boric acid, di-sodium phosphate, citric acid and mono-basic potassium phosphate were purchased from Aldrich (Poole,UK). All materials were of pharmaceutical or analytical grade as appropriate. Double-distilled water was generated in-house using a Fison's Fi-Streem still.

4.8.3.1.2 Equipment

The equipment and set-up was as described in section 4.8.2.1.2.

4.8.3.1.3 Method

Pellets were prepared and the methodology used as detailed in 4.4.3. Replicate assays were performed at a paddle speed of 50rpm in each of the following media:

- USP Buffers - pHs of 1.2, 2.0, 6.0, 7.0, 8.0, 9.0, 9.7, and 11 (the latter two included extra sodium hydroxide)
- and Citrate Buffers -pHs 3.0, 4.0 and 5.0

Compositions of buffers are as detailed in Appendix 1.

Note: USP Phthalate buffers pH 3-5 were not used due to the a large UV absorbance in the wavelength region of interest.

Data were collected at 5 minute intervals for 90 minutes. Absorbance values were obtained at a suitable wavelength in the range 295-316nm (a longer wavelength was required for alkaline solutions due to λ-max shift at higher pH values). The mass of drug dissolved (mg) *vs.* dissolution time (minutes) was calculated by comparison with a linear or polynomial equation derived from the 6-point calibration data. Standards were matrix-matched for pH.

4.8.4.2 Results and discussion

With reference to equation 4.1, a change in solubility of drug will affect the dissolution rate proportionally. Clearly, the change in IDR with pH should correspond to the change in solubility. The change in IDR as illustrated in figure 4.79 was compared to the solubility profile of paracetamol illustrated in figure 3.1. It was noted that the solubility and IDR profiles were similar, as expected. However, although the changes in solubility and IDR at the highest pH's did correlate, the measured IDR was much lower than the expected increase. This effect is likely to be the result of buffering of the boundary layer micro-environment by paracetamol to a value near the drug's own pK_a, when the pH of the bulk fluid is above its pK_a of 9.5 (Macheras *et al.* 1995). The results of the effect of pH on IDR are summarised in table 4.12. On the basis of the results the method was deemed suitable for use in investigating the role of pH-modifying excipients such as sodium bicarbonate.

Table 4.12
The effect of increasing pH on the IDR of paracetamol measured using IDR paddle apparatus. Results are the mean of at least five replicates±SD

Dissolution fluid pH	IDR mg min^{-1} cm^{-2} ±SD
1.2	1.98±0.261
2	2.077±0.203
3	1.92±0.082
4	1.77±0.112
5	1.85±0.0273
6	2.06±0.148
7	1.93±0.089
8	2.32±0.200
9	2.49±0.157
9.7	2.76±0.353
11	2.99±0.435

Figure 4.79
The effect of pH on the IDR of paracetamol using IDR paddle apparatus. Results are the mean of at least five replicates±SD

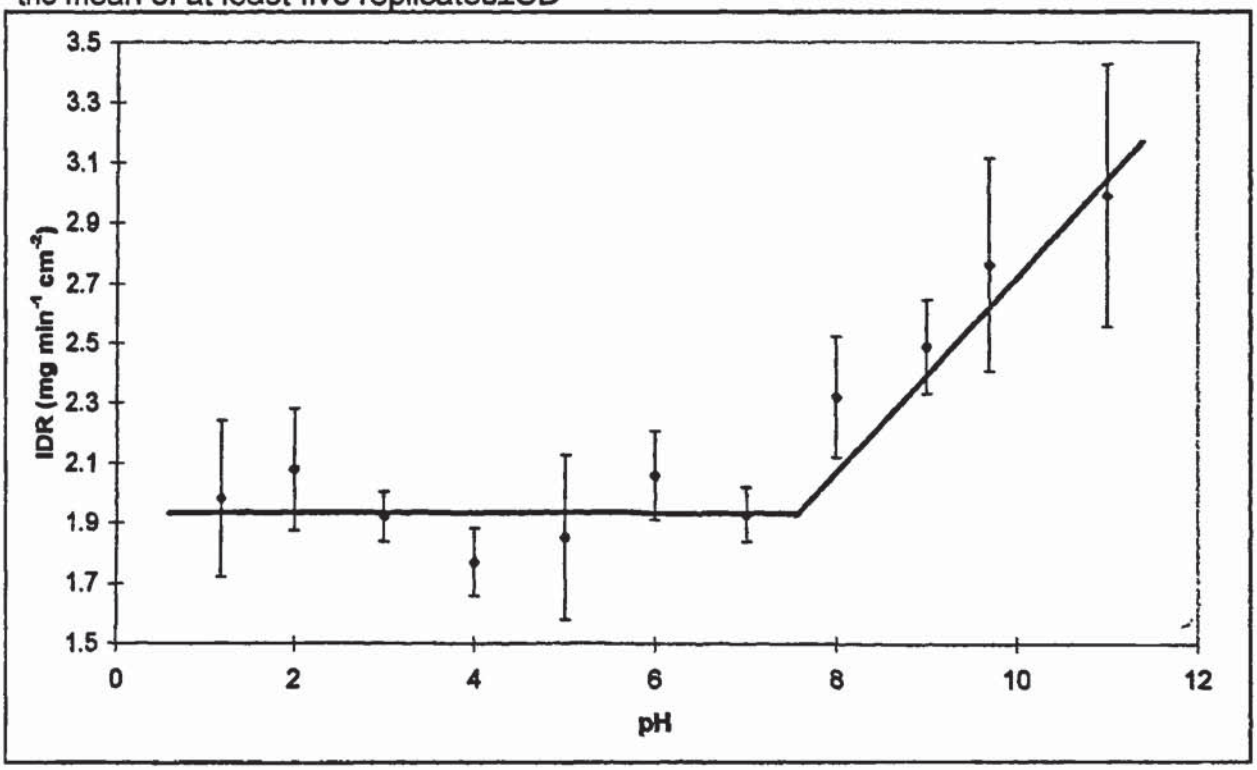

4.8.4 Effect of dissolved excipients on the IDR of model drugs

It has been shown in the controlled powder dissolution study that sodium bicarbonate appears to promote the dissolution of paracetamol by a secondary mechanism, the main mechanism being effervescence. Regardless of the importance of this mechanism, it is still important to characterise how other factors contribute to the process. With reference to equation 4.5, the saturated solubility C_s and IDR constant *k* are the two factors contributing to the IDR of a drug. To fully characterise the dissolution process, these factors were investigated, the study of the IDR being undertaken within this section. Five of the excipients utilised in section 4.6 were selected; lactose, sodium bicarbonate, potassium bicarbonate, sodium chloride and tartaric acid. This group includes a neutral non-ionic (12), two basic (23-24), a neutral ionic (9) and an acidic compound (11) covering the range of inhibition of dissolution of paracetamol through to promotion of dissolution, and a MW range of 58.4-360.3. The study aimed to determine the effect of the excipients, in solution, on the dissolution rate of the model drugs. The results could then be combined with physicochemical data obtained in section 3 to gain an understanding of the whole process.

The range chosen for excipient concentrations was 15 to 150mmol of excipient *per* 200ml, selected on the basis that the sodium bicarbonate quantity in the Zapp formulations is set at approximately 15mmol (when diluted in gastric contents) and under dissolution conditions the micro-environment around the tablet could have a higher concentration due to localised effects, hence the increase of one order of magnitude.

4.8.4.1 Experimental

4.8.4.1.1 Materials

Paracetamol, ibuprofen, lactose (Pharmatose DCL11) and sodium bicarbonate (extra fine grade) were obtained from SB Pharmaceuticals (Weybridge, UK). Hydrochloric acid, sodium hydroxide, tartaric acid, potassium bicarbonate, sodium chloride and mono-basic potassium phosphate were purchased from Aldrich (Poole, UK). All materials were of pharmaceutical or analytical grade as appropriate. Double-distilled water was generated in-house using a Fison's Fi-Streem still.

4.8.4.1.2 Equipment

The equipment and set-up was as described in section 4.8.2.1.2.

4.8.4.1.3 Method

Pellets were prepared and the methodology used as detailed in 4.4.3. Replicate IDR assays were performed at a paddle speed of 50rpm. For paracetamol experiments 0.05M HCl dissolution medium was used as the dissolution medium and for ibuprofen USP buffer pH6.8 was used. The IDR of each drug was obtained in dissolution buffer containing each excipient/concentration from the experimental series. The excipient containing dissolution fluids were used 'as is', *i.e.* without readjustment of pH to the nominal value. The experimental series were:

lactose	- 15 and 75mmol *per* 200ml
sodium chloride	- 15, 75 and 150mmol *per* 200ml
tartaric acid	- 15, 75 and 150mmol *per* 200ml*
sodium bicarbonate	- 15,75, and 150mmol *per* 200ml
potassium bicarbonate	- 15,75, and 150mmol *per* 200ml

*Excipient not used in ibuprofen investigation due to analytical limitations relating to the very low intrinsic solubility of this drug.

For paracetamol, data were collected at 5 minute intervals for 90 minutes and absorbance values were obtained at a wavelength in the range 295-298nm. For ibuprofen, data was collected at 6 minute intervals for 120 minutes at a wavelength of 233nm.The mass of drug dissolved (mg) *versus* dissolution time (minutes) was calculated by comparison with a linear or polynomial equation derived from a 6-point calibration. Standards were matrix-matched for dissolution medium.

4.8.4.2 Results and discussion

Firstly, for paracetamol it was observed that all the excipients inhibited dissolution rate at higher concentrations. Of the group lactose visually appears significantly more inhibitory, when reviewing figure 4.80, the reason for this will be discussed in section

4.8.6. For ibuprofen it is observed that at higher concentrations both sodium chloride and lactose inhibit the IDR. Both sodium bicarbonate and potassium bicarbonate are demonstrated to massively increase the dissolution rate. Again, the potential reasons for this will be explored in section 4.8.6.

The results are summarised in table 4.13 and illustrated in figure 4.80 and 4.81.

Table 4.13
The effect of dissolved excipients on the IDR of model drugs

Excipient/concentration (mmol/200ml)	Paracetamol IDR (mg min^{-1} cm^{-2}) ±SD	Ibuprofen IDR (mg min^{-1} cm^{-2}) ±SD
lactose-15	1.66±0.06	0.233±0.013
lactose-75	1.21±0.04	0.182±0.013
sodium bicarbonate-15	1.98±0.21	0.423±0.019
sodium bicarbonate-75	1.79±0.18	0.845±0.019
sodium bicarbonate-150	1.42±0.18	2.56±0.207
sodium chloride-15	1.89±0.29	0.235±0.007
sodium chloride-75	1.74±0.09	0.238±0.006
sodium chloride- 150	1.35±0.09	0.132±0.011
tartaric acid- 15	2.01±0.03	*
tartaric acid- 75	1.87±0.20	*
tartaric acid- 150	1.61±0.07	*
potassium bicarbonate-15	1.92±0.14	0.455±0.037
potassium bicarbonate-75	1.94±0.22	0.912±0.064
potassium bicarbonate-150	1.53±0.15	1.622±0.306

* not performed due to poor reproducibility at limit of method sensitivity

Figure 4.80
IDR of paracetamol in 0.05M HCl containing dissolved excipients. Results are the mean of at least five replicates

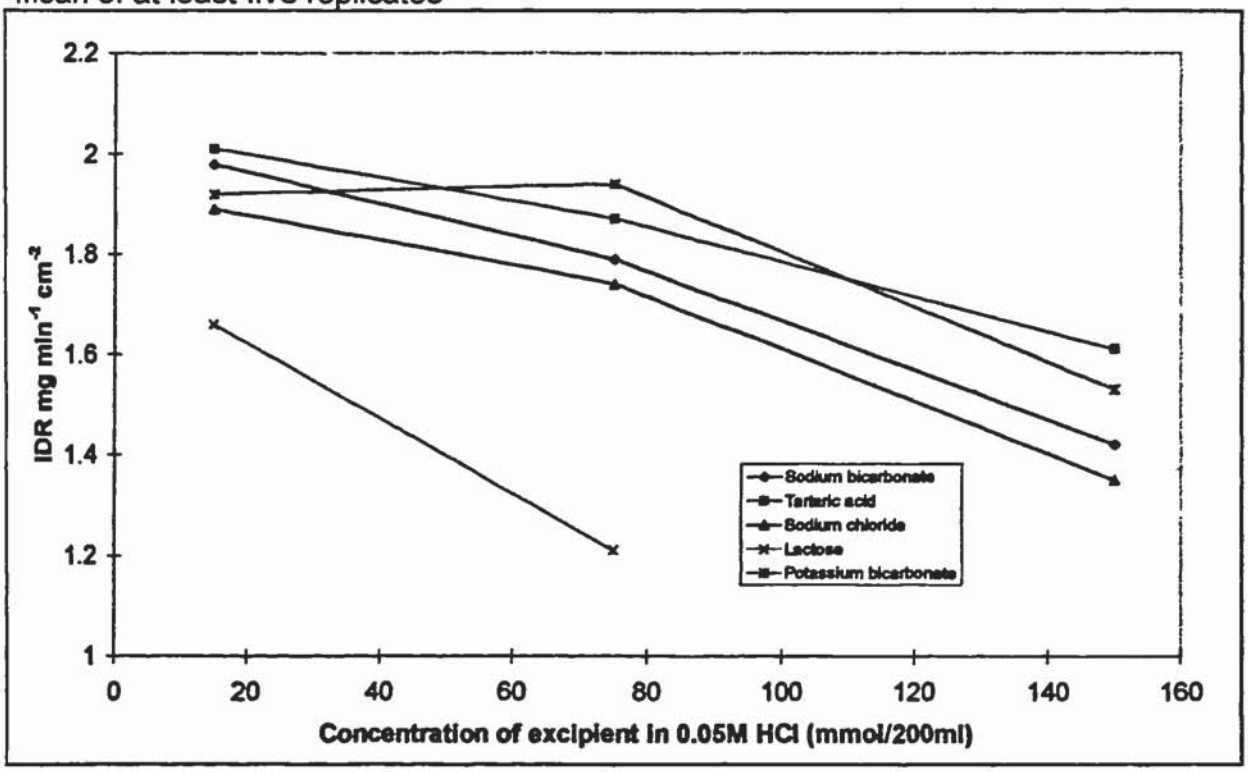

Figure 4.81
IDR of ibuprofen in 0.05M HCl containing dissolved excipients. Results are the mean of at least five replicates

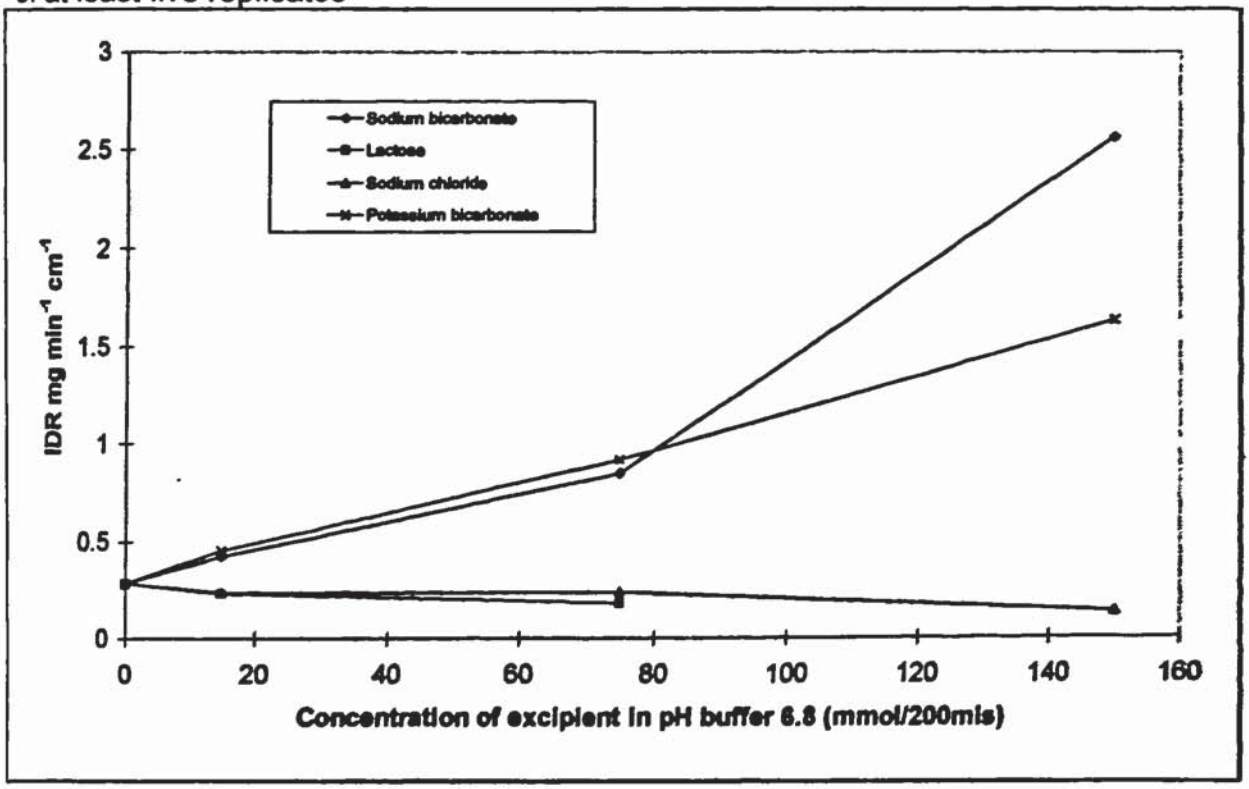

4.8.5 Comparison of a novel paracetamol formulation, containing sodium bicarbonate, *versus* commercially available paracetamol formulations

The aims of this project are based centrally on the role of excipients on the absorption of drugs. To demonstrate that selection and processing of active and excipients may affect the performance of a product, nominally identical formulations of paracetamol 500mg solid dose forms were investigated to determine the dissolution profiles in simulated stomach medium using the method developed in section 4.4.4. Secondly, as sodium bicarbonate has been postulated to increase paracetamol dissolution by modification of the dissolution hydrodynamics, the effect of reduced system hydrodynamics on the dissolution of Zapp and a typical commercial product (Panadol®) were investigated. Finally, Zapp tablets were compared to Panadol® tablets using the simulated stomach dissolution model, the data generated for use in the modelling aspect of the project conducted in Chapter 8.

4.8.5.1 Experimental

4.8.5.1.1 Materials

The following commercial products were purchased from retail outlets or supplied by SB (Weybridge, UK) as indicated by an asterisk:

- Anadin® paracetamol, Whitehall Labs, 500mg coated tablet, pack of 24, B/N E2079A, Exp. Oct 2002
- Boots® paracetamol, 500mg caplets, pack of 12, B/N 4N, Exp. Sep 00
- Panadol®, Smithkline Beecham, 500mg coated tablets, pack of 24, B/N 1SB849, Exp. Mar 2001
- Superdrug® paracetamol, Sanofi Winthrop, 500mg coated tablets, pack of 24, B/N IPN196, Exp. Nov 02
- Hedex® paracetamol, Smithkline Beecham, 500mg caplets, pack of 16, B/N INL902 Exp. Oct 99
- *Hedex® paracetamol , Stirling Health, 500mg caplets, pack of 20, B/N 95B28, Exp. Feb 02
- *Zapp paracetamol, Smithkline Beecham, 500mg caplets, prototype and B/N C328.8.003.

- *No Frills® paracetamol, Franklins Ltd, 500mg tablets, pack of 24, B/N 35771, Exp. June 2000
- *Panadol® paracetamol, Smithkline Beecham Australia, 500mg tablets, pack of 24, B/N TDO317, Exp. Apr 01
- *Panadol® paracetamol, Smithkline Beecham Australia, 500mg caplets, pack of 24, B/N TEO391, Exp. May 01
- *Herron® paracetamol, Herron Australia, 500mg tabsules, pack of 24, B/N 35995, Exp. Jul 2000
- *Herron® paracetamol, Herron Australia, 500mg tablets, pack of 24, B/N 35947, Exp. Jul 2000
- Tylenol® paracetamol, McNeil Consumer Products 500mg tablets, pack of 100, B/N BBA151

4.8.5.1.2 Equipment

The equipment and set-up was as described in section 4.8.2.1.2.

4.8.5.1.3 Method

Coarse filters (10 micron), capable of removing the particulates generated during tablet dissolution, were attached to each sampling point. 0.05M HCl dissolution medium, *i.e.* 900ml *per* flask was prepared and thoroughly degassed using helium sparging. Temperature was controlled at 37±0.5°C. After equilibration of the dissolution medium temperature and sampling flow-through system, each sampling station was background zeroed. The pump and paddles were switched off while the tablets were positioned at the bottom of the flask. The pump and paddles were restarted at 50rpm for the commercial tablet comparison and between 10-50rpm for the study into the effects of reduced system hydrodynamics, and the data collection system initiated. Absorbances were obtained at a wavelength of 300nm at 3 minute intervals for 30 minutes. The mass of the drug dissolved (mg) *vs.* dissolution time (minutes) was calculated by comparison with a linear or polynomial equation derived from the 6-point calibration data. Standards were prepared in the dissolution medium. The comparison of Zapp *versus* Panadol® in the simulated stomach model was conducted according to the method detailed in section 4.7.2.3.

4.8.5.2 Results and discussion

Summarising the commercial products comparison, for all formulations, except the Boots product, dissolution was completed within 18 minutes. Examples of some of the dissolution profiles are illustrated in figure 4.83, it is clear that the Zapp prototype formulation dissolves more quickly than all the other formulations. It can also be observed that all the tablets, except the Zapp prototype formulation, exhibit a time lag (visible from 0-3 minutes). Visually, this corresponds to the time taken for initial disintegration to occur. The Zapp prototype product began to disintegrate/dissolve immediately in the dissolution medium due to effervescence. To fully clarify the rank order and differentials between the products, the dissolution data from 3, 6 and 9 minute timepoints were transformed to obtain the difference factor F_1 with the Zapp prototype formulation as the reference product, as illustrated in figure 4.82. When comparing the F_1 fit-factors, it is noted that there is clearly a large variation between the different marketed brands of the same drug. As a guide a difference of >15 from the reference, which would indicate FDA requirement for similarity (FDA(CDRA) 1997) was not satisfied. Interestingly, the coated Zapp tablet B/N C328.8.003 shows a significant lag-time, related to the penetration of the film coat by the dissolution fluid, ensuring the F_1 value in the mid-range of the group. The Boots product appears to be, significantly, the poorest product in terms of dissolution performance.

The comparison between one of the commercial products (Panadol® B/N 1SB849) *versus* the Zapp (B/N C328.8.003) under different stirring conditions demonstrated that the Panadol® tablet's dissolution rate was reduced as the stirring speed, and hence system hydrodynamics, were reduced. Conversely, for the Zapp prototype the dissolution rate was effectively unchanged as the stirrer speed was reduced. It can be concluded that the effervescence produced by the Zapp tablet as it dissolved contributes more significantly to the hydrodynamics than the action of the stirrer, effectively the Zapp tablet is self-dissolving. The results are illustrated in figures 4.84-4.85. A comparison of Zapp (B/N C328.8.003) and Panadol® B/N 1SB849 tablets in the simulated stomach model also showed an increased absorption rate for Zapp as illustrated in figure 4.86. Overall the study illustrated that differences in dissolution characteristics are present in commercial variations of nominally the same product.

Figure 4.82
Illustrating the variation between the dissolution characteristics of commercially formulated paracetamol 500mg solid dosage forms, by transformation of the dissolution profiles to yield difference factor F_1. Reference Zapp prototype F_1=0.

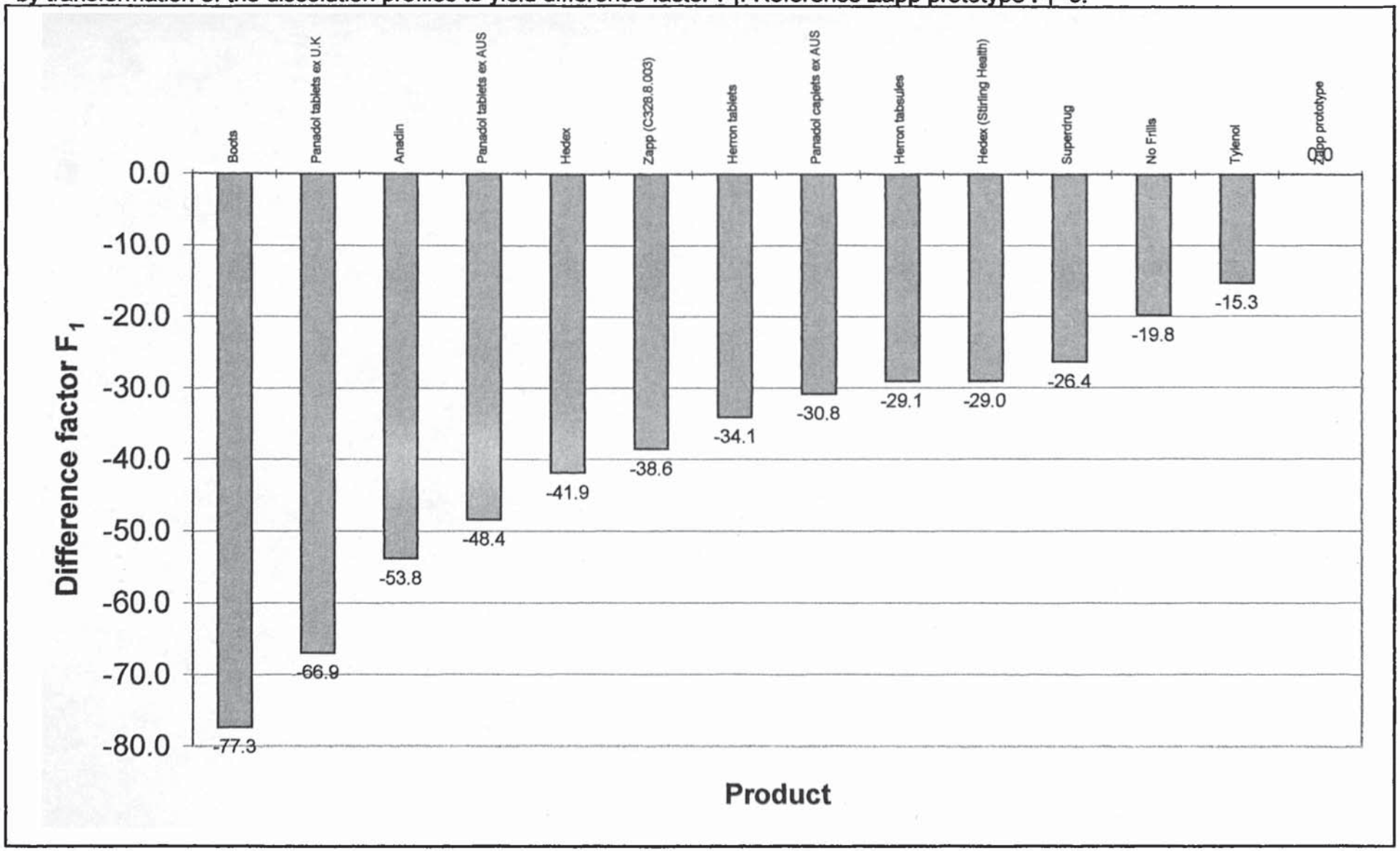

Figure 4.83
Illustrating the dissolution profiles of commercial paracetamol 500mg solid dosage forms. Results are the mean of six replicates.

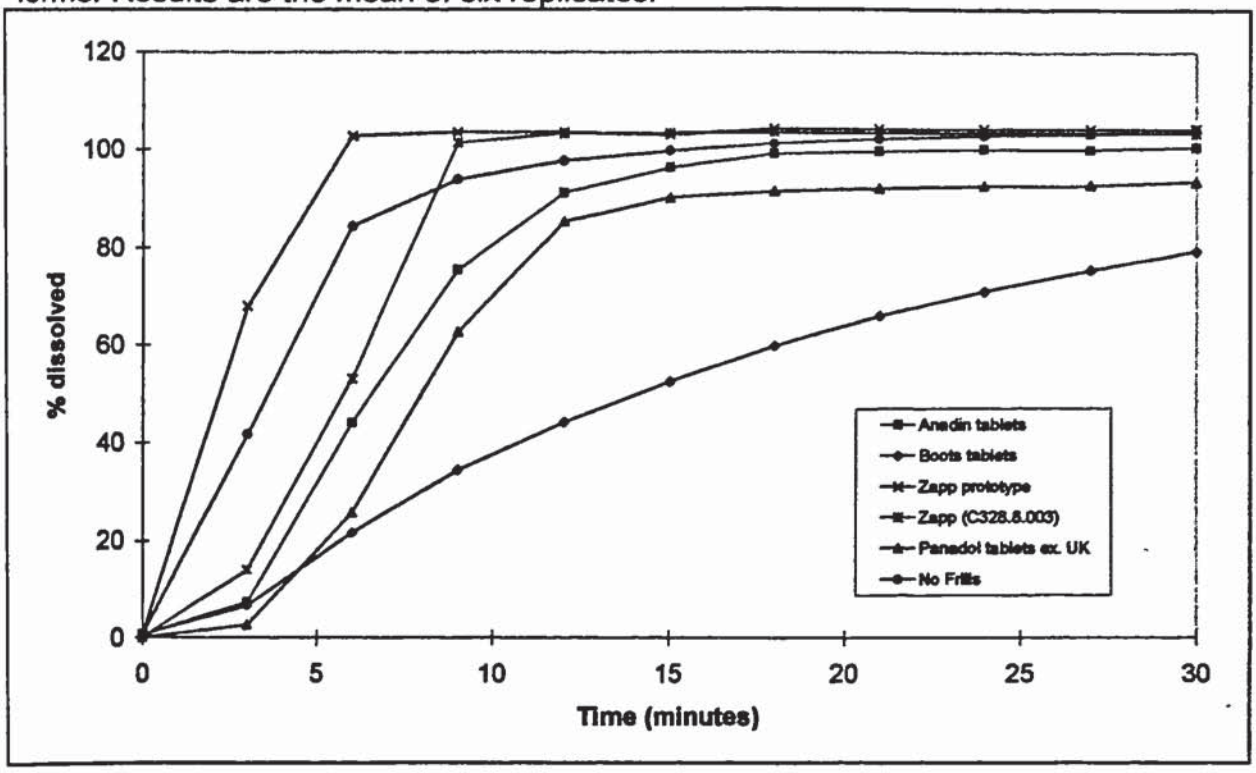

Figure 4.84
Illustrating the dissolution profiles of Panadol® tablets ex U.K. at different stirrer speeds. Results are the mean of six replicates

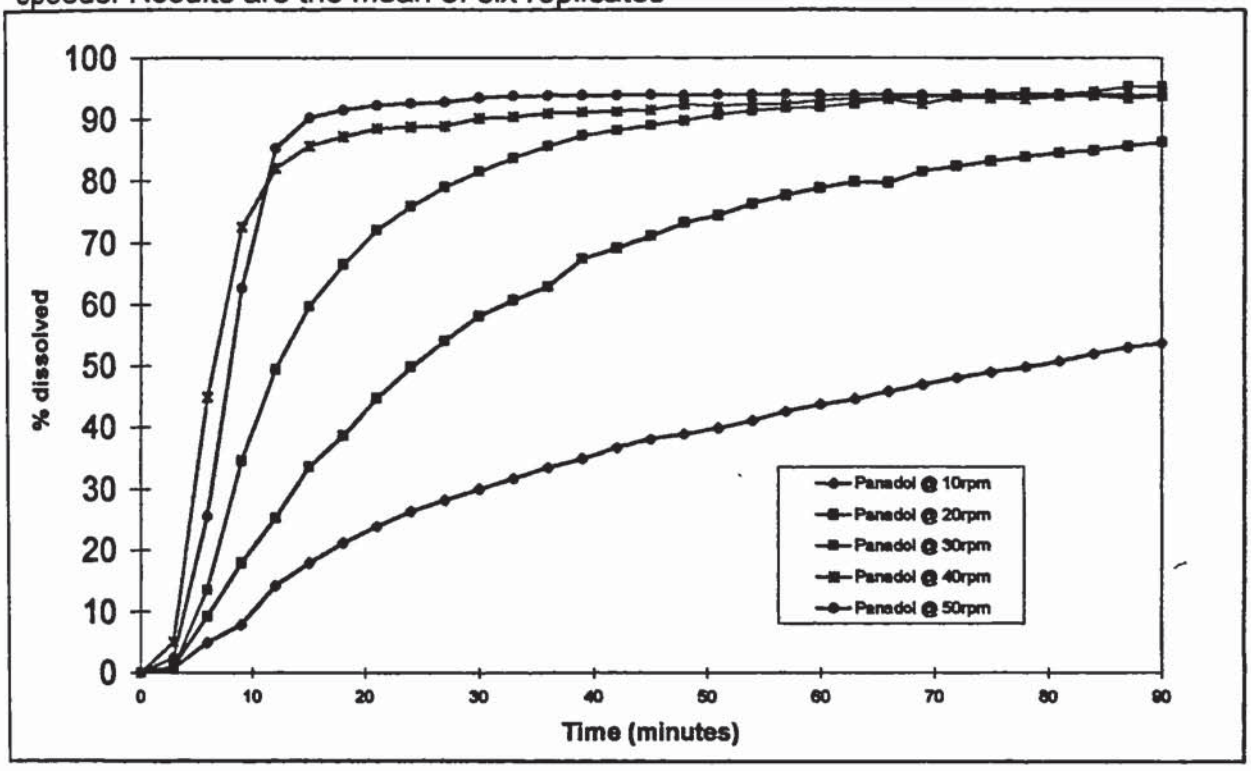

Figure 4.85
Illustrating the dissolution profiles of Zapp (C328.8.003) at different stirrer speeds. Results are the mean of six replicates

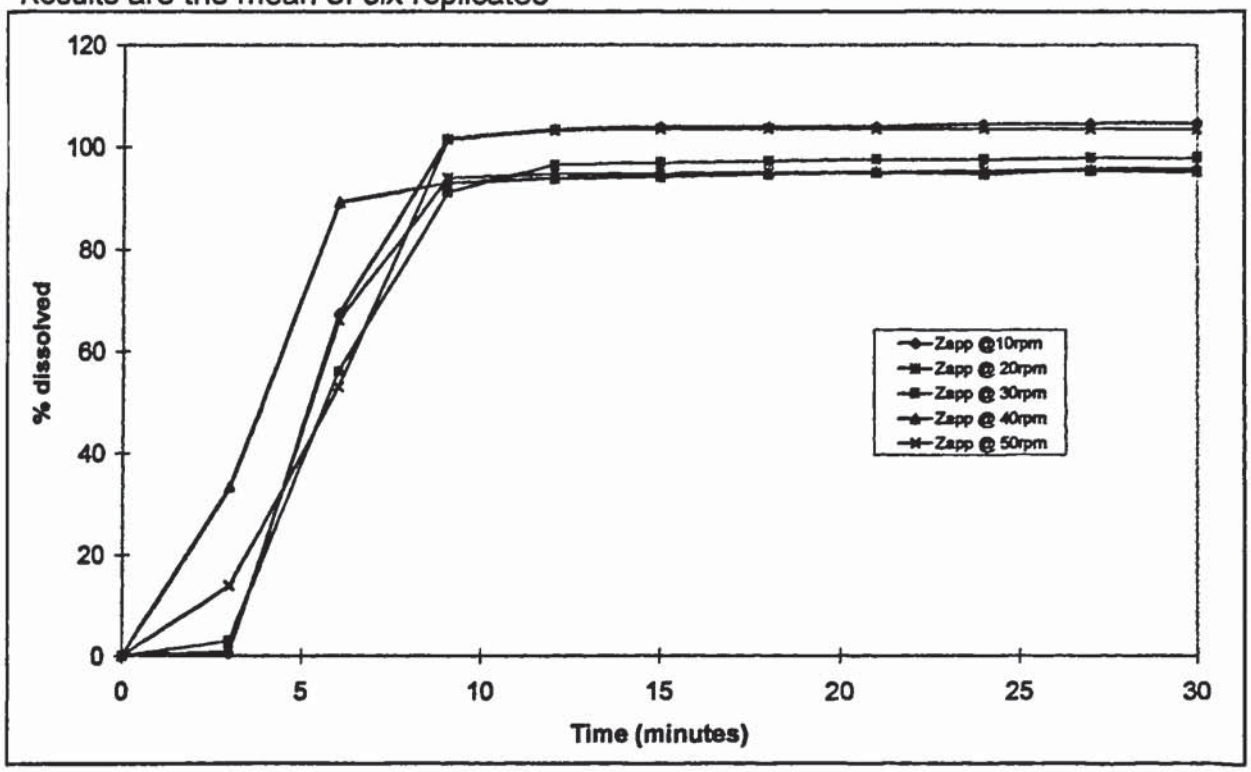

Figure 4.86
Illustrating the dissolution profiles of Zapp (C328.8.003) and Panadol ex. UK in the simulated stomach model. Results are the mean of 6 replicates with SD as appropriated for visual clarity

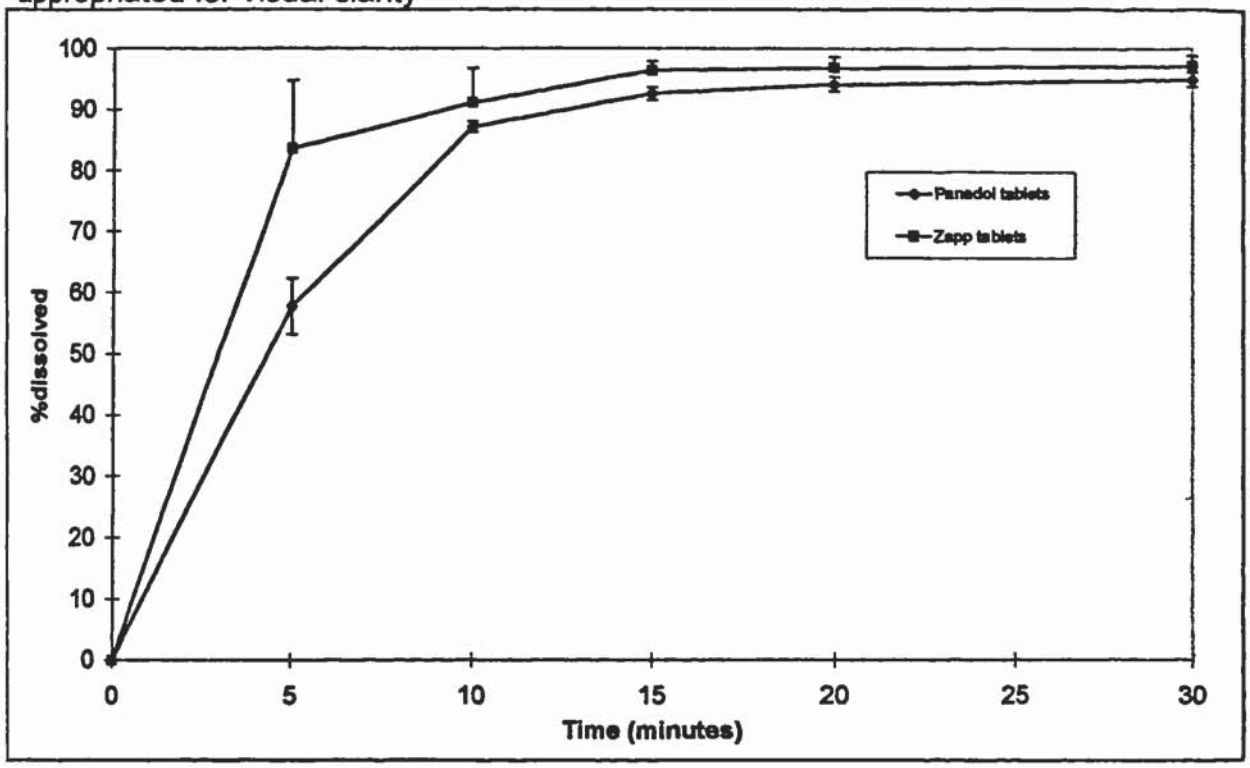

4.8.6 Characterisation of the role of sodium bicarbonate on the dissolution of model drugs

It has been shown that the model drugs dissolve according to the diffusion layer model, when they are compressed into pure drug pellets. It has also been demonstrated in the controlled powder dissolution study that, generally, alkalising excipients will promote the dissolution of the model drugs and that this is probably due to an increase in solubility of the drugs with increasing pH. Excipients that effervescence in solution, *i.e.* sodium bicarbonate and potassium bicarbonate, have also been demonstrated to significantly promote dissolution by altering the hydrodynamics of the system, *e.g.*, comparison of sodium bicarbonate:paracetamol powder mixes dissolution in water and 0.05M HCl. To further characterise the role of sodium bicarbonate, experimental work was undertaken to determine the IDR and solubility of the model drugs in excipient-containing solutions and also the viscosity of these solutions. Using the experimental data the dissolution process was reviewed.

If the surface area of the dissolving drug remains constant, as in the IDR method detailed in 4.43 equation 4.5 can be reiterated thus:

$$IDR = kCs$$

and

$$k = \frac{D}{h}$$

where

$$D = \frac{RT}{6Nr\pi\eta}$$

As η is the kinematic viscosity, it is apparent that the dissolution rate constant is inversely proportional to the viscosity of the dissolution medium (Macheras *et al.*, 1995). It has been shown that the IDR of paracetamol decreases with increasing viscosity, for solutions containing mixtures of taurine, glycine and sorbitol (Mahmud and Li.Wan.Po 1991). However, this work did not take into account changes in saturated concentration of drug in the various solutions (C_s).

By rearrangement it can be shown that

$$\frac{IDR}{Cs} * \eta = \frac{RT/6Nr\pi}{h}$$

R, *T*, *N* and π are constants, assuming the radius of the molecule in solution *r* is not measurably changed, a fair assumption on the basis that most carboxylic acids are dimeric in nature in neutral solutions, any drug-excipient interactions would form simple salts and the parameter is based on the cube root of the size) and that the hydrodynamics are unchanged, it can be deduced that, theoretically:

$$\frac{IDR * \eta}{Cs} = k_2 \qquad \text{equation 4.11}$$

where k_2 is a constant as defined in equation 4.11. The experimental data obtained for IDR, C_s and η was processed using equation 4.11. The results for paracetamol and ibuprofen are summarised in tables 4.14 and 4.15, respectively.

Table 4.14

Summary of measured factors contributing to the dissolution of paracetamol from pellets using the IDR paddle method and calculation of constant k_2. IDR and solubility results are reproduced from sections 4.84 and 3.2, viscosity results were obtained using the method described in section 2.4. k_2 values were calculated using replicate crossover analysis and by use of equation 4.11.

Excipient concentration (mmol/200ml)	IDR mg $min^{-1}cm^{-2}$ ±SD	Viscosity cm^2 min^{-1}	Saturated solubility mg ml-1 ±SD	$\frac{IDR * \eta}{Cs}$ (k_2) $min^{-2}cm^{-3}$ ±SD
lactose-15 .	1.66±0.06	0.4524	19.2 ± 1.4	0.0399±0.003
lactose- 75	1.21±0.04	0.5448	19.2 ± 0.3	0.0336±0.001
sodium bicarbonate- 15	1.98±0.21	0.4308	18.5 ± 0.2	0.0455±0.005
sodium bicarbonate-75	1.79±0.18	0.444	16.5 ± 0.2	0.0467±0.004
sodium bicarbonate-150	1.42±0.18	0.4632	14.1 ± 0.3	0.0438±0.005
sodium chloride - 15	1.89±0.29	0.4278	18.7 ± 0.4	0.0434±0.006
sodium chloride - 75	1.74±0.09	0.4272	16.5 ± 0.1	0.0452±0.002
sodium chloride - 150	1.35±0.09	0.4344	14.2 ± 0.3	0.0413±0.003
tartaric acid- 15	2.01±0.03	0.4362	19.4 ± 0.8	0.0452±0.002
tartaric acid- 75	1.87±0.20	0.4572	19.8 ± 0.8	0.0431±0.005
tartaric acid - 150	1.61±0.07	0.4872	22.0 ± 0.7	0.0338±0.002
potassium bicarbonate -15	1.92±0.15	0.4242	20.5±0.8	0.0405±0.003
potassium bicarbonate-75	1.94±0.22	0.4302	20.3±0.3	0.0426±0.006
potassium bicarbonate-150	1.53±0.15	0.4344	16.4±0.6	0.0447±0.004

Reviewing the data for paracetamol, which is illustrated in figure 4.87, it was generally noted that all the data appeared to be from the same population. This was tested by plotting the sampling distribution as illustrated in figure 4.88. The data were visually assessed as fitting a normal distribution model. From these graphs, it can be concluded that the excipients under investigation, in solution, affect the dissolution of paracetamol only through the mechanisms of modification of saturated solubility and solution viscosity. Specifically for sodium bicarbonate, it was demonstrated that, in solution, it inhibits dissolution of paracetamol by reducing the saturated solubility and by increasing the viscosity of the solution. Also, the low IDR observed for the lactose 75mmol/200ml experiment can be explained in terms of a much higher solution viscosity than all the other solutions under test (see table 4.14). Clearly, from the work undertaken in section 4.6, it has been established that the primary promotive effect of sodium bicarbonate on the dissolution of paracetamol is the effective reduction of the boundary layer due to by effervescence. The lesser promotive effect

observed when using water as the dissolution fluid, and therefore restricting effervescence, cannot be explained by this study.

Neervannan *et al.* (1994b) determined that co-compression of an effectively inert drug (phenytoin) with an ionisable drug (naproxen) did not change the dissolution mechanism in a non-dissociating (pH 2) medium and the dissolution rate decreased with increasing inert fraction in the tablet. This makes the point that if the excipient is effectively inert, the dissolution rate will decrease due to reduction of available surface area. Also, it has been demonstrated in section 4.6 that variation is seen between the dissolution of drugs from excipient:drug mixtures using neutral or 'inert' excipients. These can obviously be caused by the mechanisms studied in this investigation but also by a mechanism proposed by Neervannan *et al.* (1994a; 1994b) where the dissolution rate *versus* the calculated surface area was found to be non-linear for a series of co-compressed naproxen/phenytoin slabs. Their explanation was that the deviation was due to 'carry-over' of material from the active component to the inert component due to fluid flow, resulting in an increase in the apparent surface area of the slab. Further to this, Chakrabarti and Southard (1997) demonstrated that the use of a buffer as a co-compressate to aid dissolution of naproxen, namely calcium carbonate, increased the area-corrected dissolution flux by a factor of ≈10 whereas the inert co-compressate phenytoin increased the flux by 1.7 (in a 50:50 mixture). They concluded that both 'carry-over' and buffering action acted to promote drug dissolution. This may explain why dissolution rates of drug:inert excipient mixtures vary depending on the excipient but it cannot be used to explain a higher rate than that demonstrated by pure drug.

Figure 4.87
Illustrating calculated values of k_2 constant for dissolution of paracetamol in excipient containing solutions. Results are the mean±SD derived using cross-over analysis. Excipient concentrations expressed as mmol/200ml

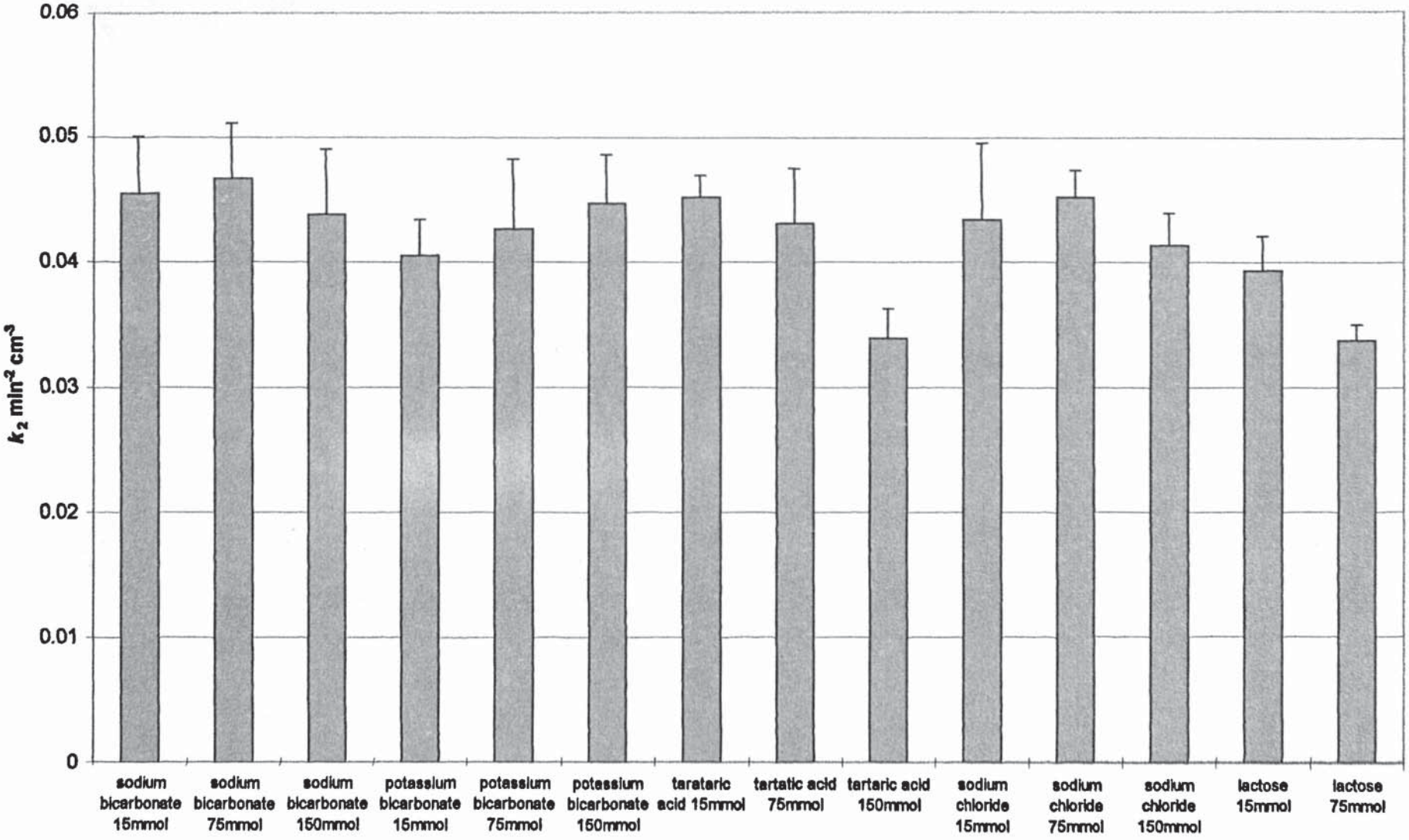

Figure 4.88
Histogram of calculated k_2 values obtained for paracetamol dissolution in excipient-containing medium. Results are all calculated values from crossover analysis, for all excipients.

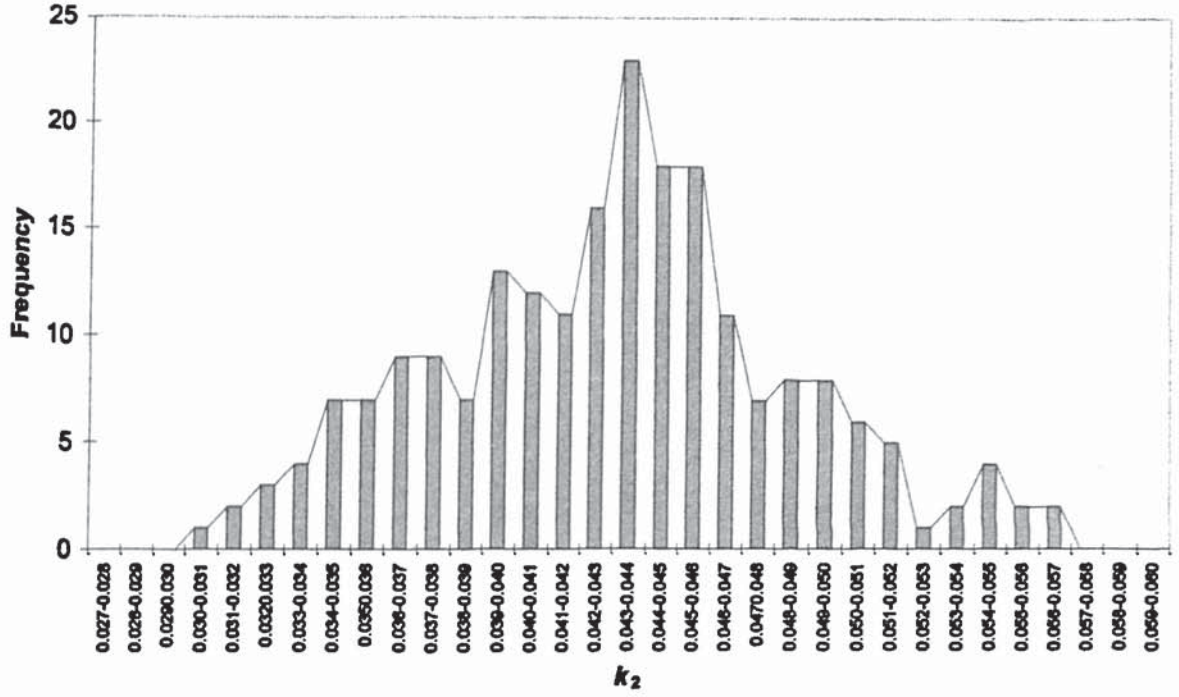

Table 4.15
Summary of measured factors contributing to the dissolution of ibuprofen from pellets using the IDR paddle method and calculation of constant k_2. IDR and solubility results are reproduced from sections 4.84 and 3.2, viscosity results were obtained using the method described in section 2.4. k_2 values were calculated using replicate crossover analysis and by use of equation 4.11.

Excipient concentration (mmol/200ml)	IDR mg $min^{-1}cm^{-2}$ ±SD	Viscosity cm^2 min^{-1}	Saturated solubility mg ml-1 ±SD	$\frac{IDR * \eta}{Cs}$ (k_2) $min^{-2}cm^{-3}$ ±SD
lactose-15 .	0.232±0.013	0.4523	3.11±0.00	0.0344±0.001
lactose- 75	0.182±0.013	0.5599	2.90±0.15	0.0355±0.003
sodium bicarbonate- 15	0.423±0.002	0.4396	11.3±0.01	0.0165±0.008
sodium bicarbonate-75	0.845±0.019	0.4441	49.9±3.0	0.0076±0.000
sodium bicarbonate-150	2.56±0.21	0.4961	109±11.4	0.0117±0.002
sodium chloride - 15	0.235±0.007	0.4342	3.08±0.21	0.0335±0.003
sodium chloride - 75	0.238±0.006	0.4256	2.35±0.27	0.0447±0.003
sodium chloride - 150	0.132±0.011	0.4297	1.77±0.25	0.0330±0.006
potassium bicarbonate -15	0.455±0.037	0.4330	9.75±1.50	0.0208±0.002
potassium bicarbonate-75	0.912±0.065	0.4334	59.5±2.8	0.0096±0.008
potassium bicarbonate-150	1.76±0.665	0.4339	205.6±9.4	0.0042±0.001

Reviewing the data for ibuprofen, which is illustrated in figure 4.90, it can generally be noted that all the data appear to separate into two distinct groups, one containing the sodium and potassium bicarbonate solutions and the other containing the sodium chloride and lactose solutions. Figure 4.91 illustrates the sample distribution which confirms the data fits a bi-modal distribution model. It is clear that the model proposed in equation 4.11 does not completely describe the dissolution process for ibuprofen in the excipient-containing solutions under investigation. Further to this, the pH-modifying and solubility-increasing excipients, *i.e.* sodium bicarbonate and potassium bicarbonate, are grouped together with much lower k_2 values than sodium chloride and lactose-containing solutions. It is known that surface dissolution of weak acids may buffer the boundary layer to a value near the pK_a of the drug and this is one reason why USP buffers, which are capable of overcoming this effect, are used in dissolution studies (Macheras *et al.* 1995). Considering this further, it is unlikely that the viscosity and IDR measurements taken are unrepresentative of the process but it is postulated that the experimental values of saturated solubility may not represent the situation *in-situ*. The saturated solubilities were measured on bulk solutions, allowed to equilibrate over several days; however, the actual saturated solubility in the boundary layer may be lower due to modification of the micro-environment by the dissolving drug as illustrated in figure 4.89. This effect may also be responsible for the lower than expected IDR of paracetamol found in the high pH solutions in the work undertaken in section 4.83 - effect of pH on IDR of paracetamol. The ability of a pH modifying-excipient to penetrate the boundary layer appears to be an important property requiring consideration in a tablet development strategy.

Figure 4.89
Representation of the dissolution process illustrating how the incomplete penetration of sodium bicarbonate into the boundary layer may alter the saturated solubility of drug compared to that within the bulk solution.

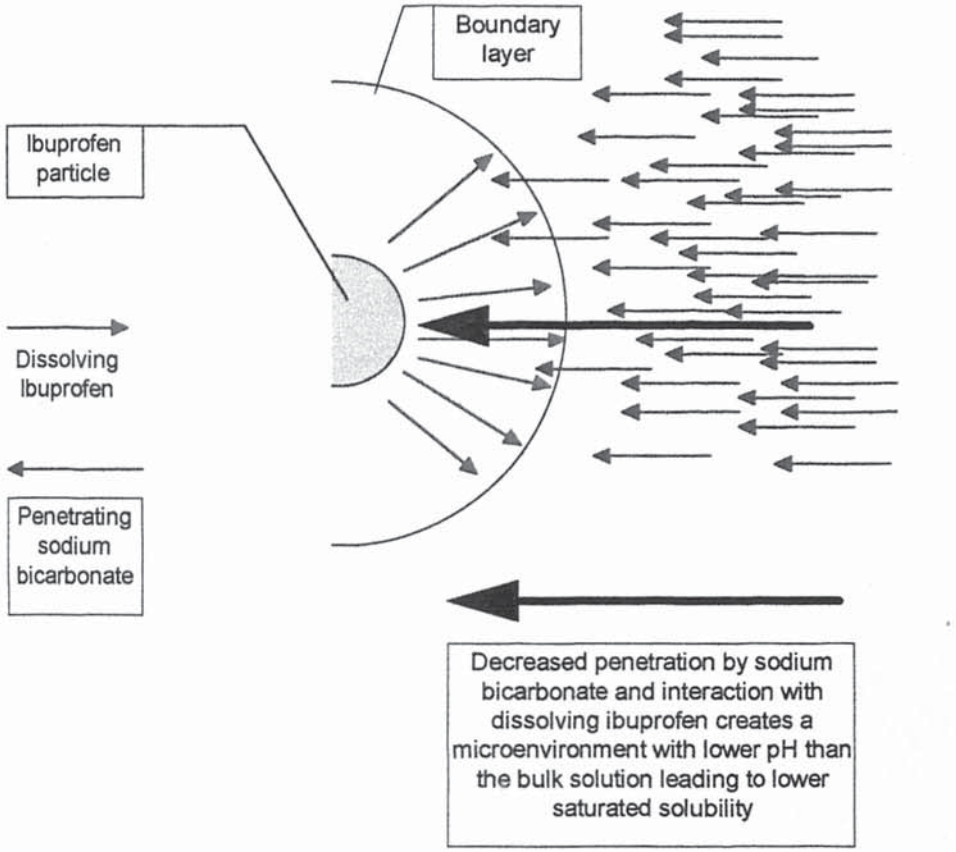

To conclude, this initial dissolution study has demonstrated that several factors have to be taken into account when developing formulations containing pH-modifying excipients. Excipients that promote dissolution and can be used in product formulations should have the following properties:

- compatibility with the drug
- sufficient alkalinity to modify bulk dissolution volume fluid pH to allow complete dissolution of drug
- sufficient alkalinity and penetration ability to modify the boundary layer microenvironment.
- modify hydrodynamics through effervescence

It is likely that an optimised dissolution- promoting tablet formulation would contain multiple pH modifying excipients encompassing all of the desired properties.

Figure 4.90
Illustrating calculated values of k_2 constant for dissolution of ibuprofen in excipient containing solutions. Results are the mean±SD derived using cross-over analysis. Excipient concentrations expressed as mmol/200ml

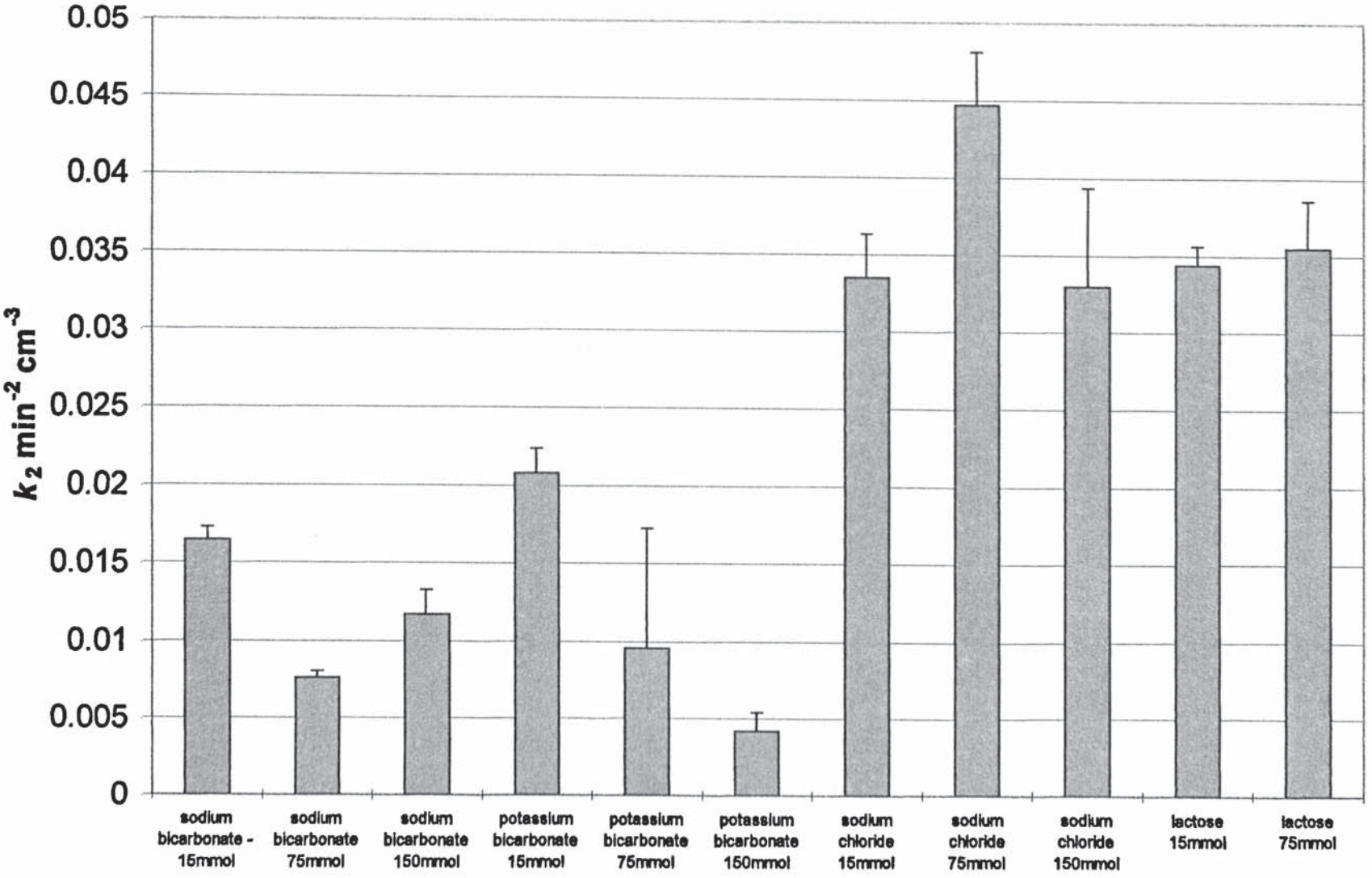

Figure 4.91
Histogram of calculated k_2 values obtained for ibuprofen dissolution in excipient-containing medium. Results are all calculated values from crossover analysis, for all excipients.

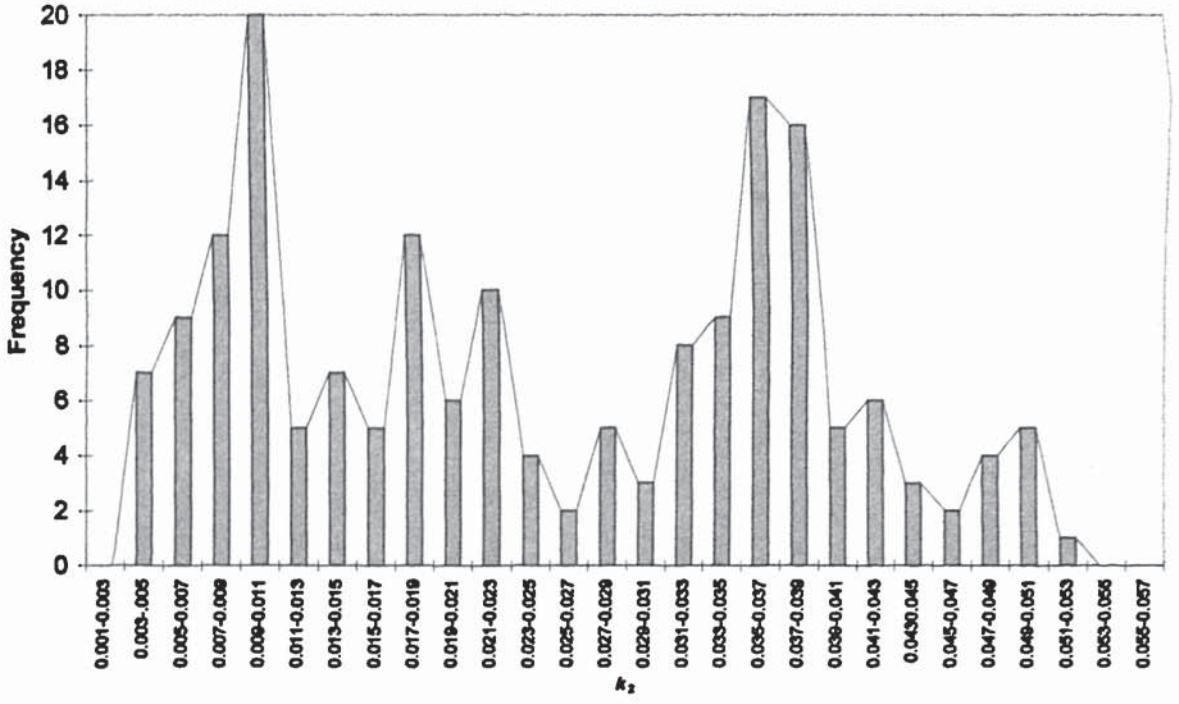

4.8.7 Summary

- A novel dissolution method with modified baskets has been developed which has been found to be suitable for the analysis of the dissolution behaviour of drug:excipient powder mixtures. The method was found to control the surface area of the dissolving powder sufficiently to linearise a substantial part of the dissolution profile. The method could also detect differences between the drug:excipient mixtures, with the dissolution rates obtained in line with expectations, based on a knowledge of the excipients properties. The dissolution rate values, calculated from the linear section of the diffusion profile, correlated with the calculated difference factors, indicating that the method is suitable for quantitative and qualitative assessment of dissolution behaviour.

- Results from the controlled powder dissolution study indicate that L-lysine, L-arginine, trisodium phosphate, sodium bicarbonate and potassium bicarbonate enhance the dissolution rate of both ibuprofen and paracetamol. Additionally,

sodium carbonate also had this effect on ibuprofen. Selected excipients were chosen for further investigation in the product formulation study.

- The role of various antacids on the dissolution of the model drugs, in tablet form, during co-administration has been characterised. The method selected for study utilised standard paddle apparatus with dissolution medium volume and composition correlating with the stomach and intestinal environment, with drug and antacid concentrations set to nominal *in vivo* levels.
- For paracetamol, the results from the experimental work in simulated stomach medium suggest that co-administered magnesium hydroxide, sodium bicarbonate, calcium carbonate or aluminium hydroxide slightly, but not significantly, improve the dissolution rate of the drug. Magnesium oxide addition caused the dissolution to plateau at between 60-70% dissolution. In the intestinal environment the effect of co-administered antacids was marginal, except for aluminium hydroxide and magnesium oxide where the dissolution reached a plateau between 70-80%.
- For ibuprofen, the results indicate that, in simulated stomach medium, aluminium hydroxide does not increase the dissolution rate of the drug. All the other antacids profoundly increase the drug dissolution rate, in line with their ability to neutralise the acid environment. In the intestinal environment, all of the antacids, with the exception of aluminium hydroxide, again act as dissolution promoters with a trend between rate and solution pH being apparent. Aluminium hydroxide had a negligible overall effect but caused the dissolution to plateau between 70-80%.
- The role of sodium bicarbonate as a dissolution-promoting excipient has been characterised.
- Using the powder-dissolution method sodium bicarbonate, along with potassium bicarbonate, were found to have the most dissolution-promoting effect of the excipients under test for both drugs. Effervescence caused by the bicarbonates reaction with the acidic medium was found be the major contributor to dissolution promotion in the paracetamol experiments. Also of interest was the observation that potassium bicarbonate produced effervescence even under dissolution conditions when the solution was not acidic whereas the sodium bicarbonate did not exhibit this effect. It is known that the potassium salt is more reactive than the sodium salt and it is postulated that a paracetamol:potassium bicarbonate acid:base reaction occurred. The results also indicated that sodium bicarbonate

appeared to promote dissolution of paracetamol by a mechanism other than effervescence and this was studied further.

- For ibuprofen, the effervescence phenomenon was observed for both bicarbonates even though the medium used was USP buffer pH6.8. It is postulated that ibuprofen was acting as the acid in the effervescence reaction.
- To study factors other than effervescence that may contribute to the promotive effect, a novel IDR method was developed based on paddle apparatus. This method was validated and was then used to determine that the dissolution process for both drugs could be best described by the diffusion-layer model.
- The effects of dissolved excipients, over a concentration range of one order of magnitude selected to mimic the effect of a co-present dissolving excipient, on the dissolution of the model drugs was studied using the IDR. The excipients were selected to cover a range of properties and included the two bicarbonate salts, tartaric acid (paracetamol only), lactose and sodium chloride. The results indicated that dissolved excipients retarded the dissolution of paracetamol. For ibuprofen, dissolved sodium chloride and lactose inhibited the dissolution rate at higher concentrations whereas both of the bicarbonates had a large promoting effect.
- Data were collated from the IDR, solubility and viscosity studies and using the equation applicable for the diffusion layer model a constant k_2 was derived which could be described in terms of IDR, viscosity and saturated solubility. Processing of the experimental data through this equation demonstrated that the paracetamol values obtained fitted a normal distribution model. From this, it was concluded that sodium bicarbonate acts to inhibit dissolution by reduction of saturated solubility and by increasing solution viscosity and that the measured effects correlated with those found for the other excipients. A review of possible other factors did not yield any mechanism that could be responsible for the dissolution-promoting effect. Therefore, it was concluded that the only dissolution-promoting property of sodium bicarbonate with respect to paracetamol was that caused by the modification of the hydrodynamic layer by effervescence. The promotive effect observed when the acid/base reaction was restricted may be attributed to paracetamol acting as an acid and reacting with sodium bicarbonate. For ibuprofen, processing of the experimental data to produce k_2 yielded a bi-modal distribution model with both bicarbonates yielding much lower k_2 values than lactose and sodium chloride. A

review of the experimental procedures led to the conclusion that the measured saturated solubility did not represent the solubility *in situ* and it was postulated that this was due to incomplete penetration of sodium or potassium bicarbonate into the boundary layer of the dissolving drug. This highlighted that it is not only an excipient's pH in solution that is important but also the ability of the excipient to modify the dissolving drug's micro-environment.

- The dissolution profile of commercial paracetamol tablets was compared to the Zapp formulation using paddle apparatus and simulated gastric fluid as the medium. The results illustrated differences in products considered to be nominally the same. The Zapp prototype was found to be the fastest dissolving product on test.
- Modifying the system hydrodynamics demonstrated no change in the dissolution behaviour of the Zapp tablets . However, a reduced stirring rate led to a decrease in Panadol® dissolution rate as would be expected. It was concluded that the Zapp tablets were 'self-dissolving'.
- Zapp tablets were demonstrated to dissolve more rapidly compared to the Panadol® commercial product, in the simulated stomach model. The dissolution rates were estimated for use in chapter 8.

CHAPTER 5
DRUG DIFFUSION THROUGH MUCUS

5.1 Introduction

As described in section 1.51, a model to describe the absorption processes of a drug must consider the role of mucus as a potential barrier and also the effects on diffusion of the drug by any co-administered material. Ideally, the model should be capable of determining the magnitude of the barrier when compared to the barrier systems as a whole and also to characterise the degree and nature of any modification to the barrier and hence absorption.

One of the earliest investigations of diffusion through mucus was performed by Heatley (1959). It was shown that there was no significant difference between diffusion of hydrochloric acid and pepsin through pyloric and duodenal mucus in comparison to diffusion through an unstirred aqueous layer of the same thickness. Therefore, it was assumed that it was the stationary nature of this layer that was of the greatest importance to drug diffusion rather than any interactions between drug and molecules comprising the mucus gel. Diluted mucus preparations were, however, used in this study at non-physiological concentrations. This idea remained undisputed until the role of gastric mucus in cytoprotection was investigated.

Several studies have subsequently been performed to investigate the diffusion of hydrogen ions through mucus from different species located at a variety of anatomical sites. All of the studies demonstrated that the diffusion rate of hydrogen ions was significantly slower through a mucus layer than through an aqueous unstirred layer of the same thickness.

To summarise these studies:

- Pfeiffer (1981) observed a two-fold reduction in the rate of diffusion of hydrogen ions using three-compartment diffusion cells and mucus collected from the rabbit small intestine, pig stomach, rat intestine and human colon.
- A similar, 2-fold reduction was also observed by Winne and Verheyen (1990) who employed rat small intestinal mucus and both three-compartment diffusion cells and capillary methodology.
- A larger, 5-fold reduction was reported by Turner *et al.* (1985) employing native porcine gastric mucus and three-compartment diffusion cells.
- A 10-fold reduction has been reported by Slomiany *et al.* (1986) with pig gastric mucus and Sarosiek *et al.* (1984) with dog gastric mucus.

Also, there have been various reports of the modification of diffusion rate of drugs by mucus when compared to an aqueous unstirred layer.

To summarise these studies:

- Matthes *et al.* (1992) found that the disappearance rate of compounds of various polarities through a diffusion chamber was reduced when buffer solutions in a drug-buffer mixture were replaced with mucus solution.
- Braybrooks *et al.* (1974) observed an 50% decrease in the apparent permeability coefficients for tetracycline in the presence of mucus using a combination of perfusion, everted gut studies and diffusion cell techniques.
- Karlsson *et al.* (1993) found, in a study of testosterone permeation through a mucus-producing human goblet cell line (HT29-H), that the permeability coefficients increased by approximately 50% when the mucus layers were removed.
- Bhat *et al.* (1995) found, for a group of three structurally diverse drugs with different binding capacities, the diffusion rate through purified mucus was reduced by approximately 50% for all compounds tested.

- Holbrook (1991) found that for a group of diverse peptides the diffusion rate was reduced to between 40-80% compared with an aqueous layer.

Further to these studies, it has it has been demonstrated that additives can act as absorption enhancers or inhibitors to the diffusion process. For example Turner *et al.* (1985) demonstrated that N-acetylcysteine could increase the diffusion rate of hydrogen ions by a factor of 1.5, through native gastric mucus. Conversely, Grubel and Cave (1998) found that the diffusion rate of clarithromycin was reduced to approximately 20-30% of the rate when antacid formulations containing aluminium and magnesium were added to the semi-purified mucus barrier.
In this study, a *in vitro* stomach mucus model was selected, developed and validated and the diffusion rates of the model drugs were determined. Also, the potential role of the antacids/excipients on the diffusion rate of the model drugs were investigated. Three-compartment diffusion cells were used for initial diffusion studies followed by a modified system, designed to model the stomach environment more closely.

5.2 Theoretical Considerations

Typically, the diffusion of a drug across a membrane, such as mucus, comprises two distinct stages; a non-linear, non-steady state diffusion stage, followed by a steady-state penetration which is linear and corresponds to a net balance in the rate of entry and exit of drug into and out of the membrane layer. A typical diffusion profile is illustrated in figure 5.1.

Figure 5.1
Schematic representation of a typical diffusion profile through a membrane

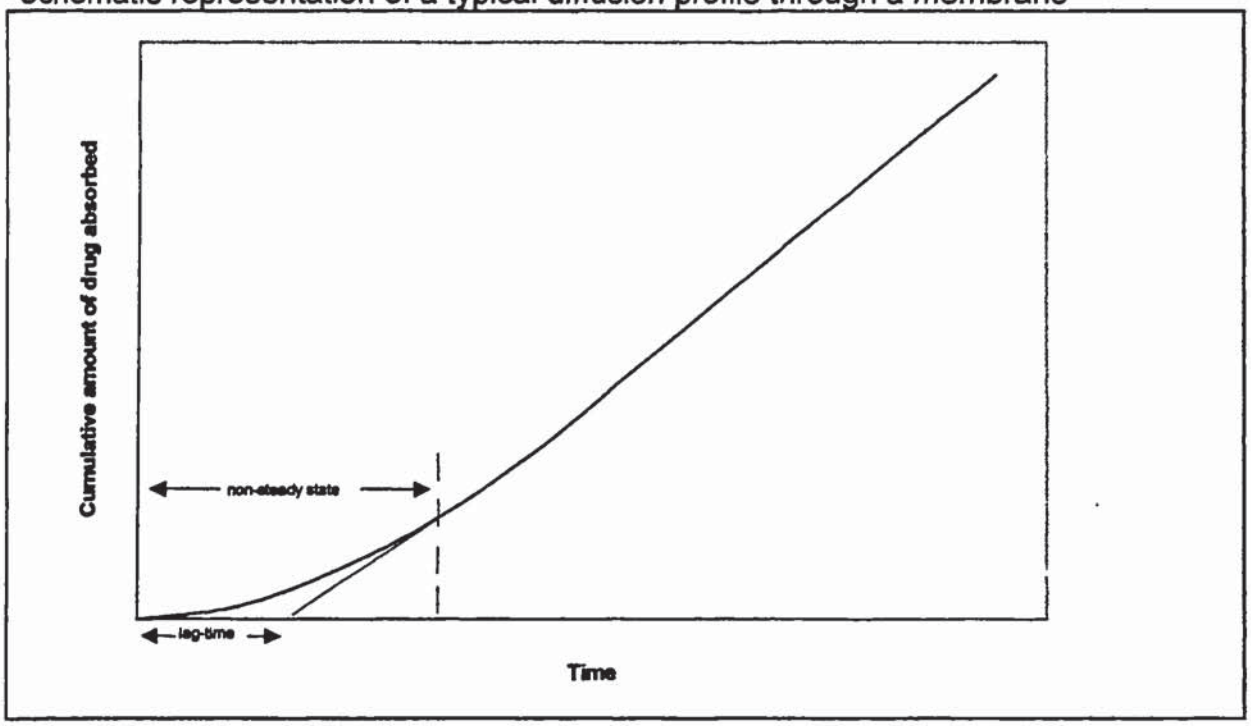

The most simple way of modelling the diffusion process is the application of Fick's first law of diffusion to the steady-state phase. The law states that the rate of transfer of a diffusing substance through a unit area of a section (the flux) is proportional to the concentration gradient across the entire barrier phase.

$$J = -D\frac{dc}{dx} \qquad \text{equation 5.1}$$

Where J is the rate of transfer *per* unit area of surface (the flux), with units of μmoles cm^{-2} min^{-1}, dc/dx is the concentration gradient across the membrane and D is the diffusion coefficient with units cm^2 min^{-1}. The flux of the penetrant corresponds to the slope of the steady-state diffusion curve in figure 5.1. For a drug diffusing across a membrane of thickness, h, the concentration gradient may be written as:

$$\frac{C_d - C_r}{-h} = -\frac{\Delta C}{h} \qquad \text{equation 5.2}$$

where C_d is the concentration at the donor side of the membrane and C_r is the concentration entering the receiver compartment. By substituting for dc/dx into equation 5.1, it can be shown that:

$$J = \frac{D.\Delta C}{h} \qquad \text{equation 5.3}$$

The factors affecting the value of the diffusion coefficient can be scrutinised by considering the Stokes-Einstein equation, derived for an approximately spherical molecule:

$$D = \frac{RT}{6N\pi\eta r} \qquad \text{equation 5.4}$$

where R is the universal gas constant, T is the temperature, N is Avogadro's number, η is the viscosity and r is the radius of the molecule in solution. From this equation it can be determined that the diffusion co-efficient is proportional to temperature and inversely proportional to viscosity.

If, however, the barrier is not simply an inert structural barrier to diffusion but one with an affinity for the applied solute, partitioning into the membrane is also important. For this reason the parameter, P, the membrane-vehicle partition coefficient, is introduced where:

$$P = \frac{C_1}{C_d} = \frac{C_2}{C_r} \qquad \text{equation 5.5}$$

and C_1 and C_2 are the concentrations within the membrane, at the donor and receiver compartment side of the membrane respectively. From equation 5.5 it follows that as:

$$dc = C_1 - C_2 = PC_d - PC_r = P(C_d - C_r) = P\Delta C \qquad \text{equation 5.6}$$

the flux may be rewritten as:

$$J = \frac{D.P.\Delta C}{h} \qquad \text{equation 5.7}$$

It is possible to combine *P*, *D* and *h* into a single proportionality constant *kp*, which is the permeability coefficient.

$$k_p = \frac{P.D}{h} \qquad \text{equation 5.8}$$

The units of *kp* are cm min^{-1}. Therefore by substituting *kp* into equation 5.7 it can be shown that:

$$J = k_p.\Delta C \qquad \text{equation 5.9}$$

If sink conditions apply, *i.e.* the concentration in the receiver compartment is negligible, ΔC approximates to C_v, the applied drug concentration remains constant and the concentration in the receiver phase remains effectively zero. Hence equation 5.4 becomes:

$$J = k_p.C_v \qquad \text{equation 5.10}$$

Using this equation it is possible to determine the permeability coefficient, k_p, by dividing the steady-state slope of figure 5.1 by the initial concentration of drug applied to the donor compartment. For two successive barriers in series, the permeability of each may contribute a resistance to the diffusion of drug molecules according to:

$$\frac{1}{k_{pobs}} = \frac{1}{k_{pa}} + \frac{1}{k_{pb}} \qquad \text{equation 5.11}$$

where k_{pobs} is the overall, combined permeability of the two membranes, and k_{pa} and k_{pb} are the permeability coefficients of membrane *a* and *b* respectively.

Likewise, the observed permeability through an aqueous unstirred layer contained within two membranes, k_p control, is a composite function of the permeability of the aqueous unstirred layer, k_{pw}, and the permeability of each membrane, k_{pmb}, according to:

$$\frac{1}{k_{pcontrol}} = \frac{1}{k_{pmu}} + \frac{2}{k_{pmb}} \qquad \text{equation 5.12}$$

A similar equation may be written for the permeability of a mucus layer contained within two membranes:

$$\frac{1}{k_{pmucus}} = \frac{1}{k_{pw}} + \frac{2}{k_{pmb}} \qquad \text{equation 5.13}$$

where k_{pmucus} , is the observed permeability through the mucus layer and k_{pmu} is the permeability of the mucus layer.

Physically, is difficult to design experiments where the diffusant has to be transported only across the membrane of interest, usually dialysis membranes or porous filters are used to provide support for the membrane under investigation. If the membrane support is selected such that its permeability is far greater than the mucus layer and aqueous control layer *i.e.* $k_{pmb} >> k_{pw}$ and $k_{pmb} >> k_{pmu}$ equations 5.12 and 5.13 can be reduced to:

$$\frac{1}{k_{pcontrol}} = \frac{1}{k_{pw}} \qquad \text{equation 5.14}$$

and

$$\frac{1}{k_{pmucus}} = \frac{1}{k_{pmu}} \qquad \text{equation 5.15}$$

respectively. This was shown to be the case for both paracetamol and ibuprofen as illustrated in figures 5.6 and 5.7. Therefore, the determination of the effect of mucus

on the diffusion rate of the model drugs, relative to an unstirred aqueous layer and also the effects of added antacid/excipient on the drug diffusion rate could be determined by calculating the ratio of the experimental permeability to the control permeability.

As illustrated in figure 5.1, prior to the establishment of steady-state there is a non-steady state phase, where the flux of the drug is gradually increasing. The linear portion of the line can be extrapolated to the x-axis in order to define a lag time, t_L, which is dependent upon the membrane diffusion coefficient D, and the thickness of the membrane, h, as shown in equation 5.16.

$$t_L = \frac{h^2}{6D} \qquad \text{equation 5.16}$$

Theoretically, the lag time permits the estimation of the diffusion coefficient, providing there is no binding. Strictly, equations 5.2-5.5 are only applicable to the steady-state phase if there are no significant interactions, such as binding between the drug and the membrane.

5.3 Selection of mucus model and diffusion method

As it is not practical to obtain mucus samples from humans, an alternative animal model is required. The animal model selected should, ideally, meet the following criteria; it should be readily available, in sufficient quantities; it should be well characterised and frequently used by other workers; and it should be from an animal where the physiology is similar to man. On this basis, pig gastric mucus (PGM) was selected as an appropriate model.

PGM consists mainly of water, between 80-95%, electrolytes and glycoproteins, commonly referred to as mucins (Macadam 1993; Bansil *et al.* 1995). Mucins are defined structurally as large (Mw 10^6-10^7), viscous proteins composed of approximately 75% carbohydrate and 25% amino acids linked *via* O-glycosidic bonds between N-acetylgalactosamine and serine or treonine residues (Bansil *et al.* 1995). The dry weight composition of pig intestinal mucus has been reported as being

approximately: 5% mucin, 37% lipids, 39% proteins, 6% DNA and 13% other by Larhed *et al.* (1998).

Generally, three mucus models are used in diffusion experiments namely:

- crude mucus, obtained and used directly. An example of this is the work conducted by Livingston and Engel (1995) to measure the pH gradient across a mucus layer.
- mucus purified and prepared to separate the high molecular weight mucin fraction, an example method being, homogenisation, treatment with a buffer, centrifugation and fractionation on a preparative column, (Kearney and Marriott 1986).
- dried crude or semi-purified mucus which is reconstituted before use.

When selecting a mucus model for this work, it is noted that the mucus itself is not under study, rather it is the transport of the drugs across a model as similar as practicable to the *in vivo* environment is of interest. However, it is also realised that the model must be both stable and consistent in order to provide meaningful results.

It is generally accepted that the mucin component of mucus is the fraction responsible for the viscous and gel-forming nature of mucus (Allen and Snary 1972; Meyer and Silberberg 1988), and this is why many workers use this purified fraction for their studies.

However, Bhaskar *et al.* (1991) demonstrated that mucus viscosity can be varied with pH, ionic strength and purification process. Of particular interest, they showed that for PGM purified by gel filtration followed by density gradient ultra-centrifugation in CsCl the viscosity decreased by a factor of approximately 100 over a pH range of 2 to 7. They also showed that this profound change was eliminated when the ionic strength (I) was increased using NaCl (range 0-2.0). Further to this, it has been shown that the swelling behaviour of mucus can vary from zero levels to enormous swelling, the degree and rate of being dependent on the pH and ionic strength (Bansil *et al.* 1995). The author's own preliminary studies showed that dried crude PGM, when reconstituted to form 5 and 10% w/w solutions, demonstrated a decrease in viscosity of approximately 30% and 25% respectively, over the pH range 2 to 7. The viscosity at all pHs was typical of those of the solutions containing higher ionic strengths in the Bhaskar study.

A detailed study of the rheological properties of crude PGM and rehydrated dried PGM conducted by Nared-Kovevar (1997) concluded that a rehydrated PGM model could not produce rheological properties equivalent to those of natural mucus.

Of course, the viscosity of the mucus is not the only consideration for drug diffusion as illustrated in section 5.2. In a recent study, conducted by Larhed *et al.* (1998), work was conducted to determine the role of various intestinal mucus components on the diffusion of drugs. They showed that the lipophilic drugs under test had reduced diffusion rates in purified intestinal mucus, relative to purified PGM, and that this decrease could be attributed to a lipid-containing fraction. They concluded that lipids play a central role in the diffusion of some drugs in native intestinal mucus.

The mucus layer in the stomach is likely to be a more considerable barrier to drug absorption than mucus in the intestine as it is much thicker, reported as being between 576±81μm in the human stomach by Bickel and Kaufmann (1981) whereas the mucus in the intestine and colon has been reported as being between 50 and 450μm, summarised by Macadam (1993), and as approximately 40μm in dogs and humans, summarised by Macheras *et al.* (1995).

Also, as the investigation involves the alkalisation of the drug environment by pH modifying excipients/antacids, it is apparent that the greatest changes will occur in the un-buffered and highly acidic environment of the stomach rather than the neutral/buffered environment of the small intestine.

Based on the above review and the models developed in section 1.51 it was decided to select fresh native PGM as the mucus layer in the experimental model, with simulated gastric juice (0.05M HCl as the chosen media). A side-on three-compartment diffusion cell system, commonly used by workers in this area, has been developed and utilised within DDRG by Holbrook (1991) and was selected as an appropriate system for these studies.

5.4 Validation of native pig gastric mucus

For the proposed mucus model to be acceptable experimentally, it must have demonstrably low inter-batch variation and some degree of stability. Therefore experiments were undertaken to determine these factors.

5.4.1 Preparation of mucus

The stomachs of a minimum of three freshly slaughtered fasted pigs (*Suis scrofa domestica*) were obtained from a local abattoir. Each stomach was opened along the greater curvature, the stomachs inverted and any food contents initially removed mechanically and finally with double-distilled water. The mucus was collected using a smooth-faced metallic laboratory spatula, ensuring no underlying mucosa was removed, from all regions of the stomach, *i.e.* cardia, fundus, body and pylorus regions as it has been shown by Nordman *et al.* that differences in some mucus characteristics, *e.g.* glycosylation, sulphation and buoyant density are apparent in mucus obtained from the different regions. The mucus was mechanically mixed until homogenous with the spatula and then stored overnight at 4°C before initial use and thereafter. The pH range of the mucus samples taken was pH4.8 to 6.2 with a mean of 5.7±0.4 (n=10).

5.4.2 Mucus inter-batch variation and stability

5.4.2.1 Experimental

5.4.2.1.1 Materials

Mucus was obtained and prepared as detailed in section 5.4.1. ^{3}H-radiolabelled paracetamol (full preparation and C of A reference Appendix 2) and paracetamol were obtained from SB (Weybridge, UK). Hydrochloric acid was obtained from Aldrich (Poole, UK). All materials were as prepared, pharmaceutical or analytical grade as appropriate. Double-distilled water was generated in-house using a Fison's Fi-Stream Still.

5.4.2.1.2 Equipment

In-house manufactured diffusion cells as illustrated in figures 5.2 and 5.3 were assembled as follows, white-soft paraffin was applied to the roughened edges of the donor and receiver compartments. The receiver compartment was placed open-end up on a bench and a polypropylene membrane support with a meshed gauze filter located into position. A Nucleopore® 0.45μm polycarbonate filter membrane was then placed. The 1mm spacer disc was then positioned on top of the filter. Sufficient

mucus was added to easily fill the volume. A second filter membrane was positioned over the mucus, followed by a second gauze and membrane support disc. Finally, the donor compartment was placed on top of the formed central compartment. Excess mucus was removed and then Parafilm® was tightened around the circumference of the assembly to ensure a good seal. Steel springs were used to clamp the cells together, a spring at each corner, straddling across the length of the cells and held in position by hooks integral to the construction of the cells (Holbrook 1991). Each combined diffusion cell was positioned onto a magnetic stirrer (Rank Brothers, Cambs, U.K) horizontally. The stirrer rates were set to the highest value where consistent stirring could still be obtained, to ensure the donor cell-aqueous/first membrane barrier drug transfer rate was maximised, ensuring the hydrodynamic conditions were not a controlling factor in the drug diffusion process. Each cell was connected serially to a Churchill circulating water pump set at a temperature of 37°C, corresponding to physiological temperature.

Figure 5.2
Diagram of side-on three-compartment diffusion cell

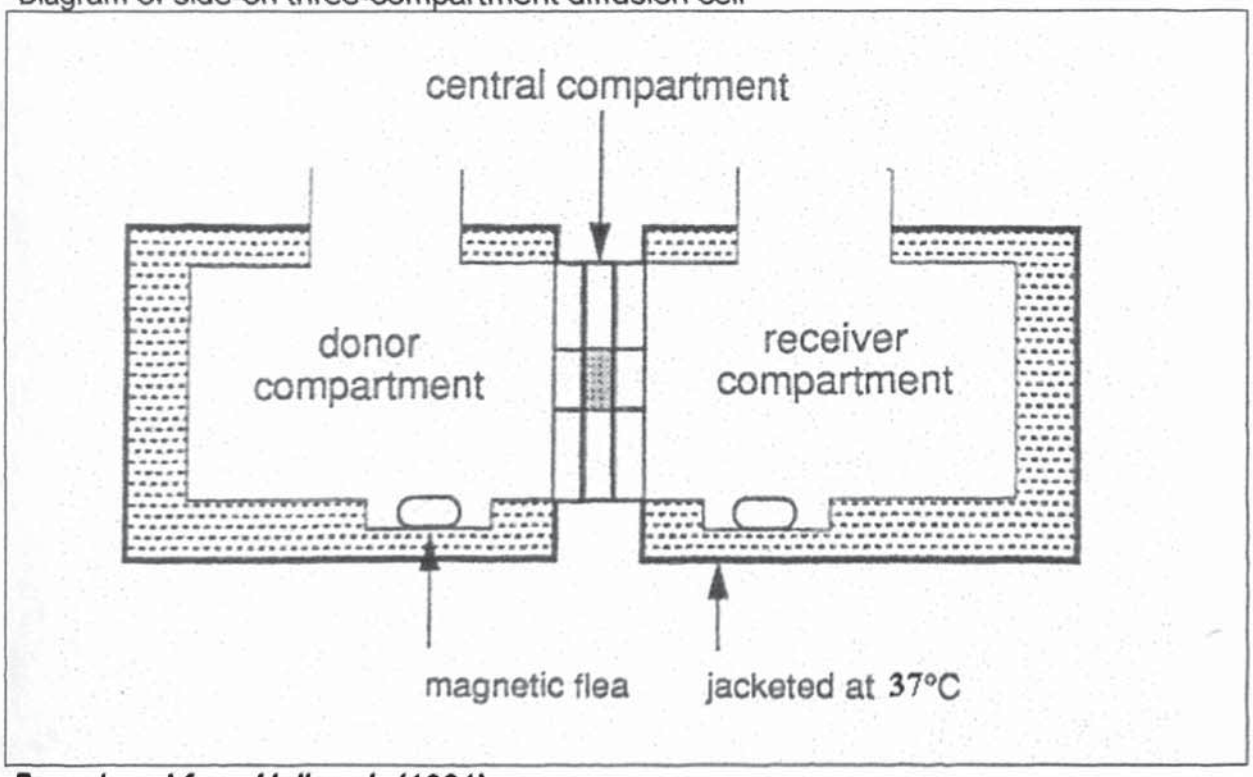

Reproduced from Holbrook (1991)

Figure 5.3
Diagram of central compartment of side-on three-compartment diffusion cell

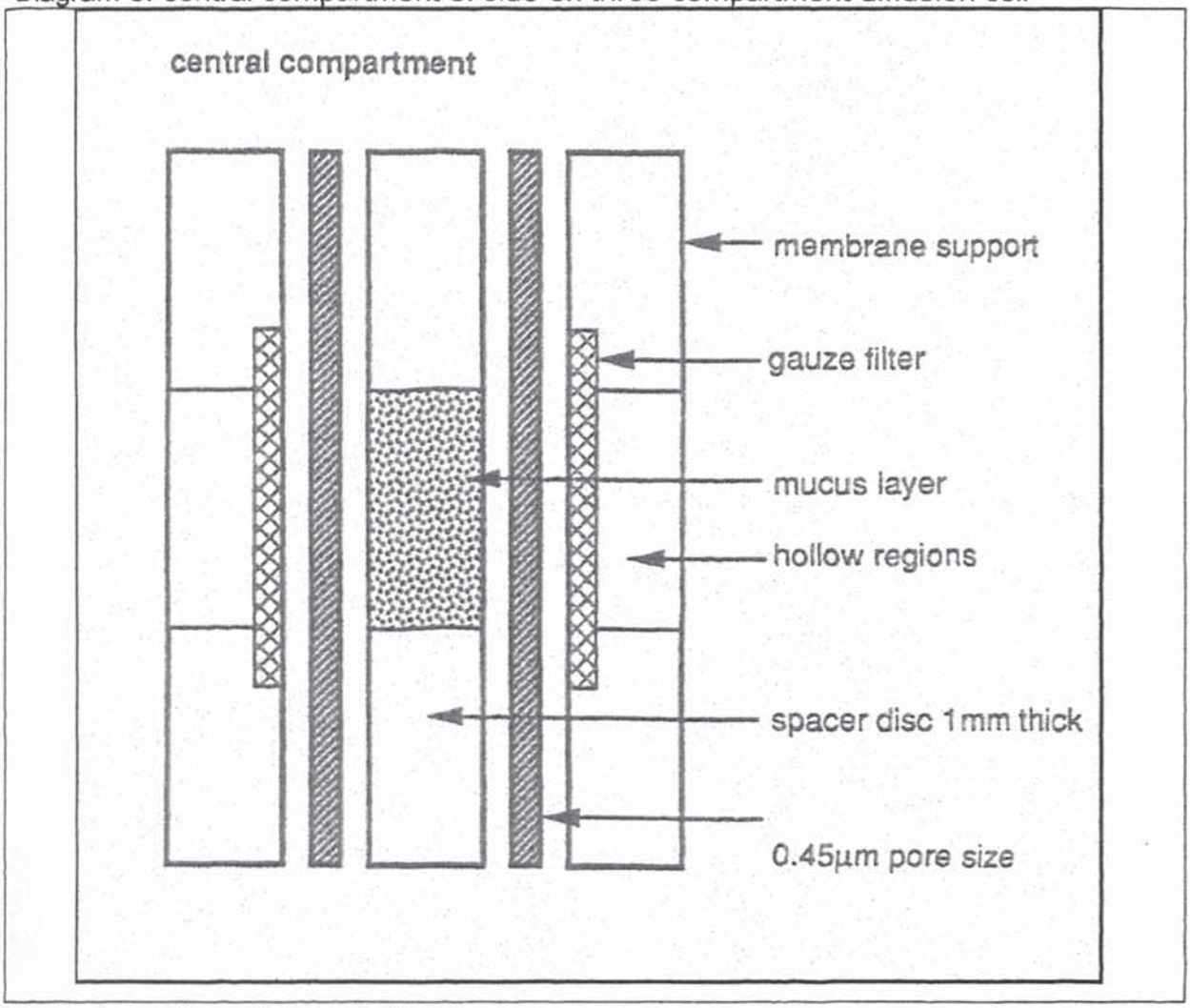

Reproduced from Holbrook (1991)

5.4.2.1.3 Method

12.0ml of 0.05M HCl was added to the receiver compartment using variable micro-pipettes. An equal volume of a 5.0mg ml^{-1} solution of paracetamol, spiked with the radio-labelled paracetamol to give a final solution activity of 15,000 DPM ml^{-1}, was added to the donor cell. Aliquots of 0.2ml were sampled every 20 minutes for 240 minutes, the sample volume being replaced with an equal volume of 0.05M HCl. The samples were assayed according to the method detailed in section 2.7, the stock solution, used in the donor cells serving as the standard solution. This procedure produced a dilution of the receiver phase. It was, therefore, necessary to adjust each successive sample concentration for the dilution caused by all the previous samples.

This was performed, using an Excel spreadsheet, by applying the correction factor detailed in equation 4.9. Three distinct and separate batches of mucus were evaluated, all on the first day after preparation of the mucus. Secondly, the first batch was tested for 4 consecutive days after preparation of the mucus.

5.4.2.2 Results and discussion

The criteria chosen to demonstrate reproducibility of diffusion through mucus are firstly, that the inter-batch variation is not more significant than the intra-batch variation, or random and systematic errors, within the experimental design. Secondly, it is desirable that the mucus does not deteriorate over time and demonstrate any significant change in diffusion rate. Ideally, the inter-day variation would not exceed the random and systematic errors within the experimental design. The results for the inter-batch variation were:

- batch 1 - flux of 2.25E-04±1.5E-05 mg cm^{-2} s^{-1}
- batch 2 - flux of 2.23E-04±2.2E-05 mg cm^{-2} s^{-1}
- batch 3 - flux of 2.03E-04±2.7E-05 mg cm^{-2} s^{-1}

Single factor ANOVA statistical analysis P=0.43 confirmed the inter-batch variation was not significant. The data are illustrated in figure 5.4.

Figure 5.4
Illustrating the diffusion of 5mg ml^{-1} paracetamol through 3 batches of mucus. Results are the mean of 4 replicates+SD

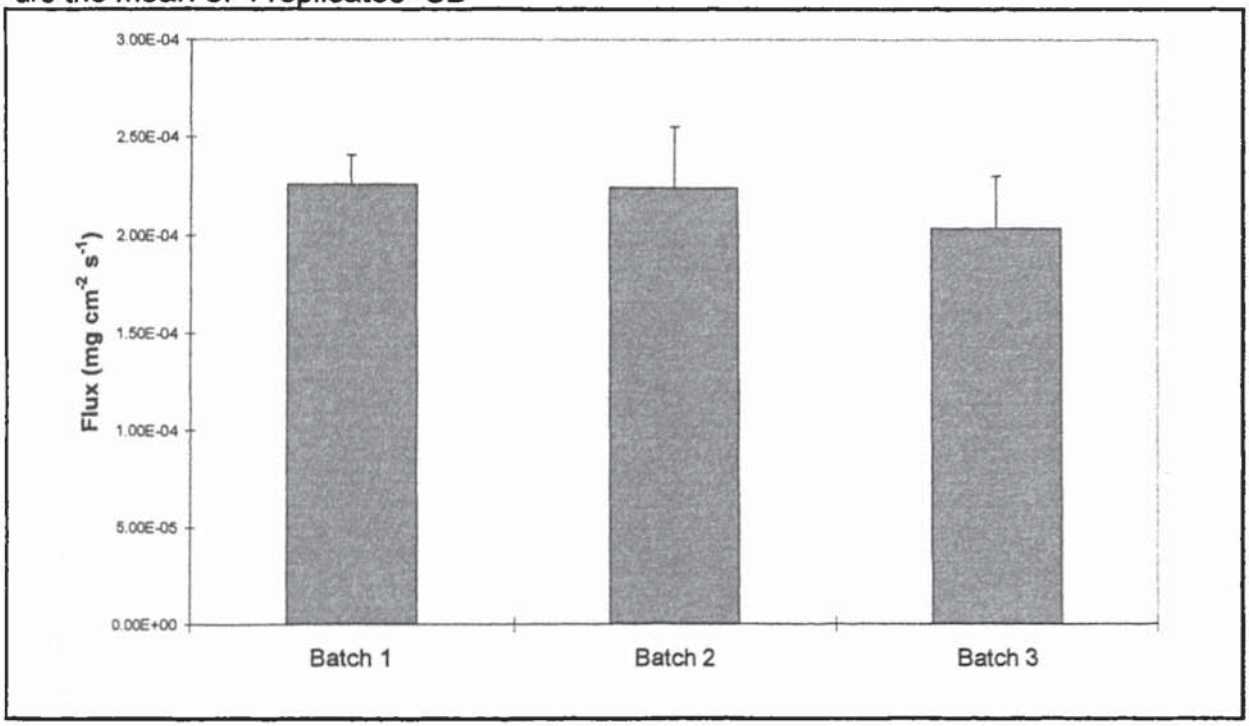

The results for the inter-day variation were:

- day 1 - flux of 2.25E-04±1.5E-04 mg cm^{-2} s^{-1}
- day 2 - flux of 2.13E-04±1.7E-04 mg cm^{-2} s^{-1}
- day 3 - flux of 2.42E-04±0.8E-04 mg cm^{-2} s^{-1}
- day 4 - flux of 2.47E-04±2.3E-04 mg cm^{-2} s^{-1}

Single factor ANOVA statistical analysis P=0.29 confirmed the inter-day variation was not significant. Also no trend is apparent from the data. The data are illustrated in figure 5.5.

Figure 5.5
Illustrating the diffusion of 5mg ml^{-1} paracetamol through 1 batch of mucus over 4 days. Results are the mean of 4 replicates+SD

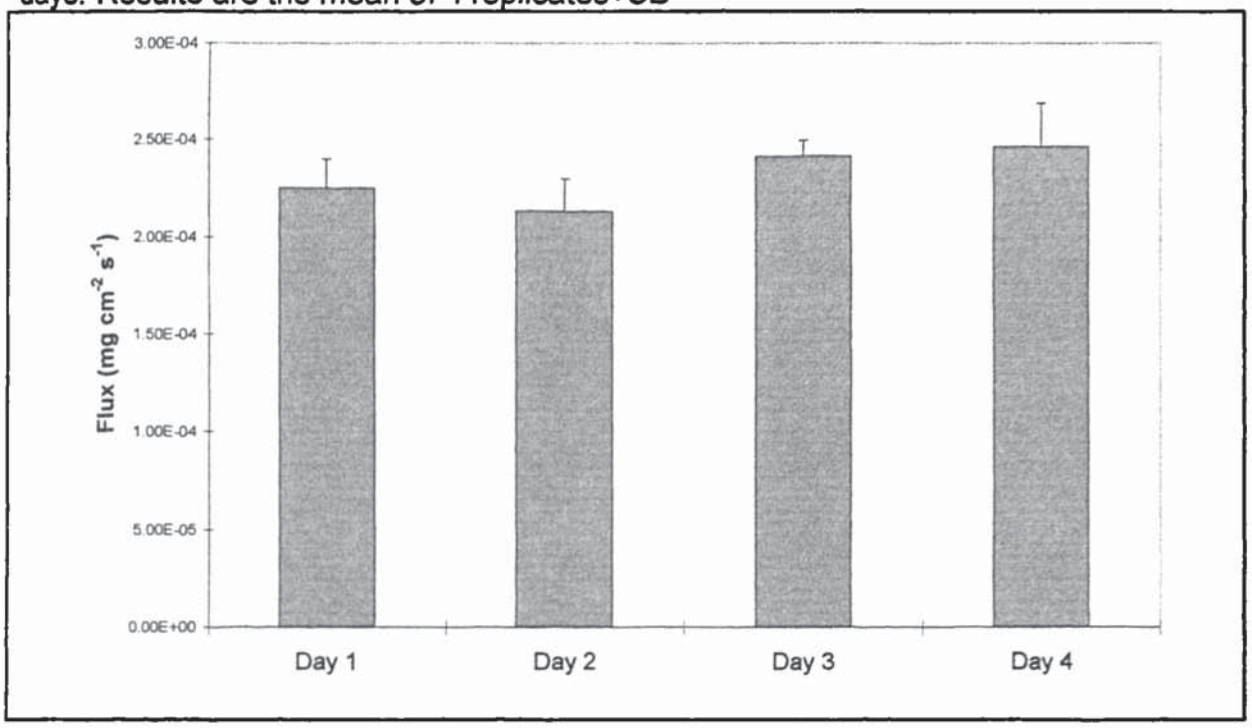

During the validation exercise the inter-sample %RSD was approximately 10%. Also, the results demonstrate that, for the mucus model selected, the preparation procedure and storage, and the use of multiple batches over four days were acceptable. These procedures were accepted as the limit of operation throughout the series of experiments. However, where possible, the use of a single batch for each experimental series, tested over the minimum number of days was adopted.

5.5 Drug diffusion through mucus layer

As discussed in the literature review (section 5.1), mucus has been shown to be a significant barrier to drug absorption for many drugs. Also, additives may either enhance, reduce or not affect the diffusion rate of the model drugs. The aim of this section was three-fold, firstly, to determine the effect of a mucus layer, relative to an unstirred aqueous layer, on the diffusion rates of paracetamol and ibuprofen, secondly, to determine the effect of dissolved additives on the diffusion rate and thirdly to characterise the effect of pH modification on the diffusion rate. Concentrations of drug and additives were set to simulate the physiological conditions.

5.5.1 Experimental

5.5.1.1 Materials

Mucus was obtained and prepared as detailed in section 5.4.1. Paracetamol, ibuprofen and sodium bicarbonate (extra fine grade) were obtained from SB (Weybridge, UK). [^{14}C] Ibuprofen was obtained from ICN, (see appendix 2 for details of manufacture and certificate of analysis). Hydrochloric acid, aluminium hydroxide, calcium carbonate, magnesium hydroxide, sodium hydroxide, potassium chloride, boric acid, di-sodium phosphate, citric acid, mono-basic potassium phosphate and magnesium oxide were obtained from Aldrich (Poole, UK). All materials were as prepared, pharmaceutical or analytical grade as appropriate. Double-distilled water was generated in-house using a Fison's Fi-Stream Still.

5.5.1.2 Equipment

The diffusion cell apparatus was assembled and used as described in section 5.4.2.1.2, except for the aqueous control experiment where the mucus layer was omitted and 0.31ml extra of the receiver solution added to fill the void volume, and for the filter experiment, the central compartment was omitted to be replaced with a filter membrane sandwiched between the two compartments.

5.5.1.3 Method

The receiver solution, as described below, was added to the receiver compartment using adjustable micro-pipettes. An equal volume of donor solution, as detailed below, was added to the donor cell. Aliquots of 0.1ml were sampled every 20 minutes for a minimum of 200 minutes, the sample volume being replaced with an equal volume of receiver solution. Ibuprofen samples were assayed according to the method detailed in section 2.7, the stock solution, used in the donor cells serving as the standard solution. Paracetamol solutions were analysed by HPLC according to the method detailed in section 2.1 and the ibuprofen solutions by the scintigraphic method detailed in section 2.5. These procedures produced a dilution of the receiver phase. It was therefore necessary to adjust each successive sample concentration for the dilution caused by all the previous samples. This was performed, using an Excel spreadsheet, by applying the correction factor detailed in equation 4.9.

For studying the mucus retardation of diffusion rate of drugs, *i.e.* mucus control, aqueous control and filter experiment, the receiver solutions consisted of 0.05M HCl. The donor solutions were 5mg ml^{-1} paracetamol in 0.05M HCl, or saturated *ibuprofen* solution (≈0.06 mg ml^{-1}) in 0.05M HCl (shaken overnight in a Techne SB 6 water bath/shaker at 37°C, agitator setting 1-corresponding to 70 cycles *per* minute) and then filtered through a 0.45µm membrane filter before being spiked with an aliquot of radio-labelled ibuprofen to give an activity of ≈150,000 DPM ml^{-1}.

For additives exhibiting incomplete dissolution, *i.e.* aluminium hydroxide, magnesium hydroxide, magnesium oxide and calcium carbonate studies, the receiver solution compositions were saturated solutions of the antacid in 0.05M HCl, prepared as detailed above. The donor solutions consisted of either 5mg ml^{-1} paracetamol in 0.05M HCl, or 0.05M HCl pre-saturated with ibuprofen and filtered before saturating with the antacid under test using the same method as detailed above. The solutions were removed from the water bath/shaker just prior to use and filtered through a 0.45µm membrane filter. The ibuprofen donor solutions were then spiked with the radio-labelled drug as before. This method ensured that, for all experiments, the drug concentration in the donor cells was unchanged.

For the soluble excipient/antacid, *i.e.* sodium bicarbonate, the receiver solution consisted of 15mmol/200ml sodium bicarbonate in 0.05M HCl and the donor cell solution was 15mmol/200ml sodium bicarbonate in 0.05M HCl containing 5mg ml^{-1} paracetamol or pre-saturated ibuprofen (≈0.06mg ml^{-1}). In each case the sodium bicarbonate was added, slowly, *in-situ.*

For studying the effects of pH-modification of diffusion rate of drugs, the receiver solutions consisted of the USP buffer at the pH under investigation. The donor solutions were 0.06mg ml^{-1} ibuprofen in the USP buffer, filtered through a 0.45µm membrane filter before being spiked with an aliquot of radio-labelled ibuprofen to give an activity of ≈150,000 DPM ml^{1}.

5.5.2 Results and discussion

5.5.2.1 Mucus retardation of diffusion rate of model drugs

The influence of a mucus layer on the diffusion of the model drugs was assessed by firstly, checking that the membrane filter did not significantly contribute to the overall permeability, which it did not in either case, and secondly, comparing the diffusion rate of each drug through a 1mm mucus layer (mucus control) to that obtained through an unstirred aqueous layer (aqueous control). The diffusion rates expressed as flux for paracetamol were:

- flux of 1.845E-03±1.0E-04 mg cm^{-2} s^{-1} through a single membrane filter
- flux of 2.27E-04±2.8E-05 mg cm^{-2} s^{-1} through a 1mm aqueous unstirred layer
- flux of 1.39E-04±4.8E-06 mg cm^{-2} s^{-1} through a 1mm mucus layer.

Using crossover analysis, where each mucus layer replicate, in turn, is ratioed against each aqueous layer replicate, from which the overall average is determined; the mucus was found to significantly (t-test, P=0.002) retard the diffusion rate to 62.2±7.3% of the diffusion rate through the unstirred layer. The diffusion rate profiles are illustrated in figure 5.6.

For Ibuprofen, the diffusion rates expressed as flux were:

- flux of 1.41E-05±7.0E-07 mg cm^{-2} s^{-1} through a single membrane filter
- flux of 1.83E-06±7.3E-08 mg cm^{-2} s^{-1} through a 1mm aqueous unstirred layer
- flux of 5.95E-07±3.6E-08 mg cm^{-2} s^{-1} through a 1mm mucus layer.

Using crossover analysis, the mucus was found to significantly (t-test, P=0.00001) retard the diffusion rate to 32.7±2.1% of the diffusion rate through the unstirred layer. The diffusion rate profiles are illustrated in figure 5.7.

The permeability coefficient, K_p, of each drug through a 1mm mucus layer was derived by dividing the steady state flux value by the concentration gradient as detailed in equation 5.10. The derived values of K_p were 2.78E-05±9.7E-07 cm s^{-1} for paracetamol and 1.19E-05±7.3E-07 cm s^{-1} for ibuprofen.

Figure 5.6
Illustrating the diffusion of paracetamol (5mg ml^{-1} solution) across a single filter membrane, through an unstirred aqueous layer of 1mm thickness and through a mucus layer of 1mm thickness. Experiments were performed in 0.05M HCl at 37°C. Data points are the mean of at least 3 replicates±SD.

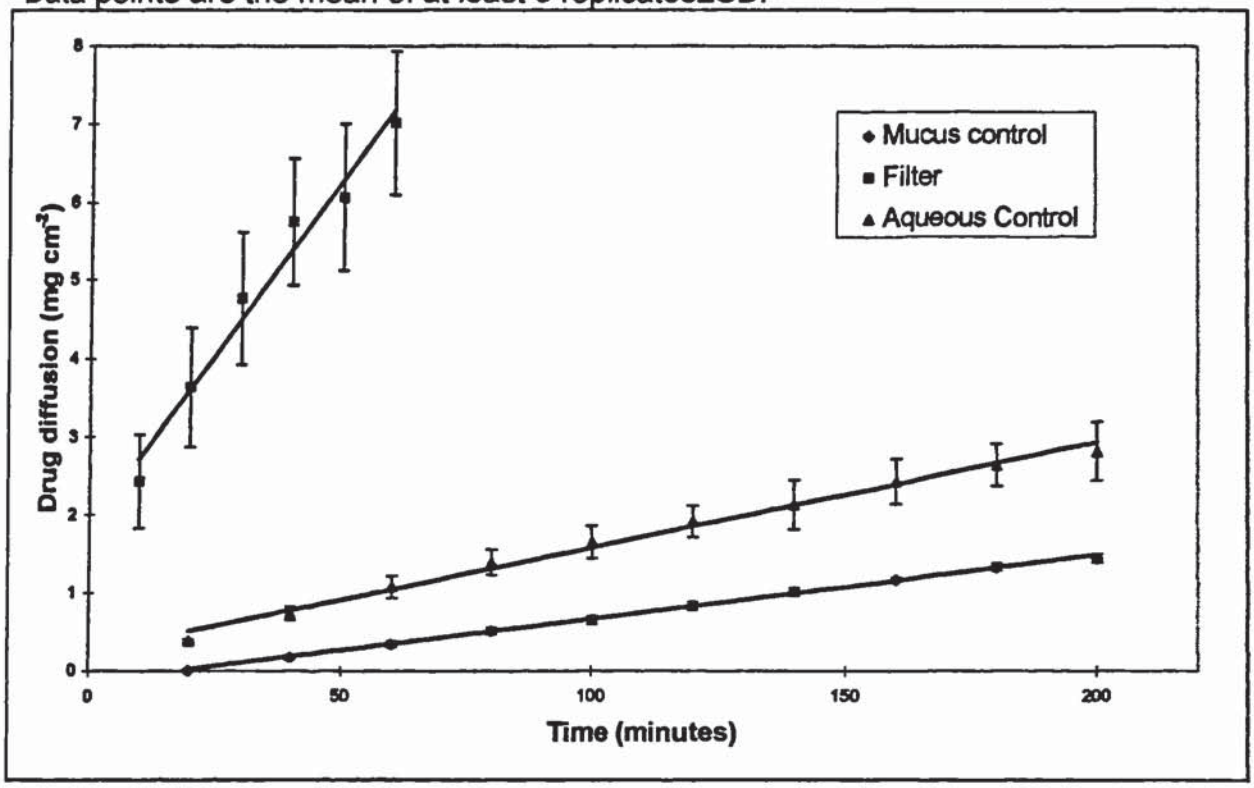

Figure 5.7
Illustrating the diffusion of ibuprofen (≈0.06mg ml^{-1}) across a single filter membrane, through an unstirred aqueous layer of 1mm thickness and through a mucus layer of 1mm thickness. Experiments were performed in 0.05M HCl at 37°C. Data points are the mean of at least 3 replicates±SD.

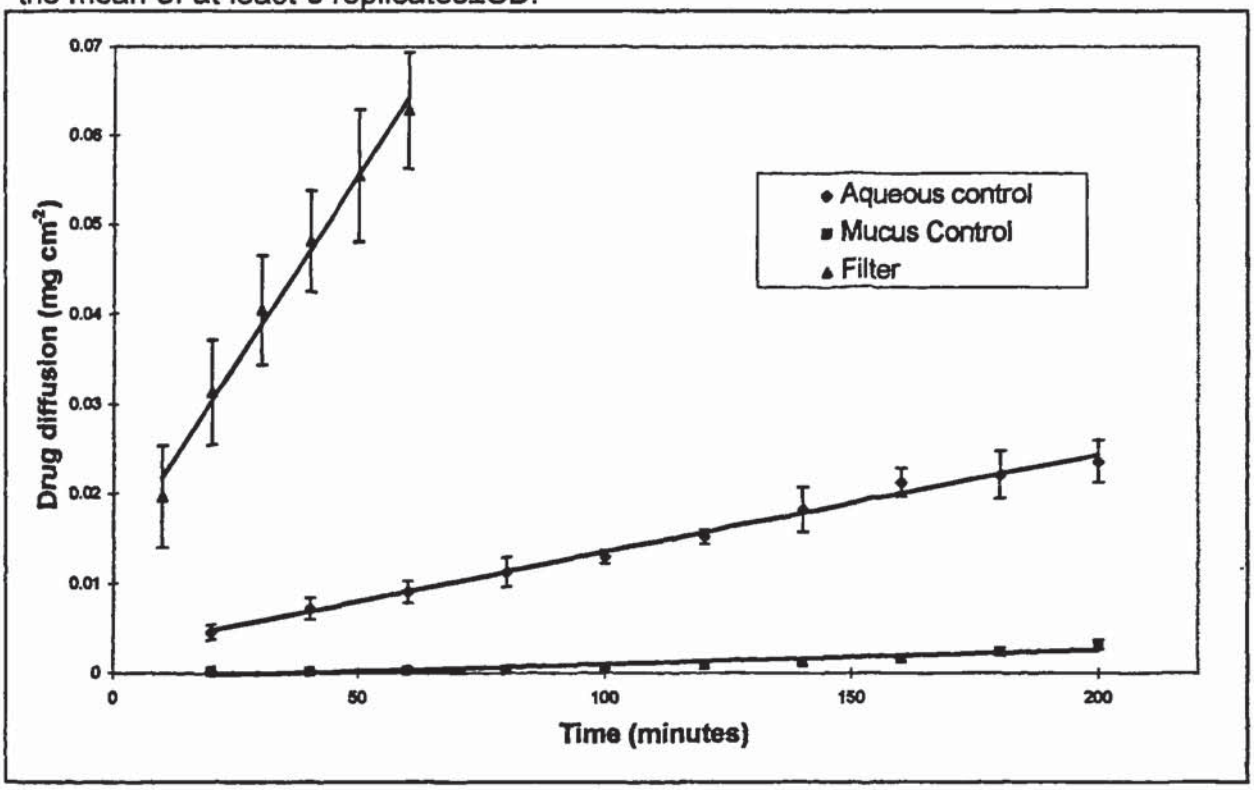

5.5.2.2 The effect of dissolved excipients/antacids on the diffusion rate of ibuprofen and paracetamol, and the role of pH

The first series of experiments were designed to reproduce the *in vivo* situation where model analgesic drugs have been co-administered with one of the selected antacids or with a tablet formulated to contain the excipient under investigation, with regard to the pH environment in the stomach with pre-dissolved drug and antacid/excipient at concentrations equivalent to those estimated *in vivo*. The second series of experiments were designed to separate the effect of pH from other factors by the use of a wide range of pH buffers, standardised to have the same ionic strength, with pre-dissolved drug at concentrations equivalent to those estimated *in vivo*.

The results from the dissolved excipients/antacids paracetamol study are summarised in table 5.1. The data includes the steady-state flux, the lag times and the calculated

permeability coefficients. The lag times and steady state fluxes are also illustrated in figures 5.8 and 5.9 respectively. Visual analysis and single-factor ANOVA analysis of the lag times, P=0.38, revealed no significant change to the lag time by any of the antacids/excipients. Visual analysis and single-factor ANOVA analysis of the diffusion rates (P=0.15) revealed that none of the antacids/excipients significantly altered the diffusion rate of paracetamol.

The diffusion profiles for each excipient/antacid under test are illustrated in figures 5.10-5.14.

Table 5.1
Summary of the effect of dissolved antacid/excipient additive on the diffusion rate of paracetamol (5mg ml^{-1}) through a 1mm mucus thickness layer. Flux and lag time values are the mean of 3 data-points±SD. k_p value and SD were determine by cross-over analysis. R^2 was determined by linear regression analysis of the mean of the replicates.

Experiment	Flux ($mg\ cm^{-2}\ s^{-1}$) ±SD	Lag time (min) ±SD	k_p ($cm\ s^{-1}$) ±SD	R^2
mucus control	1.39E-04±4.8E-06	18.3±3.9	2.78E-05±9.7E-07	0.9984
sodium bicarbonate	1.18E-04±1.9E-05	18.7±4.0	2.37E-05±3.7E-06	0.9966
magnesium hydroxide	1.49E-04±3.0E-05	10.3±2.8	3.0E-05±6.0E-05	0.9975
magnesium oxide	1.40E-04±1.2E-05	15.2±10.7	2.80E-05±2.5E-06	0.9937
calcium carbonate	1.32E-04±1.3E-05	16.5±5.8	2.63E-05±2.7E-06	0.9987
aluminium hydroxide	1.21E-04±1.1E-05	16.6±2.0	2.42E-05±2.2E-06	0.9964

Figure 5.8
Illustrating the effect of dissolved antacid/excipient on the lag times for paracetamol diffusion. Results are the mean of at least three data series+SD

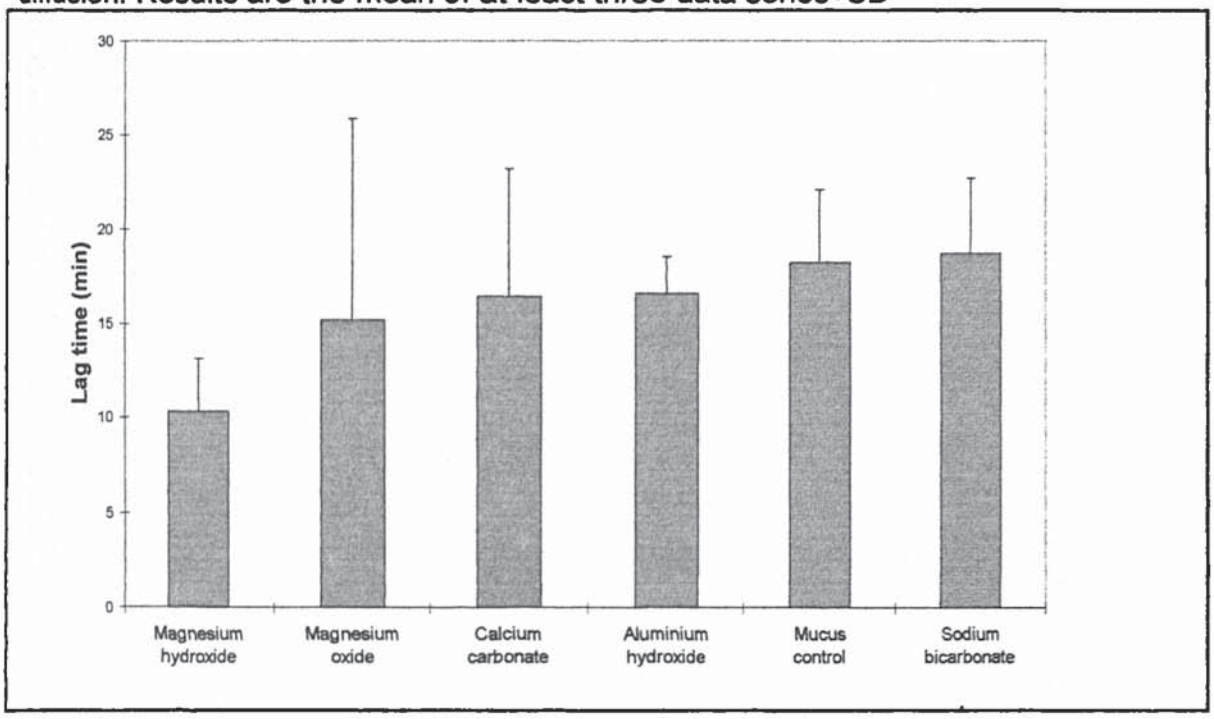

Figure 5.9
Illustrating the effect of antacid/excipient on the diffusion rate (flux) for paracetamol diffusion. Results are the mean of at least three data series+SD

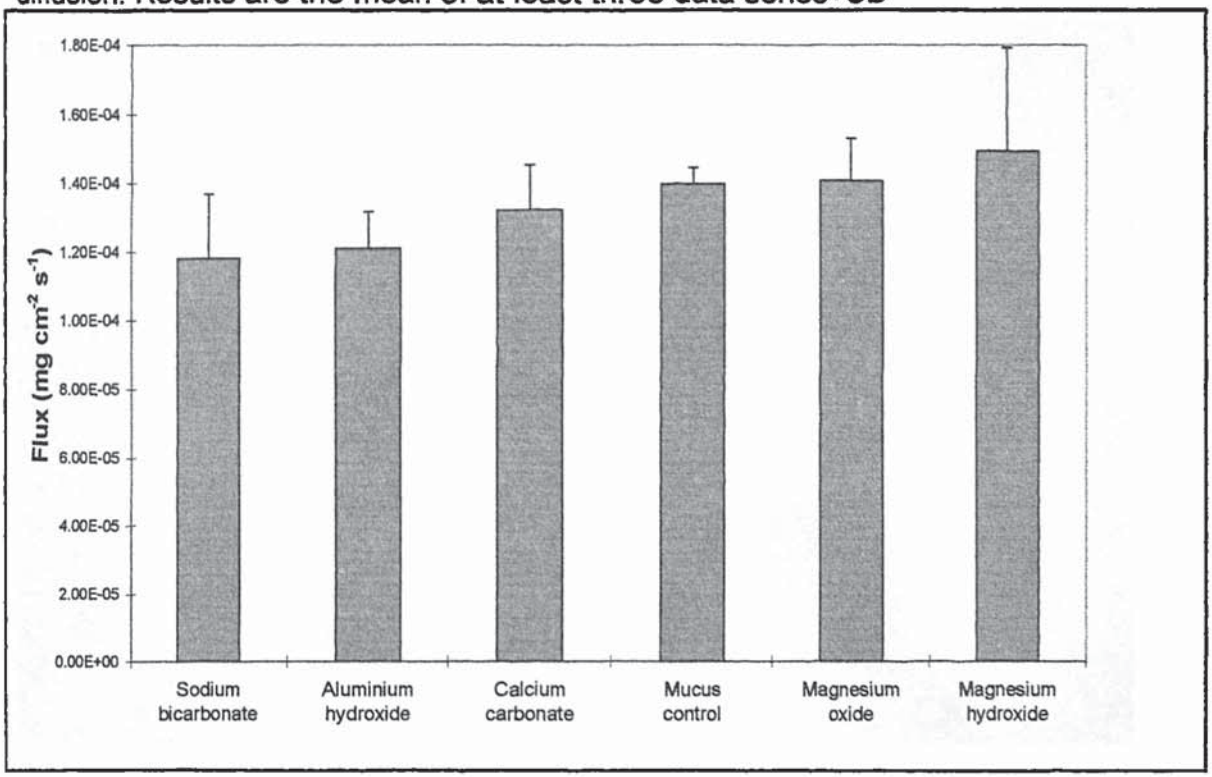

Figures 5.10-5.14

The following graphs illustrate diffusion profiles of 5mg ml^{-1} paracetamol in 0.05M HCl solutions containing dissolved antacid/excipients, compared to a paracetamol solution only (Mucus control), through a 1mm thickness mucus layer. Profiles are the mean of at least 3 replicates, with SD included as appropriate for visual clarity.

Figure 5.10
Illustrating the diffusion profile for paracetamol solution saturated with aluminium hydroxide

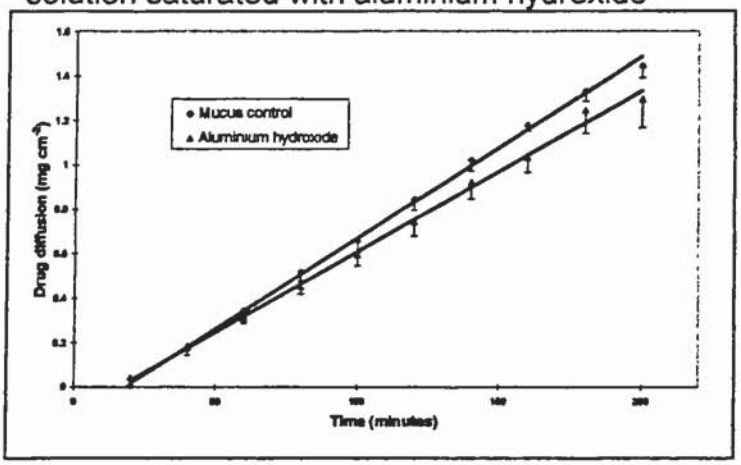

Figure 5.11
Illustrating the diffusion profile for paracetamol solution saturated with calcium carbonate

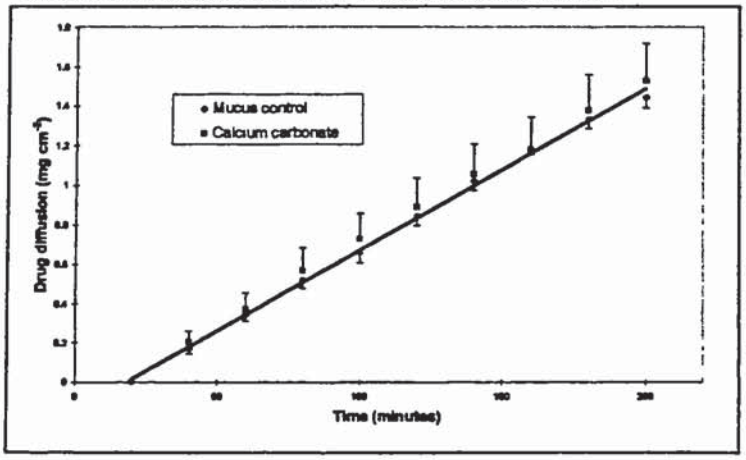

Figure 5.12
Illustrating the diffusion profile for paracetamol solution saturated with magnesium hydroxide

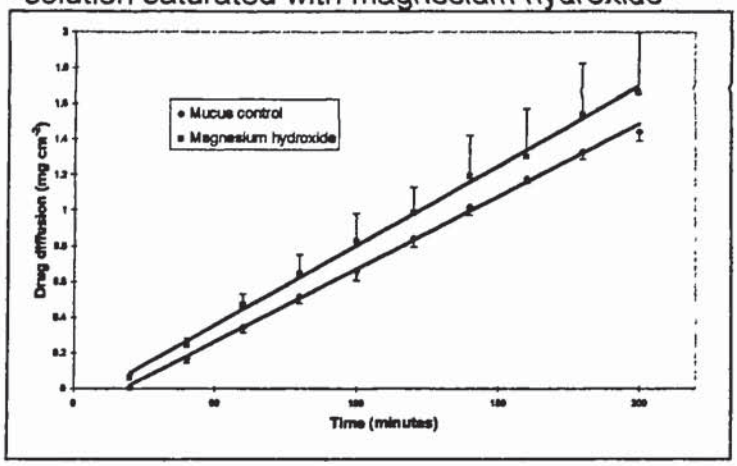

Figure 5.13
Illustrating the diffusion profile for paracetamol solution saturated with magnesium oxide

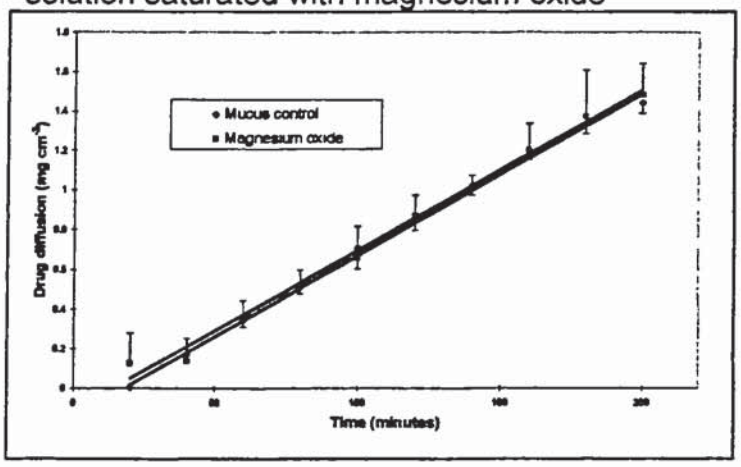

Figure 5.14
Illustrating the diffusion profile for paracetamol solution containing 15mmol/200ml sodium bicarbonate

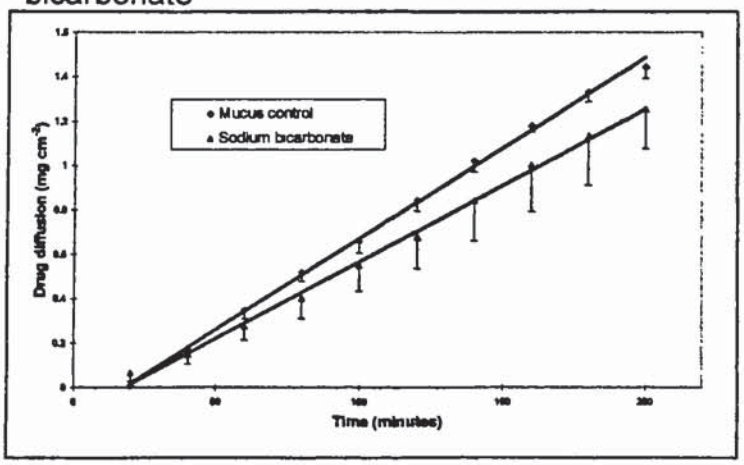

The results from the dissolved excipients/antacids ibuprofen study are summarised in table 5.2. The data includes the steady-state flux, the lag times and the calculated permeability coefficients. The lag times and steady state fluxes are also illustrated in figures 5.15 and 5.16 respectively. The following can be observed from the data (rates calculated by cross-over analysis):

- the ibuprofen steady-state diffusion rate is reduced to 43.2±12.7% of the mucus control value when the solution also contains 15mmol/200ml sodium bicarbonate. Also, the lag time is significantly reduced from ≈118min to ≈12min.
- the ibuprofen steady-state diffusion rate is reduced to 48.4±14.0% of the mucus control value when the solution is pre-saturated with magnesium oxide. Also, the lag time is reduced from ≈118min to ≈2min.
- the ibuprofen steady-state diffusion rate is increased to 145.6±31.4% of the mucus control value when the solution is pre-saturated with calcium carbonate. Also, the lag time is reduced from ≈118min to ≈29min.
- the ibuprofen steady-state diffusion rate is increased to 272.2±26.3% of the mucus control value when the solution is pre-saturated with magnesium hydroxide. Also, the lag time is reduced from ≈118min to ≈76min.
- the ibuprofen steady-state diffusion rate is effectively eliminated being 0.8±0.7% of the mucus control value when the solution is pre-saturated with aluminium hydroxide. A meaningful lag time could not be obtained due to the very low gradient of the flux.

The diffusion profiles for each excipient/antacid under test are illustrated in figures 5.17-5.21.

Table 5.2
Summary of the effect of dissolved antacid/excipient additive on the diffusion rate of ibuprofen (≈0.06mg ml^{-1}) through a 1mm mucus thickness layer. Flux and lag time values are the mean of 3 data-points±SD. k_p value and SD were determined by cross-over analysis. R^2 was determined by linear regression analysis of the mean of the replicates.

Experiment	Flux (* 10^8) (mg cm^{-2} s^{-1}) ±SD	Lag time (min) ±SD	k_p (* 10^6) (cm s^{-1}) ±SD	Average data R^2
mucus control	59.5±3.7	118.4±6.7	11.9±0.7	0.9917
sodium bicarbonate	24.8±9.1	**11.9±8.3	**5.0±1.9	0.9423
magnesium hydroxide	161.5±15.0	**76.0±7.0	**32.3±2.7	0.9888
magnesium oxide	30.2±8.8	**-2.0±14	*6.0±1.7	0.9643
calcium carbonate	88.8±18.8	**29.2±1.6	*17.8±3.8	0.9938
aluminium hydroxide	0.43±0.46	N/A	**0.09±0.09	0.7309

* Significantly different from control (Dunnett's test P<0.05)
** Significantly different from control (Dunnett's test P<0.01)

Figure 5.15
Illustrating the effect of dissolved antacid/excipient on the lag times for ibuprofen diffusion. Results are the mean of at least three data series+SD

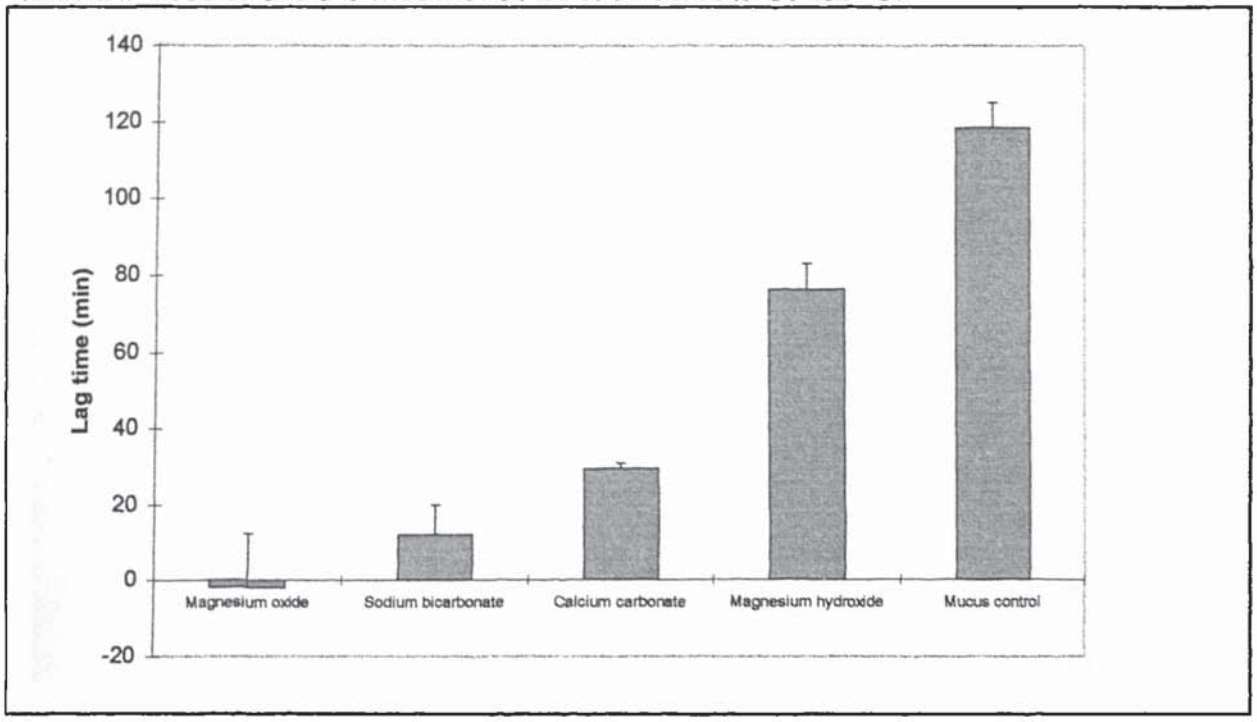

Figure 5.16
Illustrating the effect of antacid/excipient on the diffusion rate (flux) for ibuprofen diffusion. Results are the mean of at least three data series+SD

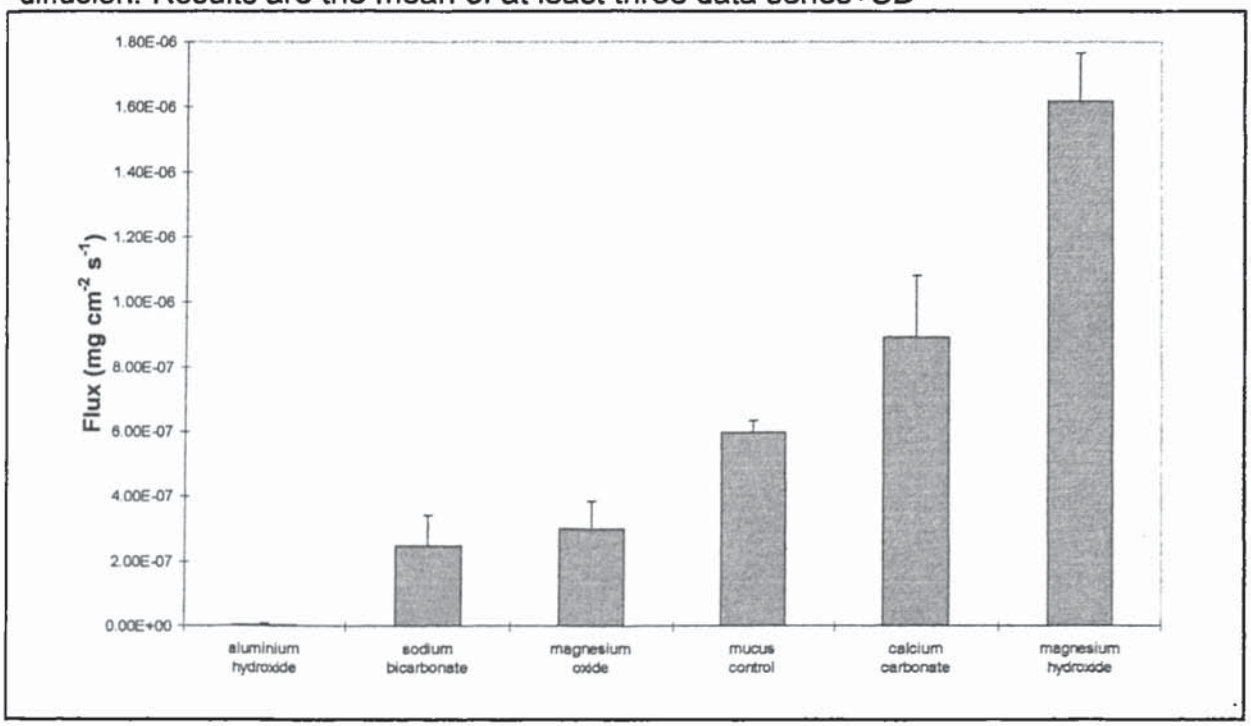

Figures 5.17-5.21

The following graphs illustrate diffusion profiles of saturated (≈0.06mg ml^{-1} in 0.05M HCl) ibuprofen solutions containing dissolved antacid/excipients, compared to a ibuprofen solution only (Mucus control), through a 1mm thickness mucus layer. Profiles are the mean of at least 3 replicates, with SD included as appropriate for visual clarity.

Figure 5.17
Illustrating the diffusion profile for ibuprofen solution containing 15mmol/200ml sodium bicarbonate

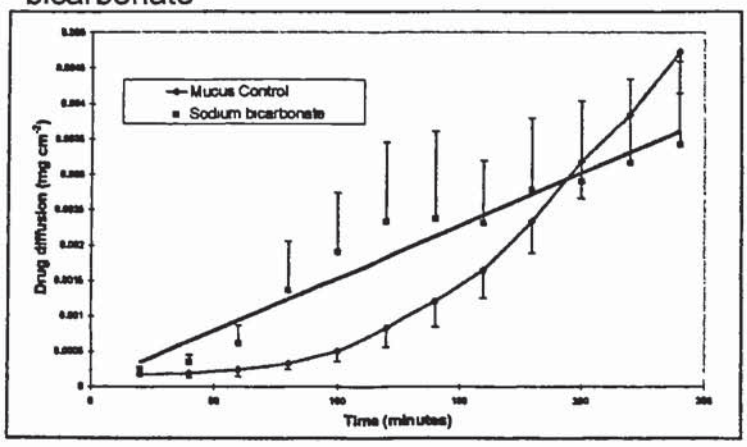

Figure 5.18
Illustrating the diffusion profile for ibuprofen solution saturated with magnesium hydroxide

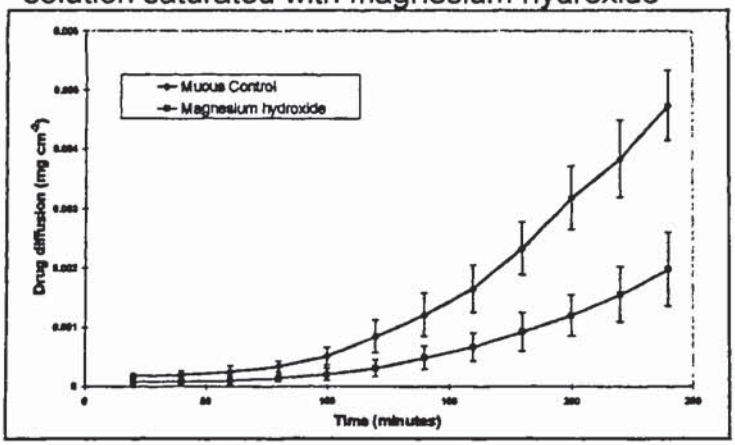

Figure 5.19
Illustrating the diffusion profile for ibuprofen solution saturated with magnesium oxide

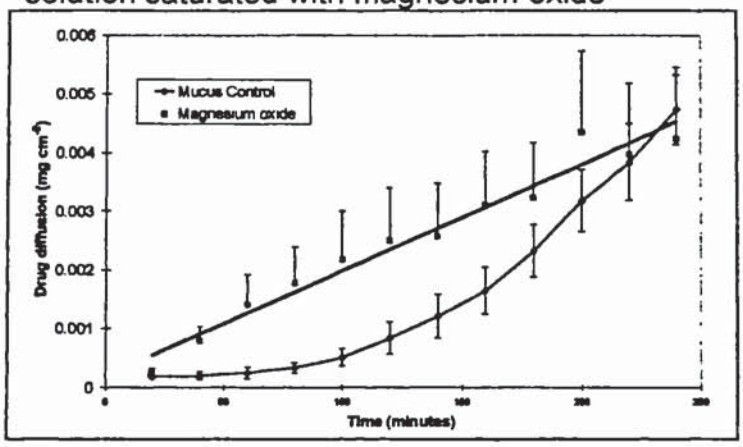

Figure 5.20
Illustrating the diffusion profile for ibuprofen solution saturated with aluminium hydroxide

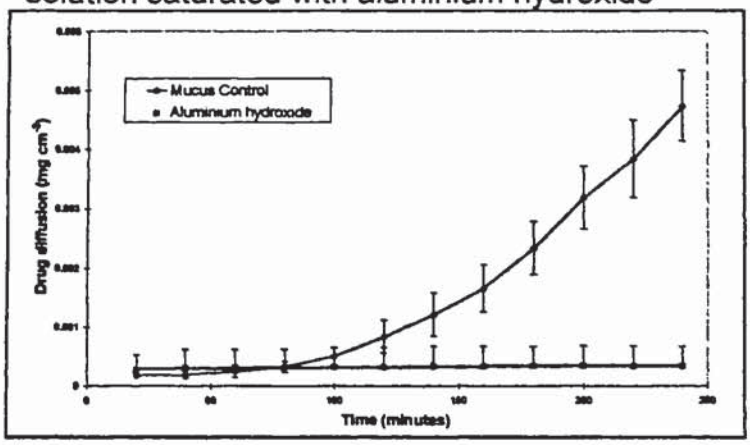

Figure 5.21
Illustrating the diffusion profile for ibuprofen solution saturated with calcium carbonate

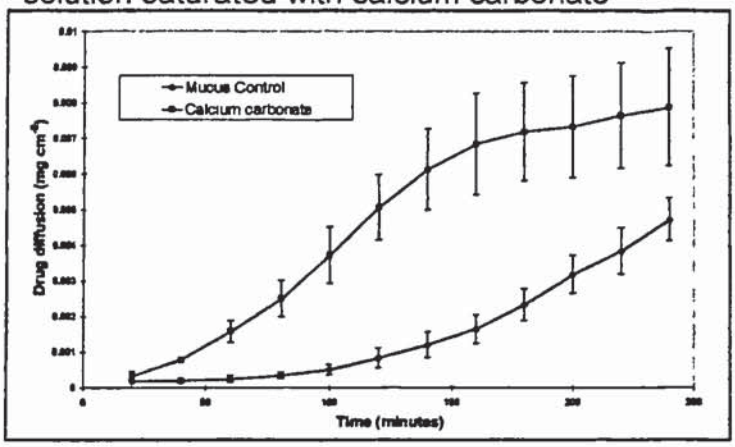

The results from the isolated pH modification study, with ibuprofen being the drug studied, are summarised in table 5.3. The data includes the steady-state flux, the lag times and the calculated permeability coefficients. The lag times and steady state fluxes are also illustrated in figures 5.22 and 5.23 respectively. The following can be observed from the data:

- there is an observed trend in reduction of lag time with increasing solution pH
- there is clear evidence that the diffusion rate of ibuprofen increases with increasing solution pH

The diffusion profiles for ibuprofen at the different pH values are illustrated in figure 5.24.

Table 5.3
Summary of the effect of pH on the diffusion rate of ibuprofen (0.06mg ml^{-1}) through a 1mm mucus thickness layer. Flux and lag time values are the mean of 3 data-points±SD. k_p value and SD were determined by cross-over analysis. R^2 was determined by linear regression analysis of the mean of the replicates.

Experiment	Flux (* 10^8) (mg cm^{-2} s^{-1}) ±SD	Lag time (min) ±SD	k_p (* 10^6) (cm s^{-1}) ±SD	Mean data R^2
pH 2	46.8±18.9	143.2±10.6	9.36±3.8	0.9901
pH 4	61.0±31.5	152.3±11.2	12.2±6.3	0.9937
pH 6	123.0±7.0	49.3±4.2	24.6±1.4	0.9982
pH 8	133.0±2.6	24.2±4.9	26.6±1.0	0.9987

Figure 5.22
Illustrating the effect of pH modification on the lag times for ibuprofen diffusion. Results are the mean of at least three data series+SD

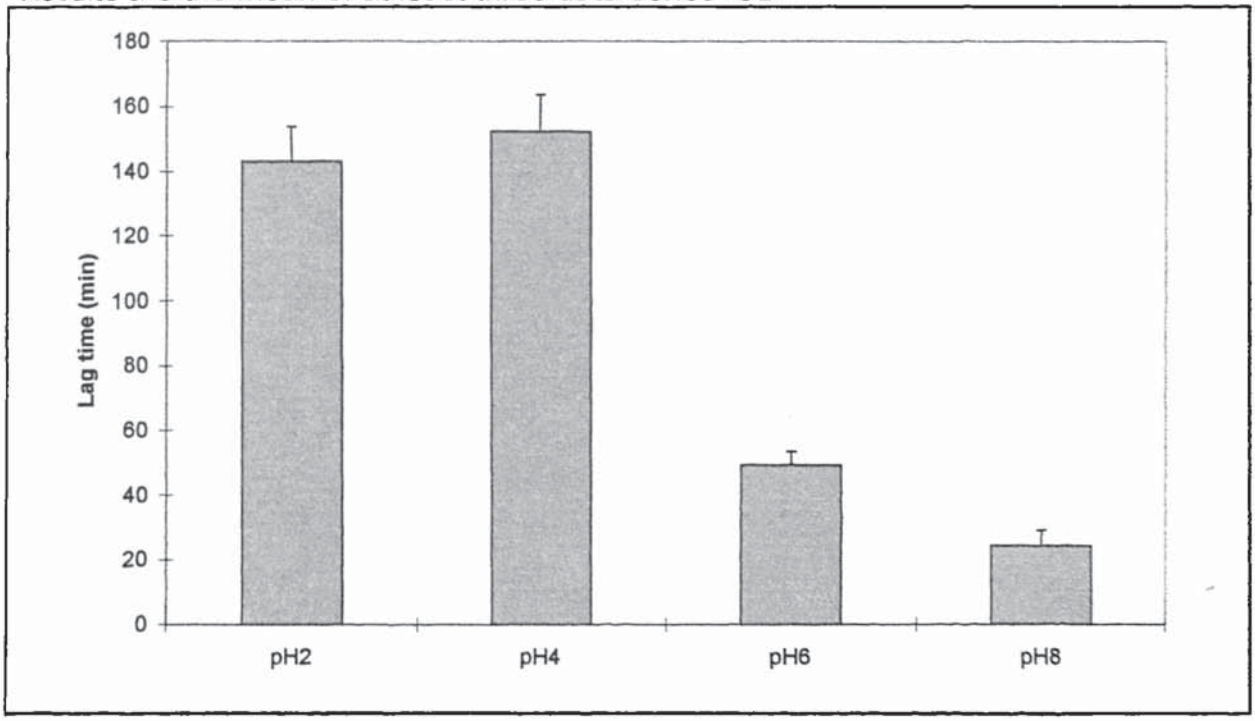

Figure 5.23
Illustrating the effect of pH on the diffusion rate (flux) for ibuprofen diffusion. Results are the mean of at least three data series+SD

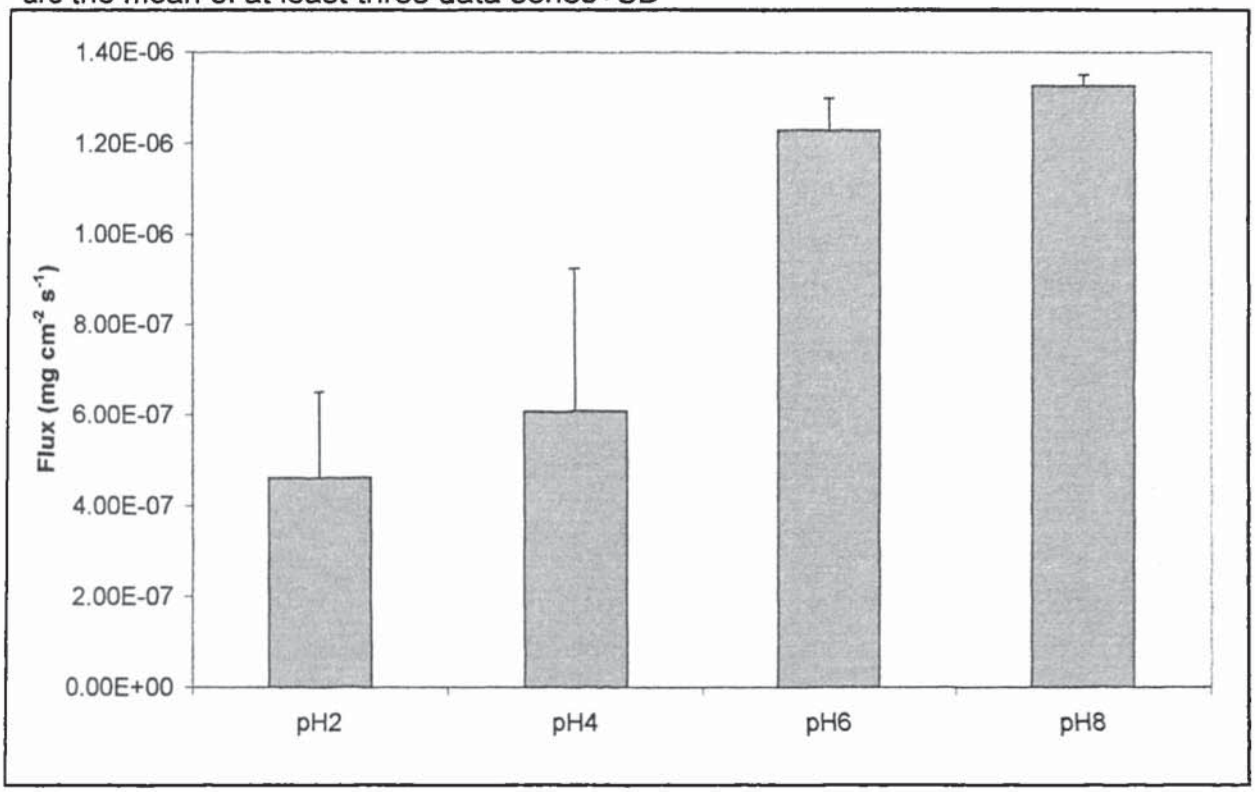

Figure 5.24
Illustrating the effects of pH on the diffusion profile for ibuprofen solution. Results are the mean of at least three data series

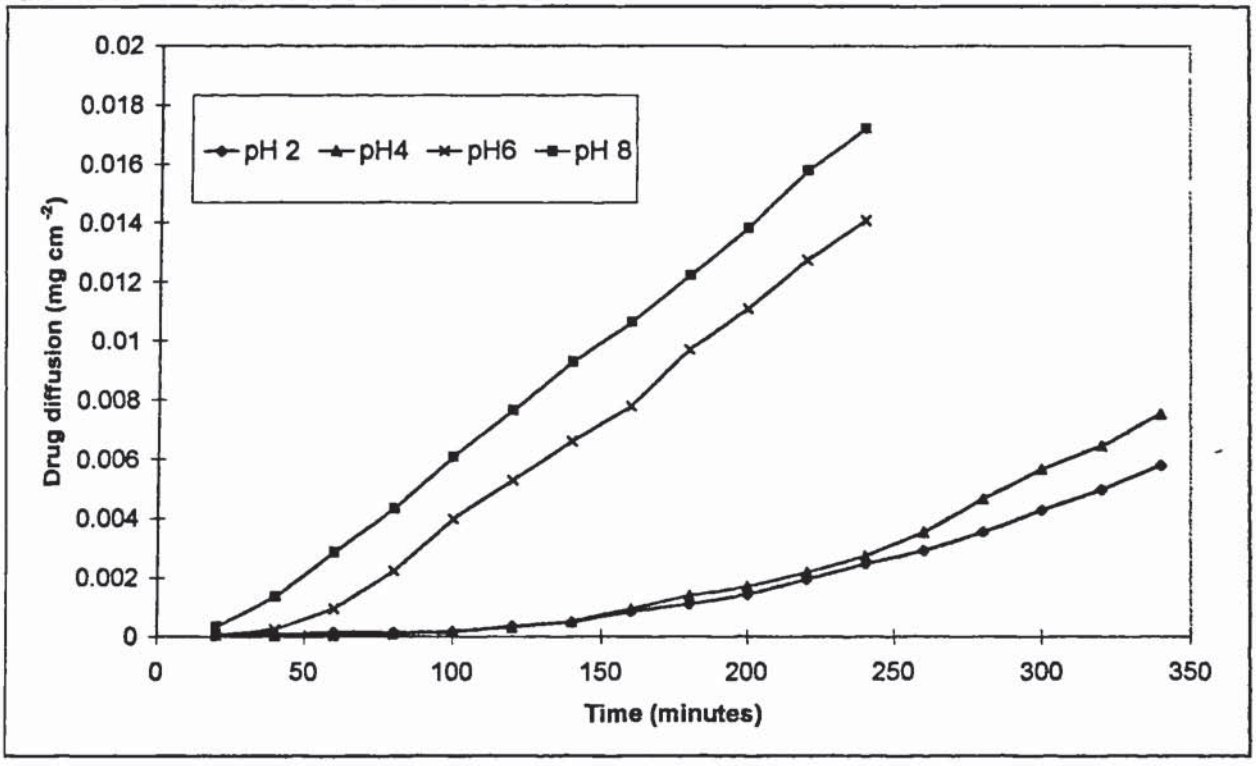

A systematic approach to explain the role of the antacids/excipients on the observed changes should, firstly, consider their role as pH modifiers *i.e.* the role of drug and mucus ionisation on mucus/drug binding and drug diffusion rate. Secondly, the role of hydrophobic interactions should to be considered and, thirdly, other known specific interactions for each antacid required review.

It is known that mucus has predominant ionisable groups within the glycoprotein, N-acetylneuraminic (sialic) acid and esterified sulphate, which both have a pK_a value of 2.6 (Kearney and Marriott 1986). It is also known that paracetamol has a pK_a of 9.5, the mean of reference values. For ibuprofen, from the reported data an mean pK_a of 5.2 was selected. As all are acidic the net charge will tend to negative above the pK_a. Using the Henderson-Hasselbalch equation thus:

$$pH = pK_a + \log \frac{[ionised]}{[unionised]} \qquad \text{equation 5.17}$$

% ionised *versus* pH plots were constructed for each drug and mucus as illustrated in figure 5.25. From these, the percentage ionised of each species could be calculated. After each experiment, the pH of the donor solution was measured and utilised to calculate the % ionised for drug and mucus.

It is recognised that, although glycoprotein is a highly soluble and extensively hydrated macromolecule, it also contains globular protein regions (Kearney and Marriott 1986) and, also, gastric mucus glycoproteins have been shown to be extensively esterified with long-chain fatty acids (Slomiany *et al.* 1983). With such lipophillic regions in the glycoprotein, a hydrophobic interaction with the drug is a realistic possibility. An extensive study by Kearney and Marriott (1986) examined the amount of tetracycline bound to purified reconstituted PGM relative to pH. For tetracycline, at low pH all ionisable groups are protonated and the net charge +1 arises from the dimethyl-amino group (pK_a=9.7). A change to a net charge of 0 occurs above pH 3 due to the ionisation of the acid group of the tricarbonyl methane system (pK_a=3.3) at which point the molecules is zwitterionic. Above pH7 the net charge changes to -1 as the acidic β-diketone system (pK_a=7.7) ionises. They postulated that, taking the two pH/charge profiles, between pH2 and 3, the drug and purified

PGM have opposite charges and hence would be able to interact electrostatically, so creating some binding. Above pH3, the drug becomes effectively neutral and although electrostatic binding is reduced, a hydrophobic interaction is now possible, leading to much more binding. A fall in the binding level above pH7 would be coincident with the reduction in the amount of the neutral species. Levels of binding, calculated theoretically, matched their observed results. As the lag time is intrinsically linked to the degree of binding, this approach will be applied to the current data in terms of lag time analysis.

Figure 5.25
Illustrating the change in percentage of species ionised with changing pH calculated using Henderson-Hasselbalch equation. pK_a mucus=2.6, pK_a ibuprofen=5.2 and pK_a paracetamol=9.5

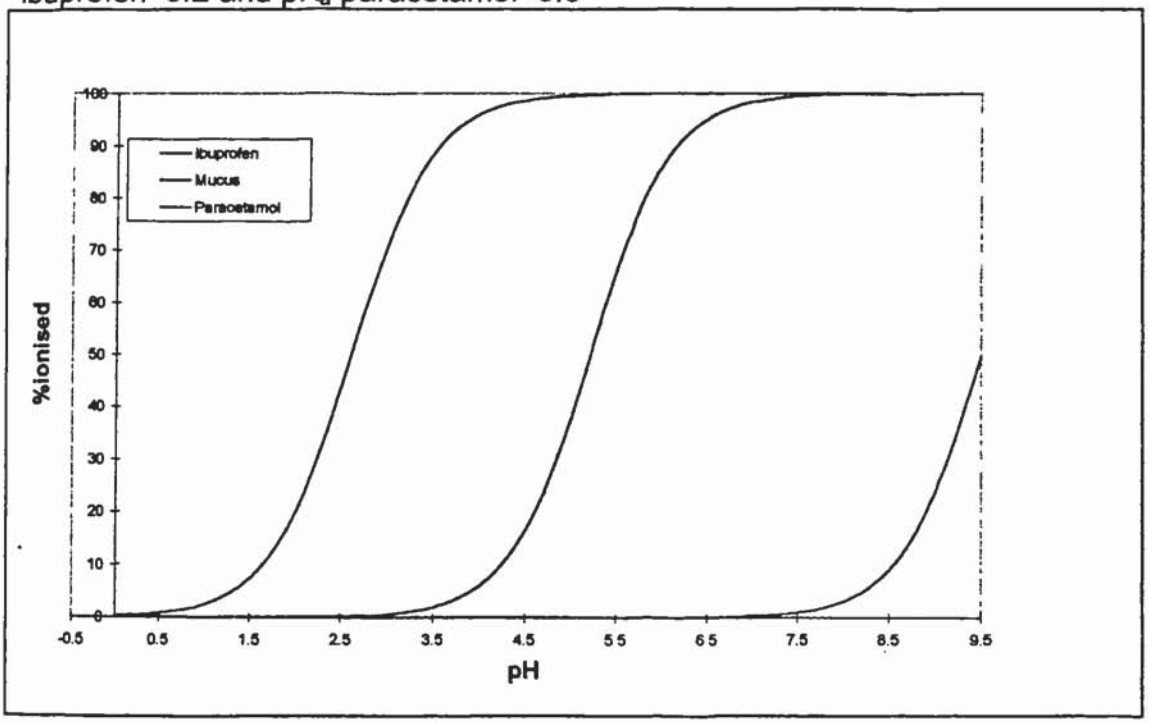

Considering paracetamol, from table 5.4 it is deduced that for all the diffusion experiments the lag times were not significantly different, being in the range of 10-19 minutes. From a knowledge of the solubility of paracetamol and its structure, *i.e.* phenolic, acetyl and amino functional groups, it can be concluded that it is unlikely to interact hydrophobically with the mucus and further, when it is becomes negatively charged, it will be electrostatically repulsed by the mucus. These points indicate that the measured lag time is a function of the diffusion coefficient as shown in equation 5.16 and that binding is insignificant, at the experimental concentrations.

For paracetamol, in terms of steady-state flux and, therefore, permeability constant, it has been concluded that no significant differences were observed by addition of any of the antacid/excipients. This implies, firstly, that any reduction in the viscosity of the mucus as pH is increased, as reported for some mucus models previously, is not sufficient to produce a measurable effect using this method, and secondly, that the vehicle-membrane coefficient *P* is not measurably changed by pH. One reason for this could be that paracetamol is predominantly unionised over the range of experiments as shown in table 5.4 and therefore none or limited electrostatic repulsion would occur, therefore not altering *P* by this mechanism. Changes to the size of the diffusing molecule, *e.g.* through complexation with metal ions, would be unlikely to be detected due to the limits of this technique. Alternatively, it is possible that changes could be occurring in the above properties with their net impact being of no significance.

Table 5.4
Summary of the calculated values of species ionised at experimental pH, for mucus and paracetamol

Antacid/ Excipient	Measured pH post-experiment	Mucus %ionised	Paracetamol %ionised
mucus control	1.3	4.8	0.0
sodium bicarbonate	7.4	100.0	0.8
calcium carbonate	6.7	100.0	0.2
aluminium hydroxide	3.8	94.0	0.0
magnesium hydroxide	9.1	100.0	28.5
magnesium oxide	9.2	100.0	33.4

Considering ibuprofen, and reviewing tables 5.1 and 5.5 the following observations can be made:

- the effect of pH on the diffusion of ibuprofen has been demonstrated. With increasing pH it was observed that the measured lag-time decreased substantially and the drug diffusion rate was greatly increased. These observations can be explained as follows. At low pH's (2-4) ibuprofen is in the unionised state and mucus is predominately unionised. Ibuprofen has a very low solubility in water, has extensive alkyl group substitution on the para position of the aromatic ring and is therefore highly lipophilic. Accordingly, there is a strong possibility that hydrophobic interactions can occur between the lipophilic groups of the glycoprotein macromolecule and the unionised ibuprofen. If so, this would lead to extensive binding of ibuprofen and mucus and, depending on the concentration of ibuprofen, a significant lag time. When the pH was raised to between pH 6-8, where mucus is 100% ionised and ibuprofen is >90% ionised in all cases. It is suggested that the hydrophobic attraction interaction would be eliminated, to be replaced by an electrostatic repulsion interaction. The consequence of this would explain the very large reduction in the lag time. In terms of the increased diffusion rate with increasing pH, for ibuprofen, this may be explained by the observations of Bhaskar *et al.* (1991), who noted a large decrease in mucus pH viscosity as the pH was raised. The fact that this effect was observed for ibuprofen and not for paracetamol may be due to the fact that mucus has been shown in section 5.5 to be a much more significant barrier to ibuprofen diffusion compared to paracetamol diffusion. It is therefore possible that this effect was not observed with paracetamol due to analytical method sensitivity limitations.
- At the pH in the mucus control experiment with ibuprofen, the lag-time was as large as expected, with the potential mechanism as explained above.
- For the experiments where magnesium oxide, magnesium hydroxide, sodium bicarbonate, and calcium carbonate were used as additives, the pHs were raised to between pH 6-8, the lag-times were reduced in line with expectations, with the potential mechanism as explained above.
- Sodium bicarbonate and magnesium oxide significantly reduced the diffusion rate, to between 40-50% of the mucus control. These results cannot be explained using the hypothesis detailed above.

- The results for calcium carbonate and magnesium hydroxide show an increase in the diffusion rate to 149% and 271% of the mucus control, respectively. In addition to the mechanism detailed above, Forstner and Forstner (1975) studied the binding of calcium to purified, calcium-free rat small intestinal mucus. There results showed that Ca^{2+} ($CaCl_2$) bound to mucus, reaching saturation at a concentration of 0.1-1.0mM, independent of temperature and with an increase with increasing pH (5.0-8.7). Their findings also suggested that Ca^{2+} combines with negative charges on mucin, especially those of sialic acid groups. They also found no evidence that $CaCl_2$ caused precipitation, polymerisation or gelation of the mucin in 0.01M Tris/HCl. This mechanism of 'neutralising' the sialic acid residues may also be a factor in the increased diffusion rate observed with the calcium carbonate additive.
- For aluminium hydroxide the antacid effectively eliminated the diffusion of ibuprofen through the mucus layer. Theoretically there are four ways that this could occur, the size of the diffusing molecule could become so large that it could not penetrate the gel structure, the liquid-vehicle membrane coefficient, *P*, could be altered such that no partitioning into the mucus occurred, the viscosity of the mucus could increase dramatically thus eliminating diffusion and finally, the aluminium hydroxide could form an insoluble complex with ibuprofen, eliminating the diffusion gradient. Of these possibilities only the final one has been verified as not being a factor, checked by assaying the donor cell contents post-experiment.

Table 5.5
Summary of the calculated values of species % ionised at experimental pH, for mucus and ibuprofen

Antacid/ Excipient	Measured pH post-experiment	Mucus %ionised	Ibuprofen %ionised
mucus control	1.3	4.8	0.0
sodium bicarbonate	6.3	100.0	92.6
calcium carbonate	6.3	100.0	92.6
aluminium hydroxide	3.5	88.8	2.0
magnesium hydroxide	8.2	100.0	100.0
magnesium oxide	8.2	100.0	100.0

5.6 Summary

- An understanding of human anatomy and physiology and the alkalising properties of the excipients/antacids used in the study leads to the conclusion that mucus is likely to be a far larger barrier to drug absorption in the stomach than in the small intestine and that the alkalising properties will create the greatest environmental change in this region.
- A diffusion method using a side-on three-compartment cell system was selected. Simulated stomach fluid was used as the medium and native PGM was selected as an appropriate mucus model.
- The mucus was validated for stability and inter-batch variation using paracetamol.
- The role of mucus as a barrier to diffusion of the model drugs was investigated. The diffusion rate of paracetamol through mucus was found to be 62.7±7.3% compared to the rate through an aqueous unstirred layer. The diffusion rate of ibuprofen was reduced to 32.7±2.1% of the rate through an aqueous unstirred layer by a mucus barrier.
- Using concentrations estimated as replicating those *in vivo* the effects of the antacids on the diffusion of the model drugs through the mucus model were investigated. For paracetamol, the antacids were found not to effect diffusion of the drug in terms of rate or lag time. Considering ibuprofen, the addition of sodium bicarbonate or magnesium oxide reduced the diffusion rate and lag time. Magnesium hydroxide was found to increase the diffusion rate and decrease the lag time. The addition of calcium carbonate was found to increase the diffusion rate and reduce the lag time. Lastly, aluminium hydroxide effectively eliminated the diffusion of ibuprofen across the barrier.
- Considering the results, it was concluded that paracetamol does not interact significantly with mucus over the experimental pH range and further to this neither the vehicle-membrane partition coefficient or the mucus viscosity were altered sufficiently by the additives to produce a measurable change in diffusion rate. A review of the drug and mucus properties indicated the results were as expected.
- To explain the ibuprofen results the mucus and drug properties were compared. It was concluded that the lag times observed correlated with a drug/mucus hydrophobic interaction that was eliminated at higher pH's. The reduction in diffusion rate observed for the sodium bicarbonate or magnesium oxide

experiments could be explained in terms of electrostatic repulsion caused by both the drug and mucus being negatively charged. An independent study into the effect of pH, in isolation, confirmed that increasing solution pH was responsible for the reduction in lag-time and increase in diffusion rate.

- From the literature a possible mechanism for the increase in ibuprofen diffusion rate in the presence of calcium carbonate was postulated. This was the ability of the antacid to bind to mucin sialic acid residues effectively neutralising the mucus and eliminating electrostatic repulsion.
- A potential mechanism for the effect of added aluminium hydroxide has not yet been elucidated.

CHAPTER 6

DRUG PERMEABILITY THROUGH THE STOMACH AND SMALL INTESTINE

6.1 Introduction

To fully understand the absorption process and drug fate following administration *via* the oral route, it is necessary to investigate drug permeability throughout the gastro-intestinal tract. The development of a model for prediction of an IVIVC, therefore, should include this factors. Specifically, for Class III drugs within the BCS, drug permeability through the human gastro-intestinal tract may be considered the limiting factor in the drug absorption process. Also, during the development process, the drug permeability is an important factor when assessing a drug candidate's suitability for administration *via* the oral route.

For these reasons, the study of drug permeability is widely undertaken, using a variety of methods. However, the ultimate aim of all methods is to correlate with drug permeability in human subjects. The methodology can be sub-divided into five main areas listed here with increasing sophistication and closeness to human oral administration:

- evaluation of drug physicochemical properties used for permeability prediction
- *in vitro* permeability through non-biological membranes
- *in vitro* permeability through biological membranes including human cell lines and animal tissues
- permeability using suitable animal models, *in-situ* and *in vivo*
- pharmacokinetic studies in human volunteers

The aims of this project required the selection of an *in vitro* model for permeability measurement, therefore the method selection was limited to the first three from the list. The determination of physicochemical properties such as the partition coefficient (logP) may be useful in an initial screening process. This may be used to screen drug candidates by use of a combinatorial approach, especially using computer modelling to predict the partition coefficient of compounds not physically produced. However, as this method does not reflect the interactions of the molecule with biological membranes or physiological properties of the membrane, it must be considered to be

the least likely method to predict drug permeability (Zheng 1999). A similar argument can be applied to the use of non-biological barriers, again limiting predictive capability. The model selection was thus narrowed to the use of animal tissues *in vitro* or human cell lines. After further review and initial experimentation, tissue sac methodology using the rat model was selected as the permeability model, the reasoning for this will be explained in section 6.3. As aspects of the model were novel, extensive validation was undertaken to determine the suitability and limitations of the developed methods. The main objective, *i.e.* the potential roles of the antacids/excipients on the permeability of the model drugs was then investigated.

6.2 Theoretical Considerations

A major function of the gastrointestinal tract is to absorb nutrients, electrolytes and water. At the same time, the membranes act as a barrier to potentially harmful compounds and micro-organisms in the lumen. The transport of drugs across biological membranes can be separated into active and passive processes.

Briefly, active transport describes a process whereby materials are complexed with 'carriers' at the surface of apical cell membrane of a columnar absorption cell which are then transported into the cell interior. This can occur against a concentration gradient and is therefore an energy-consuming process. Generally, substances of nutritional interest such as the vitamins riboflavin, thiamine, nicotinic acid and B_6, sugars and L-amino acids are transported across the gastro-intestinal membranes by active processes. Most drugs are not transported by this route although exceptions exist where the drug structurally resembles a natural substance which is actively absorbed. An example of this is levodopa, which is structurally related to the amino acids tyrosine and phenylalanine and is absorbed by the same active transport system as the amino acids, from the lumen of the small intestine into the plasma. (Aulton 1988).

Passive diffusion can be sub-divided into two routes, the paracellular and transcellular pathways. Passive diffusion of drugs across the gastrointestinal/plasma barrier can be described mathematically by Fick's first law of diffusion. Accordingly the rate of appearance of drug in the plasma at the site of absorption is given by:

$$\frac{dm}{dt} = \frac{DA(K_1C_g - K_2C_{b)}}{h} \qquad \text{equation 6.1}$$

where *dm/dt* is the rate of appearance of drug in the blood at the site of absorption, *D* is the diffusion co-efficient of the drug in the gastrointestinal membrane, *A* is the surface area of the membrane available for passive diffusion, K_1 is the apparent partition coefficient of the drug between the membrane and the gastrointestinal fluid, C_g is the concentration of the drug in the gastrointestinal fluid at the site of absorption, K_2 is the apparent partition coefficient between the gastrointestinal membrane and the plasma, C_b is the concentration of drug in the plasma at the site of absorption and *h* is the thickness of the gastrointestinal membrane. Hence K_1C_g and K_2C_b represent the concentrations of the drug inside the membrane at the gastrointestinal fluid/membrane interface and the gastrointestinal membrane/plasma interface respectively (Aulton 1988). The concentration gradient can be expressed thus:

$$\frac{(K_1C_g - K_2C_b)}{h} \qquad \text{equation 6.2}$$

As distribution of drug takes place into a large volume of blood and tissue, combined with metabolism and excretion, plasma can be considered a 'sink' and it follows that $K_1C_g >> K_2C_b$ and thus (K_1C_g-K_2C_b) approximates to K_1C_g. Equation 6.1 can therefore be rewritten as:

$$\frac{dm}{dt} = \frac{DAK_1C_g}{h} \qquad \text{equation 6.3}$$

Also, as *D*, *A*, K_1 and *h* may be regarded as constants under specified conditions and therefore can be combined into a constant known as the permeability constant, *P*. Therefore equation 6.3 becomes:

$$\frac{dm}{dt} = PC_g \qquad \text{equation 6.4}$$

The passive transcellular pathway can be explained simply by the pH-partition hypothesis of drug absorption in combination with the partitioning of a drug between the aqueous and lipid phases of the lumen and plasma, and membrane, respectively, based on the drug's polarity. The pH-partition hypothesis assumes that the gastrointestinal membrane is impermeable to the ionised (hydrophilic) form of a weak acid or basic drug but is permeable to the non-ionised (relatively lipophillic) form of the drug. The pH of the luminal medium and the plasma and the pK_a of the drug will therefore directly influence drug absorption. Therefore, the ionisation state of a drug and the inherent lipophilicity of the ionised and unionised species will contribute to the actual drug permeability (Taylor *et al.* 1989).

The paracellular route involves the convective transport of molecules across aqueous pores or channels in the membrane. This route is limited to small molecules such as water, urea and low molecular weight sugars and is limited by increasing molecular weight (Artursson *et al.* 1993).

The two constituents of the passive transport system can be incorporated into a physical model as illustrated in figure 6.1 where C_1 is the drug concentration in the gastrointestinal fluid, C_2 and C_{bound} represent the drug concentration equilibrium in mucus, J_{sm} and J_{ms} are the mucosal-to-serosal and serosal-to-mucosal water fluxes for compound C, ϕ is the sieving co-efficient, k_{trans} represents the transcellular permeability (P) and ϕJ_{ms} represents the paracellular permeability (Taylor *et al.* 1989)

Therefore the overall membrane permeability rate constant, P_{mem}, can be written as:

$$P_{mem} = \phi . J_{ms} + k_{trans} \qquad \text{equation 6.5}$$

Finally, the tissue membrane is not the only barrier to drug permeability as the unstirred aqueous layer must also be considered. The apparent permeability, which is measured experimentally, is dependent on these two factors thus:

$$\frac{1}{P_{app}} = \frac{1}{P_{mem}} + \frac{1}{P_{aq}} \qquad \text{equation 6.6}$$

where P_{aq} and P_{app} represent the permeability coefficient through the aqueous layer and the measured permeability coefficient, respectively.

Figure 6.1
Schematic representation of convective (paracellular) and diffusive (transcellular) components of passive drug absorption across the gastrointestinal mucosa

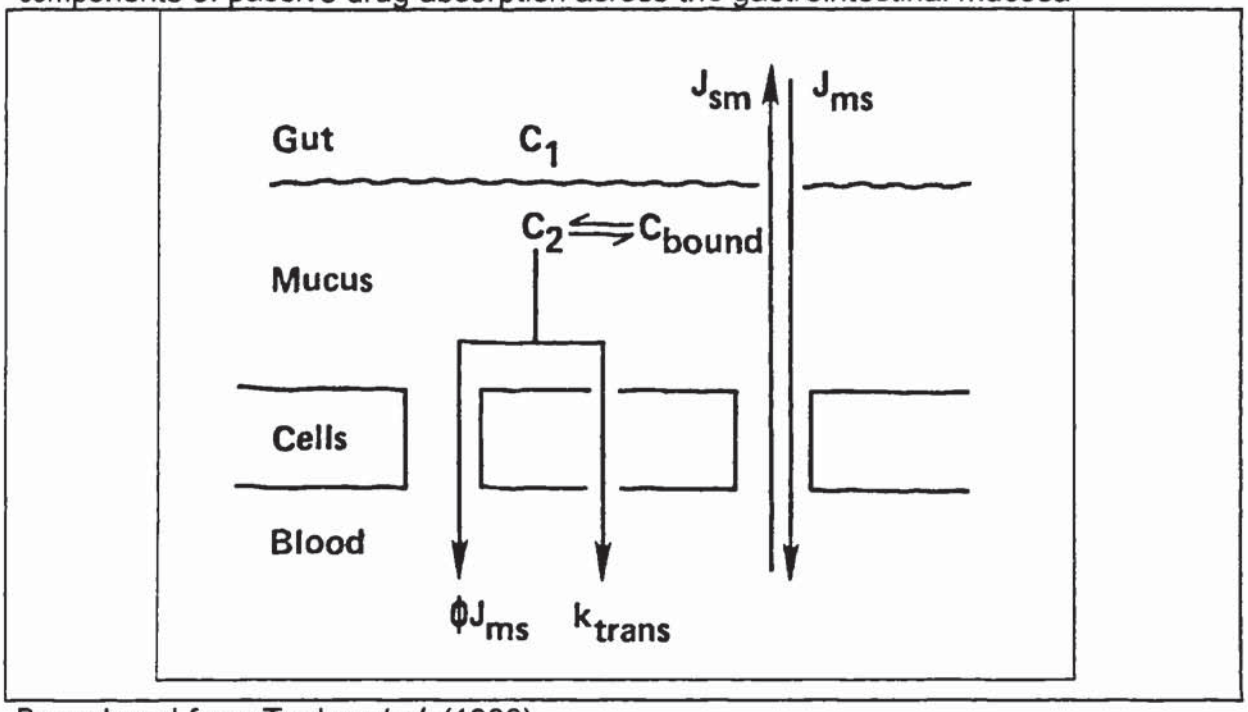

Reproduced from Taylor *et al.* (1989)

6.3 Development of *in vitro* stomach and intestine models

Individual physicochemical properties of drug molecules such as lipophilicity, represented by measurement of the partition coefficient, are roughly correlated to passive drug transport across gastrointestinal membranes. Lipophilicity has been used to predict drug permeability *in vivo*;, however, the correlations have only been significant when the compounds are from an homologous series (Martin 1981 and ter Laak *et al.* 1994). It is known that drug permeability is not solely dependent on drug lipophilicity, but combines the transcellular and paracellular pathways, and may be affected by interactions with the mucosa and membrane, This implies that factors including molecular weight, drug ionic charge, pH modification at the surface micro-environment, drug binding to mucus, mucus layer pH buffering etc. are likely to influence drug permeability. To study these factors, various biological methods have been developed to model the human *in vivo* situation more closely.

One of the most widely used technique for the measurement of drug permeability through biological tissue is the everted intestinal sac technique, developed by Wilson and Wiseman (1954). In this technique, tissues from the gastrointestinal tract are removed from the animal, with rats most frequently used, during terminal anaesthesia or after sacrifice. Usually, tissue sections are everted using, for instance, a glass rod and then tied-off at each end with the inclusion of a receiver solution, to form an everted sac. The sacs are then shaken with a donor solution, containing the drug of interest. At specified time intervals the sacs are removed, opened and the contents analysed. It has been demonstrated that the sacs are morphologically intact after eversion but progressively lose structural integrity, depending on the method used to obtain the tissue. Specifically, perfused intestines removed from anaesthetised rats, which have thus never been deprived of oxygen, maintain their structural integrity even after perfusion for 60 minutes with Krebs-Henseleit bicarbonate perfusate. Conversely, intestines removed from freshly killed rats were shown to have severe villus disruption and oedema after perfusion for only 20 minutes. It has also been shown that extensive damage to both crypts and villi is observed after a 20-minute incubation, regardless of the buffer system used (Plumb *et al.* 1987). Separately, Levine *et al.* (1970) observed that when using tissues obtained from pre-sacrificed rats, total disruption of the epithelial border had occurred after 60 minutes, but with tissues obtained from anaesthetised rats only 10-15% of the epithelial cells and been disrupted or destroyed. Clearly, the use of anaesthetised rats is preferable to sacrificed rats. However, the use of anaesthetised rats in the UK would require a specific project licence for the work to be authorised to be undertaken. The method is also limited in that the serosa and muscalaris are not removed and therefore contribute to the overall barrier. However, the advantages for the method using sacrificed rats include its widespread use, simplicity of method set-up and operation, and the absence of a requirement for specialised equipment.

A relatively new method for the study of drug permeability has been the development of human cell-culture systems. Initially, their development was limited by the lack of retention of anatomical and biochemical features of differentiated cells *in vivo*. At first, isolated, intestinal epithelial cells were used but these were found to be difficult to culture and had limited viability (Moyer 1983). This led to the use of human tumour

cell lines, particularly the human adenocarcinoma cell lines, which were found to have properties characteristic of differentiated intestinal epithelial cells (Rousset 1986, Pinto *et al.* 1983 and Neutra *et al.* 1989). Numerous studies on the characterisation of Caco-2 cell lines have shown their suitability as a tool for measuring drug permeability. For example, a high degree of cell differentiation has been observed (Zweibaum *et al.* 1989). Also, the transepithelial transport of an homologous series of six beta-blocking drugs, correlated with those published for rat ileum *in-situ*, in line with a 2000-fold range of lipophilicity (Artursson 1989). Finally, the integrity of cell tight junctions has been established by use of molecular markers (Artursson *et al.* 1993). However, Caco-2 cells are characterised by a tight, 'non-leaky' epithelial layer, the result of the tight-junction configuration. This may lead to non accurate prediction of the contribution of the transcellular route. This has been demonstrated by Artursson and Magnusson (1989) who compared the permeability of an homologous series of beta-blockers in Caco-2 cells and *in-situ* using the rat model. They found that with the lipophilic drugs, in which transport is mainly by the transcellular route, showed comparable transport rates in both models, but hydrophilic drugs such as practolol and atenolol, where the paracellular route is more significant, exhibited much slower rates in the Caco-2 system compared with the *in-situ* model. For confirmation, the transmembrane resistance of the Caco-2 monolayers was reduced from 170-400 ohms cm^2 to a resistance of 60-90 ohms cm^2, which corresponds to that of rat ileum, by use of a low extracellular calcium environment. These experiments showed an increase in the hydrophilic drug transport, which was similar to the *in-situ* rat model. While allowing elucidation of the transcellular and paracellular pathways, this characteristic may indicate that 'leaky' membranes such as rat ileum are more suitable for measuring the paracellular component of drug transport. Other practical limitations of these systems include the requirement of specific laboratory facilities, extensive protocols, coupled with substantial experience to successfully and consistently grow the cell cultures, which itself takes several weeks.

Another relatively new technique uses excised tissues, as used in the everted sac method, but involves the removal of the serosa and/or the muscularis externa from the tissue sample. The samples are mounted into Ussing chambers as a flat sheet, with a donor and receiver chamber either side. The use of this system has been

demonstrated to maintain the viability and integrity of the tissue (Polentarutti *et al.* 1999). Electrical parameters are used for monitoring the viability and integrity of the tissue in the Ussing chamber. In general, potential difference is said to reflect the voltage gradient generated by the tissue, resistance reflects the tissue integrity and the short circuit current reflects the ionic fluxes across the epithelium. Polentaruttii *et al.* (1999) found that potential difference values obtained for rat intestine correlated with those found in humans, *i.e.* the further down the intestine the measurement was performed the more negative the potential difference became. They found that over time (approx. 3 hours) both the potential difference and short circuit current decreased from the base line value at the same time as changes in tissue morphology were observed. However, the resistance was found to be stable for all intestinal segments for the experimental duration even though the total epithelial surface area decreased by approximately 50%, which they believed should lead to a doubling of resistance. It was also observed that the permeability of the paracellular marker mannitol increased over time, indicating a structural tight junction alteration which would result in decreased resistance. They concluded that the resistance measurement did not reflect tissue integrity alone and that the complexity of factors required further investigation. This study also demonstrated the selectivity of the technique by comparing the permeability of the transcellular marker propranolol with the paracellular marker mannitol. As expected, propranolol was significantly more permeable, for example the P_{app} was approximately ten-fold higher in the rat duodenum than mannitol.

Another study, conducted by Artursson *et al.* (1993), compared the selective paracellular permeability of rat ileum and colon *versus* two Caco-2 cell sub-classes (Caco-2P and Caco-2cl.40). The study compared the permeability of monodisperse polyethylene glycols with a molecular weight range of 200-500. Over this range it was observed that the P_{app} decreased from approx. 35E-06 cm s^{-1} to 5E-06 cm s^{-1} for the compounds in the ileum and 5E-06 cm s^{-1} to 1E-06 cm s^{-1} for the colon. Interestingly, both Caco-2 cell subclasses had very similar P_{app} values to the rat colon experiments. This indicates more molecular weight selectivity in the rat ileum tissue compared to the cell cultures and that the Caco-2 cell subclasses act as similar molecular weight barriers as rat colon tissue. Practically, one drawback of this method is that the dissection procedure to remove the serosa and/or muscalaris requires a significant

level of competence to produce tissue of suitable quality, as determined by the authors own experience and that omission of replicates not within limits set for electrical parameters has been used as an experimental control (Artursson *et al.* 1993).

A key objective of this project was to produce an integrated model, where dissolution and permeability data could be utilised to model drug absorption and predict bioavailability. The devised model as illustrated in figure 1.6 includes absorption in two anatomical compartments, *i.e.* the stomach and small intestine. It was therefore a prerequisite that the selected method could be used to simulate drug permeability at both these sites, using identical methodology. Work has been conducted to produce a cell-culture system that models the human stomach (Sekiguchi *et al.* 1978; Barranco *et al.* 1983). However, it was deemed that the development and validation of an appropriate cell line was beyond the scope of the project. Finally, the CaCo-2 cell line available does not contain goblet cells and is therefore limited in that no mucus layer is produced. Therefore, the use of cell-culture methods was excluded as an option in this study. The Ussing chamber method appears superior to the conventional everted sac method in that the viability and integrity of the tissue can be monitored, but may be limited in that maintenance of the mucus layer may not occur. More importantly, surgical skill is required to separate the serosa and/or muscalaris without damaging the underlying epithelium layer. Also, to reiterate, Artursson *et al.* (1993) and Curtis and Gall (1992), set criteria for short-circuit current and potential difference, excluding intestinal and stomach tissues, respectively, not meeting minimum requirements. Also, in communications with Goddard and Spiller (1997) it became apparent that the correct dissection of stomach tissues is not an easily transferable skill. It was concluded that the use of this methodology would severely limit the usefulness of the models developed in the course of this study as any future work could only be undertaken where specialised skills were available. The use of the Ussing chamber system was excluded on this basis.

It was therefore decided to base the permeability models on the everted sac method, with modifications. The rat was selected as the model and, as the rat stomach is not easily everted, a method was devised such that neither the stomach or duodenum, which was selected to represent the small intestine, were everted. Eversion is usually performed to produce a higher degree of analytical sensitivity, however within this

study no analytical deficiencies were encountered. The *in vitro* use of the stomach organ, complete with serosa and muscalaris for permeability studies has not previously been attempted, with the sac method. The utilisation of intestinal segments without the removal of the serosa/muscalaris are commonly used, for example by Barthe *et al.* (1998), Feinroth *et al.* (1982), Gershanick *et al.* (1998), Hughes *et al.* (1995) and Trenktrog *et al.* (1995). Micrographs produced by Curtis and Gall (1992) illustrated that the muscalaris layer forms approximately 20% of the total thickness the rat gastric corpus. It has also been suggested that the submucosal muscle layers do not represent a significant barrier to small molecules such as mannitol (Jackson 1987). The use of the entire stomach and a medium modified to allow dissolution of the antacids/excipients under study led to the requirement that substantial validation and characterisation of the developed methods was necessary.

6.4 Validation of stomach and intestine models

6.4.1 Tight Junction Integrity

6.4.1.1 Experimental

6.4.1.1.1 Materials

[^{3}H] Mannitol was obtained from ICN (Ca, USA), (reference appendix 2 for details of manufacture and C of A). Hydrochloric acid, Hanks balanced solution (calcium, magnesium and phenol red free), mannitol, EGTA, sodium hydroxide and calcium chloride were obtained from Aldrich (Poole, UK). HEPES was obtained from Life Technologies (Paisley, UK). CO_2-O_2 (5:95) was obtained from BOC (Manchester, UK). All materials were pharmaceutical or analytical grade as appropriate. Double-distilled water was generated in-house using a Fison's Fi-Stream Still.

6.4.1.1.2 Equipment

A Techne Tempette Junior TE-8J water bath was used to maintain the temperature throughout the experiments. 30ml disposable universals (Bibby Sterilin, Stone, UK) were used to house the tissue sacs and receiver solutions. The CO_2-O_2 gas mixture was bubbled through the receiver solution from the gas cylinder *via* rubber hosing,

with endings consisting of 1ml syringes obtained from Leuven (Belgium) and size 26 needles (Becton Dickinson, Dublin, Ireland), where the metal needles had been removed and the ends blunted. The system was designed to accommodate a maximum of 6 replicates *per* experiment.

6.4.1.1.3 Method

Male Wistar rats weighing between 250-450g, allowed food and water *ad libitum*, were sacrificed by cervical dislocation. The entire stomach and/or the duodenal part of the intestine, proximal to the stomach, were removed and transferred to the experimental area, being stored in pregassed modified buffer solution (MBS). The buffer contained 0.05M HCl, Hanks Buffer, 25mM HEPES, with adjustment to pH6.8 using 10% (w/v) sodium hydroxide solution. The buffer pH of 6.8 was selected on the basis that the mucus layer acts to form a pH gradient, especially in the stomach, whereby the pH at the mucosa/mucus interface is approximately 7 (Macadam 1993). For the control experiment the MBS contained 1.25mM calcium chloride, for the calcium-free experiment the calcium chloride was omitted and the selective calcium chelator EGTA added to bind extracellular calcium (Artursson 1989), at a concentration of 10mM. Segments of duodenum approximately 3cm in length were obtained, avoiding Peyer's patches. Silk braiding was used to tie-off each end of the intestinal segment, with 0.5ml of donor solution added into each sac. For the stomach, silk braiding was used to tie-off at the oesophageal/cardia and duodenal/pylorus interfaces, ensuring the formed sac contained only stomach tissue. 2.0ml of donor solution was included within each sac. The appropriate MBS was used as the donor and receiver solution, the donor solutions supplemented by the addition of 0.1M mannitol and spiked with an aliquot of radio-labelled mannitol to give an activity of ≈300,000 DPM ml^{-1}. The sacs were placed individually into a sterilin (30ml) with 15.0ml of the appropriate pre-warmed MBS, each sterilin (30ml) being clamped into the water bath to maintain the temperature at 37°C. The CO_2-O_2 gas mixture was bubbled through the receiver solution of each universal. Aliquots of 5.0ml were sampled every 10 minutes for 60 minutes for the intestine experiment and every 15 minutes for 105 minutes for the stomach experiment, the sample volume being replaced with the appropriate pre-warmed MBS. The samples were assayed according to the scintigraphic method detailed in section 2.7. This procedure

produced a dilution of the receiver phase. It was therefore necessary to adjust each successive sample concentration for the dilution caused by all the previous samples. This was performed, using an Excel spreadsheet, by applying the correction factor detailed in equation 4.9. On completion of the experiment the sacs were opened with scissors and/or scalpel, and pinned onto a board for determination of surface area.

6.4.1.2 Results and Discussion

The tight junction is one of the major components of absorptive and secretory epithelia. It contributes to the epithelial permeability barrier by controlling the diffusion of ions and neutral molecules through the paracellular pathway, *i.e.* the transport route through the paracellular space. This function of the tight junction can be thought of as a "gate" with highly variable permeability properties (Diamond 1977). The tight junction is crucial to the organisation of the transcellular pathway, the transport route through the cell, because it participates in the polarisation of the epithelial plasma membrane into the compositionally distinct apical and basolateral domains (Simons and Fuller 1985). The polarised distributions of ion channels, pumps, and enzymes into apical and basolateral domains is responsible for the vectorial nature of transepithelial transport. Because the tight junction forms the boundary between these membrane domains, it can also be thought to function as a "fence" in the plasma membrane (Diamond 1977, Barry 1987). Therefore, the functionality of the tight junctions should be present to ensure the integrity of the epithelial layer and suitability of the model for predicting drug permeability. The integrity of the cell tight junctions has been shown to be dependent on extracellular calcium (Ca^{2+}), (Madara and Trier; 1987; Martinez-Palomo *et al.* 1980;Gumbier *et al.* 1988 and Volberg *et al.*. Classically, the use of a Ca^{2+}-free buffer containing a Ca^{2+} chelating agent is used to 'loosen' the tight junctions. For example, this can be used to study the contribution of the paracellular and transcellular pathways to lipophillic and hydrophilic drug transport through a Caco-2 cell monolayer (Artursson and Magnusson 1989) or to validate the use of an everted sac method for the study of drug transport by the paracellular route (Barthe 1998). In both these methods, 2.5mM EGTA was used as the calcium chelating agent, the 'loosening' of the tight junctions measured by changes in membrane resistance and mannitol transport, respectively.

In order to demonstrate tight junction integrity, the transport of mannitol, a commonly used paracellular marker, was measured through the stomach and intestine sacs, using a calcium free buffer and 10mM EGTA, with comparison to a control where calcium was present in the buffer and EGTA was absent. The results from this study are detailed in table 6.1. The data included the calculated apparent permeability co-efficients, derived from the steady-state flux, and the correlation co-efficient R^2. The drug transport profiles are illustrated in figures 6.2 and 6.3.

Table 6.1
Summary of the effect of a calcium-free buffer (donor and receiver) on the transport of the paracellular marker mannitol through tissue. Results are the mean of 3 replicates±SD. R^2 was determined by linear regression of the mean of the replicates

Experiment	P_{app} ($cm\ s^{-1}$) ±SD	R^2
stomach model control	1.25E-06±9.78E-08	0.9944
stomach model 'calcium-free'	1.95E-06±2.32E-07	0.9936
intestine model control	1.54E-05±1.07E-06	0.9928
intestine model 'calcium-free'	1.92E-05±8.85E-07	0.9857

Figure 6.2
Illustrating the difference in mannitol permeability through stomach in the presence and absence of calcium ions. Results are the mean of 3 replicates ±SD

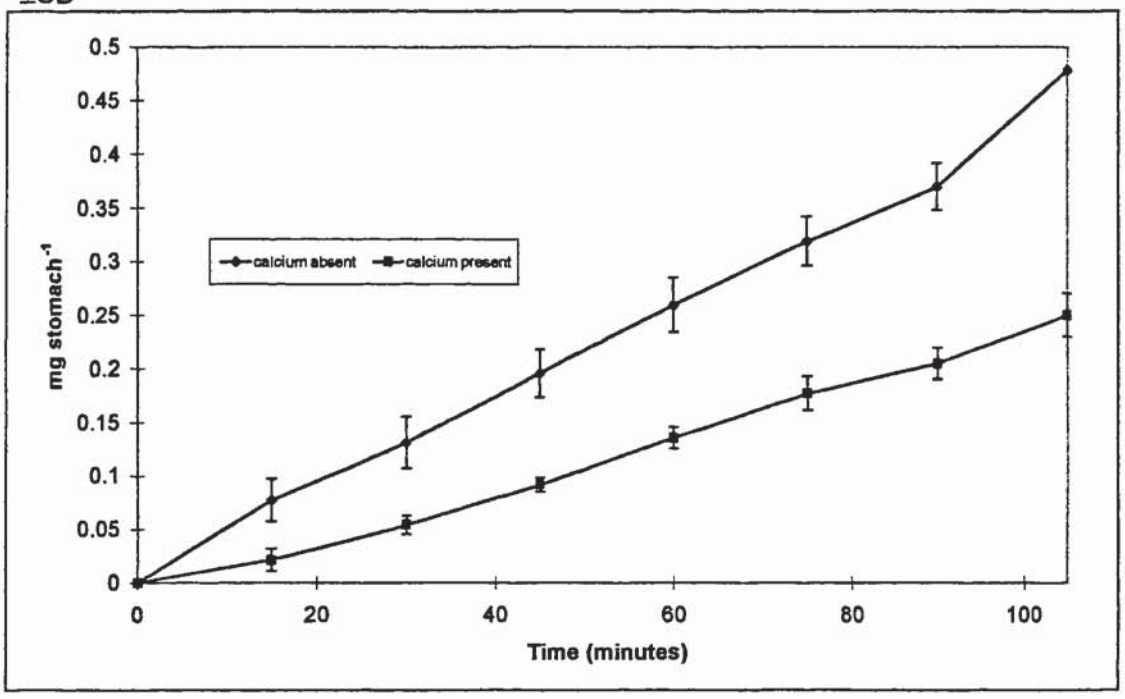

Figure 6.3
Illustrating the difference in mannitol permeability through intestine in the presence and absence of calcium ions. Results are the mean of 3 replicates with Sd appropriate for visual clarity.

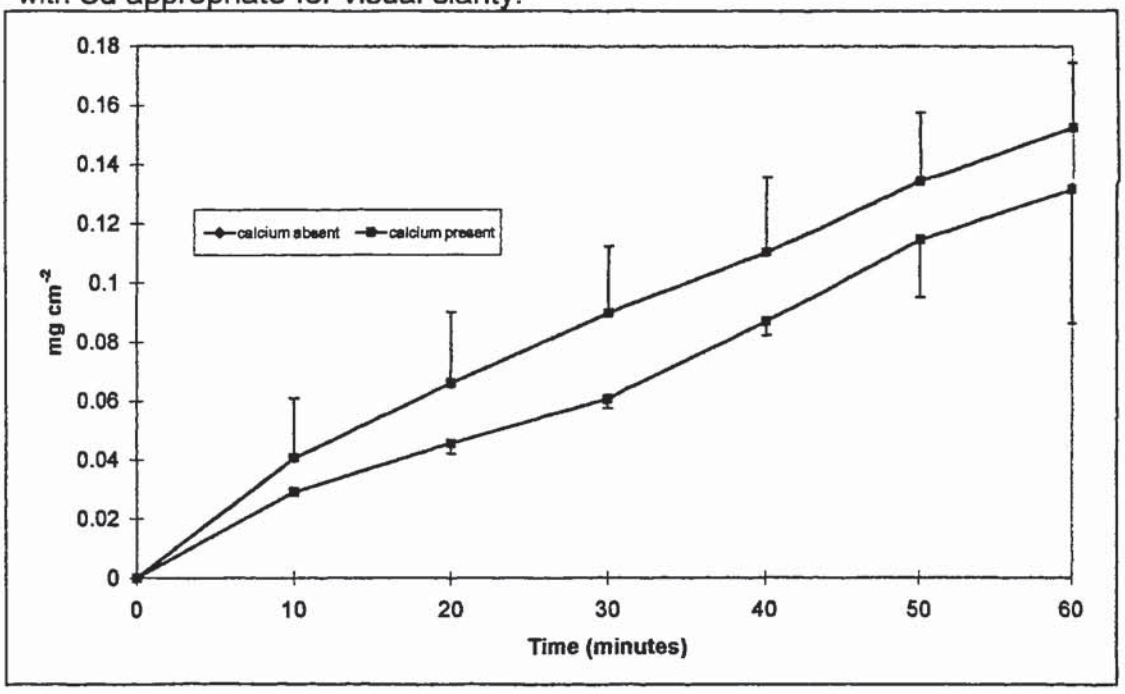

The results indicate that, under calcium-free conditions, the apparent permeability co-efficient is very significantly increased, for the stomach a 56% increase was measured (t-test, P=0.0086), and for the intestine a 25% increase was measured (t-test, P=0.0090), *vs.* controls. These data confirm the integrity of cell tight-junctions. Comparing the data to literature values, Barthe *et al.* (1998) found, using a similar protocol, employing the entire small intestine, that increases of the same order were observed, *i.e.* a 60% increase was observed when EGTA was added to the apical side only with a 90% increase observed when EGTA was added to the apical and basolateral sides. In contrast, the effect of opening tight junctions in the Caco-2 model has produces a much larger increase in mannitol transport, *i.e.* an increase from ≈1.5% to ≈15-25%, a 10-15 fold increase (Nicklin *et al.* 1995). The greater changes observed in the Caco-2 model are likely to be due to two reasons. Firstly, the Caco-2 model consists of a monolayer of epithelial cells, which represent the whole barrier, whereas in the sac model the barrier consists of mucus, mucosa, sub-mucosa, muscalaris and serosa, therefore the opening of tight junctions would be expected to increase the transport rate of mannitol much more through the Caco-2 monolayer than the sac tissue. The second reason is likely to be that the Caco-2 system is considered to contain a particularly 'tight' cell layer, where paracellular transport under control conditions may be lower than expected (Barthe *et al.* 1998 and Palm *et al.* 1996)

6.4.2 Method reproducibility and tissue stability

6.4.2.1 Experimental

6.4.2.1.1 Materials

[^{3}H]Mannitol and [^{14}C]ibuprofen were obtained from ICN (Ca, USA), [^{14}C]paracetamol was obtained from SB (USA), (reference appendix 2 for details of manufacture and C of A). Ibuprofen and paracetamol were obtained from SB (Weybridge, UK). Hydrochloric acid, Hank's balance solution (calcium, magnesium and phenol red-free), mannitol, sodium hydroxide and calcium chloride were obtained from Aldrich (Poole, UK). HEPES was obtained from Life Technologies (Paisley, UK). CO_2-O_2 (5:95) was obtained from BOC (Manchester, UK). All materials were pharmaceutical

or analytical grade as appropriate. Double-distilled water was generated in-house using a Fison's Fi-Stream Still. Details and sourcing of added excipients/antacids are detailed in section 6.5.2.1.

6.4.2.1.2 Equipment

The equipment and set-up was as described in section 6.4.1.1.2. A Techne SB-16 water bath/shaker was used for sample preparation of the saturated antacid solutions.

6.4.2.1.3 Method

The general method for tissue collection, transfer to experimental area and preparation of sacs was as detailed in section 6.4.1.1.3. The MBS contained 0.05M HCl, Hank's buffer, 25mM HEPES and 1.25mM calcium chloride with adjustment to pH6.8 using 10% (w/v) sodium hydroxide solution. For the experiments where an 'insoluble' antacid/excipient was under investigation, the MBS was prepared as follows; the suspensions were well shaken manually and then placed in the water-bath at 37°C, agitator setting 1 (70 cycles *per* minute), for 4 days. On the fifth day, and after a minimum of 96 hrs, the supernatant was decanted off. The preparation of the MBS was then completed. For investigation of the effect of added sodium bicarbonate, the excipient was added at a concentration of 15mmol *per* 200ml before adjustment to pH6.8. All donor solutions were supplemented by the addition of 0.1M (≈2.0mg ml^{-1}) mannitol and spiked with an aliquot of radiolabelled mannitol to give an activity of 300,000-1,000,000 DPM ml^{-1}. Depending on the drug under investigation the donor solution also contained paracetamol at 5.0mg ml^{-1} with a spiked aliquot of radio-labelled paracetamol to give an activity of 500,000-2,500,000 DPM ml^{-1} or, ibuprofen at 2.0mg ml^{-1} with a spiked aliquot of radio-labelled ibuprofen to give an activity of 500,000-2,500,000 DPM ml^{-1}. The sacs were placed individually into a universal with 15.0ml of the appropriate pre-warmed MBS, each universal being clamped into the water bath to maintain the temperature at 37°C. The CO_2-O_2 gas mixture was bubbled through the receiver solution of each universal. Aliquots of 5.0ml were sampled every 10 minutes for 60 minutes for the intestine experiment and every 15 minutes for upto 180 minutes for the stomach experiment, the sample volume being replaced with the appropriate pre-warmed MBS. The samples were analysed by

the scintigraphic method detailed in section 2.7. This procedure produced a dilution of the receiver phase. It was therefore necessary to adjust each successive sample concentration for the dilution caused by all the previous samples. This was performed, using an Excel spreadsheet, by applying the correction factor detailed in equation 4.9. On completion of the experiment the sacs were opened with scissors and/or scalpel, pinned onto a board for determination of surface area.

6.4.2.2 Results and discussion

Two essential requirements required for analytical/modelling methods are that the system is stable and that the results are reproducible. A suitable method should be able to distinguish true effects from random errors. As in any method, the introduction of variability was possible; for example, the use of non-fasted rats over a fairly wide weight range. ANOVA analysis is usually performed to determine whether the inter-batch variation exceeds intra-batch variation, the former being associated with random and systematic errors and the latter with random errors. High inter-batch variation indicates that the use of 'controls' is required. The use of 'controls', *e.g.* internal standards in HPLC analysis, may be used to compensate for poor reproducibility or to improve the resolving power of a given method. As the developed methods, especially the stomach model, were novel it was necessary to characterise the method reproducibility. This was performed by the addition of mannitol as a control to each of the experiments performed in section 6.5, *i.e.* during the study of the effects of the excipients/antacids on the permeability of the model drugs. The results are summarised in table 6.2., which records the apparent permeabilities calculated from the steady-state flux, which were determined from the linear portion of the drug transport profile.

Table 6.2
Summary of the calculated apparent permeability of the mannitol control during the study of the effects of added antacids/excipients on the permeability of the model drugs. Results are the mean of 3 replicates±SD. R^2 was determined by linear regression of the mean of the replicates

MANNITOL TRANSPORT THROUGH STOMACH				
Experiment (see 6.5)	**Ibuprofen**		**Paracetamol**	
	P_{app} ($cm\ s^{-1}$) ±SD	**R^2**	**P_{app} ($cm\ s^{-1}$) ±SD**	**R^2**
control	7.36E-07 ±2.26E-08	0.9901	1.25E-06 ±9.78E-08	0.9985
sodium bicarbonate	1.41E-06 ±7.91E-08	0.9977	1.45E-06 ±1.39E-07	0.9993
magnesium hydroxide	1.10E-06 ±5.91E-07	0.9968	1.58E-06 ±2.45E-07	0.9988
aluminium hydroxide	1.38E-06 ±2.91E-07	0.9987	1.58E-06 ±2.01E-07	0.9977
magnesium oxide	8.84E-07 ±3.98E-08	0.9669	1.77E-06 ±2.56E-07	0.9979
calcium carbonate	8.43E-07 ±1.88E-07	0.9988	1.38E-06 ±6.07E-08	0.9993
Form 5 (see 7.0)	1.44E-06 ±1.61E-07	0.9974	N/A	N/A

MANNITOL TRANSPORT THROUGH INTESTINE				
Experiment (see 6.5)	**Ibuprofen**		**Paracetamol**	
	P_{app} ($cm\ s^{-1}$) ±SD	**R^2**	**P_{app} ($cm\ s^{-1}$) ±SD**	**R^2**
control	2.05E-05 ±7.09E-06	0.9654	1.54E-05 ±1.10E-06	0.9714
sodium bicarbonate	1.53E-05 ±5.21E-06	0.9581	1.31E-05 ±3.45E-07	0.9590
magnesium hydroxide	1.78E-05 ±2.91E-06	0.9792	1.56E-05 ±2.28E-06	0.9941
aluminium hydroxide	1.50E-05 ±2.02E-06	0.9898	1.35E-05 ±1.93E-06	0.9804
magnesium oxide	1.87E-05 ±2.72E-06	0.9790	1.47E-05 ±2.87E-06	0.9655
calcium carbonate	1.64E-05 ±2.35E-06	0.9739	1.97E-05 ±8.46E-06	0.9758
Form 5 (see 7.0)	1.69E-05 ±5.46E-06	0.9967	N/A	N/A

From the data, it was calculated that for the stomach experiments, the mean apparent permeability of mannitol was 1.29E-06±1.50E-07 cm s^{-1}, with a range of 56-136% of the mean and the combined inter-batch and intra-batch variation (%RSD) measured as 11.6%. For the intestine experiments the mean apparent permeability of mannitol was calculated as 1.64E-05±2.28E-06 cm s^{-1}, with a range of 80-125% of the mean and the combined inter-batch and intra-batch variation (%RSD) measured as 13.9%. As inter-batch variation can be assumed to be increased by the use individual animals whose fed-state was uncontrolled, the ANOVA statistical technique was not applied. Instead, the data were analysed to determine whether the results fitted a gaussian distribution. Using the Kolmogorov-Smirnov test (Miller and Miller 1993), it was concluded that the results generated using both the stomach and intestine methods were sampled from a gaussian distribution with $P>0.10$ in both cases. The frequencies and cumulative frequencies for the stomach and intestine methods are illustrated in figures 6.4 and 6.5, the plots being typical of data sampled from a gaussian distribution. By comparison, in an everted jejenum sac system measuring aluminium permeability (Feinroth *et al.* 1982), the transport rate varied with a %RSD of between 15 and 30%; the transport rate in a duodenum sac varied with a %RSD of 12.6% (Barthe *et al.* 1998); the transport rate of mannitol through ileum mounted in an Ussing chamber varied with a %RSD estimated from a graph as 25%; the transport rate of mannitol through duodenum mounted in an Ussing chamber varied with a %RSD estimated from graphs as between 15-30% (Polentarutti *et al.* 1999); the transport rate of metronidazole through a stomach segment mounted in an Ussing chamber varied with a %RSD estimated from graphs as 7% (Goddard and Spiller 1997); the transport of mannitol through a Caco-2 monolayer varied with a %RSD of 6.3% (Nicklin *et al.* 1995) and the transport of a group of beta-blocking agents through a Caco-2 monolayer varied with a %RSD of between 5-10% (Palm *et al.* 1996). It can be concluded that the reproducibility is similar to that produced by sac and other methods, particularly as the variability may have been biased high as the data were collected during another experimental series, *i.e.* the study of the effects on excipients/antacids on the permeability of the model drugs.

The stability of the method can be measured by reviewing the mannitol transport profiles in figures 6.21-6.46 and also the linear regression analysis correlation co-efficients (R^2). R^2 values were lower for the intestine experiments, with this being

attributed to observed curvature, due to non-maintenance of sink conditions, at the experiments conclusion and an apparent 'burst' effect, due to the time taken to tie-off and form the sacs after the donor solution had been placed. The results indicate that, using the experimental conditions, the stomach sac maintained an effective and constant barrier for 180 minutes and likewise the intestine sac for 60 minutes. On the basis of these results the method was deemed suitable, in terms of stability and reproducibility, for the determination of drug permeability through the stomach and intestine tissue sacs.

Figure 6.4
Illustrating the frequency distribution of mannitol stomach permeability controls measured throughout the experimental series

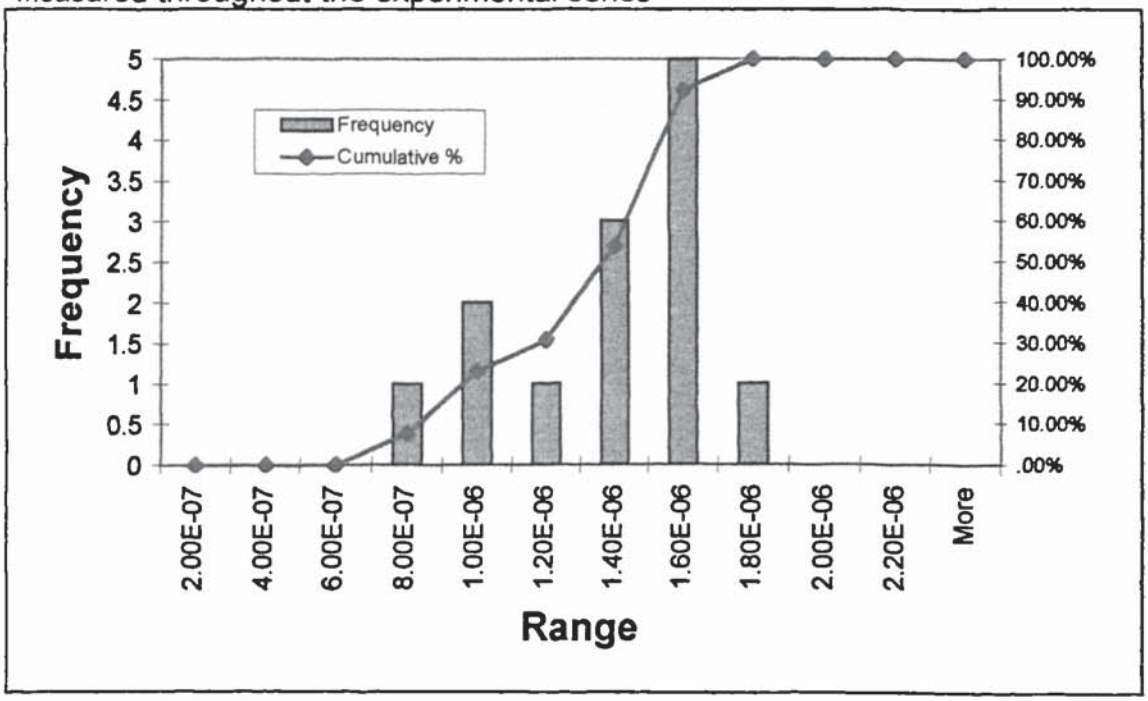

Figure 6.5
Illustrating the frequency distribution of mannitol intestine permeability controls measured throughout the experimental series

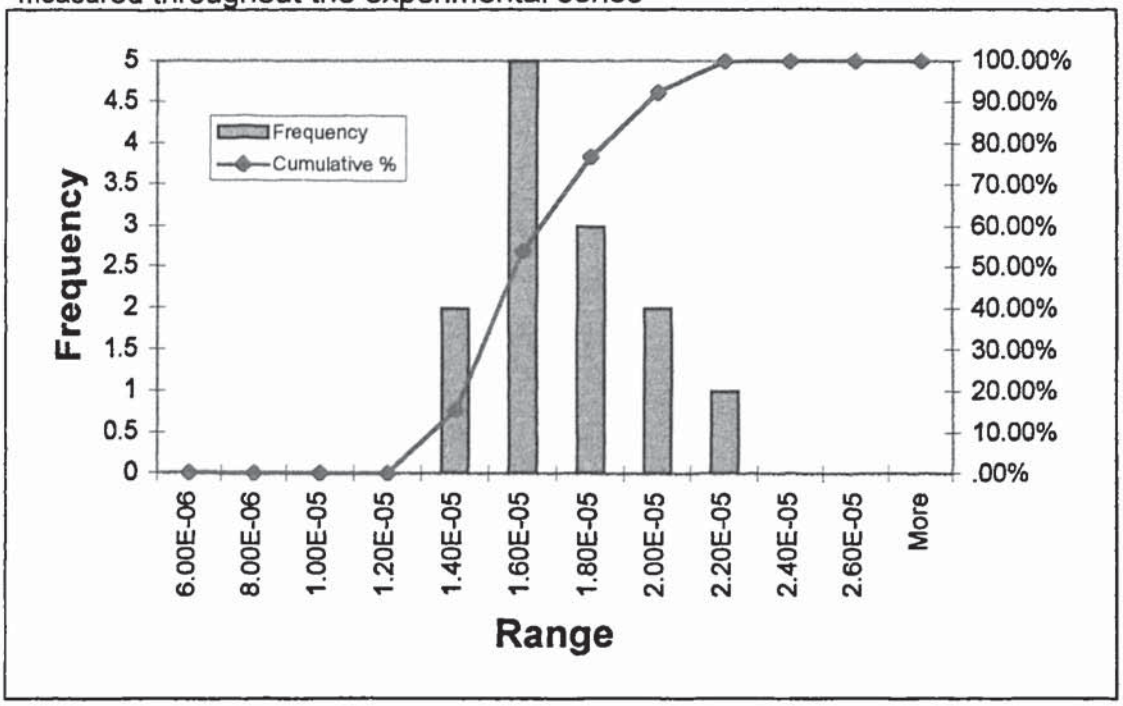

6.4.3 Membrane barrier drug permeability selectivity

6.4.3.1 Experimental

6.4.3.2 Materials

[^{3}H]Mannitol and [^{14}C]ibuprofen were obtained from ICN (Ca, USA), [^{14}C]paracetamol was obtained from SB (USA), (reference appendix 2 for details of manufacture and C of A). Hydrochloric acid, Paracetamol and ibuprofen were obtained from SB (Weybridge, UK). Cimetidine was obtained from SB (Harlow, UK). Hank's balance solution (calcium, magnesium and phenol red-free), mannitol, fluorescein, nadolol, ibuprofen, ketoprofen, propranolol, sodium hydroxide and calcium chloride were obtained from Aldrich (Poole, UK). HEPES was obtained from Life Technologies (Paisley, UK). CO_2-O_2 (5:95) was obtained from BOC (Manchester, UK). All materials were pharmaceutical or analytical grade as appropriate. Double-distilled water was generated in-house using a Fison's Fi-Stream Still.

6.4.3.1.2 Equipment

The equipment and set-up was as described in section 6.4.1.1.2.

6.4.3.1.3 Method

The general method for tissue collection, transfer to experimental area and preparation of sacs was as detailed in section 6.4.1.1.3. The MBS contained 0.05M HCl, Hank's buffer, 25mM HEPES and 1.25mM calcium chloride with adjustment to pH6.8 using 10% (w/v) sodium hydroxide solution. Depending on the drug under investigation, the donor solution also contained paracetamol at 5.0mg ml^{-1} with a spiked aliquot of radiolabelled paracetamol to give an activity of >500,000 DPM ml^{-1}, ibuprofen at 2.0mg ml^{-1} with a spiked aliquot of radiolabelled ibuprofen to give an activity of >500,000 DPM ml^{-1}, 0.1M (≈2.0mg ml^{-1}) mannitol spiked with an aliquot of radiolabelled mannitol to give an activity of >500,000 DPM ml^{-1} or the drug under investigation at a concentration of 0.1M. The sacs were placed individually into a universal with 15.0ml of the appropriate pre-warmed MBS, each universal being clamped into the water bath to maintain the temperature at 37°C. The CO_2-O_2 gas mixture was bubbled through the receiver solution of each universal. Aliquots of 5.0ml were sampled every 10 minutes for 60 minutes for the intestine experiment and every 15 minutes for 180 minutes for the stomach experiment, the sample volume being replaced with the appropriate pre-warmed MBS. The samples were analysed according to the methods detailed in chapter 2, the radio-labelled drugs concentrations were determined by a scintillation counter and the other drugs concentrations were determined by HPLC analysis, except fluorescein samples which were analysed using a Victor^2 1420 Multilabel Counter (Wallac, U.K.). This procedure produced a dilution of the receiver phase. It was, therefore, necessary to adjust each successive sample concentration for the dilution caused by all the previous samples. This was performed, using an Excel spreadsheet, by applying the correction factor detailed in equation 4.9. On completion of the experiment the sacs were opened with scissors and/or scalpel, and pinned onto a board for determination of surface area.

6.4.3.2 Results and Discussion

The gastrointestinal tract *in vivo* acts as a selective barrier to drugs. This selectivity is dependent on the physicochemical properties of the drug in the luminal environment and membrane, when the transport is by the passive diffusion mechanism. Therefore, to further validate and characterise the stomach and intestine models it was necessary to determine whether the tissues acted as selective barriers and, if so, whether the selectivity was as predicted. A wide and diverse group of drugs, with selection based on physicochemical properties and known absorption mechanism and extent, were selected for study. Drug transport was measured using the stomach and intestine models and the apparent permeabilities calculated. The results are summarised in table 6.3 and illustrated in figures 6.6-6.7, with % absorption in man data included in the table for use in method validation. The apparent permeabilities were calculated from the steady-state flux, which were determined from the linear portion of the drug transport profile. The drug transport profiles are illustrated in figures 6.13-6.16.

Table 6.3
Summary of apparent permeability of selected drugs through the stomach and intestine models. Results are the mean of 3 replicates±SD.

Drug	Stomach P_{app} (cm s^{-1}) ±SD	Intestine P_{app} (cm s^{-1}) ±SD	% absorbed in man
fluorescein	1.43E-09±3.32E-10	2.98E-06±1.90E-06	100[a]
cimetidine	5.83E-07±5.81E-08	5.41E-06±3.26E-07	62[b]
nadolol	8.68E-07±9.65E-08	9.00E-06±9.59E-07	35[b]
mannitol	1.29E-06±1.50E-07	1.80E-05±4.51E-07	17[c]
paracetamol	1.39E-06±4.64E-08	2.07E-05±5.14E-06	88[b]
ibuprofen	2.09E-06±3.85E-07	2.20E-05±7.07E-06	92[d]
ketoprofen	2.47E-06±1.12E-07	3.24E-05±2.25E-06	100[c]
propranolol	2.50E-06±2.65E-07	4.74E-05±7.51E-06	92[e]
caffeine	2.92E-06±1.89E-07	2.21E-05±1.64E-06	100[b]

[a]Barry and Behrengt (1985)
[b]Goodman Gilman *et al.* (1992)
[c]Yu and Amidon (1999)
[d]Cheng et al. (1994)
[e]Paterson *et al.* (1970)

Figure 6.6
Illustrating the permeability of drugs through the stomach model. Results are the mean of 3 replicates+SD

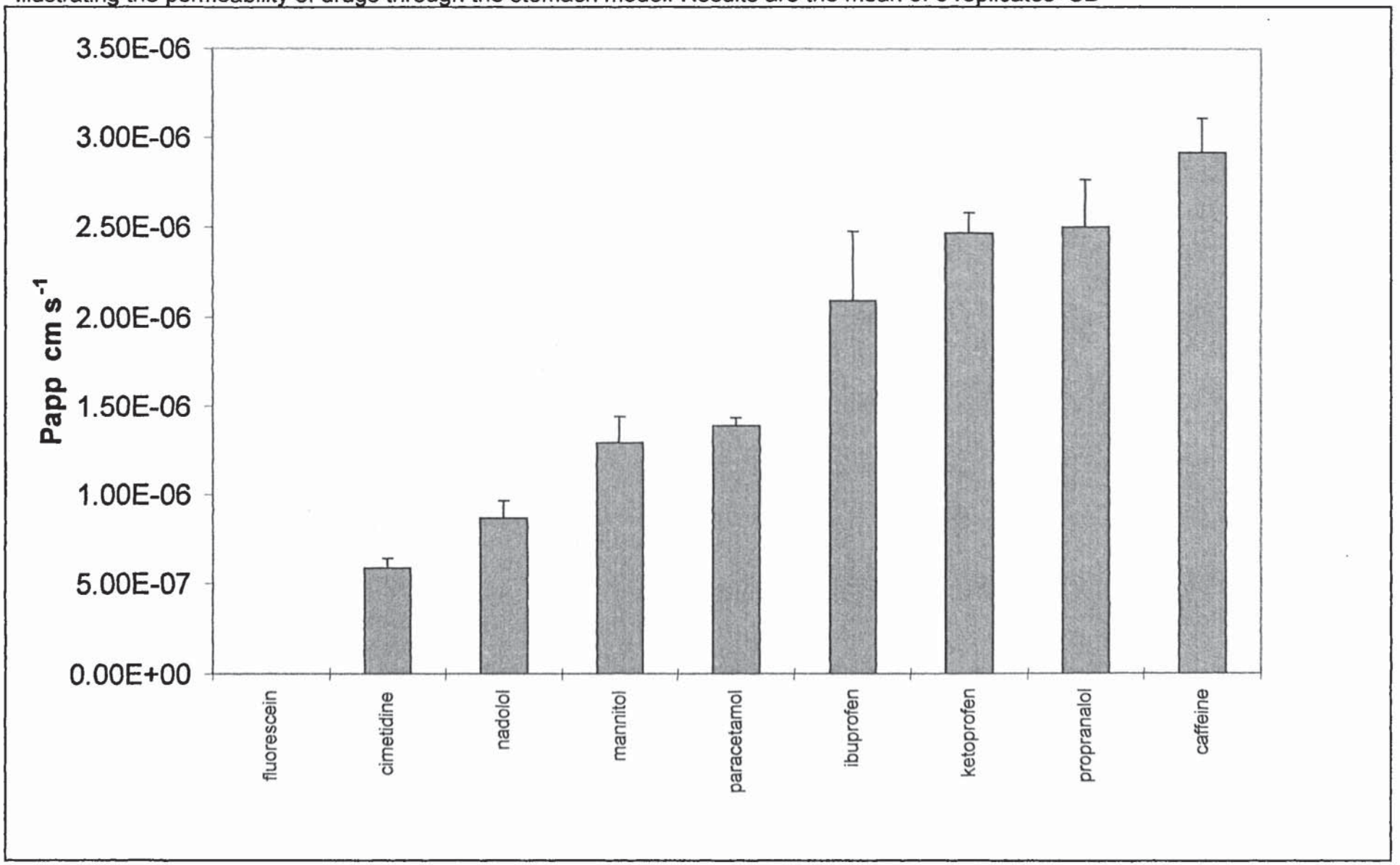

Figure 6.7
Illustrating the permeability of drugs through the intestine model. Results are the mean of 3 replicates+SD

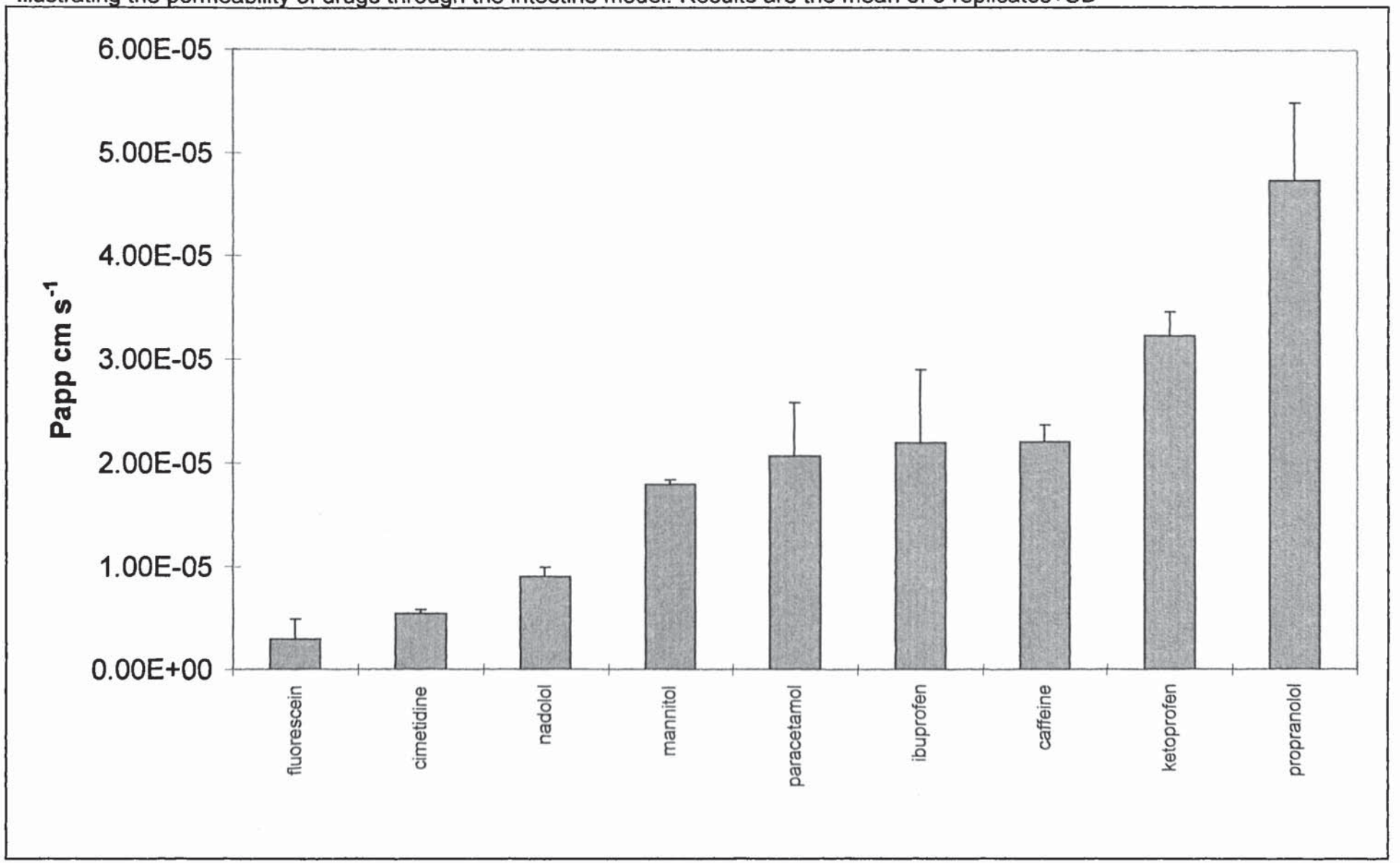

The permeability of the known paracellular and transcellular markers, mannitol and propranolol, were determined in both models. Generally, a transcellular marker would be expected to be more permeable than a paracellular marker. The calculated Papps for mannitol and propranolol were very significantly different, *i.e.* 1.29E-06±.50E-07 *versus* 2.50E-06±2.65E-07 (t-test, P=0.002) for the stomach model and, 1.80E-05±4.51E-07 *versus* 4.74E-05±7.51E-06 (t-test, P=0.002) for the intestine model. The % permeability difference was 194% and 263%, respectively. For comparison, using the Ussing chamber method, Polentarutti *et al.* (1999) found an increase of approximately 600% when comparing the rate of propranolol *versus* mannitol across a duodenum tissue section, over 60 minutes. To confirm these findings, a second study was conducted. This experiment compared two drugs from a beta-blocker homologous series, *i.e.* nadolol which is considered to be 'hydrophilic' in nature and is incompletely absorbed in man and propranolol which is considered to be 'lipophilic' in nature and is completely absorbed in man (Cruickshank 1980). The calculated Papps for nadolol *versus* propranolol were extremely significantly different, *i.e.* 8.68E-07±9.65E-08 *versus* 2.50E-06±2.65E-07 (t-test, P=0.0006) for the stomach model and, 9.0E-06±9.59E-07 *versus* 4.74E-05±7.51E-06 (t-test, P=0.0009) for the intestine model. The % permeability rate difference was 288% and 526%, respectively. Taylor *et al.* (1985) demonstrated that across a range of partition co-efficients the absorption of beta-blockers, using the *in-situ* small intestine rat model, could be divided into two groups. The first group consisted of the 'hydrophilic' drugs with absorption rate constants of between 0.30-0.36 hr^{-1} (nadolol=0.30 hr^{-1}). The second group consisted of 'lipophilic' drugs with absorption rates of between 1.5-2.87 hr^{-1} (propranolol=2.87 hr^{-1}). The % permeability rate difference between propranolol and nadolol was 956%. It was noted, that for the 'lipophilic' drugs, absorption rates began to tail-off as the logP value increased, which is likely to be due to the unstirred aqueous layer becoming the limiting factor in drug permeability.

The transport of hydrophilic drugs by the paracellular route will be affected by the molecular size. Accordingly, it has been determined that increasing molecular weight may lead to a reduction in apparent permeability (Artursson *et al.* 1993). The sieving coefficient, ϕ, indicates the efficiency of transport through the paracellular route. An estimate of the sieving coefficient plotted against molecular weight shows a steep relationship, as illustrated in figure 6.8, whereby ϕ decreases to approximately 0.1

above a molecular weight of approximately 270. Of the compounds under test, the hydrophilic marker fluorescein (MW=332) has the highest molecular weight and was found to exhibit the lowest apparent permeability of all the drugs tested, in both the stomach and intestine models, in line with expectations.

Figure 6.8
Illustrating the effect of molecular weight on the efficiency of drug transport by the paracellular route, expressed as the sieving coefficient

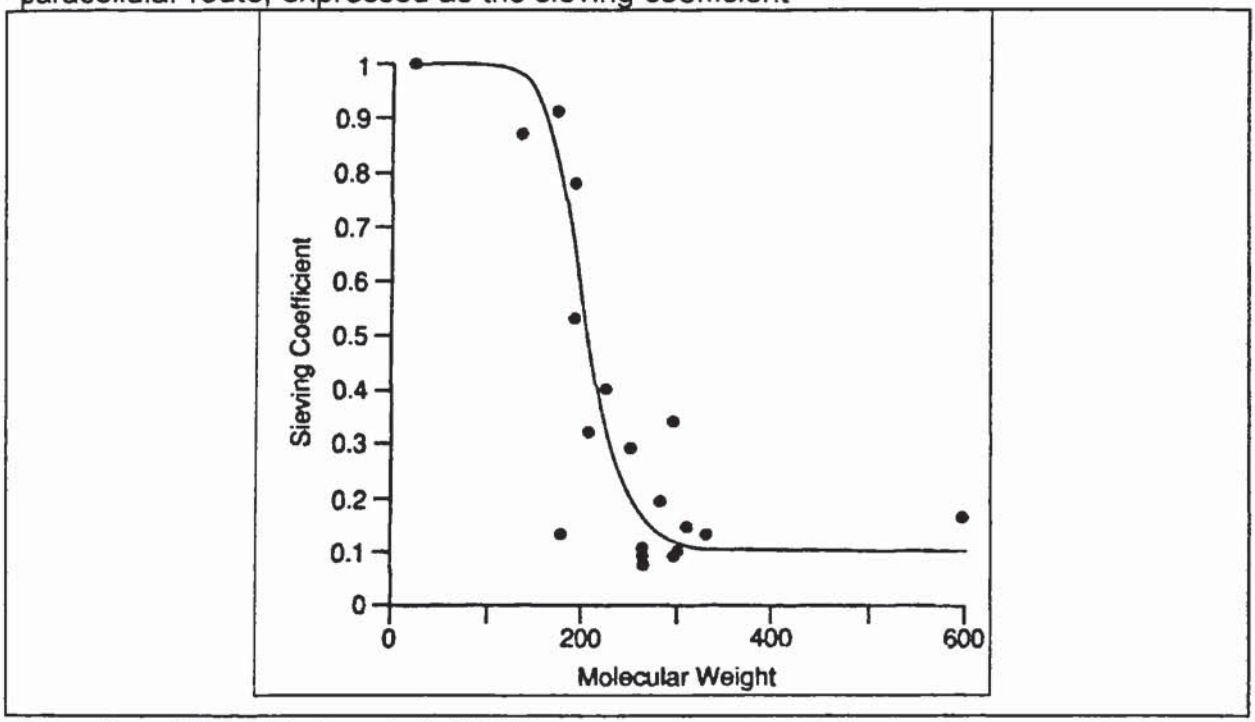

Reproduced from Taylor *et al.* (1989)

These methods were developed to model the permeability of drugs through selected regions of the gastrointestinal tract. A central project aim was the combination of *in vitro* dissolution and permeability methods to allow prediction of human absorption and ultimately the development of IVIVCs. Therefore, it was necessary to determine the level of correlation between the calculated apparent permeabilities *versus* a measure of drug permeability *in vivo*. The appropriate choice of parameter is required as a measure of permeability. Both C_{max} and t_{max} are dependent on absorption rate which will be dependent on the dissolution rate, permeability or a combination of both of these. It has been established that the fraction of dose absorbed in man, accounting for metabolism effects, is likely to be related to the drug permeability (Yu and Amidon 1999). Therefore the relationship between % drug absorbed *in vivo* and drug permeability was determined as illustrated in figures 6.9 and 6.10. It has been

demonstrated, as detailed below, that the relationship between % absorbed in man and drug physicochemical or permeability characteristics may be sigmoidal. For example, the relationship between the partition co-efficient (logD) and absorption rate *in-situ* in rat small intestine is sigmoidal (Taylor *et al.* 1985/1989). The sigmoidal relationship is explained as follows; at lower logD values, the absorption rate is very similar, for drugs with similar molecular weights, corresponding to transport primarily *via* the paracellular route. As the drugs become more lipophilic, the transcellular route becomes more dominant, corresponding to an increasing absorption rate. With increasing lipophilicity, transport through the unstirred aqueous layer becomes the rate-limiting step, leading to a plateau. This relationship is illustrated in the work of Taylor *et al.* (1989) which is reproduced in figure 6.11. A comparison of % absorbed *versus* drug permeability in vascularly perfused rat small intestine was performed in the work of Level-Trafit *et al.* (1996) as illustrated in figure 6.12. It can be observed that again the relationship is sigmoidal. The results for both the stomach and intestine model as illustrated in figures 6.9 and 6.10 clearly demonstrate two groups of compounds which may fit a sigmoidal relationship, similar to the previous work cited, and therefore concluded that the developed methods may be useful to simulate drug absorption *in vivo*, with limitations. It is noted that fluorescein appeared to be an outlier in this relationship in that it was observed to exhibit by far the lowest apparent permeability in both models but following oral dose in man it exhibits 99% bioavailability. Interestingly, fluorescein has been used as measure of tight junction integrity in cell culture systems, where a low transport rate confirms monolayer integrity (Jaehde *et al.* 1993), which concurs with the results from the present study.

Figure 6.9
Illustrating the relationship between % absorbed in humans and the apparent permeability in the stomach model, excluding fluorescein

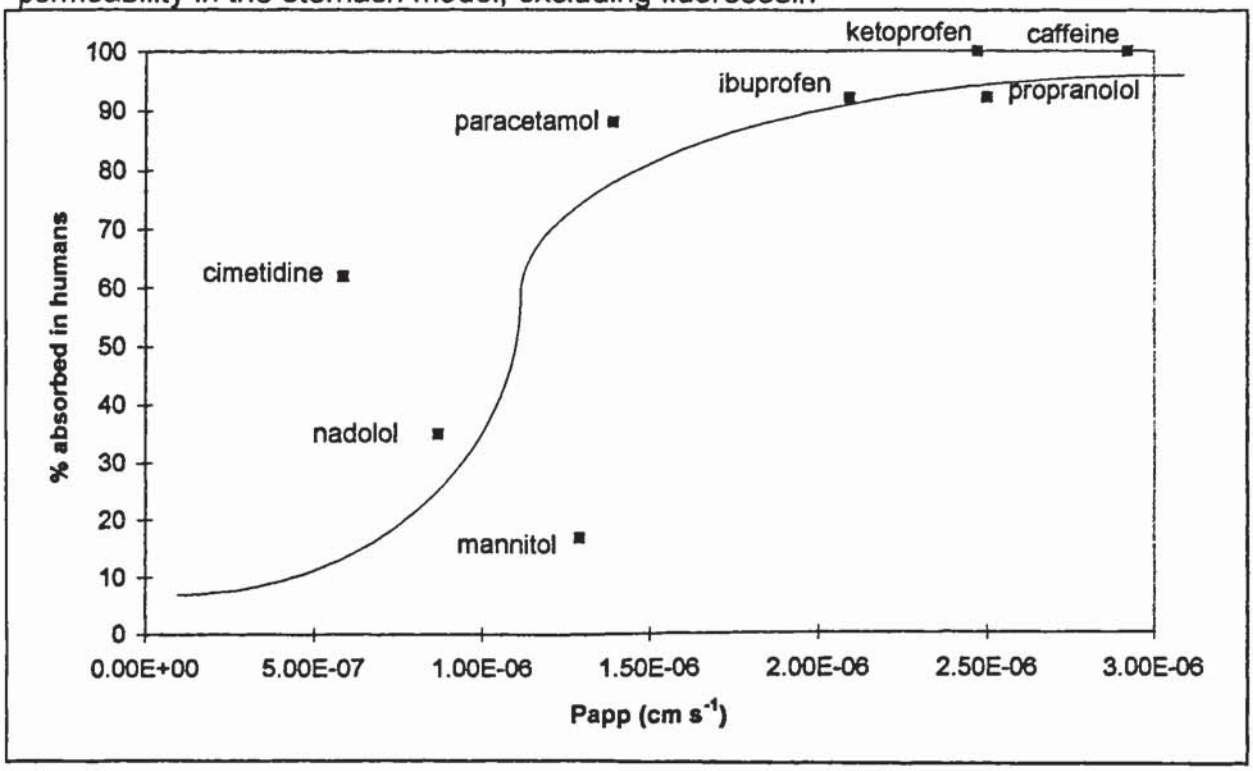

Figure 6.10
Illustrating the relationship between % absorbed in humans and the apparent permeability in the intestine model, excluding fluorescein

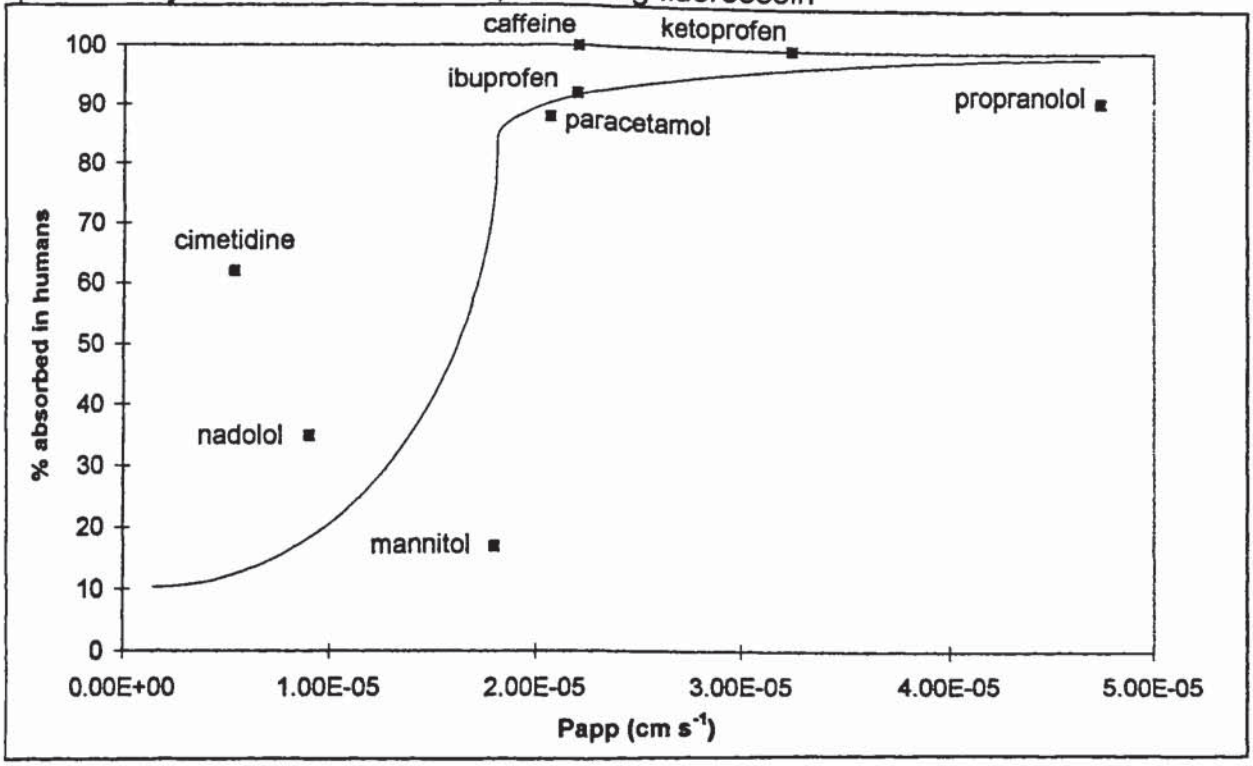

One further observation from this study is the comparison of the absorption rate of each drug in the stomach compared to the intestine. It is known that the small intestine is the major site of absorption from the gastrointestinal tract with the stomach playing only a minor role. As the method protocols for each tissue type were essentially the same it has been possible for the first time to directly compare the permeability of drugs through both the stomach and the intestine *in vitro*. Unsurprisingly, the data confirm the faster transport of all of the selected drugs in the intestine compared to the stomach. The relative increase in the drugs' permeability observed in the intestine compared to the stomach is detailed below:

- 8-fold increase in caffeine permeability
- 9-fold increase in cimetidine permeability
- 10-fold increase in ibuprofen permeability
- 10-fold increase in nadolol permeability
- 13-fold increase in ketoprofen permeability
- 14-fold increase in mannitol permeability
- 15-fold increase in paracetamol permeability
- 19-fold increase in propranolol permeability
- 2,000-fold increase in fluorescein permeability

For all drugs, except fluorescein, permeability in the intestine is between 8-19 times higher than the permeability in the stomach. Fluorescein demonstrated the lowest permeability in the stomach, and a 2000-fold increase in the intestine. The reasons for this have not been elucidated.

Figure 6.11
Illustrating the relationship between logD, determined in a water:propylene glycol dipelargonate system. Data are for a compound set with a wide range of structural diversity. Absorption determined *in-situ* in rat ileum

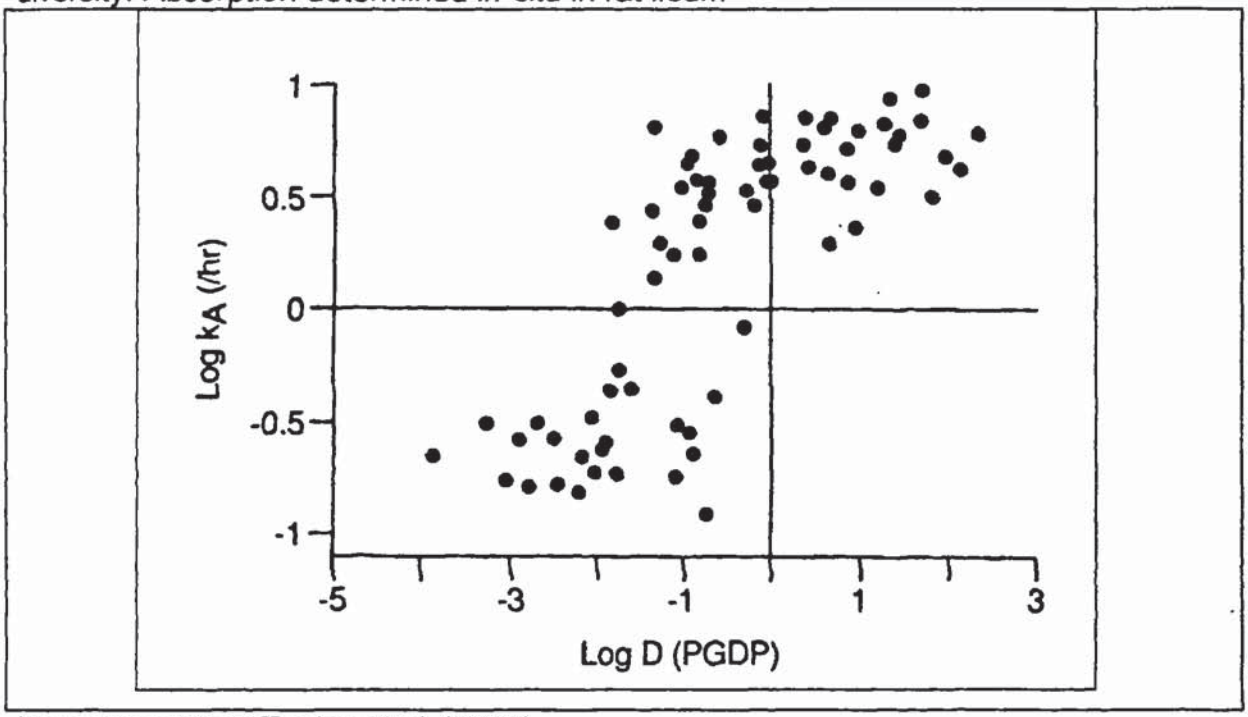

Reproduced from Taylor *et al.* (1989)

Figure 6.12
Illustrating the correlation between oral absorption in man and the permeability coefficients in vascularly perfused whole rat small intestine

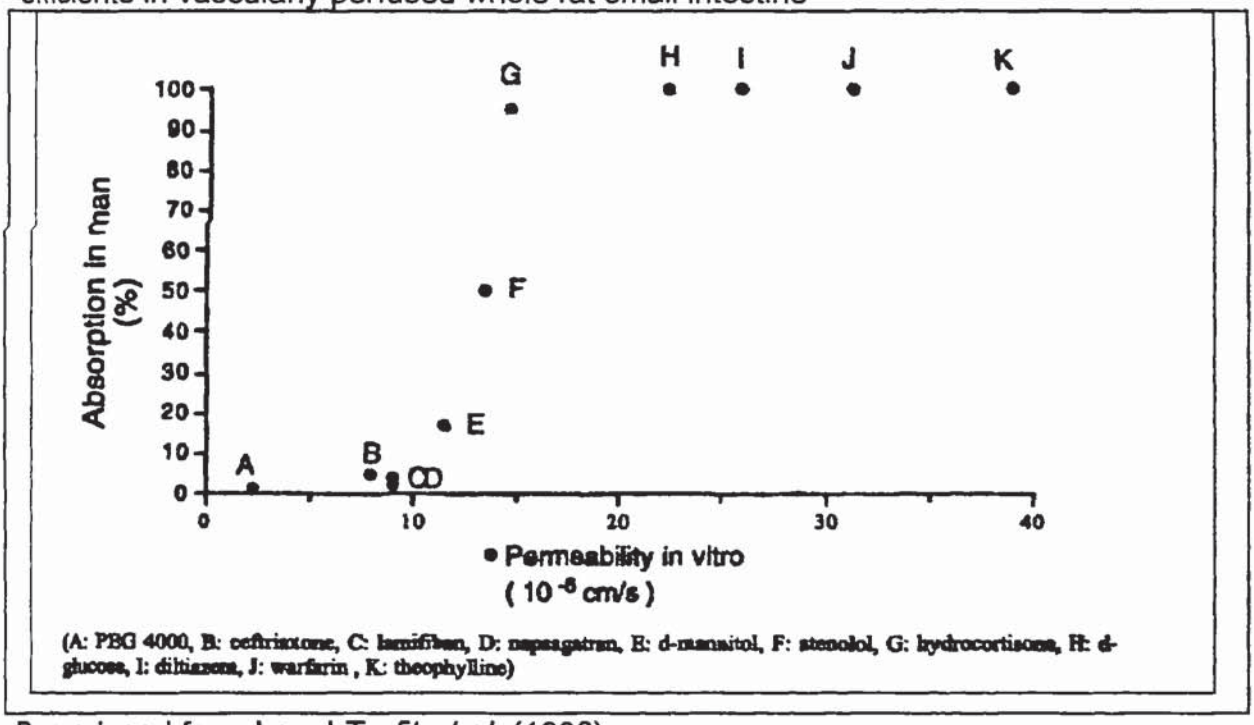

Reproduced from Level-Trafit *et al.* (1996)

Figure 6.13
Illustrating the transport of drugs through the stomach. Results are the mean of 3 replicates with SD as appropriate for visual clarity

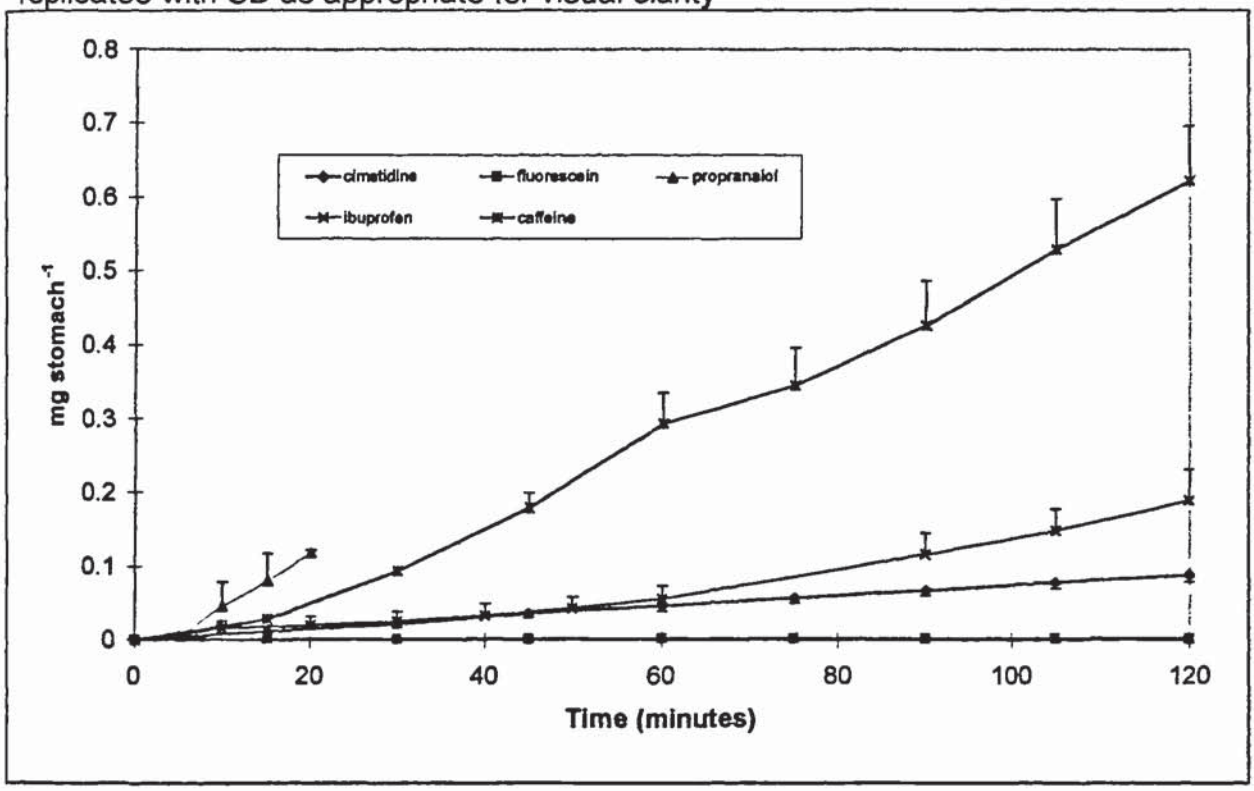

Figure 6.14
Illustrating the transport of drugs through the stomach. Results are the mean of 3 replicates with SD as appropriate for visual clarity

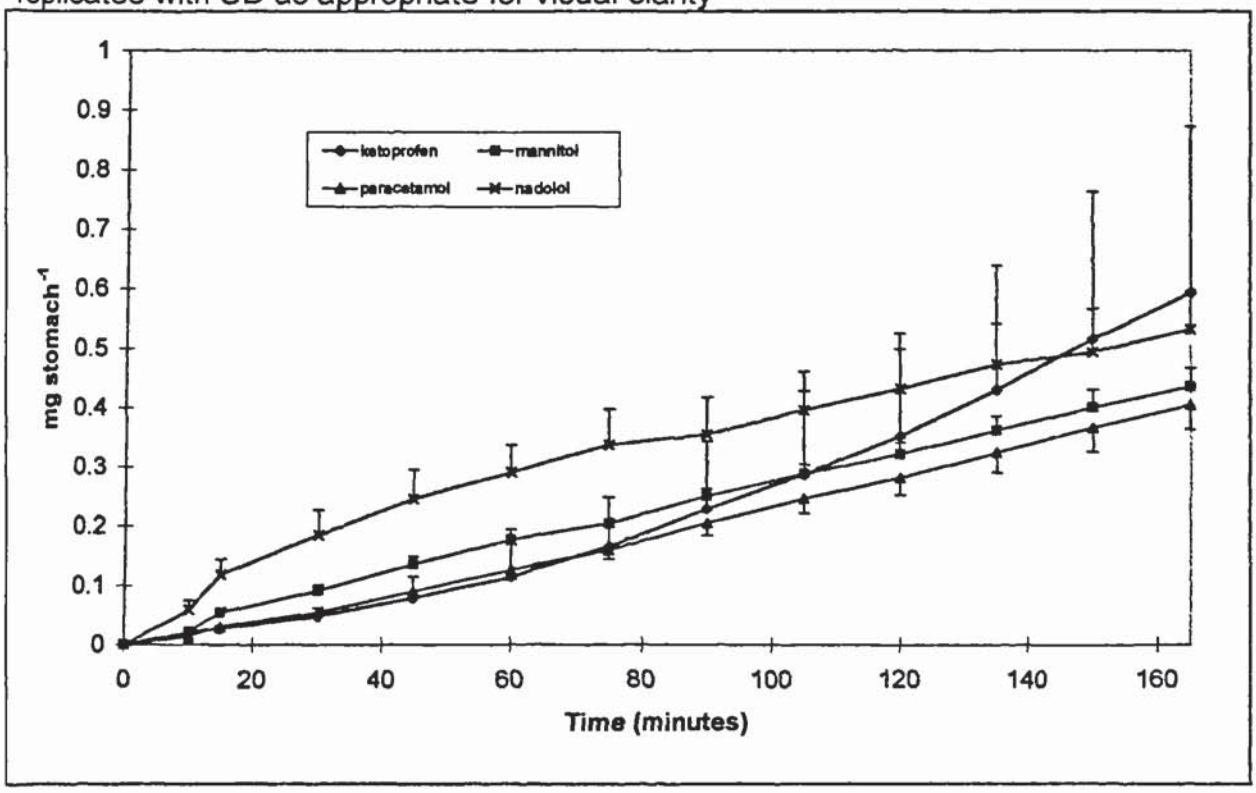

Figure 6.15
Illustrating the transport of drugs through intestine. Results are the mean of 3 replicates with SD as appropriate for visual clarity

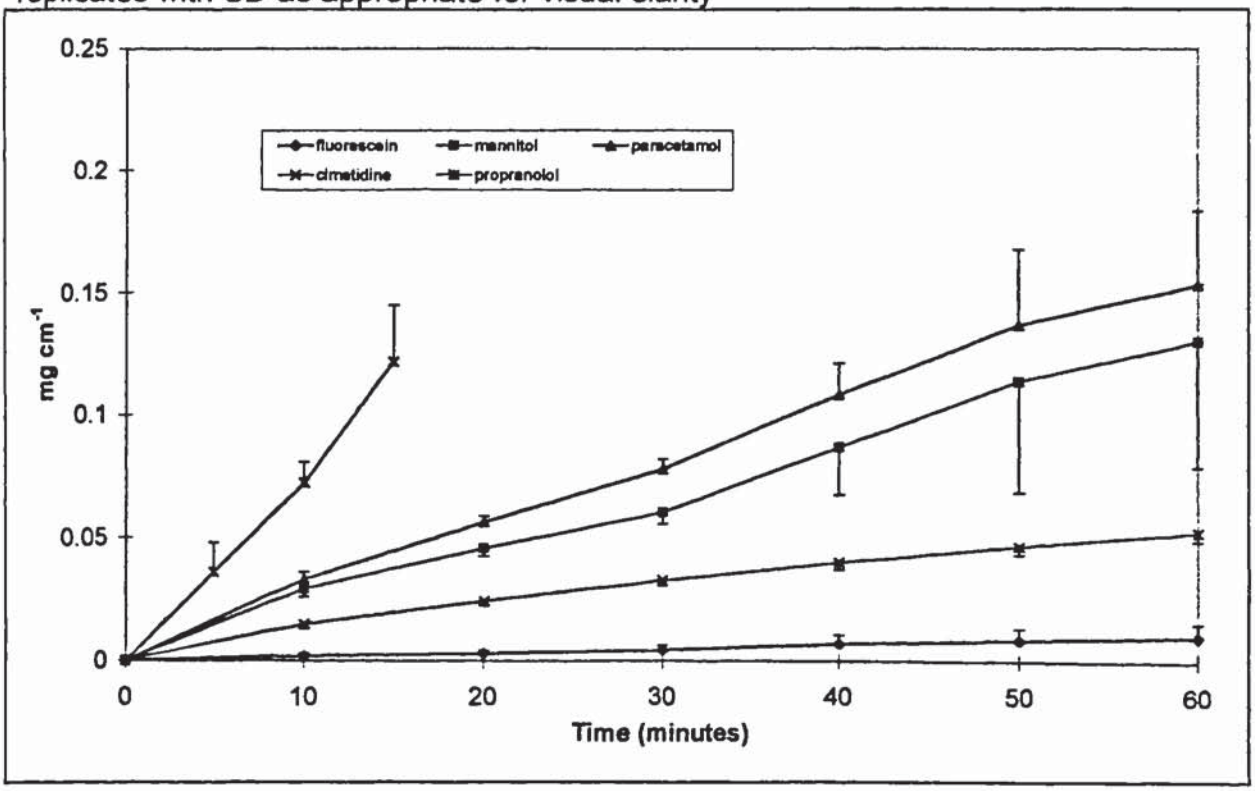

Figure 6.16
Illustrating the transport of drugs through intestine. Results are the mean of 3 replicates with SD as appropriate for visual clarity

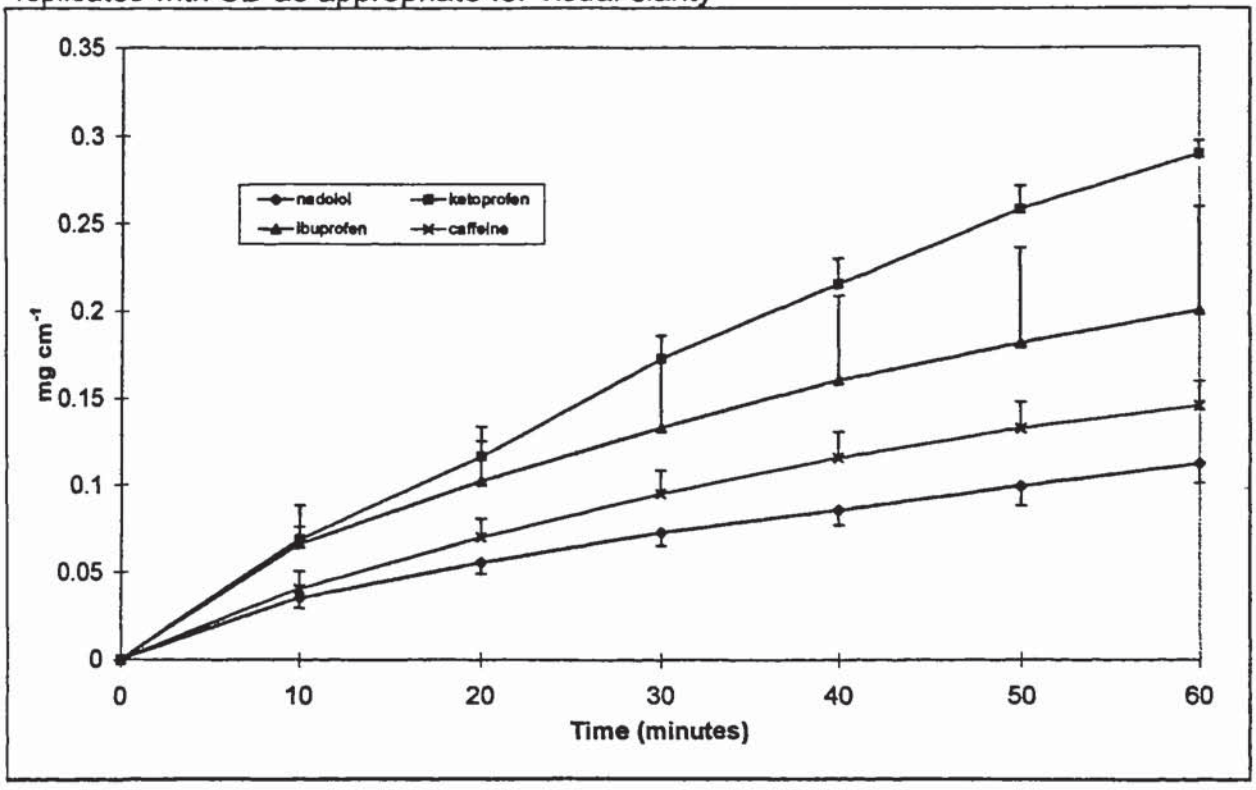

6.5 The effect of dissolved excipients/antacids on model drug permeability

6.5.1 Experimental

6.5.2.1 Materials

[^{3}H]Mannitol and [^{14}C]ibuprofen were obtained from ICN (Ca, USA). [^{14}C]paracetamol was obtained from SB (USA), (reference appendix 2 for details of manufacture and C of A). Ibuprofen, paracetamol and sodium bicarbonate (extra-fine grade) were obtained from SB (Weybridge, UK). Hydrochloric acid, Hank's balanced solution (calcium, magnesium and phenol red free), mannitol, sodium hydroxide, aluminium hydroxide, magnesium oxide, magnesium hydroxide, calcium carbonate and calcium chloride were obtained from Aldrich (Poole, UK). HEPES was obtained from Life Technologies (Paisley, UK). CO_2-O_2 (5:95) was obtained from BOC (Manchester, UK). All materials were pharmaceutical or analytical grade as appropriate. Double-distilled water was generated in-house using a Fison's Fi-Stream Still.

6.4.2.1.2 Equipment

The equipment and set-up was as described in section 6.4.1.1.2. A Techne SB-16 water bath/shaker was used for preparation of the saturated antacid solutions.

6.4.2.1.3 Method

The general method for tissue collection, transfer to experimental area and preparation of sacs was as detailed in section 6.4.1.1.3. The MBS contained 0.05M HCl, Hanks Buffer, 25mM HEPES and 1.25mM calcium chloride with adjustment to pH6.8 using 10% (w/v) sodium hydroxide solution. For the experiments where an 'insoluble' antacid/excipient was under investigation, the MBS was prepared as follows; the suspensions were well shaken manually and then placed in the water bath at 37°C, agitator setting 1 (70 cycles *per* minute), for 4 days. On the fifth day, and after a minimum of 96 hrs, the supernatant was decanted off. The preparation of the MBS was then completed. For investigation of the effect of added sodium bicarbonate, the excipient was added at a concentration of 15mmol *per* 200ml before adjustment to pH6.8. All donor solutions were supplemented by the addition of 0.1M (≈2.0mg ml^{-1}) mannitol and spiked with an aliquot of radiolabelled mannitol to give an

activity between 300,000-1,000,000 DPM ml^{-1}. Depending on the drug under investigation, the donor solution also contained paracetamol at 5.0mg ml^{-1} with a spiked aliquot of radiolabelled paracetamol to give an activity between 500,000-2,500,000 DPM ml^{-1} or, ibuprofen at 2.0mg ml^{-1} with a spiked aliquot of radiolabelled ibuprofen to give an activity between 500,000-2,500,000 DPM ml^{-1}. The sacs were placed individually into a universal with 15.0ml of the appropriate pre-warmed MBS, each universal being clamped into the water bath to maintain the temperature at 37°C. The CO_2-O_2 gas mixture was bubbled through the receiver solution of each universal. Aliquots of 5.0ml were sampled every 10 minutes for 60 minutes for the intestine experiment and every 15 minutes for upto 180 minutes for the stomach experiment, the sample volume being replaced with the appropriate pre-warmed MBS. The samples were analysed by the scintigraphic method detailed in section 2.7. This procedure produced a dilution of the receiver phase. It was therefore necessary to adjust each successive sample concentration for the dilution caused by all the previous samples. This was performed, using an Excel spreadsheet, by applying the correction factor detailed in equation 4.9. On completion of the experiment, the sacs were opened with scissors and/or scalpel, pinned onto a board for determination of surface area.

6.5.3 Results and discussion

These experiments were designed to reproduce the *in vivo* situation where model analgesic drugs have been co-administered with one of the selected antacids or with a tablet formulated to contain the excipient under investigation, with regard to the pH environment at the mucus/mucosa interface, with pre-dissolved drug and antacid/excipient at concentrations equivalent to those estimated *in vivo*.

Apparent permeabilities were calculated from the steady-state flux, which were determined from the linear portion of the drug transport profile. For each experimental replicate, the apparent permeability of the model drug was divided by the apparent permeability of mannitol to produce a apparent permeability ratio. The use of this 'control' was to increase the discriminating power of the method. The drugs' calculated apparent permeabilities are detailed in tables 6.4-6.7. The model drug/mannitol apparent permeability ratios are illustrated in figures 6.17-6.20 and the drug transport profiles are illustrated in figures 6.21-6.46.

The first step in the analysis of the effect of each antacid/excipient on the model drug's transport was to measure whether the antacid/excipient affected the transport of the control, *i.e.* mannitol. Therefore, the apparent permeability obtained for mannitol with each added antacid/excipient for the stomach and intestine experiments were paired. This was performed separately for paracetamol and ibuprofen. The Spearman rank correlation test was applied to determine whether a relationship existed between the calculated Papp for mannitol and the excipient/antacid under test. For both the paracetamol and ibuprofen experimental series it was found that the correlation coefficient (R=0.4286 with P=0.4194) was not significantly different from zero which indicated that there was no relationship between the Papp for mannitol and the added antacid/excipient. Further statistical analysis led to the following conclusions:

- all added excipients/antacids did not significantly affect the Papp of paracetamol relative to mannitol, *i.e.* (Dunnett's test $P>0.05$ *versus* control for all experiments), except calcium carbonate which significantly ($P<0.01$ *versus* control) increased the Papp paracetamol/mannitol ratio from 1.04 to 1.20, in the stomach model
- all added excipients/antacids did not significantly affect the Papp of ibuprofen relative to mannitol, *i.e.* (Dunnett's test $P>0.05$ for all experiments *versus* control), in the stomach model
- all added excipients/antacids did not significantly affect the Papp of paracetamol relative to mannitol, *i.e.* (Dunnett's test $P>0.05$ *versus* control for all experiments), except calcium carbonate which significantly ($P<0.01$ *versus* control) decreased the Papp paracetamol/mannitol ratio from 1.16 to 1.04, in the intestine
- all added excipients/antacids did not significantly affect the Papp of ibuprofen relative to mannitol, *i.e.* (Dunnett's test $P>0.05$ *versus* control for all experiments), except aluminium hydroxide which significantly ($P<0.05$ *versus* control) decreased the Papp ibuprofen/mannitol ratio from 1.08 to 0.79 and ibuprofen form 5 which significantly ($P<0.01$ *versus* control) increased the Papp ibuprofen/mannitol ratio from 1.08 to 1.46, in the intestine model.

Table 6.4
Summary of the effect of added antacids/excipients on the calculated permeability of mannitol and ibuprofen, and the relative ibuprofen/mannitol permeability ratio, in the intestine model. Results are the mean of 3 replicates±SD.

IBUPROFEN/INTESTINE			
Experiment	**Mannitol P_{app} (cm s^{-1}) ±SD**	**Ibuprofen P_{app} (cm s^{-1}) ±SD**	**Ratio**
control	2.05E-05 ±7.09E-06	2.20E-05 ±7.07E-06	1.08±0.12
sodium bicarbonate	1.53E-05 ±5.21E-06	1.91E-05 ±3.37E-06	1.29±0.24
magnesium hydroxide	1.78E-05 ±2.91E-06	1.95E-05 ±5.35E-06	1.09±0.08
aluminium hydroxide	1.50E-05 ±2.02E-06	1.18E-05 ±1.07E-06	0.79±0.05
magnesium oxide	1.87E-05 ±2.72E-06	2.09E-05 ±4.09E-06	1.11±0.07
calcium carbonate	1.64E-05 ±2.35E-06	1.69E-05 ±2.89E-06	1.03±0.03
Form 5 (see 7.0)	1.69E-05 ±5.46E-06	2.44E-05 ±5.93E-06	1.46±0.11

Table 6.5
Summary of the effect of added antacids/excipients on the calculated permeability of mannitol and paracetamol, and the relative paracetamol/mannitol permeability ratio, in the intestine model. Results are the mean of 3 replicates±SD.

PARACETAMOL/INTESTINE			
Experiment	**Mannitol P_{app} (cm s^{-1}) ±SD**	**Paracetamol P_{app} (cm s^{-1}) ±SD**	**Ratio**
control	1.54E-05 ±1.10E-06	1.78E-05 ±1.25E-06	1.16±0.01
sodium bicarbonate	1.31E-05 ±3.45E-07	1.51E-05 ±4.13E-06	1.15±0.01
magnesium hydroxide	1.56E-05 ±2.28E-06	1.79.E-05 ±2.87E-06	1.15±0.02
aluminium hydroxide	1.35E-05 ±1.93E-06	1.56E-05 ±1.36E-06	1.16±0.07
magnesium oxide	1.47E-05 ±2.87E-06	1.68E-05 ±3.41E-06	1.14±0.02
calcium carbonate	1.97E-05 ±8.46E-06	2.05E-05 ±9.10E-06	1.04±0.02

Table 6.6
Summary of the effect of added antacids/excipients on the calculated permeability of mannitol and ibuprofen, and the relative ibuprofen/mannitol permeability ratio, in the stomach model. Results are the mean of 3 replicates±SD.

IBUPROFEN/STOMACH			
Experiment	**Mannitol P_{app} (cm s^{-1}) ±SD**	**Ibuprofen P_{app} (cm s^{-1}) ±SD**	**Ratio**
control	7.36E-07 ±2.26E-08	1.19E-06 ±1.82E-07	1.62±0.29
sodium bicarbonate	1.41E-06 ±7.91E-08	1.77E-06 ±1.23E-08	1.26±0.08
magnesium hydroxide	1.10E-06 ±5.91E-07	1.51E-06 ±9.591E-07	1.36±0.33
aluminium hydroxide	1.38E-06 ±2.91E-07	1.76E-06 ±1.66E-07	1.30±0.18
magnesium oxide	8.84E-07 ±3.98E-08	1.31E-06 ±6.25E-08	1.48±0.004
calcium carbonate	8.43E-07 ±1.88E-07	1.13E-06 ±2.77E-07	1.34±0.12
Form 5 (see 7.0)	1.44E-06 ±1.61E-07	2.32E-06 ±5.69E-08	1.62±0.13

Table 6.7
Summary of the effect of added antacids/excipients on the calculated permeability of mannitol and paracetamol, and the relative paracetamol/mannitol permeability ratio, in the stomach model. Results are the mean of 3 replicates±SD.

PARACETAMOL/STOMACH			
Experiment	**Mannitol P_{app} (cm s^{-1}) ±SD**	**Paracetamol P_{app} (cm s^{-1}) ±SD**	**Ratio**
control	1.25E-06 ±9.78E-08	1.30E-06 ±1.45E-07	1.04±0.03
sodium bicarbonate	1.45E-06 ±1.39E-07	1.53E-06 ±1.39E-07	1.05±0.03
magnesium hydroxide	1.58E-06 ±2.45E-07	1.57E-06 ±2.46E-07	0.99±0.02
aluminium hydroxide	1.58E-06 ±2.01E-07	1.59E-06 ±2.07E-07	1.01±0.01
magnesium oxide	1.77E-06 ±2.56E-07	1.89E-06 ±3.00E-07	1.07±0.01
calcium carbonate	1.38E-06 ±6.07E-08	1.65E-06 ±9.92E-08	1.20±0.02

Figure 6.17
Illustrating the effect of antacid/excipient on the relative permeability of paracetamol compared to mannitol through intestine. Results are the mean of 3 replicates+SD with individual replicate controls.

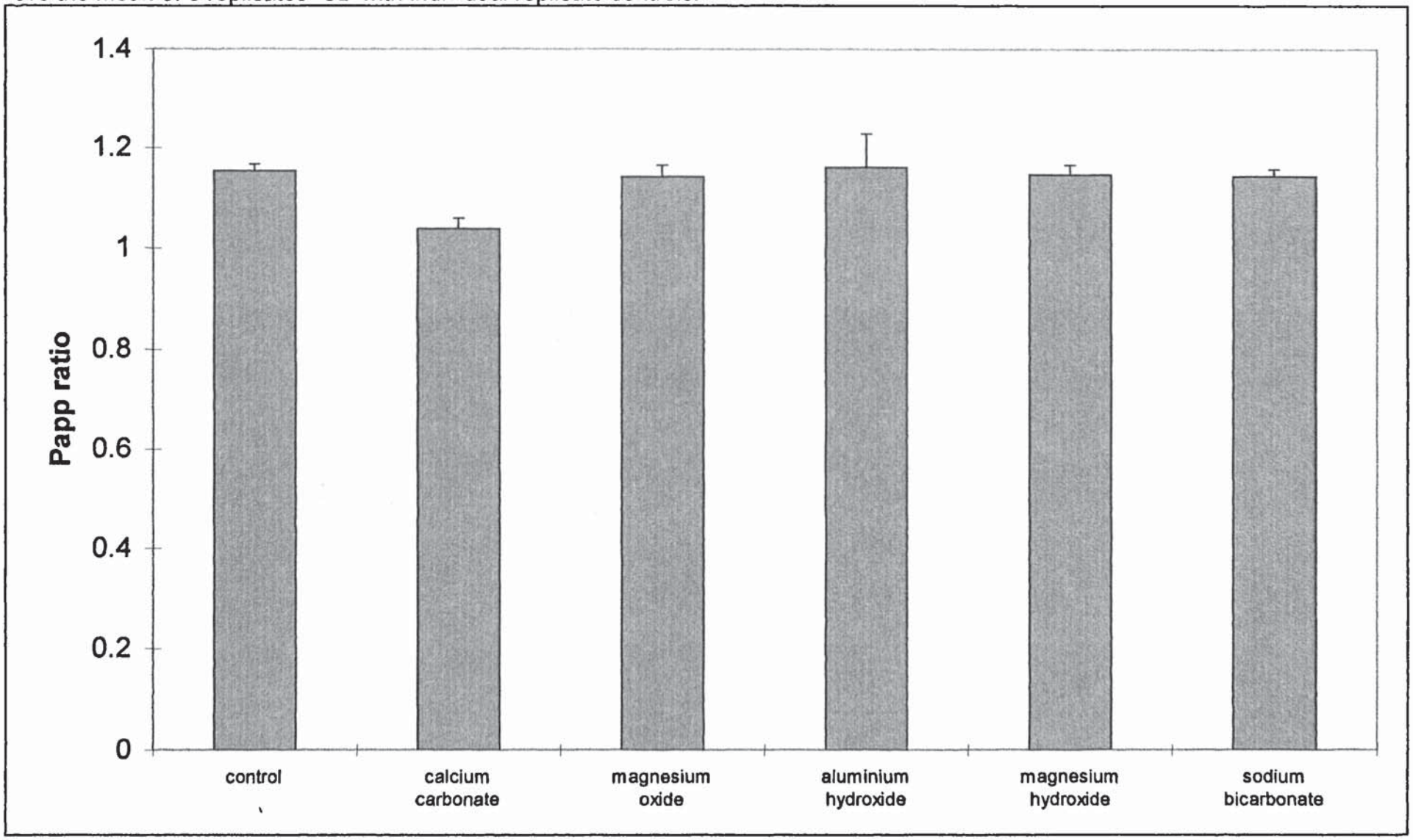

Figure 6.18
Illustrating the effect of antacid/excipient on the relative permeability of ibuprofen compared to mannitol through intestine. Results are the mean of 3 replicates+SD with individual replicate controls.

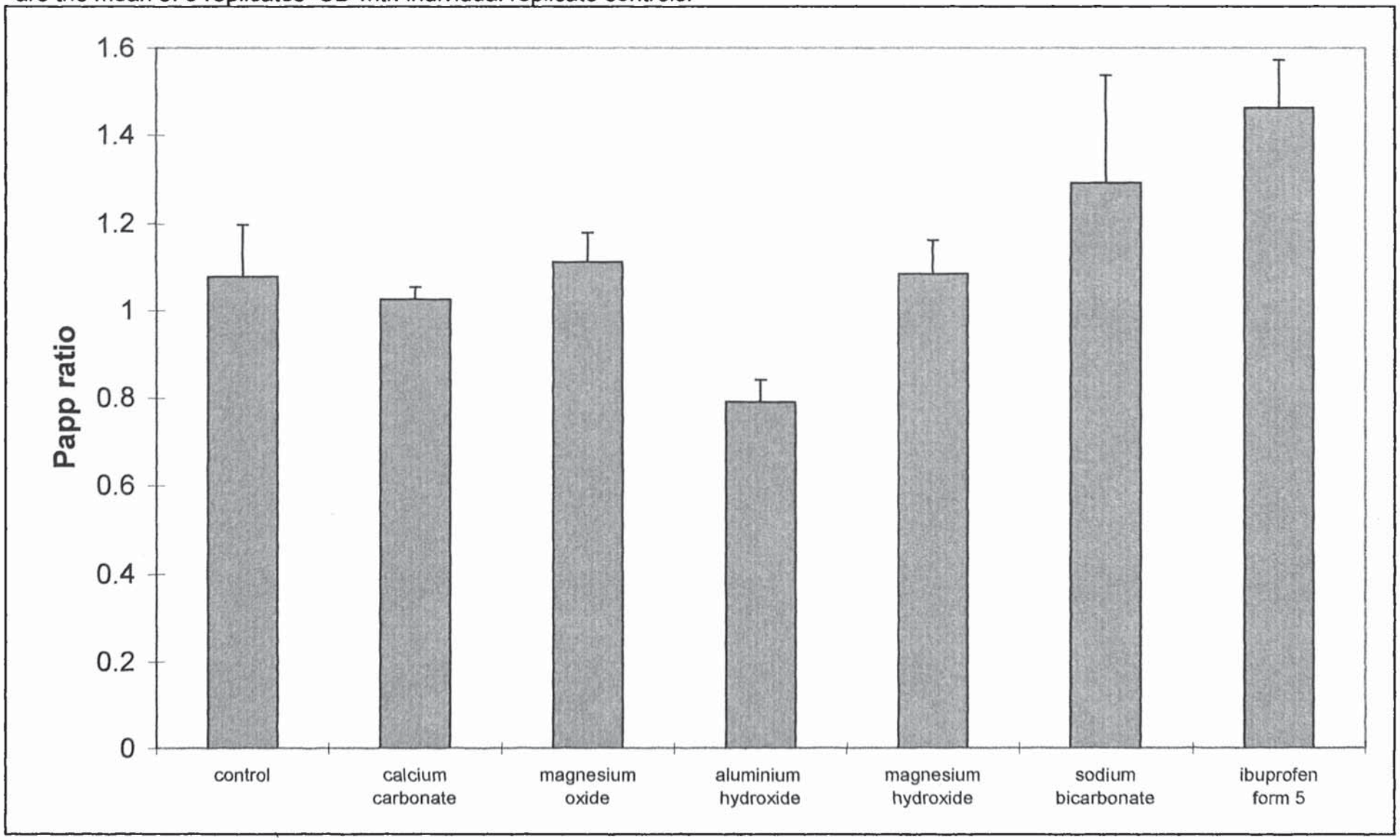

Figure 6.19
Illustrating the effect of antacid/excipient on the relative permeability of paracetamol compared to mannitol through stomach. Results are the mean of 3 replicates+SD with individual replicate controls.

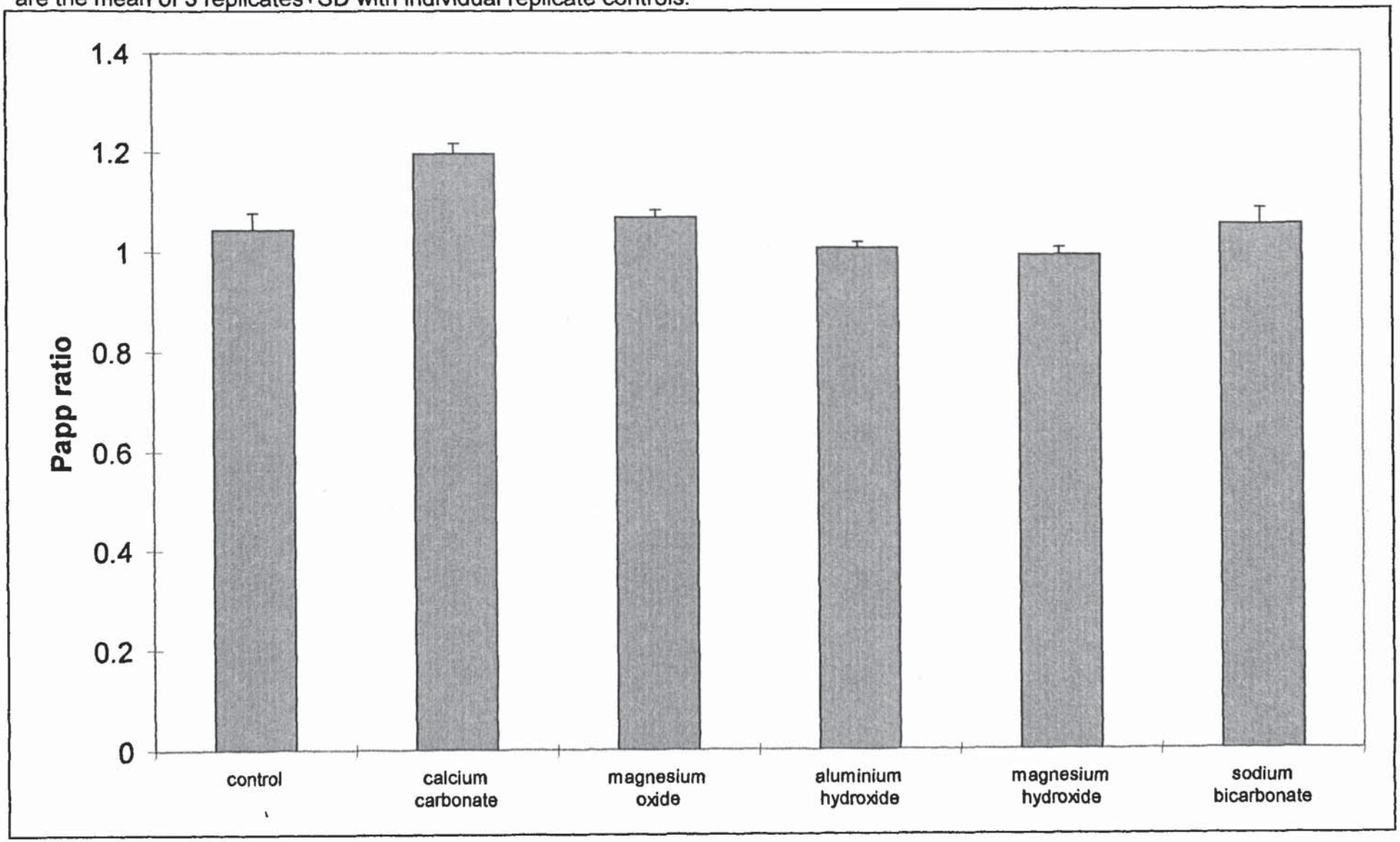

Figure 6.20
Illustrating the effect of antacid/excipient on the relative permeability of ibuprofen compared to mannitol through stomach. Results are the mean of 3 replicates+SD with individual replicate controls.

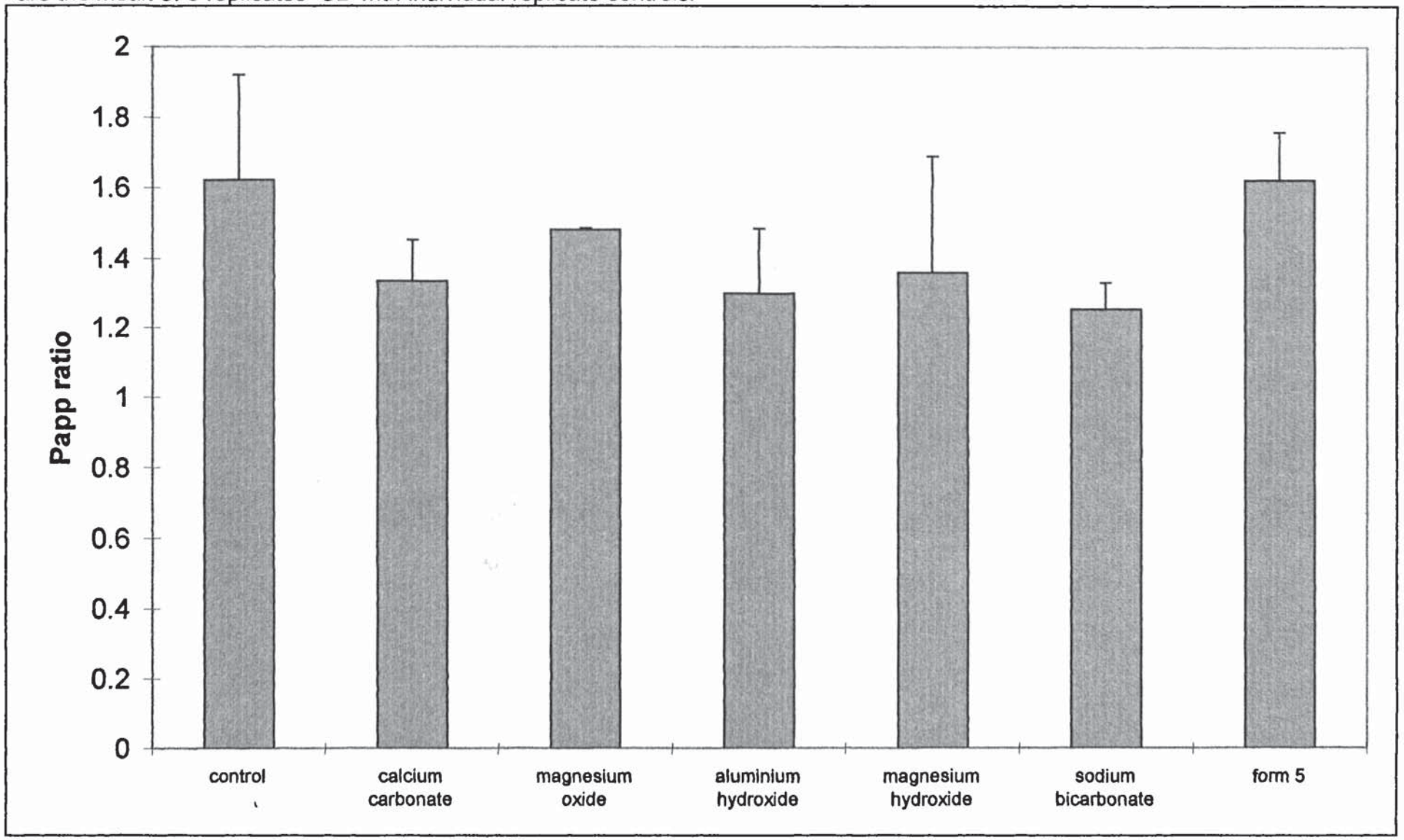

Figure 6.21-46 illustrating the transport of mannitol and either paracetamol or ibuprofen through either the stomach or the intestine. Results are the mean of 3 replicates with SD as appropriate for clarity

Figure 6.21
Illustrating the transport of mannitol and paracetamol through the stomach, with donor solution containing buffer solution only (control)

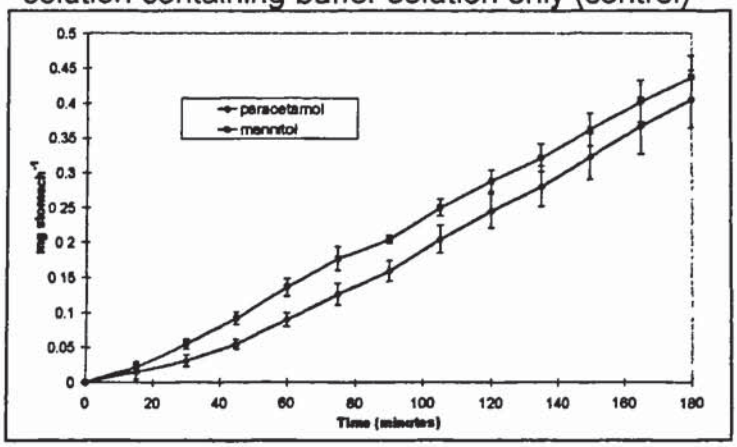

Figure 6.22
Illustrating the transport of mannitol and paracetamol through the stomach, with donor solution containing sodium bicarbonate

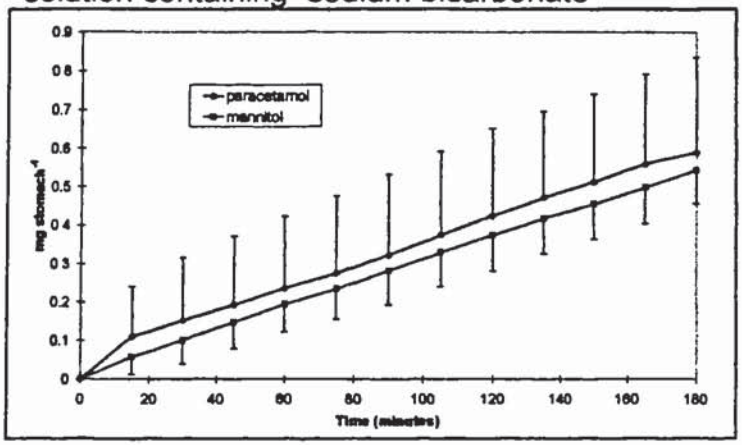

Figure 6.23
Illustrating the transport of mannitol and paracetamol through the stomach, with donor solution saturated with calcium carbonate

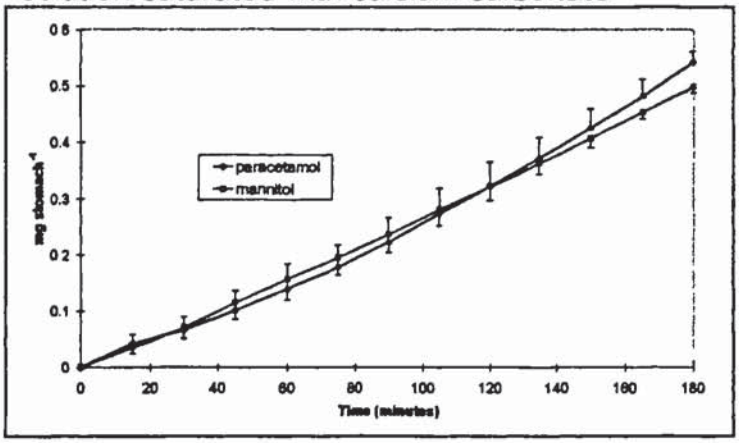

Figure 6.24
Illustrating the transport of mannitol and paracetamol through the stomach, with donor solution saturated with aluminium hydroxide

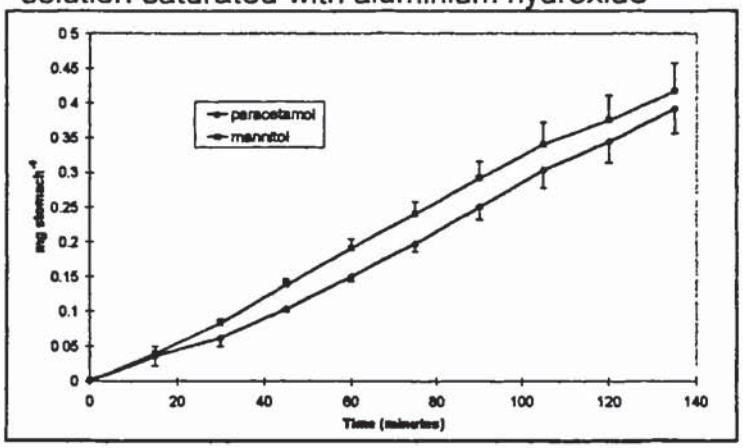

Figure 6.25
Illustrating the transport of mannitol and paracetamol through the stomach, with donor solution saturated with magnesium hydroxide

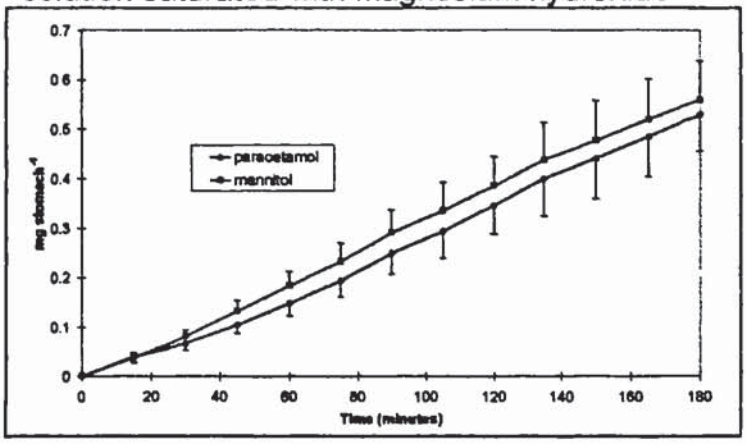

Figure 6.26
Illustrating the transport of mannitol and paracetamol through the stomach, with donor solution saturated with magnesium oxide

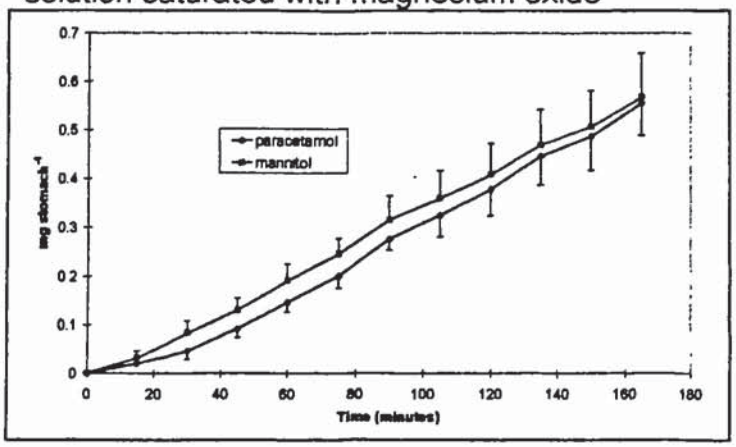

Figure 6.27
Illustrating the transport of mannitol and ibuprofen through the stomach, with donor solution containing buffer solution only (control)

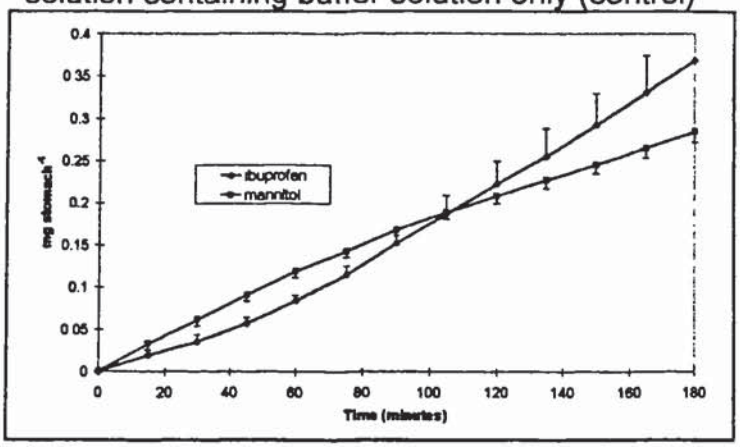

Figure 6.28
Illustrating the transport of mannitol and ibuprofen through the stomach, with donor solution containing sodium bicarbonate

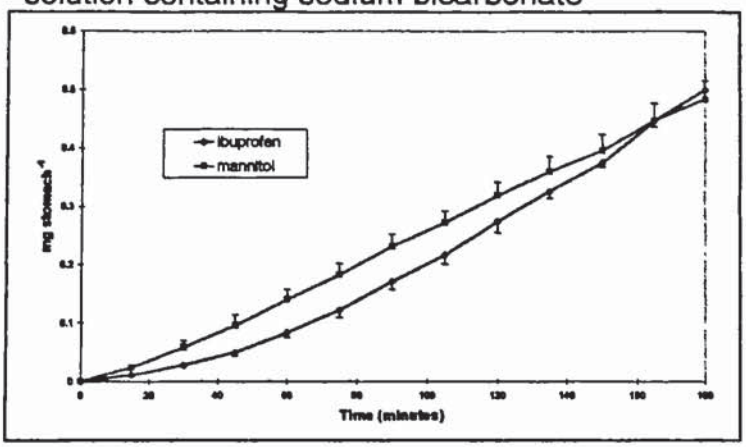

Figure 6.29
Illustrating the transport of mannitol and ibuprofen through the stomach, with donor solution saturated with calcium carbonate

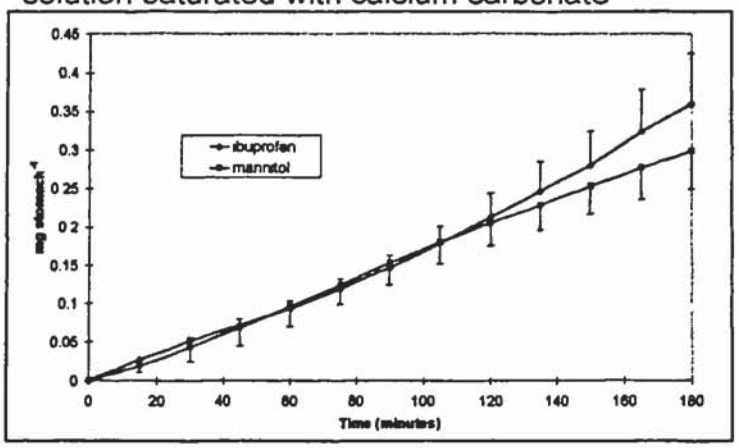

Figure 6.30
Illustrating the transport of mannitol and ibuprofen through the stomach, with donor solution saturated with aluminium hydroxide

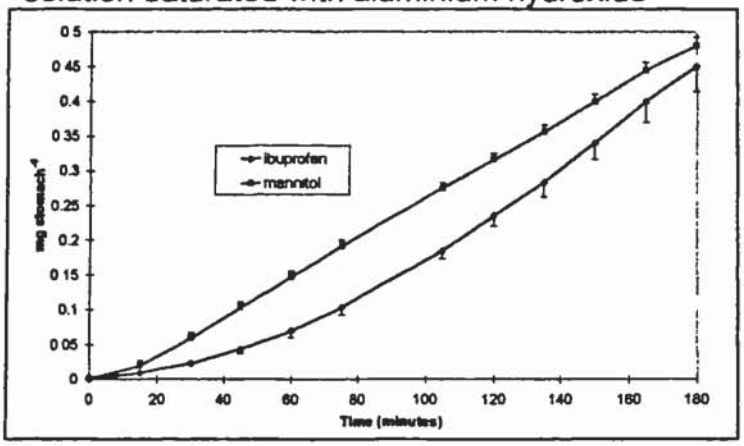

Figure 6.31
Illustrating the transport of mannitol and ibuprofen through the stomach, with donor solution saturated with magnesium hydroxide

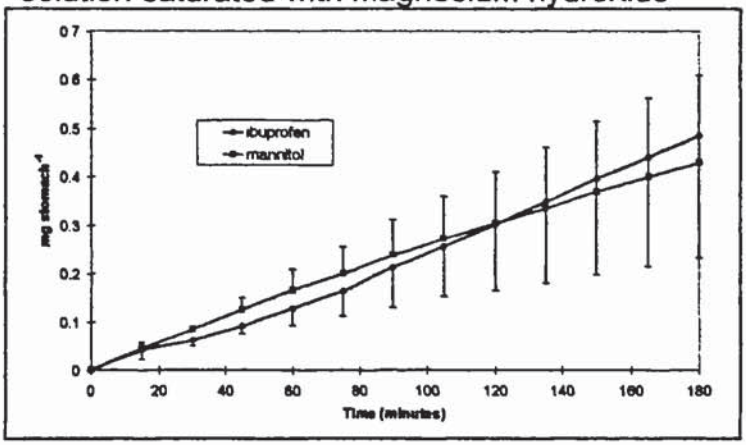

Figure 6.32
Illustrating the transport of mannitol and ibuprofen through the stomach, with donor solution saturated with magnesium oxide

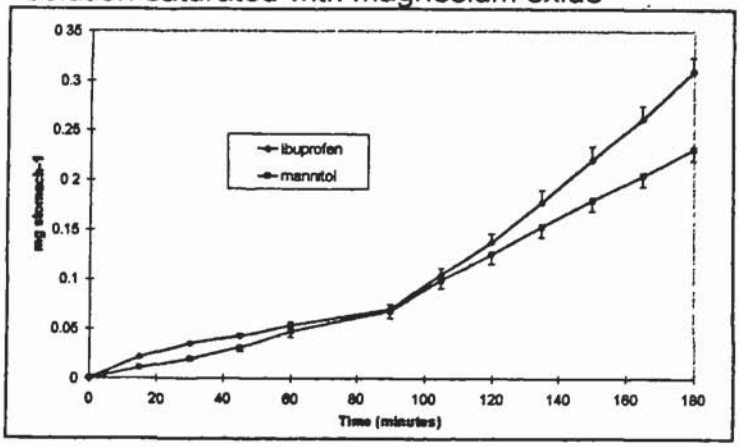

Figure 6.33
Illustrating the transport of mannitol and ibuprofen through the stomach, with donor solution containing Form 5 Ibuprofen tablet

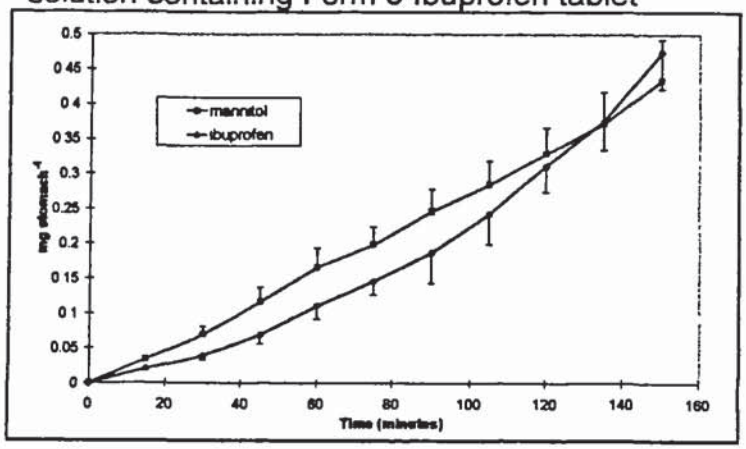

Figure 6.34
Illustrating the transport of mannitol and paracetamol through the intestine, with donor solution containing buffer solution only (control)

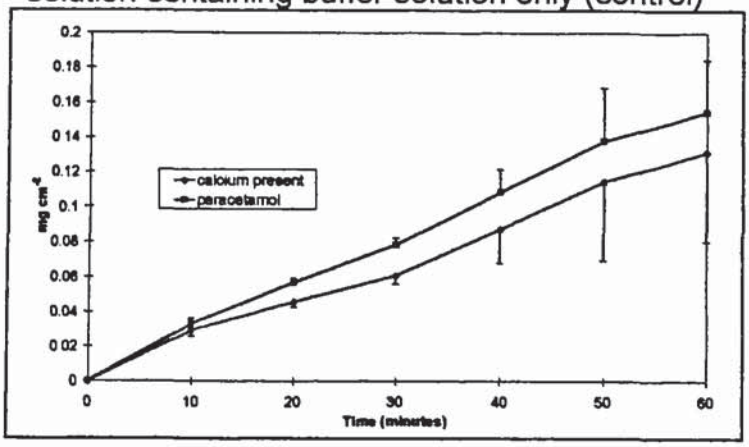

Figure 6.35
Illustrating the transport of mannitol and paracetamol through the intestine, with donor solution containing sodium bicarbonate

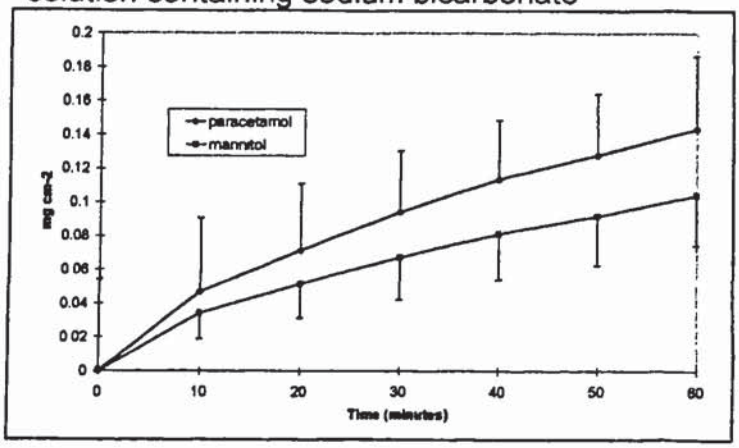

Figure 6.36
Illustrating the transport of mannitol and paracetamol through the intestine, with donor solution saturated with calcium carbonate

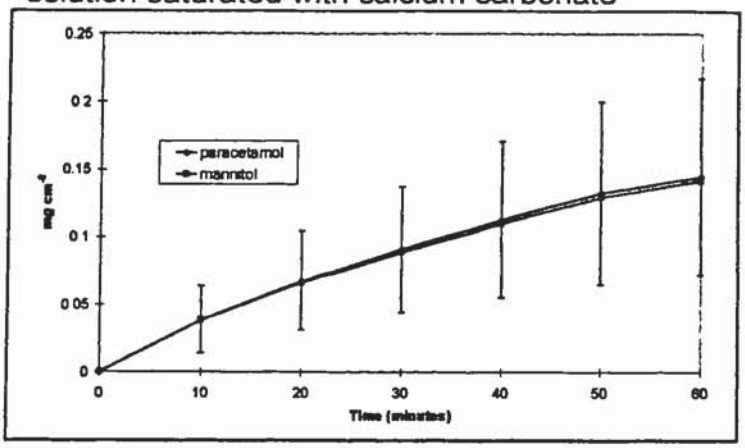

Figure 6.37
Illustrating the transport of mannitol and paracetamol through the intestine, with donor solution saturated with aluminium hydroxide

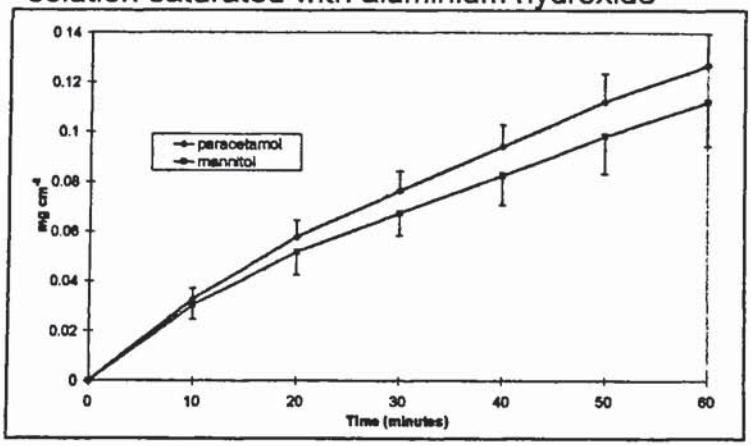

Figure 6.38
Illustrating the transport of mannitol and paracetamol through the intestine, with donor solution saturated with magnesium hydroxide

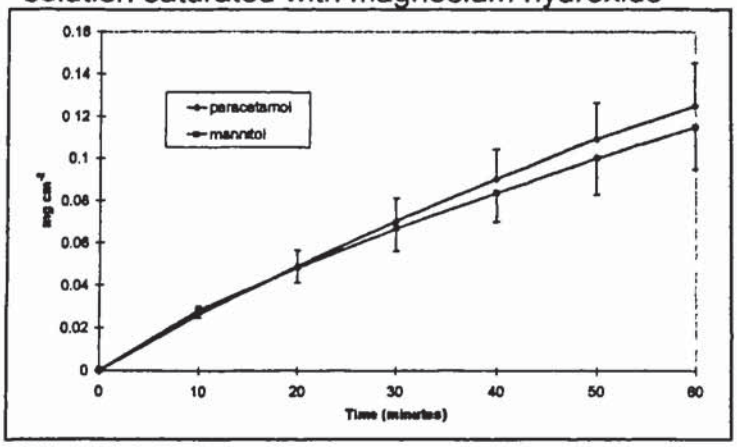

Figure 6.39
Illustrating the transport of mannitol and paracetamol through the intestine, with donor solution saturated with magnesium oxide

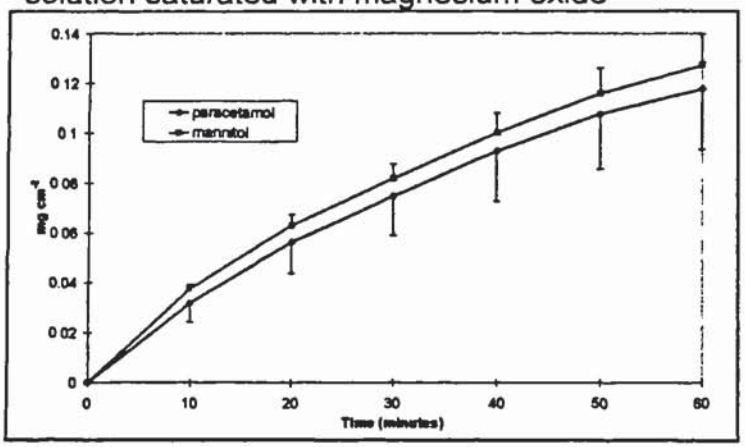

Figure 6.40
Illustrating the transport of mannitol and ibuprofen through the intestine, with donor solution containing buffer solution only (control)

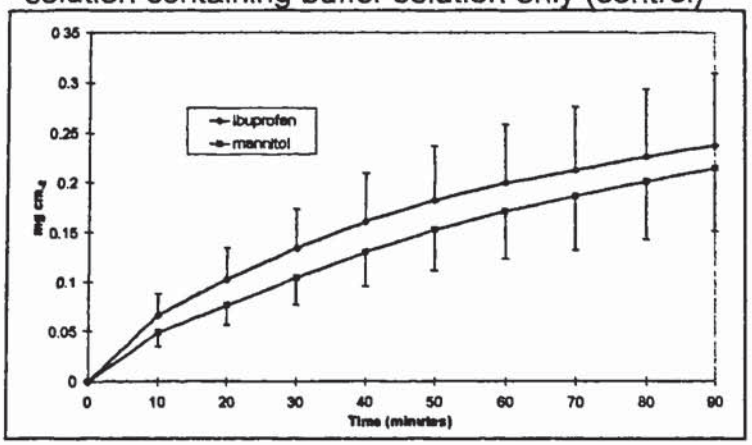

Figure 6.41
Illustrating the transport of mannitol and ibuprofen through the intestine, with donor solution containing sodium bicarbonate

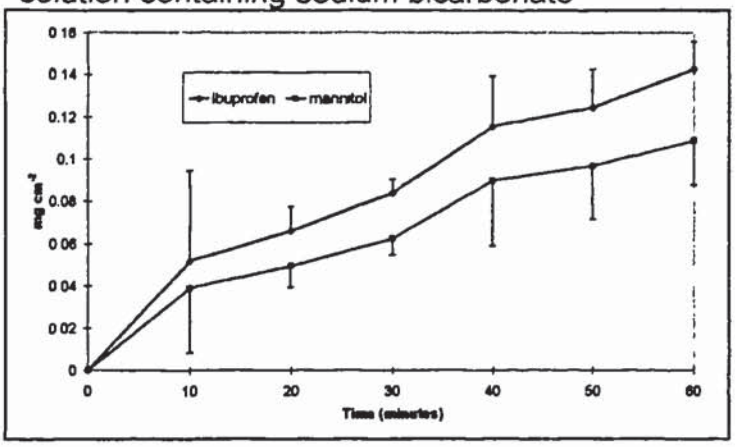

Figure 6.42
Illustrating the transport of mannitol and ibuprofen through the intestine, with donor solution saturated with calcium carbonate

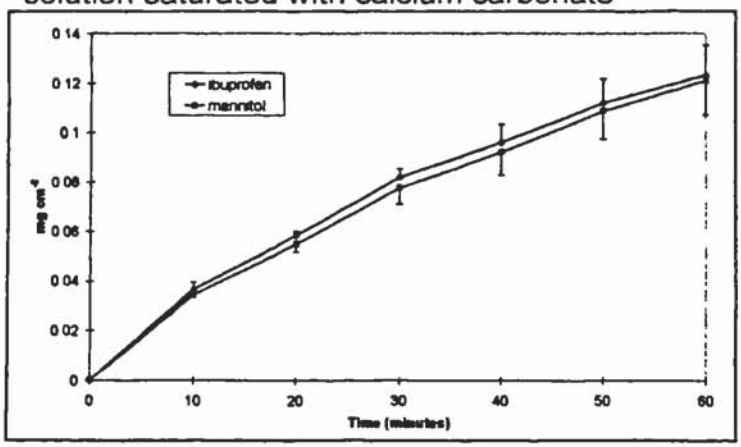

Figure 6.43
Illustrating the transport of mannitol and ibuprofen through the intestine, with donor solution saturated with aluminium hydroxide

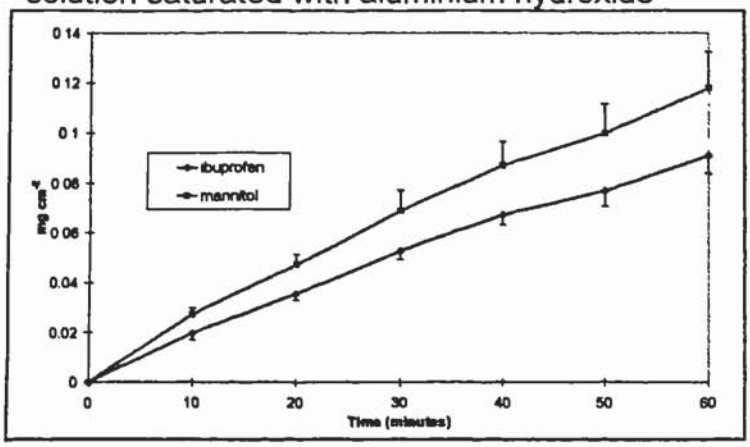

Figure 6.44
Illustrating the transport of mannitol and ibuprofen through the intestine, with donor solution saturated with magnesium hydroxide

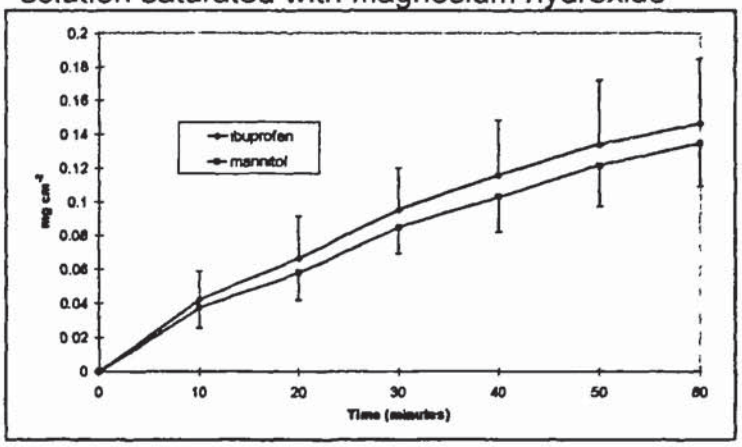

Figure 6.45
Illustrating the transport of mannitol and ibuprofen through the intestine, with donor solution saturated with magnesium oxide

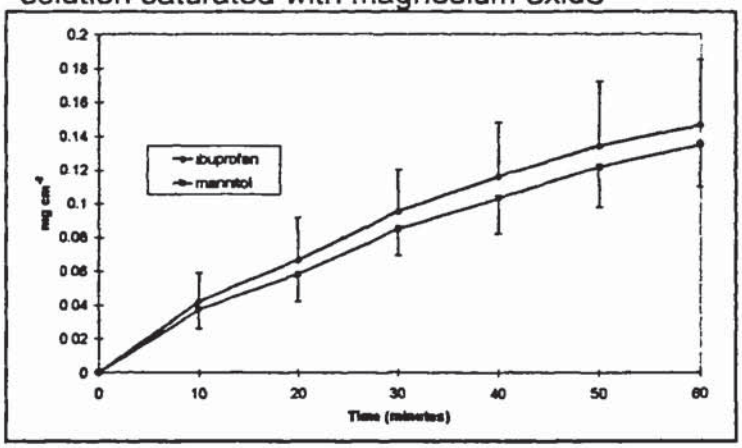

Figure 6.46
Illustrating the transport of mannitol and ibuprofen through the intestine, with donor solution containing Form 5 Ibuprofen tablet

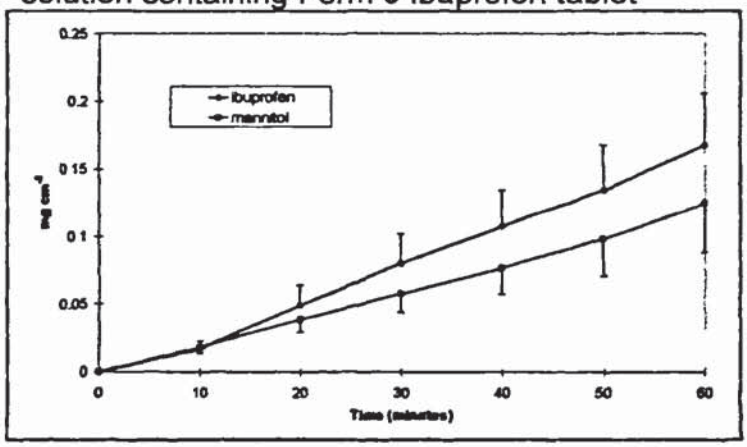

6.6 Summary

Statements refer to both stomach and intestine methods unless otherwise indicated.

- An everted tissue sac methodology was selected as an appropriate model to measure drug permeability. Analytical sensitivity allowed the method to be modified such that tissue eversion was not necessary, minimising the risk of tissue damage during sac preparation.
- Modification of the medium, which was based on a Hank's buffer system, was introduced to allow analysis of the antacids under study.
- Stomach and intestine models were developed which utilised the same method protocols, allowing the direct comparison of apparent permeability through different parts of the GI tract.
- Tissue integrity was established, by verification of integrity of cell tight junctions.
- Tissue stability was observed for the duration of the experiments.
- The use of a control marker, the measurement of the apparent permeability of mannitol in each experiment, indicated that tissue sampling, preparation and use produced barrier properties which conformed to those from a gaussian distribution.
- The method variability, incorporating intra-and-inter variation and measured as %RSD, compared favourably to those reviewed from similar methods and other techniques used to obtain permeability data.
- For both methods, the tissue sacs acted as selective barriers to drugs.
- The apparent permeability of the transcellular marker propranolol *versus* the paracellular marker mannitol was higher, in line with expectations and literature data.
- The apparent permeability of the lipophilic beta-blocker marker propranolol *versus* the hydrophilic betablocker nadolol was higher, in line with expectations and literature data.
- The molecule with the highest molecular weight, fluorescein, had the lowest apparent permeability, in line with expectations and literature data.
- A relationship was established between the apparent permeability and the % absorbed in man. Although limited data were obtained, it was observed that the

relationship approximated to a sigmoidal relationship and was similar to those observed in the literature.

- Dissolved calcium carbonate was observed to increase the apparent permeability of paracetamol in the stomach model.
- Dissolved calcium carbonate was observed to decrease the apparent permeability of ibuprofen in the intestine model.
- Dissolved aluminium hydroxide was observed to decrease the apparent permeability of paracetamol in the intestine model.
- Dissolved formulation 5 (see chapter 7) was observed to increase the transport of ibuprofen in the stomach model.
- All other antacids investigated did not significantly affect the model drugs' apparent permeability in either model.
- Overall the method was found to be stable, reproducible and selective. Further work could investigate the viability of the tissues and the contribution of the muscalaris layer to the barrier, in both models.

CHAPTER 7

NOVEL TABLET FORMULATION DEVELOPMENT

7.1 Introduction

Immediate-release products are formulated such that the delivery of the drug to the site of action is fast, ensuring the rapid onset of the therapeutic action of the drug. This may apply particularly to analgesic drugs, where the therapeutic action is the relief of acute and chronic pain. It is generally accepted that the pharmacokinetics of the drug, *i.e.* the C_{max} and t_{max}, can be correlated to the pharmacodynamic effect induced by the drug. Although enjoying enormous commercial success, conventional tablet formulations of paracetamol and ibuprofen, which are formulated according to well established formulations and methods, have been observed to have t_{max} values of approximately 1 hour and 2 hours respectively (see tables 1.1 and 1.2). The development of the Zapp paracetamol tablet by SB (t_{max} of 0.28 hours), Grattan *et al.* 2000) was influenced by the commercial opportunity of a more rapidly acting paracetamol tablet. Unsurprisingly, several groups have undertaken work to develop rapidly absorbed analgesic tablet formulations. For example, Bruna *et al.* (1998) developed an innovative oral fast dispersible tablet, which underwent rapid dissolution in the mouth, being formulated to mask the bitter taste of the paracetamol active ingredient, and was more rapidly absorbed when compared to a brand leader tablet formulation (t_{max} of 0.69hr *vs.* 0.91hr). For ibuprofen, the opportunities for formulation improvement may be greater, due to its poor gastric solubility. Altomare *et al.* (1997) produced an effervescent tablet formulation which was more rapidly absorbed than a sugar coated tablet (0.5hr *vs.* 1.1hr). It was also claimed that the effervescent formulation would aid compliance as it would be preferable for patients who had difficulty in swallowing. Gazzaniga *et al.* (1988) produced an ibuprofen formulation which also contained arginine and sodium bicarbonate with a claimed t_{max} of 15 minutes. Interestingly, ibuprofen/sodium bicarbonate granules prepared by a wet granulation method were found to liquefy during preparation (Ghosh *et al.* 1998). Finally, a tablet formulation containing ibuprofen as the lysinate salt (Nurofen Advance®) is available which has been clinically proven to be faster acting than conventional paracetamol products, in the relieve of dental pain. (Meslisch *et al.* 1995).

It has been demonstrated in chapter 3 that both paracetamol and ibuprofen are weak acids whose solubility greatly increases as the solvent pH is increased above the drugs' pK_a. It has also been explained in chapter 4 that the dissolution rate of a drug increases proportionally as the drug's saturated solubility increases. This was used as the basis of selection and assessment of potential dissolution enhancers in the work undertaken in chapter 4. It was observed that some of the excipients exhibited dissolution-enhancing properties with respect to the model drugs, in powder mixes. The aim of the tablet formulation study was to assess whether the selected excipients maintained their dissolution-enhancing properties when processed into granules and final tablet formulations. The selected excipients suitability for use in tablet formulations in terms of processing, compatibility and stability was also assessed. The development of the formulations was conducted in a structured manner by the application of statistical experimental design, where appropriate.

7.2 Granule formulation development

7.2.1 Paracetamol granule development

7.2.1.1 Experimental

7.2.1.1.1 Materials

Paracetamol, lactose, starch and sodium bicarbonate (extra fine grade were obtained from SB (Weybridge, UK). Tri-sodium phosphate and L-arginine were obtained from Aldrich (Poole, UK). All materials were pharmaceutical or analytical grade as appropriate. Double-distilled water was generated in-house using a Fison's Fi-Stream Still.

7.2.1.1.2 Equipment

A Pearless and Ericsson planetary mixer was used for mixing and granulation. A Gallenkamp Hotbox fan-assisted oven was used to dry the prepared granules. A Copley mechanical tapping device was used for the tap-density measurements. A mechanical vibrator and sieves in the range 75-710μm, both supplied by Endecotts,

were used for particle size analysis. A single-punch tabletting press supplied by Wilkinson was used to produce tablets. A Schleuniger-4M crushing strength instrument was used to measure tablet crushing strength.

7.2.1.1.3 Method

All materials were presieved through a 710μm or smaller mesh, 150g of paracetamol and 150g of the excipient mixture were added into the planetary mixer. The powders were mixed thoroughly using a 5-minute mechanical mixing cycle. 10% (w/v) starch mucilage solution was added manually until the endpoint was reached, measured visually by the virtual absence of ungranulated powder. The granules were then sieved through a 1mm sieve followed by drying overnight in the fan-assisted oven at a temperature of 45°C. The dried granules were again passed through a 1mm sieve. The dissolution properties of the granules were assessed using the dissolution equipment described in 4.6.3.2 and the 'controlled powder' method described in 4.6.3.3 with 600mg of granules used in each modified basket (n=6) and an experimental duration of 30 minutes with 0.05M HCl used as the dissolution medium. The Carr's index was determined by calculation from the bulk and tap densities, both of which were obtained in a 250ml measuring cylinder and the latter undergoing 2400 taps on the mechanical tapping device. For particle-size analysis the sieve stack was vibrated for 30 minutes. The tabletting qualities of the granules were very crudely assessed by pressing tablets weighing approximately 0.5g. The tabletting qualities were qualitatively assessed and the crushing strengths obtained using the crushing strength instrument.

7.2.1.2 Results and discussion

From the work conducted in Chapter 4, it was apparent that, of all the excipients investigated, potassium bicarbonate and sodium bicarbonate produced the most profound increase in the dissolution rate of paracetamol in an acidic medium, when added as an excipient in a 1:1 ratio. It was also concluded that both bicarbonate compounds increased paracetamol dissolution rate by a mechanism of increased agitation, and also that these excipients were not alkaline enough to increase the solubility of the weakly acidic paracetamol. Work undertaken in Chapters 3 and 4 demonstrated that dissolved sodium bicarbonate decreased the solubility and IDR of

paracetamol as illustrated in figures 3.3 and 4.75. Combining these facts, it was therefore postulated that the combination of sodium bicarbonate with an alkalising excipient, capable of increasing the solubility of paracetamol by increasing the pH above paracetamol's pK_a, within the diffusion layer surrounding each particle and/or the bulk solution, would create a dissolution enhancing excipient mixture superior to sodium bicarbonate, as used in the Zapp tablets. To determine whether this hypothesis was true, two alkalising excipients; tri-sodium phosphate and L-arginine, both of which have been demonstrated to act as paracetamol drug dissolution enhancers in powder mixtures, were selected for study along with sodium bicarbonate.

A systematic way to determine whether the individual excipients or an excipient combination produced the most rapidly dissolving granules was to use an experimental design for mixtures method (Armstrong and James 1996). A practical example where this approach was used was in work conducted by Huisman *et al.* (1984) where the crushing strengths and disintegration times of tablets containing various combinations of the diluents α-lactose monohydrate, potato starch and anhydrous α-lactose were investigated. If three factors (three excipients) are to be studied, as in the study undertaken, the factor space, which is an area representing all possible combinations of the components, can be represented by an equilateral triangle. As it was not known whether the relationship between dissolution rate and excipient mixture composition was linear or of a higher order, the experimental design selected required the investigation of 10 excipient combinations according to the experimental plan detailed in table 7.1, where the figures indicate the fraction of each excipient in the excipient mixture, noting that the excipient mixture was ratioed 1:1 (weight) with paracetamol.

Table 7.1
Factor (excipient) combinations for paracetamol granule development study. Table indicates relative amounts of each excipient in the excipient mix, which was ratioed 1:1 to paracetamol on a weight basis.

Experiment	Composition (decimal fraction)		
	sodium bicarbonate	tri-sodium phosphate	L-arginine
1	0.00	1.00	0.00
2	1.00	0.00	0.00
3	0.33	0.33	0.33
4	0.16	0.67	0.16
5	0.50	0.50	0.00
6	0.00	0.00	1.00
7	0.50	0.00	0.50
8	0.67	0.16	0.16
9	0.16	0.16	0.67
10	0.00	0.50	0.50

The dissolution properties of the granules were determined using the controlled powder method developed in chapter 4, with 0.05M HCl used as the dissolution medium. A lactose:paracetamol (1:1) granule prepared by the same method as the other granules was used as the reference material. F_1 fit-factors were calculated for each formulation using data obtained at 1 minute intervals over 30 minutes and by comparison to the reference material. The F_1 fit factors (response) were overlaid on to the factor space as illustrated in figure 7.1. Generally, data of this type are fitted to an appropriate model to allow the generation of surface response contour maps (Lewis *et al.* 1999). However, this was unnecessary as conclusions could be drawn without the generation of contour plots. Reviewing figure 7.1, it can be concluded that 100% tri-sodium phosphate actually inhibited the dissolution of paracetamol compared to lactose and that any mixture containing tri-sodium phosphate (area excluding the BC line) was at best only a marginal dissolution-promoter. As expected, 100% sodium bicarbonate had a significant dissolution-promoting effect and L-arginine exhibited a marginal promoting effect. In line with the hypothesis it was found that a granule containing equal quantities of L-arginine and sodium bicarbonate exhibited the fast dissolution rate (F_1=217), *i.e.* it is possible that the alkalising excipient L-arginine acted synergistically with sodium bicarbonate, which acts by increasing agitation, to increase the dissolution rate of paracetamol.

As part of the formulation development strategy other factors require consideration. For example, an assessment of the suitability of the produced granules for tabletting is required. Therefore, the granules produced were characterised in terms of some physical properties considered to be important during the tabletting process. These results, along with the dissolution results are summarised in table 7.2. As tri-sodium phosphate was considered unsuitable, the results from the physical characterisation of granules containing this excipient are reproduced as a matter of record only and conclusions will be drawn only for the three granule formulations containing either 100% sodium bicarbonate, 100% L-arginine or 50:50 sodium bicarbonate:L-arginine, as the added excipients. From table 7.2, it can be concluded that the Carr's index results, which are used as a measure of flowability (Aulton 1988), indicate the three granule formulations would have good flow characteristics and with a % compressibility range of 12-16 are considered as free flowing powdered granules. It is also noted that when only sodium bicarbonate was used as the excipient the granules were compressed easily into relatively hard tablets. Conversely, when the granules contained only L-arginine as the excipient, the production of tablets was not possible due to constant seizure of the tablet press. The intermediate granule formulation was found to produce only a few tablets before the tablet machine seized. These tablets were relatively soft and where found to exhibit 'capping'. This indicates that paracetamol formulations containing L-arginine may require the addition of other excipients to increase compressibility and lubrication to produce a finished tablet of acceptable quality.

The paracetamol granule development program was not progressed. However, a rational formulation development strategy would be to perform an optimisation study for the most suitable sodium bicarbonate and L-arginine combination, for example using the simplex search technique (Armstrong and James 1996), to obtain granules undergoing the most rapid dissolution.

Figure 7.1
Illustrating the relationship between the granule dissolution rate expressed as F_1 *versus* the excipient composition where A=100% tri-sodium phosphate, B=100% L-arginine and C=100% sodium bicarbonate. Data illustrated as a surface response contour map.

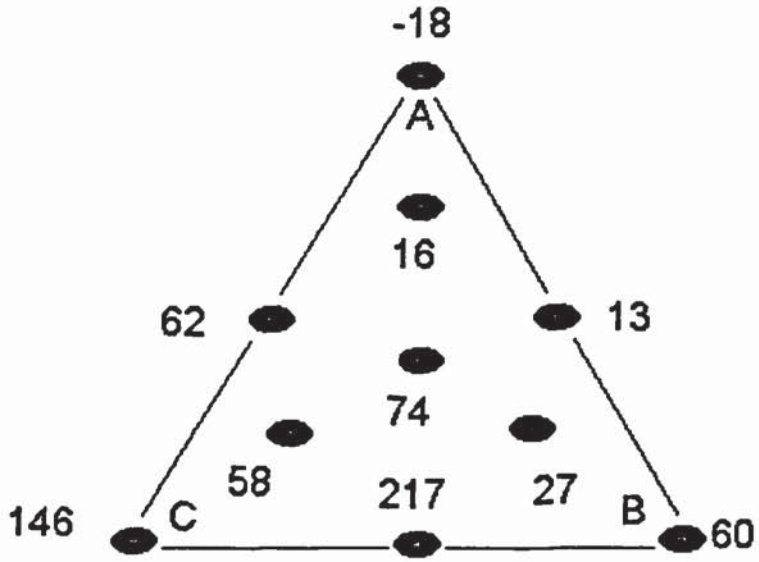

Formulation composition key for table 7.2			
Formulation identity	**Composition* (decimal fraction)**		
	sodium bicarbonate	**tri-sodium phosphate**	**L-arginine**
1	0.00	1.00	0.00
2	1.00	0.00	0.00
3	0.33	0.33	0.33
4	0.16	0.67	0.16
5	0.50	0.50	0.00
6	0.00	0.00	1.00
7	0.50	0.00	0.50
8	0.67	0.16	0.16
9	0.16	0.16	0.67
10	0.00	0.50	0.50

*Represents the composition of the excipient mixture, which was ratioed 1:1 with paracetamol, on a weight basis.

Table 7.2
Physical characterisation of paracetamol granule formulations

	Formulation*										
Parameter	**lactose**	**1**	**2**	**3**	**4**	**5**	**6**	**7**	**8**	**9**	**10**
F_1	0	-18	146	74	16	62	60	350	58	27	13
Bulk density (gcm^{-3})	0.238	0.408	0.565	0.443	0.459	0.510	0.517	0.447	0.4313	0.3475	0.544
Tap density (gcm^{-3})	0.278	0.440	0.673	0.532	0.536	0.62	0.595	0.515	0.4913	0.3798	0.5763
Carr's index	15	7	16	17	14	18	13	13	12	9	6
Particle size %retained											
>710μm	4.6	41.4	12.8	8.9	10.4	6.6	7.3	3.6	4.3	5.8	35.8
>500<710μm	9.1	27.6	13.6	10.2	12.7	7.9	15.6	9.1	11.3	8.8	11.1
>250<75μm	41.6	22.5	33.1	28	31.3	18.7	46.5	39	44.7	29.9	31.5
>75<250μm	43.2	6.1	36.8	43.2	38.2	44.4	29.6	46.9	34.7	38.1	28.9
<75μm	1.5	2.4	3.6	9.7	7.3	22.5	0.9	1.4	5.0	17.3	7.6
Tabletting**	3	4	5	3	3	3	1	2	4	2	2
Hardness (N)	56	35	76	42	37	43	N/A	20	34	15	16

*Refer to key on previous page.
**Tabletting properties of granules: 1=unable to tablet, machine seizes and tablets not formed. 5=excellent tablets, machine free running with consistent hard tablets produced.

7.2.2 Ibuprofen granule development

7.2.2.1 Experimental

7.2.2.1.1 Materials

Ibuprofen, lactose, starch and sodium bicarbonate (extra-fine grade were obtained from SB (Weybridge, UK). Tri-sodium phosphate, sodium carbonate and L-arginine were obtained from Aldrich (Poole, UK). All materials were pharmaceutical or analytical grade as appropriate. Double-distilled water was generated in-house using a Fison's Fi-Stream Still.

7.2.2.1.2 Equipment

The equipment and set-up was as described in 7.2.1.1.2.

7.2.2.1.3 Method

The granules were prepared according to the method detailed in 7.2.1.1.3 replacing the 150g of paracetamol with 150g of ibuprofen. The granules were characterised using the methods detailed in 7.2.1.1.3.

7.2.2.2 Results and discussion

Reviewing the results from chapter 4 (table 4.7), several excipients were demonstrated to act as dissolution promoters for ibuprofen. Of these, tri-sodium phosphate, sodium bicarbonate, sodium carbonate and L-arginine were selected for this study. During an initial investigation it was found that both L-arginine and sodium bicarbonate were incompatible with ibuprofen using a wet granulation technique with an aqueous based binder (starch solution) in that the mixture did not form granules but instead produced an exothermic reaction with effervescence, followed by the formation of a 'dough'. Therefore, the ibuprofen granulation study was restricted to the use of sodium carbonate and tri-sodium phosphate as the dissolution enhancing excipients. The experimental design for mixtures technique (Armstrong and James 1996) was again selected to systematically determine the most suitable excipient combination for promoting ibuprofen dissolution from granules. If two factors (two excipients) are to be studied, as in this case, the factor space is represented by a

straight line which joins the points representing pure sodium carbonate and tri-sodium phosphate and represents all proportions of the two ingredients (the abscissa on an x-y graph). Using a theoretical example illustrated in figure 7.2, examples of how crushing strength may vary with composition are portrayed. If the responses are purely additive, then the response line will be a straight line joining the crushing strengths of the pure excipients. If the relationship produces a concave line this indicates mixing of the two components has a detrimental effect. If the line is convex this indicates a beneficial or synergistic effect of mixing the components.

Figure 7.2
Illustrating an example of a response line when two factors, crushing strength and composition, are investigated. Refer to text for full explanation.

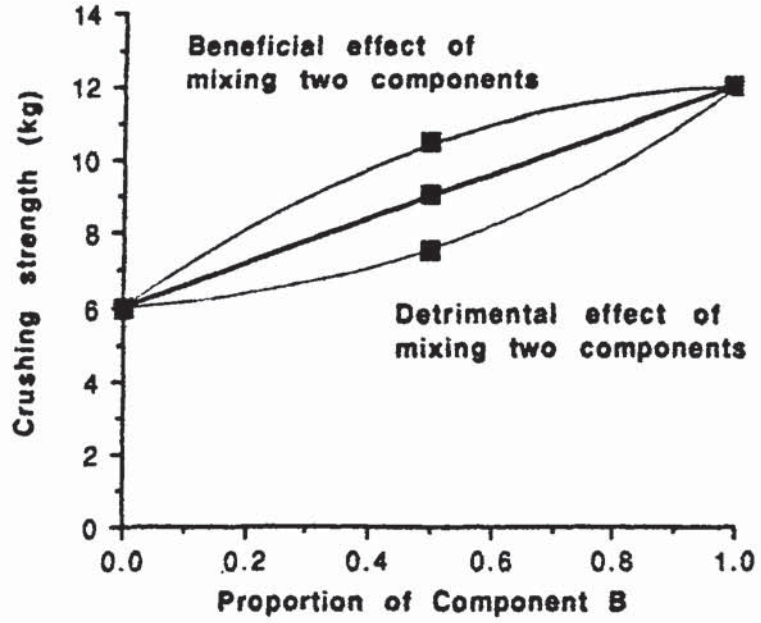

Reproduced form Armstrong and James (1996)

The experimental design for the present study is detailed in table 7.3.

Table 7.3
Factor (excipient) combinations for ibuprofen granule development study. Table indicates relative amounts of each excipient in the excipient mix, which was ratioed 1:1 to ibuprofen, on a weight basis.

	Composition (decimal fraction)	
Experiment	**sodium carbonate**	**tri-sodium phosphate**
1	1.00	0.00
2	0.00	1.00
3	0.25	0.75
4	0.75	0.25
5	0.50	0.50

The dissolution properties of the granules were determined using the controlled powder method developed in chapter 4, with USP buffer pH6.8 used as the dissolution medium. A lactose:paracetamol (1:1) granule prepared by the same method as the other granules was used as the reference material. F_1 fit-factors were calculated for each formulation using data obtained at 1 minute intervals over 60 minutes. The dissolution profiles are illustrated in figure 7.3 and the F_1 fit-factors detailed in table 7.4.

Figure 7.3
Illustrating the dissolution profiles of ibuprofen granules with varying dissolution promoting excipients compositions. Refer to key to table 7.4 for formulation composition. Results are the mean of at least 5 replicates.

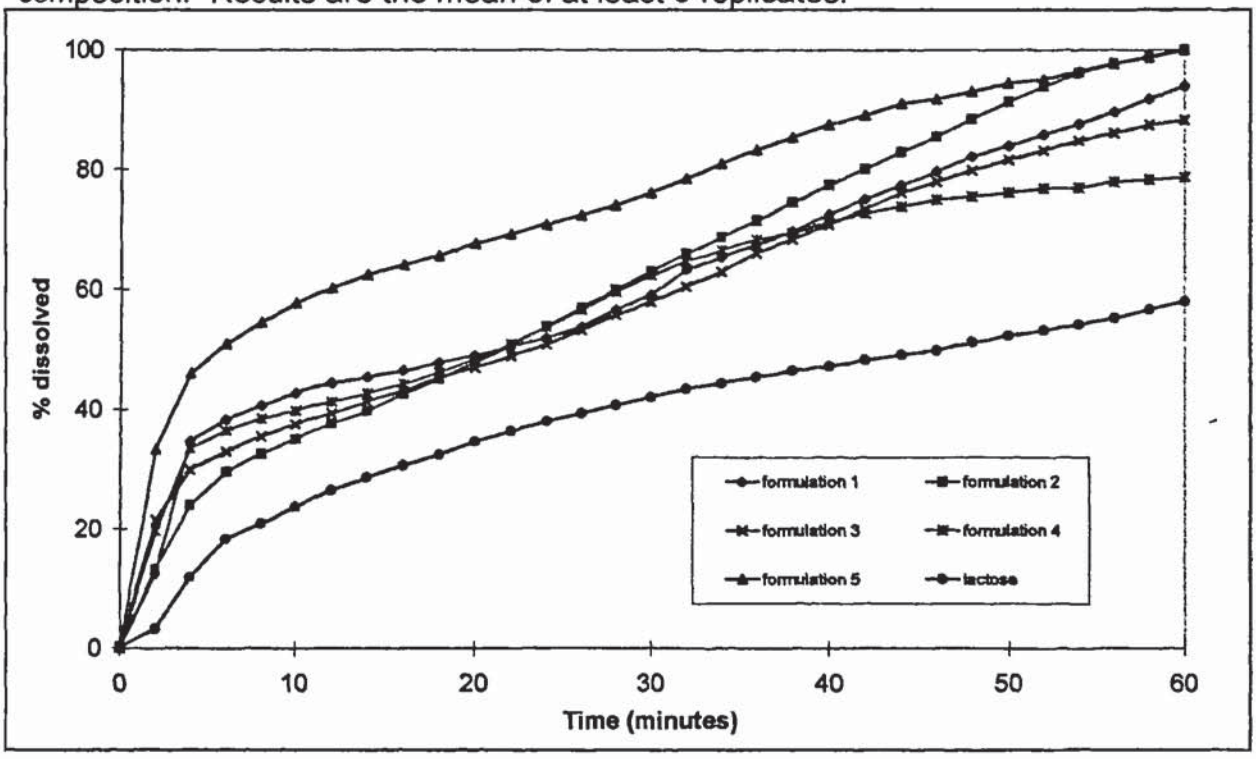

All five granule formulations exhibited increased dissolution rates compared to the reference granules. As the dissolution test was conducted using pH6.8 medium, whereby the pH differential between the medium and a solution of the excipient was lower than if simulated stomach medium (0.05M HCl) was used, the results probably underestimate the potential of the excipient combinations as dissolution enhancers. It was noted that formulation 5, which contained a 50:50 mixture of sodium carbonate and tri-sodium phosphate, had the greatest differential from the reference. However, all the other formulations were similar to each other. This indicates there maybe a synergistic effect in combining the excipients, although this evidence is far from conclusive. As for the paracetamol granule formulation study, assessment of the suitability of the produced granules for tabletting was required. Therefore, the granules produced were characterised in terms of some physical properties considered to be important during the tabletting process. These results, along with the dissolution results are summarised in table 7.4. The Carr's index results, which are used as a measure of flowability (Aulton 1988), indicate the granule formulations would have excellent flow characteristics and with a % compressibility range of 8-11 are considered as free-flowing granules. All of the granules were found to produce good tablets with no indication of machine seizure, tablet fracturing or capping. It was noted that, although all the tablets appeared hard and robust when manually handled, tablets containing increasing concentrations of tri-sodium phosphate were slightly pliable. The crushing strengths obtained for these formulations are therefore unreliable but are included as a matter of record.

The overall conclusion from the ibuprofen granule development study was that both sodium carbonate and tri-sodium phosphate, separately and in combination with each other, were demonstrated to be very suitable excipients for use in ibuprofen tablet formulations. The reasons for this are their ability to act as drug dissolution promoters and also, the physical suitability of the granules to be compressed into finished tablets. The results of this study were utilised for the development of an improved ibuprofen tablet formulation.

Formulation composition key for table 7.4		
Formulation identity	**Composition* (decimal fraction)**	
	sodium carbonate	**tri-sodium phosphate**
1	1.00	0.00
2	0.00	1.00
3	0.25	0.75
4	0.75	0.25
5	0.50	0.50

*Represents the composition of the excipient mixture, which was ratioed 1:1 with ibuprofen, on a weight basis.

Table 7.4
Physical characterisation of ibuprofen granule formulations

	Formulation*					
Parameter	**lactose**	**1**	**2**	**3**	**4**	**5**
F_1	0	56	56	51	50	104
Bulk density (gcm^{-3})	0.397	0.435	0.393	0.422	0.395	0.366
Tap density (gcm^{-3})	0.438	0.487	0.437	0.478	0.445	0.409
Carr's index	9	11	10	8	10	11
Particle size %retained						
>710μm	5.4	15.2	40.5	24.3	11.1	24.0
>500<710μm	9.9	8.2	26.4	18.3	11.0	16.3
>250<75μm	40.6	20.5	21.6	32.6	29.6	39.7
>75<250μm	33.1	47.2	9.9	19.3	35.6	17.5
<75μm	11	8.8	1.7	5.5	12.7	2.6
Tabletting**	5	5	5	5	5	5
Hardness (N)	64	69	10	10	40	10

*Refer to key on previous page.
**Tabletting properties of granules: 5= excellent tablets, machine free running with consistent hard tablets produced.

7.3 Novel ibuprofen tablet formulation development program

7.3.1 Experimental

7.3.1.1 Materials

Ibuprofen, lactose, starch, microcrystalline (Avicel®), sodium starch glycollate (Explotab®) and magnesium stearate were obtained from SB (Weybridge, UK). Tri-sodium phosphate, sodium carbonate and sodium lauryl sulphate were obtained from

Aldrich (Poole, UK). All materials were pharmaceutical or analytical grade as appropriate. Double-distilled water was generated in-house using a Fison's Fi-Stream Still.

7.3.1.2 Equipment

A Pearless and Ericsson planetary mixer was used for mixing and granulation. A Gallenkamp Hotbox fan-assisted oven was used to dry the prepared granules and for determining moisture content. A Copley mechanical tapping device was used for the tap-density measurements. A mechanical vibrator and sieves in the range 75-710μm, both supplied by Endecotts, were used for particle size analysis. A Pharmactech cube blender was used to mix the granules with the extra-granular excipients. A Manesty F3 single-punch tabletting press, located at SB (Harlow), was used for tabletting. A Schleuniger-6D crushing strength instrument was used to measure tablet crushing strength. An Erweka 2T-34 bath was used for to measure tablet disintegration time. A Friabilator supplied by Vankel was used to measure tablet friability.

7.3.1.3 Method

All materials were presieved through a 710μm or smaller mesh, 600g of ibuprofen, 2400g of the appropriate dissolution promoting excipient mixture and 600g of microcrystalline cellulose were added into the planetary mixer. The powders were mixed thoroughly using a 5-minute mechanical mixing cycle. 10% (w/v) starch mucilage solution was added manually until the endpoint was reached, measured visually by the virtual absence of ungranulated powder. The granules were than sieved through a 1mm sieve and then dried for 1 week in the fan-assisted oven at a temperature of 45°C. The dried granules were again passed through a 1mm sieve. The Carr's index was determined by calculation from the bulk and tap densities, both of which were obtained in a 250ml measuring cylinder and the latter undergoing 2400 taps on the mechanical tapping device. For the particle-size analysis, the sieve stack was vibrated for 30 minutes. The granules were assayed by the HPLC method detailed in section 2.2. The assay values were used to calculate the assigned tablet weight for each formulation, based on a tablet strength of 200mg of ibuprofen with correction for the addition of extragranular excipients. For each formulation 1000g of the granules were combined in the blender with 5g of sodium lauryl sulphate, 5g of

magnesium stearate and 30g of sodium starch glycollate, for 5 minutes using a rotation speed of 15rpm. For each formulation, the tablet press was set-up and adjusted to ensure correct tabletting weight with an acceptable hardness. The entire mix was then tabletted without interruption. Each batch of tablets was assessed for crushing strength, friability (100 rotations at 25rpm) and disintegration (30 cycles min^{-1}) using 0.05M HCl at 37°C (British Pharmacopoeia 1998), using the appropriate instrument. The dissolution behaviour of the tablets in simulated stomach and simulated small intestine were assessed using the dissolution equipment described in section 4.7.2.2, according the method described in 4.7.2.3, and with 0.05M HCl and USP buffer pH 6.8 used as the dissolution media, respectively.

The pH of the dissolution fluid was measured post-experiment. The average tablet weights were determined using 20 randomly selected tablets. The tablets were analysed for ibuprofen content according to the method detailed in 2.2 and the level of impurities assessed according to the method detailed in section 2.3. A moisture level assessment was performed on ground tablets, with a duration of 4 hours and an oven temperature of 45°C.

7.3.2 Results and discussion

The ibuprofen granules developed in section 7.2.2 were demonstrated to be suitable for tablet manufacture, during the initial tabletting assessment. Therefore, it was concluded that final tablet formulations could be based on the granule formula with the addition of some extragranular excipients, which would be beneficial to large scale tablet manufacturing. The ibuprofen tablet formulations were devised thus:

- tablet strength designated as 200mg ibuprofen *per* tablet
- intragranular dissolution-promoting excipients 800mg *per* tablet, with the compositions as detailed in the key for table 7.4, listed previously
- addition of 200mg *per* tablet compressibility aid microcrystalline cellulose
- granulation of above three ingredients using 10% (w/v) starch mucilage as the binding agent
- addition of the lubricant magnesium stearate (0.5%w/w) to dried granules
- addition of the wetting agent sodium lauryl sulphate (0.5%w/w) to dried granules
- addition of disintegrant sodium starch glycollate (3%w/w) to dried granules

with the level of dissolution-promoting excipients specified to ensure adequate neutralising capacity of the tablet.

Physicochemical analysis was performed In order to characterise the tablets and also to determine their suitability as a commercial product. Firstly, for any pharmaceutical product to be acceptable for commercial use it must comply with the relevant pharmacopoeia specification. It can be observed from table 7.5 that all five formulations would pass the USP and BP specifications for assay, impurities, dosage uniformity and disintegration time. For friability, all formulations may be considered as marginal failures. Friability is used as a measure of the tablet's ability to withstand both shock and abrasion without crumbling during the processes of manufacturing, packaging and shipping, and consumer use. Tablets that tend to powder, chip and fragment when handled lack elegance and, hence, consumer acceptance. These tablets can also create excessive dust and dirt in processing areas, and can add to a tablet's weight variation Gordon *et al.* (1990). One method to reduce the friability would be to increase the tablet's crushing strength, by increasing compression pressure, measured through the crushing strength test. The formulations could be further refined to ensure an appropriate balance between a minimally acceptable tablet crushing strength to produce an adequate friability value and a maximally accepted crushing strength to achieve adequate dissolution. However, the appearance of all formulations was satisfactory, with all exhibiting a smooth edged surface, free from cracks or chips, and a white to off-white colouration.

The use of a wet granulation method introduces water into the granules. A drying step is therefore necessary in order to reduce the moisture content to an acceptable level. The USP has a moisture limit of less than 5%, however the exact acceptable moisture level is dependent on the drug and formulation under investigation, *e.g.* water may act as a vehicle for chemical degradation and must be minimised for drugs readily undergoing hydrolysis; very dry granulations may produce very friable tablets; overdried granules may lose their cohesiveness leading to soft tablets with a tendency to cap; underdried granules may adhere to punches and stick to the die when they are compressed and if the drug forms an hydrate the water may be present in the bound form as opposed to free unbound water Gordon *et al.* (1990) and Burlinson (1968). The loss-on-drying values, which are used as an indicator of the

tablet moisture content indicate a trend, *i.e.* a measured increase with increasing concentration of tri-sodium phosphate in the granules. It is likely that the ability of tri-sodium phosphate to form a stable hydrate is responsible for this trend. It was noted that the tray-dried oven method is inefficient when compared to the more commonly used fluid-bed dryer method. The influence of the high moisture content in tri-sodium phosphate containing formulations, in terms of formulation stability, is considered in section 7.4 and would be one of the factors influencing the selection of the optimum formulation. It is noted however, that the high level of moisture in some formulations did not impede the tabletting process.

In terms of dissolution, a comparison between the pharmacopoeia specification and the results was not possible as different methodologies were employed. It can be observed that commercial products containing ibuprofen free acid do not dissolve in the stomach, referencing the solubility/pH profile in illustrated in figure 3.2 and the dissolution profile of ibuprofen tablets illustrated in figure 7.5. This is the reason that the pharmacopoeia specification is performed at pH 7.4, *i.e.* simulating intestinal pH conditions. To demonstrate the differences between the developed formulations and commercial products, in terms of dissolution, it was necessary to compare the prepared formulations with commercially available ibuprofen free acid and ibuprofen lysinate tablet formulations, in both the simulated stomach and intestine dissolution models. Drug dissolution in the stomach is strikingly increased for all developed formulations compared to both commercial formulations. It can be observed in figure 7.5 that the commercial product containing ibuprofen free acid (Hedex®) dissolved until saturation was reached when approximately 1% of the drug was dissolved, corresponding to 0.02mg ml^{-1} ibuprofen. For the ibuprofen lysinate-containing product (Nurofen Advance®) the amount of drug dissolved varies between 4-11% of the dose. For the developed formulations, it can be observed in figures 7.6-7.10 that all formulations undergo >85% dissolution in 30 minutes, except formulation 4 (68% in 30 minutes). The enormous differences in drug dissolution rate and extent are quantified as F_1 fit-factors in table 7.5. To determine whether the novel formulations would dissolve satisfactorily in the intestine, the dissolution characteristics of formulation 5, the median batch (and fastest dissolving), were compared to the two commercial formulations in the simulated intestine model. The dissolution profiles are illustrated in figure 7.4. The dissolution rate appears to be slower, but after 30

minutes the amount of drug dissolved exceeds 80% and is more than the ibuprofen free acid formulation. The impact of the substantially increased dissolution rate of the novel formulations in the simulated stomach and the similar dissolution rate in simulated intestine, compared to the two commercial formulations will be modelled in chapter 8. The post-experimental pH of the dissolution media using the simulated stomach model is listed in table 7.6. A trend exists whereby the solution pH increases from 6.8 to 9.4 as the sodium carbonate content of the dissolution-promoting excipient mixture is increased. From the F_1 fit-factors, 7219 for formulation 1 (100% sodium carbonate) and 5470 for formulation 2 (100% tri-sodium phosphate) it is observed that the dissolution profiles are similar. This can be explained by the fact that both these excipients produce solutions with similar pH values, sodium carbonate solution pH=11.6 and tri-sodium phosphate solution pH≈11-12., with reference to table 4.1. It is therefore likely that the dissolving excipients produce similar pH changes in the drug micro-environment.

It can be concluded that all formulations exhibited rapid and similar dissolution properties therefore, the optimisation of a formulation would be based on physicochemical characteristics and product stability. From the former's perspective, it is evident that formulations based on sodium carbonate as the dissolution enhancer would be preferable as the granules can be more easily dried and the friability is more satisfactory. More importantly, the fact that formulations dominated by this excipient exhibited higher post-experimental solution pHs in the stomach model allows the potential for reduction in the quantity of excipient used and hence a reduction in the final tablet weight. It is noted that alkaline solutions can cause gastric irritation and damage (Sauers *et al.* 1994) so the formulation could be modified by reduction of the sodium carbonate concentration to a level to produce a solution of approximately pH7. Finally, if this adversely affected the dissolution rate of the formulation, a more reasonable approach may be to base the final formulation development on the formulation exhibiting a balance in the moisture content, friability, and post-experimental solution pH value properties, *i.e.* formulation 5.

Formulation composition key for table 7.5		
Formulation identity	**Composition* (decimal fraction)**	
	sodium carbonate	tri-sodium phosphate
1	1.00	0.00
2	0.00	1.00
3	0.25	0.75
4	0.75	0.25
5	0.50	0.50

*Represents the composition of the excipient mixture, which was ratioed 4:1 with ibuprofen, on a weight basis.

Table 7.5
Physical and chemical characterisation of ibuprofen tablet formulations

Specification	Limits	Formulation 1	Formulation 2	Formulation 3	Formulation 4	Formulation 5
Assay (%)	95-105%[1] 90-110%[2]	99.0 (198±2.0mg)	97.6 (195.2±2.0mg)	96.5 (193.0±1.1mg)	101 (202.1±2.5mg)	101 (207.7±3.0mg)
Dissolution F_1 fit-factor	NLT 70% in 30 minutes[3]	7219	5470	6631	5113	7052
Post-dissolution media pH	N/A[4]	9.4	6.8	7.3	9.3	7.8
Impurities (%)	individual<0.3%[1] total<0.7%[1]	<0.1 <0.1	<0.1 <0.1	<0.1 <0.1	<0.1 <0.1	<0.1 <0.1
Dosage Uniformity (%)	range 85-115%[2] %RSD<6%[2]	92-109 4.7	98-102 1.9	98-103 1.1	99-101 0.6	99-102 0.8
Loss on drying 4hrs at 45°C (%)	water<5.0%[2]	1.4	12.0	15.7	2.3	7.1
Crushing strength (kpa)	N/A[4]	11.3	9.9	11.5	12.5	11.5
Friability (%)	<1%[2]	1.0	1.7	1.3	1.4	2.2
ATW (g)	N/A[4]	1.4209	1.498	1.559	1.468	1.475
Disintegration Time (min)	<15mins[2]	11.3	8.3	10.0	13.3	11.0

[1]USP (1995)
[2]BP (1998)
[3]USP (1995) method: Apparatus I, baskets@100rpm using pH7.2 dissolution medium
[4]Non-Pharmacopoeia test

Figure 7.4
Illustrating the dissolution of two commercial and one experimental ibuprofen tablet formulations in simulated intestine fluid (USP buffer 6.8) Results are the mean of three replicates±SD

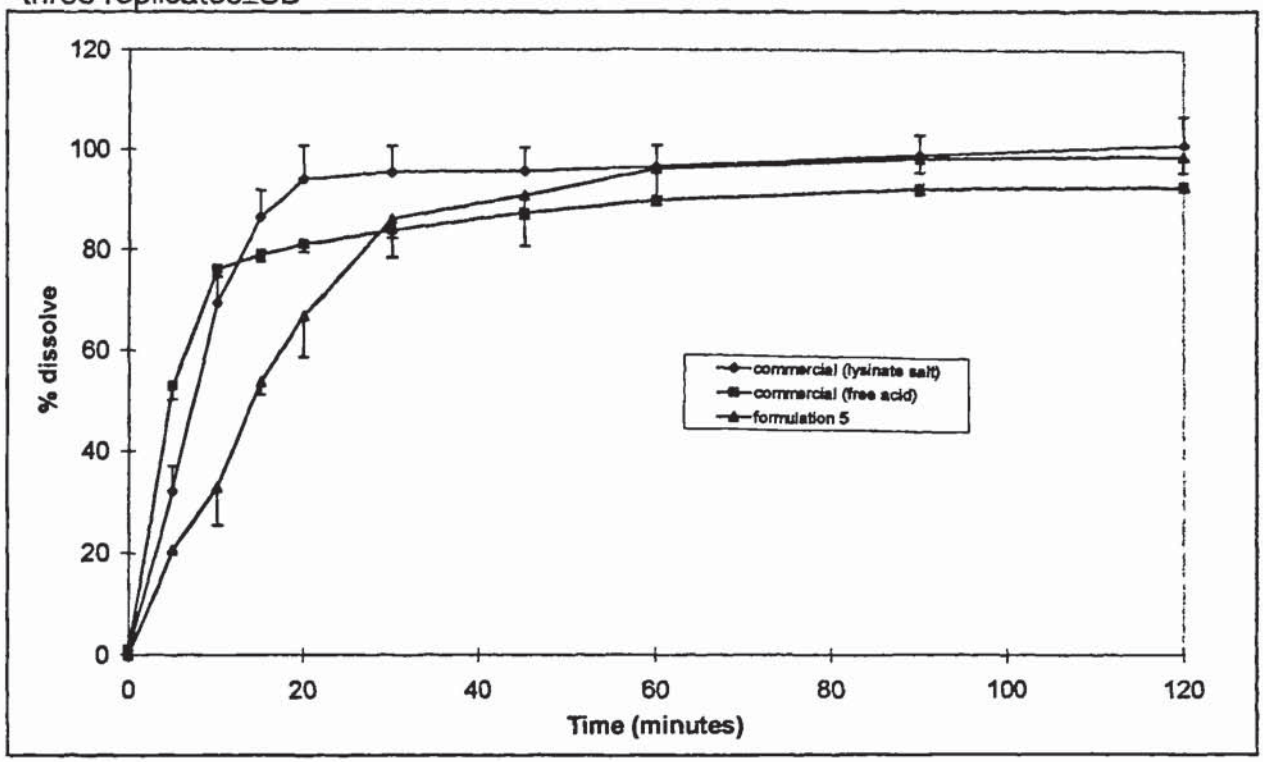

Figure 7.5
Illustrating the dissolution of two commercial ibuprofen tablet formulations in simulated stomach fluid (0.05M HCl) Results are the mean of three replicates±SD

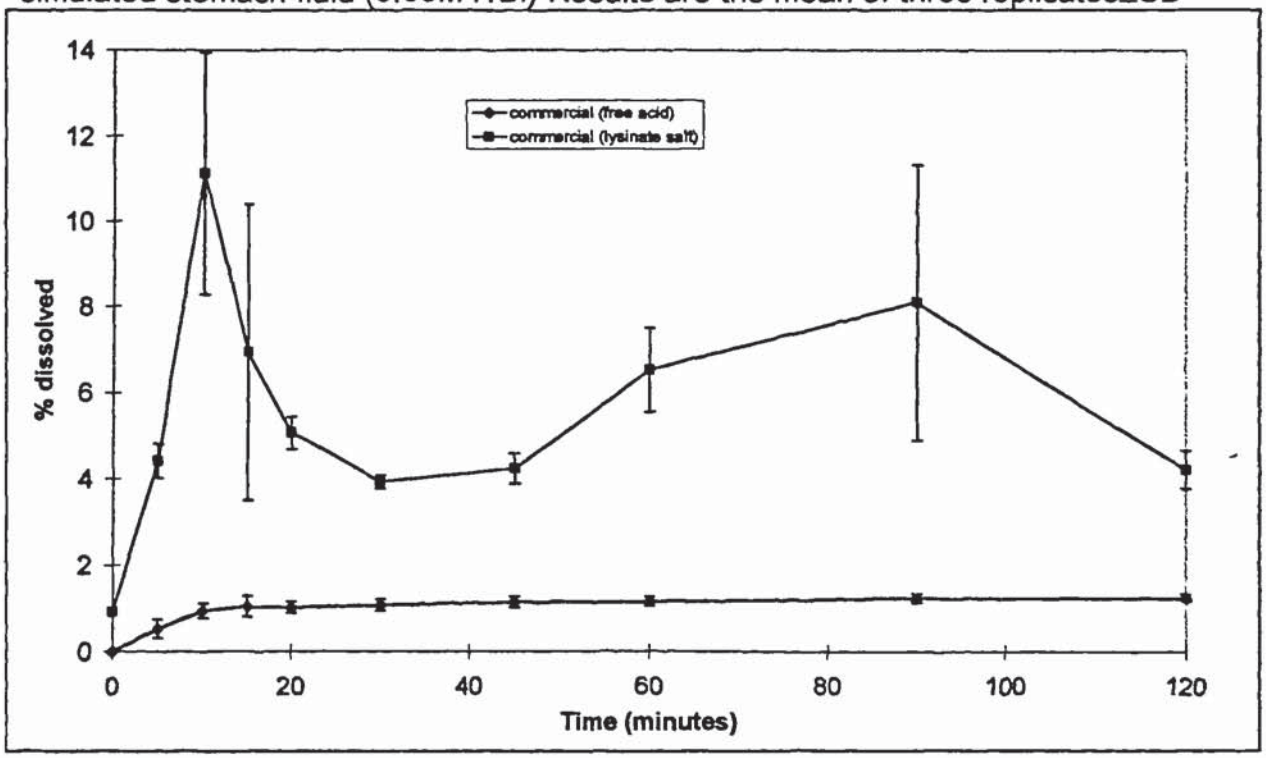

Figure 7.6
Illustrating the dissolution of formulation 1 and two commercial ibuprofen tablet formulations in simulated stomach fluid (0.05M HCl) Results are the mean of three replicates±SD

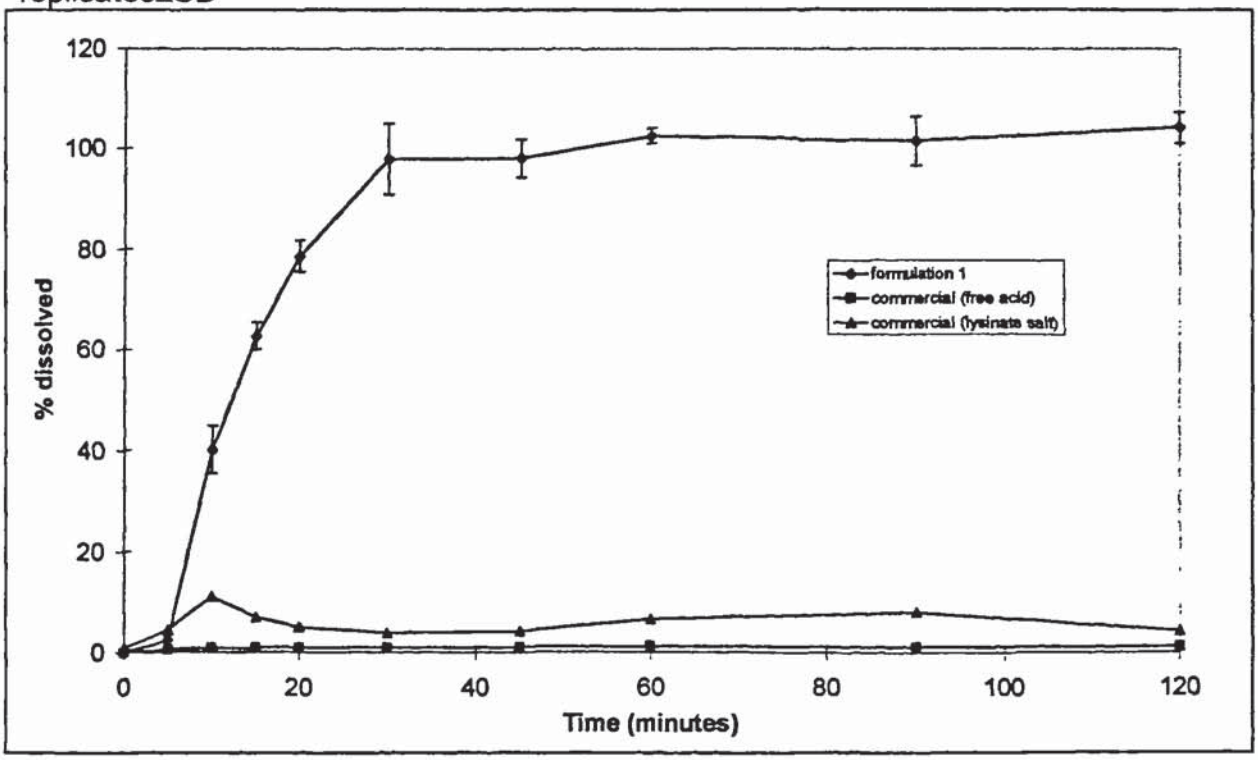

Figure 7.7
Illustrating the dissolution of formulation 2 and two commercial ibuprofen tablet formulations in simulated stomach fluid (0.05M HCl) Results are the mean of three replicates±SD

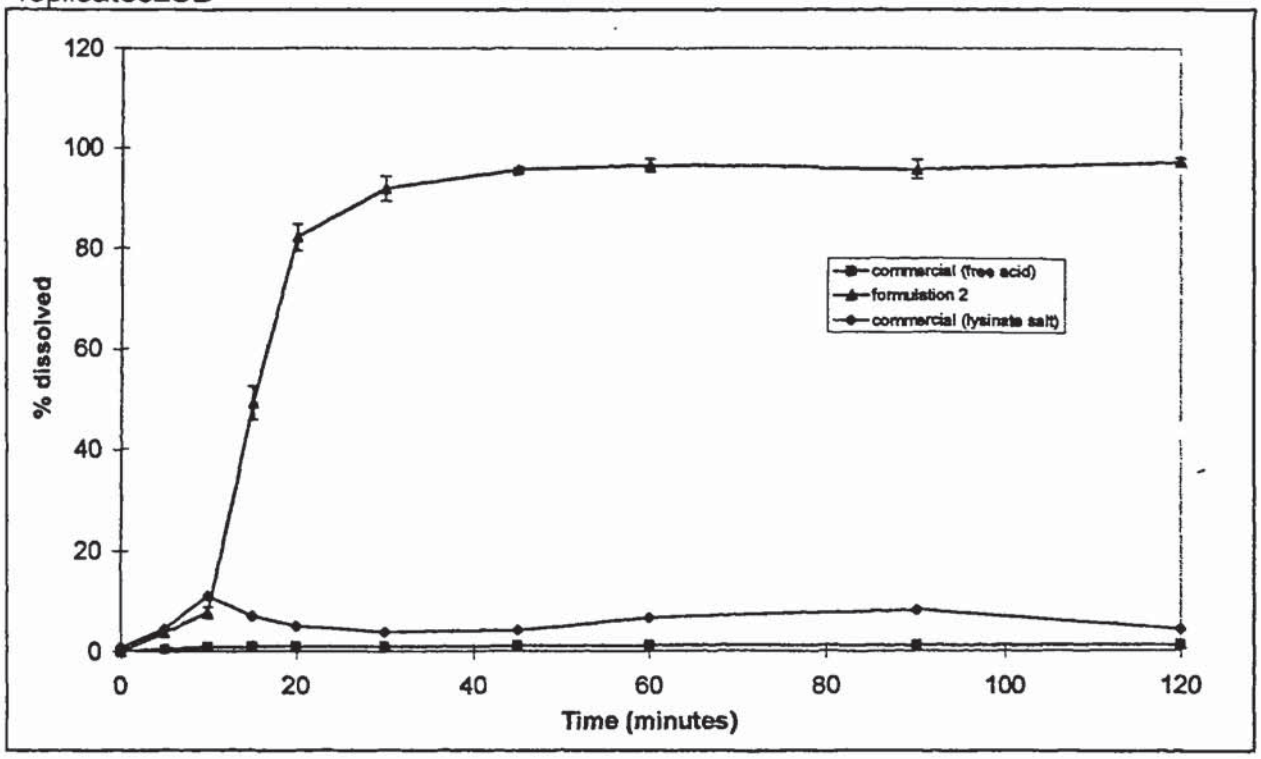

Figure 7.8
Illustrating the dissolution of formulation 3 and two commercial ibuprofen tablet formulations in simulated stomach fluid (0.05M HCl) Results are the mean of three replicates±SD

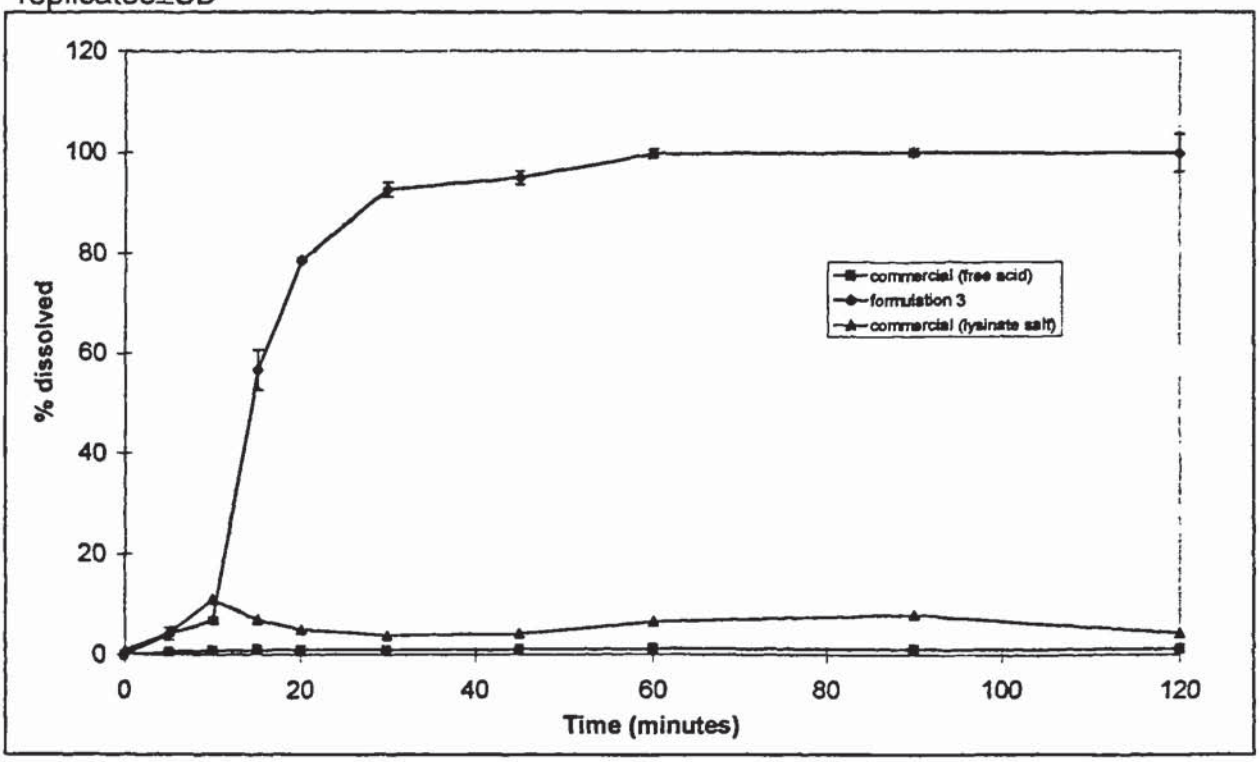

Figure 7.9
Illustrating the dissolution of formulation 4 and two commercial ibuprofen tablet formulations in simulated stomach fluid (0.05M HCl) Results are the mean of three replicates±SD

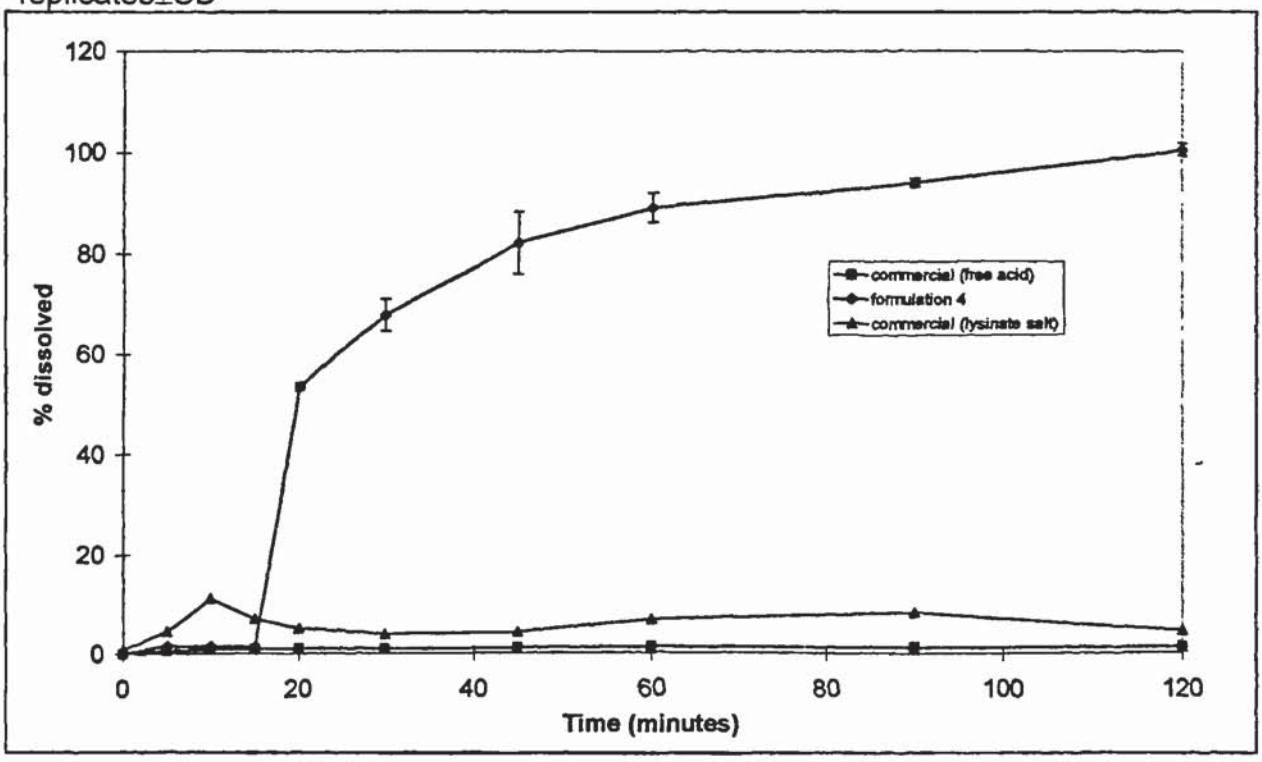

Figure 7.10
Illustrating the dissolution of formulation 5 and two commercial ibuprofen tablet formulations in simulated stomach fluid (0.05M HCl) Results are the mean of three replicates±SD

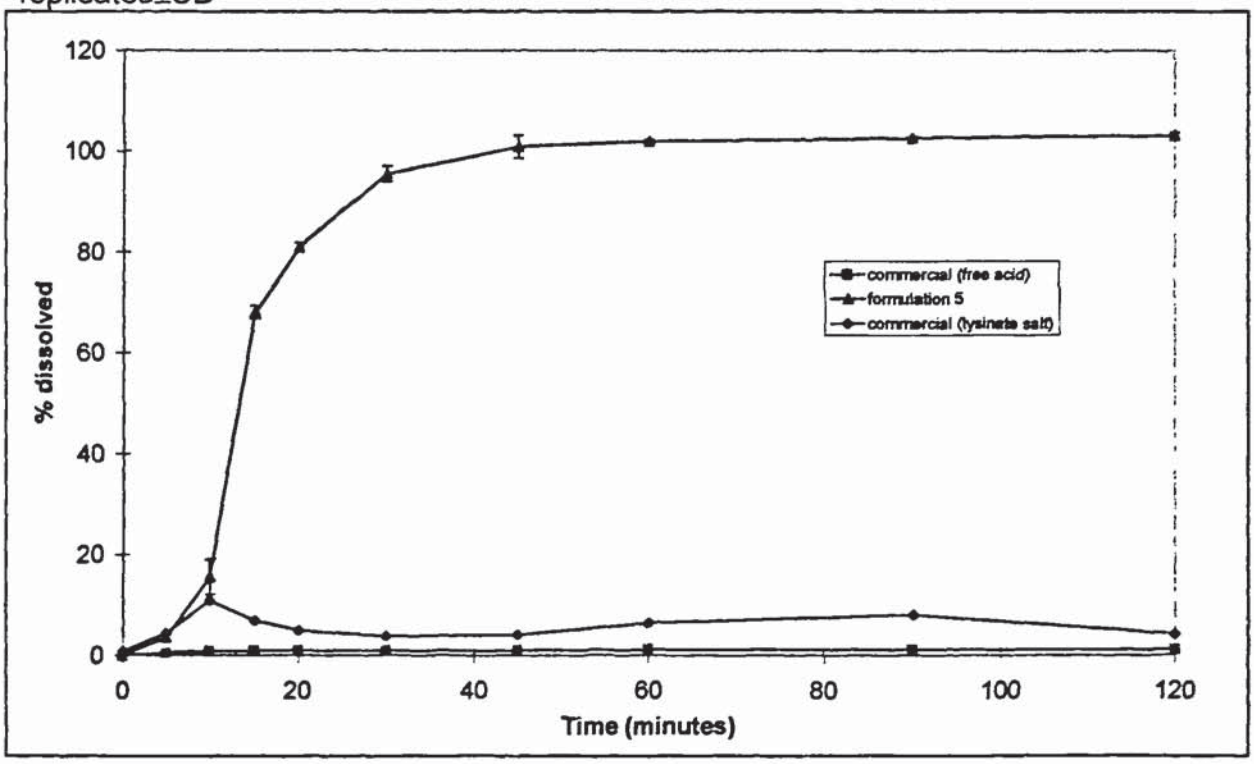

7.4 Novel ibuprofen tablet formulation stability program

7.4.1 Experimental

7.4.1.1 Materials

Samples of the ibuprofen tablets produced during the tablet development study, as recorded in section 7.3, were utilised for this study.

7.4.1.2 Equipment

The stability suite located at Aston Molecules (Birmingham, U.K.) was used for the long-term storage of the tablets. A Schleuniger-6D crushing strength instrument was used to measure tablet crushing strength. A Gallenkamp Hotbox fan-assisted oven was used to determine moisture content.

7.4.1.3 Method

A random sample of 500 tablets of each of the novel ibuprofen formulations (1-5) was obtained. The tablets were transferred to a 500ml amber glass container, with a screw cap, for storage. Samples of each formulation were stored in ovens at 25°C/60%RH or 40°C/75%RH for 12 and 6 months, respectively. At set time-points, 0,3,6,9, and 12 months for the ambient conditions and 0,2,4 and 6 months for the accelerated conditions, samples of each formulation were obtained for analysis. Each tablet formulation/time-point was analysed for assay and impurities using the HPLC methods detailed in sections 2.2 and 2.3. Dissolution testing (n=3) was performed using the simulated stomach method detailed in section 4.7.2.3 with equipment detailed in section 4.7.2.2, with the post-experimental pH of the medium also measured. The average tablet weights were determined using 20 randomly selected tablets. A moisture level assessment was performed on ground tablets, with a duration of 4 hours and an oven temperature of 45°C. Tablet crushing strength was measured using the crushing strength instrument.

7.4.2 Results and discussion

Stability is one of the most important factors to consider in evaluating tablet products. Stability is important not only from the standpoint of aesthetics and customer acceptance, *e.g.* colour changes and fading, but also in maintaining uniform drug strength, identity, quality and purity (Lierberman *et al.*1990). It is recognised that physical as well as chemical characteristics have stability profiles and that physical properties may influence a product's *in vivo* release characteristics. In establishing expiration dates for solid dosage forms, it is essential that the physical characteristics and the dissolution properties are given equal consideration with the chemical characteristics, since all of these properties may change with product age and exposure. Therefore, tests such as dissolution and crushing strength are routinely evaluated within the framework of a stability program for a solid dosage form.

When undertaking a tablet formulation development program, it is recognised that dosage form design is complex. This is due to the fact that tablets usually consist of many ingredients, which may interact to affect physical and chemical properties, both

initially and after extended storage. The uniqueness of each individual formulation means that the application of general principles are useful only upto a certain point. It is for these reasons that experimental design and optimisation techniques are utilised to develop commercially acceptable tablet formulations. The results from a stability program can be utilised in two ways. Firstly, the effect of long-term storage on the dosage form can be measured to determine a shelf-life for the product, based on certain specifications meeting regulatory requirements. For example, if the active ingredient degrades, an end-point can be calculated where the product falls below the assay specification and so a shelf-life can be determined. If several formulations are produced, as in this study, the most suitable formulation can be selected, based on the range of parameters investigated. The second method of utilising the stability results would be use a mechanistic perspective. Here, the interaction between certain properties, *e.g.* effect of a tablet's increased crushing strength on the dissolution rate could be elucidated. A more in-depth approach would also try to evaluate the mechanisms behind a change in one of the properties. With reference to the overall project scope and vast quantity of data generated during the stability study, the data analysis was restricted to comparison of the formulation composition with any change in measured properties. Some analysis was also conducted into the relationships between certain properties.

The stability parameters and sampling timepoints were chosen in accordance with current regulatory guidelines (FDA (CDER/CBER) 1998). Although several tablet characteristics are important for the stability of the product, the most important may be considered to be the chemical stability of the active drug. Two parameters are measured to determine the effect of storage on this property, the assay of the active drug and the determination of degradation impurities. All chemical and physical characterisation collected during the storage of the formulations is summarised in tables 7.6-7.10. With reference to these tables no measurable degradation impurities were observed in any of the formulations, under both storage conditions for the whole storage period. To aid the elucidation of any relationships and for visualisation of trends in the data, each parameter was plotted separately, for each stability condition, to include all formulations. These data are illustrated in figures 7.11-7.22. With reference to figures 7.11-7.12 it was observed that all formulations had assay values

>90% (BP specification) for the duration of the study and all formulations except formulation 1 (40°C/75%RH) and formulation 4 (25°C/60%RH) had assay values >95% (USP specification). In terms of dissolution, all formulations were found to deteriorate as measured by the F_1 fit-factors illustrated in figures 7.13-7.14, except formulation 4 (40°C/75%RH) where the dissolution improved due to a decrease in disintegration time. Overall, no trend was apparent relating to the promoting excipient composition. The decrease in dissolution rate may be attributed to a decrease in disintegration rate caused by an observed hardening of the tablets (Armstrong and James 1996). It can be summarised from tables 7.6-7.10 that the % dissolution at 30 minutes, in simulated stomach media, was >70% in all cases except for formulation 3 (25°C/60%RH) where the % dissolution was as low as 60%. However, contrasting this with the commercial formulations where for the free acid the % dissolution was previously found to be approximately 1% and the lysinate salt was found to between 4-11%, it can be concluded that all formulations have significantly improved dissolution compared to the commercial formulations even after prolonged storage; under accelerated and ambient conditions. It was noted from figures 7.15-7.16 that the pH of the dissolution media measured post-experiment did not alter over time and the trend across the formulations was as observed in the formulation study. Considering ATW and loss on drying together, illustrated in figures 7.17-7.20, all formulations were observed to demonstrate an increase in tablet weight except formulation 1. Formulation 1 tablets, containing 100% sodium carbonate as the dissolution-promoting excipient and having the least free moisture, were found to decrease in weight over time under the ambient conditions and exhibit no change under accelerated conditions. The low loss on drying values showed no trend over time. For the other formulations, the increase in tablet weight appeared to correspond to a decrease in loss on drying values, under ambient conditions. This apparent paradox may be explained by the fact that the loss on drying only measures the free moisture and not the bound water, for instance in the hydrated form of tri-sodium phosphate. It is possible that the tablets absorbed moisture, increasing the tablet weight, but that the moisture was in the bound form, perhaps hydrating the tri-sodium phosphate. It was also noted that moisture content generally increased under accelerated conditions. Reviewing the crushing strength, it can be observed that under ambient conditions after an initial sharp increase in all cases. However, the

trend across the formulations shows a change from a reduction with time through to a levelling and finally a steady increase in the tablet crushing strength, where the promoting excipient used varied in composition from 100% sodium carbonate to 100% tri-sodium phosphate. Under accelerated conditions, all formulations showed a steady increase in tablet crushing strength. Finally, no change in tablet appearance was noted, with all exhibiting a smooth edged surface, free from cracks or chips, and a white to off-white colouration.

Based on the above analysis, it appears from a chemical perspective that all formulations were stable. In light of some very high residual moisture values these results are encouraging. However, changes were observed in some of the physical characteristics, most notably a decrease in drug dissolution and an increase in tablet crushing strength, the latter contributing to the former. It is noted that even the worst performing formulation exhibited a far superior dissolution profile compared to two commercial formulations. It can be concluded that all formulations withstood storage satisfactorily and that they would be considered equally in terms of a formulation development strategy, from a stability perspective.

Table 7.6
Summary of the effect of long-term storage on the physical and chemical characteristics of ibuprofen tablet formulation 1

Specification	Accelerated stability conditions 40°C/75%RH				Ambient stability conditions 25°C/60%RH			
	0 months	2 months	4 months	6 months	3 months	6 months	9 months	12 months
Assay (%)	100.0	99.3	96.3	93.4	93.7	94.6	94.0	96.2
Total impurities (%)	<0.1	<0.1	<0.1	<0.1	<0.1	<0.1	<0.1	<0.1
Individual impurities (%)	<0.1	<0.1	<0.1	<0.1	<0.1	<0.1	<0.1	<0.1
Dissolution F_1 fit-factor (%)	1.0	-5.8	-31.8	-21.4	-3.7	-15.0	-18.2	-25.0
Dissolution (%) @ 30 mins	98.0	91.5	79.2	92.4	90.9	85.4	87.2	83.2
Dissolution medium pH	9.4	9.6	9.2	9.1	9.6	9.5	9.6	9.6
Loss on drying (%)	1.4	2.1	1.3	1.0	0.3	0.5	1.6	0.8
ATW (%)	100.0	98.3	99.9	99.0	98.6	96.8	95.8	95.6
Crushing strength (%)	100.0	123.9	137.2	153.1	122.1	112.4	109.7	118.0

Table 7.7
Summary of the effect of long-term storage on the physical and chemical characteristics of ibuprofen tablet formulation 2

Specification	Accelerated stability conditions 40°C/75%RH				Ambient stability conditions 25°C/60%RH			
	0 months	2 months	4 months	6 months	3 months	6 months	9 months	12 months
Assay (%)	100.0	103.2	98.5	99.7	95.5	97.7	97.7	98.0
Total impurities (%)	<0.1	<0.1	<0.1	<0.1	<0.1	<0.1	<0.1	<0.1
Individual impurities (%)	<0.1	<0.1	<0.1	<0.1	<0.1	<0.1	<0.1	<0.1
Dissolution F_1 fit-factor (%)	1.0	13.4	-26.7	-11.2	-8.7	3	-12.0	-10.2
Dissolution (%) @ 30 mins	92.0	92.8	93.1	93.1	89.6	88.6	90.0	91.0
Dissolution medium pH	6.8	7.3	6.6	6.5	7.3	6.9	6.8	6.9
Loss on drying (%)	12.0	11.6	4.3	6.4	7.8	5.5	9.5	8.0
ATW (%)	100.0	100.5	101.1	101.8	100.2	100.3	100.7	100.6
Crushing strength (%)	100.0	132.3	155.6	172.7	109.1	131.3	137.4	140.2

Table 7.8
Summary of the effect of long-term storage on the physical and chemical characteristics of ibuprofen tablet formulation 3

Specification	Accelerated stability conditions 40°C/75%RH				Ambient stability conditions 25°C/60%RH			
	0 months	2 months	4 months	6 months	3 months	6 months	9 months	12 months
Assay (%)	100.0	105.0	102.2	101.4	94.7	98.9	100	99.8
Total impurities (%)	<0.1	<0.1	<0.1	<0.1	<0.1	<0.1	<0.1	<0.1
Individual impurities (%)	<0.1	<0.1	<0.1	<0.1	<0.1	<0.1	<0.1	<0.1
Dissolution F_1 fit-factor (%)	1	-0.4	-13.6	-17.1	-29.5	-56.2	-55.3	-50.1
Dissolution (%) @ 30 mins	92.6	89.3	73.8	80.9	74.0	63.2	60.1	62.3
Dissolution medium pH	7.3	7.8	6.9	7.5	7.8	7.2	7.3	7.3
Loss on drying (%)	15.7	13.6	5.2	7.3	7.9	5.8	10.4	8.6
ATW (%)	100.0	101.7	102.5	102.5	100.9	101.2	102.0	102.1
Crushing strength (%)	100.0	133.9	148.7	150.4	102.6	127.0	148.7	151.0

Table 7.9
Summary of the effect of long-term storage on the physical and chemical characteristics of ibuprofen tablet formulation 4

Specification	Accelerated stability conditions 40°C/75%RH				Ambient stability conditions 25°C/60%RH			
	0 months	2 months	4 months	6 months	3 months	6 months	9 months	12 months
Assay (%)	100.0	104.7	98.9	99.1	94.1	94.6	95.0	96.2
Total impurities (%)	<0.1	<0.1	<0.1	<0.1	<0.1	<0.1	<0.1	<0.1
Individual impurities (%)	<0.1	<0.1	<0.1	<0.1	<0.1	<0.1	<0.1	<0.1
Dissolution F_1 fit-factor (%)	1	4	20	45.2	-1.1	-23.1	-16.2	-25.2
Dissolution (%) @ 30 mins	88.7	62.6	71.0	87.6	86.1	82.1	87.5	77.2
Dissolution medium pH	9.3	9.6	9.6	9.1	9.6	9.1	9.5	9.6
Loss on drying (%)	2.3	3.1	1.9	2.7	1.9	1.2	3.1	2.8
ATW (%)	100.0	101.0	103.1	104.3	100.5	100.7	101.0	101.1
Crushing strength (%)	100.0	136.0	182.4	194.4	125.6	124.8	144.8	149.6

Table 7.10
Summary of the effect of long-term storage on the physical and chemical characteristics of ibuprofen tablet formulation 5

Specification	Accelerated stability conditions 40°C/75%RH				Ambient stability conditions 25°C/60%RH			
	0 months	2 months	4 months	6 months	3 months	6 months	9 months	12 months
Assay (%)	100.0	101.7	104.9	98.6	95.4	95.6	95.6	95.3
Total impurities (%)	<0.1	<0.1	<0.1	<0.1	<0.1	<0.1	<0.1	<0.1
Individual impurities (%)	<0.1	<0.1	<0.1	<0.1	<0.1	<0.1	<0.1	<0.1
Dissolution F_1 fit-factor (%)	1	-2.4	-31.9	12.5	-14.8	-22.6	-20.2	-24.3
Dissolution (%) @ 30 mins	95.5	91.7	77.1	95.3	79.8	86.0	88.2	84.3
Dissolution medium pH	7.8	7.8	7.8	7.7	7.8	7.8	7.8	7.7
Loss on drying (%)	7.1	6.3	2.8	3.8	3.9	3.4	5.4	5.2
ATW (%)	100.0	101.0	102.1	103.1	100.5	100.4	100.6	100.5
Crushing strength (%)	100.0	122.6	127.0	160.0	115.7	104.3	117.4	121.0

Figure 7.11
Illustrating the effect of long-term storage at 25°C/60%RH on the assay of each ibuprofen formulation. Data aligned such that 100⇒0% sodium carbonate from L-R

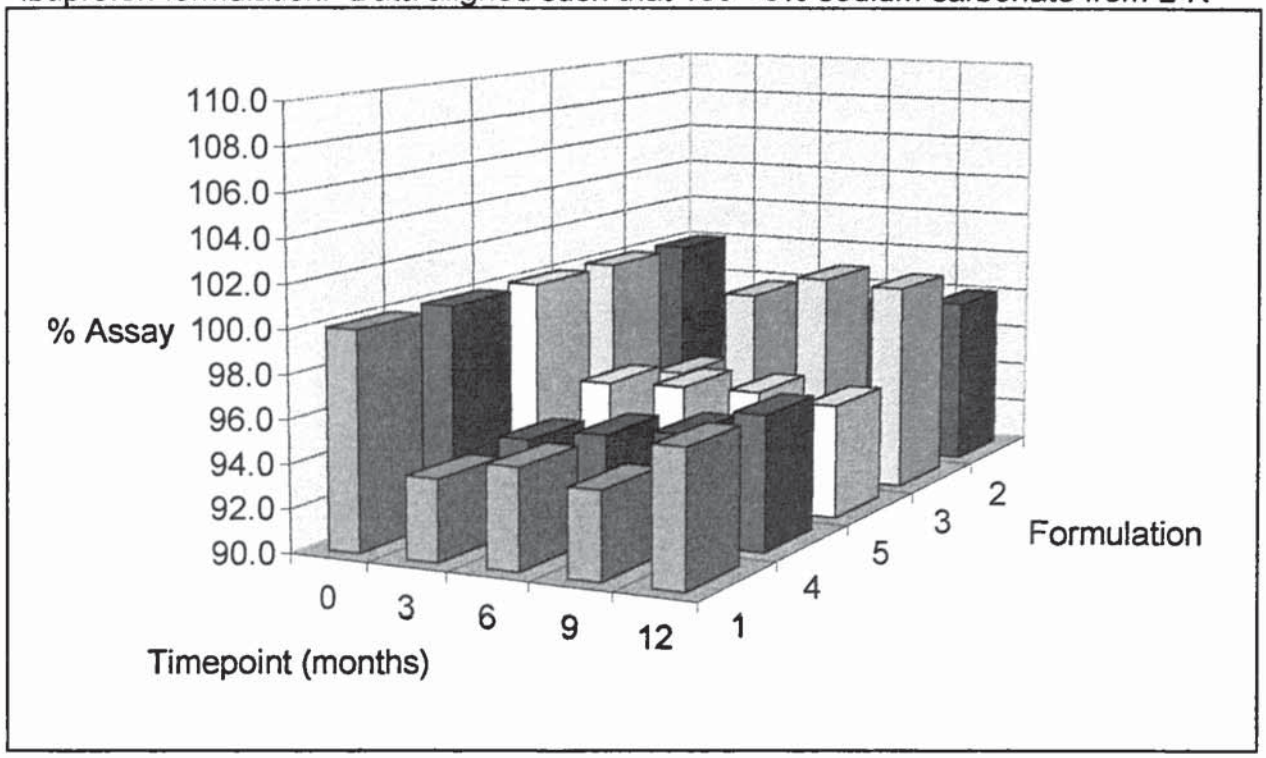

Figure 7.12
Illustrating the effect of long-term storage at 40°C/75%RH on the assay of each ibuprofen formulation. Data aligned such that 100⇒0% sodium carbonate from L-R

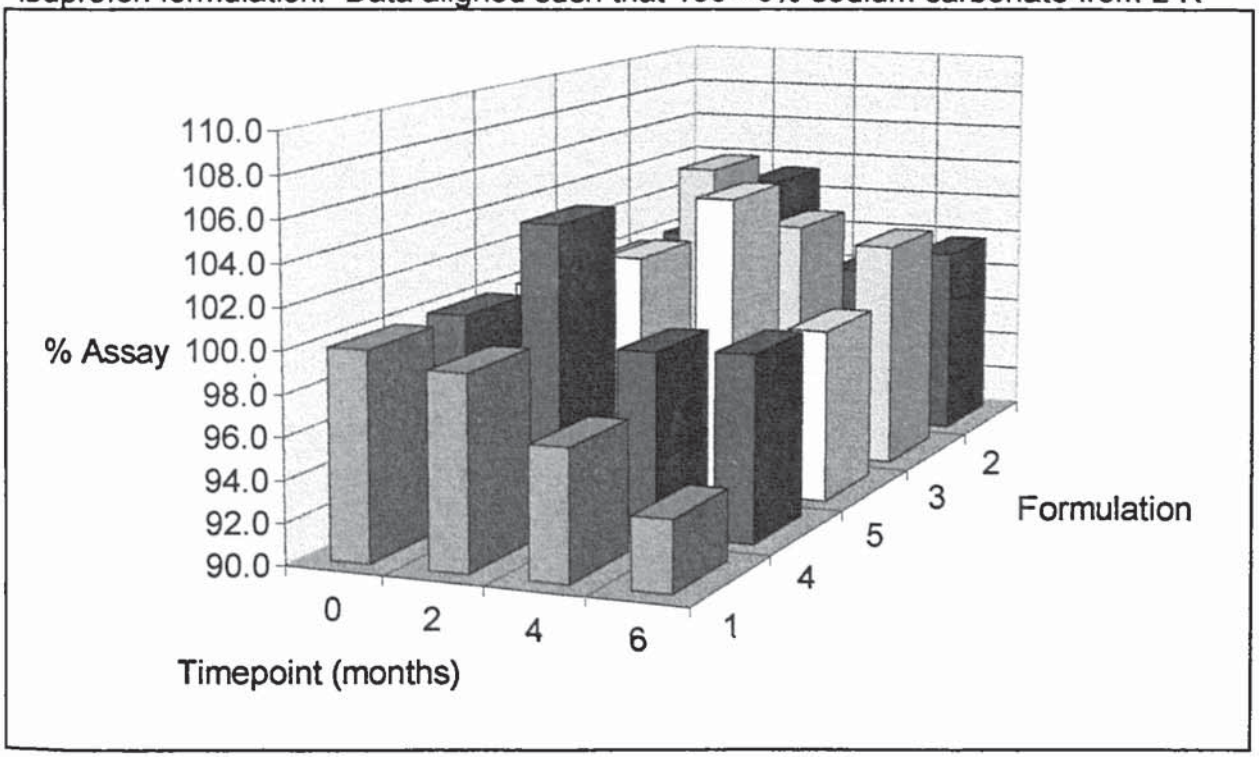

Figure 7.13
Illustrating the effect of long-term storage at 25°C/60%RH on the dissolution of each ibuprofen formulation. Data aligned such that 100→0% sodium carbonate from L-R

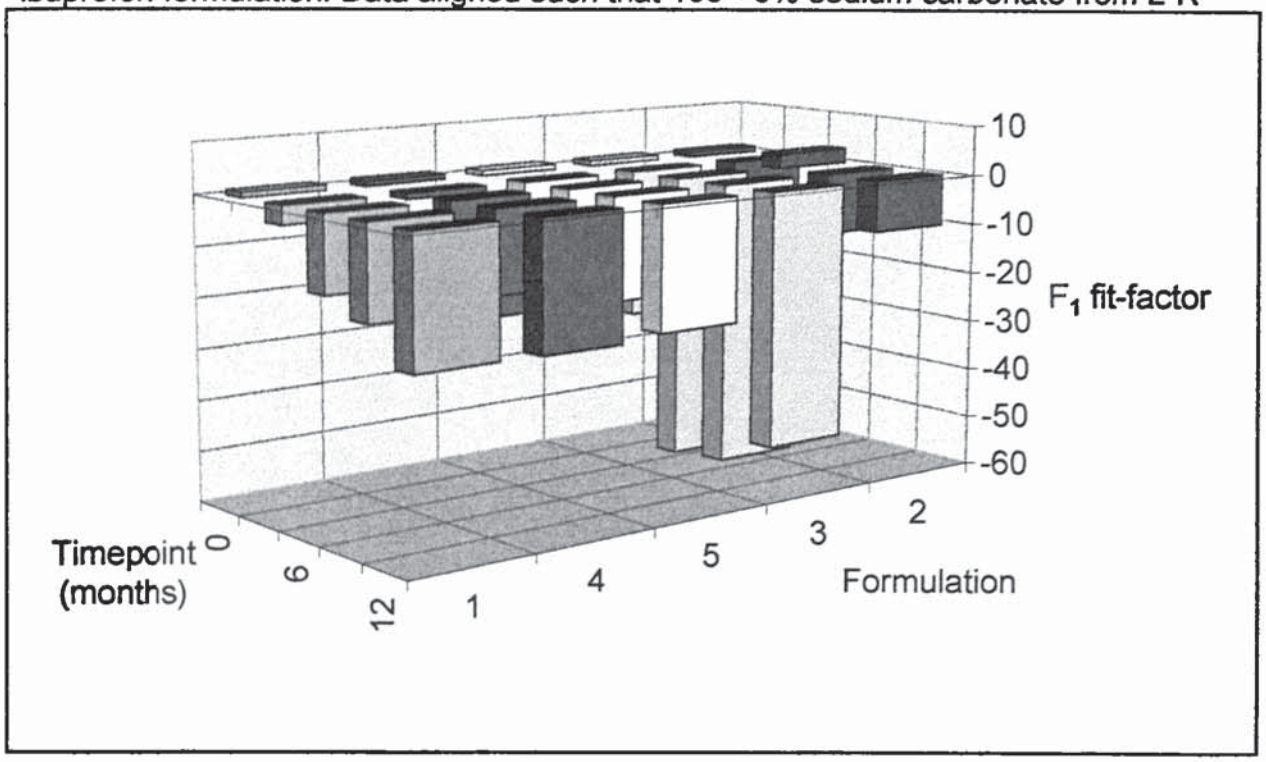

Figure 7.14
Illustrating the effect of long-term storage at 40°C/75%RH on the dissolution of each ibuprofen formulation. Data aligned such that 100→0% sodium carbonate from L-R

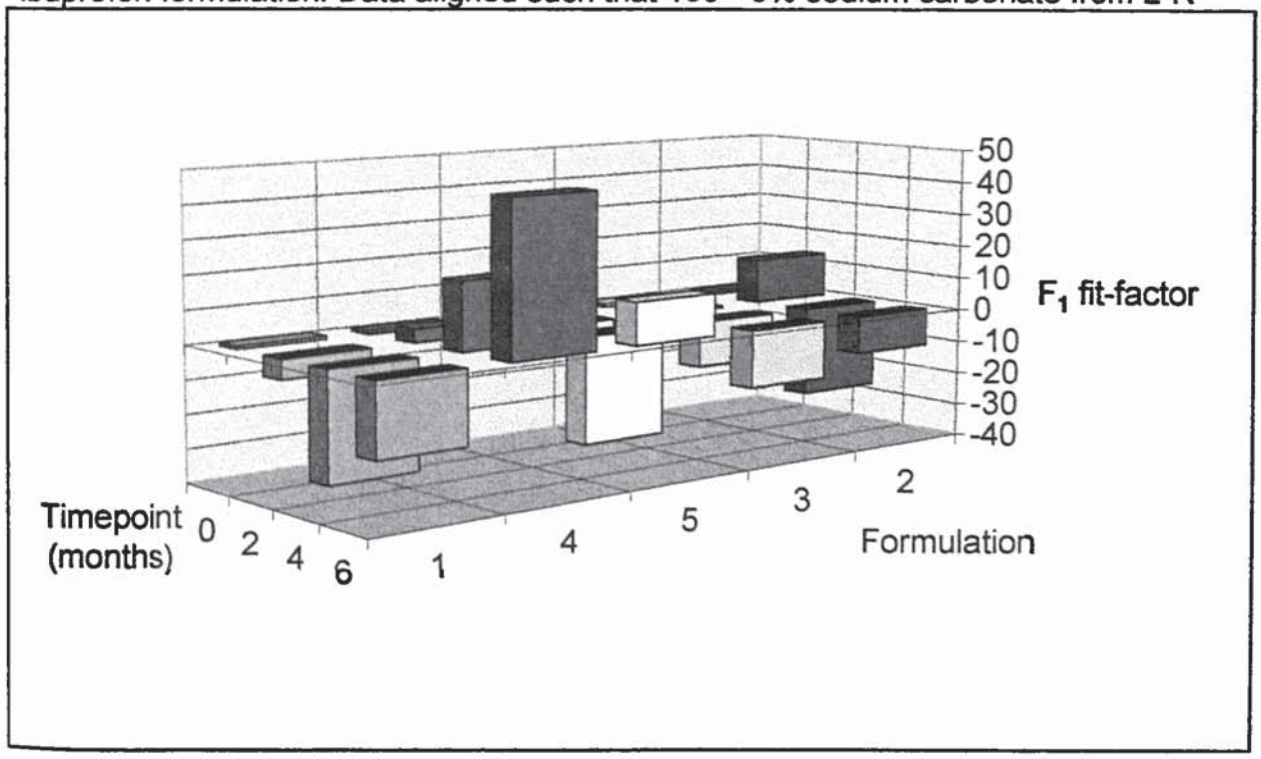

Figure 7.15
Illustrating the effect of long-term storage at 25°C/60%RH on diss^{n} pH for each ibuprofen formulation. Data aligned such that 100→0% sodium carbonate from R-L

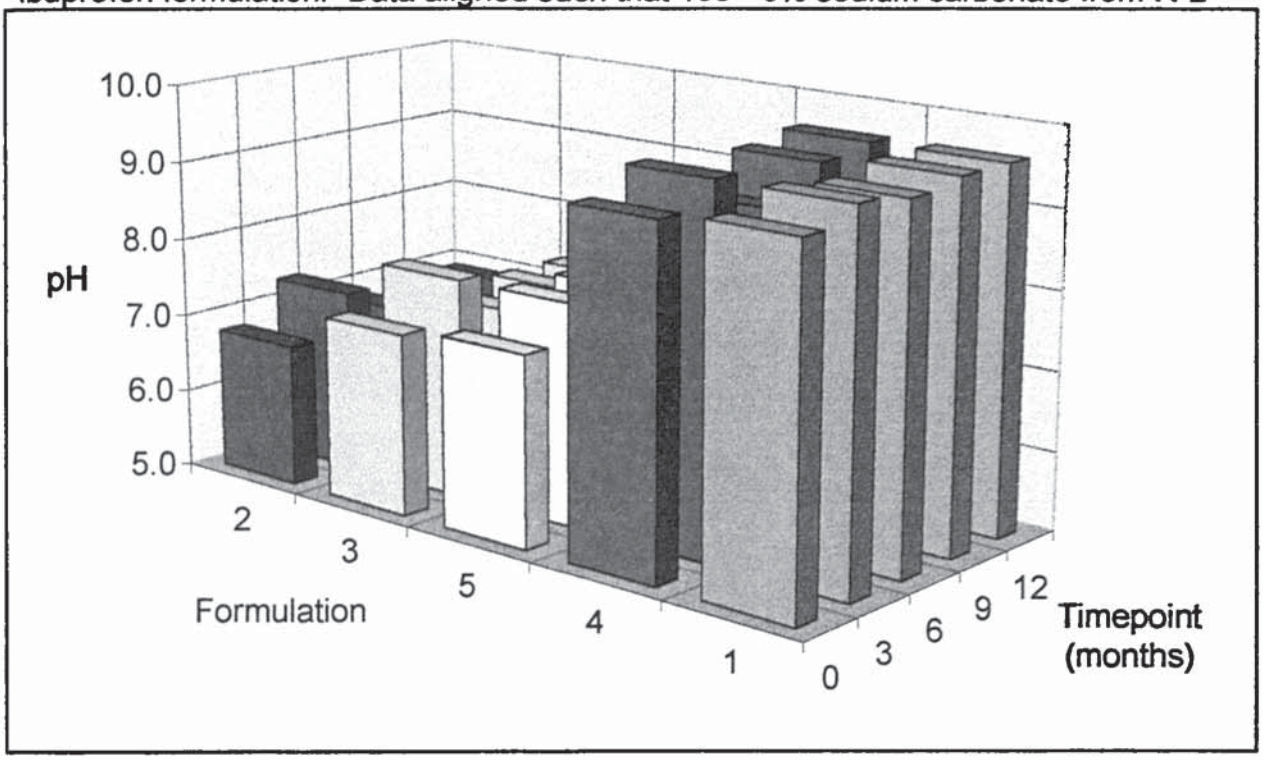

Figure 7.16
Illustrating the effect of long-term storage at 40°C/75%RH on diss^{n} pH for each ibuprofen formulation. Data aligned such that 100→0% sodium carbonate from R-L

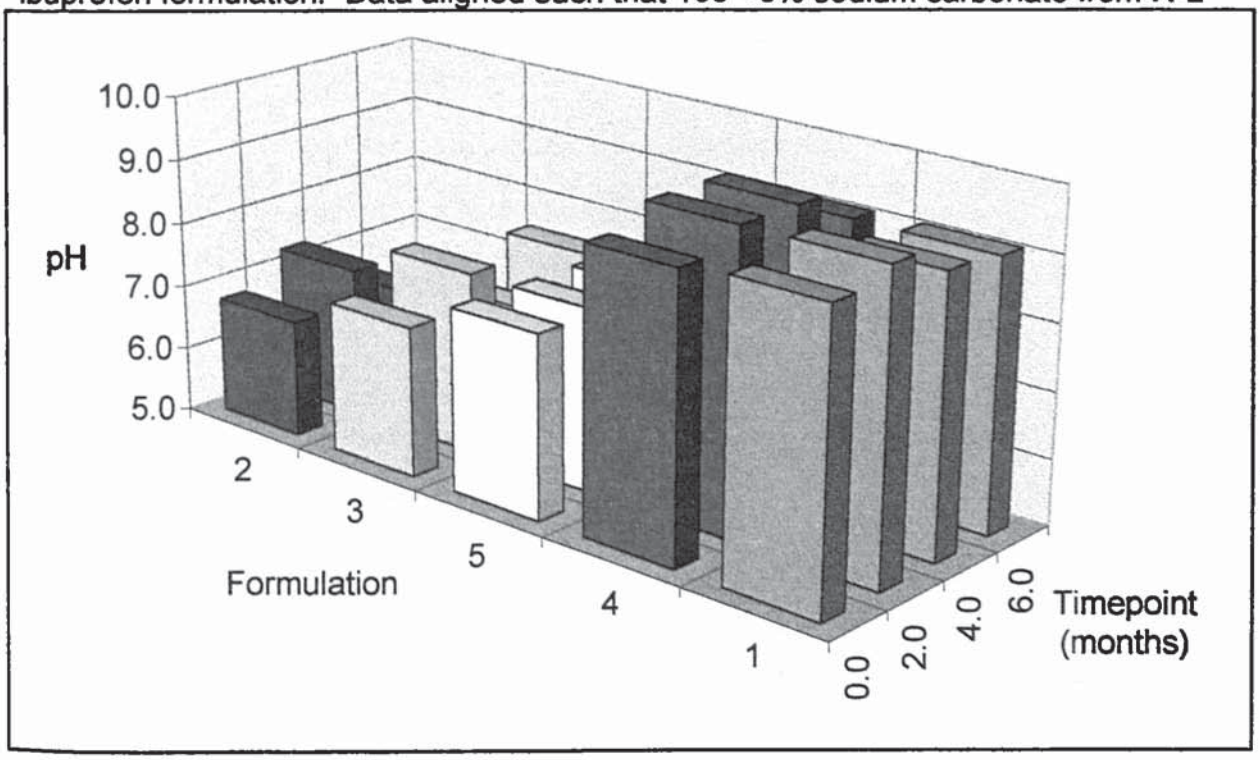

Figure 7.17
Illustrating the effect of long-term storage at 25°C/60%RH on the ATW of each ibuprofen formulation. Data aligned such that 100→0% sodium carbonate from L-R

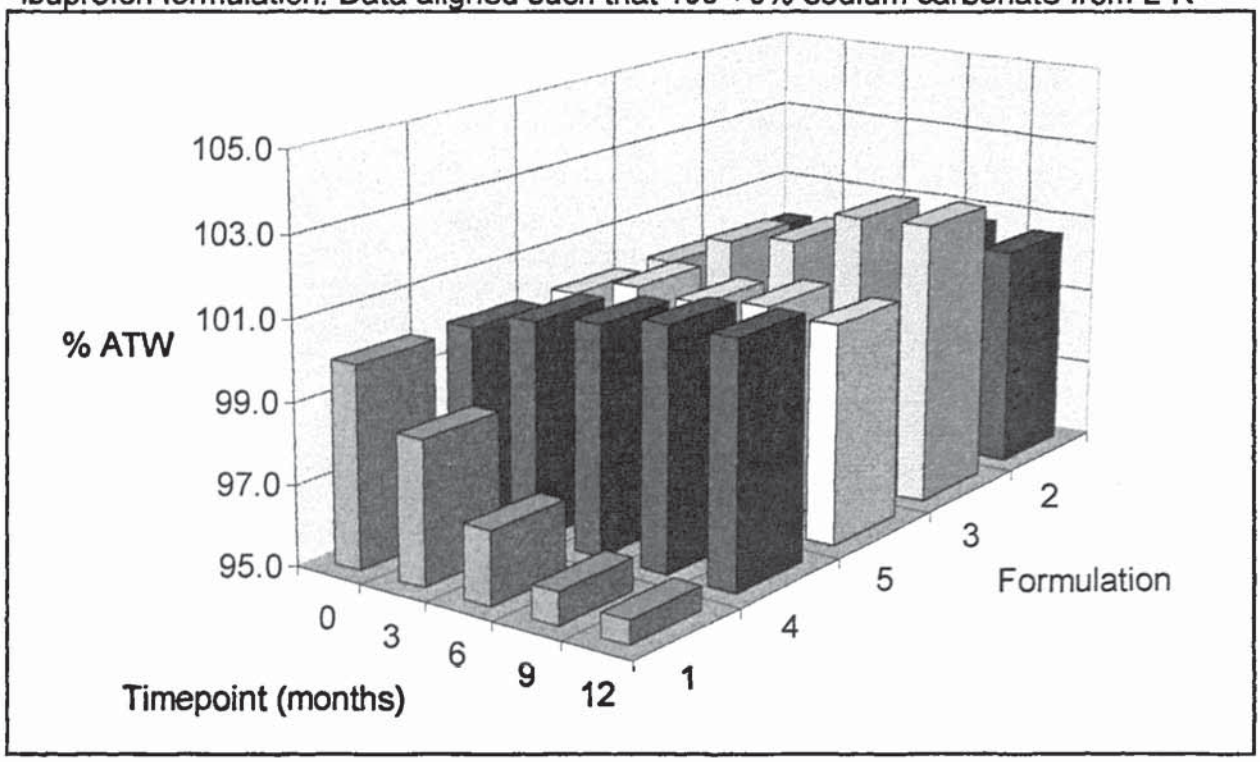

Figure 7.18
Illustrating the effect of long-term storage at 40°C/75%RH on the ATW of each ibuprofen formulation. Data aligned such that 100→0% sodium carbonate from L-R

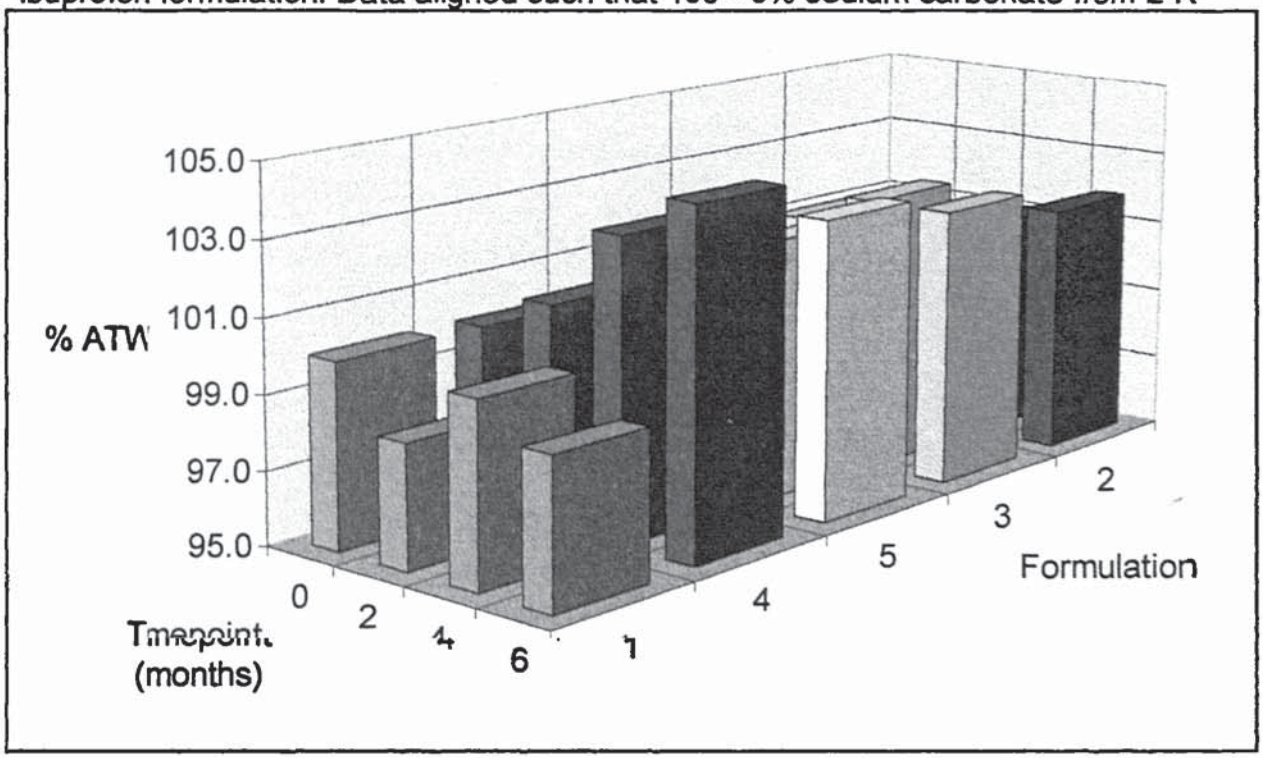

Figure 7.19
Illustrating the effect of long-term storage at 25°C/60%RH on the measured LOD for each ibuprofen form[n]. Data aligned such that 100→0% sodium carbonate from L-R

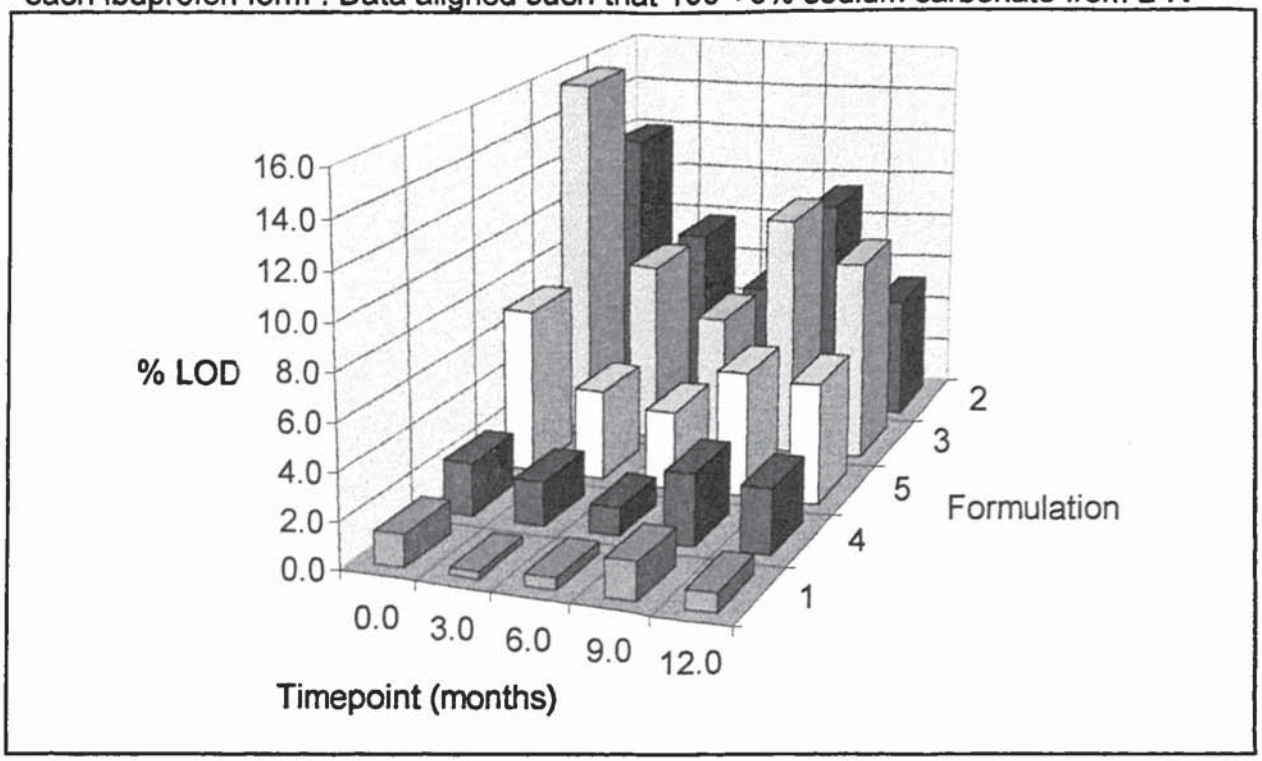

Figure 7.20
Illustrating the effect of long-term storage at 40°C/75%RH on the measured LOD for each ibuprofen form[n]. Data aligned such that 100→0% sodium carbonate from L-R

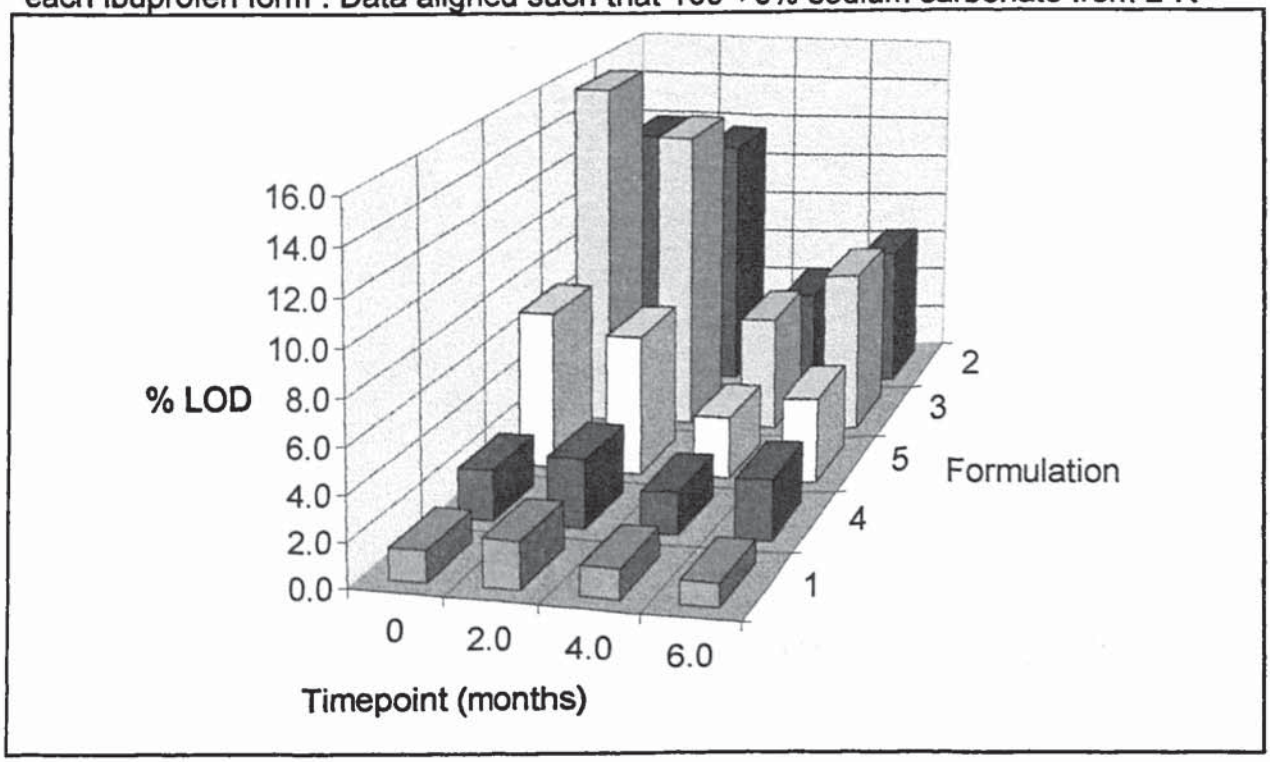

Figure 7.21
Illustrating the effect of long-term storage at 25°C/60%RH on the crushing strength for each ibuprofen form[n]. Data aligned such that 100→0% sodium carbonate from L-R

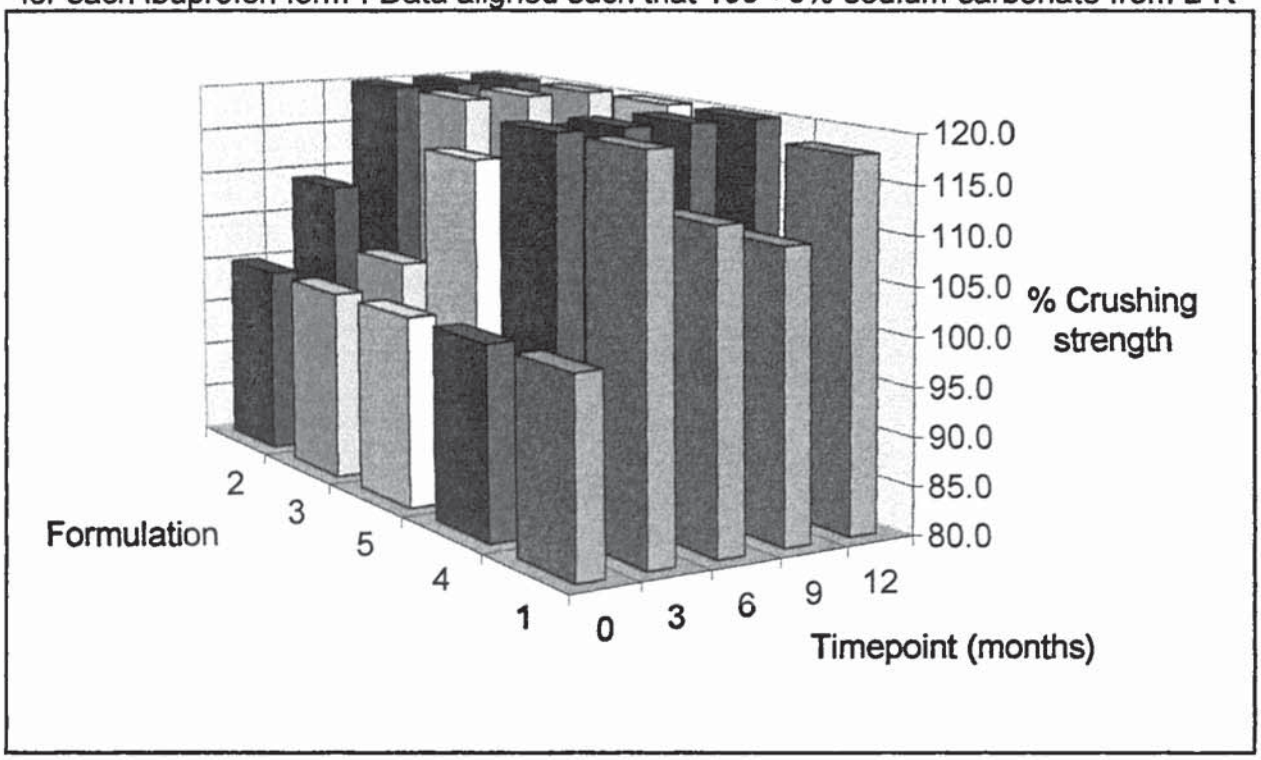

Figure 7.22
Illustrating the effect of long-term storage at 40°C/75%RH on the crushing strength for each ibuprofen form[n]. Data aligned such that 100→0% sodium carbonate from L-R

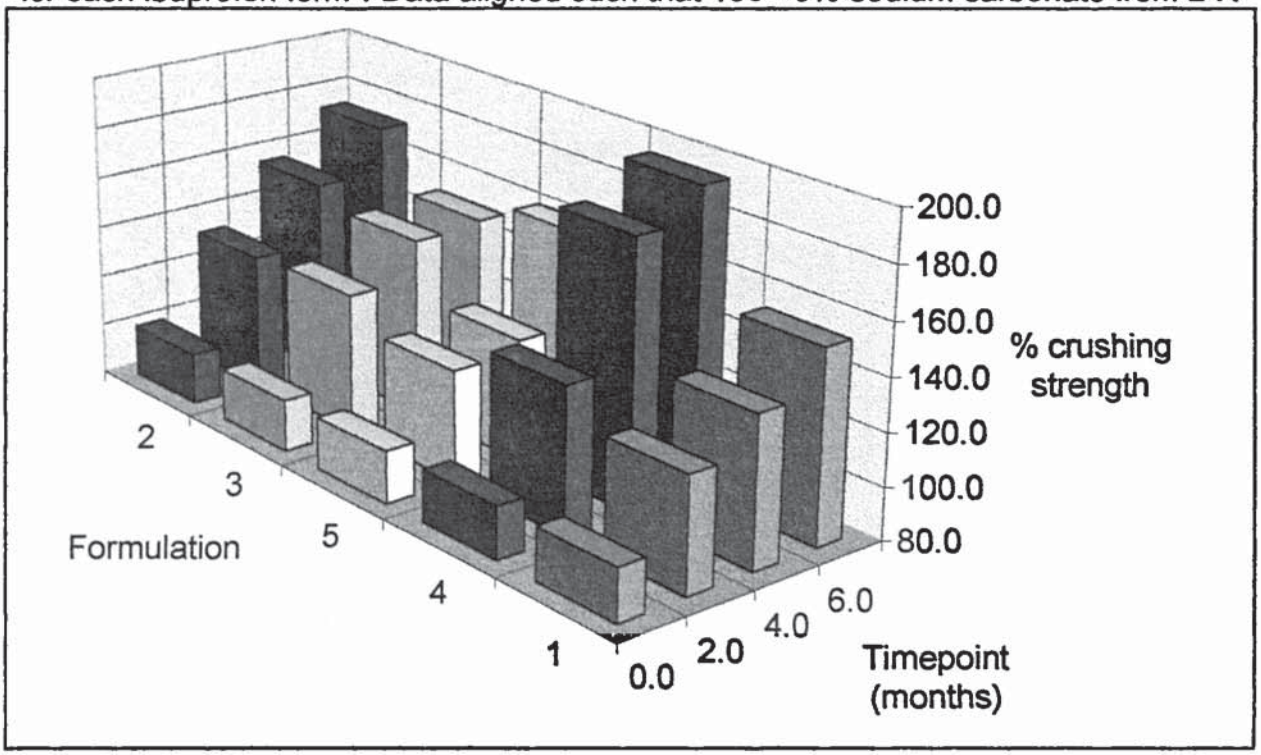

7.5 Summary

- The potential for improving the absorption rate of ibuprofen and paracetamol tablets, by inclusion of dissolution-promoting excipients into the tablet formulation, was recognised.
- It was observed that an opportunity existed to improve the dissolution of the SB Zapp prototype. This was based on the hypothesis that a combination of excipients including sodium bicarbonate, which increases dissolution rate by agitational forces, and another excipient with a solution pH above the pK_a of paracetamol, which would act by increasing the drug's solubility. It was hypothesised these two modes of action would produce a superior drug dissolution rate compared to sodium bicarbonate alone.
- For paracetamol, two alkalising excipients were selected on the basis of the results obtained in the 'controlled powder' dissolution study, *i.e.* tri-sodium phosphate and L-arginine, as well as sodium bicarbonate. An experimental design for mixtures approach was adopted to investigate the dissolution-promoting response of the excipients. Paracetamol:excipient mixtures (1:1) were processed into granules and analysed using the 'controlled powder' dissolution method. The calculated F_1 fit-factors suggested that, in granules, tri-sodium phosphate actually acted to inhibit the dissolution of the drug, compared to a reference containing lactose as the excipient. As expected, sodium bicarbonate and L-arginine, alone and in combination, increased the drug dissolution rate. It was observed, as hypothesised, that a combination of sodium bicarbonate and L-arginine (1:1) increased the dissolution rate compared to sodium bicarbonate alone. This study was not progressed to tablet formulation development.
- For ibuprofen, four alkalising excipients were selected on the basis of the results obtained in the 'controlled powder' dissolution study, *i.e.* tri-sodium phosphate, sodium bicarbonate, sodium carbonate and L-arginine. Early investigations showed that sodium bicarbonate and L-arginine were unsuitable, due to an unknown reaction with ibuprofen. An experimental design for mixtures approach was adopted to investigate the dissolution promoting response of the two remaining excipients. Ibuprofen:excipient mixtures (1:1) were processed into granules and analysed using 'controlled powder' dissolution method. The calculated F_1 fit-factors

work investigating the tabletting properties of the granules suggested that all formulations would be suitable. The five excipient combinations produced were selected for further development into tablet formulations.

- A final tablet development study for ibuprofen was undertaken. Five formulations containing either sodium carbonate, tri-sodium phosphate, or combinations of both intra-granularly were prepared. Other excipients were added to act as either a compressibility aid, disintegrant, wetting agent or lubricant. Tablets were produced using a single-punch machine without incident. Physical and chemical analysis demonstrated that the tablets produced would meet either the USP or BP Pharmacopoeia specification except for tablets containing predominantly tri-sodium phosphate which were found to contain significant quantities of moisture, post drying. It was observed that a more efficient drying method than the one used, *i.e.* fluid bed dryer *versus* trays should be able to dry the granules more satisfactorily. It was noted that the friability in some formulations was high, but that this could be improved by increasing the tablets crushing strengths. Most importantly, in terms of this study, it was observed that all the formulations dissolved much more readily and completely in the simulated stomach method than commercial formulations containing either ibuprofen free acid or lysinate salt. Also, the median formulation was found to have a similar dissolution profile to the two commercial formulations, in the simulated intestine model, having the median % dissolved after 30 minutes. It was concluded that the trends indicated that the formulation containing 100% sodium carbonate would be the most appropriate tablet formulation because it had the lowest retained moisture and friability values. This selection was strengthened by the fact that this excipient was also the most alkalising, *i.e.* the pH of the dissolution fluid measured post-experiment was highest, on a weight basis. This may give an opportunity for an a reduction in quantity of excipient required and hence a reduction in the tablet weight, which would be considered heavy at 1.4g. Of course, the final tablet formulation selection would be dependent on the outcome of the stability testing of the products.
- Overall, stability testing of the formulations under ambient and accelerated conditions demonstrated the products to be stable from a chemical perspective. Some changes were noted in the physical characteristics, most importantly, a reduction in dissolution rate, which was probably related to an increase in the

tablet's crushing strength. The dissolution rate decrease was not considered significant as all of the formulations were still superior to the two ibuprofen commercial products. From an assay perspective, the results were variable but in all cases no assay value was obtained below the BP assay limit (>90%). The variability may be associated with the fact that the work was not conducted within a GLP laboratory. Analysis of degradation products throughout, where no increase in impurities was observed, indicates that all formulations were chemically stable for the duration of the stability study. From a stability perspective all formulations were qualitatively considered to be equal.

- A rational optimisation study would be to base an ibuprofen formulation with sodium carbonate as the primary dissolution promoting-excipient.

CHAPTER 8

DEVELOPMENT OF DRUG ABSORPTION MODEL

8.1 Introduction

In vitro-in vivo correlations (IVIVC) attempt to link *in vitro* drug product performance to *in vivo* product biopharmaceutic-pharmacokinetic performance. IVIVC has been defined by the United States Pharmacopoeia subcommittee on Biopharmaceutics as: "the establishment of a relationship between a biological property produced by a dosage form, and a physicochemical characteristic of the same dosage form" (Pharmacopoeial Forum 1988). A FDA interpretation of *in vitro-in vivo* correlation has been cited (Cardot and Beyssac 1993) as: "To show a relationship between two parameters. Typically a relationship is sought between *in vitro* dissolution rate and *in vivo* input rate. This initial relationship may be expanded to critical formulation parameters and *in vivo* input rate." The use of the dissolution test has been the primary method used to develop IVIVCs, with mixed success. Dissolution rate-limited absorption *e.g.*, absorption from extended release products, in particular, has been shown to produce high IVIVCs as summarised by Polli *et al.* (1996). Far fewer studies have been shown to produce IVIVCs, for immediate-release products, a rare exception being digoxin tablets (Welling 1991). The reason for this is that, for any drug undergoing permeation-limited absorption, the dissolution of the drug is not the rate-limiting step, and therefore no correlation would be expected. As discussed in chapter 1, the BCS demonstrates that for Class III drugs (high solubility/low permeability) an IVIVC can not be generated, based on dissolution. Also, in the case of drugs in Class I drugs (high solubility/high permeability) an IVIVC would only be expected if the dissolution rate was slower than gastric emptying. However, some workers persist in trying to produce IVIVCs using drug dissolution as the *in vitro* method where it is apparent that no direct correlation can be expected. An example of this is the work conducted by Radovanovic *et al.* (1997), where the authors tried to produce an IVIVC for immediate release paracetamol tablet formulations. It is well known, and summarised in the paracetamol drug profile detailed in section 1.4, that the absorption of paracetamol is limited by gastric emptying, so much so that this drug has been used a gastric emptying marker. Although the study produced a correlation for the formulations, the method was flawed. The reason for this is that the *in vivo* 'dissolution' profile, calculated by numerical deconvolution, is in fact the resultant of

dissolution, stomach absorption, gastric emptying and intestinal absorption. The correlation of *in vitro* dissolution profiles with the generated profile may produce a correlation but the 'black-box' approach to the absorption processes severely limits the value of results. The *in vitro* dissolution method employed must be considered extremely limited in that it is only applicable to the products evaluated and could not be extended to other formulations. Recently, the focus of the development of IVIVCs has shifted to an approach where the intestinal permeation and drug dissolution are considered jointly (Polli *et al.* 1996). In this theoretical study it was demonstrated that the correlation between amount of drug dissolved and absorbed was highly non-linear when drug absorption was the rate-limiting step, however as the dissolution rate became the rate-limiting step the correlation increased. This theoretical approach has been extended to a practical example, an investigation into the dissolution specifications for metoprolol tartrate tablets, conducted by Polli *et al.* (1997). In this study it was demonstrated that four formulations with different dissolution profiles, measured using several model dependent/independent methods, were in fact found to be bioequivalent. The reasons for this were shown to be due to the fact that the dominant rate-limiting mechanism to absorption was drug intestinal permeation. Most recently and for the first time, the combination of *in vitro* methods investigating drug dissolution and permeation have been integrated to study absorption relationships (Ginski and Polli 1999). The developed combination model was utilised to predict dissolution-absorption relationships, and hence the contributions of dissolution and intestinal permeation to the overall drug process for fast and slow dissolving immediate release formulations of piroxicam, metoprolol and ranitidine. The prediction of dissolution or permeation rate-limited absorption was in agreement with the clinical results.

The objectives of this study were to produce a simulation of the drug absorption process, utilising the dissolution and permeation data generated previously. However, in terms of modelling, the work was a significant development over the work conducted by Polli and co-workers in that drug absorption in the stomach was considered as well as the gastric emptying process, the latter being utilised from references. An attempt to validate the model by determining the level of correlation between pharmacokinetic parameters generated by the model and those obtained

from drug and antacid/excipient co-administration *in vivo* studies was undertaken. Secondary objectives included an intimate profiling of the key parameters throughout the drug absorption process and, also, the determination of the rate-limiting step in the drug absorption process, for each experimental scenario.

8.2 Experimental

8.2.1 Equipment

A computer software modelling package 'Modelmaker' (V3.0 Cherwell Scientific Publishing, Oxford, U.K.) was utilised to produce the drug plasma concentrations/time simulations, parameter/time and absorption/dissolution datasets.

8.2.2 Method

The model was developed, to simulate drug absorption *via* the oral route. This involved utilising anatomical and physiological aspects of the gastrointestinal tract, combined with the biopharmaceutical parameters determined as part of this project. The dissolution, permeation and gastric emptying rates were assigned as first-order processes. For the determination of the dissolution rate constant the relevant dissolution profile, referenced from chapter 4, was visually examined and the approximate half-life observed. This was transformed into a rate constant using equation 8.1:

$$t_{½} = \frac{\ln 2}{k} \qquad \text{equation 8.1}$$

where k is the dissolution rate constant and $t_{½}$ is the estimated dissolution half-life. The permeation rate constant (P_{app}) was referenced from chapter 6. To model the situation, *in vivo* the permeation for the paracetamol control through the intestine model was transformed to correspond with a total permeation half-life of 6.8 minutes. This value was used as it had been estimated from the pharmacokinetic data obtained from eight volunteers, fasted overnight, and dosed with 20mg kg^{-1} of paracetamol, using a two-compartment model. It was noted that this model separated the drug absorption from the gastric emptying parameter (Clements *et al.* 1978). All

other permeation rate constants utilised, including those for the stomach and the model drug ibuprofen, were transformed by ratioing the permeation values to the control, followed by multiplication by the derived *paracetamol intestine model control* rate constant value. For gastric emptying, unless otherwise indicated, for dose emptying with a phase I pattern (Maceras *et al.* 1995), a lag-time of 16 minutes was used, followed by an emptying half-life of 6.7 minutes. Phase III (Maceras *et al.* 1995), emptying of solid and liquid from the stomach were assigned half-lives of 4.9 minutes and 2.9 minutes, respectively, with data obtained from a gastric emptying study conducted by Oberle *et al.* (1990). The gastric emptying of the liquid phase was limited to 6 half-lives, with a change from phase I and II to phase III emptying initiated after 60 minutes. The model assumed no absorption from the colon. Drug distribution volumes were taken as 67.5 litres for paracetamol (Prescott 1996) and 8 litres for ibuprofen, representing plasma volume, Davies (1998). Elimination rate constants were assigned as 0.007 min^{-1} and 0.0063 min^{-1} for paracetamol and ibuprofen, respectively, averaged from the drug profiles in chapter 1.

The model is illustrated in figure 8.1 and comprises six compartments, representing undissolved drug in the stomach and intestine; dissolved drug in the stomach and intestine; total drug absorbed and drug eliminated. The compartments are represented by rectangles. The flows from one compartment to another are represented by complete lines, with the flow direction indicated. Variables, represented by rounded-rectangles, are used to track parameters within the model without modification or interference *i.e.*, they represent a function of a component. The components influencing the variables are selected by use of dotted lines with the direction of influence indicated. A full explanation of the model's functionality is described in table 8.1. Experimentally obtained and referenced data for each scenario were processed through the model. The rate constants, obtained experimentally, are summarised in table 8.2.

Figure 8.1
Schematic of the model developed to simulate the drug absorption process *via* the oral route. Model designed to produce simulated drug plasma concentration/time profiles *in vivo.*

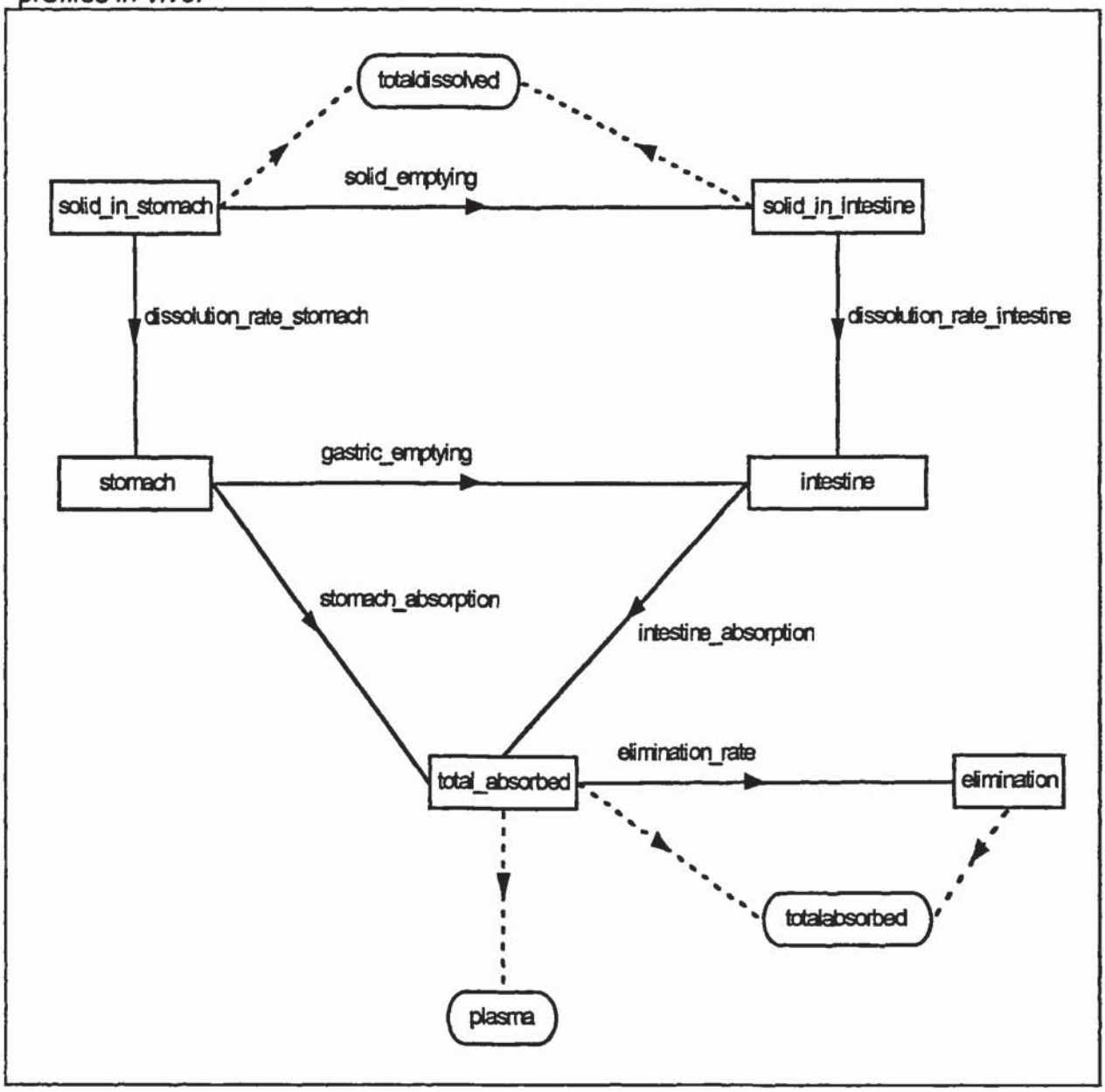

Table 8.1

Summary of developed *in vivo-in vitro* model's functionality

Model Constituent	Description	Value/ Equation (*dm/dt*)
solid_in_stomach (a)	undissolved drug in the stomach (mg)	dose -(A+B)
stomach (b)	dissolved drug in the stomach (mg)	+B-(D+E)
solid_in_intestine (c)	undissolved drug in the intestine (mg)	+A-C
intestine (d)	dissolved drug in the intestine (mg)	+C+D-F
total_absorbed	total drug absorbed (mg)	+E+F-G
elimination	total drug eliminated (mg)	+G*total_absorbed
solid_emptying (A)	phase III G.E. of undissolved drug (min^{-1})	t<=60(0*a) t>60(a*0.14)
dissolution_rate_stomach (B)	dissolution rate of drug in the stomach (min^{-1})	a*stomach $diss^n$ rate[1,2]
dissolution_rate_intestine (C)	dissolution rate of drug in the intestine (min^{-1})	c*intestine $diss^n$ rate[1]
gastric_emptying (D)	phase I + III G.E. of dissolved drug (min^{-1})	t<16(0*b) t<=56(0.104*b) t<60(0*b) t>=60(0.24*b)[1,3]
stomach_absorption (E)	drug permeation rate in the stomach (min^{-1})	b*stomach $perm^n$ rate[1]
intestine_absorption (F)	drug permeation rate in the intestine (min^{-1})	d*intestine $perm^n$ rate[1]
elimination_rate (G)	drug elimination rate (min^{-1})	total_absorbed*$elim^n$ rate[1]
totaldissolved	total drug dissolved (mg)	dose-(a+c)
totalabsorbed	total drug absorbed (mg)	total_absorbed+elimination
plasma	total drug absorbed divided by distribution volume	total_absorbed/distribution volume[1]

[1]Dissolution and permeation rates were obtained from the appropriate study. Elimination rates, distribution volumes and gastric emptying data was referenced from literature as detailed previously.

[2]Where appropriate conditional statements were included to limit the drug concentration as appropriate.

[3]For aluminium hydroxide studies, gastric emptying half-life was set to 40 minutes, with 16 minute lag-time (Sadowski 1994).For sodium bicarbonate studies gastric emptying lag time was set to 8 minutes with gastric emptying half-life set to 4.7 minutes (O'Mahoney 2000).

Table 8.2
Summary of rate constants used in modelling study. Data derived from results obtained experimentally in dissolution and permeability studies

Experimental Scenario	Stomach Dissolution Rate (min^{-1})	Intestine Dissolution Rate (min^{-1})	Stomach Permeation Rate (min^{-1})	Intestine Permeation Rate (min^{-1})
paracetamol/ control	0.139	N/A[1]	0.00679	0.102
paracetamol/ sodium bicarbonate	0.173	N/A[1]	0.00685	0.101
paracetamol/ calcium carbonate	0.277	N/A[1]	0.00781	0.0918
paracetamol/ aluminium hydroxide	0.198	N/A[1]	0.00659	0.102
paracetamol/ magnesium hydroxide	0.231	N/A[1]	0.00645	0.101
paracetamol/ magnesium oxide[2]	0.116	N/A[1]	0.00700	0.100
paracetamol/ Zapp	0.231	N/A[1]	0.0685	0.101
ibuprofen/ control[3]	0.0693	0.139	0.0102	0.108
ibuprofen/ sodium bicarbonate	0.063	0.346	0.00793	0.121
ibuprofen/ calcium carbonate	0.0121	0.116	0.00847	0.103
ibuprofen/ aluminium hydroxide[4]	0.277	0.173	0.00891	0.108
ibuprofen/ magnesium hydroxide	0.0462	0.346	0.00857	0.0857
ibuprofen/ magnesium oxide	0.0462	0.139	0.00928	0.111
ibuprofen/ Form 5	0.0693	0.0693	0.0102	0.146

[1]Rate not required as 100% dissolution occurred in the stomach in all cases.
[2]Limited to 70% dissolution in the stomach
[3]Limited to 1% dissolution in the stomach.
[4]Limited to 2.5% dissolution in the stomach and 70% in the intestine.

8.3 Results and Discussion

Bioavailability can be described as the rate and extent to which the active ingredient or therapeutic ingredient is absorbed from a drug product and becomes available at the site of drug action (Selen 1991). The pharmacokinetic parameters measuring peak plasma concentration (C_{max}) and time of peak plasma concentration (t_{max}) are used as indicators of the rate of absorption and the area under the pharmacokinetic curve (AUC) is used to measure the extent of absorption. The focus of the experimental studies conducted was on absorption rates and did not include major factors which would affect the AUC values, such as drug metabolism and first-pass effects. Therefore, the extent of absorption was not examined as part of the IVIVC development. In terms of the two parameters for measuring the drug absorption rate, it was discovered that the rapid absorption of drug may lead to a situation where the volume of distribution is not initially constant. For example, analysis of the intravenous administration of paracetamol plasma concentration/time curve (Prescott 1996) by the author led to the discovery that two apparent distribution volumes could be elucidated, the initial distribution volume estimated from the first four points was 29 litres with the steady-state distribution volume estimated to be 76 litres. An explanation of this from an *in vivo* perspective could be that the rapid absorption of the drug leads to a non-equilibrated drug concentration in the body *e.g.*, drug is rapidly absorbed into the plasma and does not fully distribute into tissues, to the equilibrium point, before some plasma samples are taken. This leads to a situation where the measured C_{max} is more concentrated than would otherwise be expected. This phenomenon is well known by pharmacokineticists, who develop models where two or more compartments represent the *in vivo* distribution volume *e.g.*, the two-compartment open model, is used to simulate this observation, with rate constants mathematically optimised to produce the most significant correlation (Welling 1986 and Wagner 1993). In fact, a model of this type has been used to explain the observed increase in C_{max} obtained for the Zapp tablet *versus* the Panadol® tablet (Rostami 2000). As the developed model is based on *in vitro* methods and physiological values, and aims to use experimental data to develop a general correlation, it would not be appropriate to use a mathematical approach to refine the model to produce a specific correlation. For this reason, the C_{max} values were not

utilised in developing an IVIVC. Therefore, the remaining indicator of drug absorption, t_{max}, was selected for IVIVC development.

When undertaking modelling exercises of this nature, it is crucial that the investigator understands the model's limitations in order to correctly interpret the results. In this model, several assumptions have been made *i.e.*, equivalence of *in vitro* and *in vivo* dissolution rates, estimation of *in vivo* permeation rates, use of selected gastric emptying rates and averaging of elimination rates. In practice, this means that comparisons with PK profiles and underlying mechanisms obtained from in vivo studies are important, and require validation. Also, the correlation level obtained, in part, reflects the effect of these assumptions on the output of the model.

Initially, experiments were undertaken to ensure that the plasma profiles generated by the model were similar to data obtained in vivo. For paracetamol, the average of the t_{max} values published, collated in chapter 1 (table 1.1), was 58±25 minutes compared to 58 minutes generated by the model. For ibuprofen the average t_{max} value from the literature was 109±73 minutes compared to 105 minutes obtained using the model. The results indicate good agreement between the theoretical and experimental data. To further investigate the validity of the model, the ability to predict whether absorption was dissolution or permeation rate-limiting was investigated. The novel approach to the analysis of IVIVC developed by Polli *et al.* (1996), assuming first-order dissolution and permeation, demonstrated the relationship between % absorbed and % dissolved as the ratio of drug permeation and dissolution rate-constants between a range of 0.001-1000. Where the dissolution rate-constant is rate-limiting (ratio>>1) the relationship between % absorbed *versus* % dissolved will result in a 'straight-line' appearance with a high correlation coefficient (R^2). Conversely, where the permeation rate-constant is rate-limiting (ratio<<1) the relationship between % absorbed *versus* % dissolved will result in a 'reverse L' appearance and low correlation coefficient (R^2). Where the relationship is intermediate between these two extremes, the shape of the curve and correlation coefficient will demonstrate transitional characteristics, constituting a family of curves. The relationship between the % absorbed and % dissolved for the paracetamol control is illustrated in figure 8.4. The relationship clearly has a 'reverse L' appearance; the model, therefore, predicts that the absorption of paracetamol is permeation-rate limited. This agrees

with the fact that the absorption of paracetamol is modulated by gastric-emptying and that it is categorised as a Class I or III drug using the BCS, indicating that dissolution is not the rate-limiting step to absorption. The relationship between the % absorbed and % dissolved for the ibuprofen control is illustrated in figure 8.25. The relationship approximates to a 'straight-line' appearance, the model therefore predicts that the absorption of ibuprofen is dissolution-rate limited Ginski and Polli (1998). This agrees with the fact that the absorption of ibuprofen is categorised as a Class II drug using the BCS, indicating that dissolution is the rate-limiting step to absorption. It was concluded that using the limited examples, the model could differentiate the rate-limiting step to absorption.

Reviewing the model's output for the experimental scenarios, in the form of plasma/concentration profiles, %absorbed *versus* %dissolved, and parameter tracking, as illustrated in figures 8.2-8.43 and summarised in table 8.3 the following observations were made:

- The simulated plasma concentration/time profiles for paracetamol were not substantially modified by co-administration of the antacids magnesium hydroxide or calcium carbonate
- The simulated plasma concentration/time profiles for paracetamol were substantially modified by co-administration of the antacids sodium bicarbonate, magnesium oxide and aluminium hydroxide, with a quicker t_{max}, a reduced AUC and a slower t_{max} being observed, respectively. The reasons for this are due to an increase in gastric emptying rate and/or increased dissolution rate, a reduction in the amount of drug dissolved and a decrease in gastric emptying rate, respectively. The Zapp formulation exhibits a quicker t_{max}, the possible reasons being an increased dissolution or gastric emptying rate, or combination of these two effects. The importance of these two factors is explored in more detail in a following section.
- For paracetamol, in all cases, the parameter tracking plots indicate that drug dissolution is completed in the stomach with no dissolution occurring in the intestine

- For paracetamol, in all cases, it was predicted that significant quantities of drug were absorbed from the stomach (7 to 25%), contrary to the assumption that no absorption occurs through this organ (Clements et al. 1978), concluded from mathematical modelling of pharmacokinetic data. It is noted that the absorption of paracetamol has been demonstrated in the rat model where approximately 22% of a dose was absorbed through the stomach in 30 minutes, compared to 70% through the small intestine Bagnall *et al.* (1979)
- For paracetamol, in all cases, the % absorbed *versus* % dissolved profiles demonstrated a 'reverse L' appearance, to varying degrees. These profiles illustrate that for all of the experimental simulations the absorption was rate-limiting. The term 'absorption' rather than 'permeation' is used deliberately as the results measuring the effect of sodium bicarbonate and aluminium hydroxide, and the Zapp formulation indicate that gastric emptying influences the absorption rate to a great extent. This finding agrees with the conclusion drawn from a pharmacokinetic study (Heading *et al.* 1973).
- The simulated plasma concentration/time profile for ibuprofen is not substantially modified by co-administration of the antacid calcium carbonate. Although the addition of calcium carbonate increases the amount of dissolution in the stomach, the rate is very slow.
- The simulated plasma concentration/time profiles for ibuprofen are substantially modified by co-administration of the antacids sodium bicarbonate, magnesium oxide, magnesium hydroxide and aluminium hydroxide, with a quicker t_{max} recorded for the first three and a reduced AUC for the latter. The reasons for this, in the first three cases, are due to an increase in drug dissolution rate in the stomach, combined with an increased GE rate for sodium bicarbonate, which leads to the dissolved drug being emptied with the liquid phase, therefore making it available to be rapidly absorbed in the small intestine. For aluminium hydroxide, the drug remains undissolved in the stomach and is emptied during phase III, as for the control; the effect of a slower liquid GE rate under these circumstances is inconsequential. It is noted that the effect of the aluminium hydroxide on the onset of the phase III cycle has not been determined, following an extensive literature search. The reduced AUC for aluminium hydroxide is due to a reduction in cumulative dissolution in the intestine model. The novel formulation 5 ibuprofen

tablet also exhibited a quicker t_{max}, again due to a increased dissolution rate in the stomach, with a contribution from an increased permeation rate in the intestine.

- For ibuprofen, in all cases, the parameter tracking plots indicate a change in the proportion of dissolution taking place in the stomach. This change can be quantified through an increase in stomach absorption. For the control approximately 1% of the drug was absorbed through the stomach, compared to a range of between 5-17%, when either magnesium oxide, magnesium hydroxide, calcium carbonate or sodium bicarbonate are co-administered and also in the case of formulation 5.
- For ibuprofen, with aluminium hydroxide co-administration the amount of drug absorbed through the stomach was 3%.
- For ibuprofen, for the control, and aluminium hydroxide or calcium carbonate co-administration the % absorbed *versus* % dissolved profiles demonstrated a 'straight line' appearance, to varying degrees. These profiles illustrate that for these experimental simulations drug permeation was the rate-limiting step.
- For ibuprofen, the co-administration of magnesium oxide, magnesium hydroxide, sodium bicarbonate, and for formulation 5, the % absorbed *versus* % dissolved profiles demonstrated a hybrid appearance which did not correspond to any of the family of curves produced by Polli *et al.* (1996). The relationship appeared to be bi-phasic, with the first ≈50% of the drug being absorbed with a permeation rate-limiting step and the last ≈50% of the drug being absorbed with a dissolution rate-limiting step. These observations correspond to relatively rapid dissolution in the stomach, compared with slower permeation through the stomach, followed by relatively slow dissolution in the intestine compared to more rapid permeation in the intestine. The change in absorption character coincided with the onset of phase I gastric emptying of solution containing dissolved drug.

Table 8.3

Summary of results generated from drug absorption model, including comparison with *in vivo* data

Experimental Scenario	t_{max} *in vivo* (mins)	t_{max} predicted (mins)	Stomach Absorption (% predicted)	Intestine Absorption (% predicted)
paracetamol/ control	58	58	12	88
paracetamol/ sodium bicarbonate	17.5	46	7	93
paracetamol/ calcium carbonate	44	58	16	84
paracetamol/ aluminium hydroxide	86	84	25	75
paracetamol/ magnesium hydroxide	-	57	13	87
paracetamol/ magnesium oxide	-	59	12	88
paracetamol/ Zapp	17.5	45	7	93
ibuprofen/ control	109	105	1	99
ibuprofen/ sodium bicarbonate	24	51	7	93
ibuprofen/ calcium carbonate	102	102	5	95
ibuprofen/ aluminium hydroxide	186	111	3	97
ibuprofen/ magnesium hydroxide	54	81	11	89
ibuprofen/ magnesium oxide	-	78	11	89
ibuprofen/ Form 5	-	60	17	83

Figure 8.2
Illustrating the predicted drug plasma conc^{n}/ time profile for paracetamol control simulated PK study

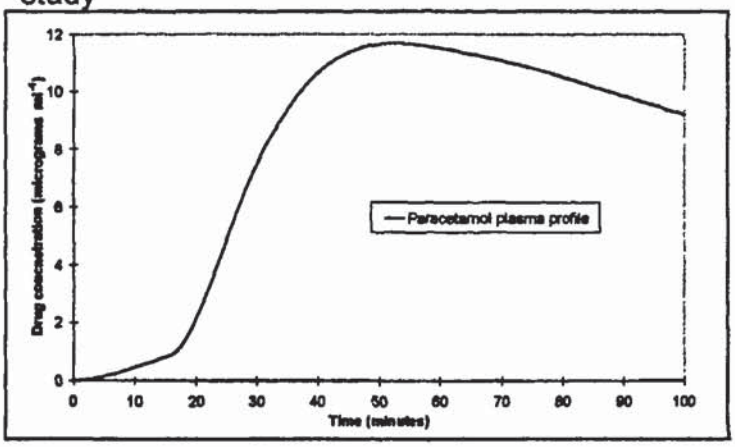

Comments

Model input:
Stomach diss^{n}= 0.139 (min^{-1})
Intestine diss^{n}= N/A
Stomach perm^{n}= 0.00679 (min^{-1})
Intestine perm^{n}= 0.102 (min^{-1})

Model output: t_{max}= 58 mins

Figure 8.3
Illustration of predicted parameter values during paracetamol control simulated PK study

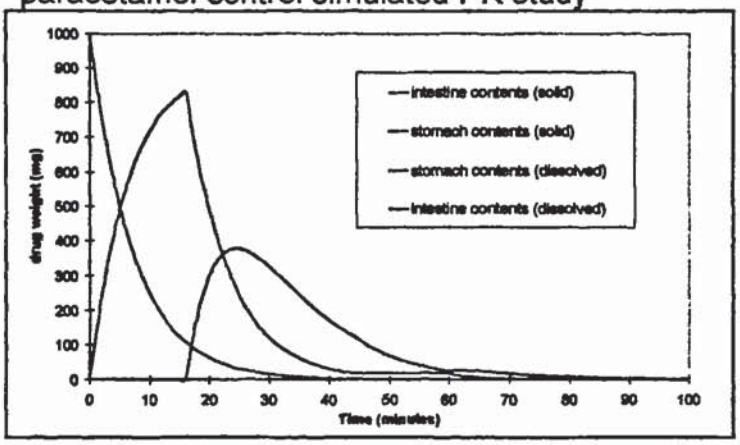

Comments

Drug undergoes rapid and complete dissolution in the stomach. Solid drug does not enter the intestine. Rapid emptying of the dissolved drug from the stomach occurs after 16 minutes.

Figure 8.4
Illustration of predicted %dissolved/%absorbed relationship during paracetamol control simulated PK study

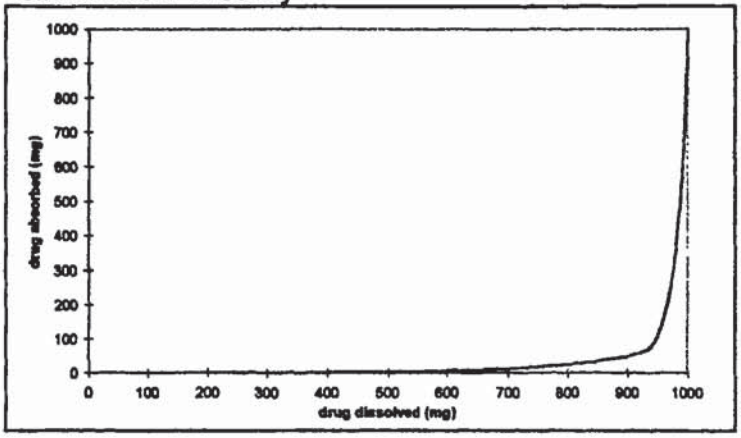

Comments

Reverse-L shape of curve indicates the absorption of paracetamol is permeability rate-limited.

Figure 8.5
Illustrating the predicted drug plasma conc^{n}/ time profile for paracetamol/magnesium oxide simulated PK study

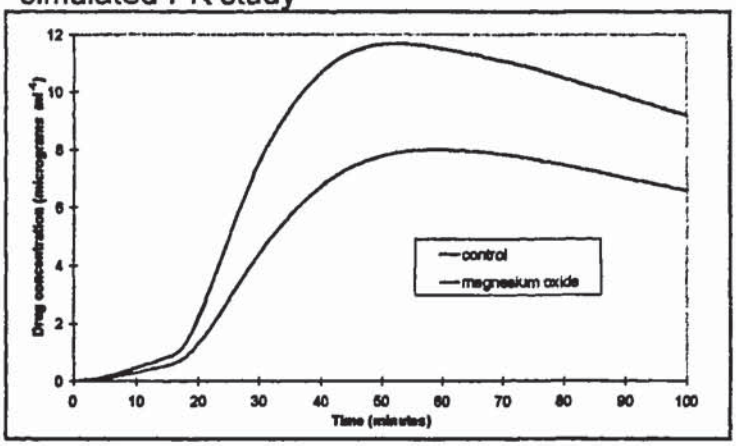

Comments

Model input:
Stomach diss^{n}= 0.116 (min^{-1})
Intestine diss^{n}= N/A
Stomach perm^{n}= 0.00700 (min^{-1})
Intestine perm^{n}= 0.100 (min^{-1})

Model output: t_{max}= 59 mins

Lower C_{max} due maximum dissolution of 70% observed in stomach model.

Figure 8.6
Illustration of predicted parameter values during paracetamol/magnesium oxide simulated PK study

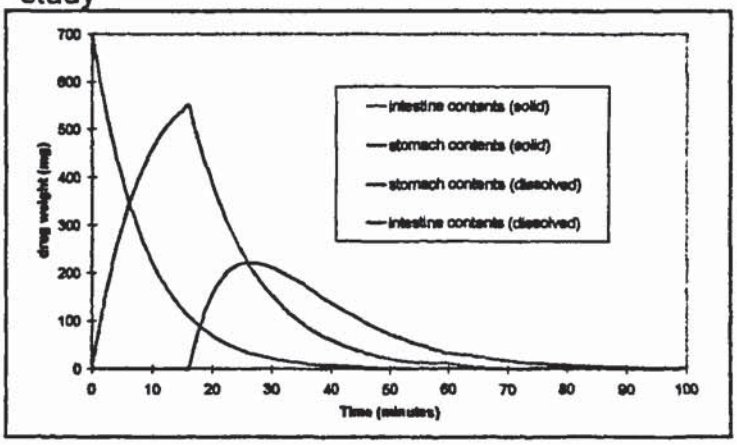

Comments

Drug undergoes rapid and complete dissolution in the stomach upto a maximum of 70%. Solid drug does not enter the intestine. Rapid emptying of the dissolved drug from the stomach occurs after 16 minutes.

Figure 8.7
Illustration of predicted %dissolved/%absorbed relationship during paracetamol/magnesium oxide simulated PK study

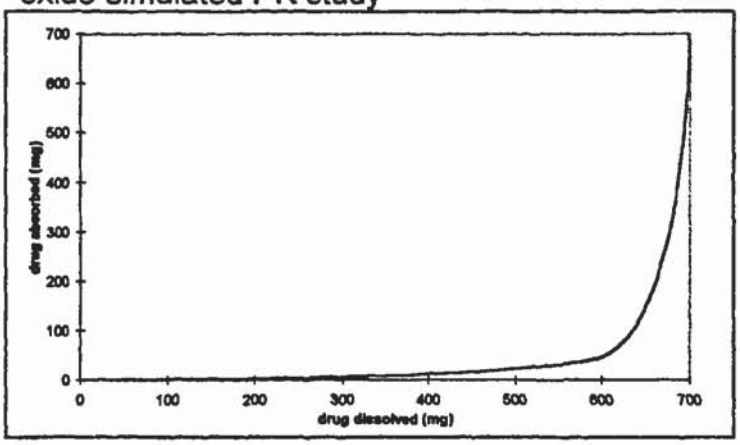

Reverse-L shape of curve indicates the absorption of paracetamol is permeability rate-limited.

Figure 8.8
Illustrating the predicted drug plasma conc^{n}/ time profile for paracetamol/magnesium hydroxide simulated PK study

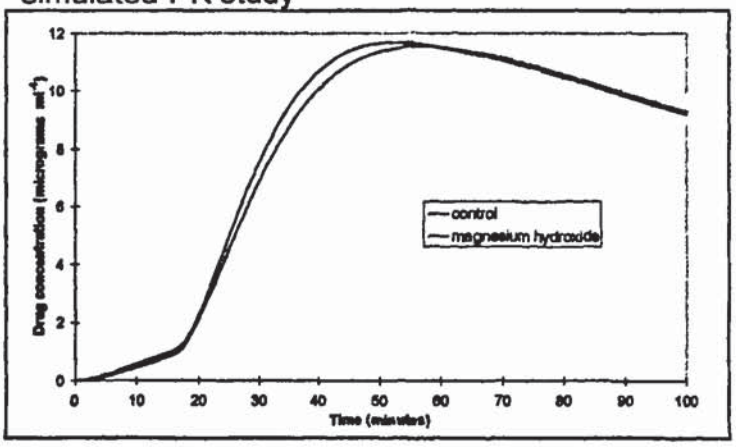

Comments

Model input:
Stomach diss^{n}= 0.231 (min^{-1})
Intestine diss^{n}= N/A
Stomach perm^{n}= 0.00645 (min^{-1})
Intestine perm^{n}= 0.101 (min^{-1})

Model output: t_{max}= 57 mins

Figure 8.9
Illustration of predicted parameter values during paracetamol/magnesium hydroxide simulated PK study

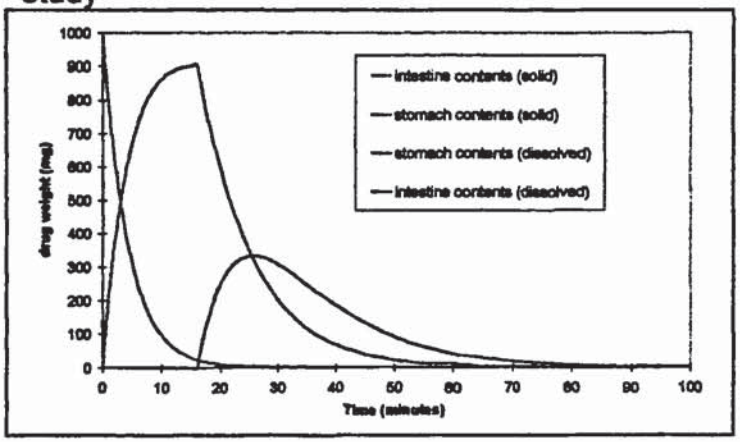

Comments

Drug undergoes rapid and complete dissolution in the stomach. Solid drug does not enter the intestine. Rapid emptying of the dissolved drug from the stomach occurs after 16 minutes.

Figure 8.10
Illustration of predicted %dissolved/%absorbed relationship during paracetamol/magnesium hydroxide simulated PK study

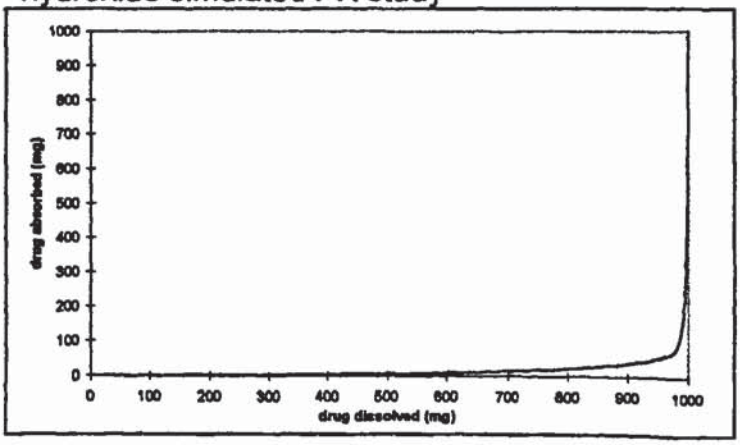

Comments

Reverse-L shape of curve indicates the absorption of paracetamol is permeability rate-limited.

Figure 8.11
Illustrating the predicted drug plasma conc^{n}/ time profile for paracetamol/aluminium hydroxide simulated PK study

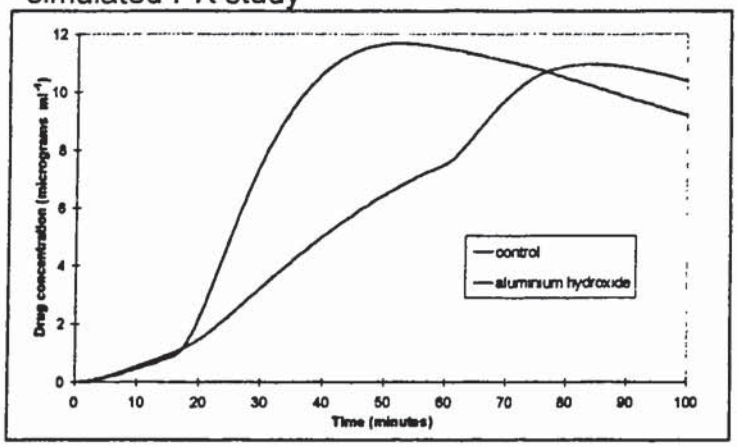

Comments

Model input:
Stomach diss^{n}= 0.198 (min^{-1})
Intestine diss^{n}= N/A
Stomach perm^{n}= 0.00659 (min^{-1})
Intestine perm^{n}= 0.102 (min^{-1})

Model output: t_{max}= 84 mins

Reduced absorption rate as a consequence of reduced GE. emptying rate

Figure 8.12
Illustration of predicted parameter values during paracetamol/aluminium hydroxide simulated PK study

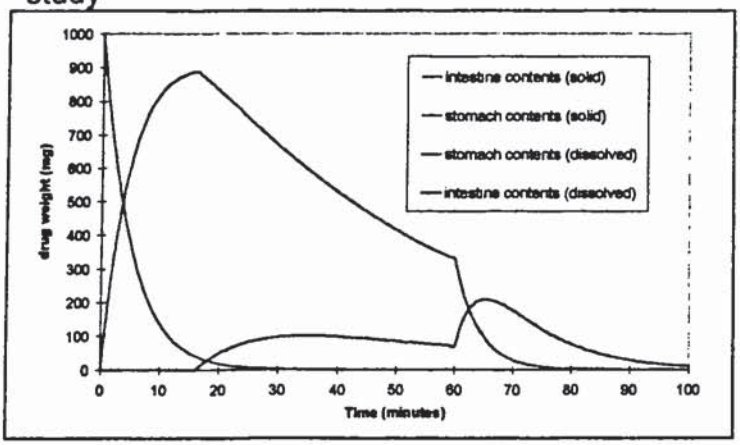

Comments

Drug undergoes rapid and complete dissolution in the stomach. Solid drug does not enter the intestine. Slower emptying of the dissolved drug from the stomach occurs after 16 minutes. After 60 minutes dissolved drug in stomach is rapidly emptied with onset of phase III of GE cycle.

Figure 8.13
Illustration of predicted %dissolved/%absorbed relationship during paracetamol/aluminium hydroxide simulated PK study

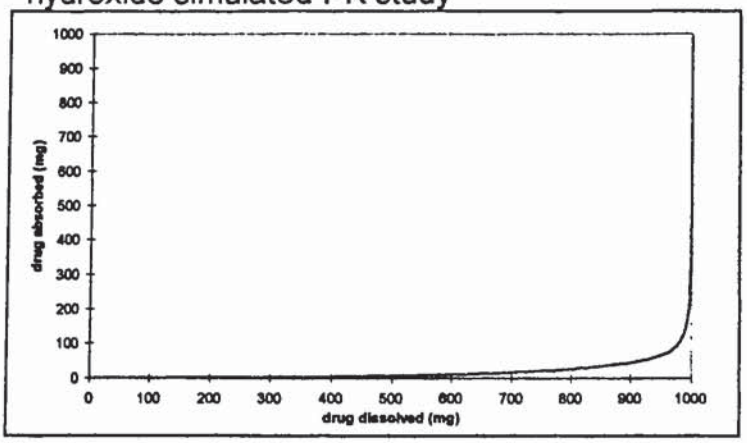

Comments

Reverse-L shape of curve indicates the absorption of paracetamol is permeability rate-limited.

Figure 8.14
Illustrating the predicted drug plasma conc^{n}/ time profile for paracetamol/calcium carbonate simulated PK study

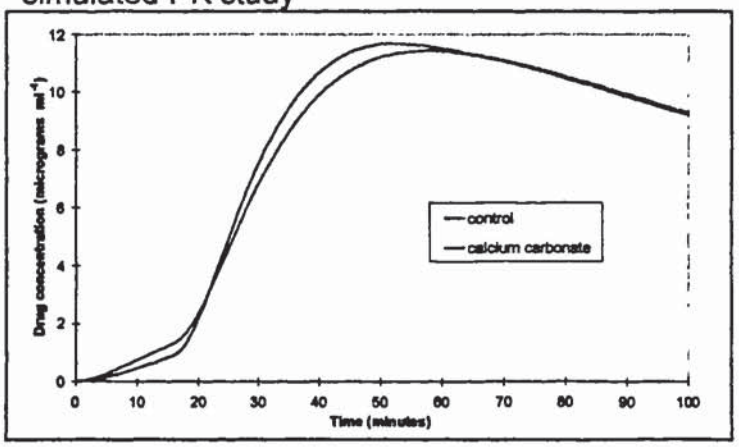

Comment

Model input:
Stomach diss^{n}= 0.277 (min^{-1})
Intestine diss^{n}= N/A
Stomach perm^{n}= 0.00781 (min^{-1})
Intestine perm^{n}= 0.0918 (min^{-1})

Model output: t_{max}= 58 mins

Figure 8.15
Illustration of predicted parameter values during paracetamol/calcium carbonate simulated PK study

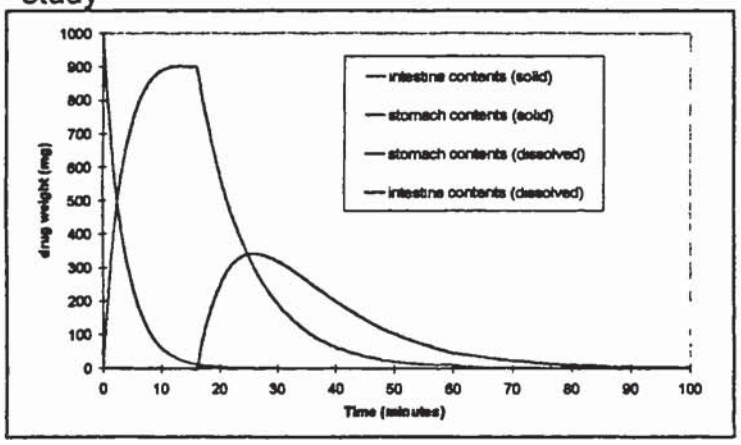

Comments

Drug undergoes rapid and complete dissolution in the stomach. Solid drug does not enter the intestine. Rapid emptying of the dissolved drug from the stomach occurs after 16 minutes.

Figure 8.16
Illustration of predicted %dissolved/%absorbed relationship during paracetamol/calcium carbonate simulated PK study

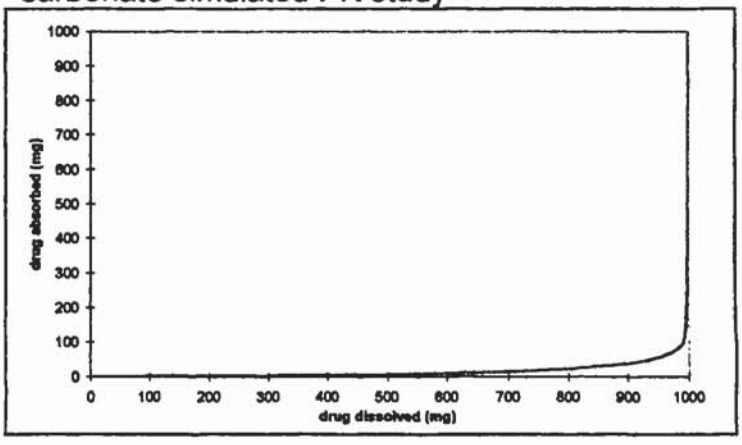

Comments

Reverse-L shape of curve indicates the absorption of paracetamol is permeability rate-limited.

Figure 8.17
Illustrating the predicted drug plasma conc^{n}/ time profile for paracetamol/sodium bicarbonate simulated PK study

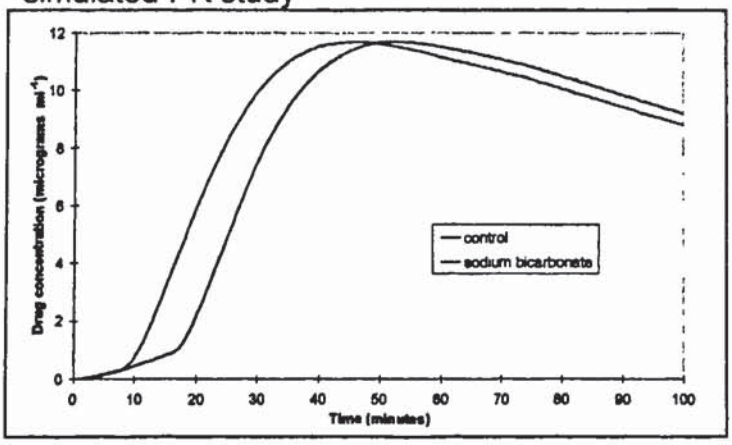

Comment

Model input:
Stomach diss^{n}= 0.173 (min^{-1})
Intestine diss^{n}= N/A
Stomach perm^{n}= 0.00685 (min^{-1})
Intestine perm^{n}= 0.101 (min^{-1})

Model output: t_{max}= 46 mins

Rapid absorption caused by reduced GE lag-time and increased GE rate.

Figure 8.18
Illustration of predicted parameter values during paracetamol/ sodium bicarbonate simulated PK study

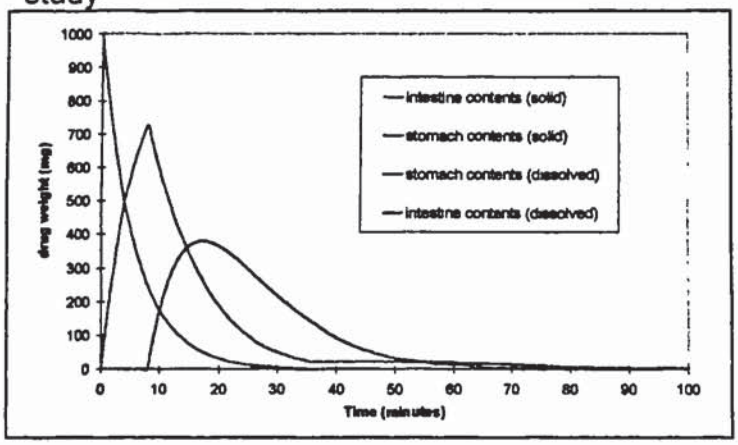

Comments

Drug undergoes rapid and complete dissolution in the stomach. Solid drug does not enter the intestine. Rapid emptying of the dissolved drug from the stomach occurs after 8 minutes.

Figure 8.19
Illustration of predicted %dissolved/%absorbed relationship during paracetamol/ sodium bicarbonate simulated PK study

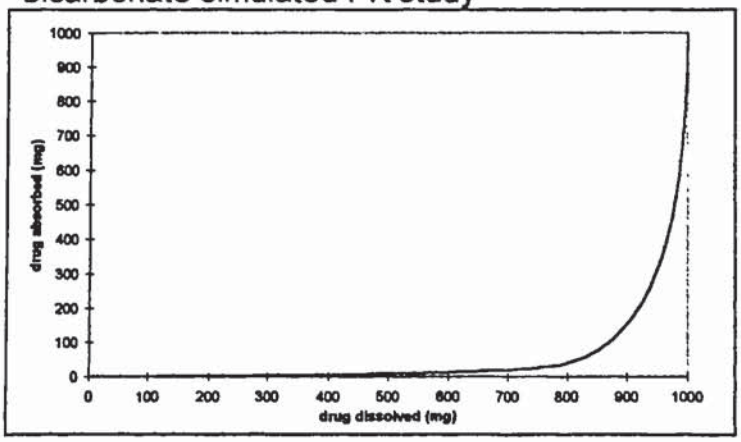

Comments

Reverse-L shape of curve indicates the absorption of paracetamol is permeability rate-limited.

Figure 8.20
Illustrating the predicted drug plasma conc^{n}/ time profile for paracetamol Zapp tablets simulated PK study

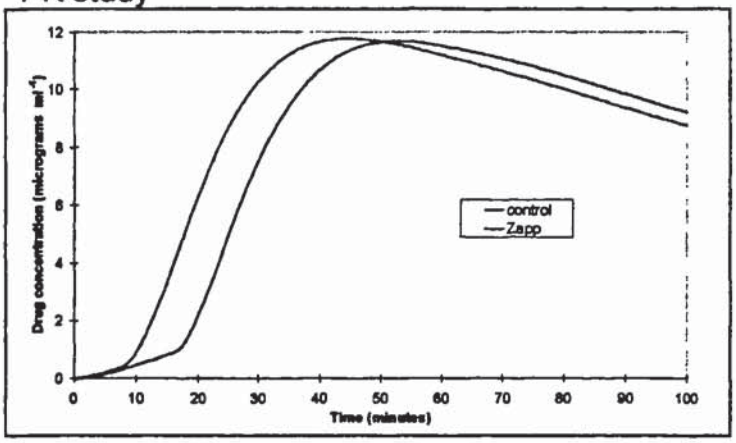

Comments

Model input:
Stomach diss^{n}= 0.231 (min^{-1})
Intestine diss^{n}= N/A
Stomach perm^{n}= 0.00685 (min^{-1})
Intestine perm^{n}= 0.101 (min^{-1})

Model output: t_{max}= 45 mins

Rapid absorption caused by reduced GE lag-time and increased GE rate.

Figure 8.21
Illustration of predicted parameter values during paracetamol Zapp tablets simulated PK study

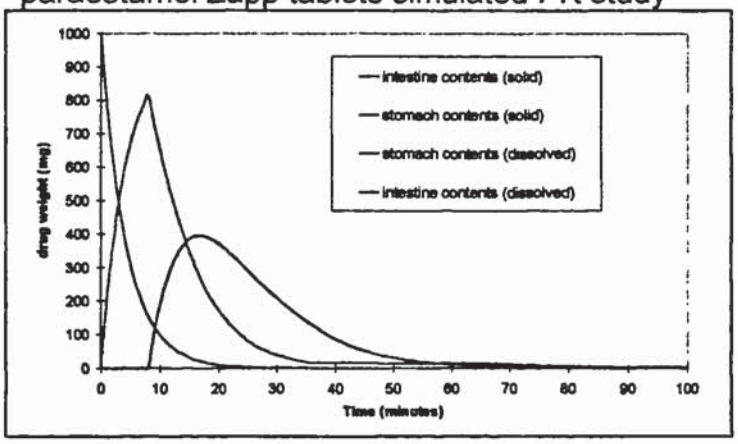

Comments

Drug undergoes rapid and complete dissolution in the stomach. Solid drug does not enter the intestine. Rapid emptying of the dissolved drug from the stomach occurs after 8 minutes.

Figure 8.22
Illustration of predicted %dissolved/%absorbed relationship during paracetamol Zapp tablets simulated PK study

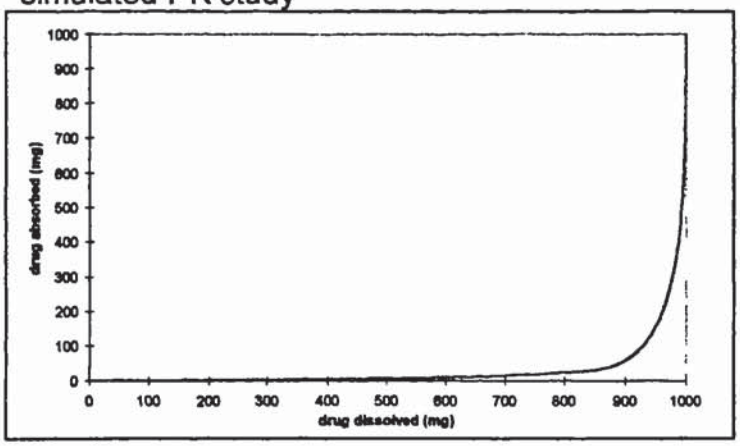

Comments

Reverse-L shape of curve indicates the absorption of paracetamol is permeability rate-limited.

Figure 8.23
Illustrating the predicted drug plasma conc^{n}/ time profile for ibuprofen control simulated PK study

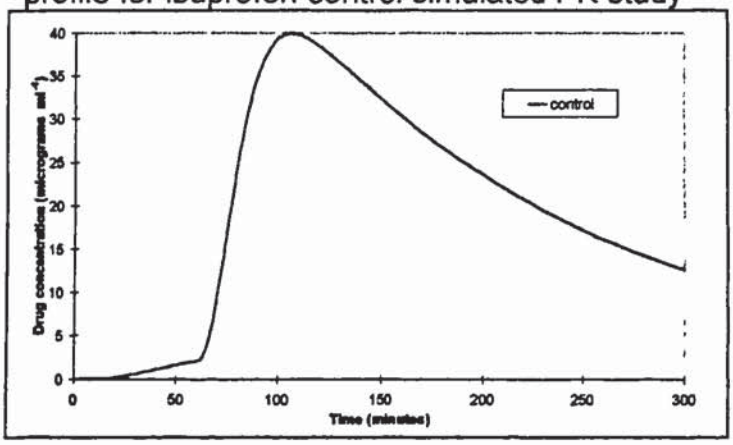

Comments

Model input:
Stomach diss^{n}= 0.0693 (min^{-1})
Intestine diss^{n}= 0.139 (min^{-1})
Stomach perm^{n}= 0.0102 (min^{-1})
Intestine perm^{n}= 0.108 (min^{-1})

Model output: t_{max}= 105 mins

Lag caused by drug insolubility and retention of undissolved drug in the stomach.

Figure 8.24
Illustration of predicted parameter values during ibuprofen control simulated PK study

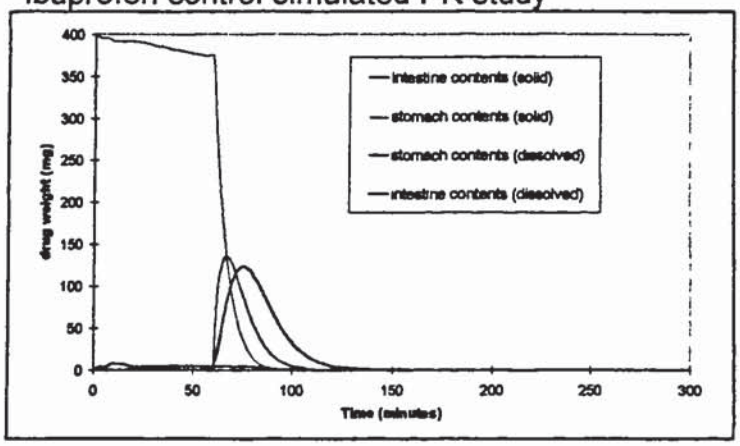

Comments

Drug undergoes minimal dissolution and absorption in the stomach. Onset of phase III of GE cycle leads to transfer of solid drug to the intestine, where dissolution and absorption occur more rapidly.

Figure 8.25
Illustration of predicted %dissolved/%absorbed relationship during ibuprofen control simulated PK study

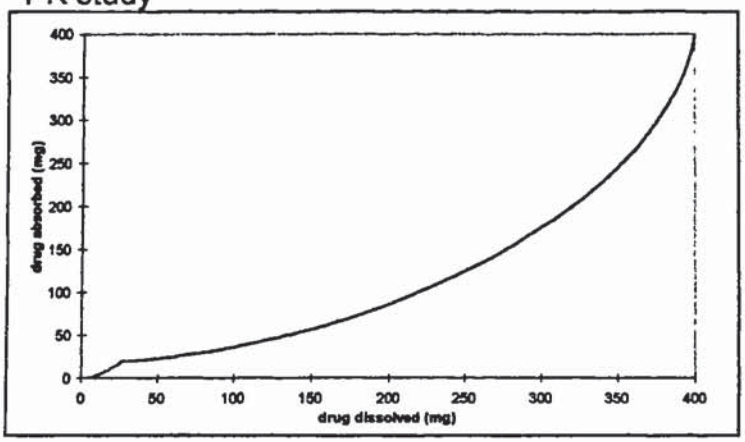

Comments

Straight-line shape of curve indicates the absorption of ibuprofen is dissolution rate-limited.

Figure 8.26
Illustrating the predicted drug plasma conc^{n}/ time profile for ibuprofen/magnesium oxide simulated PK study

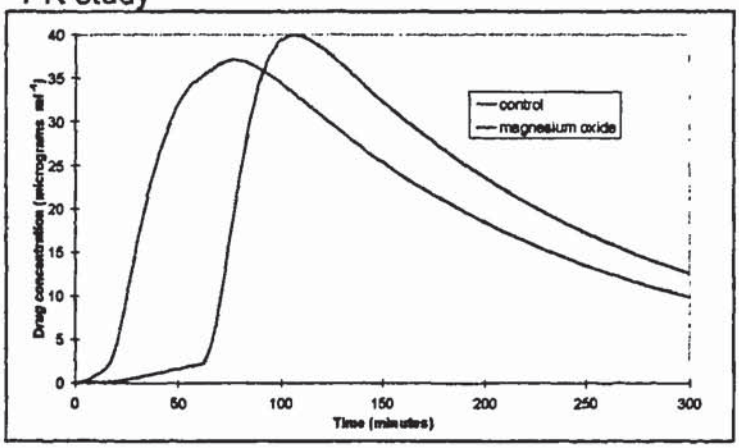

Comments

Model input:
Stomach diss^{n}= 0.0462 (min^{-1})
Intestine diss^{n}= 0.139 (min^{-1})
Stomach perm^{n}= 0.00928 (min^{-1})
Intestine perm^{n}= 0.111 (min^{-1})

Model output: t_{max}= 78 mins

Increased absorption rate due to drug dissolution in the stomach and GE of dissolved drug.

Figure 8.27
Illustration of predicted parameter values during ibuprofen/magnesium oxide simulated PK study

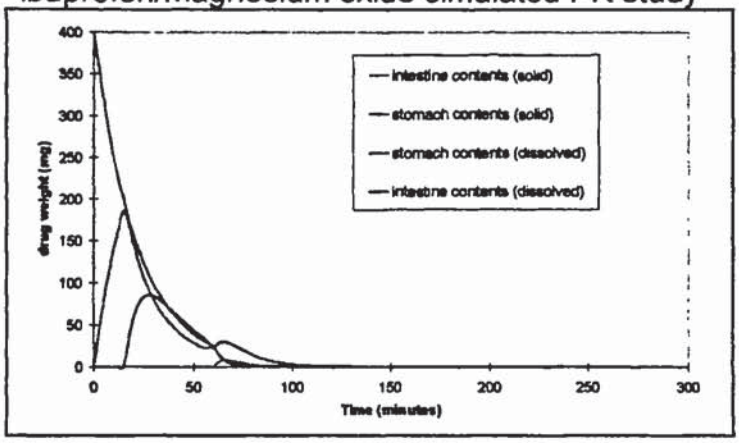

Comments

Drug undergoes increased and almost total dissolution in the stomach. Rapid emptying of the dissolved drug occurs after 16 minutes. Remaining solids are emptied after approximately 1 hour.

Figure 8.28
Illustration of predicted %dissolved/%absorbed relationship during ibuprofen/magnesium oxide simulated PK study

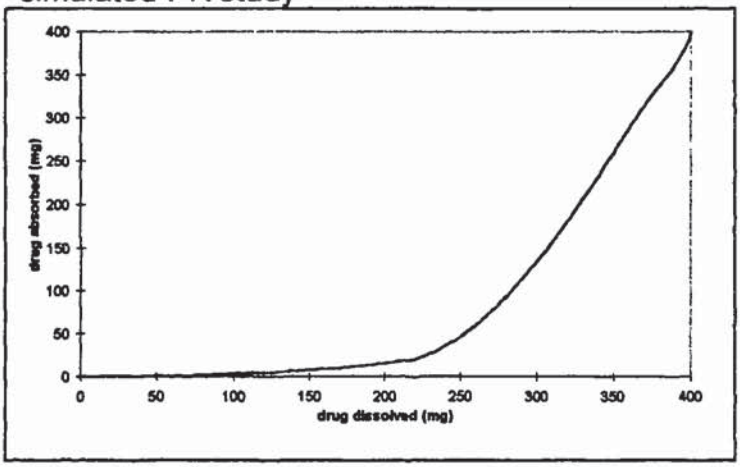

Comments

Bi-phasic relationship, first ≈50% of the drug absorbed with a permeation rate-limiting step and last ≈50% of the drug absorbed with a dissolution rate-limiting step. Corresponds to relatively rapid dissolution in the stomach, compared with slow permeation through the stomach, followed by relatively slow dissolution in the intestine compared to more rapid permeation in the intestine.

Figure 8.29
Illustrating the predicted drug plasma conc^{n}/ time profile for ibuprofen/magnesium hydroxide simulated PK study

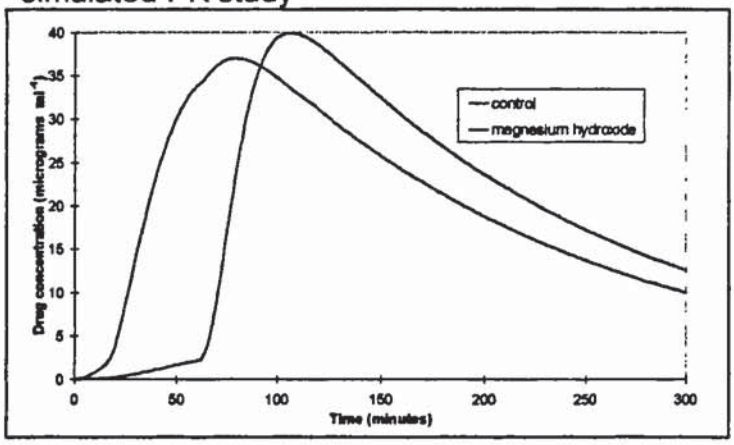

Comments

Model input:
Stomach diss^{n}= 0.0462 (min^{-1})
Intestine diss^{n}= 0.139 (min^{-1})
Stomach perm^{n}= 0.00928 (min^{-1})
Intestine perm^{n}= 0.111 (min^{-1})

Model output: t_{max}= 78 mins

Increased absorption rate due to drug dissolution in the stomach and GE of dissolved drug.

Figure 8.30
Illustration of predicted parameter values during ibuprofen/magnesium hydroxide simulated PK study

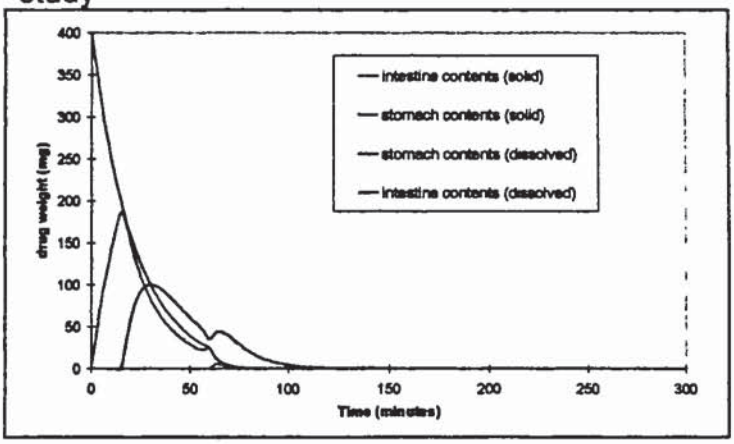

Comments

Drug undergoes increased and almost total dissolution in the stomach. Rapid emptying of the dissolved drug occurs after 16 minutes. Remaining solids are emptied after approximately 1 hour.

Figure 8.31
Illustration of predicted %dissolved/%absorbed relationship during ibuprofen/magnesium hydroxide simulated PK study

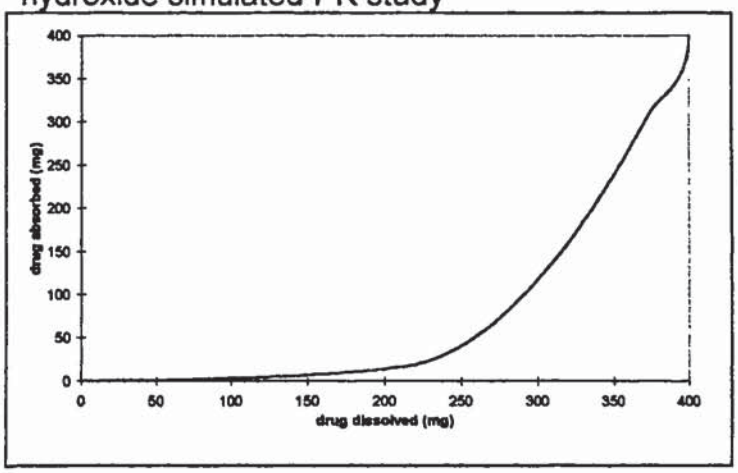

Comments

Bi-phasic relationship, first ≈50% of the drug absorbed with a permeation rate-limiting step and last ≈50% of the drug absorbed with a dissolution rate-limiting step. Corresponds to relatively rapid dissolution in the stomach, compared with slow permeation through the stomach, followed by relatively slow dissolution in the intestine compared to more rapid permeation in the intestine.

Figure 8.32
Illustrating the predicted drug plasma conc^{n}/ time profile for ibuprofen/aluminium hydroxide simulated PK study

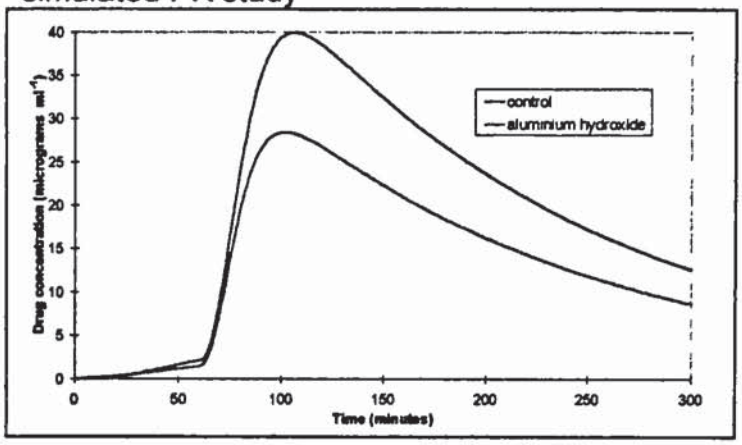

Comments

Model input:
Stomach diss^{n}= 0.277 (min^{-1})
Intestine diss^{n}= 0.173 (min^{-1})
Stomach perm^{n}= 0.00891 (min^{-1})
Intestine perm^{n}= 0.108 (min^{-1})

Model output: t_{max}= 111 mins

Decreased absorption due to maximum dissolution being limited to 70%.

Figure 8.33
Illustration of predicted parameter values during ibuprofen/aluminium hydroxide simulated PK study

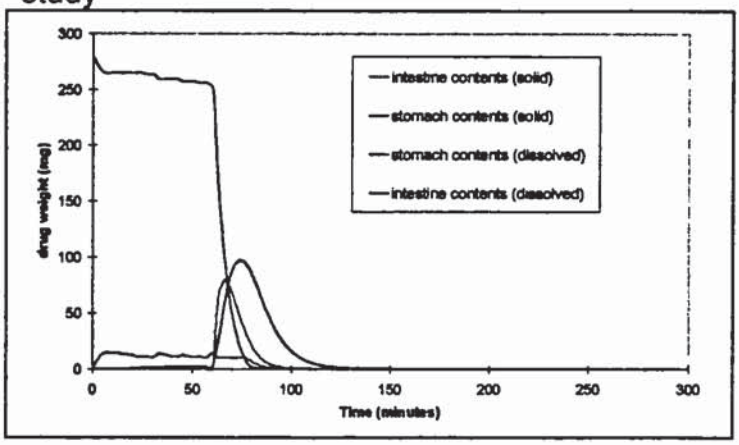

Comments

Drug undergoes minimal dissolution and absorption in the stomach. Onset of phase III of GE cycle leads to transfer of solid drug to the intestine, where dissolution and absorption occur more rapidly.

Figure 8.34
Illustration of predicted %dissolved/%absorbed relationship during ibuprofen/aluminium hydroxide simulated PK study

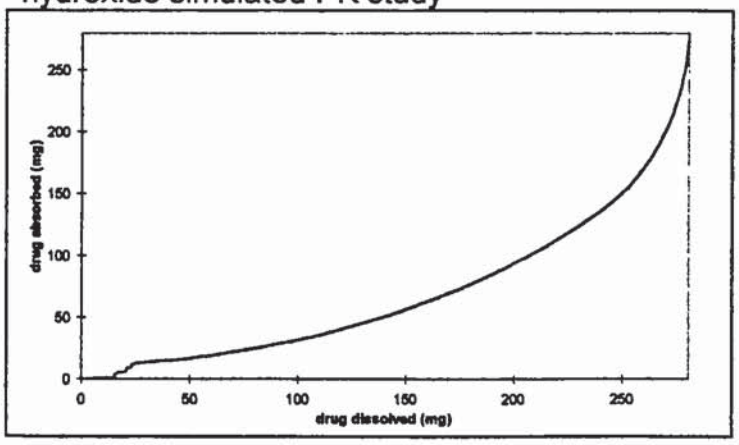

Comments

Straight-line shape of curve indicates the absorption of ibuprofen is dissolution rate-limited.

Figure 8.35
Illustrating the predicted drug plasma conc^{n}/ time profile for ibuprofen/calcium carbonate simulated PK study

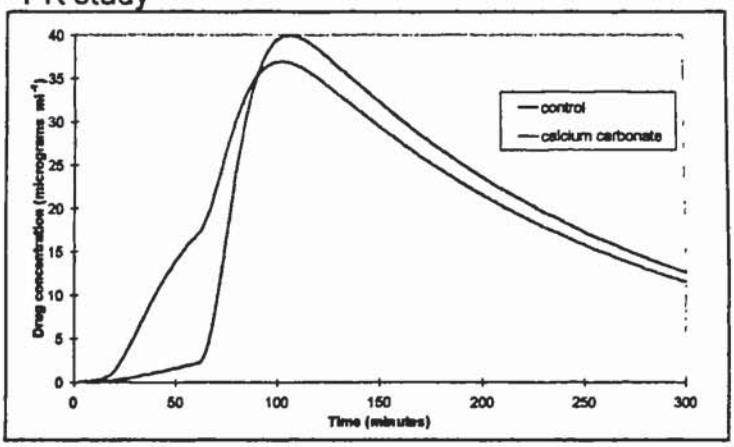

Comments

Model input:
Stomach diss^{n}= 0.0121 (min^{-1})
Intestine diss^{n}= 0.116 (min^{-1})
Stomach perm^{n}= 0.00847 (min^{-1})
Intestine perm^{n}= 0.103 (min^{-1})

Model output: t_{max}= 102 mins

Shoulder appearance a product of slow dissolution in the stomach.

Figure 8.36
Illustration of predicted parameter values during ibuprofen/calcium carbonate simulated PK study

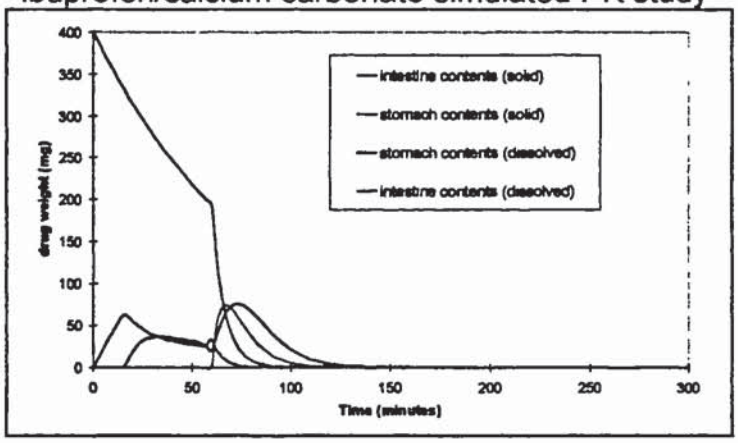

Comments

Drug undergoes slow dissolution and absorption in the stomach. Onset of phase III of GE cycle leads to transfer of solid drug to the intestine, where dissolution and absorption occur more rapidly.

Figure 8.37
Illustration of predicted %dissolved/%absorbed relationship during ibuprofen/calcium carbonate simulated PK study

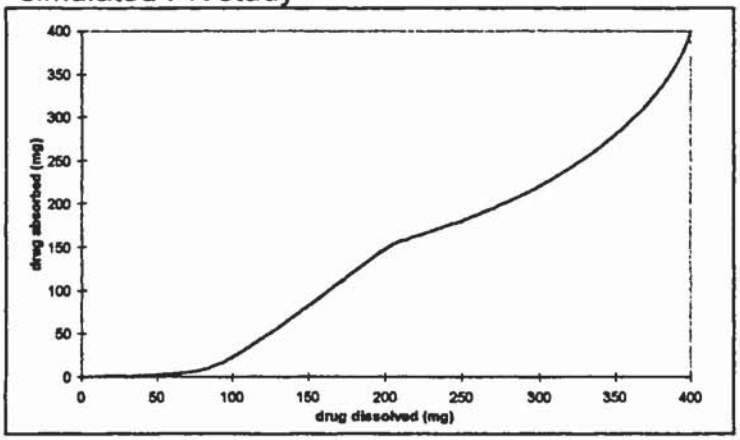

Comments

Straight-line shape of curve indicates the absorption of ibuprofen is dissolution rate-limited.

Figure 8.38
Illustrating the predicted drug plasma conc^{n}/ time profile for ibuprofen/sodium bicarbonate simulated PK study

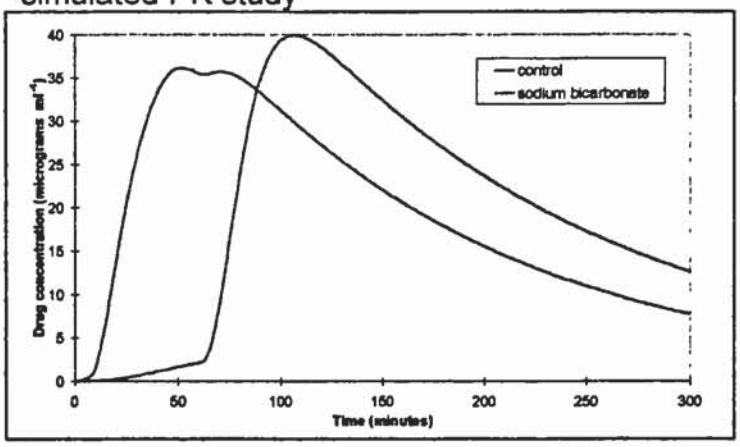

Comments

Model input:
Stomach diss^{n}= 0.063 (min^{-1})
Intestine diss^{n}= 0.346 (min^{-1})
Stomach perm^{n}= 0.00793 (min^{-1})
Intestine perm^{n}= 0.121 (min^{-1})

Model output: t_{max}= 51 mins

Double peak phenomenon observed.

Figure 8.39
Illustration of predicted parameter values during ibuprofen/sodium bicarbonate simulated PK study

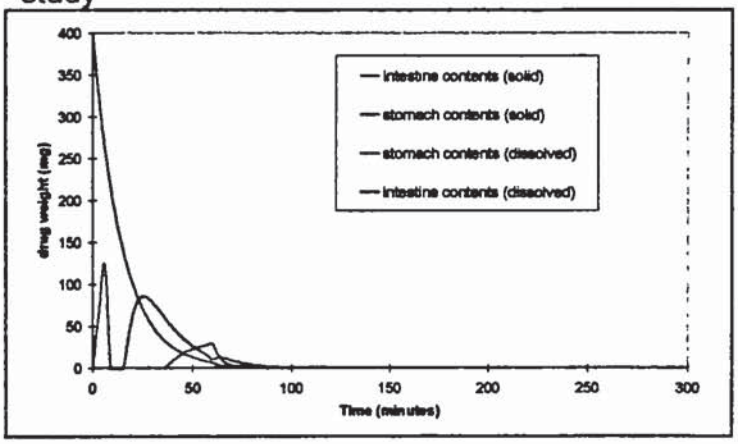

Comments

Drug undergoes increased dissolution in the stomach. Rapid emptying of the dissolved drug occurs after 8 minutes. Onset of phase III of GE cycle leads to transfer of solid/dissolved drug to the intestine, where dissolution and absorption occur more rapidly.

Figure 8.40
Illustration of predicted %dissolved/%absorbed relationship during ibuprofen sodium bicarbonate simulated PK study

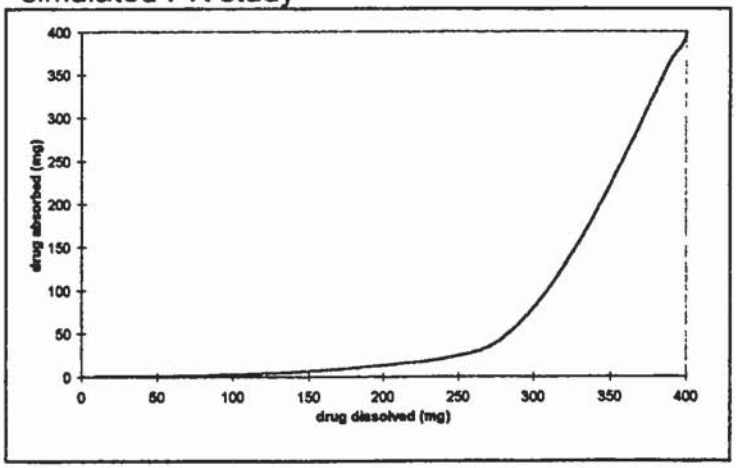

Comments

Bi-phasic relationship, first ≈50% of the drug absorbed with a permeation rate-limiting step and last ≈50% of the drug absorbed with a dissolution rate-limiting step. Corresponds to relatively rapid dissolution in the stomach, compared with slow permeation through the stomach, followed by relatively slow dissolution in the intestine compared to more rapid permeation in the intestine

Figure 8.41
Illustrating the predicted drug plasma conc^{n}/ time profile for ibuprofen formulation 5 simulated PK study

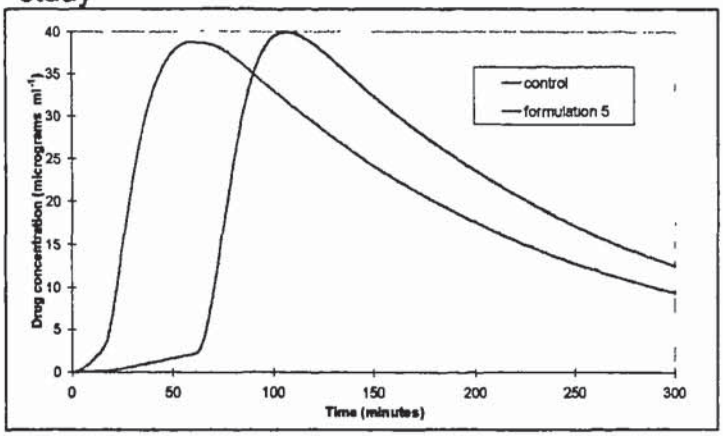

Comments

Model input:
Stomach diss^{n}= 0.0693 (min^{-1})
Intestine diss^{n}= 0.0693 (min^{-1})
Stomach perm^{n}= 0.0102 (min^{-1})
Intestine perm^{n}= 0.146 (min^{-1})

Model output: t_{max}= 60 mins

Increased absorption rate due to drug dissolution in the stomach and GE of dissolved drug

Figure 8.42
Illustration of predicted parameter values during ibuprofen formulation 5 simulated PK study

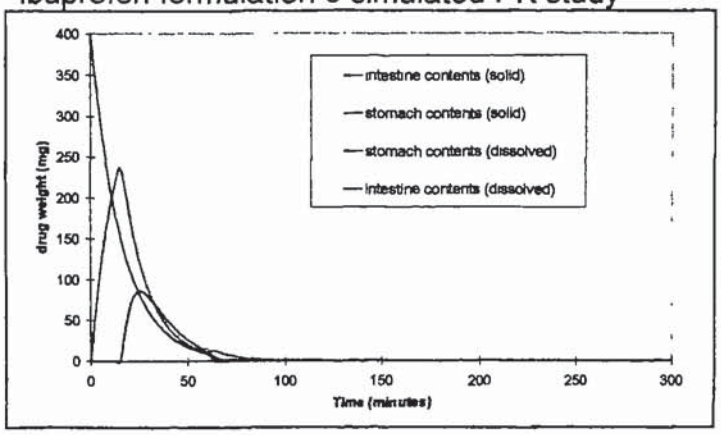

Comments

Drug undergoes increased dissolution in the stomach. Rapid emptying of the dissolved drug occurs after 16 minutes. Onset of phase III of GE cycle leads to transfer of solid/dissolved drug to the intestine, where dissolution and absorption occur more rapidly.

Figure 8.43
Illustration of predicted %dissolved/%absorbed relationship during ibuprofen formulation 5 simulated PK study

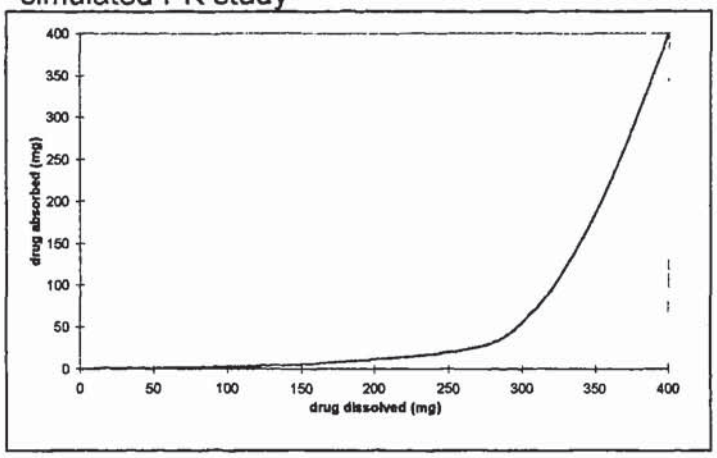

Comments

Bi-phasic relationship, first ≈50% of the drug absorbed with a permeation rate-limiting step and last ≈50% of the drug absorbed with a dissolution rate-limiting step. Corresponds to relatively rapid dissolution in the stomach, compared with slow permeation through the stomach, followed by relatively slow dissolution in the intestine compared to more rapid permeation in the intestine.

From work undertaken in the dissolution study *i.e.*, comparison of Zapp and Panadol® dissolution profiles in the simulated stomach model and, also, under reduced stirring conditions, it has been confirmed that Zapp has a more rapid dissolution rate *in vitro*. Further to this, work under taken at Strathclyde University has demonstrated that the presence of sodium bicarbonate in the stomach increased the gastric emptying rate (O'Mahoney 2000). Analysis of these data, by the author, showed that the lag-time was halved from 12 minutes in the control to 6 minutes in the presence of sodium bicarbonate. Also, the emptying rate was increased by a factor of 1.39. These factors were applied to the GE control data used in this study to produce a comparable GE rate for sodium bicarbonate solutions. It has been stated many times throughout this study that paracetamol absorption is gastric-emptying rate-limiting. However, this statement is based on work using 'standard' commercial formulations, where the formulations contain commonly used excipients and the dissolution characteristics are not extraordinary. Secondly, the excipient content of the formulations was standardised in terms of the effect on gastric emptying rate *i.e.*, excluding specific examples where the formulation does not affect gastric emptying rate. Therefore, the relative influences of the two mechanisms on an increased absorption rate was studied using the model, noting that the use of *in vitro* dissolution data combined with GE data from different literature sources limited the validity of the results obtained. Firstly, the effect of changing dissolution/gastric emptying rate was determined, with GE lag-time set to 16 minutes, which was found under controlled conditions (Oberle *et al.*1990). From the simulations, the predicted t_{max} values were obtained and are illustrated in figure 8.44. From this plot, is can be observed that with this GE lag-time, an increased dissolution rate has very little effect on the absorption rate as measured through the t_{max} value. The absorption rate is modified substantially when the GE rate is altered. Under these 'normal' conditions, the model predicts, correctly, that gastric emptying is the rate-limiting step in paracetamol absorption. The simulation was repeated with the lag-time halved to 8 minutes to simulate the conditions during sodium bicarbonate administration. From the simulations, the predicted t_{max} values were obtained and are illustrated in figure 8.45. Again, it can be observed that with this GE lag-time an increased dissolution rate has very little effect on the absorption rate as measured through the t_{max} value. The absorption rate was modified substantially when the GE rate was altered. Under these conditions, the model

predicted that GE was still the rate-limiting step to paracetamol absorption. It was also observed that if GE rate was increased sufficiently with sufficient decrease in stomach dissolution rate, the 'double peak' phenomena was observed (Mummaneni *et al.* 1995). In this instance this effect was caused by two rapid absorption phases separated by non-absorption phase, with a resultant large increase in time to t_{max}. This may indicate that increased dissolution rate observed in the Zapp product may be useful to ensure complete emptying of the dissolved drug in the liquid phase, under the condition of accelerated GE induced by the Zapp tablets.

Predicted data for the model drugs, alone and during co-administration of the antacids were compared to pharmacokinetic data referenced from literature sources. The co-administration of aluminium hydroxide with ibuprofen datapoint was observed to be an outlier with a much lower predicted t_{max} than observed t_{max}, producing a much lower correlation coefficient. Also, this datapoint was determined using the assumption that aluminium hydroxide does not interfere with the gastric emptying cycle progressing form phase I and II to phase III, which has not been demonstrated. On this basis the datapoint was excluded from the analysis. The correlation between predicted and experimentally obtained t_{max} values was R^2=0.9139, which was extremely statistically significant with $P<0.0001$, as illustrated in figure 8.46. The relationship between the predicted and observed t_{max} was found to fit the equation: y (observed)= 1.44 * x (predicted) - 43.60.

Figure 8.44
Illustrating the predicted effects of changing dissolution/gastric emptying rates on the t_{max} of paracetamol, with gastric emptying lag-time=16 minutes. Red block=Panadol®

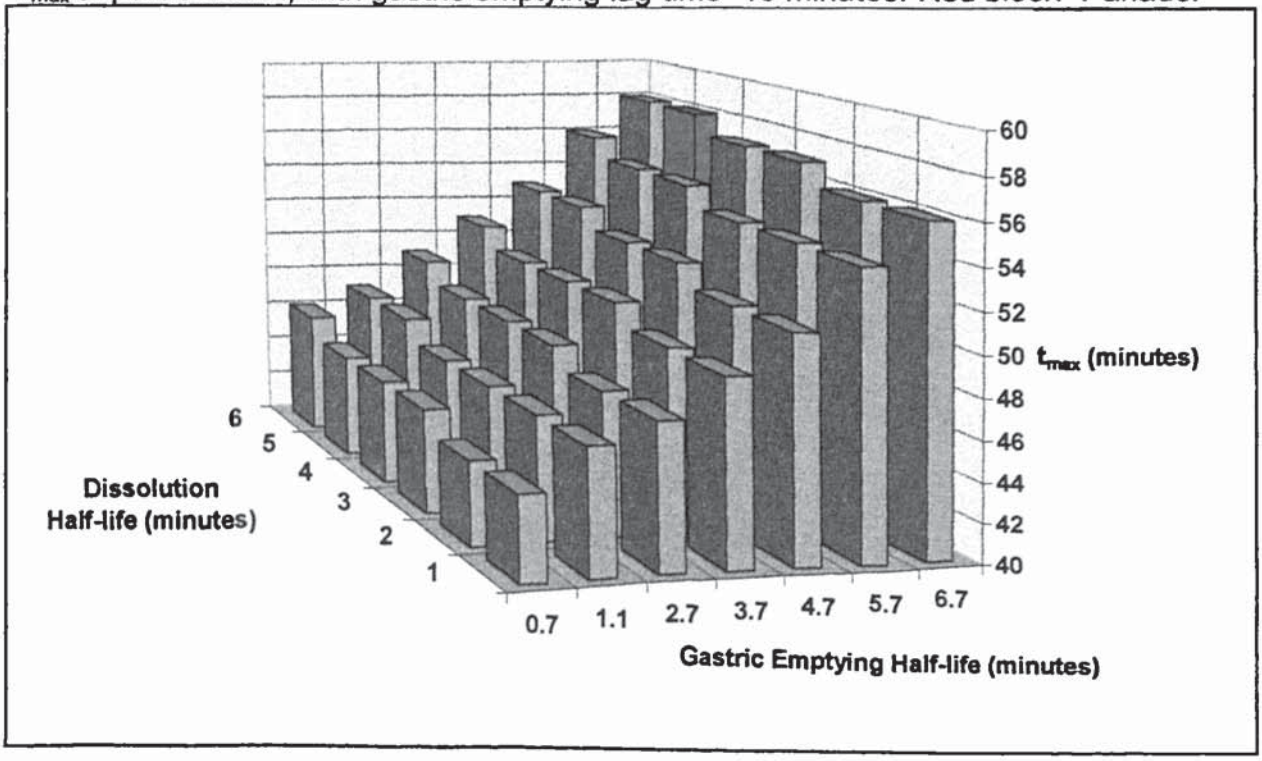

Figure 8.45
Illustrating the predicted effects of changing dissolution and gastric emptying rates on the t_{max} of paracetamol, with gastric emptying lag time set at 8 minutes. Red block=Zapp, yellow blocks indicate the appearance of double peaks (offscale).

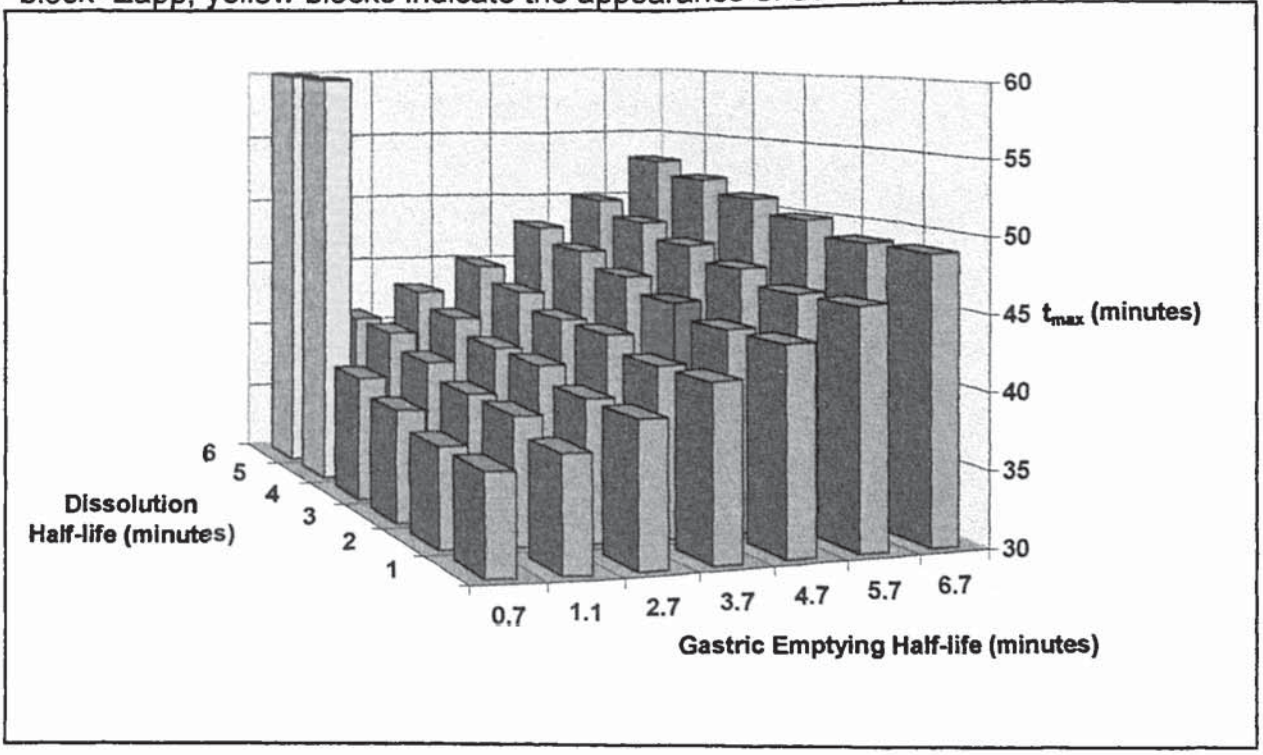

Figure 8.46
Illustrating the correlation between predicted t_{max} values, for each experimental simulation, using the developed model and values referenced from *in vivo* studies. R^2= 0.9139 and Y=1.44*X-43.60

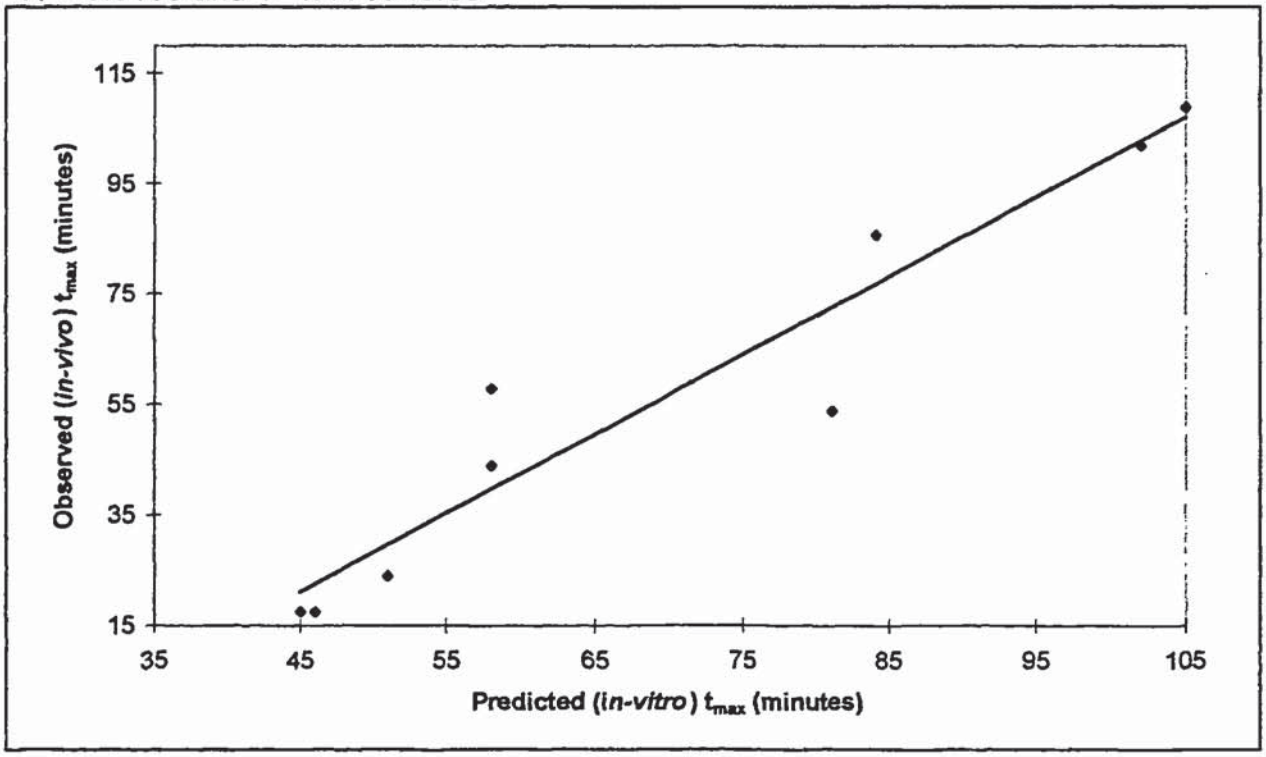

8.4 Summary

- A computer model was developed to simulate drug absorption *via* the oral route. The model was structurally based on the GI anatomy and physiology, with all absorption processes being assigned as first-order. Drug dissolution and permeation values were obtained from the studies conducted in chapters 4 and 6, with solubility limits set as appropriate. Permeation data were transformed to correspond to an absorption half-life, obtained from the literature. The dissolution data was used without transformation. Distribution volumes, gastric emptying and drug elimination rates were referenced from literature sources.
- The model output was designed to be in the form of drug plasma concentration/time profiles, simulating the output from a pharmacokinetic study with t_{max} selected as the measure of drug absorption rate. Key parameter/time data and %absorbed *versus* %dissolution was also generated.
- Limited model validation was conducted, the t_{max} values for both ibuprofen and paracetamol controls were in close agreement with the average of values obtained

from *in vivo* PK studies. Also, the model successfully predicted that the rate-limiting step for paracetamol as absorption (gastric emptying), and dissolution for ibuprofen.

- Parameter values obtained from the simulations predicted that for paracetamol all drug dissolved in the stomach and that a substantial amount (>10%) of drug would be absorbed through the stomach, for the control and in all cases of antacid administration except sodium bicarbonate. The amount absorbed was reduced to 7% for the Zapp tablets and for sodium bicarbonate co-administration, the reduction due to an increase in the GE rate and hence decrease in residence time in the stomach.
- Parameter values obtained from the simulations predicted that for ibuprofen approximately 1% of drug would be absorbed through the stomach, due to very low drug dissolution, where administered alone. The model predicted that co-administration of any antacid would cause a large increase in drug dissolution and hence absorption in the stomach.
- The model predicted that the novel tablet formulation 5 would be superior to a commercial product (Hedex®) in terms of drug absorption rate.
- For all experimental scenarios the predicted %absorbed *versus* %dissolved profiles suggested that paracetamol absorption has an absorption rate-limiting step.
- For ibuprofen, for the control, and aluminium hydroxide or calcium carbonate co-administration the %absorbed *versus* %dissolved profiles demonstrated that drug permeation would be the rate-limiting factor.
- For ibuprofen, the co-administration of magnesium oxide, magnesium hydroxide, sodium bicarbonate, and for formulation 5 the %absorbed *versus* %dissolved profiles demonstrated a hybrid appearance. The relationship appeared to be bi-phasic, with the first ≈50% of the drug being absorbed with a permeation rate-limiting step and the last ≈50% of the drug being absorbed with a dissolution rate-limiting step. These observations correspond to relatively rapid dissolution in the stomach, compared with slower permeation through the stomach, followed by relatively slow dissolution in the intestine compared to faster permeation through the intestine.
- In terms of the rate-limiting step the model predicted that for Panadol® and Zapp increased GE rate would be more significant than increased dissolution rate.

- A simulation modelling paracetamol absorption illustrated that under conditions of increasing GE rate and decreasing dissolution rate the 'double peak' phenomena appeared, the consequence being a large increase in t_{max} .
- The correlation between predicted and experimentally obtained t_{max} values was R^2=0.9139, which was statistically significant with P<0.0001.
- The relationship between the predicted and observed tmax was found to fit the equation:y (observed)= 1.44 * x (predicted) - 43.60.

CHAPTER 9
GENERAL SUMMARY

The main objective of this project was to contribute to the field of IVIVC development, through the production of novel *in vitro* methods and models useful for the characterisation of the different processes contributing to drug absorption. Secondly, an industrial partnership required the study of potential factors which may contribute to the observed rapid absorption of a novel paracetamol tablet formulation containing sodium bicarbonate as an absorption enhancer. The interaction of various antacids with the model drugs, paracetamol and ibuprofen, was selected for study for two reasons, namely the availability of pharmacokinetic data obtained during co-administration, which allowed model development and correlation determination, and the fact that sodium bicarbonate is a commonly used antacid. It was considered that that an opportunity existed for formulation development based on the use of alkalising excipients/antacids in combination with the acidic model drugs. This was undertaken using a systematic approach which included experimental design.

9.1 IVIVC Development

Based on a knowledge of the GI tract, the physicochemical properties of a drug and product formulation characteristics, it was determined that the following factors were required to characterise and model the absorption of drugs delivered *via* the oral route:

- drug dissolution in the stomach environment
- drug dissolution in the intestinal environment
- characterisation of drug diffusion through the mucus layer
- drug permeability in the stomach
- drug permeability in the intestine
- gastric emptying

Methods to study all of these factors, excluding gastric emptying (where data was obtained from literature sources) were therefore developed.

Dissolution methods were developed, based on the USP paddle method at 50 rpm, with dissolution media composition and volumes, and tablet dosing set to correspond with those under *in vivo* conditions. From the study of the dissolution of ibuprofen tablets it was observed that the minimal dissolution in the stomach model for the control was greatly increased during the co-administration of either of the antacids, sodium bicarbonate, calcium carbonate, magnesium oxide or magnesium hydroxide. It was determined that the mechanism of action was likely to be the alkalising nature of the antacids, whereby the increase in solution pH above the pK_a of ibuprofen increased drug solubility. The above antacids were found to marginally increase the dissolution of ibuprofen in the intestine model. For paracetamol in the stomach model, it was observed that the effects of the added antacids were marginal except for magnesium oxide, which reduced the maximum drug dissolved to between 60-70% of dose. In the intestine model both magnesium oxide and aluminium oxide reduced the maximum drug dissolved to between 75-85% of dose. It was postulated that this effect may have been caused by the ability of these antacids to adsorb the drug.

Characterisation of the role of mucus as a barrier to absorption was undertaken using native PGM, using 3-compartment diffusion apparatus. Validation of the mucus in terms of stability and inter-batch variation was undertaken. Mucus was found to be a statistically significant barrier compared to an unstirred aqueous layer for both model drugs. Under conditions modelling the *in vivo* situation the addition of any of the antacids did not alter the lag time or diffusion rate of paracetamol. For ibuprofen the addition of all of the antacids, except aluminium hydroxide, reduced the lag-time. Aluminium hydroxide was observed to effectively eliminate ibuprofen diffusion through the mucus barrier. Calcium carbonate and magnesium hydroxide increased the diffusion rate of ibuprofen through mucus with sodium bicarbonate and magnesium hydroxide acting to reduce the diffusion rate. Considering the results, it was concluded that paracetamol does not interact significantly with mucus over the experimental pH range and further to this neither the vehicle-membrane partition coefficient or the mucus viscosity were altered sufficiently by the additives to produce a measurable change in diffusion rate. A review of the drug and mucus properties indicated the results were as expected. To explain the ibuprofen results the mucus and drug properties were compared. It was concluded that the lag times observed

correlated with a drug/mucus hydrophobic interaction that was eliminated at higher pH's. This hypothesis was confirmed by measuring ibuprofen diffusion rates where the donor and receiver solutions consisted of standardised buffer solutions covering a wide pH range, where a correlation between increasing pH, led to reduced lag-time and increased diffusion rate for ibuprofen. The reduction in diffusion rate observed for the sodium bicarbonate or magnesium oxide experiments could be explained in terms of electrostatic repulsion caused by both the drug and mucus being negatively charged. A mechanism for the increase in ibuprofen diffusion rate in the presence of calcium carbonate was postulated,which was the ability of the antacid to bind to mucin sialic acid residues effectively neutralising the mucus and eliminating electrostatic repulsion.

The study of drug permeability was undertaken with tissue sac methodology being utilised. For the first time directly comparable methods simulating drug transport in stomach and small intestine were devised. The novelty of the methods dictated the requirement for extensive validation. Tissue integrity, stability, selectivity and variability was established as being satisfactory. A relationship between drug permeability and %absorbed in man was apparent. The inclusion of dissolved antacids was observed to have a minor effect on the model drugs permeability, in some instances.

Drug absorption *via* the GI tract was modelled using the developed *in vitro* methods, combined with literature data for gastric emptying, and drug distribution and elimination. The model was utilised to produce computer simulations of drug absorption, generating simulated pharmacokinetic profiles, specific parameter tracking *e.g.*, %dissolved drug in stomach, and drug absorbed/drug dissolved profiles, the latter useful in predicating the rate-limiting step to drug absorption. The model predicted that the novel ibuprofen formulation 5 would be more rapidly absorbed than the current commercial free-acid formulation. Also, the model predicted the rapid absorption of the Zapp formulation. Finally, the relationship between the theoretical and experimental t_{max} data demonstrated a statistically significant correlation.

9.2 Mechanism elucidation of Zapp tablets rapid absorption

Pharmacokinetic studies have shown that the novel paracetamol tablet formulation produced by SB was more rapidly absorbed than a conventional commercial formulation. Methods were developed and utilised in order to characterise the processes responsible for the observed differences.

A dissolution method utilising basket methodology, with modification to control powder dispersal, was developed which assessed the dissolution of drug:excipient powder mixes. By using different media *i.e.*, acidic or neutral dissolution fluid it was possible to elucidate that the sodium bicarbonate excipient in the Zapp tablets significantly increased the dissolution rate of paracetamol and that the mechanism responsible was the generation of carbon dioxide on contact with acidic media, leading to a modification of the hydrodynamics and hence a change in the boundary layer. This was confirmed by a study where Zapp tablets were found to dissolve independently of stirrer rate in a conventional paddle dissolution system, whereas a commercial product demonstrated a decrease in dissolution rate which corresponded to the decrease in paddle speed. It was thus demonstrated that the Zapp tablets underwent more rapid dissolution than the commercial tablets with the differences becoming more apparent as the paddle speed was reduced. It was concluded that the Zapp tablets could be considered 'self-dissolving'. A novel dissolution method for measuring IDR was developed and utilised to demonstrate the effect of dissolved sodium bicarbonate on paracetamol dissolution. The effect was observed to be inhibitory, which was further shown to be due to reduced paracetamol solubility in the excipient containing solution.

Sodium bicarbonate was demonstrated not to significantly alter the transport of paracetamol through either mucus or through the stomach and intestine models.

A literature source highlighted that sodium bicarbonate acted to rapidly increase the gastric emptying rate in humans.

The computer simulation predicted that the increased absorption rate of the Zapp product compared to the commercial product was a consequence of an increased gastric emptying rate rather than an increased dissolution rate. However, a review of the individual profiles obtained during the PK study conducted by SB, comparing Zapp with a commercial product, highlighted the presence of the 'double peak' phenomena in several subjects, leading to a longer time to the t_{max} value. This phenomena was not observed during the administration of the Zapp tablets. This difference can be explained by an increased dissolution rate in the case of the Zapp tablets. It was considered likely that a definitive elucidation of the dominant mechanism can only be obtained by studying the absorption of Zapp tablets containing a radiolabel in a pharmacokinetic study.

9.3 Tablet formulation development

It is known that for acidic drugs an increase in pH above the pK_a increases solubility and hence dissolution rate. This property was used as a strategy in the development of novel tablet formulations.

A systematic approach was adopted to tablet formulation development. This consisted of the selection of common alkalising pharmaceutical excipients which were studied using various methods to determine their suitability. Initially, a screen was undertaken whereby the chosen excipients were combined with the model drugs as simple powder mixes. The dissolution of these mixtures was assessed using the controlled dissolution powder method mentioned previously. This method had the advantage of measuring the effect of each excipient on drug dissolution without interference from factors related to granule and final tablet formulation. The initial screen indicated several excipients were suitable as dissolution promoters, for both drugs, in-line with expectations based on alkalising properties.

A study of model drug solubility and IDR in excipient containing solutions and at various pH values, combined with viscosity measurement of these solutions was undertaken. Analysis of the relationship between these parameters yielded two interesting observations. Firstly, it was noted that as previously stated, sodium bicarbonate in solution reduced the solubility and hence IDR of paracetamol and that

the pH of sodium bicarbonate solutions was below the pK_a of paracetamol. Therefore, it was considered that an opportunity existed for improving the dissolution rate observed with the Zapp formulation by the inclusion of an alkalising agent with a solution pH above the pK_a of paracetamol. It was postulated that this product design would utilise two mechanisms, increased drug solubility and increased agitation, whereas Zapp has been found to only utilise the latter mechanism. Several granule formulations were produced containing various ratios of sodium bicarbonate and L-arginine. It was found that an equal mixture of the two excipients produced more rapid paracetamol dissolution than sodium bicarbonate alone, supporting the hypothesis. The same physicochemical studies were performed with ibuprofen as the model drug. The analysis of the relationship between the various properties yielded an interesting result, when potassium bicarbonate or sodium bicarbonate were the excipient under test, it was observed that the IDR was not as high as predicted and it was hypothesised that this was probably due to reduced penetration of the alkalising agent into the boundary layer surrounding the dissolution drug particle. It was demonstrated that several alkalising excipients increased the dissolution rate of ibuprofen, by increasing the solution pH above the pK_a of the drug. Two excipient candidates, tri-sodium phosphate and sodium bicarbonate were selected. Combinations of the excipients were processed with ibuprofen to form granules. Dissolution studies conducted using the controlled powder dissolution method demonstrated all mixtures to have faster dissolution rates than a lactose containing control. On the basis of this preliminary work final tablet formulations containing the two excipients, individually and as mixtures, were prepared. Physical and chemical analysis showed the tablets would meet the USP and BP specifications for tablets except for tablets containing predominately tri-sodium phosphate, which contained large residues of moisture. It was concluded that tablets containing sodium carbonate would be most suitable due to low moisture, friability, combined with the excipient being the more basic of the two under test. Stability studies indicated all formulations were generally stable from both a chemical and physical perspective.

9.4 Future Work

The developed IVIVC model is limited in that only two drugs, combined with their interactions with co-administered antacids were studied. To improve the value of the model requires the generation of more datapoints to improve and understand the correlation between model output and PK data. Several other drugs were processed through the permeability models as part of the validation of these methods. The processing of these drugs through the dissolution models would generate several more data-sets for inclusion within the IVIVC model. Further to this work could be undertaken to determine the contribution of the muscle layer to the membrane barrier in the permeability models. The integrity of permeability models has been demonstrated, further work could be undertaken to assess the tissue viability and therefore the suitability of these methods to the assessment of drugs where active transport mechanisms are important.

For the Zapp project, potassium bicarbonate has been shown to exhibit similar properties to sodium bicarbonate in terms of acting as a dissolution promoter of paracetamol. The development of a product containing this excipient, alone and in combination with sodium bicarbonate, is worthy of investigation, to reduce/eliminate the loading of sodium in the formulation. Of the aspects studied *in vitro* sodium bicarbonate was only demonstrated to significantly affect the dissolution rate of paracetamol. Other workers have shown that GE is also modified by this excipient. A PK study using radiolabelled tablets may be required to definitively elucidate the contribution of each mechanism to the rapid absorption observed in Zapp tablets.

The tablet formulation development study introduced a rational stepwise progression of assessment for product development, whereby excipient/drug interactions could be investigated initially without formulation factor considerations. This approach may have general uses. The use of alkalising excipients as dissolution modifiers could be investigated for other drug candidates. The developed formulations have been demonstrated to be superior to current commercial products in terms of absorption and also to be stable during storage. They may be suitable for commercial development.

REFERENCES

Abernathy, D.R. and Greenblatt, D.J. "Ibuprofen disposition in obese individuals". *Arthritis Rheum.,* 1985, 28, 1117-21

Albert, K.S. and Gernaat, C.M. "Pharmacokinetics of ibuprofen". *Am. J. Med.*, 1984, July, 40-46

Albin, H., Demotes-Mainard, F., Vincon, G., Bedjaoui, A. and Begaud, N. "Effect of two antacids on the bioavailability of paracetamol". *Eur. J. Clin. Pharmacol.*, 1985, 29, 251-253

Allen, A. and Snary, D. "The structure and function of gastric mucus". *Gut,* 1972, 13, 666-672

Altomare, E., Vendemiale, G., Benvenuti, C. and Andreatta, P. "Bioavailability of a new effervescent tablet of ibuprofen in healthy volunteers". *Eur. J. Clin. Pharmacol.*, 1997, 52, 505-506

Ameer, B., Divoll, M., Abernethy, D.R., Greenblatt, D.J and Shargel, L. "Acetaminophen bioavailability". *J. Clin. Pharmacol.*, 1982, 4, A1

Ameer, B., Divoll, M., Abernethy, D.R., Greenblatt, D.J and Shargel, L. "Absolute and relative bioavailability of oral acetaminophen preparations". *J. Pharm. Sci.*, 1983, 72, 955-958

Amidon, G.L., Lennernas, H., Shah, V.P. and Crison, J.R. "A theoretical basis for a biopharmaceutic drug classification system: The correlation of *in vitro* drug product dissolution and *in vivo* bioavailability". *Pharm. Res.*, 1995, 12, 413-420

Ansel, H.C., Popovich, N.G., Allen, L.V. *Pharmaceutical dosage forms and drug delivery systems.* 6th ed. USA: Williams & Wilkins, 1995.

Armstrong, N.A. and James, K.C. *Pharmaceutical Experimental Design and Interegation.* 1st Ed. London: Taylor and Francis Ltd, 1996.

Artursson, P. "Epithelial transport of drugs in cell culture. 1: A model for studying the passive diffusion of drugs over intestinal absorptive (Caco-2) cells". *J. Pharm. Sci.*, 1989, 79, 476-482

Artursson, P. and Magnusson, C. "Epithelial transport of drugs in cell culture. 2: Effect of extracellular calcium concentration on the paracellular transport of drugs of different lipophilicities across monolayers of intestinal epithelial (Caco-2) cells". *J. Pharm. Sci.*, 1990, 79, 595-600

Artursson, P., Ungell, A. and Lofroth, J. "Selective paracellular permeability in two models of intestinal absorption: cultured monolayers of human intestinal cells and rat intestinal segments". *Pharm. Res.*, 1993, 10, 1123-1129

Aulton, M.E. Pharmaceutics - *The science of dosage form design.* 1st ed. Hong Kong: Churchill Livingstone, 1988. pp62-80, pp304-321

Bagnall, W. E., Kelleher, J., Walker, B.E. and Losowsky, M.S. "The gastrointestinal absorption of paracetamol in the rat". *J. Pharm. Pharmacol.*, 1979, 31, 157-160

Baichwal, M.R., Deshpande, S.G. and Shetty, U.C. "Comparative evaluation of four dissolution apparatus", *Drug Dev. Ind. Pharm* ,1985, 11, 1639-1656

Bansil, R., Stanley, E. and Lamont J.T. "Mucin Biophysics". *Annu. Rev. Physiol.*, 1995, 57, 635-657

Barranco, S.C., Townsend, C.M. and Casartelli, C.C. "Establishment and characterisation of an *in vitro* model system for human adenocarcinoma of the stomach". *Cancer Res.* 1983, 43, 1703-1709

Barry, G. "Structure, biochemistry and assembly of epithelial tight junctions". *Am. J. Physiol.*, 1987, 22, C749-C758

Barry, R.E. and Behrendt, W.A. "Studies on the pharmacokinetics of fluorescein and its dilaurate salt ester under the conditions of the fluorescein dilaurate test". *Arzneimittelforschung*, 1985, 35, 644-8

Barthe, L., Woodley, J.F., Kenworthy, S. and Houin, G. "An improved everted gut sac as a simple and accurate technique to measure paracellular transport across the small intestine". *Eur. J. Drug Metab.*, 1998, 23, 313-323

Bhaskar, R. K., Gong, D., Bansil, R., Pajevic, S., Hamilton, J.A., Turner, B.S. and Lamont, J.T. "Profound increase in viscosity and aggregation of pig gastric mucin at low pH". *Am. J. Physiol.*, 1991, 261, G827-32

Bhaskar, R.K., Garik, P., Turner, S.T., Bradley, J.D., Bansil, R., Stanley, H.E. and Lamont T.J. "Viscous fingering of HCl through gastrin mucin". *Nature,* 1992, 360, 458-461

Bhat P.G., Flanagan D.R., and Donovan M.D. "The limiting role of mucus in drug absorption: drug permeation through mucus solution". *Int. J. Pharm.*, 1995, 126, 179-187

Bickel, M. and Kauffman, G.L. "Gastric gel mucus thickness: 16,16-dimethyl prostaglandin E2 and carboxolone". *Gastroenterology*, 1981, 80, 770-775

Blume, H., Ali, S. H., Elze, M., Kramer, J., Wendt, G. and Scholz, M. E. "Relative bioavailability of paracetamol in suppositories preparations in comparison to tablets". *Arzneimittelforscchung.*, 1995, 44, 1333-1338

Borin , M. T. and Ayres, J. W. "Single dose bioavailability of acetaminophen following oral administration". *Int. J. Pharm.,* 1989, 54, 199-209

Bottenberg, P., Cleymaet, R., Munyck, C., Remon., J.P., Coomans, D., Michotte, Y. and Slop, D., "Comparison of salivary fluoride concentrations after administration of a bioadhesive slow release tablet and a conventional fluoride tablet". *J. Pharm, Pharmacol.*, 1992, 44, 684-686

Bouckaert, S. and Remon, J.P. "*In vitro* bioadhesion of a buccal miconazole slow release tablet". *J. Pharm. Pharmacol.* 1993, 45, 504-507

Braybrooks, M.P., Barry, B.W. and Abbs, E.T. "The effect of mucin on the bioavailability of tetracycline from the gastrointestinal tract: *in vivo in vitro* correlations". *J. Pharm. Pharmacol.*, 1974, 27, 508-515

British National Formulary. 30th ed. London: The Pharmaceutical Press 1995

Bruna, P., Leneveu, A., Abou Chacra, M.L., Delhotal, B., Chauveau, F. and Flouvat, B. "Acetaminophen flashtab formulation: Fast disintegration and optimal absorption of the active ingredient". *Proceed. Int'l. Symp. Control. Rel. Bioact. Mater.*, 1998, 25, 938-939

Budvari, S. *The Merck Index*. 12th ed. NJ. USA: Merck Research Laboratories 1996

Burlinson, H. *Tablets and Tabletting*. 1st Ed. UK: Morrison and Gibb, 1968, pp19-45

Cardot, J.M., and Beyssac, E. "*In vitro-in vivo* correlations - scientific implications and standardisation". *Eur. J. Drug Metab. Pharmacokin.*, 1993, 18, 113-120

Chakrabarti, S. and Southard, N.Z. "Control of soluble drug dissolution in conditions simulating the intestinal tract flow. 2. Cocompression of drugs with buffers". *J. Pharm. Sci.*, 1997, 86, 465-469

Charles, B.G. and Mogg, G.A.G. "Comparative *in vitro* and *in vivo* bioavailability of naproxen from tablet and caplet formulations". *Biopharm. Drug. Dispos.*, 1994, 15, 121-128

Cheng, H., Rogers, J.D., Demetriades, J.L., Holland, S.D., Seibold, J.R. and Depuy, E. "Pharmacokinetics and bioinversion of ibuprofen enantiomers in humans". *Pharm. Res.*, 1994, 11, 824-830

Clements, J.A., Nimmo, W.S., Heading, R.C. and Prescott, L.F. "Kinetics of acetaminophen absorption and gastric emptying in man". *Clin. Pharmaco. Ther.*, 1978, 24, 420-431

Clements, J.A., Critchley, J.H. and Prescott, L.F. "The role of sulphate conjugation in the metabolism and disposition of oral and intravenous paracetamol in man". *Br. J. Clin. Pharmaco.*, 1984, 18, 481-485

Cruickshank, J.M. "The clinical importance of cardioselectivity and lipophilicity in beta-blockers" *Am. Heart J.*, 1980, 100, 160-178

Curtis, G.H. and Gall, F.G. "Macromolecular transport by rat gastric mucosa", *Am. J. Phys.* 1992, 262, G1033-G1040

Dash, B.H., Blank R.G., Schachtel, B.P. and Smith A.J. "Ibuprofen tablets dissolution *versus* bioavailability". *Drug Dev. Ind. Pharm.*, 1988, 14(11), 1629-1645

Davies, N.M. "Clinical pharmacokinetics of ibuprofen: The first 30 years". *Clin Pharmacokinet.*, 1998, 32, 101-154

Desai, M.A. and Vadgama, P.M. "Bicarbonate and other buffer systems can enhance the rate of hydrogen ion diffusion through mucus *in vitro*". *Biochimica et Biophysica Acta*, 1992, 1116, 43-49

Diamond, J. "The epithelial junction:bridge, gate and fence". *Physiologist*, 1977, 20, 10-18

Dighe, S.V. and Adams, W.P. "Bioequivalence: A United State Regulatory Perspective": In Welling, P.G., Tse, F.L. and Dighe, S.V. (ed.) *Pharmaceutical equivalence.* 1st ed. New York, USA: Marcel Dekker, 1991. Drugs and pharmaceutical sciences, Vol 48

Divoll, M., Greenblatt, D.J., Ameer, B. and Abernethy, D.R. "Effect of food on acetaminophen absorption in young and elderly subjects". *J. Clin. Pharmacol.*, 1982, 22, 571-576

Dorlars, D., Schilling, D. and Riemann, J.F. "The place of ultrasonography in the assessment of abnormal gastric-motility". *Dtsch. Med. Wochenschr*, 1994, 119, 575-680

Dougall, J.R., Cunningham, B. and Nimmo, W.S., 1983, "Paracetamol absorption from Paramax, Panadol and Solpadeine". *Br. J. Clin. Pharmacol.,* 1983, 15, 487-489

Dressman, J.B., Amidon G.L., Reppas, C. and Shah, V.P. "Dissolution testing as a prognostic tool for oral drug absorption: immediate release dosage forms". *Pharm. Res.,* 1998, 15,11-22

Eichman, J.D., Yassin, A.E.B. and Robinson, J.R. "The influence of *in vivo* carbonation on GI physiological processes and drug permeability". *Eur. J. Pharm. Biopharm.*, 1997, 44, 33-38

El-Sayed, Y.M., Gouda, M.W., Al-Khamis, K.I., Al-Meshal, M.A., Al-Dhawailie, A.A., Al-Rayes, S., Bin-Salih, S.A. and Al-Rashood, K.A. "Comparative bioavailability of two tablet formulations of ibuprofen". *Int. J. Clin. Pharmacol. Ther.*, 1995, 33, 294-298

Feinroth, M., Feinroth, M.V. and Berlyne, G.M. "Aluminium absorption in the rat everted gut sac". *Mineral Electrolyte Metab.*, 1982, 8, 29-35

Florence A.T. and Attwood D. *Physiochemical principles of pharmacy.* 1st ed. Basingstoke: Macmillan Press, 1988.

Florey, K. *Analytical profiles of drugs* - volume 3. 1st ed. USA: Academic Press, 1974.

Forrest, J.A.H., Clements, J.A. and Prescott, L.F., "Clinical pharmacokinetics of paracetamol". *Clin Pharmacokinet.*, 1982, 7, 93-107

Forstner, J.F. and Forstner, G.G., "Calcium binding to intestinal goblet cell mucin", *Biochimica et Biophysica Acta*, 1975, 386, 283-292

Fritz, A.K., Benziger, D.P., Peterson, J.E., Park, G.B. and Edelson, J. "Relative bioavailability and pharmacokinetics-a combination of pentazocine and acetaminophen". *J. Pharm. Sci.*, 1984, 73, 326-331

Gazzaniga, A., Gianesello, W., Stroppolo, F. and Vigano, L. "Water soluble analgesic ibuprofen formulation - contains L-arginine and sodium bicarbonate to reduce gastric irritation". 1988, Patent GB2193039

Geisslinger, G., Dietzel, K. and Bezler, H. "Therapeutically relevant differences in the pharmacokinetic and pharmaceutical behaviour of ibuprofen lysinate as compared to ibuprofen acid. *Int. J. Clin. Ther. Toxicol.*, 1989, 27, 324-328

Gershanik, T., Benzeno, S. and Benita, S. "Interaction of a self-emulsifying lipid drug delivery system with the everted rat intestinal mucosa as a function of droplet size and surface charge", *Pharm. Res.* 1998, 15, 863-869

Ghosh, L.K., Ghosh, N.C., Chatterjee, M. and Gupta, B.K. "Product development studies on the tablet formulation of ibuprofen to improve bioavailability". *Drug Dev. Ind. Pharm.* 1988, 24, 473-477

Gillespie, W., Disanto, A., Monovich, R. and Albert, K. "Relative bioavailability of commercially available ibuprofen oral dosage forms in humans". *J. Pharm. Sci.*, 1982, 71,1034-38

Ginski, M.G. and Polli, J.E. "Prediction of dissolution-absorption relationships from a dissolution/Caco-2 system". *Int. J. Pharm.*, 1999, 177, 117-125

Goddard, A.F. and Spiller, R.C. "*In vitro* assessment of gastric mucosal transfer of anti-*helicobacter* therapeutic agents". *Antimicrob. Agents Chemother.*, 1997, 41, 1246-1249

Goodman Gilman, A., Rall, T.W., Nies, A.S. and Taylor, *Goodman and Gilman's The Pharmacological Basis of Therapeutics*. 8th Ed. Singapore: Mcgraw-Hill, 1992, p1669

Gordon, R.E., Rosanske, T.W., Fonner, D.E., Anderson, N.R. and Banker, G.S. Granulation technology and tablet characterisation: in Lierberman, H.A., Lachman, L. and Schwartz, J.B. (ed.) *Pharmaceutical Dosage Forms: Tablets:* volume II. 2nd ed. USA:Marcel Dekker, 1990

Gramatte, T. and Richter, K. "Paracetamol absorption from different sites in the human small intestine ". *Br. J. Clin. Pharmacol.*, 1993, 37, 608-611

Grattan T.J., Hickman, R.A., Darby-Dowman, A., Hayward, M.A., Boyce, M.J. and Warrington, S. "A pilot biostudy to investigate the pharmacokinetics of acetaminophen (paracetamol) from two commercially available acetaminophen products and three development formulations containing acetaminophen in combination with sodium bicarbonate or calcium carbonate" *Eur. J. Pharm. Biophar.*, 2000, 43, 225-229

Grubel. P. and Cave D.R. "Factors affecting solubility and penetration of clarithromycin through gastric mucus". *Aliment. Pharmacol. Ther.*, 1998, 12, 569-576

Gugler, G. and Allgayer, H. "Effects of antacids on the clinical pharmacokinetics of drugs: an update". *Clin. Pharmacokinet.*, 1990, 18, 210-219

Gumbier, B., Stevenson, B. and Grimaldi, A.J. "The role of cell adhesion molecule uvomarulin in the formation and maintenance of the epithelial junction complex". *Cell Biol.*, 1988, 107, 1575-1587

Hannula, A.M., Marvola, M., Rajamaek, M. and Ojantakanen, S. "Effects of pH regulators on the bioavailability of ibuprofen from hard gelatin capsules". *Acta Pharm. Fenn.*, 1990, 7, 221-7

Harasawa , S., Kikuchi, K., Senoue, I., Nomiyama, T. and Miwa, T. "Gastric emptying in patients with gastric ulcers: effects of oral and intramuscular administration of anticholinergic drug". *Tokai J. Exp. Clin. Med.*,1982,7, 551-559

Heading, R.C.,Tothill, P., Mcgloughlin G.P., and Shearman D.J.C. "Gastric emptying rate measurement in man. A double isotope scinti-scanning technique for the simultaneous study of liquid and solid components of a meal". *Gast.* , 1976, 71, 45-50.

Heading, R.C., Nimmo L.F., Prescott L.F., and Tothill P. "The dependence of paracetamol absorption on the rate of gastric emptying". *Br. J. Pharmacol.*, 1973, 47, 415-421

Healy, A.M and Corrigan O.I. "The influence of excipient particle size, solubility, and acid strength on the dissolution of an acidic drug from two-component compacts". *Int. J. Pharm.*, 1996, 143, 211-221

Heatley N.G. "Mucosubstance as a barrier to diffusion". *Gastroenterol.*, 1959, 37, 313-317

Hendriksen, B.A. "Characterization of calcium fenoprofen - 1. Powder dissolution rate and degree of crystallinity". *Int. J. Pharm.*, 1990, 60,243-252

Herzfeldt, C.D. and Kummel, R. "Dissociation constants, solubilities and dissolution rates of some selected non-steroidal anti-inflammatories", *Drug Dev. Ind. Pharm.*, 1983, 9, 767-93

Holbrook, P.A. *Biological barriers to the nasal delivery of peptide drugs*. PhD Thesis, 1991, University of Aston in Birmingham,

Holt, S., Heading R.C., Carter, D.C., Prerscott, L.F. and Tothill, P."Effect of gel fibre on gastric emptying and absorption of glucose and paracetamol". *Lancet,* 1979, I, 636-639

Hong, Z., Li, Z., Wang, Y., Li, L., Quiang, W., Wang, M. and Zou, J. "Pharmacokinetics and bioavailability study on acetaminophen oral drop in healthy volunteers". *Hua Hsi I Ko Ta Hsueh Hsueh Pao.*, 1994, 25, 410-413

Hughes, J.A., Avrutskaya, A.V., Brouwer, K.L.R., Wickstrom, W. and Juliano, R.L. "Radio-labelling of methylphoshonate and phosphorothioate oligonucleotides and evaluation of their transport in everted rat jejunum sacs". *Pharm. Res.* 1995, 12, 817-824

Huisman, R., van Kamp, H.V., Weyland, J.W., Boornbos, D.A., Bolhuis, G.K. and Lerk. "Development and optimisation of pharmaceutical formulations using a simple lattice design". *Pharm. Weekbl.* [*Sci.*] , 1984, 6, 185-194

Hunt, J.N. The regulation of gastric emptying: in Friedman, M.H.F (ed.*), Functions of the Stomach and Intestine.* 1st ed. U.K: HM+M, 1975,

Iqbal, N., Ahmed, B., Hussain-Janbaz, A., Hassan-Gilant, A. and Khan-Niazi, S. "The effect of caffeine on the pharmacokinetics of acetaminophen in man". *Biopharm. Drug. Dispos.*, 1995, 16, 481-87

Ishii, K., Saitou, K., Yamada, R., Ital, S. and Nemoto, M. "Novel approach for determination of correlation between *in vivo* and *in vitro* dissolution using optimisation technique". *Chem. Pharm. Bull.*, 1996, 44, 1550-1555

Iwuagwu, M.A., and Aloko K.S. "Adsorption of paracetamol and chloroquinine phosphate by some antacids". *J. Pharm. Pharmacol.*, 1992, 44, 655-658

Jackson, M.J. in Johnson L.R. ed. *Physiology of the gastrointestinal tract,* 2nd ed. New York: Raven Press, 1987

Jaehde, U., Goto, T., Deboer, A.G. and Breimer, D.D. "Blood-brain-barrier transport rate of quinolone antibacterials evaluated in cerebrovascular endothelial cell culture". *Eur. J. Pharm. Sci.*, 1993,1, 49-55

Jamali, F., Singh, N., Pasutto, F.M., Russel, A.S. and Coutts, R.T. "Pharmacokinetics of ibuprofen enantiomers in humans following oral administration of tablets with different absorption rates". *Pharm. Res.* 1988, 5, 40-43

James, K.C. *Solubility and related properties.* 1st ed. USA: Marcel Dekker 1986 pp395-403, Drugs and the pharmaceutical sciences volume 28

Johnson, L.R, *Gastrointestinal physiology.* 4th ed. USA: Mosby Year Book ,1991, pp23-83

Karlsson, J., Wikman, A. and Artursson, P., "The mucus layer as a barrier to drug absorption in monolayers of human intestinal epithelial HT29-h goblet cells". *Int. J. Pharm.*, 1993, 99, 209-218

Kearney, P. and Marriott, C. "The effects of mucus glycoproteins on the bioavailability of tetracycline. I. Dissolution rate". *Int. J. Pharm.,* 1986, 28, 33-40

Kelly, K.A., Code, C.F. and Elveback, L.R. "Patterns of canine gastric electrical activity". *Amer. J. Physiol.,* 1969, 217, 461-470

Kleinblesem, C. H., Ouwerkerk, M., Spitnagel, W., Wilkinson, F.E. and Kaiser R.R. *Arzneimittelforschung.*, 1995, 45, 1117-21

Koizuma, F., Ebina, H., Kawamura, T., Ishimori, A. and Satoh, M. "Relationship between plasma acetaminophen concentrations measured by fluorescence polarisation immunoassay and gastric emptying in men". *Jap. J. Gastroenterol.*, 1988, A85, 2559-2562

Koizumi, F., Kawamura, T., Ishimori, A., Ebina, H and Satoh, M., "Plasma paracetamol concentrations measured by fluorescence polarisation immunoassay and gastric emptying time". *Tohuku J. Exp. Med.*, 1988, B155, 159-164

Krieger, D.J. "Liquid chromatographic determination of acetaminophen in tablets - collaborative study ". *Assoc. Off. Anal. Chem.*, 1987, 70,212

Larhed, A.W, Artursson, P. and Bjork, E. "The influence of intestinal mucus components on the diffusion of drugs". *Pharm. Res.*, 1998, 15, 66-71

Lenhard, G., Kieferndorf, U., Berner, G., Engels, B. and Vogtlejunkert, U. "Pharmacokinetics and bioequivalence of 2 ibuprofen preparations". *Arzneimittelforscchung.*, 1990, 40, 1358-1362

Letley, E., Fowle, A.S.A., Whiteman, P. and Land, G., "Plasma paracetamol profile following oral administration of paracetamol tablets". *Edizone Pratica.*, 1980, 35, 571-574

Levet-Trafit, B., Gruyer, M., Marajanovic, M. and Chou, R.C. "Estimation of oral drug absorption in man based on intestine permeability in rats". *Life Sciences*, 1996, 58, PL359-363

Levet-Trafit, M.S., Gruyer, M.M. and Chou, R.S. "Estimation of oral drug absorption in man based on intestine permeability in rats". *Pharmaco. Letters*, 1996, 58, PL359-363

Levine, R.R., Mcnary, W.F., Kornguth, P.J. and LeBlanc, R. "Histological reevaluation of everted gut technique for studying intestinal absorption". *Eur. J. Pharmacol.* 1970, 9, 211-219

Lewis, G.A, Mathieu, D. and Phan-Tan-Luu, R. *Pharmaceutical Experimental Design.* 1st ed. USA:Marcel Dekker, 1999, Drugs in the Pharmaceutical Sciences volume 92

Liedtke, R., Berne, G., Haase, W., Nicolai, W., Staab, R. and Wagener, H.H. "Vergeichene humanpharmakokinetik von paracetamol nach oraler und rektaler einmalapplickation". *Arzneimittelforschung*, 1979, 29, 1607-1611

Livingston, E.H and Engel, E. "Modelling of the gastric gel mucus layer: Application to the measured pH gradient". *J. Clin. Gastroenterol.*, 1995, 21, S120-S124

Lockwood, G., Albert, K., Gillespie, W., Bole, G., Harkom, T., Szpunar, G. and Wagner, J. "Pharmacokinetics of ibuprofen in man. I. Free and total area/dose relationships". *Clin Pharmacol. Ther.*, 1983, 34, 97-103

Lund, W. (ed.), *The Pharmaceutical Codex*. 12th ed. London: The Pharmaceutical Press 1994

Macadam, A. "The effect of gastrointestinal mucus on drug absorption". *Adv. Drug Del. Rev.*, 1993, 11, 221-251

Macheras, P., Reppas C. and Dressman J.B. *Biopharamaceutics of orally administered drugs*. 1st ed. London: Ellis Horwood 1995. pp35-87 and p127

Macia, M.A., Frias, J., Carcas, A.J., Guerra, P., Valiente, R. and Lucero, M.L. "Comparative bioavailability of a dispersible formulation of Diclofenac and finding of plasma peaks". *Int. J. Clin. Pharmacol. Ther.*, 1995, 33, 333-339

Madara, J.L. and Trier, J.S. *Physiology of the gastrointestinal tract*. 2nd ed. New York: Raven Press, 1987, p1209

Maddern, G., Miners, J., Collins, P.J. and Jamieson, G.G. "Liquid gastric emptying assessed by direct and indirect techniques: radionuclide labelled liquid emptying compared with a simple paracetamol marker method". *Aust. & NZ J. Med.*, 1985, 55, 203-206

Mahmud, A. and Li Wan Po, A. "Investigation of the effect of additives on the dissolution rates of aspirin and paracetamol using a factorial design". *Drug Dev. Ind. Pharm*, 1991, 17, 709-724

Martin, Y.C. "A practitioners perspective of the role of quantitative structural analysis in medicinal chemistry". *Med. Chem.*, 1981, 24, 229-237

Martindale-The Extra Pharmacopoeia. 28th ed. London:The Pharmaceutical Press, 1982

Martinez-Palomo, A. Meza, I., Beaty, G. and Cerejido, M.J. "Experimental modulation of occluding junctions in a cultural transporting epithelium". *Cell Biol.* 1980, 87, 736-745

Matthes, I., Nimmerfall., F. and Sucker, H. "Mucusmodelle zur untersuchung von intestinalabsorptionmechanismen II". *Pharmazie*, 1992, 54, 203-211

Mattok, G.L., Mcgilverray, I.J. and Mainville, C.A. "Acetaminophen III: Dissolution studies of commercial tablets of acetaminophen and comparison with *in vivo* absorption parameters". *J. Pharm Sci.*, 1971, 60, 4, 561-564

Mehlisch, D.R., Jasper, R.D. and Brown, P. "Comparative study of ibuprofen lysine and acetaminophen in patients with post-operative dental pain", *Clin. Ther.* 1995, 17,852-860

Meyer, F.A. and Silberberg, A. "A model for mucus glycoprotein structure. Comparison with sunmaxillary mucins". *Biorheology*, 1978, 25, 799-801

Miller, J.C., and Miller, J.N. *Statistics for analytical chemistry.* 3rd ed. London: Ellis Horwood 1993. pp158-159

Miller, R. P. and Fischer, L. J. "Urinary excretion of acetaminophen elimination kinetics in neonates, children, and adults". *Clin Pharmacol Ther.*, 1974, 63, 969-970

Moffat, A. C. (ed.), *Clarkes isolation and identification of drugs.* 2nd ed. London: The Pharmaceutical Press 1986, pp677 and 849

Moore, J. G., Christian P. E., and Coleman, R E. "Gastric emptying of varying meal weight and composition in man. Evaluation by dual liquid and solid phase isotopic method". *Dig. Dis Sci*, 1981, 26 , 16-22

Moore, J.G., Tweedy, C., Christian, P.E. and Datz, F.L. "Effect of age on gastric emptying of liquid-solid meals in man". *Dig. Dis. Sci.*, 1983, 28, 340-344

Moore, J. G., Circadian rhythmicity in gastric emptying, acid secretion, and mucosal damage by drugs: implications for drug therapy: in Lemmer, B (ed.), *Chronopharmacology - Cellular and Biochemical Interactions.* 1st ed. USA:Marcel Dekker, 1989, Cellular Clocks Series Volume III:

Moore, J.W, and Flanner, H.H. "Mathematical comparison of dissolution profiles". *Pharm Technol.*, June 1996, 64-74

Moyer, M.P., "Culture of human gastrointestinal epithelial cells". *Proc. Soc. Exp. Biol. Med.*, 1983, 174, 11-15

Muller, M., Schmis, R., Georgopoulos, A., Buxbaum, A., Wasicek, C. and Eichler, H. "Application of microdialysis to clinical pharmacokinetics in humans". *Clin Pharmaco. Ther.*, 1995, 57, 371-379

Mummaneni, V., Amidon, G.L, Dressman, J.B. "Gastric pH influences the appearance of double peaks in the plasma concentration-time profiles of cimetidine after oral administration in dogs". *Pharm. Res.*, 1995, 12, (5), 780-786

Mumtaz, A.M. and Ch'ng, H.S., "Design of a dissolution apparatus suitable for *in-situ* release study of triamcinolone acetonide from bioadhesive buccal tablets". *Int. J. Pharm.*, 1995, 121, 129-139

Nared-Kocevar, J., Kristl, J. and Korbar-Smid, J. "Comparative rheological investigation of crude gastric mucin and natural gastric mucus". *Biomaterials*, 1997, 18, 677-681

Neervannan, S., Dias, L.S., Southard, M.Z and Stella, V.J. "A convective-diffusion model for dissolution of two non-interacting drug mixtures from co-compressed slabs under laminar hydrodynamic conditions". *Pharm. Res.*1994a, 11, 1288-1295

Neervannan, S., Southard, M.Z and Stella, V.J. "Dependence of dissolution rate on surface area: is a simple linear relationship valid for co-compressed drug mixtures". *Pharm. Res.* 1994b, 11, 1391-1395

Neutra, M. and Louvard, D. Differentiation of intestinal cells *in vitro: in Modern Cell Biology: Functional Epithelial Cells in Culture*, Alan R. Liss, New York, NY, 1989

Neuvonen, P. and Kivisto, K.T. "Enhancement of drug absorption by antacids". *Clin Pharmacokinet.*, 1994, 27, 120-128

Nicklin, P.L., Irwin, W.J., Hassan, I.F. and Mackay, M. "Development of a minimum-calcium Caco-2 monolayer model: calcium and magnesium ions retard the transport of pamidronate". *Int. J. Pharm.*, 1995, 123, 187-197

Nimmo, J., Heading, R.C., Tothill, P. and Prescott, L.F. "Pharmacological modification of gastric emptying: effects of propantheline and metoclopromaide on paracetamol absorption". *Br. Med. J.*, 1973, 1, 587-589

Nimmo, W.S., Heading, R. C., Wilson, R.C. and Prescott, L. F. "Reversal of narcotic induced delay in gastric emptying and paracetamol absorption by naloxone". *Br. Med J.*, 1979, 2, 1189

Noble, L.B. Personal Communication,1998

Nordman, H., Davis, J.R. and Carlstedt, I. "Mucus glycoprotein from pig gastric mucosa: different mucins are produced by the surface epithelium and glands". *Biochem. J.*, 1998, 331,687-694

Oberle, R.B., Tzyy-Show, C., Lloyd, C., Barnett, J. L., Owyang, C., Meyer, J. and Amidon, G.L. "The influence of the interdigestive migrating myoelectric complex on the gastric emptying of liquids". *Gastroenterology*, 1990, 99, 1275-1282

Ojantakanen, S., Hannula, A. M. and Marvola M. "Bioavailability of ibuprofen from hard gelatin capsules containing sodium bicarbonate, lactose, or dicalcium phosphate". *Acta Pharm. Fennica*, 1990, 99, 119-126

O'Mahoney, B. Personal Communication,1998

Osiescka, I., Porter, P.A., Borchardt, R.T., Fix J.A. and C.R. Gardner, "*In vitro* drug absorption models. Brush border membrane vesicles, isolated mucosal cells and everted intestinal rings: Characterisation and salicylate accumulation". *Pharm. Res.*, 1985, 2, 284-293.

Palm, K., Luthman, K., Ungell, A., Strandlund, G. and Artursson. P. "Correlation of drug absorption with molecular surface properties". *J. Pharm. Sci.*, 1996, 85, 32-39

Paterson, J.W., Conolly, M.E., Dollery, C.T., Hayes, A., Cooper, R.G. "The pharmacodynamics and metabolism of propranolol in man". *Clin. Pharmacol.*, 1970, 2, 127-133

Petring, O. U., Adelhoj, B.,Ibsen, M. and Poulsen, H.E. " The relationship between gastric emptying of semisolids and paracetamol absorption". *Br. J. Clin Pharmaco.*, 1986, 22, 659-662

Petring, O. U. and Flachs, H. "Inter- and intra-subject variability of gastric emptying in healthy volunteers measured by scintigraphy and paracetamol absorption". *Br. J. Clin. Pharmacol.*, 1990, 29, 703-708

Pfeiffer C.J. "Experimental analysis of hydrogen ion diffusion on gastrointestinal mucus glycoprotein". *Am. J. Physiol.* 1981, 240, G176-G182

Pharmacopoeial Forum: July-August, 1988, 4160

Pinto, M., Appay, M.D., Simon-Assmann, P., Dracopoli, N., Fogh, J. and Zweibaum, A. "Enterocytic differentiation of cultured human cancer cells by replacement of glucose by galactose in the medium". *Biol. Cell.*, 1983, 47, 232-330

Plumb, J.A., Burston D., Baker. T.G. and Gardner M.L.G. "A comparison of the structural integrity of several commonly used preparations of rat small intestine *in vitro*". *Clin. Sci.*, 1987, 73, 53-59

Polentarutti, B.I., Peterson, A.L., Sjoberg, A.K., Anderberg, E.I., Utter, L.M. and Ungell, A.B. "Evaluation of viability of excised rat intestinal segments in the ussing chamber: Investigation of morphology, electrical parameters and permeability characteristics". *Pharm. Res.*, 1999, 16, 446-454

Polli, J. E., Crison, J.R. and Amidon, G.L. "Novel approach to the analysis of *in vitro-in vivo* relationships". *J. Pharm. Sci.*, 1996, 85, 753-759

Polli, J.E., Singh-Rekhi, G., Augsburger, L.L. and Shah, V.P. "Methods to compare dissolution profiles and a rationale for wide dissolution specifications for metoprolol tablets". *J. Pharm. Sci.*, 1997, 86, 690-700

Prescott, L.F. " Gastrointestinal absorption of drugs". *Med. Clin. North Am.*, 1974, 58, 907-916

Prescott, L.F., "Kinetics and metabolism of paracetamol and phenacetin". *Br. J. Clin. Pharmacol.*, 1980, 10, 291S-298S

Prescott, L.F. *Paracetamol (Acetaminophen): A Critical Bibliographic Review.* 1st ed. London: Taylor and Francis Ltd, 1996.

Radovanovic, J., Duric, Z., Jovanovic, M., Ibric, S. and Petrovic, M. "An attempt to establish an *in vitro-in vivo* correlation: case of paracetamol immediate release tablets". *Eur. J. Drug Metab. Pharmacokinet.*, 1998, 23, 33-40

Ramakrishna, B.S., Gee, D., Weiss, A., Pannall, P., Roberts-Thomson, I.C. and Roediger, W.E.W. "Estimation of phenolic conjugation by colonic mucosa". *J. Clin. Pathol.*, 1989, 42, 620-623

Rashid, M.U. and Bateman, D.N., "Effect of intravenous atropine on gastric emptying, paracetamol absorption, salivary flow and heart rate in young and fit elderly volunteers". *Br. J. Clin. Pharmaco.*, 1990, 30, 25-34

Rawlins, M.D., Henderson, D.B. and Hijab, A.R. "Pharmacokinetics of paracetamol after intravenous and oral administration". *Eur. J. Clin. Pharmacol.*, 1977, 11, 283-286

Rees, W.D.W. "Mucus-bicarbonate barrier-shield or sieve". *GUT*, 1987, 28, 1553-1556

Retaco, P., Gonzalez, M., Pizzorno, M.T. and Volonte, M.G. "Bioavailability study of paracetamol tablets in saliva and urine". *Eur. J. Drug Metab. Pharmacokinet*, 1996, 21, 295-300

Robertson, D.R.C., Renwick, A.G., Wood, N.D., Cross, N., Macklin, B.S., Fleming , J.S., Waller, D.G. and George, C.F."The influence of levodopa on gastric emptying in man". *Br. J. Clin. Pharmacol.*, 1990, 29, 47-53

Robertson, D.R.C., Renwick, N., Macklin, B. Jones, S. Waller, D.G., George, C.F. and Fleming J.S. "The influence of levodopa on gastric emptying in healthy elderly volunteers". *Eur. J Clin. Pharmacol.*, 1992, 42, 409-412

Rostami, A. Personnel Communication, 2000

Rousset, M. "The human colon carcinoma lines HT-29 and Caco-2: Two *in vitro* models for the study of intestinal differentiation". *Biochimie*, 1986, 68, 1035-1040.

Saano, V., Paronen, V., Puera, P. and Vidigren, M. "Pharmacokinetics of two 200mg ibuprofen film coated tablets and an effervescent tablet". *Drug Dev. Ind. Pharm.*, 1992, 18, 491-497

Sack-Walter, I., Lucklow, V., Guserle, R. and Weber, E. "The relative bioavailability of paracetamol following administration of solid and liquid oral preparations and rectal dosage forms". *Arzneimittelforscchung.*, 1989, 39, 719-24

Sadowski, D.C. "Drug interactions with antacids. Mechanisms and clinical significance". *Drug safety*, 1994, 11, 395-407

Sanford, Paul A., *Digestive system physiology*. 1st ed. U.K: Edward Arnold, 1982, pp36-53

Sarosiek, J., Slomany, A., Takagi, A. and Slomiany, B.L. "Hydrogen ion diffusion in dog gastric mucus glycoprotein: Effect of associated lipids and covalently bound fatty acids". *Biochem. Biophys. Res. Comm.*, 1984, 118, 523-531

Sauers, L.J., Maurer, J.K., and Reer, P.J. "The rat as a model to evaluate the gastric irritation potential of alkaline products". *Toxicologic Pathology*, 1994, 22, 324-329

SB (1998a): SB internal report PM/7/84

SB(1998b): SB internal report (pharmacokinetic data for Zapp prototype)

Schuirmann, D.J. "A comparison of two one-sided tests procedure and the power approach for assessing the equivalence of average bioavailability". *J. Pharmacokinet.* 1987, 15, 657-680

Seidman, P., Alvan, G., Andrews. R. S. and Labross, A. "Relative bioavailability of a paracetamol suppository". *Eur. J. Clin. Pharmacol.* 1980, 17, 465-468

Sekiguchi, M., Sakakibara, K. and Fujji, G. "Establishment of cultured cell lines derived from human gastric carcinoma". *Jap. J. Exp. Med.* 1978, 48, 61-68

Selen, A., Factors influencing bioavailability and bioequivalence: in Welling, P.G., Tse, F.L.S and Dighe, S.V. (ed.), *Pharmaceutical Bioequivalence*. 1st Ed. USA:Marcel Dekker,1991, Drugs and the Pharmaceutical Sciences Volume 48

Simons, K. and Fuller, S.D. "Cell surface polarity in epithelia". *Annu. Rev Cell Biol.*, 1985, 1, 243-288

Sinko, P.J., Leesman, G.D. and Amidon, G.L.,"Predicting fraction dose absorbed in humans using microscopic mass balance approach". *Pharm. Res.*, 1991, 8, 979-988

Skelly, J.P., Amidon, G.L., Barr W.H., *et al.* "Workshop Report - *In vitro* and *in vivo* testing and correlation for oral controlled/modified-release dosage forms", *Pharm. Res.* 1990, 7, 975-982

Slomiany, A., Slomiany, B., Witas, H., Aono, M. and Newman, L.J. "Isolation of fatty acids covalently bound to the gastric mucuc glycoproteins of normal and cystic fibrosis patients", *Biochem. Biophys. Res. Commun.*, 1983, 113, 286-293

Slomiany, B.L, Laszewicz, W., and Slomiany, A. "Effect of sucralfate on the viscosity of gastric mucus and the permeability to H^+ ion". *Digestion*, 1986, 33, 146-151

Small, R. E., Johnson, S.,M.and Willis H.E. "Pharmacokinetic and taste evaluation of ibuprofen (Motrin®) 800mg tablets in extemporaneous solution". *J. Rheumatol.*, 1988, 15, 345-7

Sotiropoulus, J.B., Deutsch, T. and Plakogiannis, F.M., "Comparative bioavailability of three commercial acetaminophen tablets". *J. Pharm. Sci.*, 1981, 70, 442-445

Stead, J. A., Freeman, M., John, G.T., Ward, G.T. and Whiting, B. "Ibuprofen tablets: dissolution and bioavailability studies"., *Int. J Pharm.*,1983, 14, 59-72

Supabphol, R. and Stewart, P.J. "Influence of the carrier on the intrinsic rate of dissolution of diazepam in interactive mixtures". *J. Pharm. Pharmacol.*, 1996, 48, 1249-1255

Swarbrick, J. "*In vitro* dissolution, drug bioavailability and the spiral of science". *Pharm. Technol.*, 1997, June, 68-70

Taylor D.C., Pownall, R. and Burke, W. "The absorption of beta-adrenoreceptor antagonists in rat in-situ small intestine; the effect of lipophilicity". *J. Pharm. Pharmacol.*, 1985, 37, 280-283

Taylor, D.C., Lynch, J. and Leahy, D.E. Models for intestinal permeability to drugs: in Hardy, J.G., Davis, S.S. and Wilson, C.G. (ed.), *Drug delivery to the gastrointestinal tract*, 1st ed. Chichester, U.K: Ellis Horwood Ltd, 1989

TerLaak, A.M., Tsai, R.S., Donne-Op den Kelder, G.M, Carupt, P.A., Testa, B. and Timmerman, H. "Lipophilicity and hydrogen bonding capacity of H_1-antihistamic agents in relation to their sedative side effects". *Eur. J. Pharm, Sci.*, 1994, 2, 373-384

Theobald, A.E. *Radiopharmacy and radiopharmaceuticals*, 1st ed. London, U.K: Taylor and Francis 1985

Thomas, M., Michael, M.F., Andrew, P. and Scully, N. "A study to investigate the effects of ranitidine on the metabolic disposition of paracetamol in man". *Br. J. Clin. Pharmacol.*, 1988, 25, 671P

Tortora, G.J. *Principles of anatomy and physiology*. 8th ed. USA: Harper Collins 1996

Trenktrog, T. Muller, B.W. and Seifet, J. "*In vitro* investigation into the enhancement of intestinal peptide absorption by emulsion systems". *Eur. J. Biopharm.*, 1995, 41, 284-290

Turner, N.C., Martin, G.P. and Marriott C. "The influence of native porcine gastric mucus gel on hydrogen ion diffusion: the effects of potentially ulcerogenic agents". *J. Pharm. Pharmaco.*, 1985, 37, 776-780

UK, *The British Pharmacopoeia (1998)*. United Kingdom Stationary Office - Crown Copyright, WK, 1998

USA, *The United States Pharmacopoeia (USP* 23). United States Pharmacopoeial Convention, Inc., Rockville, USA, 1995.

USA, U.S Department of Health and Human Services, Food and Drug Administration, Centre for Drug Evaluation and Research (CDER). "Guidance for Industry - Immediate release oral dosage forms. Scale-up and post-approval changes: Chemistry, manufacturing and controls, *in vitro* dissolution testing, and *in vivo* bioequivalence". November 1995

USA, U.S Department of Health and Human Services, Food and Drug Administration, Centre for Drug Evaluation and Research (CDER). "Guidance for Industry - Dissolution testing of immediate release solid oral dosage forms". August 1997

USA, U.S Department of Health and Human Services, Food and Drug Administration, Centre for Drug Evaluation and Research (CDER), Centre for Biologics Evaluation and Research (CBER). "Guidance for Industry - Stability Testing of Drug Substances and Drug Products". Draft - June 1998

Vist, G.E. and Maughan, R.J. "Gastric emptying of ingested solutions in man - effect of beverage glucose concentration", *Medicine and science in sports exercise*, 1994, 26, 1269-1273

Volberg, T., Geiger, B., Kartenbeck, J. and Franke, W.W. "Changes in membrane microfilament interaction in intracellular adherons junctions upon removal of extracellular ca^{2+} ions", *Cell Biol.*, 1986, 102, 1832-1842

Wade A. and Weller P.J. *Handbook of Pharmaceutical Excipients*. 2nd ed. London: The Pharmaceutical Press, 1994.

Wagner, J.G. *Pharmacokinetics for the Pharmaceutical Scientist*. 1st ed. USA: Technomic Publishing, 1993, pp15-44

Walter, K., Weiss, G., Laicher, A. and Stanislaus, F. "Pharmacokinetics of ibuprofen following a single administration of a suspension containing enteric-coated microcapsule". *Arzneimittelforschung.*, 1995, 45. 886-90

Walter-Sack, I.E., de Vries, J. X., Nickel, B., Stenzhorn, G and Webber, E. "The influence of different formula diets and different pharmaceutical formulations on the systemic availability of paracetamol, gall bladder size, and plasma glucose", *Int. J. Clin. Pharm.*, 1989, 27, 544-550

Weikel, J. H., and Lish, P.M. "Gastrointestinal pharmacology of antipyretic-analgesic agents. II. Absorption and smooth muscle effects". *Arch. I. Pharm.* 1959,119, 398-408

Welling, P.G., *In vitro* methods to determine bioavailability: in Welling, P.G., Tse, F.L.S and Dighe, S.V. (ed.), *Pharmaceutical Bioequivalence*. 1st ed. USA:Marcel Dekker, 1991, Drugs and the Pharmaceutical Sciences Volume 48

Welling, P.G., *Pharmacokinetics: Processes and Mathematics*. 1st ed. USA: American Chemical Society, 1986, pp213-240

Williams, R.L., Bioequivalence and therapeutic equivalence: In Welling, P.G., Tse, F.L.S and Dighe, S.V. (ed.) *Pharmaceutical Bioequivalence*. 1st ed. USA:Marcel Dekker, 1991, Drugs and the Pharmaceutical Sciences Volume 48

Williams, S. E., and Turnberg, L. A. "Demonstration of a pH gradient across mucus adherent to rabbit gastric mucosa evidence for a 'mucus-bicarbonate' barrier". *GUT*, 1981, 22, 94-96

Wilson, T.H. and Wiswman, G. "The use of everted small intestine for the study of the transference of substances from the mucosal to the serosal surface", *J. Physiol.*, 1954, 123, 116-125

Winne, D. and Verheyen, W. "Diffusion coefficient in native mucus gel of rat small intestine". *J. Pharm. Pharmacol.*,1990, 42, 517-519

Wong, C., Yeh, M. and Wang, D. "High performance liquid chromatographic determination of ketoprofen in pharmaceutical dosage forms and plasma" *J. Chromatogr.*, 1992, 15, 1215-1225

Wood, C.W. and Holiday, A.K, *Inorganic Chemistry: an intermediate text* . 3rd ed. London: Butterworths 1967. p56

Yu, L.X. and Amidon, G.L. "A compartmental absorption and transit model for estimating oral drug absorption". *Int. J. Phar.*, 1999, 18, 119-125

Zheng, Y., Qiu, Y., Fu Lu, M., Hoffman, D. and Reiland, T. "Permeability and absorption of leuprolide from various intestinal regions in rabbits and rats". *Int. J. Pharm.*, 1999, 185, 83-92

Zweibaum, A., Laburthe, Grasset, E. and Louvard, D., Use of cultured cell lines in studies of intestinal cell differentiation and function: in Field, M. and Frizzell, R.A. (ed.) *Handbook of Physiology, The gastrointestinal system, IV*, American Physiological Society, Oxford University Press, New York, NY, 1989

APPENDIX 1

Composition of Buffers

Buffer	Component 1	Component 2	Final Volume
pH 1.2	50ml 0.2M Potassium Chloride	85ml 0.2M hydrochloric acid	200ml
pH2.0	50ml 0.2M potassium chloride	13ml 0.2M hydrochloric acid	200ml
pH 3.0	80.3ml 0.1M citric acid	19.7ml 0.2M disodium phosphate	100ml
pH 4.0	62.0ml 0.1M citric acid	38.0ml 0.2M disodium phosphate	100ml
pH 5.0	49.0ml 0.1M citric acid	51.0ml 0.2M disodium phosphate	100ml
pH 6.0	50ml 0.2M monobasic potassium phosphate	5.6ml 0.2M sodium hydroxide	200ml
pH 7.0	50ml 0.2M monobasic potassium phosphate	29.1ml 0.2M sodium hydroxide	200ml
pH8.0	50ml 0.2M boric acid and potassium chloride	3.9ml 0.2M sodium hydroxide	200ml
pH 9.0	50ml 0.2M boric acid and potassium chloride	20.8ml 0.2M sodium hydroxide	200ml
pH9.7 (modified)	50ml 0.2M boric acid	20.8 ml 0.5M sodium hydroxide	200ml
pH 11 (modified)	50ml 0.2M boric acid and potassium chloride	adjusted to pH 11 with concentrated sodium hydroxide	200ml

APPENDIX 2

Radio-labelled materials manufacture and certificates of analysis

[^{3}H]Paracetamol

The labelled compound was prepared *via* a palladium mediated bromine/tritium exchange. The dibromo precursor (SB 288330) was prepared via the bromination of acetaminophen with Br21CH3COOH, followed by flash chromatography on silica. In the tritiation, SB 288330 (1 mg, 3.24 μmol) was dissolved in ethyl acetate (3 ml) and treated with Et_3N (1.64 mg, 16.2 μmol, 5 eq) and 10% PdC (2 mg, 200 wt%). The mixture was stirred under 2.7 Ci of tritium gas at room temperature for 21 h. After removal of the catalyst and evaporation of the solvent in vacuo, the labile tritons were exchanged with a proton source (CH_3OH) by static distillation. The ensuing residue was taken up in ethanol to give 135 mCi of product having a radiochemical purity of about 80% by radio-TLC scanning analysis. This material was subsequently chromatographed by semi-preparative HPLC on a 10 mm ID Microsorb Si column eluting with 5% CH_30H in CH_2Cl_2. The eluate fraction containing the product was collected, pooled, and evaporated to dryness 1.n vacuo. The ensuing residue was taken up in abs ethanol (10 ml) affording Lot AV41590-020BI having the following analytical profile.

Lot AV41590-020B 1

Assay	Result
Total activity	100.0 mCi
Radiochemical purity by HPLC	99.5 %
Specific activity by mass spectrometry	38 Ci/mmol

Storage and Stability

The compound is stored at -143 °C under an inert atmosphere. The stability of the compound is not known, therefore the material should be reanalysed before use.

[^{14}C]Ibuprofen

ICN Biomedicals, Inc. A Subsidiary of ICN

Data and Analyses

Catalogue Number: 16022 RS-IBUPROFEN [Carboxyl-^{14}C]
MW 206.27

Lot Number: 612311

Specific activity: 50.3 mCi/mmol
1.86 GBq/mmol

Concentration: 0. 1 mCi/ml
3.7 MBq/ml

Packaging: In ethanol in a screw top vial.

Preparation: This was made according to the methods in the following reference Chen, C., S., et al. Anal. Biochem. 212, 143. (1993). J. L. C. R., Vol. XXVIII, No. 9, 1017.

QUALITY CONTROL ANALYSIS:

Radiochemical Purity: The radiochemical purity is initially determined to be 99% on July 9, 1998 when determined by the following methods:

1. HPLC on a Zorbax SB-CI8 column, 5 microns, 250 x 4.6 mm, using 50% Acetonitrile, 50% Aq H_3PO_4 as the mobile phase, at a flow rate of 1.0 ml/min. Detector 1 = Beta Ram. Detector 2 = UV at 220 nm.
2. TLC (silica gel) using Hexane:Ethyl acetate (1: 1).
3. TLC (silica gel) using Ether:Hexane (1: 1).
4. TLC (silica gel) using Benzene:Hexane (1: 1).

Stability and Storage Conditions:
The product exhibits decomposition at a rate of <l% per month when stored between 0-5°C.This ships ambient, please refrigerate upon arrival.

It is recommended that the product be analysed for radiochemical purity in at least one of the above systems if it is used more than two months beyond the date of receipt.

[^{3}H]D-Mannitol

ICN Pharmaceuticals, Inc

Data and Analyses

Catalogue Number: 27040

D-MANNITOL, [2-^{3}H]
MW 182.2

Lot Number: 54620302

Specific activity: 27 Ci/mmol
999 GBq/mmol

Concentration: 1 mCi/ml
3.7 MBq/ml

Packaging: Ethanol:Water (2:8) in a multi-purpose vial.

Preparation: D-mannitol, 2-[^{3}H] is prepared by the reduction of D-mannose [2-^{3}H] with NaB^3H_4. D-mannitol, 2-[^{3}H] is purified by paper chromatography and HPLC.

QUALITY CONTROL ANALYSIS:

Radiochemical Purity: The radiochemical purity is initially determined in the following systems. The purity is rechecked every two months. On May 22,1999 the purity was >99%.

1. HPLC using a Phenomenex Rezex ROA column with a mobile phase of 0.005M H_2S0_4 at a flow rate of 0.6 ml per minute and 35°C.
2. Paper chromatography in n-BuOH:EtOH:H_20 (52:18:30)
3. Paper chromatography, descending, in n-PrOH:EtAc:H_20 (7:1:2).
4. Paper chromatography, descending, in 80% phenol.
5. TLC on cellulose in n-BuOH:pyridine:H_20 (6:4:3).
6. Paper electrophoresis in 0.015 M Na.Citrate, 0.04% EDTA, pH 4.05.

Stability and Storage Conditions:
This product exhibits less than 1 % decomposition per month when stored at 4°C.

It is recommended that the product be analysed for radiochemical purity in at least one of the above systems if it is used more than two months beyond the date of receipt.